Death Receptor 3: A Regulator of Bone Turnover and New Target for Therapy for Osteoporosis?

A thesis submitted in candidature for the degree of

Doctor of Philosophy

By

Fraser Leigh Collins

2013

Section of Rheumatology

School of Medicine

Cardiff University

DECLARATION

This work has not been submitted in substance for any other degree or award at this or any other university or place of learning, nor is being submitted concurrently in candidature for any degree or other award.

Signed.....(Fraser Collins) Date.....

STATEMENT 1

This thesis is being submitted in partial fulfilment of the requirements for the degree of PhD.

Signed.....(Fraser Collins) Date.....

STATEMENT 2

This thesis is the result of my own independent work/investigation, except where otherwise stated. Other sources are acknowledged by explicit references. The views expressed are my own.

Signed.....(Fraser Collins) Date.....

STATEMENT 3

I hereby give consent for my thesis, if accepted to be available for photocopying and for inter-library loan, and for the title to be made available to outside organisations.

Signed.....(Fraser Collins) Date.....

STATEMENT 4

I hereby give consent for my thesis, if accepted to be available for photocopying and for inter-library loans **after expiry of a bar on access previously approved by the Academic Standards & Quality Committee.**

Signed.....(Fraser Collins) Date.....

Acknowledgements

The work performed throughout the duration of this thesis would not have been possible without the help, support and guidance of a number of people whom I would like to thank, as well as the financial support from Arthritis Research UK (ARUK).

I am deeply grateful to my supervisors Dr Anwen Williams and Dr Eddie Wang whose advice, encouragement, support and most importantly patience have helped me through the past few years. Thank you to Dr Michael Stone and the doctors and nurses at the Bone Research Unit (University Hospital, Llandough) who helped collect the post-menopausal patient blood samples.

Next I would like to thank Anja Bloom for all the help she provided as a friend and lab partner during the course of my Ph.D. William Perks and Ravinder Singh who always managed to make me smile and Kate Mumford for her helpful advice, support and optimism. I must also express gratitude to many of my colleagues in the section of Rheumatology and the Tenovus building who provided support, advice and research facilities but more importantly made it a fun and enjoyable place to work.

Special thanks have to go to my family. My Mum and Dad, who have always provided me with unconditional support, and my brothers James and Richard who have given me helpful advice throughout my research and write up, as well just helping me relax from time to time.

Finally and most importantly I have to thank my wife Stephanie whose patience, support and belief have kept me smiling (and relatively sane) throughout the duration of this thesis.

Summary

Death receptor 3 (DR3) is a member of the TNFRSF and has one confirmed TNFSF ligand - TNF-like protein 1A (TL1A). Recent studies have suggested a role for DR3/TL1A in osteoclast (OC) and osteoblast (OB) biology. However, the mechanism through which they acted and the consequences in diseases characterised by adverse bone pathology were not investigated. This thesis investigated the role of DR3/TL1A in OC formation and resorptive function (murine and human), diseases characterised by OC hyper-activity and homeostatic OB differentiation and function (murine) using cell culture and molecular biology techniques.

DR3/TL1A were demonstrated for the first time to have a direct effect on *in vitro* OC formation and resorptive function in both murine and human models. DR3 was revealed to be critical for OC resorptive function (murine) while TL1A dose-dependently increased osteoclastogenesis and resorptive function in the human system. Studies into the mechanism identified that DR3/TL1A regulated expression of the chemokines CCL2 and CCL3 as well as the activation of MMP-9. In rheumatoid arthritis patient serum TL1A was significantly increased, with levels linked to the presence of rheumatoid factor and erosive disease. Intriguingly, DR3/TL1A were shown to have no direct significant role in the increased OC activity associated with post-menopausal osteoporosis; DR3 was not detected on patient-derived OC precursors and serum levels of TL1A were not elevated. Analysis of murine osteoprogenitors and OB revealed expression of DR3 and TL1A and suggested a novel autocrine role in OB differentiation. This was supported by the OB mineralisation assay results which demonstrated reduced differentiation, MMP-2 and MMP-9 activation and mineral deposition in $DR3^{ko}$ cultures.

The results presented in this thesis identify a novel, complex and multi-factorial role for DR3/TL1A in controlling OC and OB differentiation and function; imbalances in which can lead to the pathogenesis of adverse bone pathology.

Table of Contents

List of Tables

List of Figures

Abbreviations

AA	Ascorbic acid
ACR	American College of Rheumatology
AIA	Antigen induced arthritis
ALP	Alkaline phosphatase
αMEM	Alpha Modification Minimum Essential Medium
AP-1	Activator protein-1
AS	Ankylosing spondylitis
ATF4	Activating transcription factor 4
BCIP	5-bromo-4-chloro-3-indolyphosphate
βGP	β-glycerophosphate
BM	Bone marrow
BMCs	Bone marrow cells
BMD	Bone mineral density
BMM	Bone marrow macrophages
BMPRs	BMP receptors
BMPs	Bone morphogenetic proteins
BMU	Basic multicelluar unit
BRU	Bone remodelling unit
BSA	Bovine serum albumin
CatK	Cathepsin K
cbfa 1	Core-binding factor subunit alpha-1
CFU-Fs	Single colonies
CIA	Collagen induced arthritis
CMP	Common myeloid progenitor
CRD	Cysteine rich domain
DAPI	4', 6-diamidino-2-phenylindole
DD	Death domain
Dex	Dexamethasone
DISCs	Death-inducing signalling complexes
DKK1	Dickkopf-related protein 1
DMARDs	Disease-modifying anti-rheumatic drugs

DMF	Dimethylformamide
DMSO	Dimethyl sulphoxide
dNTPs	Deoxyribonucleotide triphosphates
DR	Death receptor
DR3	Death receptor 3
DTT	Dithiothreitol
DXA	Dual x-ray absorptiometry
ECD	Extracellular domain
ECM	Extracellular matrix
EDTA	Ethylenediaminetetraacetic acid
ERK	Extracellular-signal-regulated kinase
EULAR	Eurpoean League Against Rheumatism
F-actin	Filamentous actin
FCS	Foetal calf serum
FISH	Fluorescence in situ hybridisation
FLICE	FADD-like interleukin-1β-converting enzyme
FSD	Functional secretary domain
GM-CSF	Granulocyte-macrophage colony-stimulating factor
GMP	Granulocyte/macrophage progenitor
GRB 2	Growth-factor-receptor-bound protein 2
GST	Glutathione-S-tranferase
HBSS	Hank's balanced salt solution
IBD	Irritable bowel disease
IC	Immune Complex
ICD	Intracellular domain
IFNγ	Interferon-gamma
IL-8	Interleukin-8
JNK	Jun-N-terminal kinase
LARD	Lymphocyte associated receptor of death
LDL	Low-density lipoprotein
LIGHT	Homologous to lymphotoxins exhibiting inducible expression and competing with herpes simplex virus glycoprotein D for herpes-virus entry mediator [HVEM], a receptor expressed by T lymphocytes

LT	Lympohtoxin
mAb	Monoclonal antibody
MAPKS	Mitogen-activated kinases
MCP-1	Monocyte chemoattractant protein-1
MCSF	Macrophage colony stimulating factor
MDP	Macrophage/dendritic cell progenitor
MDSREC	Medical / Dental School Research Ethics Committee
MFI	Median fluorescent intensity
MIP-1α	Macrophage inflammatory protein-1α
MITF	Microphthalmia-associated transcription factor
MMP-9	Matrix metalloproteinase-9
MSC	Mesenchymal stem cells
NBT	Nitro blue tetrazolium
NFATc1	Nuclear factor of activated T cells, cytoplasmic 1
NF-κB	Nuclear factor-κB
NRTK	Non-receptor tyrosine kinase
NSAIDs	Non-steroidal anti-inflammatory drugs
OA	Osteoarthritis
OB	Osteoblast
OC	Osteoclast
OP	Osteoporosis
OPC	Osteoprogenitor cell
OPG	Osteoprotegerin
OSX	Osterix
P13K	Phosphoinositide 3-kinase
PBMCs	Peripheral blood mononuclear cells
PBS	Phosphate buffered saline
PCR	Polymerase chain reaction
PKB	Protein kinase B
PsA	Psoriatic arthritis
PTH	Parathyroid hormone
QuOPs	Cell-cycle-arrested quiescent osteoclast pre-cursors

RA	Rheumatoid arthritis
RANK	Receptor activator of nuclear factor κB
RANKL	Receptor activator of NF-κB ligand
REC	South East Wales Research Ethics Committee
RF	Rheumatoid factor
RGD	Arg-Gly-Asp
RIP	Receptor-interacting protein
RPMI-1640	Roswell Park Memorial Institute 1640 basal medium
R-Smads	Receptor signalling mothers against decapentaplegic
SDF-1	Stromal cell-derived factor-1
SFRPs	Secreted frizzled related proteins
SNPs	Single nucleotide polymorphism
SOST	Sclerostin
SpAs	Spondyloarthritides
TGF-β	Transforming growth factor-beta
TL1	TNF-like molecule
TL1A	TNF-like protein 1A
TMB	Tetramethylbenzidine
TNF	Tumour necrosis factor
TNFR1	Tumour necrosis factor receptor 1
TNFRSF	TNF receptor super family
TNFRSF25	TNF receptor superfamily member 25
TNFSF	Tumour necrosis factor super family
TR3	TNF receptor-like 3
TRADD	TNFR-associated death domain protein
TRAF	TNF-associated factor
TRAMP	TNF related-receptor apoptosis-mediating protein
TRANCE	TNF related activation-inducing cytokine
TRAP	Tartrate resistant acid phosphatase
VEGF	Vascular endothelial growth factor
VEGI	Vascular endothelial growth inhibitor

Chapter 1

Introduction

1 Introduction

1.1 Bone

The adult human skeleton is comprised of 206 bones. Depending on its location each bone has one or more specific functions including structural support and movement, protection of vital organs and maintenance of mineral homeostasis. Bone is split into two main types: flat bone, such as the skull and scapula, and long bone such as the femur and tibia. Long bone (Fig 1.1) consists of a hollow diaphysis which flairs at the end to form the metaphysis, the region below the growth plate, and the epiphyses, the region above the growth plate. The shaft is mainly composed of dense, solid bone known as cortical bone, whereas, the metaphysis and epiphysis contain a honeycomb-like network of interconnected trabecular plates surrounding bone marrow known as cancellous bone.

Bones are surrounded by an outer fibrous sheath known as the periosteum. This is an envelope of fibrous connective tissue that covers all bone surfaces, except at joints. The periosteum provides nourishment to the bone via blood vessels as well as containing nerve endings and the bone cells – the osteoclast and the osteoblast. The inner surface of bone, which is in contact with the marrow, is known as the endosteum. This is a membranous sheath that contains blood vessels, osteoclasts and osteoblasts (1). Rather than being solid and inanimate, bones are dynamic organs that are continuously changing via a process known as bone remodelling.

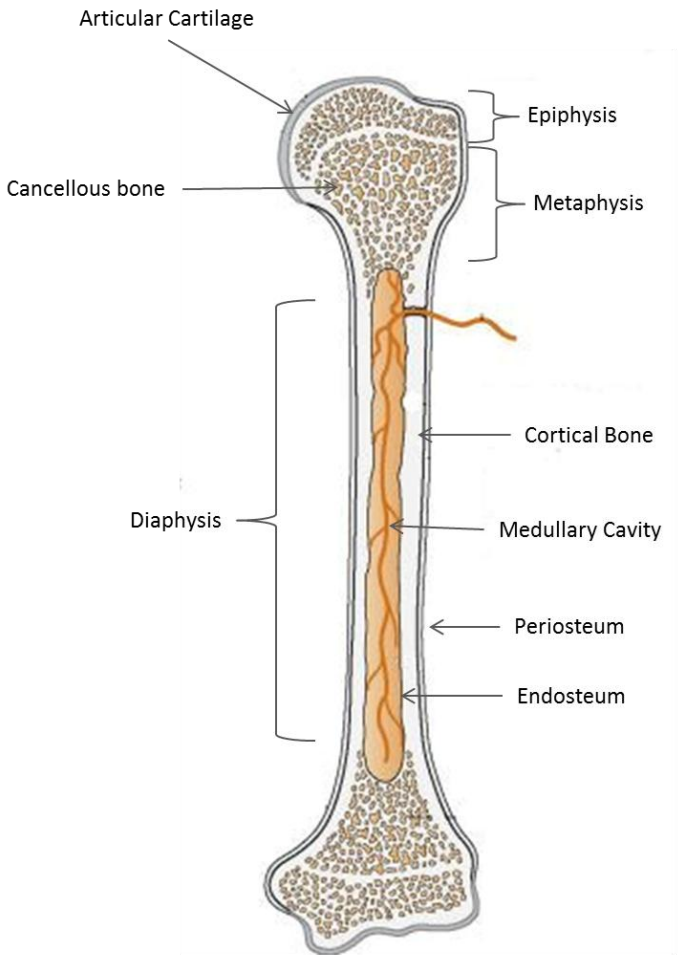

Fig 1.1. Schematic Representation of a Long Bone

Long bones are composed of two bone types. Dense cortical bone surrounds the medullary cavity making the diaphysis, while the metaphysis and epiphysis are composed of a spongy cancellous bone. A thin fibrous sheath, the periosteum, covers the outside of the bone while the inner surface in contact with the marrow is the endosteum. Image adapted from Aspinall et al, 2004. Introduction to Veterinary Anatomy and Physiology: Butterworth-Heinemann Limited.

1.2 **Bone Remodelling**

Throughout a lifetime the skeleton is subjected to a variety of stresses and strains leading to the formation of cracks and micro-damage. To maintain the integrity of the skeleton it is continuously remodelled; in the adult human skeleton, approx. 5 – 10% of the existing bone is replaced every year (2). Remodelling is accomplished by the coupled activities of a group of cells collectively termed the bone remodelling unit (BRU) or basic multicelluar unit (BMU). The cells that constitute the BMU are the osteoblast (OB), a cell that produces the organic bone matrix and aids in its mineralisation (3); the osteoclast (OC), a cell responsible for the degradation of bone and extracellular matrix (ECM) (4); the osteocyte, an osteoblast-derived cell that lies within the bone matrix which acts as a mechanosensor and an endocrine cell (5); and the bone lining cell, a cell that helps couple bone formation to resorption (6). There are four distinct phases in the bone remodelling cycle (7): i) initiation, ii) resorption, iii) reversal and iv) formation (Fig 1.2).

1.2.1 **Initiation**

The initiation phase of bone remodelling is induced by mechanical strain, damage or by signals from cytokines or systemic factors. This generates local signals that lead to the digestion of the thin layer of non-mineralised matrix under the lining cells, exposing the mineralised matrix to which the OC can attach (8-10). OC and their precursors are recruited to the site of bone remodelling from the circulatory system and the 'osteoclast niche'; an area on the bone surface near osteoblasts that contains cell-cycle-arrested quiescent osteoclast precursors (QuOPs) (11, 12). Initiation of resorption is induced through osteoclast-osteoblast communication within the BMU; with osteoblast-lineage produced receptor activator of NF-κB ligand (RANKL) and macrophage colony stimulating factor (MCSF) driving the differentiation and survival of the OC and their precursors (13-16).

1.2.2 **Resorption**

Once the remodelling process is initiated resorption of the bone occurs. OC attach to the exposed surface of the mineralised matrix where they polarise and form a sealed microenvironment. This sealed microenvironment is acidified to breakdown the inorganic component of bone followed by release of the enzymes cathepsin K, matrix metalloproteinase-9 (MMP-9) and tartrate resistant acid phosphatase (TRAP) to

breakdown the organic component (4, 17). Following resorption of the old damaged bone the process undergoes reversal.

1.2.3 **Reversal**

Toward the end of the resorption phase of the bone remodelling cycle mononuclear cells of OB-lineage move into the resorption pit. These mononuclear cells remove the old demineralised collagen while laying down a new thin layer (18-20). During this phase EphB4-receptor expressing OB interact with ephrinB2-expressing OC in a process known as 'coupling'. Apoptosis of the OC subsequently follows while the OB-lineage cells are stimulated to differentiate and form new bone.

1.2.4 **Formation**

Bone formation is a two-step process and proceeds slowly, taking approximately 3 months (compared to resorption which typically takes 3 weeks). The OB first secretes the unmineralised osteoid. This is composed of 90% type I collagen, the remaining 10% being made up of some minor types of collagen, proteoglycans and specific bone proteins such as osteopontin, bone sialoprotein and osteocalcin. Once the osteoid is secreted the OB triggers mineralisation by releasing matrix vesicles. These establish suitable conditions for initial mineral deposition by concentrating phosphate and calcium ions. When the OB has completed the matrix formation they undergo a number of possible fates.

The majority of OBs become apoptotic; however, some undergo further differentiation. The terminal differentiation stage of the OB is the osteocyte. Osteocytes are encased in bone and support its structure and viability, while also acting as mechanosensors. Through the production of sclerostin (SOST), an inhibitor of Wnt signalling, the osteocyte regulates the amount of new bone formation that takes place. The remaining OBs that haven't undergone apoptosis or differentiation into osteocytes form the bone lining cells. The differentiation and function of the OC and the OB are covered in more detail in sections 1.3 and 1.4.

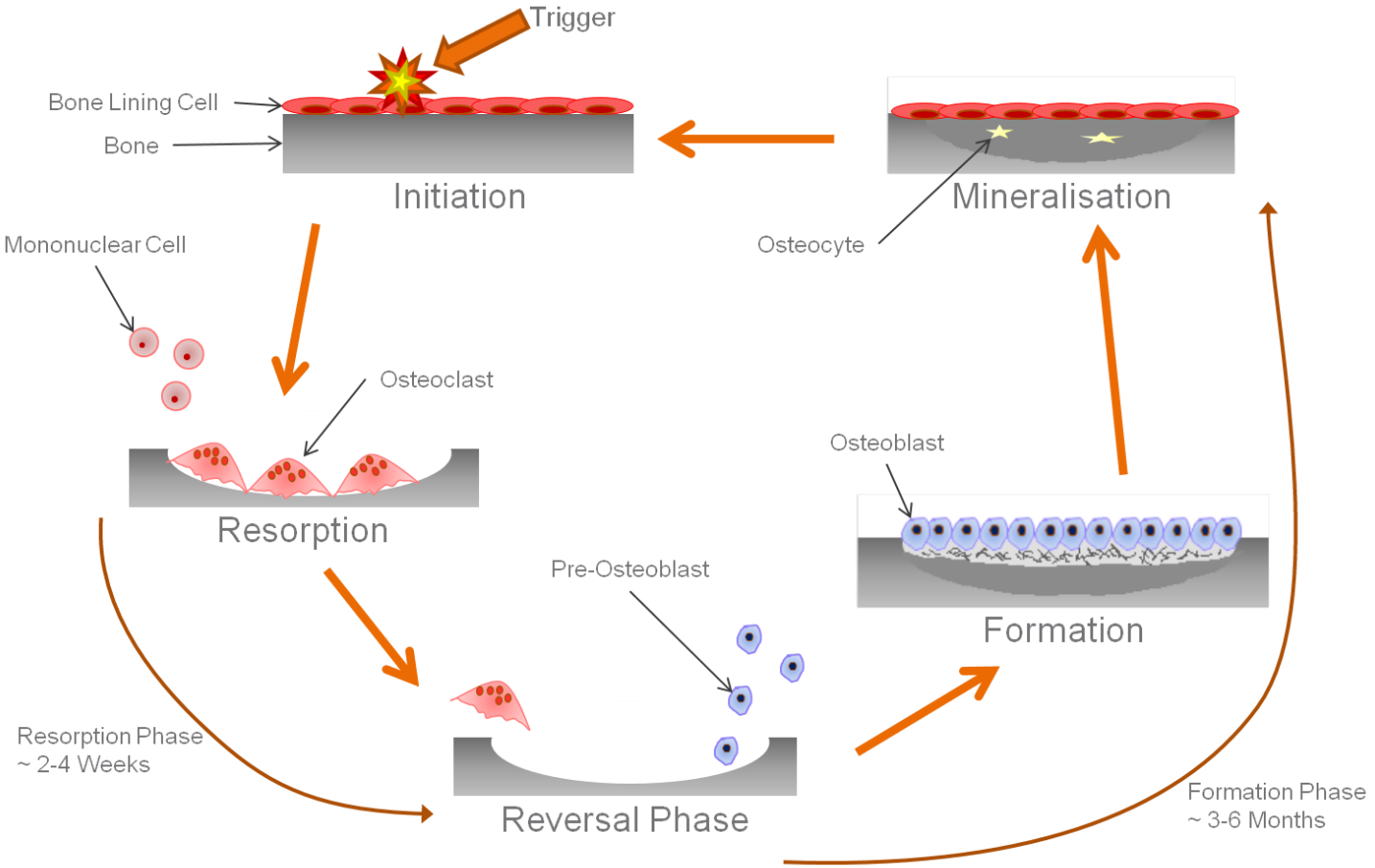

Fig 1.2. The Bone Remodelling Cycle

A representative diagram of the bone remodelling cycle. Bone remodelling is initiated by a trigger leading to the recruitment and differentiation of osteoclasts. Osteoclast resorb the old bone which is followed by the recruitment and differentiation of osteoblasts. Osteoblasts lay down new osteoid which is subsequently mineralised forming new bone.

1.3 **The Osteoclast**

The OC is a terminally differentiated, highly motile, multinucleated cell; they can contain between 3 – 100 nuclei but typically contain 10 – 20 nuclei (21). They come from an haematopoietic origin (22, 23) and are formed by the fusion of monocyte / macrophage precursors. Mature osteoclasts have several features that distinguish them from other macrophage polykaryons (large multinucleated macrophages such as Langhans' giant cells (24)) that are also useful in their identification (Table 1.1); however, the most commonly employed are their multinuclear appearance and the expression of tartrate resistant acid phosphatase (TRAP) (25, 26).

Although OC are derived from the monocyte / macrophage lineage their precise origin remains unclear. Monocytes develop from haematopoietic stem cells in the bone marrow that go through a series of intermediate multipotential stages; the common myeloid progenitor (CMP), the granulocyte/macrophage progenitor (GMP) and the macrophage/dendritic cell progenitor (MDP) stages (27). There is some uncertainty, however, about what constitutes the point of divergence of the OC lineage from the macrophage lineage. The phenotype of murine and human OC precursors is explored in more detail below.

1.3.1 **Murine Osteoclast Precursors**

Early *in vitro* work by Kurihara et al (28), used isolated spleen cells and identified the colony-forming unit (CFU)-blast as the earliest identifiable hematopoietic precursor that could form OC. This was built upon by Arai et al (29) who revealed by flow cytometry that c-Kit^{+} CD11b^{dull} cells in the BM contained the OC progenitors; compared to the c-Kit^{+} CD11b^{hi} population which contained macrophages and granulocytes. The c-Kit^{+} CD11b^{dull} cells could be further divided into c-FMS^{+} and c-FMS^{-} subsets with the c-FMS^{-} cells demonstrating a higher degree of immaturity and multipotency, taking longer to differentiate into OC. This was supported by Jacquin et al (30) who showed that CD3^{-} CD45R^{-} CD11b$^{-/lo}$ c-FMS^{+} c-Kit^{hi} cells rapidly formed OC when cultured in the presence of MCSF and RANKL. In recent studies by de Vries et al (31), CD31^{+} Ly6C^{+} myeloid blasts were demonstrated to respond quickly to MCSF and RANKL, when compared to CD31^{hi} Ly6C^{-} early blasts and CD31^{-} Ly6C^{hi} monocytes. In a study by Geissmann et al (32), murine blood monocytes were divided into two functional subsets; short lived CX3CR1^{lo} Gr1^{+} inflammatory monocytes and CX3CR1^{hi} Gr1^{-} long-lived resident macrophages that gave

rise to OC. A summary of the current paradigm for murine OC precursors is shown in Fig 1.3.

1.3.2 **Human Osteoclast Precursors**

The phenotypic identification of the human OC precursor in the bone marrow is less defined compared to the murine OC precursor. *In vitro* co-culture assays by Mbalaviele et al (33) demonstrated that isolated $CD34^{+}$ haematopoietic stem cells could be differentiated into OC. Further work by Koizumi et al (34) identified OC precursors and immature OC (1-3 nuclei) to be positive for CX3CR1, while mature multinucleated OC were CX3CR1-negative. Human peripheral blood monocytes are a readily accessible alternative source of OC precursors (12, 35, 36). Initial studies by Fujikawa et al (26), Quinn et al (37) and Massey, Flanagan et al (38) identified that $CD14^{+}$ monocytes isolated from peripheral blood could readily differentiate into bone resorbing OC. Further studies have added to the clarification of the circulating OC precursor phenotype. Human peripheral monocytes consist of two major subsets $CD16^{+}$ and $CD16^{-}$. These cells additionally differ in their expression of CX3CR1 (32) and CD33 (39); with $CX3CR1^{lo}$ $CD16^{-}$ $CD14^{hi}$ $CD33^{hi}$ monocytes readily differentiating into OC and $CX3CR1^{hi}$ $CD16^{+}$ $CD14^{lo}$ $CD33^{lo}$ monocytes forming few OC. These results demonstrate that the human and murine OC precursors differ in their phenotypic receptor expression. A summary of the human OC precursor phenotype is depicted in Fig 1.3.

Feature	Function	Ligand	Role
c-Fms	Receptor	MCSF	Proliferation and survival
RANK	Receptor	RANKL	Differentiation
Calcitonin Receptor	Receptor	Calcitonin	Inhibits osteoclast activity
$\alpha_v\beta_3$ integrin	Receptor	arginine-glycine-aspartic acid (RGD) motif	Mediates cell – substrate attachment
OSCAR	Receptor	-	Differentiation
CCR1	Chemokine Receptor	CCL3, CCL5, CCL7, CCL9	OC migration / differentiation
CCR2	Chemokine Receptor	CCL2	OC migration / differentiation
CCR4	Chemokine Receptor	CCL2, CCL5	OC migration / differentiation
CCR5	Chemokine Receptor	CCL3, CCL5	OC migration / differentiation
V-ATPase (ATP6i complex)	Proton pump	-	Acidification of resorption lacunae
Carbonic Anhydrase II (CAII)	Proton pump	-	Generation of H^+ ions
MMP-9	Gelatinase	-	OC migration and bone resorption
Cathepsin K	Protease	-	Bone resorption
TRAP	Enzyme	-	Bone resorption
ADAM8	A Disintegrin And Metalloproteinase	-	Differentiation
c-src	Tyrosine Kinase	-	Formation of ruffled border
Actin Ring	Structure	-	Bone resorption

Table 1.1. Osteoclast Features for use in Identification (adapted from (4, 17, 40-42))

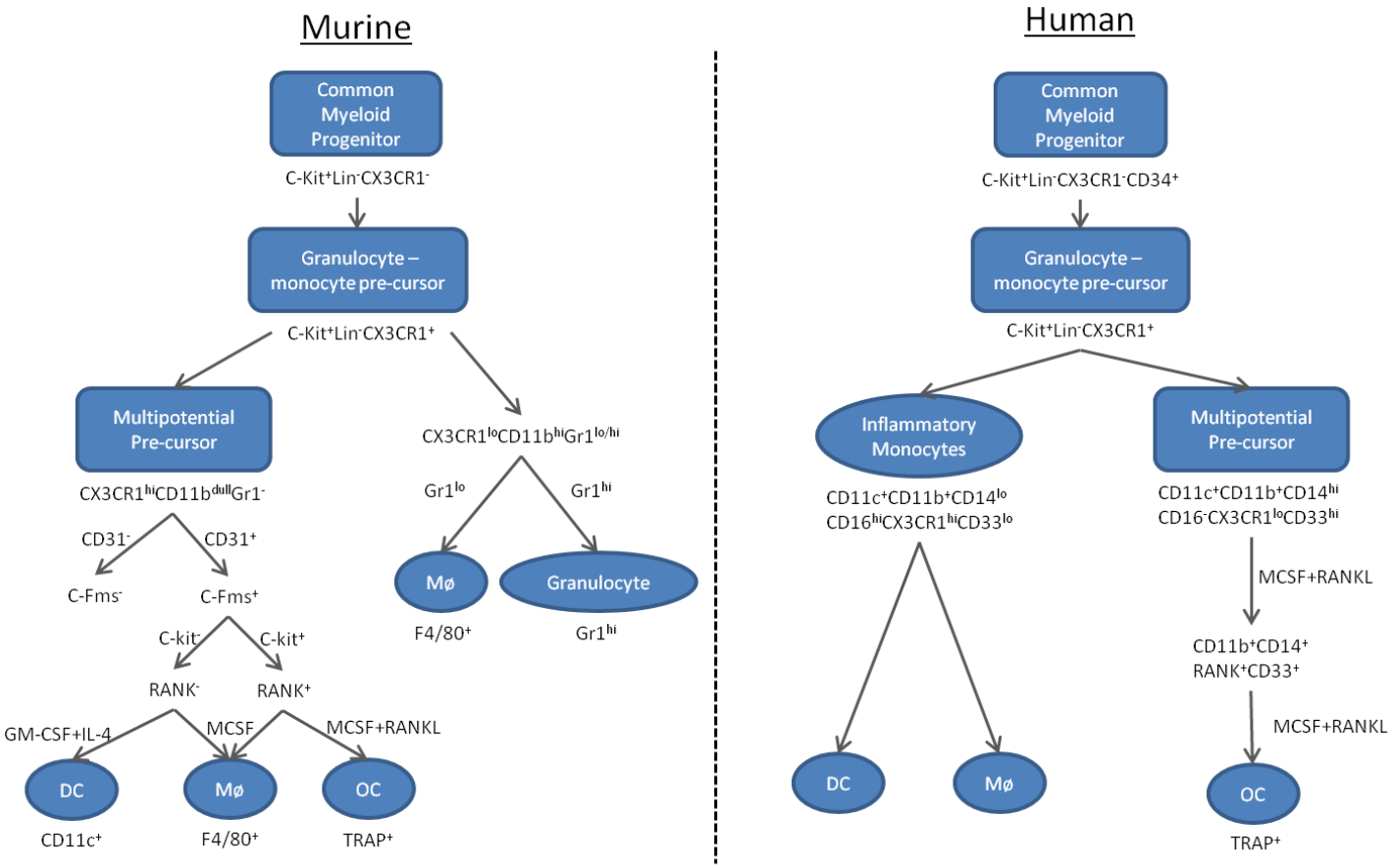

Fig 1.3. Cell Surface Markers Differentiating Murine and Human Osteoclast Pre-Cursor Populations

A representative diagram providing an outline of the cell surface markers present on cells in the osteoclast pre-cursor pathways in the murine and human systems. Image adapted from Lorenzo J, Choi Y, Horowitz M, Takayanagi H. *Osteoimmunology: interactions of the immune and skeletal systems*: Academic Press.; 2010.

1.3.3 **Osteoclast Differentiation**

While differences are observed in human and murine OC precursor phenotype, the differentiation pathways are comparable. Osteoclast differentiation is the process by which mononuclear cells undergo fusion into the multinucleated OC. The process involves a number of cytokines and hormones, from different cellular sources, that stimulate or inhibit differentiation (Table 1.2). The two critical cytokines required for OC differentiation have been identified as MCSF and RANKL. These are discussed in further detail in sections 1.3.3.1 and 1.3.3.2. The current model for OC differentiation is depicted graphically in Fig 1.4. Osteoclasts precursors are recruited to sites of bone remodelling from the circulation following chemokine gradients. At these sites the precursor cells proliferate in response to MCSF. The precursor cells then undergo differentiation following interaction between receptor activator of nuclear factor κB (RANK), expressed on the precursor cell and its ligand RANKL, which is primarily expressed on the surface of osteoblasts but can also be cleaved into a soluble form by metalloprotease. The precursor cells fuse together following chemokine gradients forming the multinucleated OC. Chemokines involved in OC differentiation are discussed in section 1.3.5. Control of OC differentiation is via the soluble receptor osteoprotegerin (OPG) which is produced by T cells and osteoblasts (43). This competes with RANK for RANKL binding, inhibiting OC differentiation.

Cytokines	Main Source	Effect on OC Formation	Direct / Indirect
Macrophage Colony Stimulating Factor (MCSF)	Osteoblasts, activated T cells	↑	Direct
Receptor Activator of Nuclear Factor-κB (RANKL)	Osteoblasts, T cells	↑	Direct
Osteoprotegerin (OPG)	Osteoblasts	↓	Direct
Tumour Necrosis Factor (TNF)	Macrophages, T_H1 cells	↑	Direct and indirect
Interferon-gamma (IFNγ)	T_H1 cells, NK cells	↓	Direct

Interleukins (IL-)	Main Source	Effect on OC Formation	Direct / Indirect
IL-1	Monocytes, Fibroblasts	↑	Direct and indirect
IL-3	Activated T cells	↑	Direct
IL-4	T_H2 cells, NKT cells	↓	Direct
IL-6	T_H2 cells, Dendritic cells, Osteoblasts	↑	Direct and Indirect
IL-10	T_H2 cells	↓	Direct
IL-11	Haematopoietic tissue	↑	Indirect
IL-17	T_H17, memory T cells	↑	Indirect
IL-18	Macrophages, Dendritic cells	↓	Indirect

Hormones and Prostaglandins	Main Source	Effect on OC Formation	Direct / Indirect
1,25-dihydroxy-vitamin D	Kidneys	↑	Indirect
Parathyroid Hormone (PTH)	Parathyroid glands	↑	Indirect
Prostaglandin E_2 (PGE2)	Most nucleated cells	↑	Direct
Oestrogen	Ovaries, fat cells	↓	Direct and indirect

Table 1.2. Factors that directly or indirectly affect OC formation (adapted from (2, 12, 44, 45)).

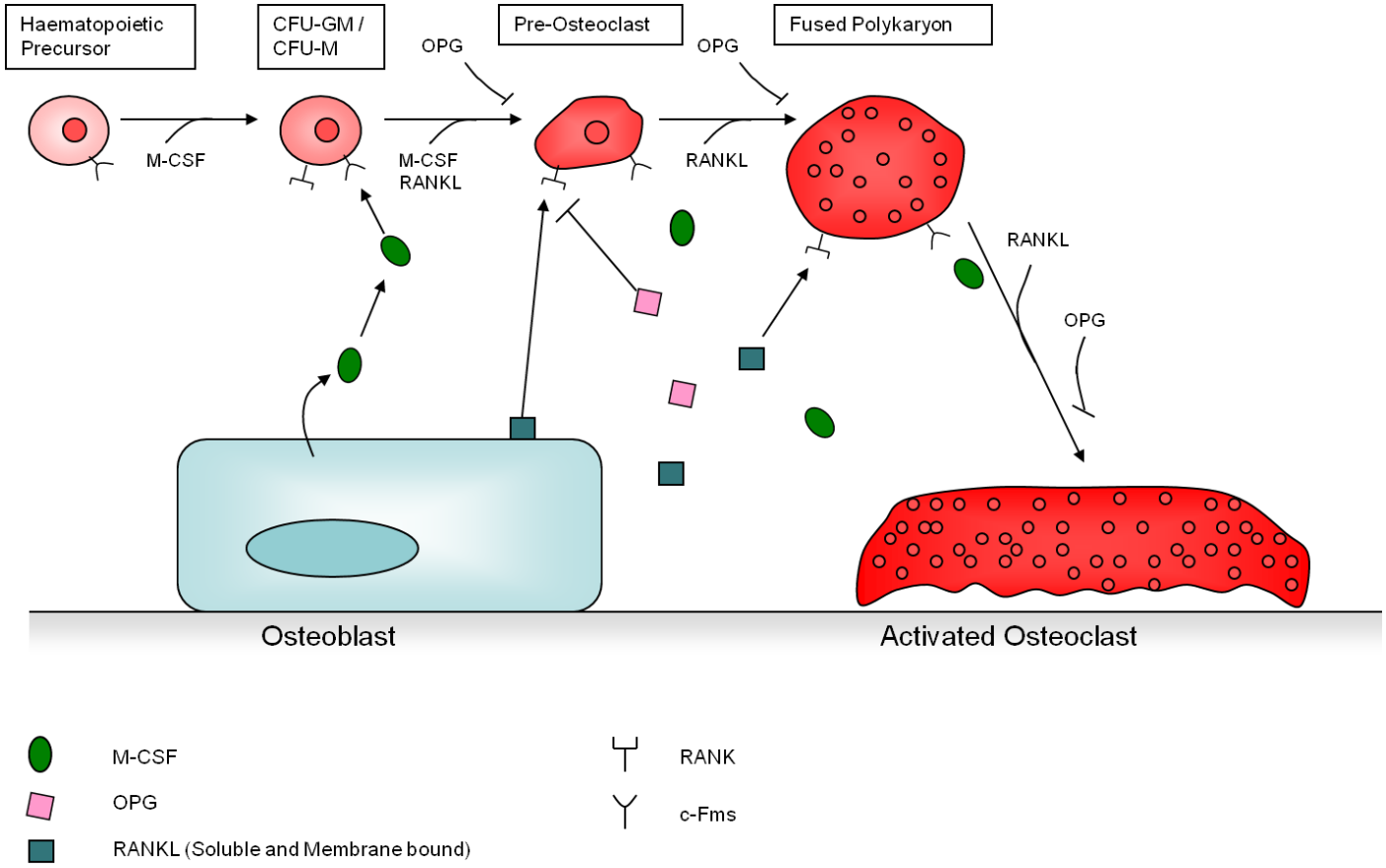

Fig 1.4. Osteoclast Differentiation

Haematopoietic precursors are recruited from the bone marrow to sites of bone remodelling. Under the influence of MCSF and RANKL cells undergo proliferation and differentiation into multinucleated osteoclasts. Control of OC differentiation is via the soluble decoy receptor OPG that competes with RANK for RANKL binding.

1.3.3.1 **MCSF / c-Fms**

Early *in vitro* systems of OC formation from marrow and circulating mononuclear precursors established the necessity for contact with an osteoblast / bone stromal cell population (46, 47). Studies with the osteopetrotic *op/op* mouse identified osteoblast / stromal cell-derived MCSF as an absolute requirement for the differentiation and proliferation of OC precursors with *op/op* mice unable to form multinucleated OC (48). The importance of MCSF signalling in OC formation was further supported by Dai et al (49). In their study, the targeted disruption of c-Fms, the MCSF receptor, resulted in a more extreme osteopetrotic phenotype than the *op/op* mice.

1.3.3.2 **OPG / RANKL / RANK**

Direct cell-cell contact was demonstrated to be essential for osteoclastogenesis in early *in vitro* studies (46, 47). This led to attempts to discover the membrane-bound factor on stromal cells. Initial attempts were unsuccessful; however, in 1997 two groups discovered a protein that blocked osteoclast formation *in vitro* and *in vivo.* This protein was subsequently termed OPG (50, 51). OPG was determined to be a soluble decoy receptor belonging to the TNF receptor super family (TNFRSF) (50). Studies using transgenic mice expressing rat OPG showed a systemic osteopetrotic phenotype, while *in vitro* addition of OPG to osteoclast cultures inhibited OC formation. Ovariectomised rats treated with recombinant OPG were observed to exhibit an increase in bone volume and a decrease in OC numbers relative to controls (50); while OPG deficient mice exhibited severe osteoporosis resulting from excessive osteoclast differentiation and activity (52, 53). From these studies it was speculated that OPG was a receptor for an unidentified TNF-related protein that normally acts as an osteoclast maturation factor.

The major breakthrough in OC biology was the discovery by Lacey et al (54) in 1998 of a membrane-bound and soluble ligand for OPG that was capable of directly affecting osteoclastogenesis. Named OPGL, it was subsequently identified as the previously characterised tumour necrosis factor super family (TNFSF) member TNF related activation-inducing cytokine (TRANCE; TNFSF11) (55). In addition to OPG, the ligand was also demonstrated to activate the TNFRSF member RANK (TNFRSF11A). TNFSF11 is now generally named after its receptor, RANK-ligand or RANKL (56, 57). The initial study by Lacey et al (54) demonstrated that stimulation of *in vitro* co-cultures and OC precursors with RANKL and MCSF stimulated the development of numerous large, functionally active osteoclasts. Administration of RANKL to mice also resulted in the significant increase in

blood-ionised calcium (hypercalcaemia), while co-administration of OPG significantly reduced the effects of RANKL. Histomorphometric and radiographic analysis of the tibia from the RANKL-treated mice revealed reduced bone volume. However, no change in the number of OC was observed between the control and treated animals, though a significant increase in the size and nuclearity of OC in the RANKL-treated group was seen (54). Further evidence for the importance of RANKL in OC formation was provided by Kong et al. (58). In their studies RANKL knockout mice were observed to exhibit osteopetrosis and defects in tooth eruption that were associated with an absence / deficiency of osteoclasts (58).

RANK, the receptor for RANKL, was originally described in dendritic cells by Anderson et al (56). It was subsequently identified on the surface of OC precursors and mature OC *in vivo* by Hsu et al (59). Recombinant RANK-Fc was observed to bind with high affinity to RANKL and inhibit OC differentiation and activity *in vitro* and *in vivo* (59). Furthermore, in a study by Dougall et al (60), $RANK^{-/-}$ mice were demonstrated to exhibit severe osteopetrosis, highlighting the importance of this receptor in OC formation and bone remodelling. OC precursor survival and differentiation induced by c-Fms / MCSF, and RANK / RANKL signalling, is via the activation of a number of signalling pathways. This results in the transcription and activation of numerous OC specific genes. These pathways are outlined below.

1.3.4 **MCSF and RANKL Signalling Pathways**

Phosphorylation of the receptor c-FMS by MCSF activates two main signalling pathways (Fig 1.5): i) the extracellular-signal-regulated kinase (ERK) pathway via growth-factor-receptor-bound protein 2 (GRB 2) and ii) the protein kinase B (PKB, also known as Akt) pathway via phosphoinositide 3-kinase (P13K) (61). Prolonged activation of ERK by MCSF also promotes its nuclear translocation where it induces c-FOS and nuclear factor of activated T cells, cytoplasmic 1 (NFATc1) expression (62). Activation of these pathways promotes osteoclast precursor proliferation and stimulates the expression of the receptor RANK (2).

Binding of RANKL to RANK induces the trimerisation of RANK and the adaptor molecule TRAF-6, activating a number of downstream signalling cascades (Fig 1.5). NFATc1 is activated via the NF-κB and c-FOS pathways (63, 64) while activator protein-1 (AP-1) is induced through the action of mitogen-activated kinases (MAPKS); including Jun-N-terminal kinase (JNK), p38 (63) and its component c-FOS (65). Robust induction of

NFATc1 during osteoclastogenesis is driven by auto regulation of its promoter (66), along with continued activation of calcium signalling and AP-1 (64). NFATc1 is subsequently translocated to the nucleus, in a process mediated by calcineurin, where in co-operation with other transcription factors such as AP-1, PU.1 and microphthalmia-associated transcription factor (MITF), it regulates a number of osteoclastogenic specific genes; CatK, TRAP, calcitonin receptor and B_3 integrin (64, 67, 68).

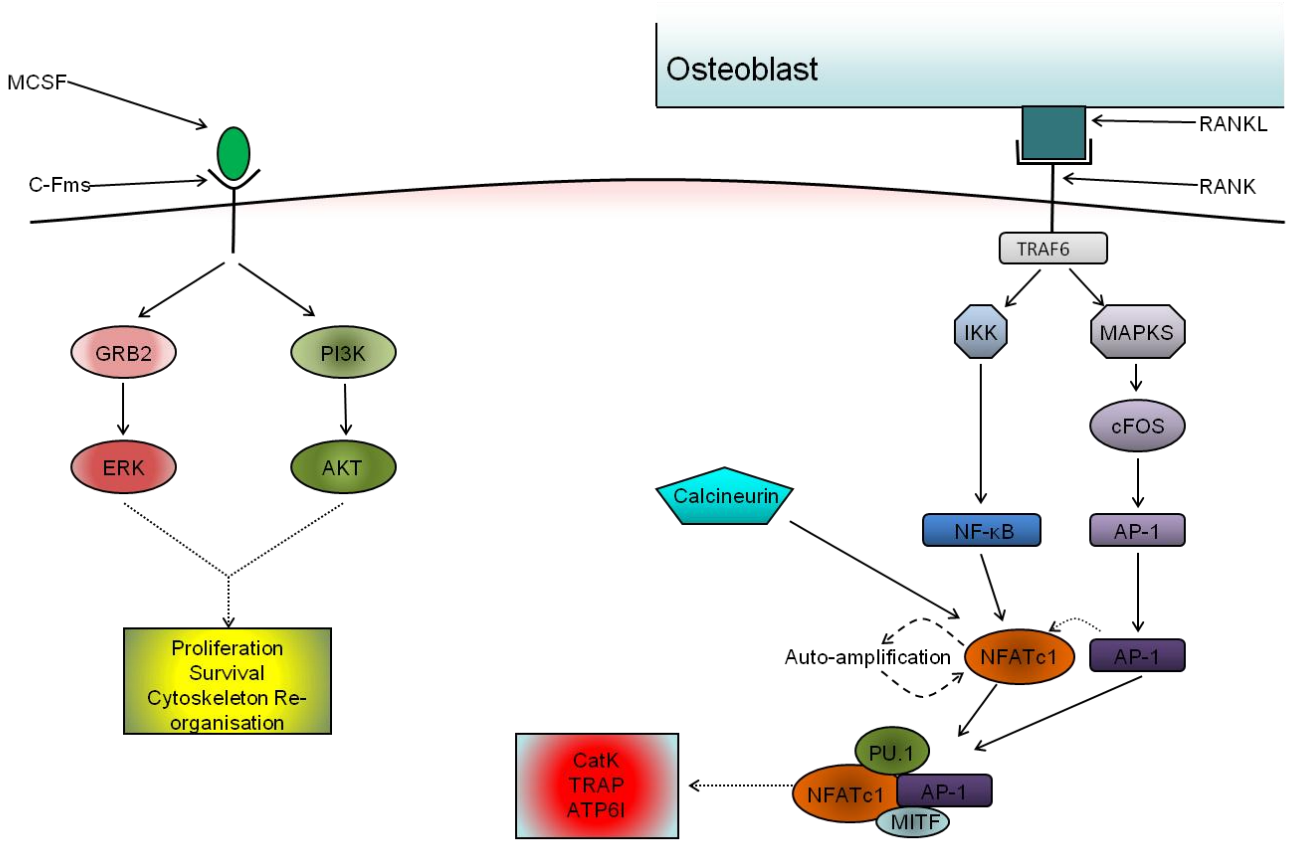

Fig 1.5. MCSF / c-Fms and RANKL / RANK Signalling Pathways

Schematic representation of MCSF / c-Fms and RANKL / RANK signalling pathways. MCSF binds to its receptor c-FMS leading to proliferation and survival of OC pre-cursors via activation of the ERK and AKT pathways. Binding of RANKL to RANK leads to activation of the NF-κB and AP-1 pathways via TRAF6. Translocation of NFATc1 to the nucleus leads to the expression of the genes involved in bone resorption such as Cathepsin K and TRAP

1.3.5 **Osteoclast Chemokines**

OC precursor migration involves at least two major steps: i) release of the cells from the bone marrow into the circulation and ii) homing from the peripheral blood to sites of bone resorption. This mobilisation of the precursor cells is a complex process involving proteolytic enzymes, stromal cells, cytokines and chemokines (69). Chemokines are small chemotactic cytokines that function as key mediators in the migration of cells. They can be divided into four branches, depending on the spacing and sequence motifs of their first cysteine (C) residues; these are C, CC, CXC and CX_3C, where X is another amino acid.

OC precursors are retained in the BM through the interaction of CXCL12 (stromal cell-derived factor-1, SDF-1) and its receptor CXCR4, expressed on OC precursors (70). Reduction of CXCL12 concentration or CXCR4 expression in the bone marrow leads to the release of OC precursors into the peripheral blood (71). In the peripheral blood stream the precursors are directed to sites of bone resorption via chemokine gradients. Chemokine signalling via their respective receptors (Table 1.3) is also required for the induction of fusion, differentiation and maturation of the mononuclear precursor cells into the multinucleated OC. The effect of the chemokines CXCL8, CXCL1, CCL2 and CCL3 on OC precursor migration and differentiation are explored in more detail below.

1.3.5.1 **CXCL8 / Interleukin-8 (IL-8)**

CXCL8 is a chemokine produced at high basal levels by osteoclasts (72). It exerts its effects through the receptors CXCR1 and CXCR2. Studies into the effects of CXCL8 on OC migration and function have yielded contrasting results. Addition of exogenous CXCL8 to rat OC cultures was demonstrated to stimulate cell spread and motility while suppressing resorption (73). In a human model, however, studies by Bendre et al (74, 75) demonstrated that exogenous CXCL8 stimulated osteoclastogenesis and bone resorption; by mechanisms dependent and independent of the RANKL pathway.

1.3.5.2 **CXCL1 / Mouse Keratinocyte-derived cytokine (KC)**

CXCL1 has been proposed as a murine functional homologue of human CXCL8, and it functions as the major pro-inflammatory alpha chemokine in mice. The receptor for CXCL1, CXCR2 is highly expressed in osteoclast precursors (76). CXCL1 is a chemoattractant for macrophages (77), suggesting that it may act as a chemoattractant for murine osteoclast precursors.

1.3.5.3 **CCL2**

CCL2 (monocyte chemoattractant protein-1, MCP-1) is a potent chemokine for monocytes, with high levels of its receptor CCR2 expressed on the cells (78, 79). Initial indications for a role of CCL2 in OC precursor recruitment were provided by observations from Wise et al (80). They demonstrated that dental follicle cells, at the site of tooth eruption, express CCL2 prior to the influx of monocytes and formation of OC (81). Studies by Kim et al (82, 83) demonstrated that CCL2 is induced by RANKL in mononuclear cells, and enhances OC-like cell formation. However, cells induced by treatment of cultures with CCL2 alone, while multinucleated and calcitonin receptor positive, could not resorb bone unless stimulated by RANKL (83). Additional support for the role of CCL2 in osteoclastogenesis, acting in an autocrine / paracrine manner, was provided by Miyamoto et al (84). In their studies OC formation was significantly reduced in CCL2-deficient mice, with DC-STAMP, NFATc1, and CatK down-regulated in the OC that did form.

1.3.5.4 **CCL3**

CCL3 (macrophage inflammatory protein-1α, MIP-1α) and its receptors CCR1 and CCR5 are expressed by OC and their precursors (85, 86). CCL3 is a direct stimulator of RANKL-induced osteoclastogenesis in bone and bone marrow cells, acting in a dose dependent manner (85, 87-89). Blockage of CCL3 (90, 91) or its receptors (86) has been shown to inhibit OC formation. Serum levels of CCL3 have also been demonstrated to correlate with the level of bone destruction in multiple myeloma patients (92) and are significantly elevated in synovial fluid from rheumatoid arthritis patients (93).

Chemokine	Alternative Nomenclature	Receptor(s)	Action
CXCL12	Stromal cell-derived factor-1 (SDF-1)	CXCR4	Recruitment of pre-cursors from bone marrow to peripheral blood
CX_3CL1	Fractalkine	CX3CR1	OC migration and attachment
sphingosine-1-phosphate	S1P	S1P receptors	Recruitment of precursors from peripheral blood to bone
CXCL8	Interleukin-8 (IL-8)	CXCR1, CXCR2	OC differentiation and / or motility
CXCL2	Macrophage Inflammatory Protein-2α (MIP-2α)	CXCR2	OC maturation
CXCL10	Interferon-γ-inducible 10kDa protein (IP-10)	CXCR3	OC maturation
CCL2	Macrophage chemoattractant protein-1 (MCP-1)	CCR2	OC differentiation
CCL3	Macrophage Inflammatory Protein-1α (MIP-1α)	CCR1, CCR5	OC differentiation
CCL9	Macrophage Inflammatory Protein-1γ (MIP-1γ)	CCR1	OC differentiation and survival
CCL5	RANTES	CCR1, CCR5	OC migration

Table 1.3. Chemokines involved in Osteoclast / OC precursor Migration and Differentiation (adapted from (27, 94)).

1.3.6 **Osteoclast Bone Resorption**

The main function of the OC is the degradation and resorption of bone. Bone degradation requires physical contact between the osteoclast and the bone matrix. It is now clear that the principal integrin mediating osteoclast attachment to the bone matrix is the $\alpha_v\beta_3$ integrin. This was demonstrated in β_3 deficient mice who displayed osteopetrosis due to dysfunctional osteoclasts (95). The $\alpha_v\beta_3$ heterodimer recognises the amino acid motif Arg-Gly-Asp (RGD) which is present in bone residing proteins such as osteopontin and sialoprotein (61), allowing the osteoclast to attach and spread on the bone substrates in an RGD-dependent manner. Osteoclasts that lack the $\alpha_v\beta_3$ integrin are still able to attach to bone, however, they are unable to organise their cytoskeleton into a sealing zone and have abnormal ruffled membranes (95). Attachment of the OC to bone causes it to undergo a number of intracellular changes, generating two polarised structures; the ruffled membrane and the actin ring. Formation of these structures enables the OC to initiate bone resorption.

In the generation of the first polarised structure, the ruffled membrane, acidified vesicles containing CatK and MMPs are transported to the bone-apposed plasma membrane (96, 97). These vesicles fuse to the membrane, in a manner regulated by the small GTPase Rab 3D (98). This fusion results in the formation of the ruffled membrane, an organelle unique to the osteoclast. Experiments have shown that the non-receptor tyrosine kinase (NRTK) c-Src is also critical for the formation of the ruffled membrane (99, 100). A high level of c-Src expression in osteoclasts is consistent with the importance of this kinase. In addition to the formation of the ruffled membrane, contact with bone prompts the osteoclast to polarise its filamentous actin (F-actin) into a circular structure known as the actin ring (101). This creates a sealed zone around the ruffled border (102).

The sealed compartment under the OC formed by the generation of the sealing zone is known as the resorption pit or Howship's lacunae. This pit is acidified to a pH of ~4.5 by the fusion of acidic vesicles to the ruffled border and an electrogenic proton pump (H^+ATPase); generated by the ATP6i complex (103) coupled to a Cl^- channel. The formation of HCl in the sealed microenvironment dissolves the inorganic solid hydroxyapatite, exposing the organic matrix beneath. Further secretion from the osteoclasts ruffled membrane continues with the export of lytic enzymes such as CatK and MMP-9 into the resorption pit to digest the organic matrix (104-106). The enzymes involved in OC resorption are covered in section 1.3.7. Efficient osteoclast activity

requires the transport and removal of the degraded ions and collagen fragments from the resorption pit into the extracellular fluid.

A specific plasma membrane domain located in the upper part of the cell, called the functional secretary domain (FSD) is the area of the cell where degradation products are targeted (101). Degradation products are endocytosed in to the osteoclast through a specific section of the ruffled membrane. They are transcytosed through the cell and finally secreted into the extracellular fluid through the FSD. This transcytotic pathway is supported with thick bundles of microtubules, which originate from the ruffled membrane and continue towards the FSD (107, 108). The extent to which the degradation of collagen and other matrix components is extracellular and the extent to which this takes place in intracellular transcytotic vesicles is not completely known. Results suggest that TRAP is localised in the transcytotic vesicles of resorbing osteoclasts and that it can generate highly destructive reactive oxygen species able to destroy collagen (109). This activity together with the co-localisation of TRAP and collagen fragments in the transcytotic vesicles suggest TRAP functions in the destruction of matrix-degradation products in these vesicles (110).

Although the events involved in the initiation of bone resorption (Fig 1.6) are relatively well understood the signals that arrest the process are less well known. Recent developments in the field suggest that the osteoblast and osteoclast are 'coupled', with reverse signalling through OC ephrinB2 by OB EphB4 suppressing OC function and initiating OB differentiation and bone formation (111, 112).

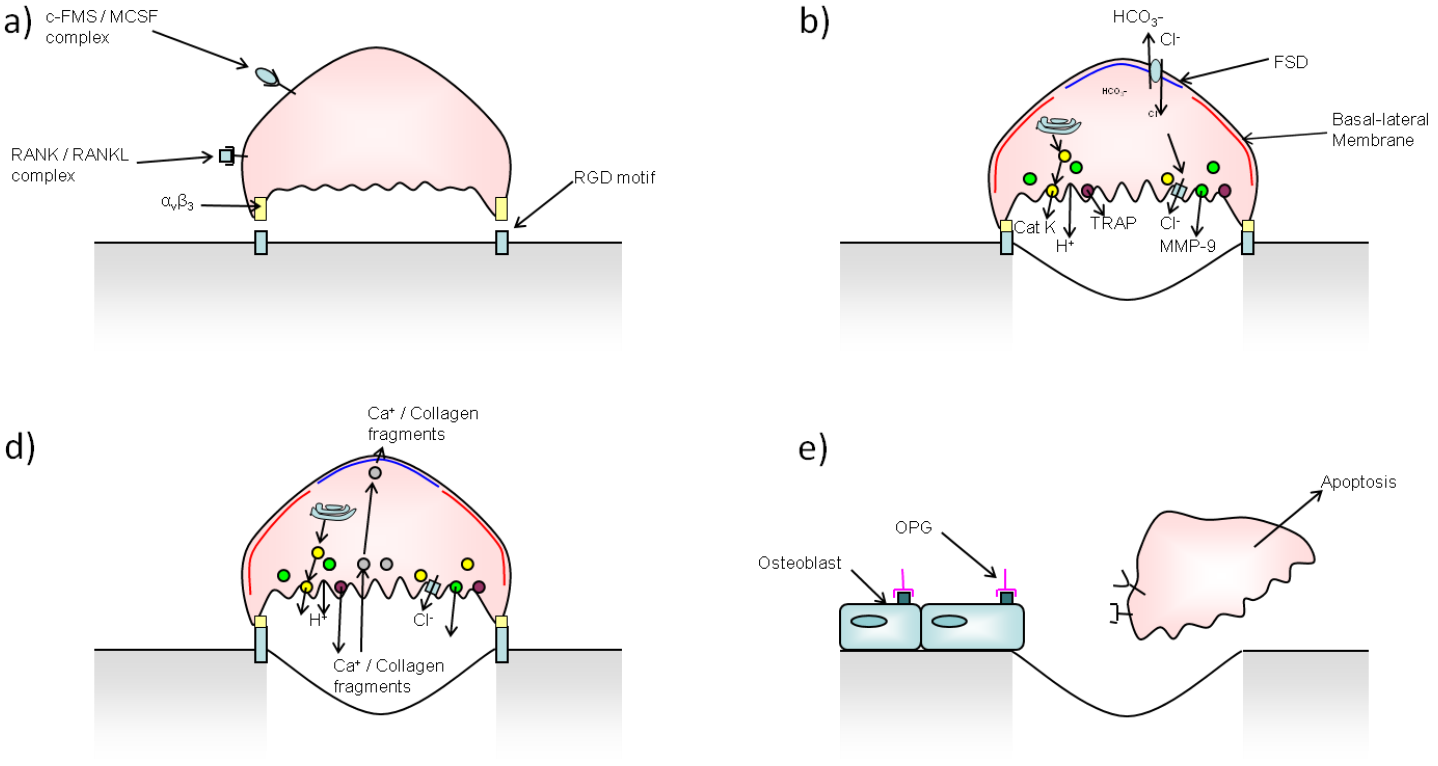

Fig 1.6. Osteoclast Resorption

Schematic diagram depicting osteoclast resorption. a) Activated osteoclasts bind via the αvβ3 integrin to the RGD amino acid motif present in bone. b) Once bound the osteoclast forms the ruffled border, actin ring and functional secretary domain. H^+ and Cl^- ions are pumped into the resorption pit to digest the inorganic bone matrix. Cathepsin K, MMP-9 and TRAP then breakdown the organic bone matrix. c) Ca^{2+} and broken collagen fragments are taken back in to the osteoclast via endocytosis and transcytosed through the cell and secreted in to the extracellular space through the FSD. d) Reverse signalling by the osteoblast induces OC apoptosis.

1.3.7 **Osteoclast Bone Degradation Enzymes**

Degradation of bone by the OC involves a number of enzymes that are responsible for the processing of the organic matrix (Table 1.4). These include members of the matrix metalloproteinase (MMP) family, cysteine proteinases (Cathepsin K) and metalloenzymes (TRAP).

Cathepsins	**Alternative Nomenclature**	**Latent / Active (kDa)**	**Substrate**
Cathepsin K	CatK	43 / 29	Type I collagen, Osteopontin, Osteonectin

Metalloenzymes	**Alternative Nomenclature**	**kDa**	**Substrate**
Tartrate Resistant Acid phosphatase	TRAP	35	Degradation products

MMP Designation	**Alternative Nomenclature**	**Latent / Active (kDa)**	**Collagen Substrate**
MMP-9	Gelatinase B 92 kDa gelatinase 92 kDa type IV collagenase	92 / 86	IV, V, VII, X, XIV
MMP-14	MT1-MMP Membrane Type 1 – MMP	66 / 56	I, II, III
MMP-1	Collagenase-1 Fibroblast collagenase Interstitial collagenase	55 / 45	I, II, III, VI, VII, X
MMP-3	Stromelysin-1 Transin-1	57 / 45	III, IV, IX, X, XI
MMP-2	Gelatinase A 72 kDA gelatinase 72 kDa type IV collagenase	72 / 66	I, III, IV, V, VII, X, XI, XIV
MMP-10	Stromelysin-2 Transin-2	57 / 44	III, IV, V,IX, X

Table 1.4. Principal enzymes and MMPs involved in OC bone degradation (adapted from (113-115)).

1.3.7.1 **Osteoclast derived MMP's and MMP-9**

Matrix metalloproteinase's (MMPs), also known as matrixins, are a class of extracellular and membrane-bound proteases. They play a central role in the breakdown of extracellular matrix (ECM) in embryonic development, morphogenesis, reproduction, and tissue resorption and remodelling (113). All members of the MMPs are synthesised as prepro-enzymes and, in the majority of cases, secreted as inactive pro-MMPs. OC MMPs have the ability to process both helical and denatured type I collagen; the most well characterised being the gelatinase matrix metalloproteinase-9 (MMP-9; (114, 116, 117).

MMP-9 is predominantly expressed by OC and OC precursors in adult bone. The contribution that MMP-9 activity plays in OC biology is only just being understood, with dual roles in bone resorption and cell migration. Evidence for the classical role of MMP-9 in bone resorption was provided by Everts et al (118, 119) and Tezuka et al (106). In these studies high levels of expression of MMP-9 mRNA in OC were shown along with secretion of the enzyme into the resorption lacuna, demonstrating a role in bone resorption. MMP-9, however, wasn't found to be rate limiting, as the resorptive activity of OC in MMP-9 null mice compares to that of wild type mice (120). This revealed that MMP-9 is not the principal enzyme involved in matrix solubilisation (121).

The additional role for MMP-9 in OC migration has evolved from a number of studies. In experiments by Vu et al (121) using MMP-9 null mice, the invasion of OC into the growth plate was delayed, resulting in the formation of lengthened growth plates. This observation that MMP-9 is involved in OC migration was supported in a study by Cackowski et al (122) who demonstrated that OC formation in MMP-9 null mice was due to reduced OC migration. Evidence that the MMPs involved in OC invasion were osteoclastic in origin came from work performed by Sato et al (123). Their experiments showed that OCs were able to migrate through collagen in the absence of other cells and that osteoclastic MMPs appear, therefore, unique amongst the OC proteinases for migration of OCs through collagen. A role for the involvement of MMP-9 in the migration and invasion of OC is also consistent with the early expression of the gelatinase during OC differentiation (117, 121, 124, 125). While the studies into MMP-9 have demonstrated that it is not the principal enzyme involved in bone degradation, the proteinase Cathepsin K is critical.

1.3.7.2 **Cathepsin K**

Cathepsin K (CatK) is a cysteine protease active at low pH that plays a key role in the degradation of bone. It is highly expressed in OCs compared to the other cathepsins (105, 126). It is largely responsible for cleaving and removing the organic matrix during OC resorption (104, 127). The importance of CatK in bone remodelling can be seen in the rare human disease pycnodysostosis and CatK-deficient mice. Pycnodysostosis results from mutations in the *Ctsk* gene, leading to decreased CatK enzymatic activity. Bones in these patients are characterised by defective remodelling and poor structure. High levels of collagen fibres are found to remain in the resorption pit as well as accumulation of non-digested collagen fibrils in vesicles inside the OC (128). CatK-deficient mice also demonstrate a mild osteopetrotic phenotype due to a high number of OC with impaired function (104, 129).

1.4 **The Osteoblast**

The osteoblast is the principal cell involved in the formation of new bone (130). They arise from pluripotent stem cells found in the BM. These stem cells have the proliferative potential to form single colonies (CFU-Fs) with the capacity to form bone, cartilage and fibrous tissue (131, 132). The CFU-Fs are commonly referred to as mesenchymal stem cells (MSC) and are separate from the haematopoietic stem cell lineage. Enrichment of the MSCs from BM preparations takes advantage of the adherent nature of the stem cells. Analysis of these cells demonstrated that the STRO-1^+ fraction contained the osteogenic precursors in human and rat, however, this lineage marker is not expressed in mouse marrow (133, 134). In a murine system the markers Sca1 and CD34 have been successfully used to identify the BM MSCs (134). Differentiation of the stem cells into mature bone forming OB is controlled under a spectrum of signalling proteins, hormones, cytokines, growth factors and transcription factors (Table 1.5). OB differentiation is discussed in further detail in section 1.4.1.

Determinant	Effect
Adrenomedullin	Mitogenic effects on OB
Androgen	Increases differentiation of post-proliferative OB and mineralisation
Activating transcription factor 4 (ATF4)	Required for bone formation
β-Catenin	High levels stimulate OB differentiation
Bone morphogenetic Proteins (BMPs)	Support OB differentiation
CXCL12 (Stromal-derived factor-1, SDF-1)	Promotes growth and survival of marrow stromal cells
Epidermal Growth Factor (EGF)	Stimulates MSCs to differentiate
Oestrogen	Increases IGF-1; stimulates osteoprogenitor proliferation and collagen synthesis
Glucocorticoid	Promotes OPC differentiation, increases apoptosis of mature OB
Insulin-like growth-factor (IGF-1/IGF-2)	Anabolic regulators; IGF-1 required for anabolic effects of PTH
Immobilisation	Inhibits bone formation
Mechanical load	Stimulates bone formation
Oncostatin M	Increases IGF-1 and alkaline phosphatase, promoting OPC differentiation
Osterix (OSX)	Required for OB differentiation and bone formation
Parathyroid hormone (PTH)	Numerous anabolic effects via regulation of OB genes
Peroxisome proliferator-activated receptor gamma (PPARγ2)	Inhibits OB differentiation, promotes adipocyte differentiation
Prostaglandin E2 (PGE2)	Increases BMP2 expression
Runx2	Required for OB differentiation and bone formation
Sclerostin (SOST)	BMP antagonist secreted by osteocytes, inhibits OB differentiation and activity, suppressed by intermittent PTH
Thyroid stimulating hormone	Decreases Wnt/LRP5 signalling, inhibits OB differentiation and collagen synthesis
$1,25(OH)_2D_3$	Upregulates OB genes that are components of the ECM

Table 1.5. Factors regulating OB differentiation and function (Adapted from (135, 136))

1.4.1 **Osteoblast Differentiation**

The initial stage of OB differentiation is the generation of the osteoprogenitor cell (OPC) from the MSCs. OPCs are multi-potential and are directed to specific cell fates by transcriptional regulators. At an early stage of differentiation members of the canonical Wnt / β-catenin pathway and bone morphogenetic proteins (BMPs) shift the cell fate of the MSC towards the osteoblast lineage, suppressing adipogenic transcription factors while inducing the osteogenic transcription factors. Expression of the transcription factor Runx2, also known as core-binding factor subunit alpha-1 (*cbfa 1*), is essential for MSC differentiation into the OPC (137). Still under the influence of the Wnt pathway and BMPs a second transcription factor, osterix (OSX), is induced. Induction of OSX drives the differentiation of the OPC towards the pre-osteoblast (or immature OB) (138). The pre-OB still has the potential to divide and expresses low levels of alkaline phosphatase (ALP) activity, an early marker of the OB phenotype. The final stages of OB differentiation and mineralisation are dependent on the transcription factors OSX and activating transcription factor 4 (*ATF4*) (139). Induction of these transcription factors leads to the generation of the non-proliferating mature cuboidal OB that actively synthesises bone matrix. The role and function of key pathways and transcription factors involved in OB differentiation are explored further in sections 1.4.1.1, 1.4.1.2 and 1.4.1.3. At the end of mineralisation the mature OBs are subjected to a number of different outcomes. The majority undergo apoptosis while the remainder become trapped in the matrix and become osteocytes or remain on the surface and become bone-lining cells (Fig 1.7). While the processes involved in OB differentiation and function *in vivo* are complex, MSCs can be persuaded to undergo osteogenesis *in vitro*.

In vitro osteogenic differentiation of marrow derived MSCs from the mouse was demonstrated by Schoeters et al (140). In this set of experiments they demonstrated that MSC differentiation and OB mineralisation could be induced in the presence of foetal calf serum, β-glycerophosphate and ascorbic acid. The ascorbic acid initiates the formation of the collagenous extracellular matrix and the synthesis of several OB-related proteins (141). β-glycerophosphate provides an exogenous phosphate source, required for induction of mineralisation. Addition of the synthetic glucocorticoid dexamethasone (Dex) is also added to *in vitro* cultures as it has been demonstrated to stimulate OB differentiation and function in mouse (142), rat (143) and human (144) MSCs.

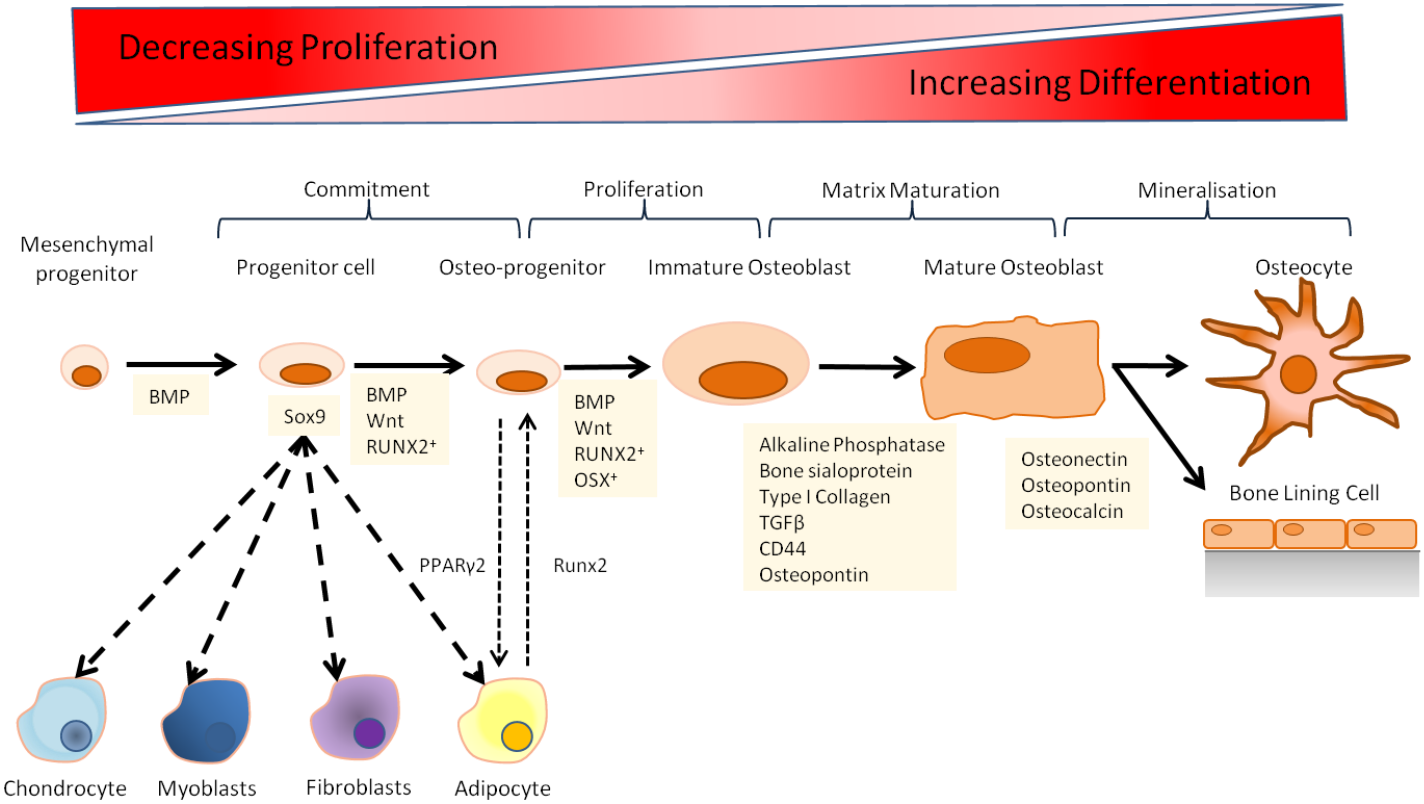

Fig 1.7. Osteoblast Differentiation

Schematic representation of osteoblast differentiation. Osteoprogenitor cells arise from mesenchymal stem cells under the influence of BMPs, Wnt signalling and the Runx2 transcription factor. These OPCs then undergo differentiation into mature mineralising osteoblasts following induction of osterix. Immature OB generate the osteoid through secretion of proteins and enzymes. The osteoid is then mineralised by the mature OB. Following the formation of the new bone the mature OB undergoes apoptosis, or differentiates into the osteocyte or bone lining cell. Image adapted from Aubin JE et al, 2006. Bone Formation: Maturation and Functional Activities of Osteoblast Lineage Cells. 6th ed: American Society for Bone and Mineral Research.

1.4.1.1 **The Canonical Wnt / β-Catenin Pathway**

The first stage in MSC differentiation towards the mature OB is dependent on the canonical Wnt / β-Catenin pathway. Canonical Wnt signalling is a key event in normal bone development and the regulation of bone mass in adults. Wnt ligands transduce their signal through cell surface frizzled receptor interactions, which are regulated by the transmembrane LRP co-receptors. The binding of Wnt ligands triggers a chain of events, which leads to the dephosphorylation of β-catenin. The freed β-catenin then enters the nucleus where it forms a complex with transcriptional regulators. The discovery of the importance of the canonical Wnt / β-catenin pathway came from studies by Boyden et al (145) and Little et al (146). They demonstrated that a high bone mass phenotype human genetic disorder was due to an activating mutation in the canonical Wnt ligand co-receptor LRP5. This role of Wnt signalling in bone formation was further supported by the observation that inactivating mutations of the LRP5 gene resulted in osteoporosis pseudoglioma syndrome (147). Additional support for the importance of the canonical Wnt / β-catenin pathway in OB development has come from a number of genetic mouse models. Work by Hill et al (148) and Day et al (149) demonstrated that a high level of β-catenin differentiates mesenchymal cells towards the OB lineage while low / moderate levels promotes chondrogenesis. Activity of canonical Wnt signalling is controlled by a number of extracellular and intracellular inhibitors. The association of Dickkopf-related protein 1 (DKK1) with LRP5, sclerostin with LRP5/6 and secreted frizzled related proteins (SFRPs) with Wnt ligands, inhibit the signalling process by stopping the formation of the receptor complex (150).

1.4.1.2 **Bone Morphogenetic Proteins**

BMPs are members of the transforming growth factor-beta (TGF-β) family. Studies have demonstrated that BMP-2, -4 and -7 are potent inducers of osteogenesis *in vivo* and *in vitro* (151). BMPs interact with specific BMP receptors (BMPRs) on the cell surface mobilising the intracellular receptor signalling mothers against decapentaplegic (R-Smads) that heterodimerise with the DNA binding Smad4. The activated Smad complex enters the nucleus where it induces the transcription of key genes involved in the commitment to the osteogenic lineage (138). The activity of the BMPs is regulated by a number of inhibitory Smads as well as the secreted factors Chordin and Noggin (152). Elucidation of the precise function of the BMPs in osteoblastogenesis and bone formation has been done through the analysis of deficiencies and mutations in the receptors and intracellular

Smad signalling components. BMP-null mice cannot be generated due to early embryonic lethality (153, 154).

1.4.1.3 **Transcription Factors – Runx2/Cbfa1, Osterix and *ATF4***

Additional to Wnt and BMP signalling, differentiation of OB from the MSCs requires the induction of a number of critical transcription factors. The transcription factors are expressed and function at different stages during the differentiation process, defining the developmental stages of the OB lineage. The initial transcription factor identified as critical for OB differentiation was Runx2/Cbfa1.

Induction of Runx2/Cbfa1 is subsequent to Sox9 expression (155); a transcription factor marker of MSCs. The significance of Runx2 was demonstrated in a murine knockout model. Mice deficient in the Runx2 gene were non-viable due to a lack of OB, resulting in a complete lack of ossification (156, 157). In humans, mutations in the Runx2 gene results in the disorder cleidocranial dysplasia (158); which is characterised by hypoplasia / aplasia of the clavicles, patent fontanelles, supernumerary teeth and short stature. In studies by Ducy et al (159) transgenic mice overexpressing Runx2 DNA-binding domain (ΔCbfa1) in postnatal differentiated OB were observed to have a normal skeleton at birth. However, these mice later developed osteopenia. This phenotype was caused by a decrease in bone formation while OC number and activity remained at a normal level. These studies revealed Runx2 also regulates differentiated OB function as well embryonic ossification. The second transcription factor shown to be critical for OB formation and function was the zinc finger protein Osterix.

Induction of OSX occurs downstream of Runx2. This was demonstrated in Runx2-deficient mice, who also exhibited no OSX expression. The importance of OSX in OB development was identified by Nakashima et al (138). In their study they revealed that deletion of OSX resulted in the complete absence of OB in murine embryos, despite normal expression of Runx2. Further studies by Zhou et al (160) using conditional OSX knockouts revealed that, like Runx2, OSX was essential for OB differentiation and new bone formation in growing and adult bones. The final key transcription factor shown to regulate OB function is ATF4.

The transcription factor ATF4 has been shown to have an important role in mature OB lineage cells. In a study by Yang et al (139) misregulation of ATF4 activity was linked to the skeletal abnormalities observed in patients with Coffin-Lowry syndrome. ATF4-deficient mice were also observed to have a high perinatal death rate. Analysis of the

mice that survived at multiple timepoints over a year showed a severe reduction in bone volume and thickness of trabeculae. This phenotype was due in part to the OB failing to reach terminal differentiation and a defect in OB function (139). ATF4 functions in OB through two mechanisms. The first is by the direct regulation of the expression of OB-derived osteocalcin, the second by promoting efficient amino acid import to ensure correct protein synthesis by the OB (139).

1.4.2 **Bone Formation**

Before bone formation starts, OB-lineage cells are recruited to the resorption pit where they remove old demineralised collagen left by the OC (18-20). Removal of the collagen is via a number of MMPs secreted by cells of the OB-lineage (Table 1.6). Bone formation can be split into 2 main phases of activity: i) osteoid synthesis and iii) matrix mineralisation. At each step the OB expresses different proteins and enzymes, which enable the process to be performed successfully.

1.4.2.1 **Osteoid Synthesis**

Initial steps in bone formation, and also one of the earliest markers of OPCs, is the synthesis of type I collagen. This makes up 90% of the organic component of bone; however, trace amounts of type III and type V collagens may be present at certain stages of bone formation (161). Non-collagenous proteins, including proteoglycans, glycosylated proteins such as tissue nonspecific alkaline phosphatase, Gla-containing proteins (osteocalcin) and lipids compose the remaining organic material, and are synthesised by the bone forming cells and are exogenously-derived from the serum (Table 1.7). Following osteoid synthesise the OB mineralises the organic matrix.

1.4.2.2 **Mineralisation**

Mineralisation of bone is completed by the incorporation of hydroxyapatite ($Ca_{10}(PO_4)_6(OH)_2$) into the newly deposited osteoid. The exact mechanism by which mineralisation occurs is not fully understood. Membrane bound extracellular bodies (extracellular matrix vesicles) released from OB facilitate initial mineral deposition by accumulating calcium and phosphate ions in a protected environment. Clusters of these ions come together to form the first stable crystals. Addition of ions to these crystals follows, resulting in their growth (162). An important role for the non-collagenous proteins in mineralisation has been suggested by a number of groups, with osteonectin

linking the bone mineral and collagen phases (163), and ALP-deficient mice showing impaired mineralisation (164).

MMP Designation	Alternative Nomenclature	Latent / Active (kDa)	Collagen Substrate
MMP-2	Gelatinase A 72 kDA gelatinase 72 kDa type IV collagenase	72 / 66	I, III, IV, V, VII, X, XI, XIV
MMP-8	Collagenase 2	55 / 46 - 42	I, II, II
MMP-9	Gelatinase B 92 kDa gelatinase 92 kDa type IV collagenase	92 / 86	IV, V, VII, X, XIV
MMP-13	Collagenase 3	65 – 60 / 55 - 50	II
MMP-14	MT1-MMP Membrane Type 1 – MMP	66 / 56	I, II, III

Table 1.6. Members of the MMP family produced by osteoblasts (adapted from (19, 113, 165, 166)).

Protein	Function
Aggrecan	Storage of water and ions, matrix organisation
Albumin	Inhibits the growth of hydroxyapatite crystals
Alkaline Phosphatase	Carries Ca^{2+} and increases local phosphate concentration by hydrolyzing pyrophosphates
Asporin	Regulates collagen structure
Biglycan	Associates with collagen and TGF-β and other growth factors
Decorin	Associates with collagen and may regulate TGF-β activity and fibril diameter. Blocks cell attachment to fibronectin
Fibromodulin	Associates with collagen and TGF-β, may regulate fibril arrangement
Fibronectin	Binds to cells, fibrin, heparin, gelatine and collagen
Glypican	Regulates cell development through BMP-SMAD signalling
Lumican	Associates with collagen may regulate fibril arrangement
Matrix Gla protein	Negative regulator of mineralisation
Osteoadherin	Possible role in cell attachment
Osteocalcin	Regulates activity of OC and their pre-cursors, possible role in the switch between bone formation and resorption. Suggested to be a hormone.
Osteonectin	Positive regulator of bone formation binding growth factors, regulating collagen organisation and mediates hydroxyapatite deposition
Osteopontin / Bone sialoprotein	Associates with cells, may regulate mineralisation and cell proliferation. Blocks nitric oxide synthase.
Perlecan	Regulates cell signalling
Secreted Phosphoprotein	Associates with regulators of mineralisation in the serum
Tetranectin	Possible role in matrix mineralisation
Type I Collagen	Serves as scaffolding, binds and orients other proteins that nucleate hydroxyapatite deposition
Type III Collagen	Present in trace amounts. May regulate collagen fibril diameter
Type V Collagen	Present in trace amounts. May regulate collagen fibril diameter
Vitronectin	A cell attachment protein

Table 1.7. Proteins associated with the bone matrix (Adapted from (161)).

1.5 **Bone Disease**

Like any other organ of the body, bone is susceptible to disease. Diseases of the bone (Table 1.8) are typically characterised by a direct or indirect effect on the balance of remodelling, leading to an increase or decrease in bone resorption and bone formation. The aetiology of these diseases is varied with nutrition, physical activity, inflammation, genetic abnormalities and hormonal changes all playing a role. The pathogenesis of inflammatory arthritides and osteoporosis are explored in more detail next.

Disease	**Genetic / Metabolic**	**Symptoms**
Osteoporosis	Metabolic	Reduced bone mineral density leading to increased risk of fracture
Osteopenia	Metabolic	Reduced bone mineral density
Osteopetrosis	Genetic	Increase in bone mass due to defective bone resorption
Paget's Disease	Metabolic	Excessive bone resorption and bone formation
Osteomalcia and Rickets	Metabolic	Softening of bone due to deficiency or impaired metabolism of Vit D, phosphate and calcium
Renal Osteodystrophy	Metabolic	Bone mineral deficiency
Osteogenesis Imperfecta	Genetic	Brittle bone due to deficiency in Type I collagen
Osteitis Fibrosa Cystica	Metabolic	Increased osteoclast activity caused by hyperparathyroidism leading to bone pain and fractures
Inflammatory Arthritides	Metabolic	Increased bone destruction and bone formation
Non-union Fracture	Metabolic	Fracture does not heal due to movement, poor blood supply, OB mal-regulation and low OPCs.
Osteochondroma	Genetic	Benign bone tumour
Osteosarcoma	Genetic	Malignant bone tumour

Table 1.8. Overview of diseases of the bone. (Adapted from (167))

1.5.1 **Inflammatory Arthritis**

Inflammatory joint diseases are a group of diverse rheumatic disorders, which have inflammation and adverse destructive structural and functional changes of the bone tissue in common. Inflammatory joint diseases can be broadly split into two categories; i) those that are seropositive for rheumatoid factor (RF) e.g. rheumatoid arthritis (RA) and ii) those that are seronegative for RF e.g. the spondyloarthropathies (SpAs) which include, ankylosing spondylitis (AS) and psoriatic arthritis (PsA) (168).

1.5.1.1 **Spondyloarthropathies**

Joint inflammation in the SpAs affects the axial skeleton in addition to the diarthrodial joints. Characteristically the joint inflammation is asymmetrical with proximal and distal joints affected (27). The SpAs share a number of common features including inflammatory back pain, peripheral arthritis, enthesitis, dactylitis, and uveitis. In contrast to RA the SpAs are also characterised by increased bone formation; with delicate marginal syndesmophytes common in AS, and bulky, non-marginal syndesmophytes more common in reactive arthritis and psoriatic arthritis (169). The exact aetiology of the SpAs is unknown though characteristics include increased T cell and macrophage numbers, as well as greater expression of pro-inflammatory cytokines, IL-1, TNF and IFNγ, at sites of inflammation (169).

1.5.1.2 **Rheumatoid Arthritis**

Rheumatoid arthritis is a common systemic chronic inflammatory disease that affects approximately 1% of the global population, and is associated with significant morbidity and increased mortality (170). RA is characterised by persistent inflammation of multiple joints and the infiltration of immune cells (Fig 1.8 (a)); mainly macrophages, T cells and plasma cells (171). These cells initiate structural changes within the joint; hyperplasia of the synovial lining and eventual cartilage and bone damage that cause loss of mobility at later stages of the disease. Diagnosis of RA is performed according to the criteria jointly published by the American College of Rheumatology (ACR) and the European League Against Rheumatism (EULAR) as shown in Table 1.9 (172). A score of $\geq$6/10 is required for classification of a patient as having definite RA.

Section A	Joint Involvement	Score
	1 large joint	0
	2 – 10 large joints	1
	1 – 3 small joints (with or without involvement of large joints)	2
	4 – 10 small joints (with or without involvement of large joints)	3
	10 joints (at least 1 small joint)	5
Section B	**Serology (at least 1 test required)**	
	Negative RF and negative ACPA	0
	Low-positive RF or low-positive ACPA	2
	High-positive RF or high-positive ACPA	3
Section C	**Acute-phase Reactants (at least 1 test required)**	
	Normal CRP and normal ESR	0
	Abnormal CRP or abnormal ESR	1
Section D	**Duration of Symptoms**	
	< 6 weeks	0
	$\geq$ 6 weeks	1

Table 1.9. ACR/EULAR Rheumatoid Arthritis Classification Criteria. RF = rheumatoid factor. ACPA = anti-citrullinated protein antibody. CRP = C-reactive protein. ESR = erythrocyte sedimentation rate. (Reproduced from (172)).

The exact aetiology of RA is unknown, however, in the last 30 years giant strides have been made in the characterisation of the intracellular mediators, or cytokines, that drive this disease (170, 171, 173, 174). Initial cytokine analysis of RA verified that a large number of pro-inflammatory cytokines such as; IL-1, TNF, IL-6 and granulocyte-macrophage colony-stimulating factor (GM-CSF) were produced by the rheumatoid synovial membrane (173, 175, 176). The significance of TNF in RA was identified by Brennan et al (177). In their study they showed that culturing RA synovium cells in the presence of TNF specific antibodies abrogated IL-1 production. This work was further supported through subsequent experiments that showed use of anti-TNF antibodies also downregulated the expression of other pro-inflammatory cytokines, such as IL-6, GM-CSF and IL-8 (178, 179) indicating that TNF may be at the top of a pro-inflammatory cascade.

This increase in pro-inflammatory cytokines associated with RA has a knock on effect on OC formation and activity leading to increased bone destruction. Levels of the TNFSF members RANKL (TNFSF11) (180), TNF (TNFSF2) (181) and homologous to lymphotoxins

exhibiting inducible expression and competing with herpes simplex virus glycoprotein D for herpes-virus entry mediator [HVEM], a receptor expressed by T lymphocytes (LIGHT, TNFSF14) (182, 183) are upregulated in the serum and synovial fluid of RA patients. While RANKL induces osteoclast formation directly (15, 16, 60), TNF and LIGHT have been shown to synergistically enhance its effects (182, 184, 185). To abrogate the damage caused by the inflammation associated with RA, patients are given a range of treatments.

Traditionally RA is treated with non-steroidal anti-inflammatory drugs (NSAIDs), glucocorticoids and disease-modifying anti-rheumatic drugs (DMARDs). Only the DMARDs can impede or halt the destructive disease processes, while NSAIDs are used for the daily control of pain. Development of anti-TNF therapies has made significant improvements in the treatment of RA. Anti-TNF treatments such as adalimumab (human monoclonal antibody), etanercept (TNF receptor-IgG fusion protein) and infliximab (mouse-human chimera antibody) work by blocking TNF signalling via its receptor TNFR1 preventing the negative effects of TNF in RA patients (186). However, there are some patients who do not respond to the treatment. Reasons for a lack of response are generally unknown, due to RA being such a complex and heterogeneous disease, but targets must include inflammatory cell types and other as of yet uncharacterised cytokines.

1.5.2 **Osteoporosis**

Osteoporosis (OP) is a well established medical and socioeconomic problem characterised by a low bone mineral density (BMD), deteriorated bone microarchitecture (Fig 1.8 (b)) and an increased risk of fracture (187). It is considered a silent disease because bone loss occurs without symptoms and approximately two thirds of vertebral fractures are asymptomatic (188). Approximately 40% of white, postmenopausal women and 13% of men are affected by OP, and with an aging population in western society this number is expected to increase over the coming years (189-191). Fractures most commonly occur in the spine, hip or wrist but other bones can be affected, such as the humerus or ribs. Osteoporotic fracture leads to a loss of mobility and subsequent decrease in quality of life. More worrisome, however, osteoporotic fractures of the spine or hip lead to an increase in mortality; due to hospitalisation and the enhanced risk of other complications such as pneumonia or thromboembolic disease (192). Due to OP being a silent disease diagnosis can be problematic.

Historically diagnosis of OP was through the presence of non-traumatic fractures on a setting of low bone mass, detected through radiographic examination (193). While clinically useful in the past this method had low sensitivity and was based on complications of the disorder rather than the underlying pathology; the imbalance in osteoclast and osteoblast activity. Development of dual x-ray absorptiometry (DXA) allowed the measurement of bone mass at any site in the skeleton with a high level of precision (2% - 4%) (194). The technique provided a clearer clinical definition of OP (Table 1.10). Even though methods for the detection and diagnosis of OP have improved it is still often only diagnosed after the first clinical fracture (195, 196).

Level	**Definition**
Normal	Bone density is within 1 standard deviation (SD) (+1 or -1) of the young adult mean.
Low Bone Mass	Bone density is between 1 and 2.5 SD below the young adult mean (-1 to -2.5 SD).
Osteoporosis	Bone density is 2.5 SD or more below the young adult mean (12.5 SD or lower)
Severe (Established) Osteoporosis	Bone density is more than 2.5 SD below the young adult mean, and there have been one or more osteoporotic fractures

Table 1.10. World Health Organisation (WHO) Definitions Based on Bone Density

The aetiology and pathogenesis of OP are not fully defined. A major cause is an imbalance in the bone remodelling process, where increased OC activity leads to excessive bone resorption compared to bone formation (52, 197). A number of studies have also suggested that decreased bone formation plays a significant role (198, 199). In the female population, onset of menopause is the major factor that contributes to the development of post-menopausal OP with the associated oestrogen deficiency linked to a subtle increase in expression of the cytokines RANKL, TNF, IL-1 and IL-6 in *ex vivo* cultures (197, 200-204). The significance of these increases in the pathogenesis of the disease *in vivo*, however, is less clear. Low body-mass index, a family history of fractures, smoking, low dietary calcium intake, vitamin D deficiency and the use of glucocorticoids also have a role in the pathogenesis of the disease (205). A variety of treatments can be prescribed for OP, with the aim of increasing bone density and correcting the imbalance in remodelling.

Current baseline therapies for the treatment of OP include lifestyle modifications (increased physical activity and cessation of smoking), and vitamin D and calcium

supplementation (206, 207). In higher risk groups, pharmacological interventions are employed. These fall into two classes: i) those that inhibit bone resorption (antiresorptive) and ii) those that stimulate bone formation (anabolic). The main group of antiresorptive drugs is the bisphosphonates. Bisphosphonates have a long half-life in the skeleton meaning treatment can be daily, weekly, monthly or yearly, depending on the drug and the route of administration (intravenous versus oral). They act upon the OC inhibiting their activity either by a direct toxic effect or by altering their cytoskeleton (208). More recently drugs that stimulate bone formation have been approved for treatment. Anabolic drugs such as intact PTH (1-84) and teriparatide exert their effect by directly increasing bone formation by the OB (209). The mechanism of action of Strontium ranelate is unclear though it most likely acts via a combination of physiochemical effects and modest effects of increased bone formation and decreased bone resorption (210). In recent years the first monoclonal antibody (mAb) for the treatment of OP has been developed and approved for use. Denosumab is a fully humanised mAb directed against RANKL (211). Denosumab works by inhibiting the differentiation of osteoclasts, mimicking the natural action of OPG and leads to a progressive rise in bone strength (212).

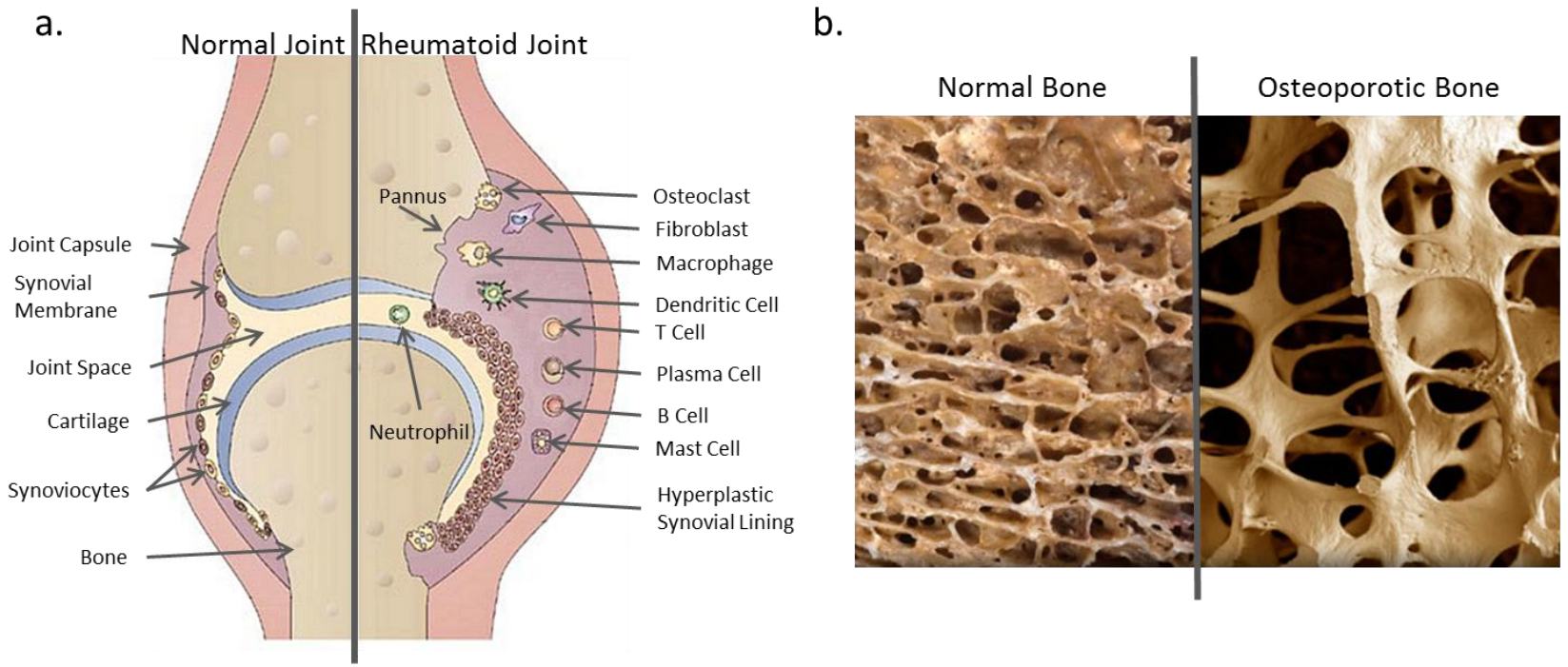

Fig 1.8. Comparison of a Rheumatoid Joint and Osteoporotic Bone to Normal

a) The rheumatoid joint is characterised by an influx of immune cells leading to inflammation and synovial hyperplasia. This leads to the development of cartilage degradation and bone destruction. Image adapted from Strand et al 2007 (Biologic Therapies in Rheumatology: Lessons learned, future Directions, Nature Reviews Drug Discovery).

b) Osteoporosis is characterised by a reduction in bone mineral density and deterioration in bone micro-architecture. Osteoporotic bone has a spongy appearance compared to normal healthy bone, giving rise to an increased risk of fracture.

1.6 **The Tumour Necrosis Factor Superfamily**

The cytokines RANKL and OPG and their receptor RANK are members of the tumour necrosis factor superfamily (TNFSF). As discussed in section 1.3, these TNFSF members play a critical role in bone homeostasis and as such have been targeted for therapy; Denosumab is a monoclonal antibody against RANKL used in the treatment of OP. The impact of some, but not all of the TNFSF members on bone homeostasis has been described in the literature. In the following sections the close structural homology and signalling events related to function in the TNFSF are discussed, with focus on death receptor 3 (DR3) and its ligand TNF-like protein 1A (TL1A).

The origins of the TNFSF date back to 1962 with the discovery by O'Malley et al (213) of an LPS induced factor in serum that was capable of tumour regression; named tumour-necrotising factor (213). This was subsequently re-named in 1975 by Carswell et al (214) to tumour necrosis factor (TNF). In 1968 lympohtoxin (LT) was first described by Williams, Granger et al (215) as a protein produced by lymphocytes that could kill tumour cells. Characterisation of the two proteins by Aggarwal et al (216, 217), in 1984 / 1985, revealed that they were homologous and shared common cell-surface receptors. This finding indicated the possibility of a TNF superfamily. To date the TNF superfamily consists of 29 receptors and 18 ligands, all with similar structures (Table 1.11).

TNFSF ligands are type II trans-membrane proteins characterised by a conserved C-terminal domain known as the 'TNF homology domain' (THD). This trimeric domain is responsible for receptor binding and its sequence identity between family members is between 20 – 30% (218). Although most of the ligands are synthesised as membrane-bound proteins, they may also be cleaved and released as soluble proteins to exert their effect (218, 219). Like the TNFSF, members of the TNF receptor superfamily (TNFRSF) also share a high degree of homology.

Members of the TNF receptor superfamily (TNFRSF) are characterised by their repeated cysteine-rich extracellular sequence homology (218, 220). They are type I trans-membrane proteins, though there are some exceptions. BCMA, TACI, BAFFR and XEDAR are type III trans-membrane proteins while DcR1, DcR2, DcR3 and OPG are secreted proteins (219, 221). Receptors of the TNFSF can be split into 3 groups based upon their cytoplasmic sequence and signalling properties: i) Receptors containing one or more TRAF Interacting Motifs (TIMs), ii) receptors containing a death domain (DD) in the cytoplasmic

tail – death receptors and iii) receptors that do not contain a functional intracellular signalling domain or motif – decoy receptors (222). The structure and function of the TNFRSF death receptors are detailed below.

Receptor	TNFRSF Designation	Expression	Ligand	TNFSF Designation	Expression	Effect
CD27	TNFRSF7	T Cells	CD27L	TNFSF7	T Cells, B Cells, NK Cells	Activation of T cells
TNFR2	TNFRSF1B	Immune Cells, Endothelial Cells	TNF / LT	TNFSF2 / TNFSF1	Immune Cells	Immune Defence
LTβR	TNFRSF3	T Cells, NK Cells	LT	TNFSF1	Immune Cells	Immune Defence
FN14	TNFRSF12A	Endothelial Cells, Fibroblasts	TWEAK	TNFSF12	Monocytes	Inflammation, Proliferation
HVEM	TNFRSF14	T Cells	LIGHT	TNFSF14	Immune Cells	Viral Entry
CD30	TNFRSF8	Reed-Sternberg Cells	CD30L	TNFSF8	T Cells, Monocytes	Th2 Cell Function
CD40	TNFRSF5	Reed-Sternberg Cells	CD40L	TNFSF5	T Cells, B Cells	Immune Cell Homeostasis
4-1BB	TNFRSF9	Activated T Cells, Monocytes, NK Cells	4-1BBL	TNFSF9	B Cells, DCs, Macrophages	T Cell, B Cell Activation
OX40	TNFRSF4	T Cells	OX40L	TNFSF4	T Cells, B Cells	T Cell, B Cell Homeostasis
GITR	TNFRSF18	$CD4^+CD25^+$ T Cells	GITRL	TNFSF18	?	T Cell Homeostasis
RANK	TNFRSF11A	Osteoclasts	RANKL	TNFSF11	Activated T Cells and Osteoblasts	Osteoclastogenesis
BCMA	TNFRSF17	Immune Cells	APRIL / BAFF	TNFSF13 / TNFSF13B	Immune Cells	B Cell Homeostasis
TACI	TNFRSF13B	Immune Cells	APRIL / BAFF	TNFSF13 / TNFSF13B	Immune Cells	B Cell Homeostasis
BAFFR	TNFRSF13C	Immune Cells	BAFF	TNFSF13B	Immune Cells	B Cell Homeostasis
XEDAR	TNFRSF27	Ectodermal derivative	EDA2	?	Skin	Hair / Teeth morphogenesis
TROY	TNFRSF19	Embryo Skin, Epithelium, Hair follicles, Brain	?	?	?	Embryonic Development
RELT	TNFRSF19L	Lymphoid Tissues	?	?	?	T Cell Homeostasis

Table 1.11. Members of the TNF receptor super family, their ligands and function. (Adapted from (219, 220, 223, 224)).

Death Receptors	TNFRSF Designation	Expression	Ligand	TNFSF Designation	Expression	Effect
CD95	TNFRSF6	Most Normal Cells	CD95L	TNFSF6	Splenocytes, Thymocytes	Immune Defence
TNFR1	TNFRSF1A	Most Normal Cells	TNF / LT	TNFSF2 / TNFSF1	Immune Cells	Immune Defence, Inflammation
DR3	TNFRSF25	Activated T Cells, Osteoblasts, Macrophages	TL1A	TNFSF15	Endothelial Cells, T Cells, Macrophages	T Cell Homeostasis and Activation, Inflammation
DR4	TNFRSF10A	Most Normal Cells	TRAIL	TNFSF10	NK Cells, T Cells, DCs	Immune Defence
DR5	TNFRSF10B	Most Normal Cells	TRAIL	TNFSF10	NK Cells, T Cells, DCs	Immune Defence
DR6	TNFRSF21	Resting T Cells	?	?	?	?
EDAR	TNFRSFEDAR	Ectodermal derivative	EDA1	?	Skin	Hair, Teeth Morphogenesis
NGFR	TNFRSF16	Nervous System	?	?	?	CNS Development

Decoy Receptors	TNFRSF Designation	Expression	Ligand	TNFSF Designation	Expression	Effect
OPG	TNFRSF11B	Osteoblasts, Most Normal Cells	RANKL / TRAIL	TNFSF11 / TNFSF10	Activated T Cells and Osteoblasts	Decoy Receptor
DcR1	TNFRSF10C	Most Normal Cells	TRAIL	TNFSF10	NK Cells, T Cells, DCs	Decoy Receptor
DcR2	TNFRSF10D	Most Normal Cells	TRAIL	TNFSF10	NK Cells, T Cells, DCs	Decoy Receptor
DcR3	TNFRSF6B	T Cells	TL1A	TNFSF15	Endothelial Cells, T Cells, Macrophages	Decoy Receptor

Table 1.11 (Cont.). Members of the TNF receptor super family, their ligands and function. (Adapted from (219, 220, 223, 224)).

1.7 **Death Receptors**

The death receptor (DR) group of the TNFRSF are so called due to the presence of a cytoplasmic region of approximately 80 residues termed the death domain. When this is triggered it results in the transduction of either apoptotic or survival signals (223). Death receptors can be further split based upon their signalling complex. The first group comprises the death-inducing signalling complexes (DISCs; CD95, DR4 and DR5), which results in the activation of caspase-8 and the transduction of the apoptotic signal. The second group of receptors (TNFR1, DR3, DR6 and EDAR) recruit a different set of molecules which can transduce both apoptotic and survival signals (219, 223).

Transduction of signal via the DR requires the recruitment of a number of intracellular adaptor molecules (Fig 1.9). Generation of the DISC consists of an oligomerised receptor, which recruits the adaptor molecule Fas-associated death domain (FADD) and isoforms of procaspase 8. The interaction between these molecules results in caspase 8 being released into the cytosol to propagate the apoptotic signal. Signalling via TNFR1 differs from above in that it can form two signalling complexes. The first complex, formed at the membrane, comprises the adaptor molecules TNFR-associated death domain protein (TRADD), receptor-interacting protein (RIP) and TNF-associated factor (TRAF). This triggers the nuclear factor-κB (NF-κB) pathway, promoting cell survival. The second signalling complex works in a manner similar to the DISC using FADD and caspase 8 to induce apoptosis (223, 225-228). Death receptor 3 (DR3) is a member of the TNFRSF that has a high degree of homology to TNFR1. The role and function of DR3 and its ligand TL1A in inflammation, immunity and bone is only just starting to be discovered. The remainder of this introduction will focus on what is currently known about DR3 and TL1A.

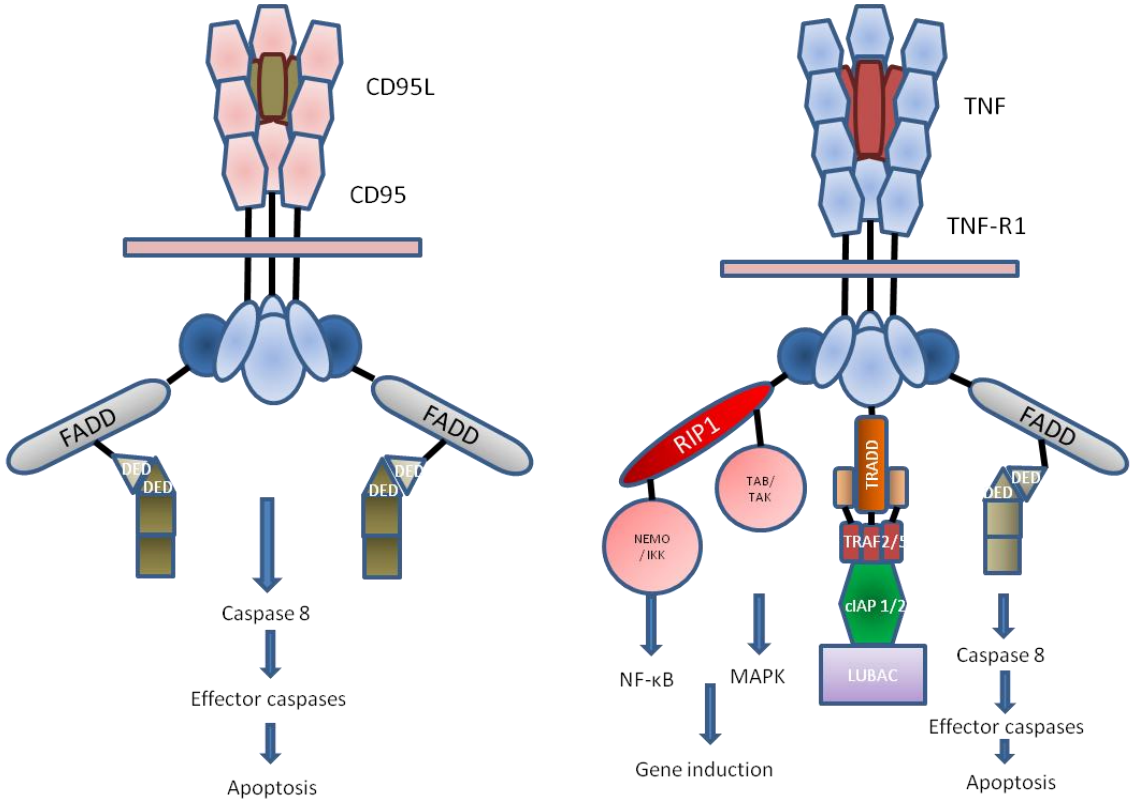

Fig 1.9. Death Receptor Signalling

Schematic representation of signalling by the TNFRSF members CD95 and TNFR1. Trimerisation of the receptor and ligand results in the recruitment of adaptor molecules for signal transduction. CD95 recruits FADD to form the DISC resulting in activation of caspase 8 and apoptosis. TNFR1 can form two different signalling pathways. Recruitment of FADD results in caspase 8 activation and apoptosis. Recruitment of TRADD, TRAF and RIP results in the induction of NF-κB and genes for cell survival.

1.8 **Death Receptor 3**

Death Receptor 3 (also known as wsl-1, APO-3, TNF related-receptor apoptosis-mediating protein (TRAMP), lymphocyte associated receptor of death (LARD), TNF receptor-like 3 (TR3), TNF receptor superfamily member 25 (TNFRSF25)) was identified in 1996 / 1997 by a number of groups (229-233); Kitson et al (229), Screaton et al (230), Marsters et al (231), Chinnaiyan et al (232) and Bodmer et al (233). With the exception of Kitson et al (229), who used a yeast two-hybrid system utilising the death domain of TNFR1 as a binding target and PCR, the discovery of DR3 was based on searching expressed sequence tag (EST) databases. Genes that had extracellular cysteine-rich domains and intracellular death domains with a homology to TNFR1, CD95 and FAS (230-233) were screened for. The DR3 gene was mapped to human chromosome 1p36.3 by Bodmer et al (233) using fluorescence in situ hybridisation (FISH) analysis. DR3 was found to be overall highly homologous to TNFR1, CD95 and FAS, with sequence identity reported as 26% - 29%, 22% - 23% and 27% respectively (229-232). The homology to TNFR1 increased to 40% - 48% in the death domain (230-233). The structure of DR3 was determined to have a signal sequence followed by an extracellular region, making up the extracellular domain (ECD), a transmembrane domain and an intracellular domain (ICD), with two N-linked glycosylation sites at amino acid positions 67 and 106. The ECD contains four cysteine-rich pseudorepeats, while the ICD contained a sequence, which resembled the death domains found in the ICD of TNFR1 and CD95. Notably, four out of the six amino acid residues in the death domain of TNFR1 that are essential for signalling are identical in DR3 with the remaining two semi-conserved (231).

The murine DR3 gene was identified in 2001 by Wang et al (234) through probing genomic mouse DNA with full-length human DR3 gene cDNA. Murine DR3 was found to be overall 63% homologous to human DR3; 94% in the death domain and 53% in the ECD. Murine DR3 was found to contain two putative N-linked glycosylation sites in the ECD, which were conserved in human DR3. 25 of the 28 ECD cysteines found in human DR3 were also conserved. However, a 9 amino acid deletion in the second half of the third cysteine rich domain (CRD) of murine DR3 was found, resulting in the absence of two conserved cysteine residues. In addition two significant amino acid substitutions were found within the 3rd CRD of murine DR3; with the sixth conserved cysteine replaced by threonine and phenylalanine replaced by a cysteine. Despite these differences the binding properties of

murine DR3 were predicted to be the same as human DR3 (234). Having identified DR3 as a new member of the TNFRSF the authors went on to detail its expression.

1.8.1 **DR3 Expression**

Initial northern blot analysis identified human DR3 expression to be mainly restricted to lymphoid organs; with 3.5 – 4kb mRNA transcripts detected in the adult spleen, thymus and peripheral blood lymphocytes (229-233). Additional studies, however, identified low levels of DR3 gene expression in the small intestine, lung, colon and foetal kidney (231). Gene expression was also identified in activated T cells, primary monocytes and early myeloid cell lines (235). While not as ubiquitously expressed as other members of the TNFRSF, recent studies have shown that expression of DR3 is not as restricted as previously thought. Cell surface receptor expression has been detected on $CD4^+$ T cells (236), $CD8^+$ T Cells (237), NK cells (238), NKT Cells (237), monocytes / macrophages (OC precursors; (239, 240)) and osteoblasts (241). Murine DR3 was demonstrated to have a similar expression pattern to human DR3. Murine DR3 mRNA has been detected in the heart, kidney, spleen, liver, thymus, brain (234) and bone marrow macrophages (242). Cell surface receptor has also been shown on NKT cells, $CD4^+$ T Cells and $CD8^+$ T cells (243). In describing DR3 expression a number of splice variants were identified.

The initial studies into human DR3 by Screaton et al (230) identified 12 splice variants. The isoform missing exon 3 was shown to include the trans-membrane and death domains, whereas the remaining isoforms potentially encoded soluble receptors. In their study, it was suggested that all but 3 of the DR3 isoforms were generated by the skipping of one or more complete exons, with two variants having a 101- and 200-bp insert. The remaining DR3 isoform was found to contain three additional nucleotides. The isoform detected by Warzocha et al (244), termed DR3β, differed from the full length receptor by a 20- and a 7-bp insert. The predicted translated products showed that DR3 and DR3β have identical intracytoplasmic and trans-membrane domains but differed in their extra-cellular domains. In the murine system, 3 DR3 splice variants were described by Wang et al (234). Variant 1 was observed to be the largest isoform and encoded a protein 55kDa in size. Variant 2 was described as a soluble form of the receptor with a missing exon 6, resulting in an early stop site before the transmembrane domain. The third variant consisted of variant 1 lacking exons 5 and 6 resulting in a protein with both a

transmembrane and cytoplasmic domain, but without the fourth cysteine rich domain. The effect that this has on its capacity for ligand binding and signalling has yet to be determined.

1.8.2 **The DR3 Signalling Pathway**

The conservation in structure between DR3 and TNFR1 suggested that they must have similar signalling pathways. This hypothesis was confirmed in a study by Chinnaiyan et al (232) using glutathione-S-transferase (GST) fusion protein binding studies. DR3 associated specifically with TRADD but not with FADD or RIP *in vitro;* a truncated death domain mutant of DR3 did not demonstrate any interaction with TRADD. When DR3 was expressed in 293 human embryonic kidney cells in the presence of TRADD, however, enhanced binding of RIP, FADD and TRAF2 were detected (232). Further support for the important role of TRADD in the DR3 signalling pathway was published by Pobezinskaya et al (245). Failure of DR3 signalling in TRADD deficient mice was due to lack of recruitment of the adaptor proteins TRAF2 and RIP1, leading to a non-functional DR3 signalling complex. Upon formation of the complete signalling complex DR3 can induce both the apoptotic pathway and the NF-κB pathway (Fig 1.10).

Induction of the apoptotic pathway by DR3 signalling has been demonstrated by a number of groups. Overexpression of full length DR3 in 293 cells resulted in morphological changes; blebbing, rounding, condensing and detachment from the dish, all indications of apoptosis (229-232). Overexpression of a truncated from of DR3, lacking the cytoplasmic domain, was not able to induce cell death (229). Apoptosis induced by DR3 could be blocked by dominant negative versions of FADD or FADD-like interleukin-1β-converting enzyme (FLICE), indicating that they are necessary components of the DR3 apoptotic pathway (232). Activation of NF-κB by DR3 was identified with a luciferase reporter gene assay (229, 233). This showed DR3 expression to strongly induce NF-κB in a dose-dependent fashion, however, truncated forms of DR3 were not able to activate NF-κB (232). Use of dominant negative derivatives of RIP and TRAF2 blocked DR3-induced NF-κB activation; it was not affected however, by a dominant negative derivative of FADD (232). These initial studies into the DR3 signalling pathway were obtained with transient systems where DR3 and / or the signalling molecule were overexpressed. Whether they were representative of the natural signalling response remained unknown.

To address this Wen et al (246) studied DR3 signalling in TF-1 cells, which naturally express the receptor. Activation of DR3 by TL1A consistently recruited the adaptor molecules TRADD, TRAF2 and RIP. Very little FADD or procaspase-8 was detected in the complex (246). Stimulation of the cells with TL1A, in addition to the NF-κB pathway, also activated the JNK, p38 and ERK1,2 MAPK pathways in a dose- and time-dependent manner. Induction of apoptosis by DR3 signalling was only observed following treatment of the TF-1 cells with a NF-κB inhibitor, or a general protein synthesis inhibitor, stopping the synthesis of the anti-apoptotic molecule c-IAP2, which was potently induced by TL1A signalling (246). The results demonstrated that while in transient systems DR3 signalling can actively induce the apoptotic and NF-κB pathways, in cells expressing natural levels of DR3 induction of NF-κB is favoured.

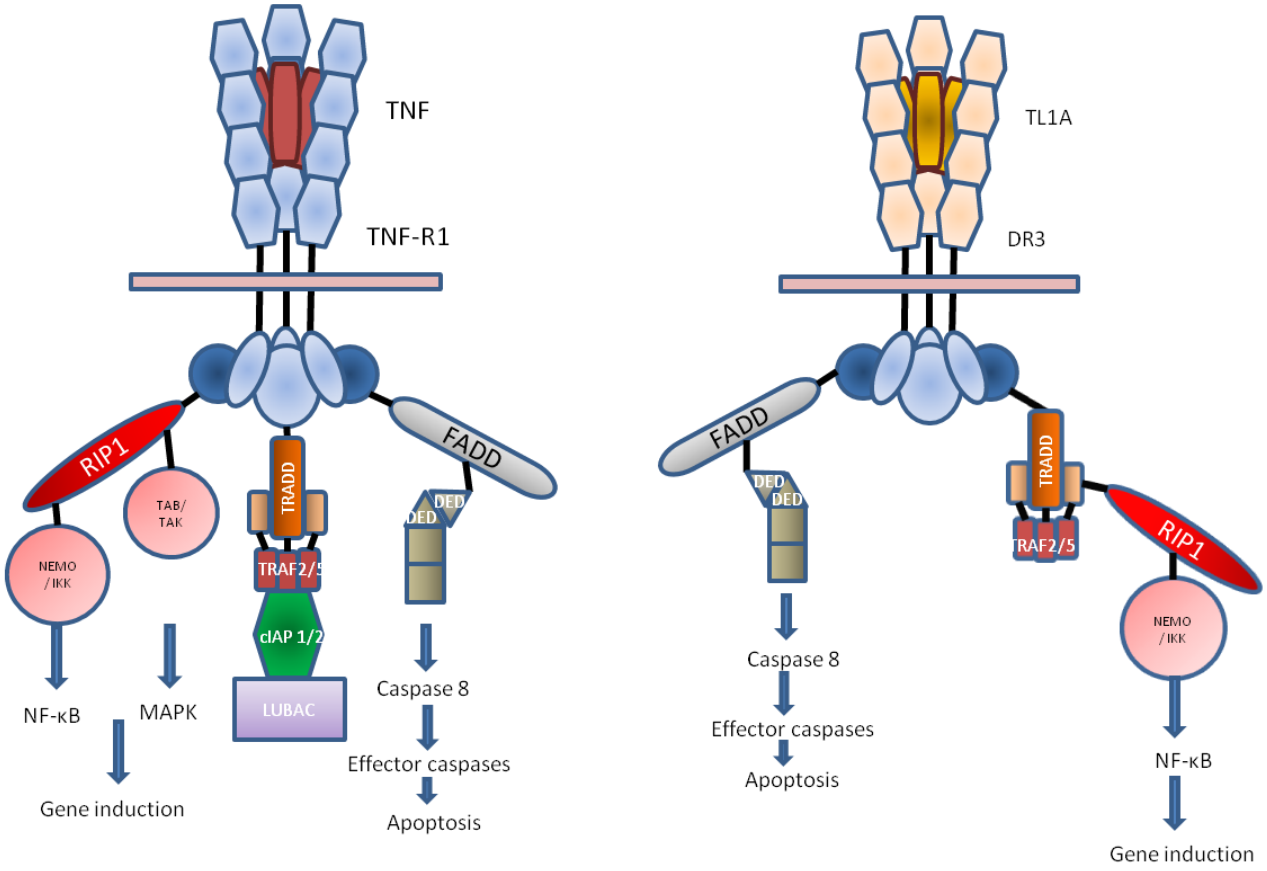

Fig 1.10. Schematic Representation of Signalling via DR3 and TL1A

Like TNFR1, DR3 recruits the adaptor molecules TRADD, FADD, RIP and TRAF2 initiating either the NF-κB pathway or the apoptotic pathway. Image reproduced from Ashkenazi et al, 1998. Death receptors: Signaling and modulation. Science. [Review].

1.8.3 **The DR3 Ligand**

Following the discovery of DR3, work into the identification of its ligand(s) began. To date three potential ligands for DR3 have been reported; the TNFSF members Apo3L/TWEAK (TNFSF12; (247)) and TL1A (TNFSF15; (248)), and the adhesion molecule E-selectin (249). This thesis will focus on the TNFSF member ligands of DR3.

1.8.3.1 **The DR3 Ligand – Apo3L / TWEAK**

The first suggested ligand for DR3 was Apo3L (247). Apo3L was identified following a search of an EST database for sequences, which had a similarity to TNF. It was subsequently shown to have a type II trans-membrane protein topology. Northern blot analysis identified a broad range of expression of Apo3L in foetal and adult tissue (247). Analysis of the function of Apo3L demonstrated it could induce apoptosis in cells by activating caspases through FADD, as well as being able to activate the NF-κB pathway using the same cytoplasmic elements as TNF (247). Apo3L was also identified independently by Chicheportiche et al (250) and named TWEAK. However, in this study it did not bind DR3. Confirmation that TWEAK / Apo3L was not the true ligand for DR3 was put forward in a study by Kaptein et al in 2000 (251). Using an ELISA-based *in vitro* assay no significant binding of TWEAK to DR3 was detected. Consistent to the ELISA method no TWEAK / Apo3L was co-immunoprecipitated using DR3-Fc. In cell based assays, treatment of DR3 transfected cells with TWEAK / Apo3L had no effect on NF-κB or apoptosis induction. Furthermore no significant difference in the ability of TWEAK / Apo3L to bind to peripheral blood lymphocytes isolated from $DR3^{wt}$ and $DR3^{ko}$ mice was detected (251). Taken together this data strongly suggested that Apo3L / TWEAK was not the true ligand for DR3. Work by Migone et al (248) in 2002 identified the endothelial cell-derived TNF-like factor, TL1A, as the ligand for DR3.

1.8.3.2 **The DR3 Ligand – TL1A**

TL1A was identified through EST databases and found to be a longer variant of TNF-like molecule (TL1), also known as vascular endothelial growth inhibitor (VEGI). TL1A mRNA was found to be expressed predominantly by endothelial cells though low levels were detected in the kidney, intestine, lung, spleen and thymus (248). It was shown to bind successfully to a DR3-Fc and DcR3-Fc fusion proteins as well as a membrane bound form of DR3, while no association was detected with any other receptors tested (248). In addition to endothelial cells (248, 252) expression of TL1A has been shown on monocytes

and dendritic cells following FcγR activation (253), activated $CD4^+$ and $CD8^+$ T cells (237) and plasma cells (254). TL1A is currently the only identified TNFSF ligand for DR3. However, it can also bind to the decoy receptor DcR3 (248). Upon binding DcR3 the effects of TL1A are neutralised. Binding to DR3, however, can initiate a variety of responses depending on the cell type.

1.9 **Effects of DR3/TL1A Signalling**

Like other members of the TNFSF, TL1A has been shown to enhance T cell proliferation and cytokine production by activated T cells. The proliferative effect of TL1A is enhanced in sub-optimally activated cells with a more pronounced effect in memory T cells versus naïve T cells (255, 256). Co-stimulation with TL1A also enhances production of a range of cytokines in both naïve and total T cells including IFNγ, IL-2, -4 and -13 (248, 256, 257). Early studies demonstrated that TL1A is associated with the expansion of T-helper subsets and can synergise with IL-12 and IL-18 to affect development of IFNγ T cells (248, 258). More recently in a study by Jones et al (236) TL1A has been shown to differentially regulate distinct outcomes in naïve and activated T cells; affecting Th17 generation, maintenance and proliferation. TL1A signalling in naïve and pre-activated effector cells was demonstrated to suppress the initial commitment of naïve T cells into Th17 cells. The effector characteristics of pre-conditioned Th17 cells, however, was maintained (236).

Less is known about the role of TL1A in $CD8^+$ T cells. In a study by Slebioda et al (259) addition of soluble TL1A was shown to co-stimulate $CD8^+$ T cell proliferation and IL-2 production. Work by Twohig et al (243) demonstrated that TL1A signalling on $CD8^+$ T cells was essential for efficient development of antiviral $CD8^+$ T cell immunity. Additional to any effects on T cells TL1A has been shown to synergise with IL-12 and IL-18 increasing IFNγ production and cytotoxicity by natural killer (NK) cells (258, 260). In NKT cells TL1A promotes a more restricted cytokine release compared to T cells, with enhanced expression of IL-4 and IL-13 but not IFNγ (237). The role that DR3 / TL1A play in bone biology has only recently come to prominence and has not been fully investigated. Currently there are only two papers that directly examine the functional role of DR3/TL1A in OB and OC biology.

1.9.1 **Effects of DR3/TL1A Signalling in Osteoclast Biology**

The role of DR3/TL1A in OC biology was touched upon in a study by Bull, Williams et al (242). In this study, DR3-deficient mice were protected from bone erosion in an antigen induced arthritis (AIA) model. Histological analysis of the arthritic joint demonstrated comparable TRAP expression in $DR3^{wt}$ and $DR3^{ko}$ mice in the femoral head and growth plate. However, at sites of bone erosion TRAP staining was significantly greater in $DR3^{wt}$ mice. These data implicated a role for DR3 in *in vivo* osteoclast formation at sites of bone pathology, but not in areas away from the pannus. This hypothesis was supported by their *in vitro* studies. Addition of TL1A to murine BMM cultures and human PBMC cultures significantly enhanced RANKL-induced OC formation. The mechanism involved, however, was not investigated in their study. While DR3 / TL1A have been shown to have an effect on primary OC formation, their role in OB biology is less well defined.

1.9.2 **Effects of DR3/TL1A Signalling in Osteoblast Biology**

Expression of DR3 on the cell surface of primary human OB and the MG63 OB cell line was demonstrated by Bu et al (261) and Borysenko et al (241). The function that DR3 plays in OB biology however, is unclear. In the study by Borysenko et al (241) cross-linking of DR3 on MG63 cells induced apoptosis, but only at low cell density. Addition of TL1A to MG63 cells was also demonstrated to increase levels of apoptosis 4-fold. However, when TL1A was added to primary human OB no difference in apoptosis was observed. Only after sensitisation of primary OB with cycloheximide, an inhibitor of protein bio-synthesis, was TL1A observed to have any effect on apoptosis. The results from the Borysenko et al (241) study suggest a role for DR3 / TL1A in the regulation of OB apoptosis. This regulation however, is only present under very specific conditions. The main focus of this thesis will be investigating the functional role of DR3 / TL1A in OC and OB biology.

1.10 **DR3 / TL1A and Inflammatory Disease**

Since their initial discovery, DR3 and TL1A have been linked to the pathogenesis of a number of inflammatory diseases in clinical studies and experimental models; including Crohn's disease (262), ulcerative colitis (263), irritable bowel disease (IBD) (254, 263), rheumatoid arthritis (264-266), ankylosing spondylitis (267, 268), psoriatic skin lesions (269), arthrosclerosis (239, 270, 271), allergic lung inflammation (237) and renal inflammation (272). The majority of these studies have focused on the effects of

DR3/TL1A on the T cell response. Early studies by Bamias et al (254) demonstrated an up-regulation of TL1A and DR3 in intestinal lamina propria $CD4^+$ and $CD8^+$ T cells isolated from patients with IBD. Addition of TL1A to T cells involved in small intestinal immune and inflammatory responses ($CCR9^+$) have also been demonstrated to enhance IL-12/IL-8 IFNγ production (257, 273), suggesting an important role for DR3/TL1A in the pathogenesis of IBD. This is supported by studies that have identified a strong genetic link between TL1A and IBD with a number of *TNFSF15* single nucleotide polymorphisms (SNPs) that confer significant risk (274-276). In animal models of IBD DR3/TL1A interactions have been shown to exacerbate intestinal inflammation via stimulation of Th1 and Th17 pathways (277), and by providing co-stimulatory signals to lymphocytes (255). In an animal model of allergic lung inflammation DR3 was identified as the trigger for amplified Th2 cytokine production by polarised CD4 cells and for IL-13 production by NKT cells. Blockage of DR3 in this model was shown to inhibit the allergic lung inflammation (237). While the majority of studies have looked at T cell response to DR3 and TL1A in inflammatory disease, studies investigating the effects on other cell types have been performed.

Work by Kim et al (239), demonstrated the presence of DR3 in atherosclerotic plaques. This was built upon by Kang et al (278) and Kim et al (271) who showed that foam cells within the plaques express both DR3 and TL1A. The importance of this in the pathogenesis of atherosclerosis was identified by McLaren et al (270), who demonstrated that TL1A promotes foam cell formation in human macrophages *in vitro*. DR3 was also revealed to regulate foam cell formation and contributed significantly to the actions of TL1A. In a 2013 study, Bamias et al (279) showed an association between TL1A levels and atheromatic plaque formation in RA with dysregulated TL1A-induced signalling potentially associated with the risk of accelerated atherosclerosis. In psoriatic skin lesions up-regulation of DR3 and TL1A were observed in the cell populations critically involved in the pathogenesis of the skin inflammation, such as keratinocytes and macrophages. The role that they played in the initiation of the inflammation was not investigated (269). Evidence for the involvement of DR3/TL1A in the pathogenesis of bone related disease has arisen from recent clinical and animal studies.

The association between DR3/TL1A and the inflammatory arthritides has been reported in a number of studies. Elevated levels of TL1A have been reported in the serum of rheumatoid arthritis (RA) and ankylosing spondylitis (AS) patients (264, 267). While in RA

patients increased duplication of the DR3 gene has been identified (265). In an animal model of antigen-induced arthritis (AIA) Bull, Williams et al (242) demonstrated that DR3-deficient mice were protected from bone erosion. Co-administration of TL1A in AIA (242) and collagen induced arthritis (CIA; (266)) was also shown to significantly exacerbate bone destruction and deformation. These data all indicated an important role for DR3 and TL1A in the pathogenesis of bone-related disease; however, the mechanisms through which it acts are unknown. The role of DR3/TL1A in the pathogenesis of diseases characterised by OC over-activity is explored in more detail in chapter 5.

1.11 **Aims of the Thesis**

Expression of DR3 has been demonstrated on the surface of osteoclast precursors and osteoblasts. The effect exerted on these cells by DR3/TL1A signalling and their role in bone-related disease however, is poorly defined. While addition of TL1A to murine BMM macrophage cultures and human PBMC cultures has been shown to significantly enhance osteoclast formation, it is unknown whether this is due to a direct or indirect effect, or the mechanisms involved. The effect of DR3 and TL1A on OB biology is even less well defined.

The aims of this thesis were three-fold: Firstly, to determine the direct effect of DR3/TL1A on osteoclast formation and function and to elucidate the mechanisms involved. Secondly, to assess the role of DR3/TL1A in the pathogenesis of disease characterised by OC over-activity; namely rheumatoid arthritis and osteoporosis. Thirdly, identify the role of DR3 in osteoblast formation and function. The specific objectives of this thesis are:

- **To establish the mechanism by which DR3 / TL1A induces osteoclastogenesis in a murine system.**

  Osteoclast formation and function will be evaluated in mice genetically deficient in DR3 ($DR3^{ko}$) and wild-type mice ($DR3^{wt}$). Markers of osteoclast formation and function will be analysed to determine the mechanism through which they act.

- **To establish the mechanism by which DR3 / TL1A induces osteoclastogenesis in man.**

  Osteoclast formation and function will be evaluated in human $CD14^{+}$ monocyte cultures ± TL1A. Markers of osteoclast formation and function will be analysed to determine the effect of TL1A.

- **To determine whether the DR3 / TL1A axis is a central determinant in the pathogenesis of disease characterised by increased osteoclast activity.**

  Serum from arthritis patients will be analysed to assess whether changes in TL1A levels may have a role in the pathogenesis of the disease. DR3 expression, osteoclast formation and function will be evaluated in $CD14^{+}$ cell cultures ± TL1A derived from post-menopausal patients. Markers of osteoclast formation and function will be analysed to determine whether DR3/TL1A have a role in the development of osteoporosis and fracture.

- **To assess the role of DR3 / TL1A in osteoblast differentiation and function.**

  Osteoblast formation and function will be evaluated in mice genetically deficient in DR3 ($DR3^{ko}$) and wild-type mice ($DR3^{wt}$).

Chapter 2

Materials and Methods

2.1 **Materials**

All materials used in this project are listed alphabetically below. A list of suppliers is described in section 2.3.

2.1.1 **Antibodies**

Antibodies used throughout this study for flow cytometry, immunohistochemistry and the collagenase bio-assay are shown in Table 2.1.

Antibody	**Clone**	**Supplier**	**Purpose**
Anti-human CD14 - FITC	61D3	eBioscience	Flow Cytometry
Anti-human DR3 - PE	JD3	eBioscience	Flow Cytometry
Mouse IgG_1 – FITC	MOPC-31C	BD Biosciences	Flow Cytometry
Mouse IgG_1 – PE	P3.6.2.8.1	eBioscience	Flow Cytometry
Polyclonal Goat anti-murine DR3 - Biotinylated	-	R&D Systems	Flow Cytometry
Goat IgG	-	Vector Labs	Flow Cytometry
Rat anti-mouse CD16/CD32 (Fc Block)	-	BD Biosciences	Flow Cytometry
Anti-mouse CD44 – FITC	IM7	eBiosciences	Flow Cytometry
Anti-mouse RANKL – PE	IK22/5	Santa Cruz	Flow Cytometry
Streptavidin - APC	-	Life Technologies, Invitrogen	Flow Cytometry
Alexa Fluor® 594 Phalloidin	-	Life Technologies, Invitrogen	Immunocytochemistry
Anti-Cathepsin K	-	Abcam	Immunocytochemistry
Rabbit IgG	-	DAKO	Immunocytochemistry
Goat anti- Rabbit IgG - FITC	-	Life Technologies, Invitrogen	Immunocytochemistry
Rabbit IgG	-	Sigma-Aldrich	Rheumatoid Factor ELISA
Anti-human IgM (F(ab)'2-Peroxidase	-	Sigma-Aldrich	Rheumatoid Factor ELISA
Rheumatoid Factor	-	DiAgam	Rheumatoid Factor ELISA
Anti-type I collagen	-	Sigma-Aldrich	Collagenase Bio-assay
Goat anti-mouse IgG - Peroxidise	-	Sigma-Aldrich	Collagenase Bio-assay

Table 2.1. List of antibodies used throughout the study

2.1.2 **Chemicals**

All chemicals were purchased from Sigma-Aldrich unless otherwise stated.

2.1.3 **Culture Medium**

Medium used for the culture of murine and human osteoclasts and osteoblasts throughout this study are listed below:

2.1.3.1 Murine Osteoclast Medium

Heat-inactivated foetal calf serum (FCS) (10%; Biosera) and Penicillin-Streptomycin (50 units/ml - 50µg/ml; Life Technologies, Invitrogen) were added to Alpha Modification Minimum Essential Medium (αMEM; Life Technologies, Invitrogen).

2.1.3.2 Human Osteoclast Medium

Heat-inactivated FCS (10%), L-glutamine (20mM; Life Technologies, Invitrogen) and Penicillin-Streptomycin (50 units/ml - 50µg/ml) were added to Roswell Park Memorial Institute 1640 basal medium (RPMI-1640; Life Technologies, Invitrogen).

2.1.3.3 Murine Osteoblast Medium

Heat-inactivated FCS (20%) and Penicillin-Streptomycin (50 units/ml - 50µg/ml) were added to αMEM medium.

2.1.3.4 Murine Osteoblast Mineralising Medium

Heat-inactivated FCS (10%), Penicillin-Streptomycin (50 units/ml - 50µg/ml), dexamethasone (DEX; 10nM), β-glycerophosphate (βGP) stock solution (10mM) and ascorbic acid (AA) stock solution (50µg/ml) were added to αMEM medium.

L-Ascorbic acid (AA) stock solution (12.5mg/ml) – 125mg of AA was dissolved in 10ml of sterile PBS.

Dexamethasone (DEX) stock solution (10mM) – 39.2mg of DEX was dissolved in 10ml of absolute ethanol.

DEX working solution (10µM) – 1ml of 10mM DEX stock was diluted in 999ml of sterile PBS.

β-Glycerophosphate (βGP) stock solution (1M) – 2.16g of βGP was dissolved in 10ml of sterile PBS.

2.1.4 **Distilled Water (dH_2O)**

dH_2O was obtained from a Millipore reverse osmosis system followed by filtration through two ion exchange resin columns using a Millipore Milli-Q system. dH_2O was used for the preparation of buffers, reagents and stains throughout this study.

2.1.5 **DR3 Genotyping Primers**

Three primers (AV1, 2R and 4F) were used to differentiate $DR3^{wt}$ and $DR3^{ko}$ from $DR3^{het}$ littermates. The specific sequence for each primer was identified in advance of the studies and is previously described (234). The specific primer sequence needed to identify each DR3 genotype is provided below (Table 2.2):

Primer Name	Product	Primer Sequence	Predicted Size (bp)
AV1	KO DR3 gene	CAT CGC CTT CTA TCG CCT TC	320
2R	WT + KO DR3 gene	GAA AGG ATG AAA CTT GCC TGT TGG	280 / 320
4F	WT DR3 gene	AGA AGG AGA AAG TCA GTA GGA CCG	280

Table 2.2 Primers used in murine DR3 genotyping

DR3 genotyping primers were supplied by Life Technologies, Invitrogen. Primers were reconstituted in dH_2O at a concentration of 100μm.

2.1.6 **Equipment and Software**

Equipment and software used for analysis throughout this study is listed below.

2.1.6.1 Flow cytometry

Flow cytometry was performed using the BD Accuri™ C6 flow cytometer and analysed using BD CFlow® Plus software (BD Biosciences).

2.1.6.2 Pictures and Analysis

Visualisation of cells, OC and resorption pits in this study was performed with an Olympus BX41 Microscope (Olympus UK). Photographs were taken with an Olympus Camedia C-3030 Digital Camera (Olympus UK) and analysed with Corel Paint Shop Pro x (Corel UK Ltd), Image J (National institute of Health (NIH)) and Carestream Molecular Imaging Software (Carestream).

2.1.7 **Gels**

The reagents used for the manufacture of gels used for the separation of DNA and proteins throughout this study are listed below:

2.1.7.1 Agarose Gel (1.6%)

Agarose gel (1.6%) – 2.4g agarose (1.6%; Life technologies, Invitrogen) was dissolved in 150ml of 1X TBE by heating in a microwave, at full power. Ethidium bromide (7.5µl at 10mg/ml), required for the visualisation of bands, was added to the gel as it cooled. Gels were poured into a mould and allowed to cool until set.

2.1.7.2 Zymogram Gel (12%)

Zymogram Gel (12%) – 2.5ml 1.5M Tris pH 8.8 (25% v/v), 4.17ml Acrylamide (41.7% v/v; Bio-Rad), 1ml 2% gelatine (10% v/v), 0.1ml 10% SDS (1% v/v), 50µl ammonium persulfate (0.5% v/v), 20µl TEMED (0.2% v/v; Bio-Rad) and 2.16ml dH_2O (21.6% v/v) were mixed together. Gel mixture was pipette into the mould and allowed to set before use.

2.1.8 **General Labware**

2.1.8.1 CD14 Isolation Kit

All materials used for the isolation of $CD14^+$ cells (CD14 microbeads, MiniMACS™ Separator, MS Column, 30µm pre-separation filter) were supplied by Miltenyi Biotec.

2.1.8.2 ELISA Plates

All 96 well ELISA plates used for the analysis of soluble mediators in culture supernatants were obtained from Nunc International.

2.1.8.3 Plastic ware

All microcentrifuge tubes (0.5ml and 1.5ml) and Petri dishes were supplied by Grenier Bio One. 5ml polystyrene round bottom test tubes used for flow cytometry were supplied by VWR International.

2.1.8.4 Surgical Tools

Stainless steel forceps, scissors and disposable scalpels used to obtain and clean murine femora were obtained from Fisher Scientific.

2.1.8.5 Tissue Culture Flasks

All tissue culture flasks (T25 and T75) used for the culture of cells were obtained from Nunc International.

2.1.8.6 Tissue Culture Plates

All tissue culture plates (6 well, 12 well and 48 well) used for the culture of cells were obtained from Grenier Bio One.

2.1.9 **Mouse Strains**

The mouse strains used for the analysis of DR3 in OC and OB formation and function in this study are listed below:

C57BL/6 - DR3 heterozygous ($DR3^{het}$), DR3 wildtype ($DR3^{wt}$) and DR3 knockout ($DR3^{ko}$)

DBA/1 - DR3 heterozygous ($DR3^{het}$), DR3 wildtype ($DR3^{wt}$) and DR3 knockout ($DR3^{ko}$)

2.1.10 **Recombinant Cytokines and Enzymes**

Recombinant MCSF, RANKL, TL1A and polyHistidine used for the differentiation and stimulation of murine and human *in vitro* osteoclast cultures were supplied by R&D Systems Europe. MMP-9 standard was supplied by R&D Systems Europe. Recombinant human cathepsin K was supplied by Dr Vera Knäuper (School of Dentistry, Cardiff University) and Enzo Life Sciences. Cathepsin K control was supplied by Biomedica Gruppe.

2.1.11 **Solutions and Buffers**

All solutions and buffers used in this project are listed below.

Phosphate buffered saline (PBS) pH7.2 used throughout this study was supplied by Life Technologies, Invitrogen.

2.1.11.1 Cathepsin K Bio-assay and Zymogram Reagents

Acetic acid (50mM) - 300µl of acetic acid was diluted in 100ml of dH_2O.

Assay buffer – 1g of bovine serum albumin (BSA; 1%) and 50µl of Tween-20 (0.05%) were added to 100ml of PBS.

Blocking buffer – 1g of BSA (1%) was dissolved in 100ml of PBS.

Buffer A – 4.1g of sodium acetate (NaOAC; 50mM), 584.5mg of Ethylenediaminetetraacetic acid (EDTA; 2mM), 308.5mg of Dithiothreitol (DTT; 2mM), 20.5g of sodium chloride (NaCl; 350mM) and 1.5ml of Chondroitin 4-Sulfate Sodium Salt (0.15%) was dissolved in 1L of dH_2O.

Cathepsin K Development buffer – 141.96g of sodium phosphate dibasic (Na_2HPO_4; 0.1M), 292.25mg of EDTA (1mM) and 308.5mg of DTT (2mM) was dissolved in 1L of dH_2O.

Cathepsin K Renaturation buffer – 7.87g of Tris (65mM) and 200ml of glycerol (20%) was dissolved in 1L of dH_2O. pH was adjusted to pH7.4 with hydrochloric acid (HCl) solution.

Cathepsin K Sample buffer – 476mg of leupeptin (0.1mM) was dissolved in 10ml of zymogram sample buffer.

Citrate buffer - 4.2g of citric acid (0.2M) was dissolved in 100ml of dH_2O. The pH of the solution was adjusted to 3.95 with potassium hydroxide (KOH) solution.

Development solution - 10µl of 30% w/v hydrogen peroxide (H_2O_2; 0.03%) and 100µl Tetramethylbenzidine (TMB; 1%) were added to 10ml of citrate buffer.

TMB - 240mg of TMB (0.1M) was dissolved in 5ml of dimethyl sulphoxide (DMSO; 50%) and 5ml of absolute ethanol (50%).

Type I collagen stock – 2mg of type I collagen (2mg/ml) was dissolved in 1ml of 50mM acetic acid.

Wash buffer - 500µl of Tween-20 (0.05%) was added to 1L of PBS.

2.1.11.2 $CD14^+$ Isolation Reagents

MACS buffer / Murine DR3 flow cytometry buffer – 0.5g of BSA (0.5%) and 58mg of EDTA (2mM) was dissolved in 100ml of PBS.

2.1.11.3 DNA and Protein Gel Reagents

Ammonium persulfate (10%) – 100mg of ammonium persulfate was dissolved in 1ml of dH_2O.

Gelatine (2%) – 2g of gelatine was dissolved in 100ml of dH_2O.

Tris pH8.8 solution (1.5M) – 181.7g of Tris was dissolved in 1L of dH_2O. pH was adjusted to 8.8 with HCl.

2.1.11.4 DR3 Genotyping Buffers and Solutions

DNA Loading Buffer Orange G - 250mg of Orange G loading dye (2.5mg/ml) and 30ml of glycerol (30%) was added to 100ml of 2x TBE.

DR3 Genotyping Master Mix – All master mix reagents were purchased from Life Technologies, Invitrogen. 5µl of 1mM deoxyribonucleotide triphosphates (dNTPs), 4µl of 10x polymerase chain reaction (PCR) buffer, 1.2µl of 50mM magnesium chloride ($MgCl_2$), 0.2µl of AV1 primer, 0.4µl of 4F primer, 0.8µl of 2R primer and 0.5µl of *Taq* DNA polymerase were mixed per genotyping sample.

EDTA (1M) – 292.24g of EDTA was dissolved in 1L of dH_2O.

Ethanol (70%) – 700ml of absolute ethanol (70%) was diluted with 300ml of dH_2O (30%).

Lysis buffer – 2ml of 5M NaCl (2% v/v), 5ml of 1M Tris pH8 (5% v/v), 10ml of 1M EDTA (10% v/v), 10ml of 10% Sodium dodecyl sulphate (SDS; 10% v/v) and 1.333ml of proteinase k (1.3%v/v; Roche) were made up to 100ml in dH_2O.

NaCl (5M) – 292.2g of NaCl was dissolved in 1L of dH_2O.

SDS (10%) – 100g of SDS was dissolved in 1L of dH_2O.

1x Tris/Borate/EDTA (TBE) – 10ml of 10x TBE (Fisher Scientific) was diluted in 90ml of dH_2O.

2x TBE – 20ml of 10x TBE was diluted in 80ml of dH_2O.

1M Tris pH8 – 121.14g of Tris was dissolved in 1L of dH_2O, pH was adjusted to pH8 with HCl.

2.1.11.5 ELISA Buffers and Solutions

Coating Buffer (0.1 M Sodium Carbonate, pH 9.5) - 7.13g of Sodium bicarbonate ($NaHCO_3$; 85mM), 1.59g of sodium carbonate (Na_2CO_3; 15mM) was dissolved in 1L of dH_2O, pH was adjusted to 9.5 with sodium hydroxide (NaOH) solution.

Development solution – made up as section 2.1.11.1.

Wash buffer – made up as section 2.1.11.1.

2.1.11.6 Flow Cytometry Reagents

Flow Cytometry buffer – 100µl of FCS (1%) was added to 10ml of PBS.

4% Formaldehyde – 10.8ml of 37% formaldehyde was added to 89.2ml of PBS.

2.1.11.7 MMP-9 Zymogram Reagents

Development buffer – 2ml of 10x zymogram development buffer (Bio-Rad) was added to 18ml of dH_2O.

Renaturation buffer – 2ml of 10x zymogram renaturation buffer (Bio-Rad) was added to 18ml of dH_2O.

2.1.11.8 Murine TL1A RT-PCR Reagents

TL1A master mix – All master mix reagents were purchased from Life Technologies, Invitrogen. 5µl of 1mM dNTPs, 4µl of 10x PCR buffer, 1.2µl of 50mM $MgCl_2$ and 0.5µl of *Taq* DNA polymerase were mixed per sample.

2.1.12 **Solvents**

All solvents used in this study (absolute ethanol, glacial acetic acid, dimethylformamide (DMF), iso-propanol and methanol) were supplied by Fisher Scientific unless otherwise stated.

2.1.13 **Stains and Histological Materials**

The reagents and materials used in the manufacture of stains for the visualisation of cells, resorption pits and gels throughout this study are listed below:

2.1.13.1 Actin Immunocytochemistry

Actin stain - 100µl of Alexa Fluor® 594 Phalloidin (Life Technologies, Invitrogen) at 200units/ml (0.5units/ml) was diluted in 10ml of PBS.

Blocking solution – 1g of BSA (1%) was dissolved in 100ml of PBS.

4', 6-diamidino-2-phenylindole (DAPI) nucleic acid stain - 1.5µl of DAPI stock at 5mg/ml (300nM; Life Technologies, Invitrogen) was diluted in 10ml of PBS.

4% Formaldehyde – made up as section 2.1.11.6.

Permabilisation solution – 10µl of Triton X-100 (0.1%) was added to 10ml of PBS.

2.1.13.2 Additional Histological Materials

Round glass coverslips (5mm diameter) were supplied by Waldemar Knittel Glasbearbeitungs- GmbH. Glass slides were supplied by Fisher Scientific. Ivory discs (6mm diameter) were supplied by Cardiff University. DPX mountant was supplied by Sigma-Aldrich.

2.1.13.3 Alizarin Red Stain

Alizarin Red - 1g of alizarin red stain (1%) was dissolved in 100ml of dH_2O, pH was adjusted to pH4.2 with KOH.

50% methanol – 50ml methanol (50% v/v) was diluted with 50ml dH_2O (50% v/v).

4% Formaldehyde – made up as section 2.1.11.6.

2.1.13.4 Alkaline Phosphatase (ALP) Stain

Alkaline phosphatase (ALP) stain – 33.4µl of BCIP solution (0.334%) and 44µl of NTB solution (0.44%) were added to 10ml of Tris buffer.

5-bromo-4-chloro-3-indolyphosphate (BCIP) solution – 7.5mg of BCIP (0.75mg/µl) was dissolved in 100µl of 70% DMF.

DMF (70%) – 7ml of DMF was diluted in 3ml of dH_2O.

Nitro blue tetrazolium (NBT) solution – 5mg of NBT was dissolved in 100µl of 100% DMF.

4% Formaldehyde – made up as section 2.1.11.6.

Tris buffer – 1.22g of Tris (100mM), 0.58g of NaCl (100mM) and 0.476g of $MgCl_2$ (50mM) was dissolved in 100ml of dH_2O.

2.1.13.5 Differential Stain

Giemsa Stain – 11ml of Giemsa stain (11%) was diluted in 89ml of PBS pH6.8.

May-Grunwald Stain – 50ml of May-Grunwald stain (50%) was diluted in 50ml of PBS pH6.8 (50%).

PBS pH6.8 – One PBS tablet (VWR) was dissolved per 100ml dH_2O.

2.1.13.6 MMP-9 and Cathepsin K Zymogram Stain

Coomassie blue stain – 0.25g of Brilliant Blue R Coomassie (0.25%) was dissolved in 100ml of destain.

Destain – 450ml of methanol (45%) and 100ml of acetic acid (10%) were added to 450ml of dH_2O (45%).

2.1.13.7 Resorption Pit Staining

Calcein solution (0.8mM) – 5mg of calcein was dissolved in 10ml of dH_2O.

Hydrogen Peroxide Solution (1%) - 333µl of H_2O_2 (30% w/v) was added to 10ml of dH_2O.

Toluidine Blue Stain (0.5%) - 0.50g of Toluidine Blue stain was dissolved in 100ml of dH_2O.

2.1.13.8 TRAP Stain

Acetate Buffer (0.1M) - 3.52ml of 0.2M sodium acetate solution (35.2% v/v) and 1.48ml of 0.2M acetic acid solution (14.8% v/v) was added to 5ml dH_2O (50%v/v).

Acetic Acid Solution (0.2M) - 0.115ml Acetic Acid was diluted in 9.885ml of dH_2O.

Fixative – 4ml of 25% grade 1 gluteraldehyde (10%) was diluted in 10ml of dH_2O.

Harris' haematoxylin Stain (VWR)

Naphthol AS-MX Phosphate Disodium Salt (10mg/ml) - 10mg of Naphthol AS-MX Phosphate Disodium Salt was dissolved in 1ml of dH_2O.

1x Scott's tap water – 1ml of 10x Scott's tap water was diluted in 9ml of dH_2O.

Sodium Acetate Solution (0.2M) - 0.164g of Sodium Acetate was dissolved in 10ml of dH_2O.

Sodium Tartrate (0.3M) - 0.69g of Sodium Tartrate was dissolved in 10ml of dH_2O.

TRAP Stain - 5ml of 0.1M acetate buffer (50%v/v), 1ml of 0.3M sodium tartrate (10%v/v), 100µl of 10mg/ml Naphthol AS-MX Phosphate Disodium Salt (1%v/v) and 100µl of Triton X-100 (1%v/v) was added to 3.80ml of dH_2O (38%v/v). 3mg of Fast red Violet LB salt (0.3mg/ml) was dissolved per 10ml.

2.1.14 **TL1A RT-PCR Primers**

Four primers were designed for the detection of murine TL1A by RT-PCR. Primers were designed by W. Perks (Dr E. Wang Laboratory). The primer sequences and predicted product size are provided in Table 2.3:

Primer Name	**Product**	**Primer Sequence**	**Predicted Size (bp)**
P1	TL1A	F - CCC CGG AAA AGA CTG TAT R – GGT GAG TAA ACT TGC TGT	75
P2	TL1A	F – GCT GCC TGT TGT CAT TTC C R – TCT GGG AGG TGA GTA AAC TTG	149
P3	TL1A	F – TCA TTT CCC ATC CTC GCA GGA CTT R – TAA TTG TCA GGT GTG CTC TCG GCT	166
P4	TL1A	F – CAG CAG AAG GAT GGC AGA R – CTC TGG CCT GTG TCT ACA	91
β-actin	β-actin	F – CGG CCA GGT CAT CAC TAT TG R – CTC AGT AAC CCG CCT AG	450

Table 2.3. Primers used in murine TL1A mRNA PCR

2.2 **Methods**

The methods used throughout this study are outlined below.

2.2.1 **Animals**

Animals were housed in the Joint Biological Services Unit (Cardiff University) at constant temperature and humidity on a 12 hour light/dark cycle. All animals were kept in filter top containers. Food and water were available *ad libitum*. $DR3^{ko}$ animals were initially generated using 129/Sv mouse strain stem cells and backcrossed onto a C57BL/6 background (280). The DBA/1 $DR3^{ko}$ mouse strain was generated through backcrossing C57BL/6 $DR3^{het}$ mice with DBA/1 wildtype mice for 7 generations, generating a $DR3^{ko}$ mouse with less than 1% C57BL/6 DNA. All C57BL/6 and DBA/1 $DR3^{ko}$ animals were generated *in house*.

2.2.2 **Murine DR3 Genotyping**

In order to determine the DR3 genotype of the C57BL/6 and DBA/1 mice used throughout this study PCR was performed on ear snips obtained from individual animals on a weekly basis.

Ear snips were taken from individual mice, by trained operators, and placed into labelled micro centrifuge tubes. Lysis buffer (750µl) was added to the microcentrifuge tube containing the ear snip and incubated overnight at 56°C in a water bath. Salt extraction was performed by adding 310µl of 5M NaCl to the samples, vortexing and incubating for 30 minutes at room temperature. Samples were spun at 13,250g for 25 minutes and 800µl of the aqueous phase removed and placed into a new labelled tube. Ice-cold iso-propanol (500µl) was added and the samples vortexed before being spun for 10 minutes at 13,250g. Supernatant was removed from the samples and 500µl of 70% ethanol added. Samples were incubated for 30 minutes at room temperature before being spun for 10 minutes at 13,250g. Supernatant was removed from the samples which were placed at 37°C for an hour until dry. dH_2O (50µl) was added to each sample and placed at 37°C for 2-3 hours to re-dissolve DNA.

For PCR 8µl of DNA was added to a thin walled PCR tube along with 20µl of dH_2O. Required volume of DR3 genotyping master mix was made up and 12.1µl added to each tube. Tubes were placed into the MyGene™ Series Peltier thermal cycler (LongGene Scientific Instruments) and run through the DR3 genotyping program, as defined in Table 2.4.

Step	Temperature (°C)	Time	Number of Cycles
Initial denaturation	94	5 minutes	1
Annealing	60	45 seconds	
Elongation	72	45 seconds	
Denaturation	94	45 seconds	33
Annealing	60	45 seconds	
Elongation	72	45 seconds	
Denaturation	94	45 seconds	1
Annealing	60	45 seconds	
Elongation	72	5 minutes	

Table 2.4. DR3 genotyping PCR settings

Samples were removed from the PCR thermal cycler and 4µl of DNA loading buffer orange G added to each sample. A 1.6% agarose gel was made up. The gel was placed into the running tank and covered with 1x TBE buffer. 5µl of 1KB DNA ladder (Life Technologies, Invitrogen) was added to the first well of the gel followed by 15 - 20µl of sample to subsequent wells. Gels were run at 100V for 90 minutes after which bands present in the gel were visualised using a UVP BioDoc It™ imaging system.

2.2.3 **Cell Count**

Cell counts on murine bone marrow cells, human cells and osteoblasts were performed using a standardised method. Cell suspension (10µl) was diluted 1:1 with Trypan Blue (Sigma-Aldrich) and applied to a haemocytometer. Viable cells were identified under a white light by the exclusion of blue dye. Cells were counted in 4 sections of the haemocytometer (Fig 2.1) and the total number of cells present calculated using the following equation:

Total No. cells / ml = (No. cells / No. of sections counted) x 2 (dilution factor) x ($1x10^4$)

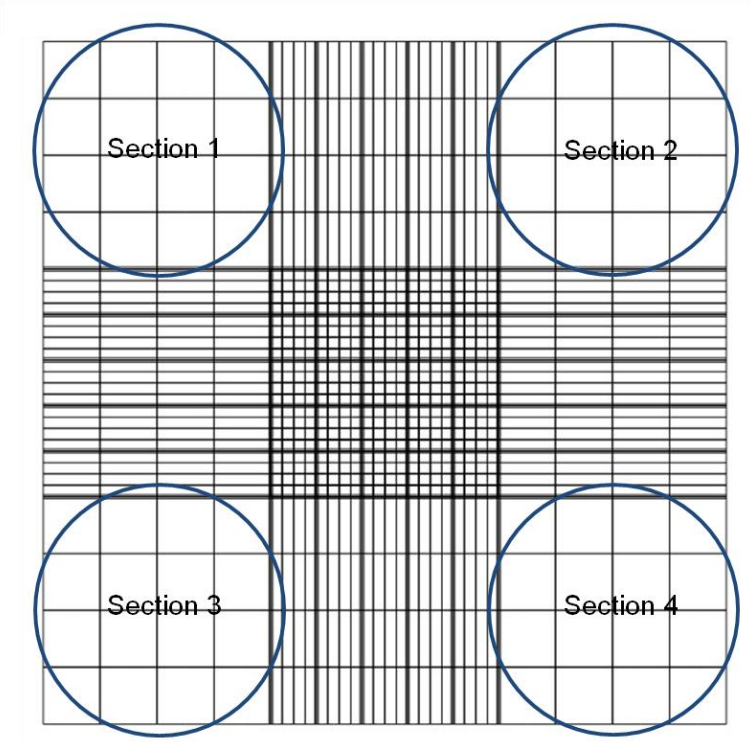

Figure 2.1. Sections of Haemocytometer used for Cell Counts.

For all cell counts 10µl of cell solution was diluted 1:1 with trypan blue and added to the haemocytometer. Viable cells were counted in 4 sections and the total cell number calculated.

2.2.4 **Murine Bone Marrow Cell Isolation**

Murine bone marrow cells were used as a source of precursor cells for the murine osteoclast and osteoblast differentiation assays reported in this thesis. Bone marrow (BM) was isolated from C57BL/6 and DBA/1, male and female mice, aged between 8 – 18 weeks. Mice were sacrificed by schedule I; an overdose of carbon dioxide (CO_2) followed by cervical dislocation. Hind legs were removed. Cleaned femurs were excised using a scalpel and the head (*caput femoris*) removed. Bones were placed into a 0.5ml micro centrifuge tube, into which a hole had been made in the base. The 0.5ml micro centrifuge tube was placed inside a 1.5ml micro centrifuge (Fig 2.2) and centrifuged at 13,250g for 1 minute, causing the bone marrow to pellet in the 1.5ml micro centrifuge tube. Isolated

bone marrow was re-suspended in 500µl murine osteoclast medium (for OC assays) or 500µl murine osteoblast medium (for OB assays).

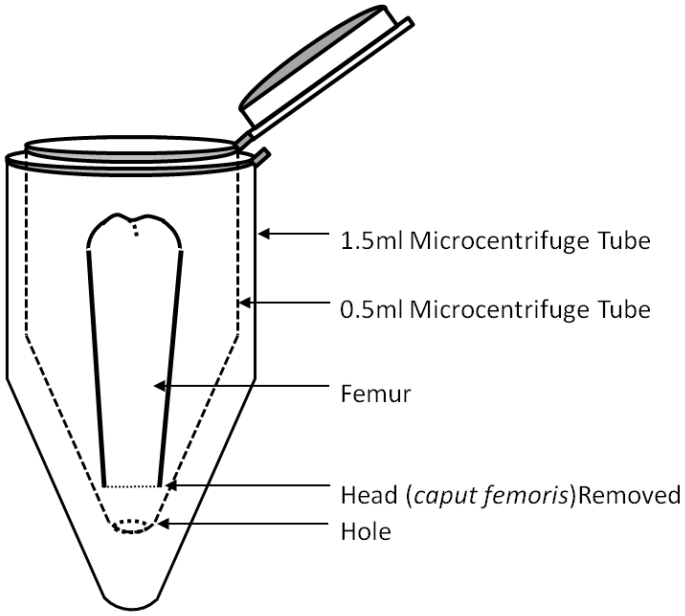

Figure 2.2. Set-up of Microcentrifuge Tube for the Isolation of Bone Marrow from Murine Femora

A hole was made in the base of 0.5ml microcentrifuge tube. The 0.5ml microcentifuge was then placed into a 1.5ml microcentrifuge tube. The head (*caput femoris*) of the femur was removed and the femur placed cut end down in the 0.5ml microcentrifuge tube.

2.2.5 **Murine Bone Marrow Differential Staining**

In advance of performing OC differentiation assays it was important to determine the cellular phenotype of $DR3^{wt}$ and $DR3^{ko}$ bone marrow. Differential cell counts were performed using a small proportion of cells (10µl of $6.4x10^6$ cells / ml cell suspension) from 5 aged-matched DBA/1 $DR3^{wt}$ and $DR3^{ko}$ mice (10-16 weeks) used in OC assays. Sterilised glass coverslips were placed into a Petri dish and 10µl of cell suspension added to the surface and incubated for 2 hours at 37°C 5% CO_2. After 2 hours non-adherent cells were removed by washing the coverslips twice in PBS pH7.2. Cells were fixed by

immersion in methanol for 15 minutes. Methanol was removed and discs immersed in May-Grunwald stain for 15 minutes then Giemsa stain for 15 minutes. Stain was removed and the cells washed in PBS then dH_2O before being allowed to air dry. Dried coverslips were then mounted onto slides using DPX and placed at 60°C overnight to dry.

Images of the mounted coverslips were taken at 20x magnification and cropped to represent a size of 1000µm^2. Cell type was defined by its morphology. Numbers of lymphocytes, monocytes, neutrophils, erythrocytes, myoblasts and megakaryocytes were analysed and frequency calculated as a % of all cells.

2.2.6 **Murine Osteoclast Differentiation Assay**

Osteoclast differentiation assays were established using bone marrow cells harvested from aged matched DBA/1 or C57BL/6 DR3^{wt} and DR3^{ko} mice (10 – 18 weeks). Initially OC assays were set-up on glass coverslips for looking at the relative contribution of DR3 and TL1A. In order to look at the functional role assays were set-up on an ivory substrate. Bone marrow was isolated as described in section 2.2.4. Cells were counted (section 2.2.3) and re-suspended in murine osteoclast medium at a concentration of 6.4x10^6 cells / ml (glass coverslip assays) or 3.2x10^6 cells / ml (ivory disc assays), to give a final volume of approx. 3ml.

2.2.6.1 Glass Coverslip Assay

Bone marrow was isolated from 3 age-matched DR3^{wt} and DR3^{ko} male DBA/1 mice (aged 10 – 16 weeks). Cells were adhered onto glass coverslips as above. Coverslips were placed into a 48 well tissue culture plate and 500µl of murine osteoclast medium supplemented with one of four conditions (Table 2.5) was added (Fig 2.3); each condition was set-up in triplicate:

	Condition 1	**Condition 2**	**Condition 3**	**Condition 4**
MCSF 25ng/ml	+	+	+	+
RANKL 2ng/ml	-	-	+	+
TL1A 10ng/ml	-	+	-	+

Table 2.5. Supplemented murine osteoclast medium conditions

Cells were incubated at 37°C 5% CO_2. On day 3 supernatants were removed and replenished with fresh media and the experiment run to day 7. OC were identified by TRAP staining (Section 2.2.13) and total cell count and OC size calculated. A summary of the procedure is shown in Fig 2.4.

2.2.6.2 Ivory Disc Assay

Before OC assays could be performed on ivory discs development of the method was required. Bone marrow was obtained from the femora of a DBA/1 $DR3^{wt}$ mouse (12 weeks). Bone marrow cells were plated onto glass coverslips as above, at the two cell concentrations cited in Table 2.6. Each condition was run in triplicate:

Volume	Cell Concentration
10µl	$6.4x10^6$ cells / ml
20µl	$3.2x10^6$ cells / ml

Table 2.6. Volumes and cell concentrations added to coverslips

Cells were stained and analysed for differential analysis as defined in section 2.2.5 with the following modifications; cell number per $1mm^2$ was calculated for each sample. Subsequent experiments, on ivory discs, were set-up using 20µl of cell suspension at $3.2x10^6$ cells / ml.

The final protocol used for the culture of murine OC on ivory discs was as follows. Bone marrow was isolated from 6 age-matched $DR3^{wt}$ and $DR3^{ko}$ female DBA/1 mice (aged 10 – 18 weeks). Cells were plated onto ivory discs and experiment set-up as glass coverslip assay (section 2.2.6.1). On day 3 and day 7 supernatants were removed, aliquoted and stored at -70°C for subsequent analysis by ELISA (CCL2, CXCL1, CCL3 and pro MMP-9). Wells were replenished with fresh media and the experiment run to day 10. All outcome measures were as above (section 2.2.6.1) with the addition of resorption pit analysis (section 2.2.14.3). A summary of the procedure is shown in Fig 2.5.

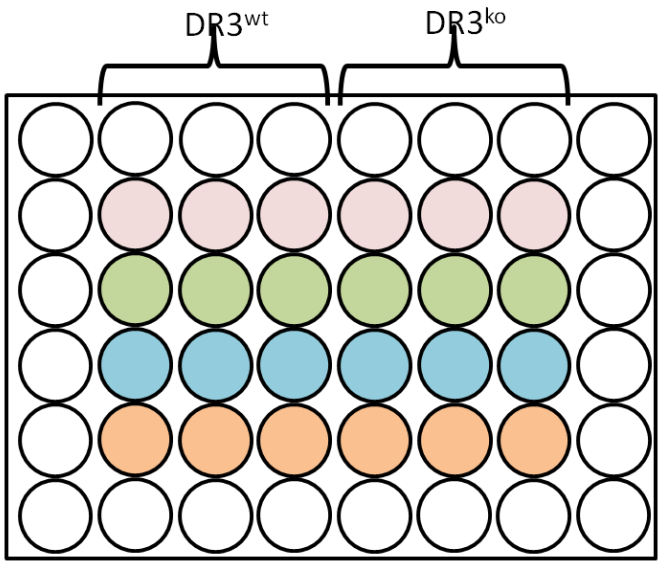

Figure 2.3. Plate Layout for Murine Osteoclast Assays.

For murine OC assays, glass coverslips and ivory discs were placed into a well of a 48 well plate. Plates were divided into 2 with one half containing the $DR3^{wt}$ cells and the other the $DR3^{ko}$cells. OC medium added to the cells either contained MCSF (pink), MCSF + TL1A (green), MCSF + RANKL (blue) or MCSF + RANKL + TL1A (orange). Outer well were filled with PBS (white) to ensure no drying effect was observed.

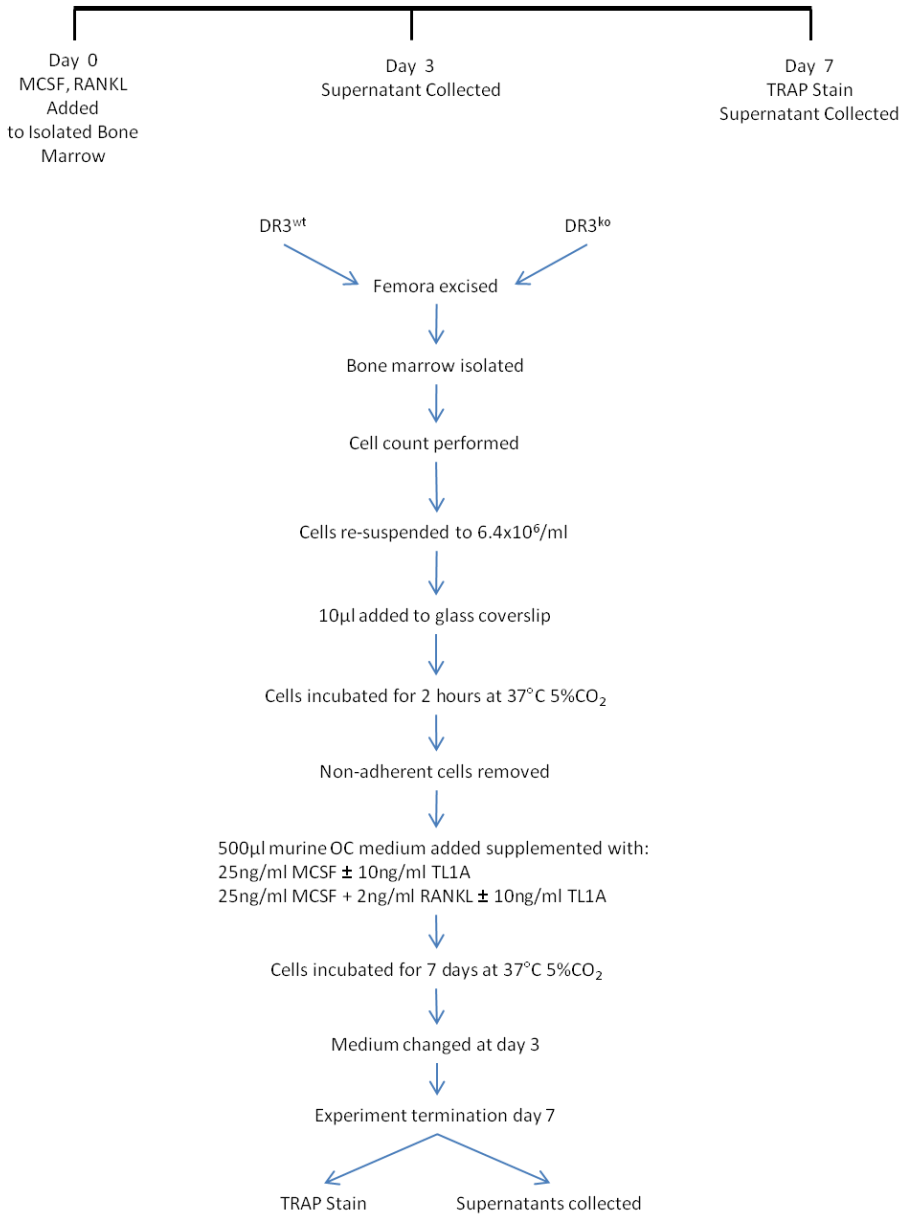

Figure 2.4. Experiment Timeline and Flow Chart of Murine Osteoclast Differentiation Assay Performed on Glass Coverslips

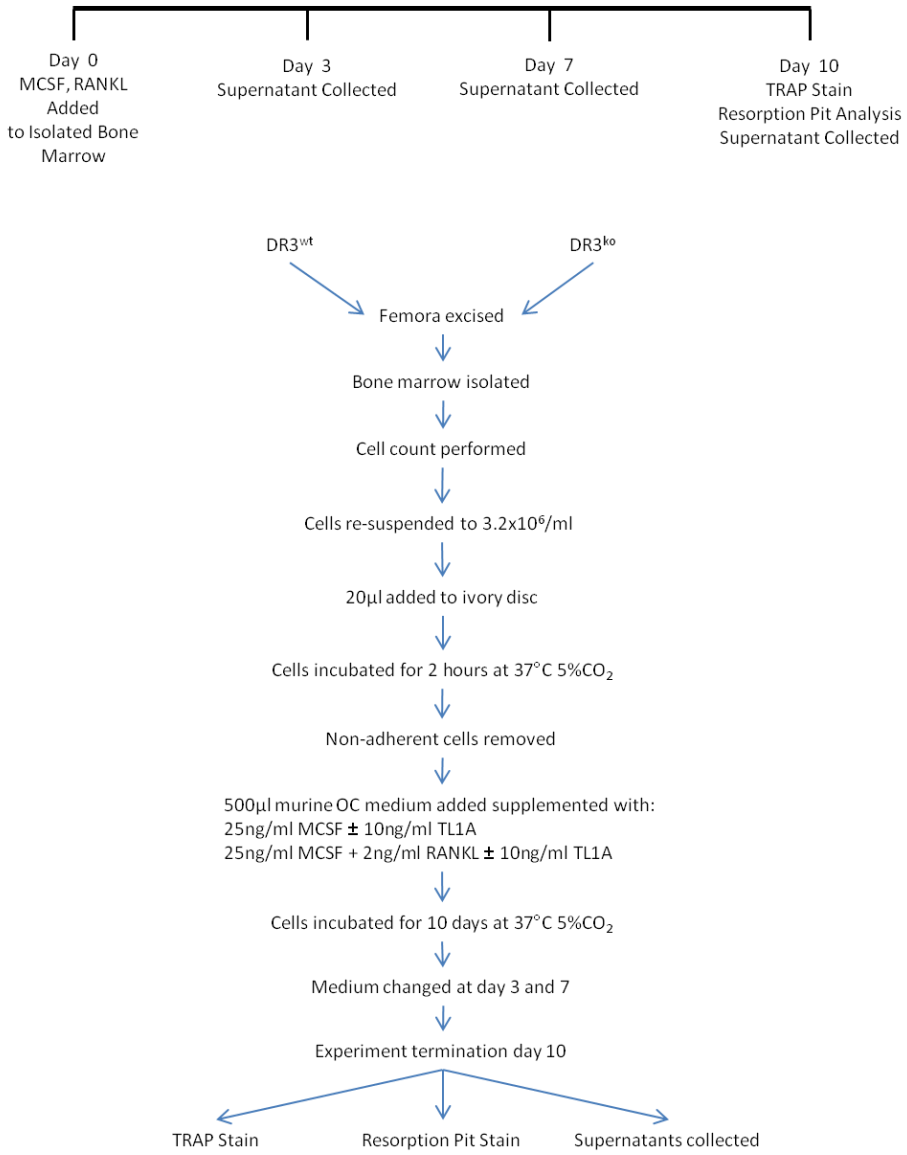

Figure 2.5. Experiment Timeline and Flow Chart of Murine Osteoclast Differentiation Assay Performed on Ivory Discs

2.2.7 **Isolation of $CD14^+$ Cells (Osteoclast Precursors) from Peripheral Blood of Healthy Females**

In order to perform human osteoclastogenesis assays $CD14^+$ cells were first isolated from peripheral blood mononuclear cells (PBMCs). Ethical approval was obtained from the Medical / Dental School Research Ethics Committee (MDSREC Reference Number: 09/21) for the collection of venous peripheral blood from healthy female volunteers. Peripheral blood (40ml) was collected and mixed with heparin (Sigma-Aldrich), to stop coagulation. A separate 10ml peripheral blood sample was collected and allowed to clot at room temperature for 30 minutes before serum was harvested and stored.

For the isolation of the $CD14^+$ cells from peripheral blood 5ml Histopaque -1077 (Sigma-Aldrich) was added to a 15ml centrifuge tube and 10ml of blood gently overlaid ensuring blood and histopaque did not mix. Four x 15 ml were used for each blood preparation. PBMCs were separated from the red blood cells and the plasma by centrifugation (samples were spun at 400g for 30 minutes). Plasma was removed and discarded. PBMCs, located at the interface of the plasma and histopaque, were carefully removed and transferred to a clean sterile 15ml centrifuge tube. PBMCs were washed 3 times by adding 10ml Hank's balanced salt solution (HBSS; Life Technologies, Invitrogen) and spinning at 300g for 10 minutes. HBSS was removed after each spin and replaced with fresh HBSS. After the third wash all HBSS was removed and replaced with 5ml human osteoclast medium, cells were kept on ice and a cell count performed (section 2.2.3). Approx. $1x10^5$ cells were removed for testing by flow cytometry for CD14 and DR3 expression (section 2.2.8). Cells were passed through a pre-separation filter into a new 15ml centrifuge tube and spun at 300g for 10 minutes. Medium was removed and replaced with 80µl MACS buffer and 20µl CD14 microbeads per 10^7 cells and incubated on ice for 15 minutes. Cells were passed through the magnetic column according to the manufacturer's protocol. $CD14^-$ cells passed through the column and were discarded. $CD14^+$ cells were removed from the column by flushing with MACS buffer and collected in a new 15ml centrifuge tube and a cell count performed (section 2.2.3). Cells were spun at 300g for 10 minutes and re-suspended in human OC medium to a final concentration of $3.2x10^6$ / ml for use in ivory disc assays, $6.4x10^6$ / ml for use in glass coverslip assays and $1x10^6$ / ml for use in plastic tissue culture plate assays. Approximately $1x10^5$ cells were removed for testing by flow cytometry for CD14 and DR3 expression (section 2.2.8).

2.2.8 **Flow Cytometric Analysis of CD14 and DR3 Expression on Isolated $CD14^+$ Cells**

Cells from two sources were analysed; (i) immediately prior to adherence onto ivory discs (section 2.2.7) or (ii) cells removed from the surface of the substrate, after 7 days culture in MCSF (section 2.2.9). These cells were rubbed gently with a cell scraper and added, along with culture medium, to a 5ml round bottom test tube. Cells were spun at 800g for 3 minutes and the medium replaced with 600µl flow cytometry buffer before being split equally between 3 round bottom test tubes (200µl per tube / ~30,000 cells). 5µl (1µg/test) of anti-human CD14-FITC, 5µl (0.125µg/test) anti-human DR3-PE or corresponding isotype antibody was added to the relevant test tube and incubated on ice for 30 minutes. Cells were spun at 800g for 3 minutes and supernatant removed and replaced with fresh flow cytometry buffer. Wash procedure was repeated 3 times. After final wash cells were re-suspended in 200µl flow cytometry buffer and 200µl 4% formaldehyde. Cells were run through the BD Accuri™ C6 Flow Cytometer and data analysed using BD CFlow® Plus software. 20,000 events were acquired per sample. Forward scatter-area (FSC-A) against forward scatter-height (FSC-H) plots were generated and doublets excluded by gating on the single cells. FSC-A against side scatter-area (SSC-A) plots were then generated and cell debris excluded by gating. Monocytes were positively selected for by gating, and expression of CD14 and DR3 calculated from scatter plots or histograms.

2.2.9 **Expansion of $CD14^+$ Cells (OC Precursors) and Induction of DR3 Expression**

In order to determine conditions for $CD14^+$ cell expansion and $CD14^+$ DR3 expression isolated $CD14^+$ cells were plated and adhered onto substrates as shown in Table 2.7.

	Glass Coverslip	**48 Well Plastic Tissue Culture Plate**	**Ivory Disc**
Volume of Cell Suspension	10µl	100µl	20µl

Table 2.7. Volume of cell suspension added to substrate

Coverslips and ivory discs were transferred to a 48 well plate. Human OC medium (500µl) supplemented with 5ng/ml MCSF was added to each well. Cells were incubated at 37°C 5% CO_2. On day 3 supernatants were removed and replenished with fresh media and experiment run to day 7. Cells were tested for DR3 expression according to section 2.2.8. A summary of the procedure is shown in Fig 2.6.

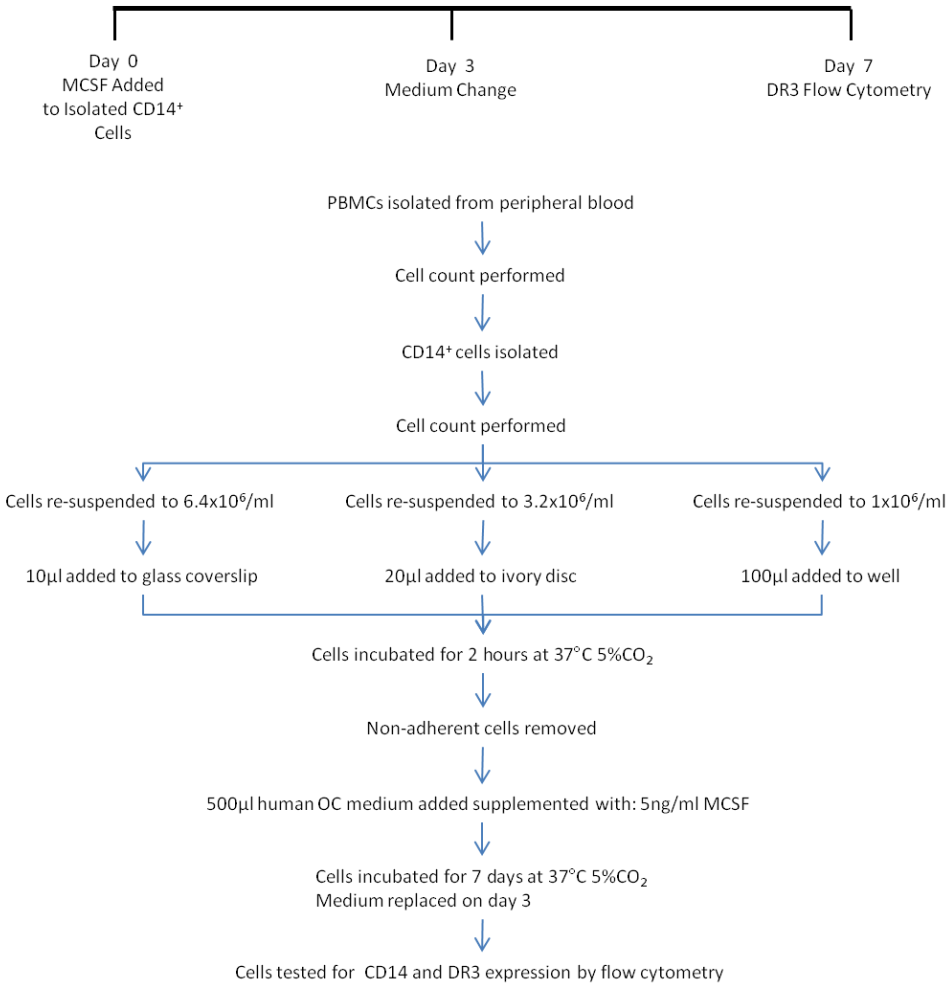

Figure 2.6. Experiment Timeline and Flow Chart of DR3 Expression on Different Support Matrices

2.2.10 **Human Osteoclastogenesis Assay**

Initially OC assays were set-up in plastic tissue culture plates for looking at the effect of TL1A on OC differentiation. In order to look at the functional role assays were set-up on an ivory substrate. Human OC differentiation assays were established using $CD14^+$ cells isolated from PBMCs, as described in section 2.2.7. Cell counts were performed (section 2.2.3) and cells re-suspended in human osteoclast medium at a concentration of $3.2x10^6$ cells / ml.

2.2.10.1 Plastic TC Plate Assays

$CD14^+$ cells were isolated from the peripheral blood (section 2.2.7) of 5 healthy females. Cells were adhered to 48 well plates as above. Human OC medium (500µl) supplemented with 5ng/ml MCSF was added per well. Cells were incubated at 37°C 5% CO_2 with medium removed and replenished with fresh media on day 3. DR3 expression was tested for on day 7 (referred to as Day 0 of osteoclastogenesis assay; section 2.2.8). Supernatants were removed and replaced with 500µl medium supplemented with one of four conditions (Table 2.8); each condition was set-up in duplicate:

	Condition 1	**Condition 2**	**Condition 3**	**Condition 4**
MCSF 5ng/ml	+	+	+	+
RANKL 5ng/ml	-	-	+	+
TL1A 10ng/ml	-	+	-	+
polyHistidine 2.5µg/ml	-	-	+	+

Table 2.8. Supplements added to human OC medium in plastic TC plate assays

Wells were terminated on days 1, 2, 3, 4 and 5 and cells stained for TRAP (section 2.2.13). Supernatants were collected, aliquoted and stored at -70°C for subsequent analysis by ELISA (CCL2 and CXCL8).

2.2.10.2 Ivory Assays

Initial assays were performed to determine the experiment termination time point; allowing analysis of OC numbers and function. $CD14^+$ cells were isolated from the peripheral blood of a healthy female (section 2.2.7). Cells were adhered to ivory discs as in section 2.2.9. Ivory discs were placed into a 48 well tissue culture plate and 500µl

supplemented human OC medium (Table 2.9) was added, each condition was set-up in duplicate:

	Condition 1
MCSF 5ng/ml	+
RANKL 5ng/ml	+
polyHistidine 2.5µg/ml	+

Table 2.9. Supplements added to human OC medium in development of assay

Cells were incubated at 37°C 5% CO_2. On day 3, 7, 10, 14 and 18 supernatants were removed and replenished with fresh media and experiment run to day 21. OC were identified by TRAP staining (section 2.2.13) and total cell count calculated. Resorption pits were identified by staining (section 2.2.14.3) and % disc resorbed calculated. A summary of the procedure is shown in Fig 2.8. Subsequent human osteoclast assays on ivory discs were run to day 14 where sufficient OC and resorption pits were detected.

The final protocol used for the culture of human OC from $CD14^+$ cells was as follows. $CD14^+$ cells were isolated from the peripheral blood (section 2.2.7) of 6 healthy females (Fig 2.9). Cells were plated onto ivory discs as above. Discs were transferred to two 48 well plates (Fig 2.7) and 500µl human OC medium supplemented with 5ng/ml MCSF added. Cells were incubated at 37°C 5% CO_2 with medium removed and replenished with fresh media on day 3. DR3 expression was tested for on day 7 (referred to as Day 0 of osteoclastogenesis assay; section 2.2.8). Supernatants were removed and replaced with 500µl medium supplemented with one of six conditions (Table 2.10); each condition was set-up in duplicate:

	Condition 1	**Condition 2**	**Condition 3**	**Condition 4**	**Condition 5**	**Condition 6**
MCSF 5ng/ml	+	+	+	+	+	+
RANKL 5ng/ml	-	-	-	+	+	+
TL1A 10ng/ml	-	+	-	-	+	-
TL1A 100ng/ml	-	-	+	-	-	+
polyHistidine 2.5µg/ml	-	-	-	+	+	+

Table 2.10. Human OC assay conditions

On day 3, 7 and 10 supernatants were removed, aliquoted and stored at -70°C for subsequent analysis by ELISA (CCL2, CXCL8, CCL3, TL1A, TNF and total MMP-9). Wells were replenished with fresh media and the experiment run to day 14.

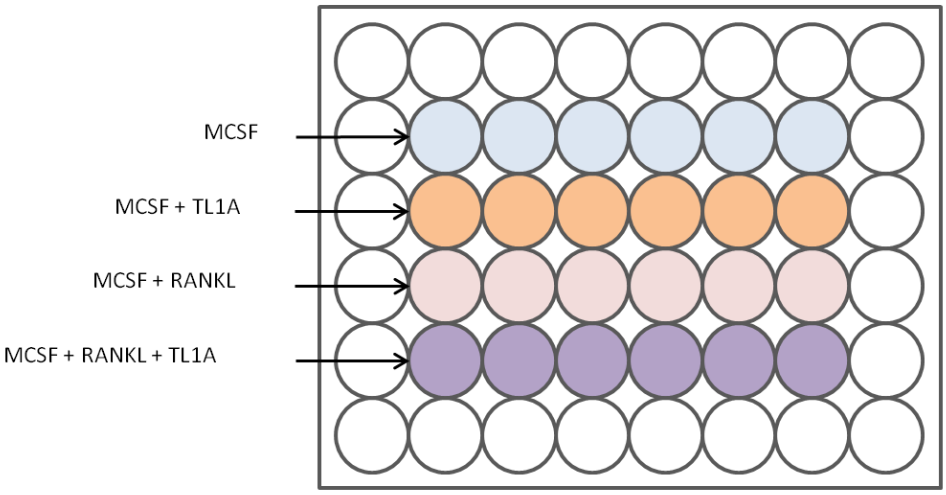

Figure 2.7. Human Osteoclast Differentiation Assay Plate Layout

For human OC assays, ivory discs were placed into wells of 48 well plates for the duration of the experiment. OC medium added to the cells was supplemented with MSCF (blue), MCSF+TL1A (orange), MCSF+RANKL+polyHistidine (pink) or MCSF+RANKL+polyHistidine+TL1A (purple). Outer wells were filled with PBS (white) to ensure no drying effect was observed

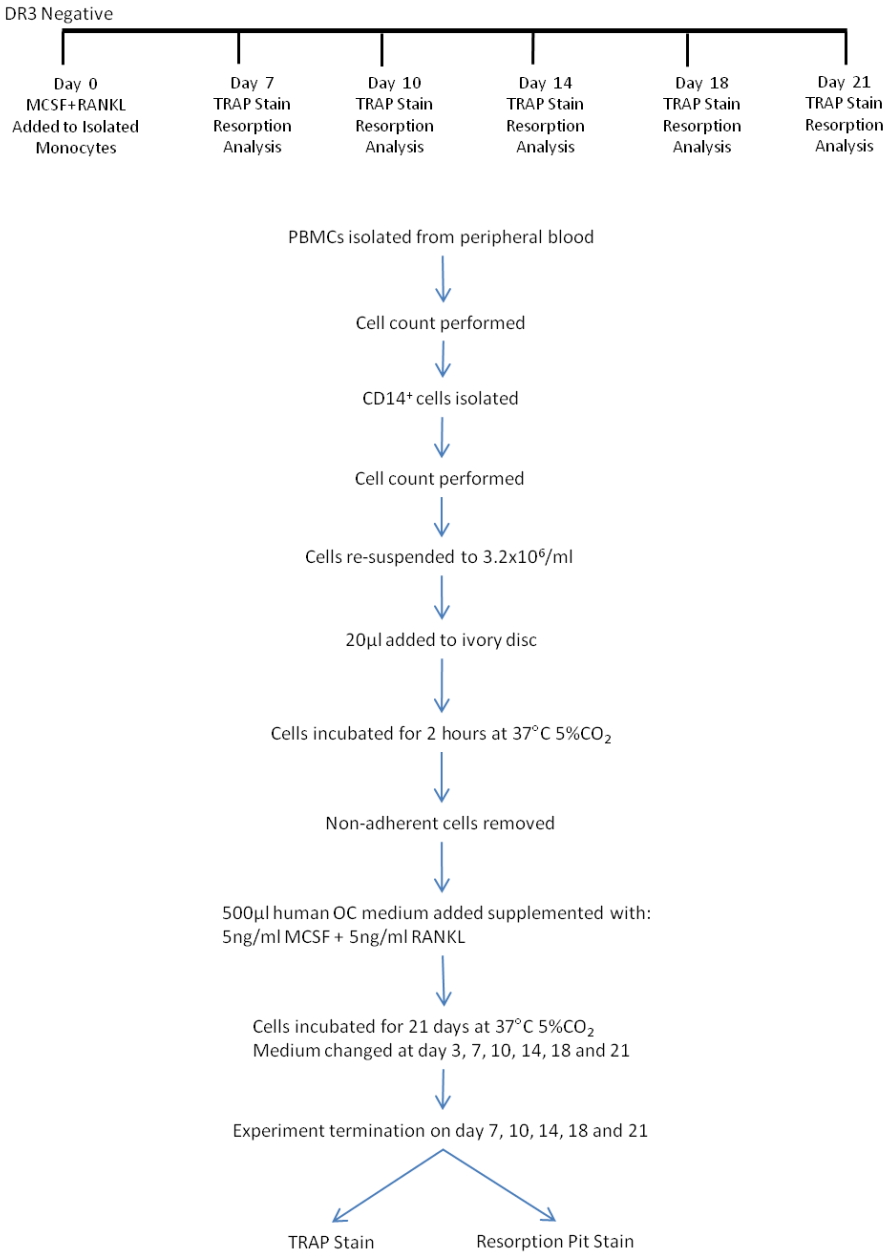

Figure 2.8. Experiment Timeline and Flow Chart of Optimisation of Osteoclast Cultures from CD14⁺ Cells on Ivory Discs

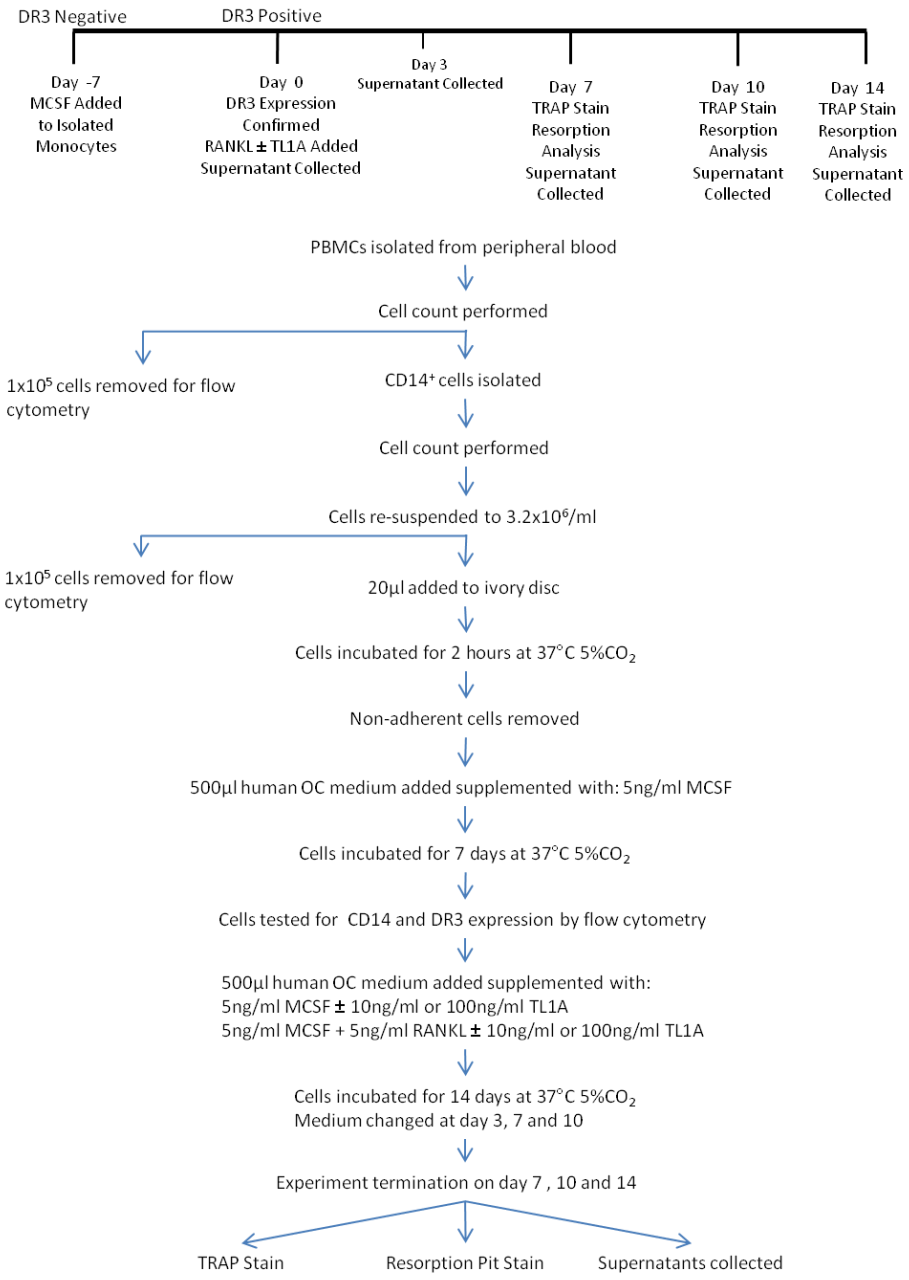

Figure 2.9. Experiment Timeline and Flow Chart of Normal Female Osteoclast Differentiation Assay Performed on Ivory Discs

2.2.11 **Isolation of $CD14^+$ Cells (Osteoclast Pre-cursors) from Peripheral Blood of Post-Menopausal Patient Cohorts**

Ethical approval was required for the acquisition of peripheral blood in patients attending fracture clinics to determine the level of TL1A and TNF in the serum. The application for ethical approval was initially submitted to the South East Wales Research Ethics Committee and reviewed on 12 May 2010. Additional amendments to the application were requested. The application was resubmitted and a favourable ethical opinion was given for the study on the 15 October 2010, 5 months after the initial application (REC reference number: 10/WSE02/44). Post-menopausal patients were to be recruited to one of three cohorts:

- - Osteoporosis, - Fracture (OP^-Frac^-)
- - Osteoporosis, + Fracture (OP^-Frac^+)
- + Osteoporosis, + Fracture (OP^+Frac^+)

Patients were either included or excluded from the study using the criteria below:

Inclusion criteria

- Attending for first bone density scan
- Adult
- Female
- Post-Menopausal

Exclusion criteria

- Recent fracture (in the past 3 months)
- History of corticosteroid use (except inhaled or topical) or
- Anti-TNF therapy.
- Patients with known seropositive rheumatoid arthritis, inflammatory bowel disease
- Recent history of continuous treatment with bisphosphonate, calcitonin, Strontium ranelate or parathyroid hormone (i.e. for more than 3 months).
- Patients with known primary hyperparathyroidism
- Currently taking part in another study

Nurses at the fracture liaison service or the Open Access Primary Care service obtained consent from each patient. Peripheral blood (40ml) was collected and mixed with heparin,

to stop coagulation. A separate 10ml peripheral blood sample was collected and was allowed to clot at room temperature for 30 minutes before serum was harvested and stored. $CD14^+$ cells were isolated as in section 2.2.7.

2.2.12 **Post-Menopausal Patient Cohort Osteoclast Assays**

Patient cohort OC assays were performed on ivory discs using $CD14^+$ cells isolated from PBMCs. Assays were performed as in section 2.2.10.2 with the following modifications; human OC medium was supplemented with the conditions in Table 2.11. A summary of the procedure is outlined in Fig 2.10.

	Condition 1	**Condition 2**	**Condition 3**	**Condition 4**
MCSF 5ng/ml	+	+	+	+
RANKL 5ng/ml	-	-	+	+
TL1A 100ng/ml	-	+	-	+
polyHistidine 2.5µg/ml	-	-	+	+

Table 2.11. Patient cohort OC assay conditions

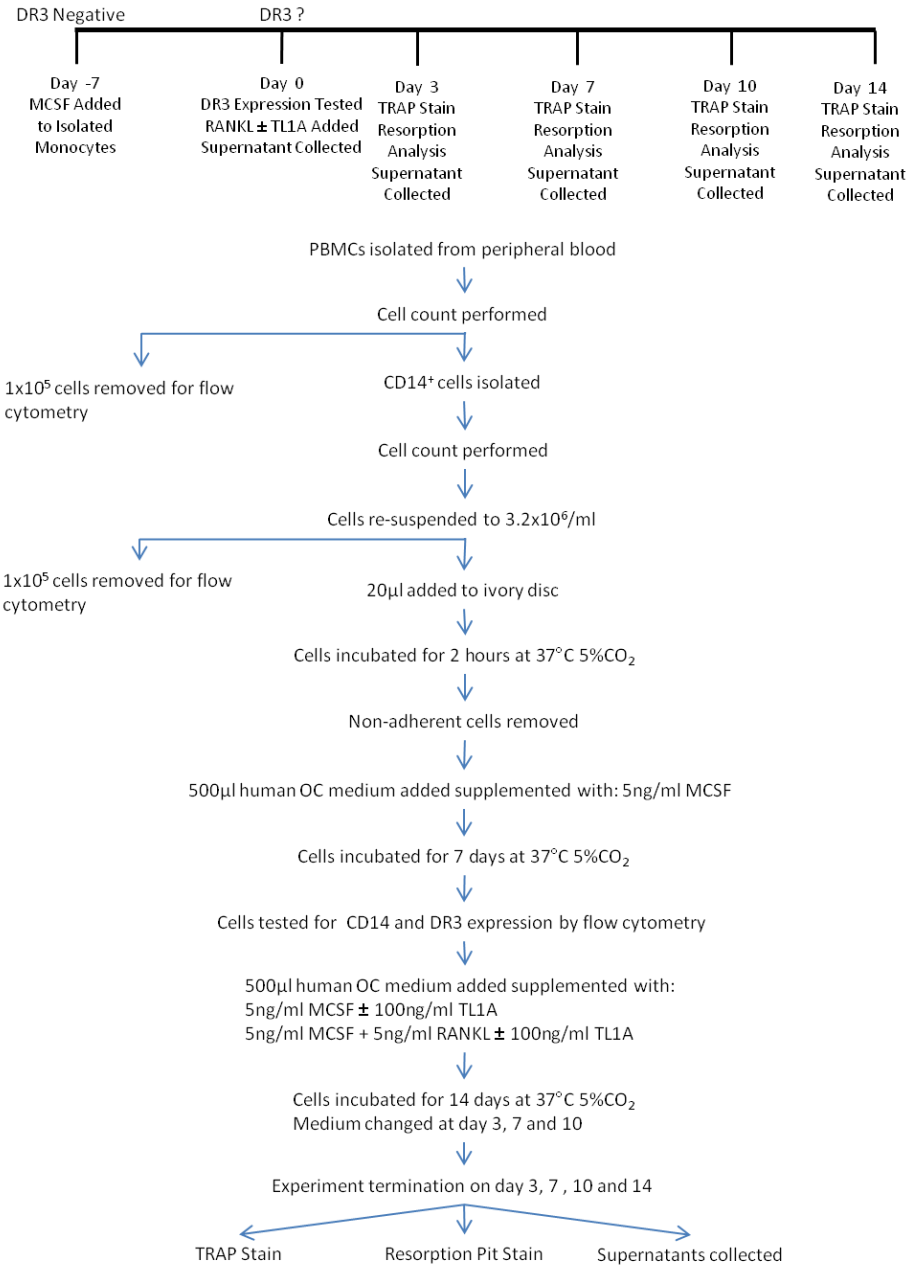

Figure 2.10. Experiment Timeline and Flow Chart of Patient Cohort Osteoclast Differentiation Assay Performed on Ivory Discs

2.2.13 **Identification of Mononuclear Cells and Osteoclasts in Culture**

Murine BM cells (section 2.2.6) or human $CD14^+$ cells (section 2.2.10) grown on plastic, glass and / or ivory were visualised by staining with haematoxylin. Osteoclasts were identified by their morphology (>3 nuclei) and positive TRAP stain. Cultures were washed twice with PBS and 150µl of fixative added per well. After 15 minutes incubation fixative was removed and the cells were washed a further 2 times with PBS. TRAP stain (300µl) was added per well and incubated for 5 minutes. TRAP stain was removed and cells washed twice with PBS. After staining for TRAP ivory discs were photographed for analysis as below. Haematoxylin stain (150µl) was added to each coverslip / disc and incubated for 1 minute before being removed and cells washed with PBS. 1x Scott's Tap Water (150µl) was added and incubated for 1 min before being removed and cells washed twice with PBS. Glass coverslips were mounted onto slides using DPX and dried overnight at 60°C. Coverslips and discs were photographed for analysis.

Stained coverslips, plates and ivory discs were visualised at 10x magnification and five images per disc (Fig 2.11) taken. Images were cropped to represent a size of $1000\mu m^2$ and the number of OC counted. OC were then outlined in black using the paintbrush tool. The brightness and contrast of the image was adjusted to remove all background leaving the black outline of the OCs. Outlined OC were filled in black using the flood fill tool and the image saved for the calculation of OC area using Image J. Images were opened in Image J and the scale set at 1440pixels = 1000µm. The threshold of image was adjusted so all OCs were detected. The area of the OCs was then calculated and the results copied into Microsoft Office Excel.

Total cell count was performed on cropped images, after haematoxylin staining, using Carestream Molecular Imaging Software. Briefly images were loaded and the auto-region of interest (ROI) tool selected from the navigation bar. New ROI set was selected and the following parameters set; edge detection, edge gradient = 20%, restrict size – Min=50, Max=no restriction. ROI's were found by selecting add.

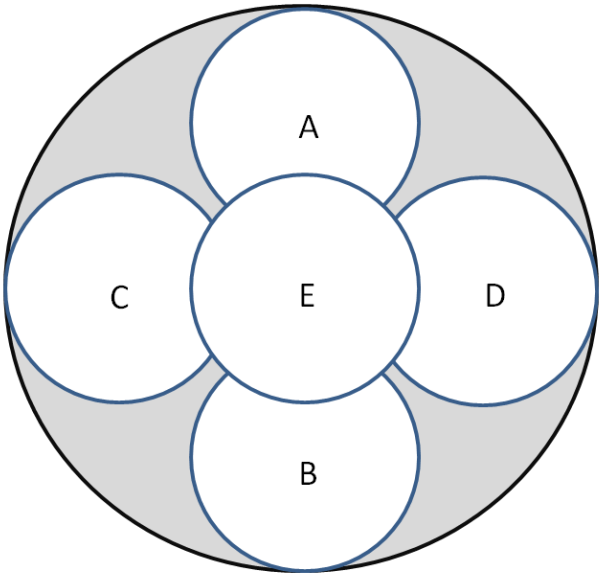

Figure 2.11. Glass Coverslip / Ivory Disc Photograph Layout

Glass coverslips and ivory discs were photographed for the analysis of cells and resorption pits. Five images per coverslip / disc were taken as shown. Microscope field of view (FoV) was placed at the top of the coverslip / disc and image taken, picture A. FoV was moved to the bottom (B), left (C), right (D) and centre (E) of the coverslip / disc and images taken.

2.2.14 **Assessing Mediators of Osteoclast Formation and Function**

A variety of methods were used to assess mediators of OC formation and function on ivory discs. They are listed below.

2.2.14.1 Chemokine Analysis

A number of chemokines associated with OC differentiation are released as soluble mediators. The chemokines CCL2, CXCL1, CXCL8 and CCL3 were measured in the culture supernatants or serum by ELISA (R&D Systems). A general method is provided, with specifc buffers and concentrations outlined in Table 2.12.

96 well ELISA plates were coated with 100µl of specific capture antibody and incubated overnight at room temperature. Following incubation the capture antibody was discarded

and the plate washed 4 times with wash buffer. The plates were blocked at room temperature, with mechanical shaking, with 300µl of blocking buffer. After 2 hours the plates were washed 4 times with wash buffer. Diluted specific standards (100µl) for the ELISA were added, in duplicate. Samples were either used neat or diluted in dilution buffer and 100µl added in duplicate. Samples were incubated for 2 hours at room temperature with mechanical shaking. After 4 washes with wash buffer 100µl of specific detection antibody was added to each well and the plate incubated for 2 hours at room temperature with mechanical shaking. Plates were washed 4 times with wash buffer and 100µl of streptavidin-HRP added and incubated at room temperature for 20 minutes. After 4 final washes, 100µl of development solution was added and the colour developed at room temperature. Reaction was terminated by the addition of 50µl of 12% sulphuric acid (H_2SO_4). The optical density of the plate was measured as 450nm.

ELISA	Coating Buffer	Wash Buffer	Blocking Buffer	Dilution Buffer	Capture Antibody	Detection Antibody	Standard
Murine CCL2	PBS	0.05% Tween in PBS	1% BSA in PBS	1% BSA in PBS	0.2µg/ml in PBS	50ng/ml in Dilution Buffer	250pg/ml – 3.9pg/ml
Murine CXCL1					2.0µg/ml in PBS	200ng/ml in Dilution Buffer	1000pg/ml – 15.63pg/ml
Murine CCL3					0.4µg/ml in PBS	100ng/ml in Dilution Buffer	500pg/ml – 7.8pg/ml
Human CCL2					1.0µg/ml in PBS	100ng/ml in Dilution Buffer	1000pg/ml – 15.625pg/ml
Human CXCL8					4.0µg/ml in PBS	20ng/ml in Dilution Buffer	2000pg/ml – 31.3pg/ml
Human CCL3					0.4µg/ml in PBS	200ng/ml in Dilution Buffer	500pg/ml – 7.8pg/ml

Table 2.12. ELISA buffers and antibody concentrations used in chemokine analysis

2.2.14.2 Cytokine Analysis

Levels of the cytokines TNF (BD Bioscience) and TL1A (Peprotech) were measured in culture supernatants and serum by ELISA. The method is described in section 2.2.14.1. Specific buffers and antibody concentrations are outlined in Table 2.13.

ELISA	Coating Buffer	Wash Buffer	Blocking Buffer	Dilution Buffer	Capture Antibody	Detection Antibody	Standard
Human TL1A	PBS	0.05% Tween in PBS	1% BSA in PBS	0.1% BSA, 0.05% Tween in PBS	1.0µg/ml in PBS	0.5µg/ml in Dilution Buffer	4000pg/ml – 62.5pg/ml
Human TNF	Coating buffer	0.05% Tween in PBS	10% FCS in PBS	10% FCS in PBS	1:250 dilution in coating buffer	1:250 dilution in dilution buffer	500pg/ml – 7.8pg/ml

Table 2.13. Buffers and antibody concentrations used in the human TNF and TL1A ELISAs

2.2.14.3 Resorption Pit Analysis

Two methods were used for the analysis of resorption pits made by murine and human OC on ivory discs; they are outlined below.

2.2.14.3.1 Light Microscope

Resorption pits made by osteoclasts cultured on ivory discs were visualised by staining with toluidine blue. Discs were individually sonicated for 1 minute at 22Hz, using a Soniprep 150 (MSE) to disrupt adherent cells. Remaining cells were removed from the discs by gentle rubbing with a cotton bud. 1% hydrogen peroxide solution (200µl) was added to each disc and incubated overnight at room temperature with mechanical shaking to remove haematoxylin stain from the disc. Discs were washed twice with dH_2O and 200µl 0.5% toluidine blue stain added. Discs were incubated for 1 minute at room temperature before the stain was removed and discs washed twice with dH_2O. Discs were photographed and analysed as above for osteoclasts (section 2.2.13).

2.2.14.3.2 Confocal Microscope

In order to obtain more detailed analysis of resorption pits a method using confocal microscopy was developed. Cultured cells were removed from the discs as in section

2.2.14.3.1. Initially discs were placed onto a glass slide for visualisation of the resorption pits, using a Leica TCS SP2 AOBS spectral confocal microscope (Leica Microsystems Ltd) and Leica confocal software (Leica Microsystems Ltd). Discs were imaged using reflective light, at x10 and x40 magnification. After identification of areas for improvement the following modifications were made; following removal of haematoxylin stain discs were washed twice in dH_2O. Calcein fluorescent dye solution (200µl) was added to each well and incubated at room temperature for 10 minutes. Discs were washed twice with dH_2O and mounted onto glass slides with DPX; discs were covered with a coverslip and dried overnight at 60°C. Discs were scanned using a 495nm wavelength laser, exciting the calcein dye. Images were taken at x10 and x40 magnification. To measure the depth of resorption pits a 'z series' was performed, creating a 3D reconstruction of the pits. Start point of the 'z series' was set at the surface of the ivory disc. Z position was adjusted until just the base of the resorption pit was in focus, and set. 'z series' was configured to take 50 images per scan. 3D reconstruction of the 'z series' images were performed using the Leica confocal software.

2.2.14.4 Tissue Degrading Enzymes

OC utilise enzymes to degrade the organic component of bone. Levels of MMP-9 and cathepsin K were analysed in culture supernatants.

2.2.14.4.1 MMP-9

Murine and human pro MMP-9 were measured in culture supernatants by ELISA (R&D Systems), following the method outlined in 2.2.14.1. Specific buffers and antibody concentrations can be found in Table 2.14.

ELISA	Coating Buffer	Wash Buffer	Blocking Buffer	Dilution Buffer	Capture Antibody	Detection Antibody	Standard
Murine pro MMP-9	PBS	0.05% Tween in PBS	1% BSA in PBS	0.1% BSA, 0.05% Tween in PBS	4.0µg/ml in PBS	250ng/ml in Dilution Buffer	20,000pg/ml – 312.5pg/ml
Human Total MMP-9				1% BSA in PBS	1.0µg/ml in PBS	100ng/ml in 2% *HI NGS in Dilution Buffer	2000pg/ml – 31.3pg/ml

Table 2.14. Buffers and antibody concentrations used in the MMP-9 ELISAs.

Active and inactive MMP-9 present in culture supernatnats was assessed by zymogram using the following method.

A 15 well 10% 'Ready Gel' zymogram gel (Bio-Rad) was attached to the gel frame and electrode and placed into the gel tank. The comb was removed from the gel and zymogram running buffer (Bio-Rad) pipetted into the wells of the gel and added to the gel tank. Samples were diluted 1:5 with zymogram sample buffer (Bio-Rad) and 15µl added to the relevant sample well. MMP-9 standard (15µl) diluted to 10ng/ml in zymogram sample buffer was added to an empty well. Broad range pre-stained protein ladder (5µl) (Bio-Rad) was added to an empty well. The gel tank was topped up with running buffer until the gel was completely covered. The lid was placed on the gel tank and the gel run at a constant 100V for 2 hours. After completion of running time the gel was removed from the gel tank and gel frame and placed into a plastic tray where it was incubated for 15 minutes in renaturation buffer. After the incubation period the renaturation buffer was discarded and replaced with fresh renaturation buffer for a further 15 minutes. Following incubation the renaturation buffer was discarded and the gel placed in development buffer and incubated at 37°C for 20 hours. After 20 hours incubation the incubation buffer was discarded and replaced with destain for 10 minutes. Destain was removed and the gel placed in coomassie blue stain for 30 – 60 minutes at room temperature with mechanical shaking. When the gel was sufficiently stained it was placed back into destain to allow the visualisation of bands before being placed in dH_2O to be analysed.

Visualisation of bands present on MMP-9 zymogram gels was performed with the Carestream *In Vivo* FX Pro (Carestream) and Carestream Molecular Imaging Software. Images were taken using the settings outlined in Table 2.15. Analysis of the images was performed using Carestream Molecular Imaging Software.

Setting	Value
Exposure	4 seconds
UV Epi	Illumination
f-Stop	2.50
FoV	120.92
Focal Plane	Tray

Table 2.15. Carestream In Vivo FX Pro Zymogram Imaging Settings

2.2.14.4.2 Cathepsin K

Measurement and visualisation of cathepsin K in OC cultures supernatants was analysed using a number of methods.

For the Cathepsin K Collagenase Bio-assay, 96 well ELISA plates were coated with 50µl type I collagen at a concentration of 10µg/ml (25µl type I collagen stock solution in 5.5ml PBS) overnight at 4°C with mechanical shaking. Following incubation the type I collagen was discarded and the plate washed 4 times with wash buffer. Plates were blocked at room temperature, with mechanical shaking, with 300µl of blocking buffer. After 2 hours the plates were washed 4 times with wash buffer. Bacterial collagenase (100µl; Clostridiopeptidase A; Sigma-Aldrich) was used as a standard and added in duplicate (sensitivity range: 10,000pg/ml – 3.2pg/ml). Buffer A (100µl) was added in duplicate as a blank. Recombinant human Cathepsin K (100µl) at 460ng/ml was added in duplicate. Samples were diluted 1:10 and 1:100 in buffer A and 100µl added to the plate in duplicate. Samples were incubated at 37°C for 24 hours. After 4 washes with wash buffer 100µl of detection antibody (1:15,000 of stock dilution of anti-type I collagen in assay buffer) was added to each well and the plate incubated for 1 hour at room temperature with mechanical shaking. Plates were washed 4 times with wash buffer and 100µl of a secondary antibody (1:10,000 dilution of anti-mouse IgG peroxidase conjugated in assay buffer) was added to each well. Plates were incubated for 1 hour at room temperature, with mechanical shaking, before being washed 4 times with wash buffer. Development solution (100µl) was added and the colour developed at room temperature. Reaction was terminated by the addition of 50µl of 12% sulphuric acid (H_2SO_4). The optical density of the plate was measured as 450nm.

Analysis of sample optical density (OD) allowed for the calculation of % collagen left in well. Blanks were taken as having 100% of collagen remaining as no enzymes were present for degradation. % of collagen remaining in each well, compared to the blank was calculated as follows:

$$\frac{OD_{Sample} \times 100}{OD_{Blank}}$$

Analysis of the effect of FCS on the collagenase bio-assay was tested following the procedure above with the following modifications; buffer A was made up containing a range of FCS concentrations: 10%, 5%, 2% and 1%. Cathepsin K controls were made up

using modified buffer A so that they contained the final concentrations of FCS: 10%, 5%, 2%, 1%, 0.5%, 0.25%, 0.1% and 0.05%. Two sets of standard were made up as above with the second containing 10% FCS. Blanks were run in duplicate with and without 10% FCS.

The Cathepsin K zymogram was adapted from work by Li et al (281). A gel frame was constructed and a 12% acrylamide gel made up. The Cathepsin K was set-up and run as per the procedure outlined in section 2.2.14.4.1 with the following modifications; Cathepsin K control sample from Biomedica Cathepsin K ELISA was diluted 1:5, with Cathepsin K sample buffer, to give a final concentration of 107pmol/L. Initial sample was serial diluted 1:5 to give the final concentrations: 21.4pmol/L, 4.28pmol/L, 0.856pmol/L, 0.171pmol/L, 0.034pmol/L and 0.007pmol/L. After completion of running, gels were added to Cathepsin K renaturation buffer followed by Cathepsin K development buffer.

For additional Cathepsin K zymograms the following modifications were made; recombinant human Cathepsin K (Enzo Life Sciences) was diluted 1:5 in sample buffer to give a concentration of 0.023µg/ml. Initial sample was serial diluted 1:5 to give the final concentrations: 4.6ng/ml, 0.92ng/ml, 184pg/ml, 36.8pg/ml, 7.36pg/ml and 1.472pg/ml. Incubation buffer was adjusted to pH 4 and pH 5 with HCl. Cathepsin K zymograms were analysed as in section 2.2.14.4.1.

Cathepsin K was visualised *in situ* using immunocytochemistry. Human osteoclasts were cultured in a 48 well plate according to the procedure outlined in section 2.2.10 with the following modifications; after adherence 500µl supplemented human OC medium (Table 2.16) was added to the cells.

	Condition 1
MCSF 5ng/ml	+
RANKL 5ng/ml	+
polyHistidine 2.5µg/ml	+

Table 2.16. Medium supplements used in culture of cells for CatK immunocytochemistry

Cells were incubated at 37°C 5% CO_2 with medium replenished every 3 to 4 days. On day 14 cultures were terminated and cells stained. Cells were fixed, permeabilised, blocked and stained for actin as in section 2.2.14.5. Anti-Cathepsin K antibody (200µl) or isotype control (Rabbit IgG), at 1µg/ml, 2µg/ml, 3µg/ml and 4µg/ml (diluted in blocking solution), was added to each well and incubated for 1 hour at room temperature. Cells were washed twice with PBS and 200µl Goat anti-Rabbit-FITC conjugated (diluted 1:50 in

blocking solution) was added to each well, and incubated at room temperature for 30 minutes. Cells were washed twice with PBS and 200µl DAPI nucleic acid stain was added to each well for 3 minutes at room temperature. Cells were washed twice with PBS. Cells were visualised under a Leica DM IRBE fluorescent microscope with Openlab 3.1.7 software.

2.2.14.5 Actin ring Formation

Formation of the actin ring plays a key role OC resorption. To determine whether DR3 affects actin ring formation cells were stained using immunocytochemistry. Murine $DR3^{wt}$ osteoclasts were cultured in a 48 well tissue culture plate as per the procedure outlined in section 2.2.6 with the following modifications; $3.2x10^5$ cells were added per well. After 10 days culture cells were washed twice with PBS. 200µl of 4% formaldehyde was added per well and incubated at room temperature for 10 minutes. Cells were washed a further 2 times with PBS. Permabilisation solution (200µl) was added and cells incubated for 3-5 minutes at room temperature. Cells were washed twice with PBS and 300µl of blocking solution was added and incubated for 30 minutes at room temperature, blocking solution was removed and cells washed twice with PBS. Actin stain (200µl) was added to each well and incubated at room temperature for 20 minutes. Cells were washed twice with PBS and 200µl DAPI nucleic acid stain was added to each well for 3 minutes at room temperature. Cells were washed twice with PBS. Cells were visualised under a Lecia DM IRBE fluorescent microscope (Lecia Microsystems Ltd) with Openlab 3.1.7 software (Perkin Elmer).

2.2.15 **Assessing TL1A Levels in Serum from Patients with Inflammatory Arthritis**

In order to determine whether DR3 and TL1A have a role in the pathogenesis of inflammatory arthritis levels of TL1A and rheumatoid factor (RF) were measured in serum from rheumatoid arthritis (RA), osteoarthritis (OA) and psoriatic arthritis (PsA) patients and healthy normal serum. Ethical approval was obtained from the Bro-Taf Health Authority (Reference 02/4692-Cardiff, Wales, UK) for the collection of venous peripheral blood from consenting RA patients and healthy normal subjects. Peripheral blood (20ml) was collected and allowed to clot at room temperature for 30 minutes before serum was harvested and stored.

2.2.15.1 Serum TL1A

Serum TL1A levels were measured by ELISA (section 2.2.14.2). Grouping of RA patients into those displaying erosive or non-erosive disease was carried out by Rheumatology doctors at Cardiff and Vale University Health Board, Heath Hospital; based on analysis of x-rays taken at time of sample collection.

2.2.15.2 Rheumatoid Factor

To analyse serum levels of RF an *in-house* ELISA was developed. ELISA was performed according to the method in section 2.2.14.1. Capture antibody used was Rabbit IgG, detection antibody was anti-human IgM (F(ab)'2-Peroxidase and standard was rheumatoid factor. Specific buffers and antibody concentrations are found in Table 2.17.

ELISA	Coating Buffer	Wash Buffer	Blocking Buffer	Dilution Buffer	Capture Antibody	Detection Antibody	Standard
Rheumatoid Factor	PBS	0.05% Tween in PBS	1% BSA in PBS	1% BSA, 0.05% Tween in PBS	10µg/ml in PBS	1:5000 dilution in Dilution Buffer	500 – 15.625 units

Table 2.17. Buffers and antibody concentrations used in the RF ELISA

2.2.16 **Murine Osteoblast Assays**

Osteoblast assays were established using bone marrow cells harvested from aged matched DBA/1 or C57BL/6 $DR3^{wt}$ and $DR3^{ko}$ mice (8 – 12 weeks). Bone marrow was isolated as described in section 2.2.4. Cells were re-suspended in murine osteoblast medium and added to a T75 tissue culture flask. Medium was removed and replenished with fresh media every 3 – 4 days until cells were 90% - 100% confluent.

2.2.16.1 Osteoblast Mineralisation Assay

Confluent osteoprogenitors were removed from the culture vessel by gentle scraping with a cell scraper. Cells were added to a 15ml centrifuge tube and spun at 800g for 3 minutes. Medium was removed, cells re-suspended in 5ml fresh murine osteoblast media and a cell count performed (section 2.2.3). Cells were re-suspended to a final concentration of 4 x 10^5 / ml and 1ml of cell suspension added per well of a 12 well tissue culture plate (Fig 2.12). Cells were incubated overnight at 37°C 5% CO_2. Murine osteoblast medium was

removed and replaced with murine osteoblast mineralising medium and cells incubated at 37°C 5% CO_2. On day 3, 7, 10, 14, 17, 20 and 23 supernatants were removed, aliquoted and stored at -70°C for subsequent analysis by ELISA (pro MMP-9). Wells were replenished with fresh media and the experiment run to day 26. Plates were removed at day 17, 20, 23 and 26 for staining for mineralisation (section 2.2.19.1) and ALP (section 2.2.19.2).

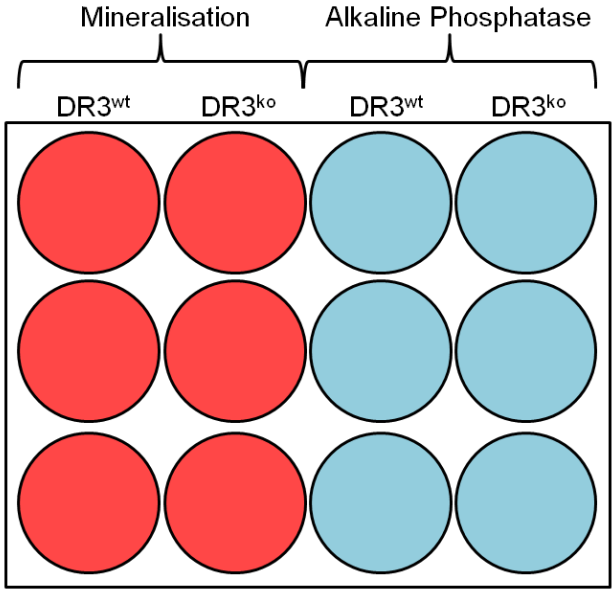

Figure 2.12. Murine Osteoblast Mineralisation Assay Plate Layout

For murine osteoblast mineralisation assays, cells were plated into wells of a 12 well tissue culture plate. Layout of plate for OB mineralisation assays. Left hand side of the plates were stained for mineralisation (red) with alizarin red stain. Right hand wells were stained for alkaline phosphatase activity (blue) with ALP stain.

2.2.17 **Flow Cytometric Analysis of DR3, RANKL and CD44 Expression on Osteoprogenitors and Mineralising Osteoblasts**

Bone marrow was isolated from two C57BL/6 and 2 DBA/1 age-matched $DR3^{wt}$ and $DR3^{ko}$ mice (8-12 weeks). Osteoprogenitors were cultured in T25 culture flasks according to section 2.2.16. When cells were 70% confluent medium was removed from half of the flasks and replaced with murine osteoblast mineralising medium. Cells were cultured for a further 7 days when mineralisation was visible in the flasks containing murine osteoblast mineralising medium. Cells were removed from the surface of the T25 tissue culture flasks by gentle scraping and added, along with culture medium, to a 5ml round bottom test tube. Cells were spun at 800g for 3 minutes and the medium replaced with 1.5ml murine DR3 flow cytometry buffer before being split equally between 6 round bottom test tubes (200µl per tube). Cells were spun at 800g for 3 minutes, supernatant removed and replaced with 200µl PBS containing Fc block (1/500 dilution). Cells were incubated for 15 min at 4°C before being spun at 800g for 3 minutes. Fc block was removed and cells re-suspended in 200µl murine DR3 flow cytometry buffer containing 2% normal goat serum. Cells were incubated for 30 min at 4°C before being spun at 800g for 3 minutes. Supernatant was removed and replaced with 200µl murine DR3 flow cytometry buffer containing 0.5% normal goat serum and either 2µl Polyclonal Goat anti-murine DR3 (1/100 dilution), 2µl anti-murine CD44 (1/100 dilution), 2µl anti-murine RANKL (1/100 dilution or isotype control at the same concentration. Cells were incubated for 30 – 45 min at 4°C. Cells were spun at 800g for 3 minutes, supernatant removed and washed three times in murine DR3 flow cytometry buffer. Murine DR3 flow cytometry buffer (200µl) containing streptavidin-APC (1/500 dilution) was added to the cells and incubated for 30 min at 4°C. Cells were washed three times before being re-suspended in 200µl murine DR3 flow cytometry buffer and fixed with 200µl 4% formaldehyde. Cells were run through the BD Accuri™ C6 Flow Cytometer and data analysed using BD CFlow® Plus software. 50,000 events were acquired per sample. Forward scatter-area (FSC-A) against forward scatter-height (FSC-H) plots were generated and doublets excluded by gating on the single cells. FSC-A against side scatter-area (SSC-A) plots were then generated and cell debris excluded by gating. Osteoprogenitors were positively selected for by gating, and expression of CD44, RANKL and DR3 calculated from scatter plots or histograms.

2.2.18 **TL1A RT- PCR**

Reagents for the detection of murine TL1A were not available at the time of this study. To determine whether cells produced TL1A, primers were designed and tested on cDNA isolated from immune complex stimulated RAW cells, osteoprogenitors and mineralising osteoblasts.

2.2.18.1 Immune Complex (IC) Stimulated RAW Cells

RAW cells were added to a T75 tissue culture flask and cultured until confluent in murine osteoclast medium. Plate bound immune complexes were generated by coating a 48 well plate with 500µl of mouse IgG (0.1µg/ml) and incubated overnight at 4°C. Following incubation the mouse IgG was discarded and the plate washed twice with PBS. 500µl of anti-mouse IgG (0.1µg/ml) was added to each well and incubated overnight at 4°C. Anti-mouse IgG was removed and plates washed twice with PBS. RAW cells were removed from the tissue culture flask by gentle scraping and added to a 15 centrifuge tube. Cells were spun at 800g for 3 minutes and re-suspended in 5ml murine osteoclast medium. A cell count was performed (section 2.2.3) and cells re-suspended to a final concentration of $2x10^5$ / ml. Cell suspension (500µl; $1x10^5$ cells) was added to each well containing plate bound immune complexes and incubated at 37°C 5% CO_2 for 3 days. Medium was removed from the wells and cells washed twice with PBS. mRNA was extracted from the cells using a Qiagen RNeasy Mini kit, following the manufacturer's instructions. The concentration of mRNA was calculated using a NanoDrop 3300 (Thermo Scientific). For conversion of RNA into cDNA by RT-PCR 2µg RNA was added to a thin walled PCR tube with 1µl 250ng oligo dT primers and 1µl 10mM dNTPs and the volume made up to 11µl with RNase free dH_2O. Samples were incubated at 65°C for 5 minutes then placed on ice for 1 minute. Samples were centrifuged at 12,000g for 1 minute and 4µl 5x 1^{st} strand buffer and 2µl 0.1M DTT added. Reverse transcriptase (1µl) was added to each sample and samples placed into the thermal cycler and run through the RT-PCR program as defined in Table 2.18. All reagents used for conversion of RNA into cDNA were supplied by Life Technologies, Invitrogen.

Step	Temperature (°C)	Time	Number of Cycles
Annealing	25	10 minutes	1
Elongation	42	50 minutes	
inactivation	70	15 minutes	

Table 2.18. RT-PCR thermal cycler settings for conversion of RNA into cDNA

2.2.18.2 TL1A Gradient PCR

For TL1A gradient PCR 1µl of IC stimulated RAW cell cDNA (section 2.2.18.1) was added to a thin walled PCR tube with 8µl of dH_2O. The required volume of TL1A master mix was made up and 12.1µl added to each tube along with 1µl of the primer to be tested (P1 – P4). Tubes were placed into the PCR thermal cycler and run through the TL1A gradient PCR program, as defined in Table 2.19. Sample products were run on a 1.6% agarose gel and visualised as outlined in section 2.2.2. Subsequent TL1A RT-PCR was performed using primer 4 and an annealing temperature of 59°C.

Step	Temperature (°C)	Time	Number of Cycles
Initial denaturation	94	5 minutes	1
Annealing	53.2 / 55.6 / 58 / 59 / 60	45 seconds	
Elongation	72	45 seconds	
Denaturation	94	45 seconds	33
Annealing	53.2 / 55.6 / 58 / 59 / 60	45 seconds	
Elongation	72	45 seconds	
Denaturation	94	45 seconds	1
Annealing	53.2 / 55.6 / 58 / 59 / 60	45 seconds	
Elongation	72	5 minutes	

Table 2.19. TL1A gradient PCR thermal cycler settings

2.2.18.3 Osteoprogenitor / Mineralising Osteoblast TL1A RT-PCR

Osteoprogenitors and mineralising osteoblast were cultured according to section 2.2.16 with the following modifications; mineralisation medium was added to the cells and mRNA extracted and converted to cDNA (section 2.2.18.1) on days 0, 5, 10 and 15. TL1A RT-PCR was performed according to section 2.2.18.2.

2.2.19 **Assessing Murine Osteoblast Function**

A variety of methods were used to assess the function of OB in culture. These are listed below.

2.2.19.1 Visualisation of Osteoblast Mineralisation

Mineralisation in murine osteoblasts cultures was visualised by staining with alizarin red stain. Cultures were washed twice with PBS and 300µl of 4% formaldehyde added per well. After 15 minutes incubation fixative was removed and the cells were washed a further 2 times with PBS. Alizarin red stain (300µl) was added per well and incubated for 30 minutes. Stain was removed and cells washed 4 times with 50% methanol. On the 4^{th} wash methanol was left in wells for 10 minutes to remove all non-specific staining before being removed and cells washed with dH_2O and allowed to air-dry.

Stained plates were scanned using a flatbed scanner at 300dpi. Corel Paint Shop Pro X was used to crop the individual wells for analysis. Background of the plate was removed from each image leaving just the stained area. Images were opened in image J and the scale set to 8.2 pixels = mm. Pictures were changed to 8-bit colour and the threshold adjusted so all mineralisation was detected. The area of the well that was stained was calculated and reported as a percentage of the well.

2.2.19.2 Visualisation of Alkaline Phosphatase Activity

Alkaline phosphatase (ALP) activity in osteoblast cultures was visualised by staining with the ALP stain. Cultures were washed and fixed as in section 2.2.19.1. ALP stain (300µl) was added per well and incubated for 30 minutes. Stain was removed and cells washed with dH_2O and allowed to air-dry. Staining was analysed as in section 2.2.19.1.

2.2.19.3 MMP-2 and MMP-9

Levels of pro MMP-9 were measured in culture supernatants by ELISA, with active MMP-2 and MMP-9 detected in culture supernatants by zymography. The methodology is described in section 2.2.14.4.1.

2.2.19.4 Visualisation of Osteoblast Cell Number

DBA/1 $DR3^{wt}$- and $DR3^{ko}$-derived osteoblasts were cultured to day 26 and cell numbers visualised by staining with DAPI as in section 2.2.14.5

2.2.20 **Analysis of DBA/1 *In Vivo* Bone Phenotype**

Analysis of DBA/1 *in vivo* bone phenotype was performed to determine whether there is any difference between $DR3^{wt}$ and $DR3^{ko}$ mice. $DR3^{wt}$ and $DR3^{ko}$, male and female mice (6 per group) were aged to either 8 or 20 weeks. At the selected time point mice were sacrificed by schedule 1; an overdose of carbon dioxide (CO_2) followed by cervical dislocation. Mouse weights were recorded before the lower half of the body was removed and stored in 70% alcohol to fix tissues. Excess flesh was removed from the femurs. X-rays of the femora and spines were taken with the Carestream In Vivo FX Pro and Carestream Molecular Imaging Software. Regions of Interest were selected using the Carestream Molecular Imaging Software and femur length and bone density calculated.

2.2.21 **Statistical Analysis**

All results were graphically illustrated as the mean ± standard error of the mean (SEM) and were statistically analysed using Graphpad Prism v5. *P* values of ≤ 0.05 were considered significant while those of ≤ 0.01 were considered highly significant. The statistical tests used in this study were the Mann-Whitney-U test, used for comparing the means of two unpaired groups of non-normally distributed data. Students unpaired T-test, used for comparing the means of two groups of normally distributed data. One-way and two-way ANOVAs were used when comparing more than two groups or variables respectively, followed by a Bonferroni post hoc test. Graphpad QuickCalcs outlier calculator (Grubb's test) was used to detect significant outliers.

2.3 **Supplier Addresses**

Abcam (Cambridge, UK)

BD Biosciences (Oxford UK)

Biosera (East Sussex, UK)

Bio-Rad (Hertfordshire, UK)

Biomedica Gruppe (Austria)

Carestream (Hertfordshire, UK)

Corel UK Ltd (Maidenhead, UK)

DAKO (Cambridgeshire, UK)

DiAgam (Ghislenghien, Belgium)

Enzo Life Sciences (Exeter, UK)

eBioscience (Hatfield UK)

Fisher Scientific (Loughborough, UK)

Graphpad (LaJolla, CA)

Life Technologies Invitrogen (Paisley, UK)

Leica Microsystems Ltd (Milton Keynes, UK)

LongGene Scientific Instruments (China)

Miltenyi Biotec (Surrey, UK)

MSE (London, UK)

Nunc International (New York, USA)

Olympus UK (Southend-on-sea, UK)

Perkin Elmer (Buckinghamshire, UK)

Qiagen (Manchester, UK)

R&D Systems Europe (Abingdon, UK)

Roche (Burgess Hill, UK)

Sigma-Aldrich (Dorset, UK)

Taicaan Technologies (Southampton, UK)

UVP (Cambridge, UK)

VWR (Leicestershire, UK)

Waldemar Knittel Glasbearbeitungs- Gmb (Braunschweig, Germany)

Chapter 3

The Role of Death Receptor 3 and TL1A in Murine Osteoclast Differentiation and Function

3.1 **Introduction**

Bone remodelling is a balanced cycle of bone breakdown and bone formation that maintains the integrity and strength of the skeleton, throughout a person's life. The two main cell types that regulate this process are; (i) the osteoclast, the cell responsible for the degradation and resorption of bone and (ii) the osteoblast, a cell that produces the organic bone matrix and aids in its mineralisation. The process of bone remodelling is controlled by a number of different factors. Key among them are members of the TNFSF, both receptors and ligands. Signalling through the TNFRSF member RANK by its ligand RANKL is critical for OC formation (15, 54, 56), and without this trigger OC differentiation will not take place. Other members of the TNFSF have also been shown to act synergistically with RANK / RANKL signalling enhancing OC formation and bone turnover; such as TNF (TNFSF2) and its receptor tumour necrosis factor receptor 1 (TNFR1) (282, 283). Although these receptors and ligands are important, the functionality of all the members of the TNFSF in bone is not known. The primary focus of this chapter is to explore the impact of DR3 and its ligand TL1A upon OC formation and function in the mouse.

To date there is only one paper that explores the effect of DR3 and TL1A on OC function. Work published by Bull, Williams et al (242) demonstrated that in a C57BL/6 AIA model of experimental arthritis, $DR3^{ko}$ mice displayed mild pathological features of arthritis; showing general absence of synovial hyperplasia, lack of pannus formation, and no evidence of bone erosion when compared to their $DR3^{wt}$ counterparts. Confirmation that this resistance to AIA was DR3 specific was shown through the co-administration of TL1A upon the induction of AIA, in $DR3^{het}$ mice. Co-administration of TL1A resulted in a significant dose-dependent exacerbation of disease in $DR3^{het}$ mice. In contrast, TL1A had no significant effect on arthritis progression in $DR3^{ko}$ mice. To determine whether the observed effects were due to DR3/TL1A signalling acting upon OC and their precursors they carried out *in vitro* assays using bone marrow cells (BMCs). These assays showed that $DR3^{wt}$ and $DR3^{ko}$ mice exhibited no significant difference in their ability to generate osteoclasts, in the presence of soluble RANKL and MCSF. However, the addition of TL1A to the cultures significantly enhanced the development of osteoclasts in $DR3^{wt}$ but not $DR3^{ko}$ BMC cultures. The data demonstrates a role for TL1A in promoting osteoclastogenesis, in the presence of RANKL and MCSF, in a DR3 dependent manner. However, the mechanism through which it drives OC formation is unknown.

The study by Bull and Williams was the first to demonstrate the impact of DR3 and TL1A upon OC formation *in vitro*. These studies were conducted using BMCs from the C57BL/6 strain of mouse. In this current study the C57BL/6 strain was used as our control, while investigating the response of BMCs from the DBA/1 strain. The DBA/1 strain of mouse provides an excellent background to study bone biology, and is the benchmark for the CIA model, which shares several pathogenic features with human rheumatoid arthritis. These features include synovial hyperplasia, mononuclear cell infiltration and cartilage and bone degradation (284). In addition a number of groups have demonstrated that aging male DBA/1 mice spontaneously developed an ankylosing phenotype (285-287), highlighting the strain as a model of the spondyloarthritides. A major difference between RA and the main subtype of spondyloarthritis, ankylosing spondylitis (AS), is the formation of new bone in AS. However, RA and AS share a number of common features. Both are inflammatory diseases, they display focal bone erosions and exhibit reduced bone density leading to osteopenia and osteoporosis (288-292). While the development of osteopenia is partly due to a reduction in bone formation, an increase in OC activity is also observed. The reasons for the differences between the C57BL/6 and DBA/1 strains of mice, in the development of bone / OC-related diseases are unknown. This chapter will determine whether there are any phenotypic differences in DR3 driven bone biology and OC response to TL1A.

Functional analysis of OC formation and activity is traditionally done through analysis of OC numbers and resorption pits, though a number of other factors can also be investigated to try and determine the mechanism of action. The chemokines CXCL1 (mouse kc, which shares many similar functions to human CXCL8) (76), CCL2 (79, 293, 294) and CCL3 (85, 90) have been shown to be involved in and enhance OC precursor recruitment, migration and fusion. Analysis of (i) actin ring formation, a marked cytoskeletal rearrangement that necessarily precedes bone resorption (295); (ii) MMP-9 expression, a gelatinase that is found in high levels in the resorption pit (105, 106); (iii) Cathepsin K, the most prominent proteinase in human osteoclasts and the main bone degrading enzyme (104), all provide additional information on the mechanisms of OC resorptive function. An effect of TL1A on two of these factors (CXCL8 and MMP-9) has already been shown (240, 278). Work by Kang et al (278) and Su et al (240) demonstrated that signalling through DR3 by TL1A, on the THP-1 macrophage cell line, induced CXCL8 and MMP-9 expression *in vitro*. The effect of TL1A on CXCL8 and MMP-9 expression by OC however, has currently not been investigated.

The aim of this chapter was to explore DR3 biology in the context of OC using BMCs from DBA/1 mice. The ability of BMCs from $DR3^{wt}$ and $DR3^{ko}$ mice to differentiate in to OC and resorb a bone substrate, namely ivory discs, was investigated. To determine the mechanism through which DR3/TL1A signalling acts culture supernatnats were analysed. Levels of specfic mediators involved in OC differentiation and tissue degrading enzymes involved in resorption were measured. The specific objectives of this chapter are:

- To undertake phenotypic characterisation of bone marrow cells from DBA/1 $DR3^{wt}$ and $DR3^{ko}$ mice.
- To isolate BMCs from DBA/1 $DR3^{wt}$ and $DR3^{ko}$ mice and develop an *in vitro* culture system for osteoclasts grown on glass coverslips and ivory discs.
- To assess the impact of DR3 on osteoclast formation on glass coverslips and ivory discs
- To assess the impact of DR3 on osteoclast resorptive function on ivory disc.
- To determine if TL1A modulates osteoclast differentiation in a DR3-dependent manner and to assess the impact of TL1A upon resorptive function *in vitro*.

3.2 **Results**

3.2.1 **Murine DR3 Genotyping**

The colony of $DR3^{wt}$ and $DR3^{ko}$ (C57BL/6 and DBA/1) mice employed for all the studies outlined in this thesis were generated from Heterozygous / Heterozygous ($DR3^{het}$) breeding pairs. For this reason each new litter of mice was screened by PCR to determine the genotype of each mouse. The PCR methodology was developed in-house by Dr E Wang (Co-supervisor); the methodology is described in section 2.2.2. One of three PCR products were generated, this was dependent upon the genotype of the mouse. One band at a molecular weight (MW) of 280 base pairs (bp) was produced for $DR3^{wt}$ mice, corresponding to a section of the coding region of the DR3 gene. One band at a MW of 320bp was expected for $DR3^{ko}$ mice, corresponding to the inserted *neo* portion of the vector used to replace the DR3 coding region. Two bands at MWs of 280bp and 320bp were used to identify $DR3^{het}$ mice, which possessed both $DR3^{wt}$ and $DR3^{ko}$ alleles. A typical genotyping screen is shown in Fig 3.1. While the number of mice obtained per week was highly variable the genotype was typically split into 25% $DR3^{wt}$, 25% $DR3^{ko}$ and 50% $DR3^{het}$. For each PCR run 95% of samples yielded a result to determine the genotype of the mouse. In 5% of cases a second PCR run was required for successful determination of genotype.

3.2.2 **Comparison of $DR3^{wt}$ and $DR3^{ko}$ Bone Marrow Cellular Phenotype**

To ensure that the cell population used at the initiation of the assay was matched between $DR3^{wt}$ and $DR3^{ko}$ bone marrow, differential cells counts (Fig 3.2 (b)) were performed (section 2.2.5) using male DBA/1 mice (n=5). Cells were identified by their size, granularity and nucleus size and shape. Data is presented as a percentage of the total bone marrow cells (mean±SEM). Erythrocytes were found to be the most common cell type present in $DR3^{wt}$ and $DR3^{ko}$ bone marrow (51.5±2.4% versus 53.5±3.1%). Leukocytes accounted for 48.1±2.69% ($DR3^{wt}$) and 46.2±4.7% ($DR3^{ko}$) of the population; of these neutrophils were the most common (35.7±2.2% versus 31.6±2.7%) and monocytes the least (2.6±0.2% versus 3.0±0.9% - Fig 3.2 (a)). The data observed for $DR3^{ko}$ mice were comparable to $DR3^{wt}$ mice with no significant differences for any of the cell types evaluated.

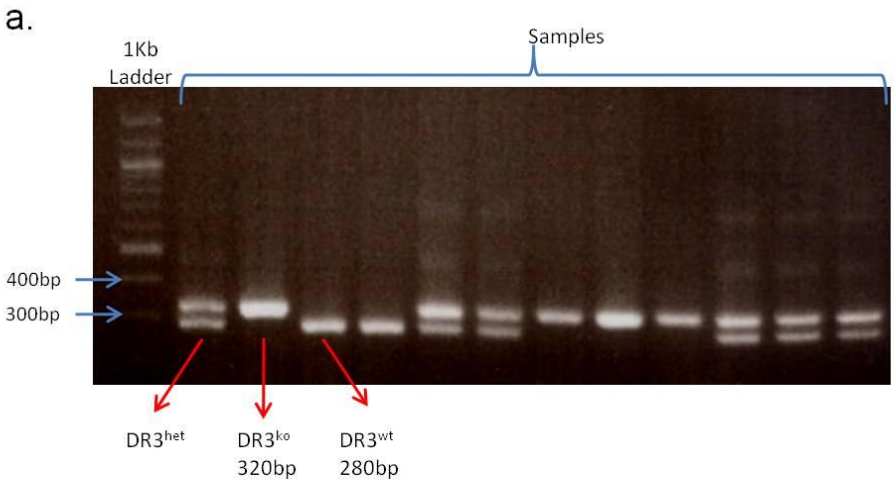

Figure 3.1 DR3 Genotyping.

PCR products were run on a 1.6% agarose gel and visualised under a UV light. $DR3^{wt}$ mice produced a single band at a MW of 280bp, corresponding to the coding region of the DR3 gene. $DR3^{ko}$ mice produced a single band at a MW of 320bp, corresponding to the inserted *neo* portion of the vector used to replace the DR3 coding region. $DR3^{het}$ mice produced a double band at MW 280 and 320bp as they possess both $DR3^{wt}$ and $DR3^{ko}$ alleles.

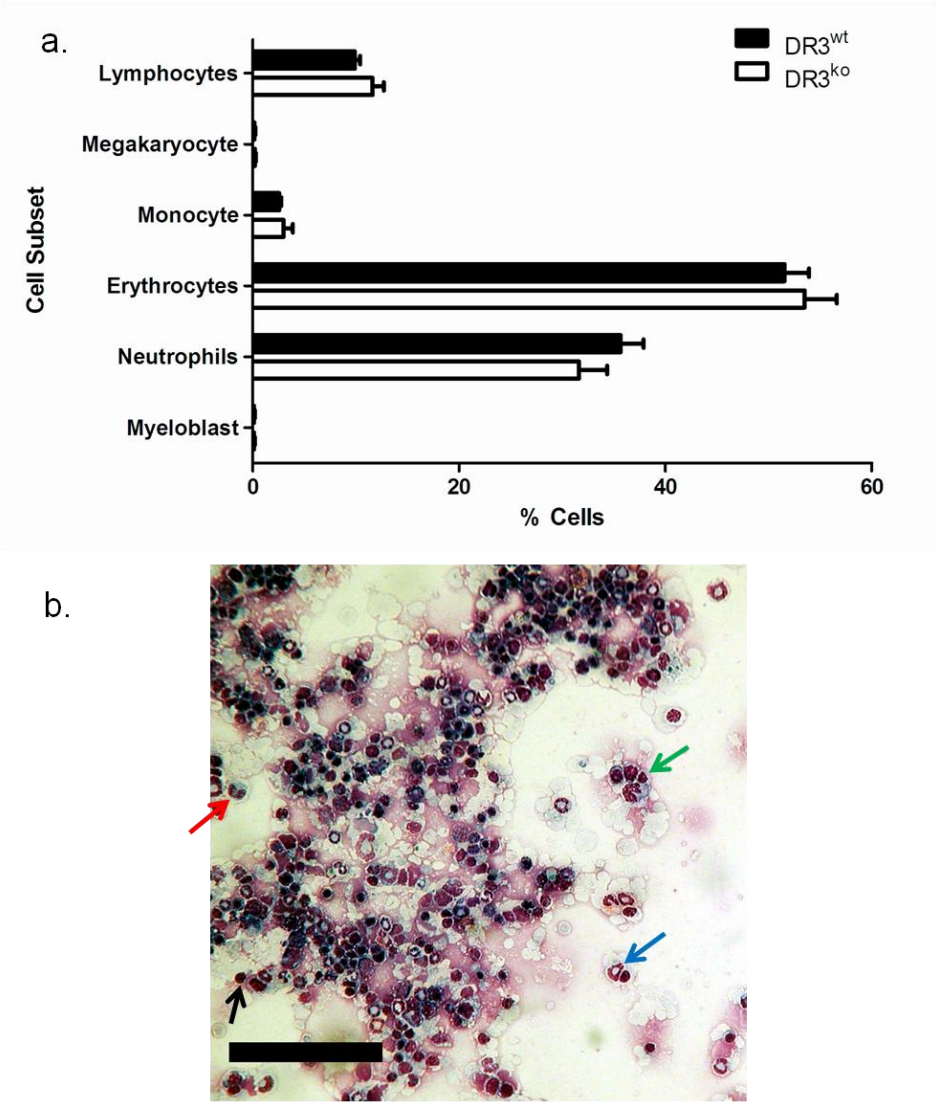

Figure 3.2. The Cellular Phenotype of Freshly Extracted BMCs was Similar in DR3^{wt} and DR3^{ko} Femora.

BMCs were extracted from the femora of DR3^{wt} and DR3^{ko} mice. Cells were dried down onto glass coverslips and stained with May-Grünwald and Giemsa stain. (a) The number of cell subsets were expressed as a percentage of the total bone marrow cells + SEM (n=5). No significant difference was observed in any cell subset. Statistical analysis was performed using a Mann-Whitney test. (b) Representative picture of stained DR3^{wt} BMC; Red arrow = monocyte, Green arrow = lymphocyte, Black arrow = erythrocyte and Blue arrow = neutrophil. Scale bar = 100µm.

3.2.3 **Assessing the Impact of DR3 upon the Development of Osteoclasts on Glass Coverslips**

A reproducible osteoclastogenesis assay had been established in the laboratory prior to the initiation of this project. This method used glass coverslips to support the cells during their expansion and differentiation. Bone marrow cells, isolated from the femora of age-matched male DBA/1 $DR3^{wt}$ and $DR3^{ko}$ mice (n=3) were used as a source of precursor cells. The culture methodology is outlined in section 2.2.6.1. Osteoclasts were successfully cultured from both $DR3^{wt}$ and $DR3^{ko}$ BMCs (Fig 3.3). The numbers of macrophages and $TRAP^{+}$ OC per glass coverslip are expressed as cells/mm^2 (mean±SEM) for graphical presentation (Fig 3.4 (a)). Comparison between $DR3^{wt}$ and $DR3^{ko}$ cultures demonstrated no significant difference at endpoint on day 7 (900±49/mm^2 versus 766±47/mm^2). Differential counts were also performed. When $TRAP^{+}$ osteoclasts were reported as a percentage of total cells (mean±SEM), no significant difference was observed between $DR3^{wt}$ and $DR3^{ko}$ (Fig 3.4 (b)). Finally, osteoclast diameter (in µm, mean±SEM) was measured. This parameter has previously been reported to be an indirect measure of osteoclast resorptive function (296-299). Osteoclast diameter in $DR3^{wt}$ (110±5µm) and $DR3^{ko}$ (96±8µm) cultures were not significantly different (Fig 3.4 (c)). These data demonstrate that DR3 does not affect osteoclastogenesis when cells are cultured on glass coverslips.

3.2.4 **Assessing the Impact of TL1A upon the Development of Osteoclasts on Glass Coverslips**

TL1A is the only known TNFSF ligand for DR3. The impact of TL1A upon osteoclastogenesis in $DR3^{wt}$ and $DR3^{ko}$ cultures was assessed. At experiment endpoint on day 7 TL1A was observed to significantly decrease the total cell number in $DR3^{wt}$ cultures (-TL1A=900±49/mm^2 versus +TL1A=648±105/mm^2, P=<0.05; Fig 3.4 (a)). Cell numbers in $DR3^{ko}$ cultures remained unaffected by TL1A, indicating the specificity of the ligand for DR3 in this system. TL1A was also observed to affect the size of osteoclasts generated in culture. In $DR3^{wt}$ cultures mean OC diameter increased from 110±5µm to 135±15µm (-TL1A versus +TL1A; Fig 3.4 (c)). When $DR3^{ko}$ cultures were treated with TL1A, osteoclasts were larger (109±8µm) than those observed in untreated cultures (96±8µm). The change in osteoclast size induced by TL1A, however, was not significantly different in either $DR3^{wt}$ or $DR3^{ko}$ cultures.

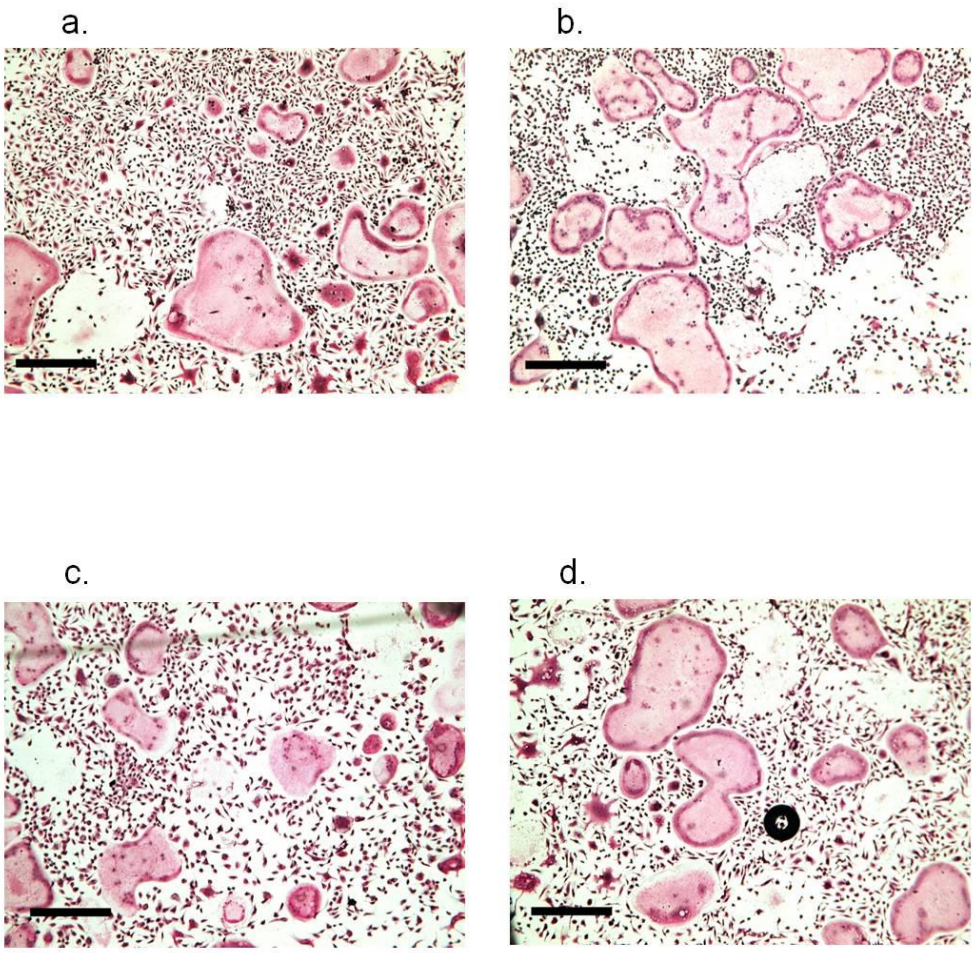

Figure 3.3. TRAP and Haematoxylin Stained Coverslips.

Coverslips were stained for TRAP and with haematoxylin for analysis of total cell and osteoclast numbers. Images were captured at 10x magnification. Representative pictures for $DR3^{wt}$ (a) MCSF and RANKL, (b) MCSF, RANKL and TL1A, and $DR3^{ko}$ (c)MCSF and RANKL, (b)MCSF, RANKL and TL1A cultures. Scale bar = 250µm.

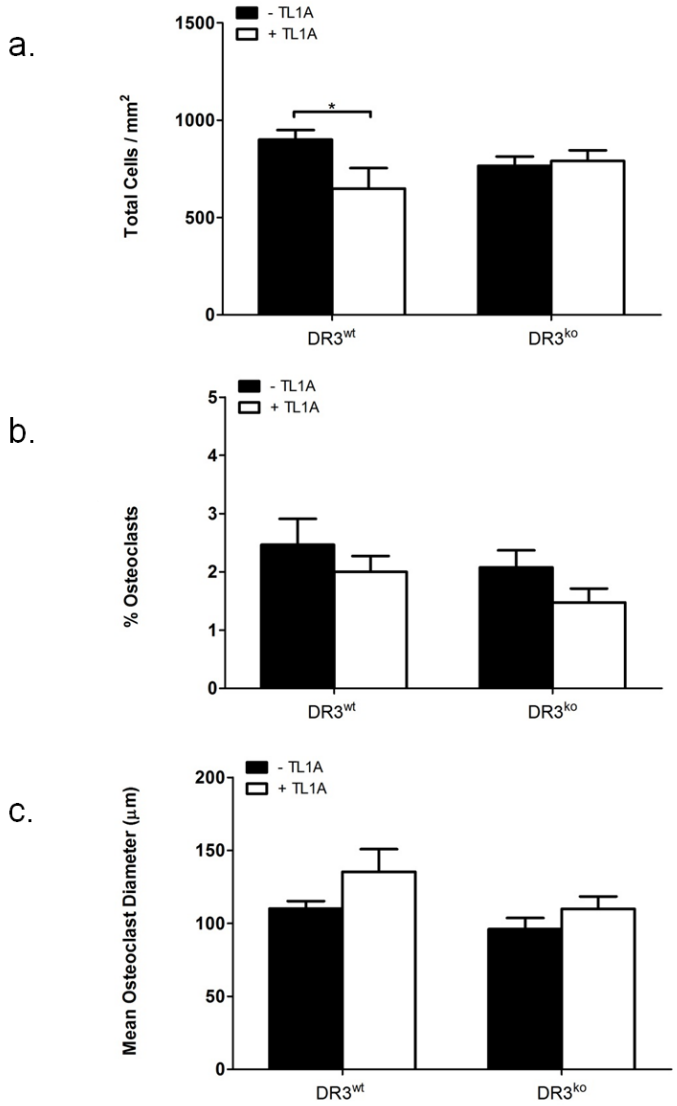

Figure 3.4. DR3 has no Effect on Total Cell Number , Osteoclast Number or Osteoclast Size. TL1A Reduces Total Cell Number in a DR3 Dependent Manner.

BMCs were extracted from the femora of $DR3^{wt}$ and $DR3^{ko}$ mice and cultured for 7 days, on glass coverslips, in the presence of MCSF and RANKL ± TL1A. Mature multinucleated osteoclasts were visualised by intense red TRAP stain. $TRAP^{+}$ multinucleated cells and mononuclear cells were counted on 5 random fields per disc; mean (a) total cell number, (b) % osteoclasts and (c) osteoclast diameter were measured and plotted (n=3, 3 reps per animal). A significant decrease in total cell number was observed in the $DR3^{wt}$ cultures following addition of TL1A (* P=<0.05). Statistical analysis was performed using a 2-way Anova with Bonferroni post test.

3.2.5 **Development of Murine Osteoclast Differentiation Assay on Ivory Discs**

In order to assess the effect of DR3 and TL1A on osteoclast resorptive function it was first necessary to establish a reproducible *in-house* osteoclastogenesis assay on a bone substrate (section 2.2.6.2). The substrate chosen was ivory; it is composed of hydroxyapatite, a substance that osteoclasts recognise and can resorb. In contrast to glass, ivory is porous and absorbs a certain volume of liquid when cells are dispensed onto its surface. The ivory discs used were slightly larger than the glass coverslips used in section 3.2.3 and 3.2.4 (6mm versus 5mm in diameter). For this reason, addition of 10µl of cell suspension to the ivory disc resulted in undesirable, uneven concentration of cells in the centre of the disc and excessive dehydration that rendered the cells unviable. To overcome these problems the volume of cell suspension added to the disc was increased from 10µl to 20µl. The concentration of the cells in the suspension was reduced from $6.4x10^6$ / ml to $3.2x10^6$ / ml to compensate for this increase in volume. Cell number / mm^2 was measured. There was no significant difference in cell density when glass and ivory culture conditions were compared (217±36 versus 242±66 cells/mm^2; Fig 3.5). 20µl of cell suspension ($3.2x10^6$ cells/ml) was used in all subsequent osteoclast assays on ivory discs.

a.

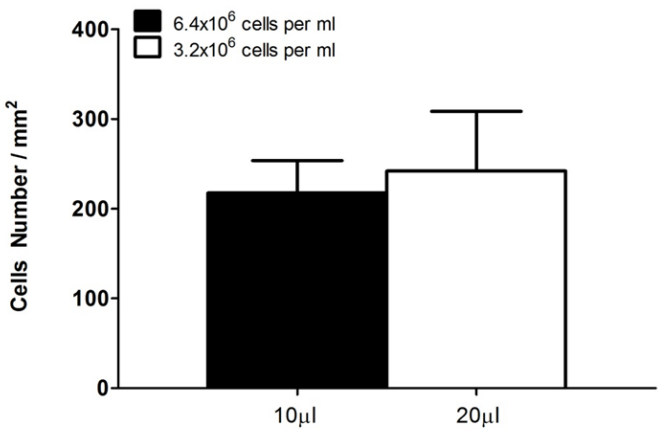

Figure 3.5. Change of Sample Volume has no Effect on Plated Cell Number.

BMCs were extracted from the femora of $DR3^{wt}$ mice (n=1, 3 reps) and re-suspended at a concentration of $6.4x10^6$ and $3.2x10^6$ cells per ml. 10µl of $6.4x10^6$ and 20µl of $3.2x10^6$ were added to glass coverslips. Cells were dried down and stained with May-Grünwald and Giemsa stain. (a) Cell number / mm^2 was calculated. No significant difference in plated cell number was observed. Statistical analysis was performed using an unpaired t-test.

3.2.6 **Assessing the Effect of DR3 on Osteoclast Differentiation (Ivory Discs)**

BMCs were isolated from the femora of age-matched female DBA/1 $DR3^{wt}$ and $DR3^{ko}$ mice (n=6). Osteoclastogenesis assays were performed using identical cytokine concentrations (MCSF, RANKL and TL1A) as previously described for the glass coverslip assays (section 2.2.6.2) with MCSF ± TL1A cultures run as controls. Osteoclasts were successfully cultured from both $DR3^{wt}$ and $DR3^{ko}$ BMCs in cultures containing RANKL, with no OC observed in the control cultures (Fig 3.6). The total number of cells (macrophages and $TRAP^{+}$ OC) per ivory disc were visualised by staining with haematoxylin, counted and expressed as cells/mm^2 (mean±SEM) for graphical presentation. Comparison between $DR3^{wt}$ and $DR3^{ko}$ control cultures (573±46 versus 527±51; Fig 3.7 (a)) and OC cultures (515±60 versus 463±45; Fig 3.7 (b)) demonstrated no significant difference at endpoint on day 10. Differential counts were also performed. $TRAP^{+}$ osteoclasts reported as (mean±SEM) osteoclast number/mm^2 (35±4 and 30±3; Fig 3.8 (a)) and as a percentage of total cells (8.2±1.4% and 7.8±1.1%; Fig 3.8 (b)) demonstrated no significant difference between the $DR3^{wt}$ and $DR3^{ko}$ OC cultures. Finally osteoclast area (µm^2, mean±SEM) was measured. Osteoclast area in $DR3^{wt}$ (925±116) and $DR3^{ko}$ (776±49) OC cultures were not significantly different (Fig 3.8 (c)).

3.2.7 **Assessing the Effect of TL1A on Osteoclast Differentiation (Ivory Discs)**

The results reported for glass coverslips (section 3.2.4) demonstrate that TL1A affects osteoclast differentiation. The effect of TL1A on osteoclast differentiation on ivory discs was assessed. BMCs were isolated from the femora of age-matched female DBA/1 $DR3^{wt}$ and $DR3^{ko}$ mice (n=6) and cultured in osteoclastogenesis assays on ivory disc. The culture methodology is outlined in section 2.2.6.2. At experiment end point on day 10 the total number of cells (macrophages and $TRAP^{+}$ OC, reported as cells/mm^2 (mean±SEM)) was significantly reduced in $DR3^{wt}$ OC cultures following addition of TL1A (-TL1A=515±60 versus +TL1A=332±29, *P*=<0.05; Fig 3.7 (b)). No significant difference in total cell number was observed in the control cultures (Fig 3.7(a)). Differential counts were also performed. TL1A was found to significantly reduce osteoclast numbers (OC/mm^2, mean±SEM) in $DR3^{wt}$ cultures (-TL1A=35±4 and +TL1A=20±4, *P*=<0.05; Fig3.8 (a)), though this did not translate into a significant reduction in % osteoclasts (-TL1A=8.2±1.4% versus +TL1A=5.2±0.7%; Fig 3.8 (b)). The increase in osteoclast area (µm^2 mean±SEM) induced

by TL1A was not significantly different (-TL1A=925.4±115.6 versus +TL1A=1275.7±170.2; Fig 3.8 (c)). The addition of TL1A to $DR3^{ko}$ cultures had no effect on osteoclast numbers or size; however, it a significant increase in the total number of cells/mm^2 was observed (-TL1A=463±45/mm^2 versus +TL1A=627±59/mm^2 *P*=<0.05; Fig 3.7 (b)).

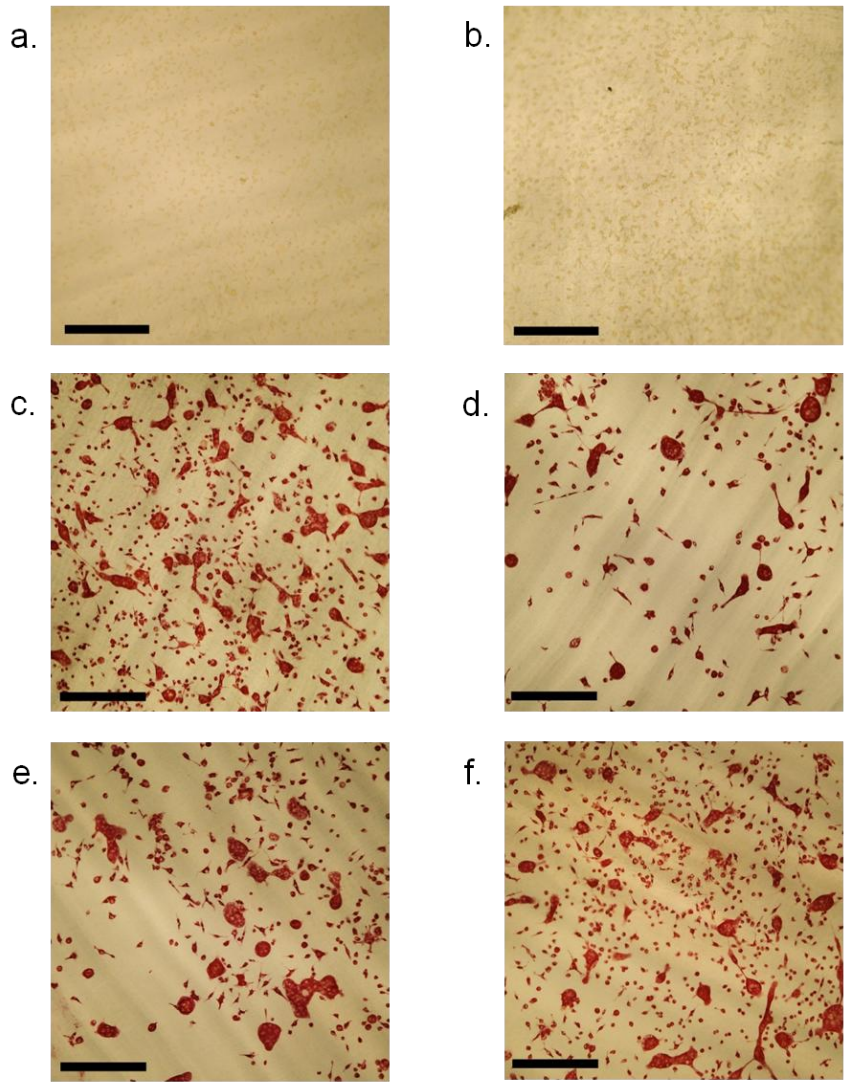

Figure 3.6. TRAP Stained Cultures on Ivory Discs.

Ivory disc cultures were stained for TRAP. Images were captured at 10x magnification. Representative pictures of control cultures for $DR3^{wt}$ (a) MCSF and (b) MCSF and TL1A. Representative pictures of osteoclast cultures for $DR3^{wt}$ (c) MCSF and RANKL, (d) MCSF, RANKL and TL1A and $DR3^{ko}$ (e) MCSF and RANKL, (f) MCSF, RANKL and TL1A cultures. Scale bar = 250µm.

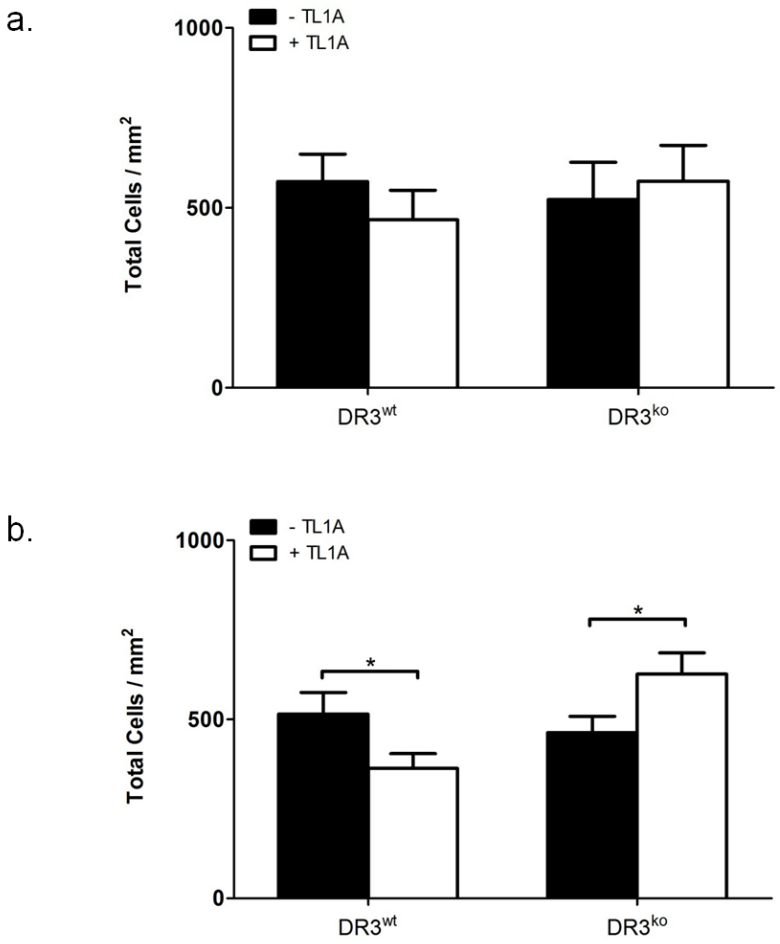

Figure 3.7. DR3 has no Effect on Total Cell Number in Control or Osteoclast Cultures. TL1A Reduces Total Cell Number in DR3^{wt} Osteoclast Cultures.

BMCs were extracted from the femora of DR3^{wt} and DR3^{ko} mice and cultured for 10 days, on ivory discs, in the presence of MCSF ± TL1A or MCSF and RANKL ± TL1A. Mature multinucleated osteoclasts were visualised by intense red TRAP stain. TRAP^{+} multinucleated cells and mononuclear cells were counted on 5 random fields per disc; mean (a) total cell number in control cultures and (b) total cell number in osteoclast cultures were measured and plotted (n=6, 3 reps per condition). A significant decrease in total cell number was observed in the DR3^{wt} osteoclast cultures following addition of TL1A (* P=<0.05). Statistical analysis was performed using a Mann-Whitney test.

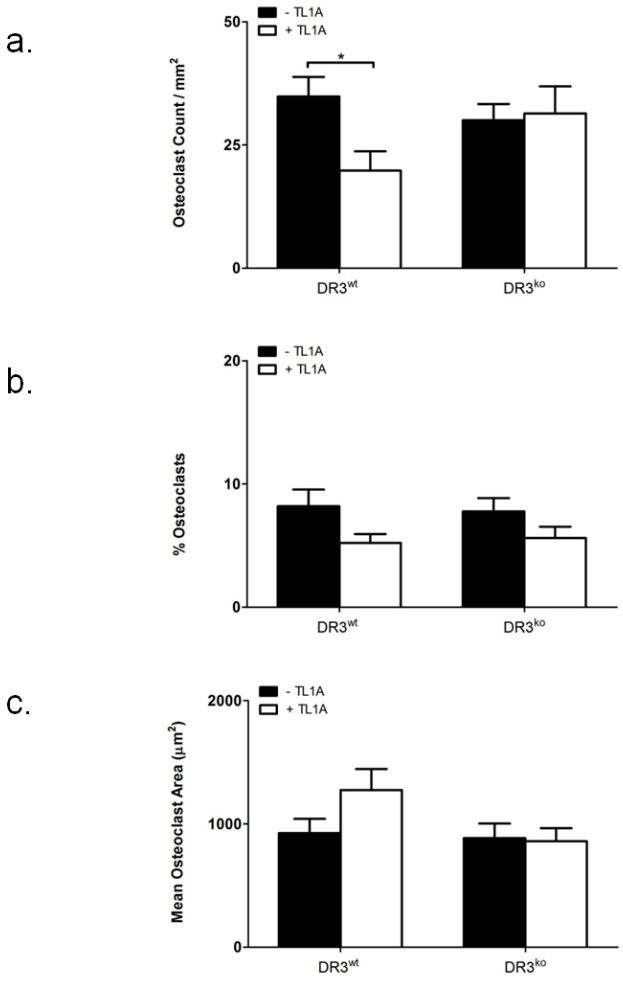

Figure 3.8. DR3 has no Effect on Osteoclast Number, % Osteoclasts or Osteoclast Size. TL1A Reduces Osteoclast Number in DR3^{wt} Cultures.

BMCs were extracted from the femora of DR3^{wt} and DR3^{ko} mice and cultured for 10 days, on ivory discs, in the presence of MCSF ± TL1A or MCSF and RANKL ± TL1A. Mature multinucleated osteoclasts were visualised by intense red TRAP stain. TRAP^{+} multinucleated cells and mononuclear cells were counted on 5 random fields per disc; mean (a) osteoclast number (b) % osteoclasts and (c) osteoclast area were measured and plotted (n=6, 3 reps per condition). A significant decrease in osteoclast number was observed in the DR3^{wt} cultures following addition of TL1A (* *P*=<0.05). Statistical analysis was performed using a Mann-Whitney test.

3.2.8 **Impact of DR3 on Osteoclast Resorptive Function**

To assess whether DR3 affected OC resorptive function the area of the ivory disc resorbed was measured. Data was expressed as the number of resorption pits/mm^2 and % area resorbed (mean±SEM) for graphical presentation. Comparison of DR3^{wt} and DR3^{ko} ivory discs showed that the absence of DR3 had a very significant effect on osteoclast resorptive function. While resorption pits were present on discs from DR3^{wt} OC cultures a very low number were observed on discs from DR3^{ko} OC cultures (2.3±0.5/mm^2 versus 0.05±0.04/mm^2, *P*=<0.001; Fig 3.9 (a)). This translated into a very significant difference in % area resorbed between the two (8.5±4.8% versus 0.02±0.02%, *P*=<0.001; Fig 3.9 (b)); this result shows that DR3 plays an important role in osteoclast resorptive function.

3.2.9 **Impact of TL1A on Osteoclast Resorptive Function**

The impact of TL1A upon osteoclast resorptive function was assessed. Data was reported as number of resorption pits/mm^2 and % area resorbed (mean±SEM) for graphical presentation. Addition of TL1A to DR3^{wt} OC cultures was found to have no overall significant effect on osteoclast resorptive function. An increase in the number of resorption pits/mm^2 was observed following the addition of TL1A (2.3±0.5/mm^2 versus 4.0±2.1/mm^2; Fig 3.9 (a)), however this was coupled with a decrease in the % area resorbed (8.5±4.8% versus 1.3±1.1%; Fig 3.9 (b)). This result shows that % area resorbed is a better measurement of OC resorptive function than the number of pits. Suggesting the decrease in resorption observed, following addition of TL1A, is due to the reduced number of OC present rather than a reduction in OC resorptive function.

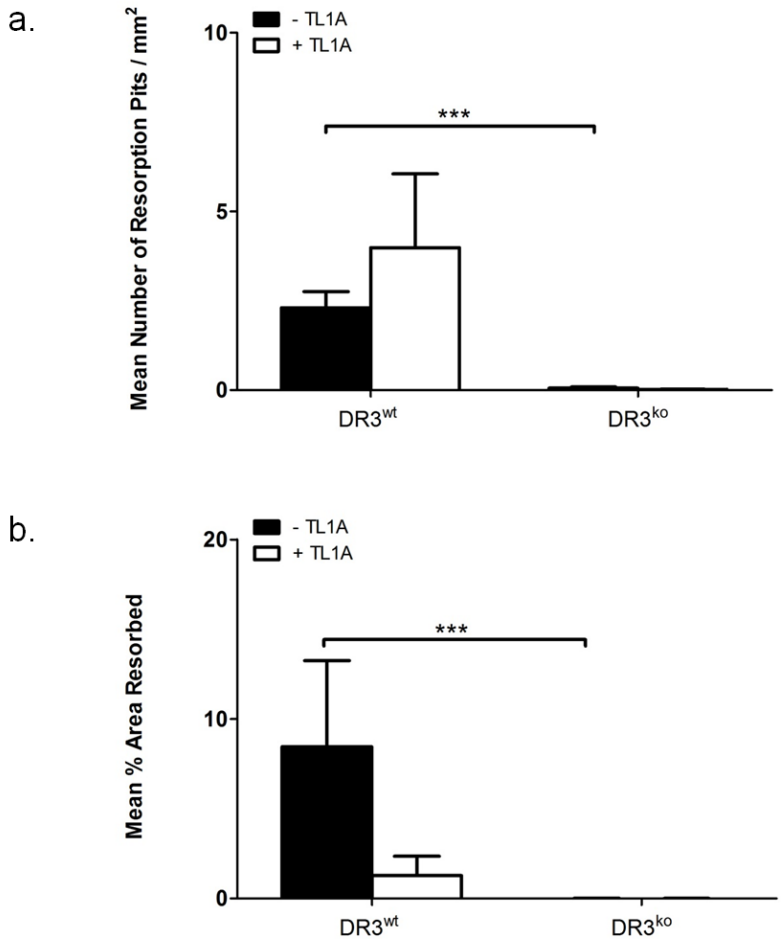

Figure 3.9. DR3 has an Important Role in Osteoclast Resorptive Function.

BMCs were extracted from the femora of $DR3^{wt}$ and $DR3^{ko}$ mice and cultured for 10 days, on ivory discs, in the presence of MCSF and RANKL ± TL1A. Cells were removed from the ivory discs which were stained with toluidine blue to visualise resorption pits. Resorption pits were counted on 5 random fields per disc; mean (a) number of resorption pits, (b) % area of disc resorbed were measured and plotted (n=6, 3 reps per condition). Absence of DR3 significantly reduced the number of resorption pits and the % area of disc resorbed (***P=<0.001). Statistical analysis was performed using a Mann-Whitney test.

3.2.10 **Assessing the Effect of DR3 on Chemokine Production**

As an assessment of osteoclast activity chemokines involved in the formation of OC were measured in the supernatants of $DR3^{wt}$ and $DR3^{ko}$ control and OC cultures (section 2.2.14.1).

3.2.10.1 CCL2

In $DR3^{wt}$ and $DR3^{ko}$ control cultures (n=6, 3 reps per condition) levels of CCL2 peaked at day 7 with a maximum level of 835.5±129pg/ml ($DR3^{wt}$) and 646.1±143pg/ml ($DR3^{ko}$) detected (Fig 3.10 (a, i). Levels of CCL2 in OC cultures (n=6, 3 reps per condition) increased across the time course with a maximum level of 94.8±19pg/ml in $DR3^{wt}$ cultures and 105.4±20pg/ml in $DR3^{ko}$ cultures detected at day 10 (Fig 3.10 (a, ii)). There was no significant difference in CCL2 levels between the $DR3^{wt}$ and $DR3^{ko}$ in either the control or OC cultures.

3.2.10.2 CXCL1

Levels of CXCL1, in $DR3^{wt}$ and $DR3^{ko}$ control cultures (n=6, 3 reps per condition) increased across the time course to a maximum level of 288.4±72pg/ml ($DR3^{wt}$) and 240.7±72pg/ml ($DR3^{ko}$) detected at day 10 (Fig 3.10 (b, i)). In $DR3^{wt}$ and $DR3^{ko}$ OC cultures (n=6, 3 reps per condition) levels of CXCL1 peaked at a maximum level of 129.4±39pg/ml ($DR3^{wt}$) and 139.7±29pg/ml ($DR3^{ko}$), detected on day 10 (Fig 3.10 (b, ii)). No significant difference in CXCL1 levels was detected between the $DR3^{wt}$ and $DR3^{ko}$ in either the control or OC cultures.

3.2.10.3 CCL3

CCL3 was detected across the time course in both $DR3^{wt}$ and $DR3^{ko}$ control cultures (n=3, 3 reps per condition), with no significant difference in expression detected between the genotypes (Fig 3.10 (c, i)). In OC culture supernatants, CCL3 (n=3, 3 reps per condition) was only detected at day 3. Levels were observed to be over three-fold higher in $DR3^{wt}$ cultures compared to $DR3^{ko}$ cultures (mean±SEM) (164.9±59.9pg/ml versus 44.8±14.9pg/ml; Fig 3.10 (c, ii)) though this difference was not significant due to variation and the small sample size.

3.2.11 **Assessing the Effect of TL1A on Chemokine Production**

Results from section 3.2.7 showed that TL1A has an effect on osteoclastogenesis; significantly reducing the number of osteoclasts formed. Levels of CCL2, CXCL1 and CCL3 were measured in control and OC culture supernatants to determine whether TL1A affects chemokine expression.

3.2.11.1 CCL2

Addition of TL1A to $DR3^{wt}$ control cultures (n=6) had no significant effect on CCL2 levels (Fig 3.11 (a, i)). In $DR3^{wt}$ OC cultures (n=6, 3 reps per condition) addition of TL1A caused a significant decrease in CCL2 levels (mean±SEM) across the time course (*P*=<0.0001). Levels of CCL2 were lower in $DR3^{wt}$ cultures containing TL1A at day 3 (-TL1A=23.1±10pg/ml versus +TL1A=0pg/ml), day 7 (-TL1A=69.8±20pg/ml versus +TL1A=27.4±8pg/ml) and day 10 (-TL1A=94.8±19pg/ml versus +TL1A=59.2±13pg/ml; Fig 3.11 (a, ii)).

3.2.11.2 CXCL1

Levels of CXCL1 in $DR3^{wt}$ control cultures (n=6) increased across the time course with a maximum level of 288.4±72pg/ml (-TL1A) and 349.9±79pg/ml (+TL1A) detected at day 10 (Fig 3.11 (b, i)). Addition of TL1A to $DR3^{wt}$ OC cultures (n=6) had no significant affect on CXCL1 expression, with a maximum level of 129.4±39pg/ml (-TL1A) and 96.9±31pg/ml (+TL1A) detected on day 10 (Fig 3.11 (b, ii)).

3.2.11.3 CCL3

Levels of CCL3 were comparable between $DR3^{wt}$ and $DR3^{wt}$ +TL1A control cultures (Fig 3.11 (c, i)). In $DR3^{wt}$ OC cultures (n=3, 3 reps per condition) addition of TL1A resulted in a greater than four-fold reduction in CCL3 at day 3 (-TL1A=164.9±60pg/ml versus +TL1A=37.1±14pg/ml; Fig 3.11 (c, ii)). As with the $DR3^{wt}$ / $DR3^{ko}$ comparison this difference was not significant due to variation and small sample size.

The data show, within statistical limitations, CCL2 to be a target of DR3/TL1A signalling. While CCL3 is a good candidate further testing and scientific rigour is required to prove that it is also a target. This reduction in chemokine expression is RANKL dependent as no change in expression was observed in the control cultures.

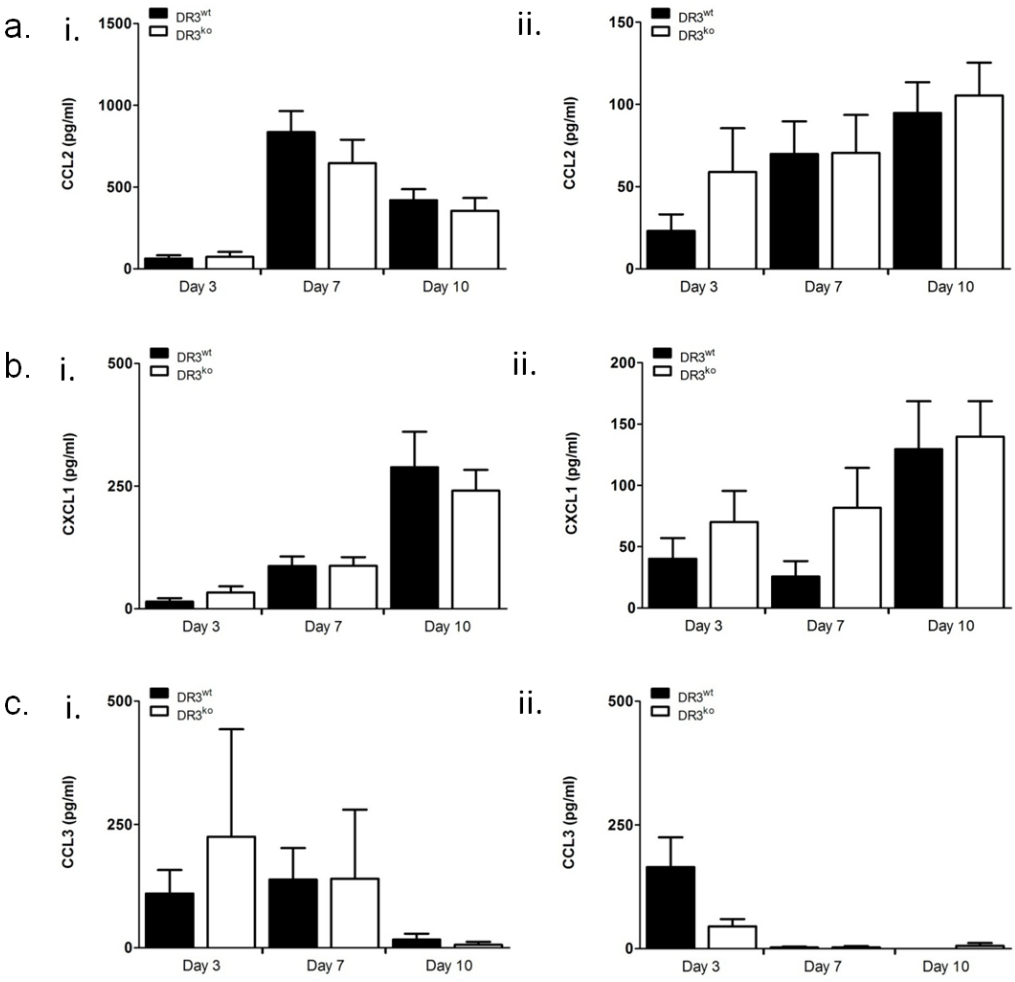

Figure 3.10. DR3 has no Effect on Levels of CCL2 or CXCL1 but causes a Reduction in CCL3 Levels in Osteoclast Cultures.

BMCs were extracted from the femora of $DR3^{wt}$ and $DR3^{ko}$ mice and cultured for 10 days, on ivory discs, in the presence of (i) MCSF or (ii) MCSF and RANKL. Supernatants were collected at the indicated time points and tested for (a) CCL2 (n=6, 3 reps per condition), (b) CXCL1 (n=6, 3 reps per condition) and (c) CCL3 (n=3, 3 reps per condition) by ELISA. No significant differences were observed, though reduced levels of CCL3 were detected in the $DR3^{ko}$ osteoclast cultures. Statistical analysis was performed using a One-way ANOVA.

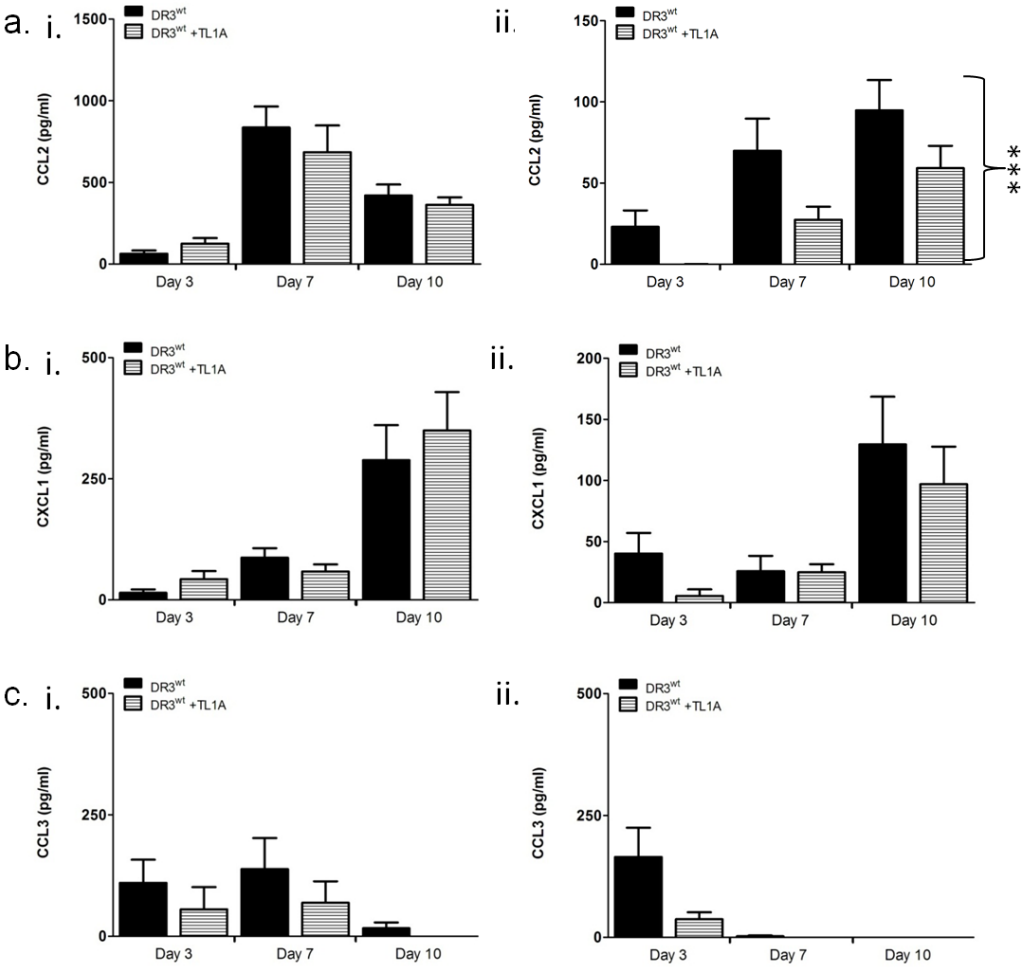

Figure 3.11. TL1A Significantly Reduces Levels of CCL2, Reduces Levels of CCL3 but has no Effect on Levels of CXCL1 in DR3^{wt} Osteoclast Cultures.

BMCs were extracted from the femora of DR3^{wt} mice and cultured for 10 days, on ivory discs, in the presence of (i) MCSF ± TL1A or (ii) MCSF and RANKL ± TL1A. Supernatants were collected at the indicated time points and tested for (a) CCL2 (n=6, 3 reps per condition), (b) CXCL1 (n=6, 3 reps per condition) and (c) CCL3 (n=3, 3 reps per condition) by ELISA. A significant reduction in CCL2 levels was observed across the time course in + TL1A osteoclast cultures (***P=<0.0001). Reduced levels of CCL3 were detected in +TL1A osteoclast cultures. Statistical analysis was performed using a One-way ANOVA.

3.2.12 **Assessing the Effect of DR3 and TL1A on pro MMP-9 Release**

To explain the observed differences in OC function (section 3.2.8), levels of the inactive (pro) form of MMP-9, a gelatinase involved in the breakdown of the organic component of bone, were measured in both control and OC culture supernatants by ELISA (n=6, 3 reps per condition). Levels of pro MMP-9 were found to be drastically reduced in control cultures, compared to OC cultures, with maximum levels of approx. 0.5ng/ml detected at day 3 (Fig 3.12 (a)). No significant difference in pro MMP-9 was detected between the $DR3^{wt}$ and $DR3^{ko}$ control cultures. In $DR3^{wt}$ and $DR3^{ko}$ OC cultures levels of pro MMP-9 (mean ±SEM) were shown to increase over time (Fig 3.12 (a, ii)). A significant decrease in pro MMP-9 was detected at day 10 in $DR3^{wt}$ compared to $DR3^{ko}$ OC cultures (8.9±9.1ng/ml versus 24.0±6.9ng/ml, P=<0.05). Addition of TL1A to the $DR3^{wt}$ control and OC cultures had no significant effect on levels of pro MMP-9 (Fig 3.12 (b)). These results show that while OC precursors can produce relatively low levels of pro MMP-9, stimulation of the cells by RANKL is required for up-regulation of its expression. A limitation of this test however, is that it can only show levels of the inactive enzyme. To overcome this limitation a gelatine zymogram was employed to look at both the pro and active forms of MMP-9.

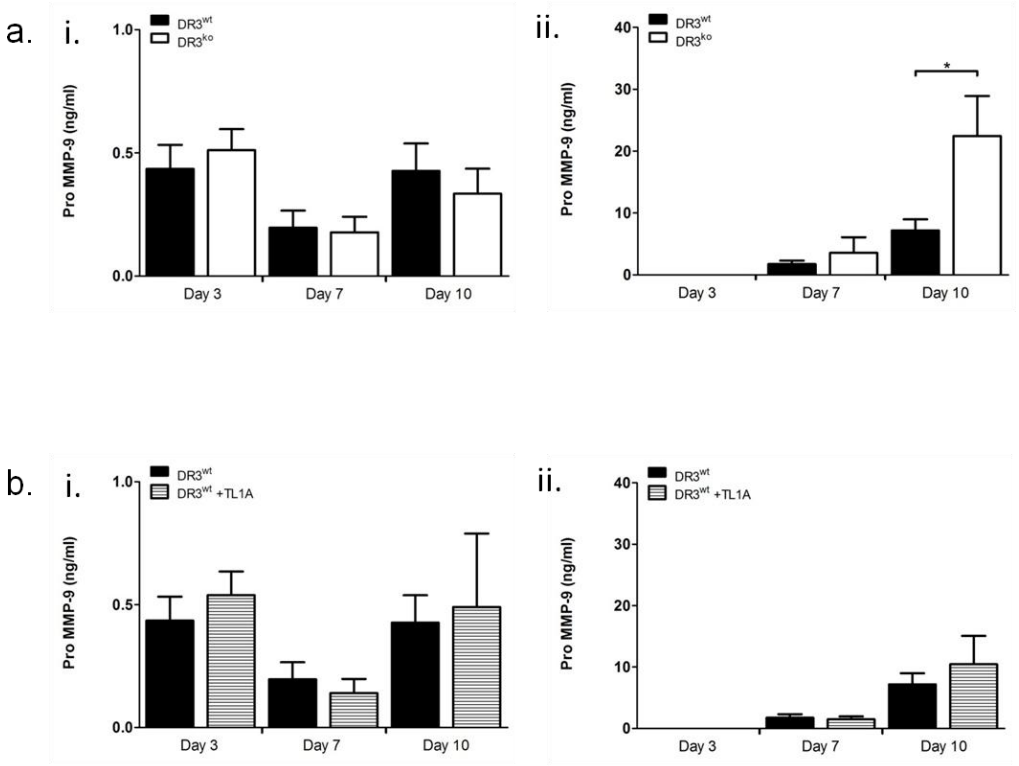

Figure 3.12. DR3-dependent Signalling Significantly Decreases Levels of Pro MMP-9, while TL1A has no Effect on Pro MMP-9 Levels in Osteoclast Cultures.

BMCs were extracted from the femora of $DR3^{wt}$ and $DR3^{ko}$ mice and cultured for 10 days, on ivory discs, in the presence of (i) MCSF ± TL1A or (ii) MCSF and RANKL ± TL1A. Supernatants were collected at the indicated time points and tested for pro MMP-9 by ELISA (n=6, 3 reps per condition). (a) DR3-dependent signalling significantly decreased levels of pro MMP-9 (*P=<0.05) in osteoclast cultures. (b) TL1A has no effect on pro MMP-9 level. Statistical analysis was performed using a One-way ANOVA.

3.2.13 **Analysis of pro and Active MMP-9 in DR3^{wt} and DR3^{ko} Osteoclast Culture Supernatants by Zymography**

Analysis of culture supernatants in section 3.2.12 showed a significant difference in pro MMP-9 levels in DR3^{wt} and DR3^{ko} OC cultures. The test however, was unable to determine whether the DR3^{ko} cultures produce more inactive MMP-9; or whether the DR3^{wt} and DR3^{ko} cultures produce equal levels, with the DR3^{wt} cultures converting more to the active form. To determine whether DR3 had a role in MMP-9 activation a gelatine zymogram (section 2.2.14.4.1) was used to semi-quantitatively measure the levels of both pro and active MMP-9 in DR3^{wt} and DR3^{ko} OC culture supernatants (n=6; Fig 3.13). Equal levels of pro MMP-9 (mean±SEM) were detected in both DR3^{wt} and DR3^{ko} supernatants at day 7 (2.9±0.8ng/ml versus 2.7±0.3ng/ml) and day 10 (9.6±3.2ng/ml versus 7.7±2.5ng/ml, Fig 3.14 (a)). Levels of active MMP-9 were comparatively lower when compared to the pro form. At day 7 low levels of active MMP-9 were detected in both DR3^{wt} and DR3^{ko} cultures. At day 10 the amount of active MMP-9 in the DR3^{wt} cultures was increased compared to the DR3^{ko} (1.6±1.3ng/ml versus 0.4±0.3ng/ml), though this difference was not significant (Fig 3.14 (b)). This result suggests that DR3 may have a role in the conversion of the inactive MMP-9 enzyme into its active form and that this partially explains some of the differences observed in osteoclast resorptive function.

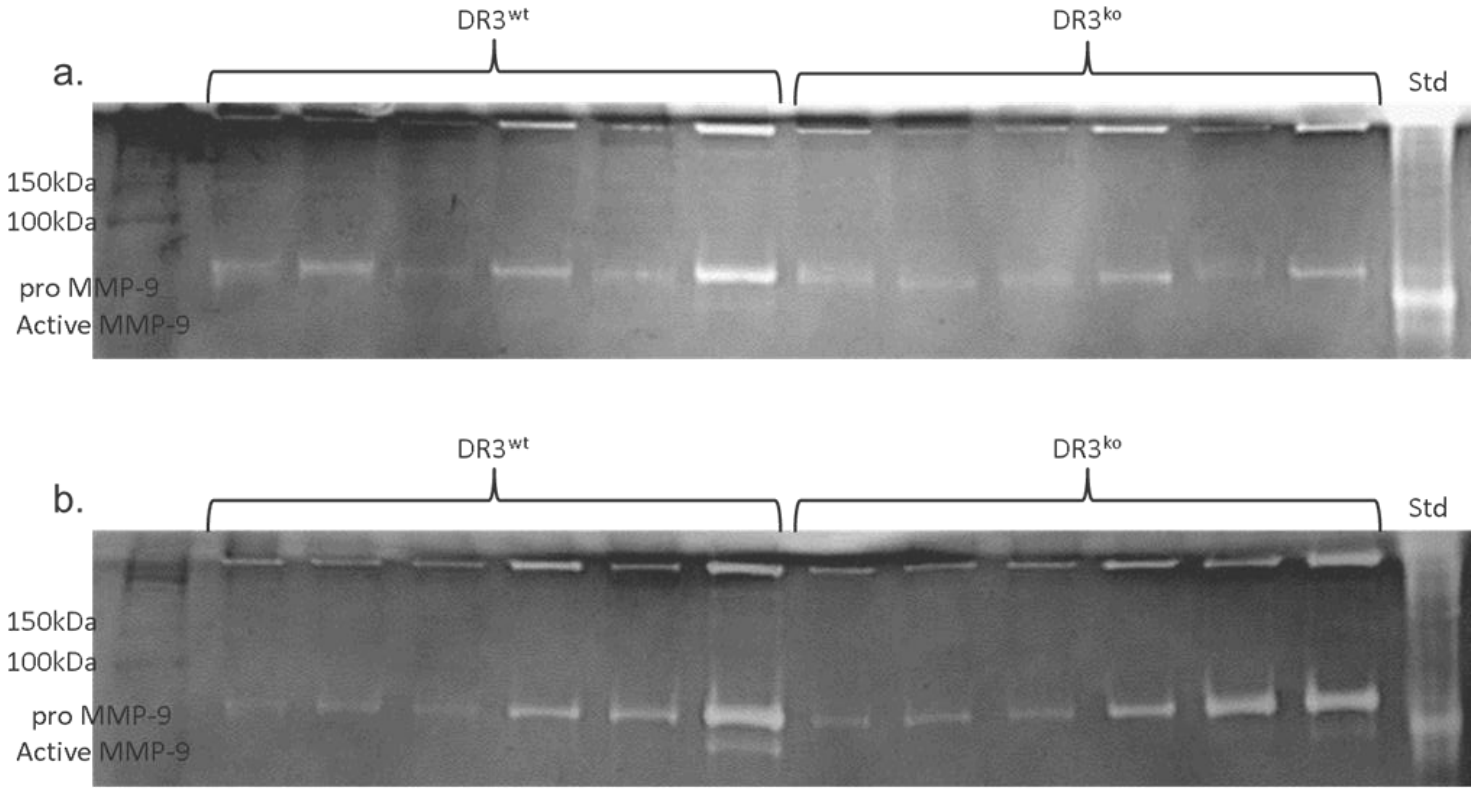

Figure 3.13. Semi-quantative Analysis of pro and active MMP-9 by Gelatine Zymography.

Supernatants from DR3^{wt} and DR3^{ko} osteoclast cultures were tested for levels of pro MMP-9 and active MMP-9 by gelatine zymography (n=6). (a) At day 7 bands were observed at approximately 80kDA, for all samples, corresponding to pro MMP-9. (b) At day 10 bands were observed at approximately 80kDa and 78kDa corresponding to both the pro and active forms of MMP-9. A standard of MMP-9 at 10ng/ml was run on each gel.

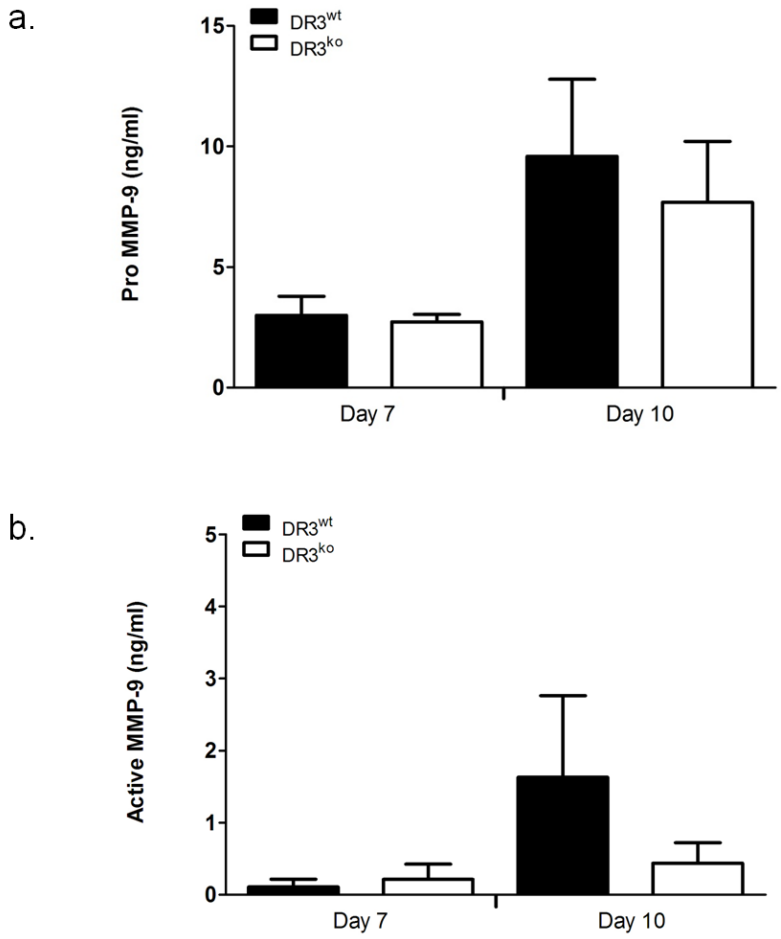

Figure 3.14. DR3 Increases Levels of Active MMP-9.

Supernatants (n=6, 1 rep per condition) were tested for levels of pro MMP-9 and active MMP-9 by gelatine zymography. Levels were calculated semi-quantitatively using a standard at known concentration (10ng/ml). No significant difference was observed in pro MMP-9 levels. At day 10 an increase in active MMP-9, though not significant, was observed in the $DR3^{wt}$ samples. Statistical analysis was performed using a One-way ANOVA.

3.2.14 **Effect of DR3 on C57BL/6 Osteoclast Differentiation**

Results in this chapter have demonstrated for the first time functional data highlighting how DR3/TL1A signalling affects OC formation and function, with DR3 shown to be involved in OC function and the addition of exogenous TL1A reducing OC formation. However, these results are in contrast to those published by Bull, Williams et al (242), who showed that addition of TL1A enhanced OC formation. To determine whether the strain of mouse used had a role in the contrasting results an osteoclast differentiation assay was performed using the C57BL/6 strain of $DR3^{wt}$ and $DR3^{ko}$ mice (n=1). The culture methodology is outlined in section 2.2.6.2. Comparison in total cell number (macrophages and $TRAP^{+}$ OC, expressed as cells/mm^2) between $DR3^{wt}$ and $DR3^{ko}$ OC cultures demonstrated no significant difference at endpoint on day 10 (397±103/mm^2 and 432±114/mm^2; Fig 3.15 (a)). Differential counts were also performed. $TRAP^{+}$ osteoclasts reported as (mean±SEM) osteoclast number/mm^2 (26±11/mm^2 versus 20±2/mm^2, Fig 3.15 (b)) and as a percentage of total cells (6.1±2.0% versus 5.9±2.3%, Fig 3.15 (c)) demonstrated no significant difference between the $DR3^{wt}$ and $DR3^{ko}$ cultures.

3.2.15 **Assessing the Effect of TL1A on C57BL/6 Osteoclast Differentiation**

Results from section 3.2.7 showed that addition of TL1A to DBA/1 $DR3^{wt}$ OC cultures inhibited OC formation, in contrast to previously published work (242). To determine whether this effect is due to the strain of the mouse TL1A was added to C57BL/6 OC cultures (n=1). The culture methodology is outlined in section 2.2.6.2. The total number of cells (macrophages and $TRAP^{+}$ OC) per ivory disc are expressed as cells/mm^2 (mean±SEM) for graphical presentation (Fig 3.15 (a)). Comparison between cultures ± TL1A demonstrated no significant difference at endpoint on day 10. Differential counts were also performed. A trend towards an increase in mean osteoclast number/mm^2 (26±11/mm^2 versus 36±3/mm^2; Fig 3.15 (b)) and mean % osteoclasts (6.1±2.0% versus 8.8±1.8%; Fig 3.15 (c)) was detected in the $DR3^{wt}$ cultures following the addition of TL1A. No difference was detected in the $DR3^{ko}$ cultures. These results support the report by Bull, Williams et al (242), confirming that the contrasting results were due to the difference in mouse strain used.

3.2.16 **Effect of TL1A on CCL3 Release in C57BL/6 Osteoclast Cultures**

Levels of CCL3 were measured in supernatants from C57BL/6 $DR3^{wt}$ cultures ± TL1A, to determine whether an increase in this chemokine is partially responsible for the increase observed in OC formation. CCL3 was detected across the time course in all cultures tested (Fig 3.16). A 3-fold increase in CCL3 levels at day 3 (mean±SEM), was observed following the addition of TL1A (44.1±11pg/ml versus 159.2±125pg/ml). This difference however was not significant due to low sample number.

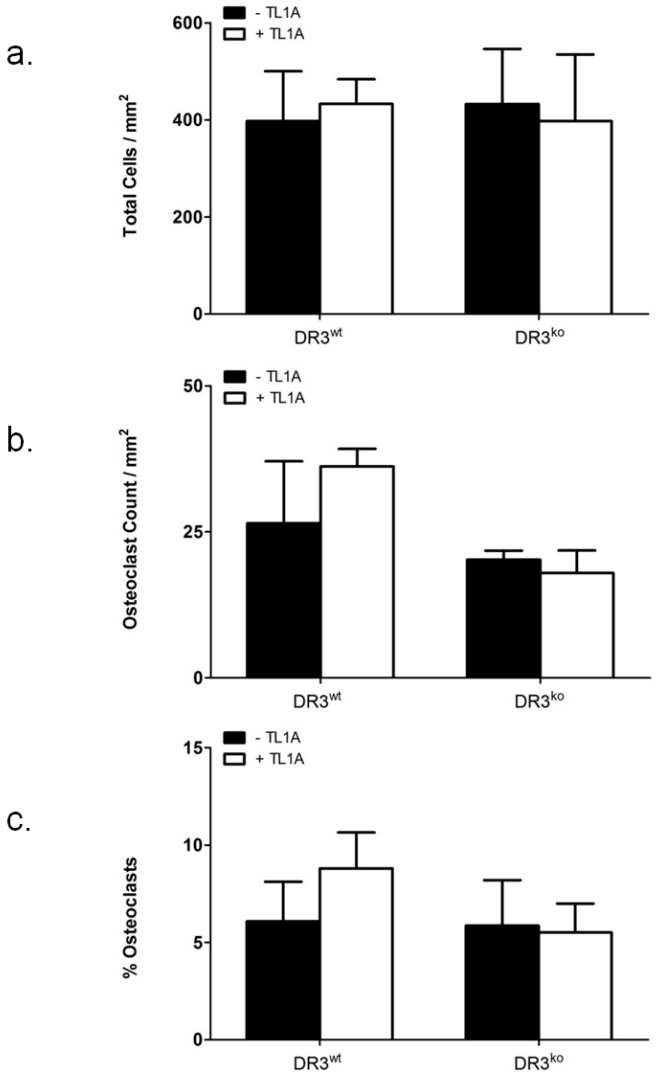

Figure 3.15. DR3 has no Effect on Total Cell Number or Osteoclast Number. TL1A Increases Osteoclast Number in DR3^{wt} C57BL/6 Cultures.

BMCs were extracted from the femora of DR3^{wt} and DR3^{ko} C57BL/6 mice and cultured for 10 days, on ivory discs, in the presence of MCSF and RANKL ± TL1A. Mature multinucleated osteoclasts were visualised by intense red TRAP stain. TRAP^{+} multinucleated cells and mononuclear cells were counted on 5 random fields per disc; mean (a) total cell number, (b) osteoclast number and (c) % osteoclastogenesis were measured and plotted (n=1, 3 reps per condition). An increase in osteoclast numbers and % osteoclastogenesis was observed in the DR3^{wt} cultures following addition of TL1A but was not significant. Statistical analysis was performed using a Mann-Whitney test.

a.

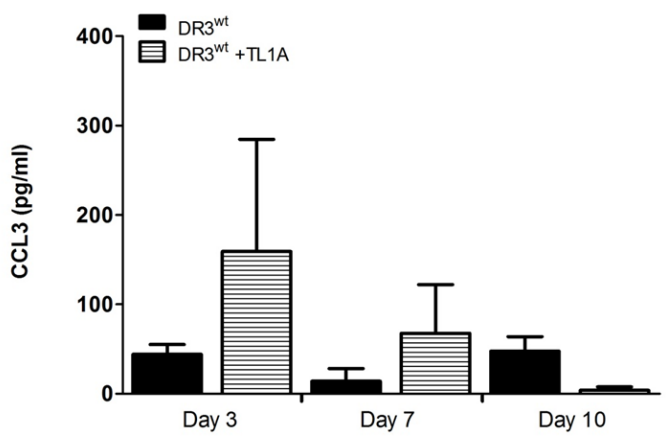

Figure 3.16. TL1A Increase Levels of CCL3 in C57BL/6 Osteoclast Cultures.

BMCs were extracted from the femora of $DR3^{wt}$ and $DR3^{ko}$ C57BL/6 mice and cultured for 10 days, on ivory discs, in the presence of MCSF and RANKL ± TL1A. Supernatants were collected at the indicated time points and tested for CCL3 by ELISA (n=1, 3 reps per condition). (a) TL1A increases levels of CCL3. Statistical analysis was performed using a One-way ANOVA.

3.2.17 **Measurement of Cathepsin K in Culture Supernatant by Collagenase Bio-assay**

The results from the C57BL/6 experiment (section 3.2.14 and 3.2.15) agreed with the previously published data by Bull, Williams et al (242); that TL1A enhances OC formation. This established that the difference between the DBA/1 and C57BL/6 results, in response to TL1A, is not due to the reagents used but a difference between the two strains. Having confirmed this further functional analysis was undertaken. While MMP-9 has been shown to be involved in the degradation of the organic component of bone (106, 300, 301), it is not the most prominent bone degrading enzyme in osteoclasts; the principal bone degrading enzyme being the proteinase CatK (104, 105). At the time of writing, commercial reagents for the analysis of CatK in murine culture supernatants were limited, so a collagen bio-assay was developed to measure CatK activity. The assay methodology is outlined in section 2.2.14.4.2. Results are expressed as % binding of blank (mean±SEM) for graphical representation. Comparison of the CatK control against the blank showed a reduction in binding of 24% (76±22% versus 100%) demonstrating that the assay can detect CatK activity. However, when culture supernatants were tested at a 1:10 dilution (Fig 3.17 (a)) and a 1:100 dilution (Fig 3.17 (b)) an increase in % binding of >500% was detected for all samples. The result suggests an unidentified substance in the sample, cross-reacting with the assay, masking any potential CatK activity. To determine the cause of the cross-reactivity the effect of FCS on the assay was investigated.

3.2.18 **The Effect of Foetal Calf Serum on Detection of Cathepsin K Activity in the Collagen Bio-assay**

Results from section 3.2.17 suggested that a component of the osteoclast supernatants was cross-reacting with the collagen bio-assay, increasing the % collagen bound to over 100%. To determine whether the FCS present in the medium was the cause of the increased binding, FCS was titrated into the CatK control and blank. The assay methodology is outlined in section 2.2.14.4.2. Results are expressed as % binding (mean±SEM) for graphical representation. In samples containing no FCS, comparison of % binding between the CatK control and blank were calculated to be 22±9.7 %. Increasing the FCS levels, in the CatK control, up to 0.25% had no effect on the % binding (24±3.0%). When levels of FCS were increase to 0.5% a dramatic effect on the % binding was observed, with levels increasing to 138±5.2%. Further increases in the level of FCS in the CatK control led to additional increases in % binding: 1% FCS – 245±10%, 2% FCS –

244±20%, 5% FCS – 275±8% and 10% FCS – 285±2% (Fig 3.18 (a)). FCS was added to the blank control to determine whether this would negate the observed effect on % binding. When calculated against a blank control containing 10% FCS the % binding observed for the CatK control, for all FCS concentrations, was reduced > 2-fold. Cat K with 0% FCS was observed to have an initial level of 9±5%. Increasing the concentration of FCS to 0.25% had no effect on the level of binding (9.8±1%). At a concentration of 0.5% FCS the % binding was observed to increase to 58±2%. Subsequent increases in FCS concentration produced further increases in % binding, as observed previously; 1% FCS – 102±6%, 2% FCS – 102±11%, 5% FCS – 114±3% and 10% FCS – 118±0% (Fig 3.18 (b)).

The results showed that, via this method, CatK cannot be measured in culture supernatant due to the presence of FCS. All cultures were performed using 10% FCS in the medium which has been shown to cross-react with the assay, producing high levels of % binding and false negatives.

3.2.19 **Detection of Cathepsin K in Culture Supernatants by Zymogram**

Results from section 3.2.17 and 3.2.18 highlighted that CatK cannot be measured in culture supernatants using a collagen bio-assay, due to cross-reactivity with FCS present in the medium. To determine whether CatK could be detected by zymogram, an assay was adapted from the work by Li et al (281) (section 2.2.14.4.2). Initial optimisation was performed using a CatK control supplied by Biomedica. Analysis of the zymogram showed that the Biomedica control failed to produce any clear bands, which are indicative of CatK activity (Fig3.19). Non-specific dark bands were visible on the gel at a molecular weight (MW) of 54kDa. These did not correspond to the MW of the pro and active forms of CatK (37kDa and 27kDa respectively). Further optimisation of the CatK zymogram was performed using a second recombinant human CatK and tested at pH 4 and pH 5. Use of the new control at lower pH values was able to produce some evidence of CatK activity. At pH 5 clear streaking was visible in the channels containing CatK at concentrations: 4.6ng/ml, 0.92ng/ml, 184pg/ml and 36.8pg/ml (Fig 3.20 (a)). At pH 4 an increase in streaking was observed with a lower level of detection of 7.36pg/ml. Bands were also visible at a MW of approximately 36kDa corresponding to that of pro CatK, at concentrations of 184pg/ml, 36.8pg/ml and 7.36pg/ml (Fig 3.20 (b)).

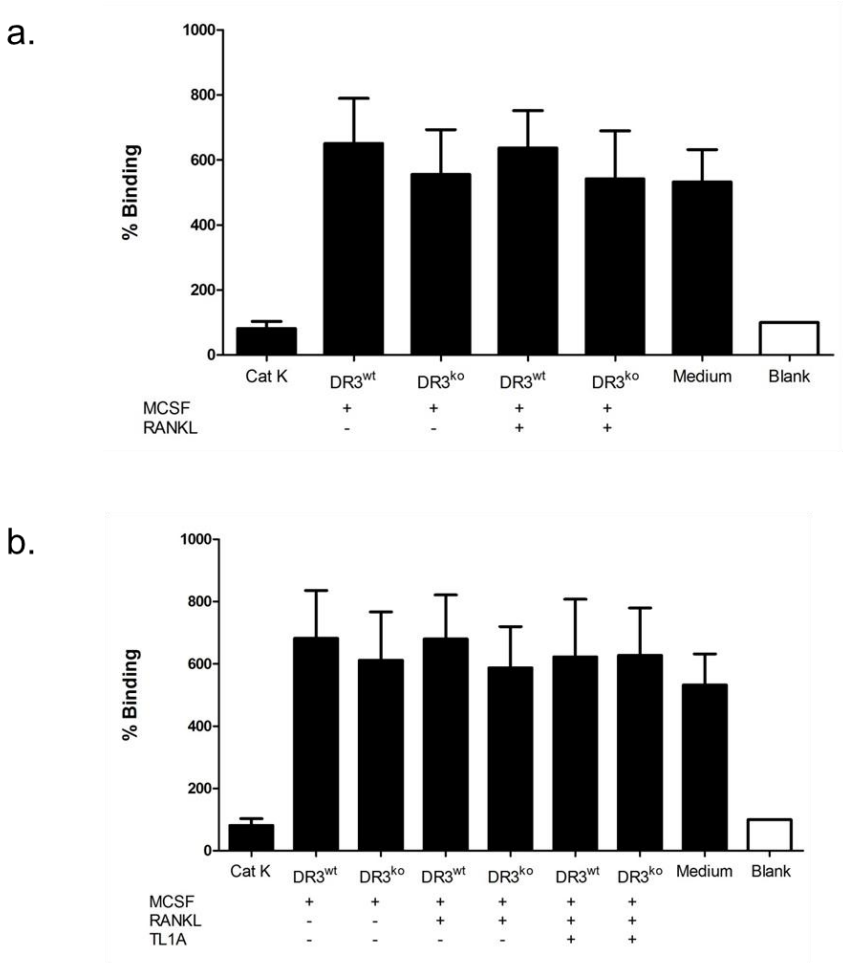

Figure 3.17. Degradation of Collagen by Cathepsin K was not Detected in Collagen Bio-Assay

Supernatants from ivory disc osteoclast cultures were incubated, in a collagen coated well, to analyse cathepsin k activity through the degradation of the collagen. (a) samples were diluted 1:10 and (b) 1:100. No cathepsin k activity was detected in any of the samples.

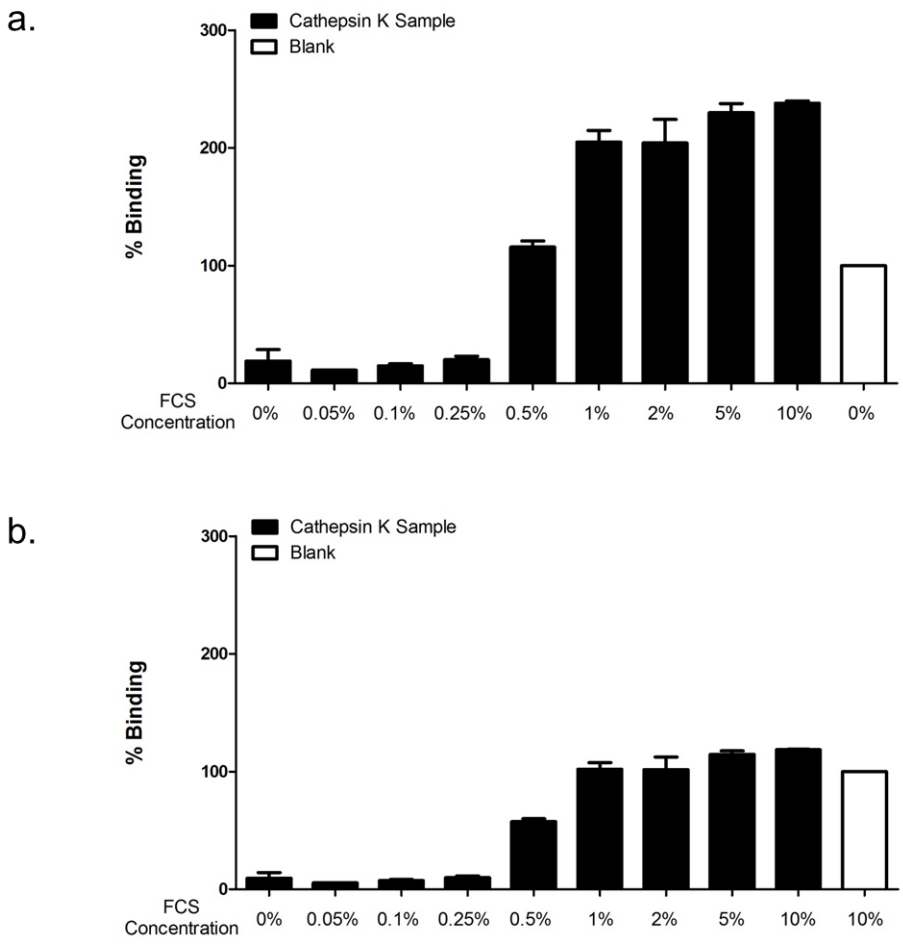

Figure 3.18. FCS has a Detrimental Effect on the Analysis of Cathepsin K Activity in a Collagen Bio-Assay.

Fetal calf serum was added to a cathepsin K control sample in increasing concentrations. % binding was compared to a (a) blank sample with no FCS and (b) a blank sample containing 10% FCS. FCS was found to have a detrimental effect on the ability to detect cathepsin K activity in a sample.

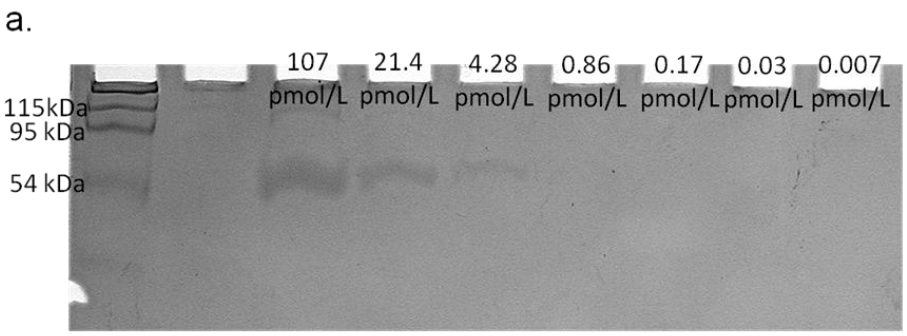

Figure 3.19. Gelatine Zymography at pH6, Using Biomedica Cathepsin K, Does Not Allow for the Detection of Bands that Corresponds to the Molecular Weight of Cathepsin K. .

A gelatine zymogram was run using a Cathepsin K control at decreasing concentrations. After running the gels were incubated at pH6 in incubation buffer overnight. Gels were stained with comassie blue to visualise any bands. Dark bands were visualised at a MW of 54kDa. No clear bands were observed corresponding to the MW of cathepsin K.

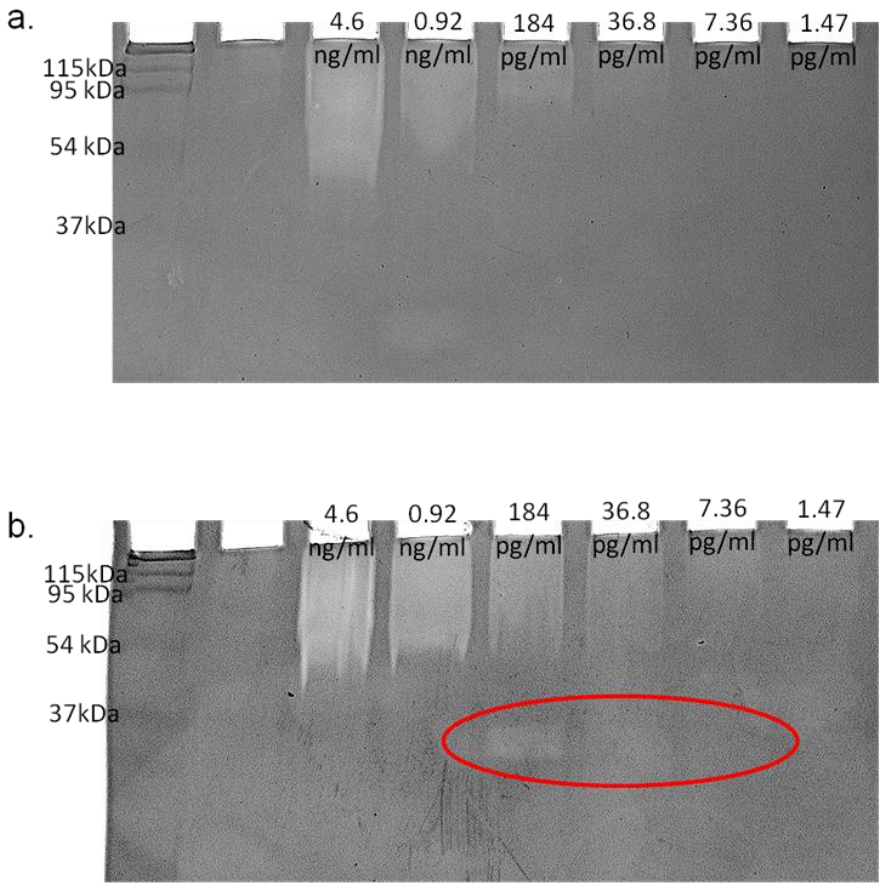

Figure 3.20. Gelatine Zymography at pH 4, but not pH 5, Allows the Detection of Bands that Corresponds to the Molecular Weight of Cathepsin K.

A gelatine zymogram was run using a recombinant human cathepsin K at decreasing concentrations. After running the gels were incubated at (a) pH5 and (b) pH4 in incubation buffer overnight. Gels were stained with comassie blue to visualise any bands. At (a) pH5 streaking was visible in a number of the wells but no bands were present on the gel at a molecular weight similar to that of cathepsin K. At (b) pH4 increased levels of streaking were observed in the wells. Bands corresponding to that of cathepsin k (37 – 27kDa) were visible at three concentrations.

3.3 **Discussion**

The discovery in the 1990's of the osteoclast differentiation factor, now commonly known as RANKL (15, 54, 56), has helped scientists gain an understanding of the role played by OC in bone remodelling and disease. For the first time, pure populations of OC could be generated *in vitro* from the haematopoietic precursors present in bone marrow (302) without co-culture with other cell types. The discovery has allowed scientist to study the direct effect of receptors, cytokines and chemokines on OC differentiation and function. Previously published work by Bull, Williams et al (242) showed a role for the TNFRSF member DR3 and its ligand TL1A in OC biology, though the mechanism through which they acted was not elucidated in this report. The aim of this chapter was to determine the role of DR3/TL1A in OC differentiation and function.

DR3 has been shown to play a role in T cell maintenance; through negative selection and anti-CD3-induced apoptosis during thymocyte development (280), though its role if any in bone marrow maintenance is unknown. A review of the current literature also doesn't yield any clues into the effects of the TNFSF cytokines and receptors on the bone marrow cell population. With BM used as the source of haematopoietic precursors for all murine osteoclastogenesis assays, the effect of DR3 on the BM cell population was first determined. No differences were observed between the $DR3^{wt}$ and $DR3^{ko}$ BM cell populations. The data suggest that while DR3 may have a role in the maintenance of certain cell types at later stages of development; it does not affect the frequency of cell types in the BM, meaning any differences observed in future experiments can be attributed to a direct effect on OC differentiation and function. Having confirmed that the starting populations of $DR3^{wt}$ and $DR3^{ko}$ assays were comparable the ability of the BM cells to differentiate into OC was investigated, using a standard system as a benchmark.

Numerous studies have been conducted generating osteoclasts on glass coverslips *in vitro* using recombinant MCSF and RANKL. The concentration of RANKL employed, ranges from 1 to over 30ng/ml (303-305), depending on the source of the cytokine and the levels required to induce OC differentiation. Concentrations of MCSF required for precursor proliferation were more consistent between groups. Levels of 20 - 30ng/ml (37, 303-307) were routinely used ensuring that MCSF is a non-limiting factor in the assays. For this study the concentrations of MCSF and RANKL used (25ng/ml and 2ng/ml) were pre-determined from work previously carried out in the laboratory by Anja Bloom (308).

No difference was observed in total cell number or % osteoclasts in $DR3^{wt}$ and $DR3^{ko}$ glass coverslip cultures. However, the differentiated osteoclasts were found to be very large, with some having a diameter >500µm (approximate surface area of >196,350µm^2). *In vivo* murine osteoclasts have been shown to have an area of approximately 300 - 400µm^2 (307). Studies looking at OC surface area on glass coverslips are limited, though a study by Saltel et al (309) demonstrated OC cultured on glass grew to disproportionally large sizes (mean surface area of approximately 14000µm^2) when compared to cells cultured on apatite (mean surface area approximately 3000µm^2). The reasons for the difference in size have not been extensively studied. The work by Saltel et al (309) however, points to the inability of OC cultured on glass coverslips to polarise and generate an actin ring or sealing zone causing the OC to be thinner and more spread out. Addition of TL1A to $DR3^{wt}$ cultures reduced total cell number while leading to a trend to increased OC size. It is possible that in this system TL1A is enhancing osteoclastogenesis; increasing the number of precursor cells fusing together, lowering the total cell number and increasing osteoclast size. To confirm this the number of nuclei / cell would have to be counted, to determine if following addition of TL1A there is an increase in cells fusing together to form the multinucleated OC.

An alternative explanation for the decrease in cell number may be due to an apoptotic effect of DR3/TL1A signalling. Work by Chinnaiyan et al (232) demonstrated that over-expression of DR3 in MCF7 breast carcinoma cells and 293 cells induced rapid apoptosis. Additional work by Wen et al (246) and Borysenko et al (241) have shown that TL1A signalling can induce apoptosis in TF-1 cells and osteoblasts respectively. However, these effects were only observed under certain regulated conditions. The increased numbers of gaps (absence of cells) present in the $DR3^{wt}$ + TL1A cultures suggests an increase in cell death. However, to determine whether this is due to TL1A signalling inducing cell death additional apoptosis assays would be required. While enabling the easy visualisation of cells, the major limitation of using a glass substrate for osteoclastogenesis assays is that it does not allow the study of osteoclast resorptive function. To determine whether DR3 and TL1A had an effect on osteoclast differentiation and resorptive function, ivory (dentine) was chosen as a new substrate for culture. Like bone, ivory is comprised of the mineral hydroxyapatite; a substrate osteoclasts can recognise and resorb and has been shown to be an affective substrate in osteoclast assays (41).

Osteoclasts, when cultured on ivory, were observed to be greatly reduced in size when compared to the glass coverslip assays. This result is in-line with the surface area of OC

reported by Redey et al (310) and Saltel et al (309), when cultured on a similar substrate (natural calcium carbonate = 1379±273μm^2 and apatite = approximately 3000μm^2 respectively). Analysis of the experimental outcomes showed that DR3 has no effect on osteoclastogenesis confirming what was observed in the glass coverslip assays. Contrary to the work published by Bull, Williams et al (242) however, which showed *in vitro* TL1A enhanced osteoclastogenesis, TL1A reduced osteoclast differentiation in DR3^{wt} cultures. The reasons for the difference in TL1A response between the two studies were not instantly obvious, but may be due to the difference in mouse strain used. This will be discussed in further detail at a later point in this chapter. TL1A was also found to significantly increase the total cell number in DR3^{ko} cultures. Reasons for this increase are currently not clear, as the only confirmed cellular receptor for murine TL1A is murine DR3. A 2008 study by Al-Lamki et al (272) however, suggested that TL1A may additionally signal through an as yet unidentified receptor. In their study addition of TL1A to an organ culture of DR3-deficient mouse kidneys induced TNFR2 expression but did not activate NF-κB and did not increase apoptosis of tubular epithelial cells. Further experimentation is required to conclusively determine whether there is an alternative receptor for TL1A. Additionally, experimentation would be required using TL1A at different concentrations to determine whether the levels being used are having a blocking effect. While signalling through RANK by its ligand RANKL is known to be crucial for OC differentiation (54) another member of the TNFSF, LIGHT (TNFSF14) has been suggested to be able to induce OC differentiation in its absence (182). The study by Bull, Williams et al (242) showed that TL1A in the absence of RANKL and MCSF could not generate osteoclasts, however, it is unknown whether signalling by TL1A in the presence of MCSF is sufficient to induce osteoclast differentiation. DR3 and TL1A were found to have no effect on cell number or on the induction of osteoclast formation, in control cultures. The result confirms those reported by Bull, Williams et al that signalling by TL1A, in the absence of RANKL, is not sufficient for osteoclast differentiation.

Having shown that TL1A has an effect on OC differentiation the effect of DR3/TL1A on osteoclast resorptive function was investigated. The resorptive function of osteoclasts can be analysed through the number and area of the resorption pits they produce on the ivory surface. DR3 was found to have a significant effect on osteoclast function. In the absence of DR3, osteoclasts were found to be functionally inactive at the time point analysed with very low numbers of resorption pits produced, resulting in a mean of <0.5% of the ivory discs resorbed. This data suggests that DR3 must play an important role in

osteoclast resorption; either through the process of osteoclast attachment, actin ring / sealing zone formation, acidification or enzyme release as there is no difference in osteoclast differentiation between the $DR3^{wt}$ and $DR3^{ko}$ cultures. Failure in any of the aforementioned would result in the cellular phenotype observed, as demonstrated by a number of groups (103, 311-314). Care must be taken when analysing the resorption pit data however, as levels were relatively low even in the $DR3^{wt}$ cultures. This could make accurate interpretation of the role of DR3 in OC resorptive function difficult and raises the possibility that resorption by the $DR3^{ko}$ OC could be delayed rather than being functionally inactive.

The role of TL1A in osteoclast resorptive function is less clear. The increase in the number of resorption pits observed in the $DR3^{wt}$ cultures is off-set by the reduction in the mean % area resorbed. The data suggests that TL1A does not play a role in OC function; the increase in resorption pit numbers and reduction in area resorbed could be attributed to the reduction in osteoclasts numbers. Fewer osteoclasts would result in small individual resorption pits rather than the larger, merged resorption pits observed in the $DR3^{wt}$ –TL1A cultures. This would then create the observed effect where there is an increase in resorption pit number but a decrease in the % area resorbed. Analysis of OC numbers and resorption pits has demonstrated a role for DR3 in OC resorptive function and TL1A in OC differentiation. To determine the mechanism through which the effects were being driven, culture supernatants were analysed for soluble mediators involved in OC formation and activity. The migration, recruitment and fusion of mononuclear precursor cells into multinucleated OC, is controlled by a family of small cytokines known as chemokines; so called as they have the ability to induce chemotaxis in nearby responsive cells. The effect of DR3/TL1A upon chemokine release from murine OC precursors (monocytes / macrophages) and osteoclasts is currently unknown.

As discussed in the introduction the chemokines CXCL1 (1.3.5.2), CCL2 (1.3.5.3) and CCL3 (1.3.5.4) are involved in osteoclastogenesis. The results from the supernatant analysis of this study showed DR3 to have no effect on CCL2 or CXCL1 expression in control or OC cultures, however the trend towards a 3-fold decrease in CCL3 levels in $DR3^{ko}$ OC cultures highlights expression of this chemokine as a target of DR3. Perhaps surprisingly the reduction in $DR3^{ko}$ CCL3 levels did not correspond to a reduction in OC numbers. This suggests that there may be redundancy in the chemokine system. Further experiments, blocking either the receptors for CCL3 (CCR1 and CCR5) or the chemokines CCL4 and CCL5 (which signal through the same receptors) (315), would be required to prove this. If there

is redundancy then blocking either the receptors or the chemokines should result in a reduction in OC numbers.

The reduction observed in CCL2 and CCL3 levels, following addition of TL1A to $DR3^{wt}$ cultures, provides a possible mechanism for the reduction in OC differentiation observed. Studies in CCL2-deficient mice, which have been shown to have inhibited OC formation (84), highlight the importance of this chemokine in the migration and fusion of OC precursors. Additional experiments are required however, to determine which of these chemokines has the more dominant role. CCL2 and CCL3 add-back experiments, to restore the $DR3^{wt}$ phenotype, would identify which of the chemokines is responsible for the reduction in OC numbers. The addition of TL1A to $DR3^{wt}$ cultures had no effect on CXCL1 levels. While in a human macrophage cell line TL1A induces CXCL8 secretion (240) the same is not true of the murine ortholog.

Analysis of soluble mediators identified CCL2 and CCL3 as targets of TL1A signalling. The mechanism through which DR3 affects osteoclast resorptive function was then investigated. Two enzymes involved in the degradation of bone by osteoclasts are the gelatinase MMP-9 (106) and the proteinase Cathepsin K (104), though some debate exists about the exact role of MMP-9 in osteoclast function. Evidence for a role of MMP-9 in bone resorption has been shown by a number of groups (106, 118, 119), though work by Chen et al (120) has shown that it is not rate limiting, as the resorptive activity of OC in MMP-9 null mice compares to that of wild type mice (121). Emerging evidence also suggests an alternative role for MMP-9, in osteoclast migration. Evidence that MMPs have a role in osteoclastic invasion was provided by Sato et al (123) who showed that OCs are able to migrate through collagen in the absence of other cells and that inhibitors of these MMPs inhibited osteoclast migration. Comparison of $DR3^{wt}$ and $DR3^{ko}$ OC cultures showed a significant increase in the inactive form of MMP-9 (pro MMP-9) in the $DR3^{ko}$ cultures by ELISA, suggesting that DR3 possibly inhibits MMP-9 release. To determine the source of the MMP-9 the OC precursor's cultures were tested. Levels of MMP-9 were found to be greatly reduced in both the $DR3^{wt}$ and $DR3^{ko}$ cultures ± TL1A. The result shows that while the OC precursors express background levels of MMP-9, the majority of the enzyme is produced by cells that have been activated by RANKL and are differentiating / differentiated into osteoclasts. A limiting factor of the ELISA used for the analysis however, is that it did not measure the active form of the enzyme, which is the component involved in the degradation of bone. This means that such data was unable to differentiate between $DR3^{ko}$ cultures producing more inactive MMP-9 or whether $DR3^{wt}$

and DR3^{ko} cultures produce the same level but the DR3^{wt} cultures convert more to the active form. To measure the active form of MMP-9 a gelatine zymogram was employed. The zymogram showed equal levels of pro MMP-9 between the two cultures, but levels of the active form were raised in the DR3^{wt} cultures at day 10, suggesting that DR3 has a role in MMP-9 activation.

Activation of MMP-9 is a stepwise process requiring the activation and activity of a number of other MMPs. Studies by Toth et al (316) demonstrated that the activation of pro MMP-9 can be accomplished via a cascade of zymogen activation initiated by MT1-MMP and mediated by MMP-2. Activation of pro MMP-9 through an interacting protease cascade involving plasmin and MMP-3 has also been demonstrated *in vitro* and in human tumour cells (317). In the study by Dreier et al (318) addition of plasmin, a partial activator of pro MMP-1 and pro MMP-3 was found to enhance the activation of pro MMP-9. Blockade of MMP-3 activity through an inhibitor was also observed to dose-dependently prevent activation of pro MMP-9 (318). The MMPs -7 (319), -13 (320) and -26 (321) were also shown to activate pro MMP-9, albeit with different efficiencies. A schematic representation of the mechanism involved in the activation of osteoclast pro MMP-9 is shown in Fig 3.22. How DR3 influences the activation of MMP-9 is however, currently unknown. The observed difference in levels of active MMP-9 between the DR3^{wt} and DR3^{ko} cultures would not fully account for the very significant difference observed in osteoclast resorptive function, therefore DR3 must have an effect on another aspect of osteoclast resorptive function.

The main proteinase involved in osteoclastic resorption is Cathepsin K (104). Commercial methods for the quantitative measurement of murine CatK levels in culture were not readily available and so methods were developed *in-house*. Development of the collagen bio-assay initially showed some success when using a CatK control. Reduction in collagen binding was detected compared to the blank suggesting that enzyme activity could be measured. However, when samples were used, levels of binding increased >500%. Further analysis showed that this was due to the foetal calf serum present in the culture supernatant which was cross-reacting within the assay, rendering it unsuitable for the detection of CatK in supernatant. Work on detecting CatK by zymogram was adapted from a method by Li et al (281), who developed a technique for the detection of fentomole quantities of mature CatK from osteoclasts. Optimisation of the method produced promising results with a CatK standard being detected down to levels of 7.36pg/ml, when the gel was incubated at pH 4. Problems arose however, in sample

testing. CatK is tightly controlled by the osteoclast and so is only released in to the resorption pit (322, 323) after the actin ring has formed the sealed zone. To free the CatK into the culture supernatant the cells would require lysis. Correspondence with Li also confirmed that, for their method to work successfully the culture medium must be serum free and the cells lysed to free the CatK, thus further work into the optimisation of the CatK zymogram was halted.

Another component of osteoclast resorptive function is the rearrangement of the intracellular actin to form the actin ring, enabling the cell to create a tight seal with the bone surface. An immunocytochemistry technique was developed for the staining of the actin and nuclei of multinucleated osteoclasts and their precursors, to determine whether $DR3^{ko}$ cells are able to successfully form a sealed zone (Appendix I). The method was optimised successfully in $DR3^{wt}$ cultures, with the actin and nuclei being readily visualised under a fluorescent microscope. Further work is required however, to determine whether DR3 has an effect on actin ring formation.

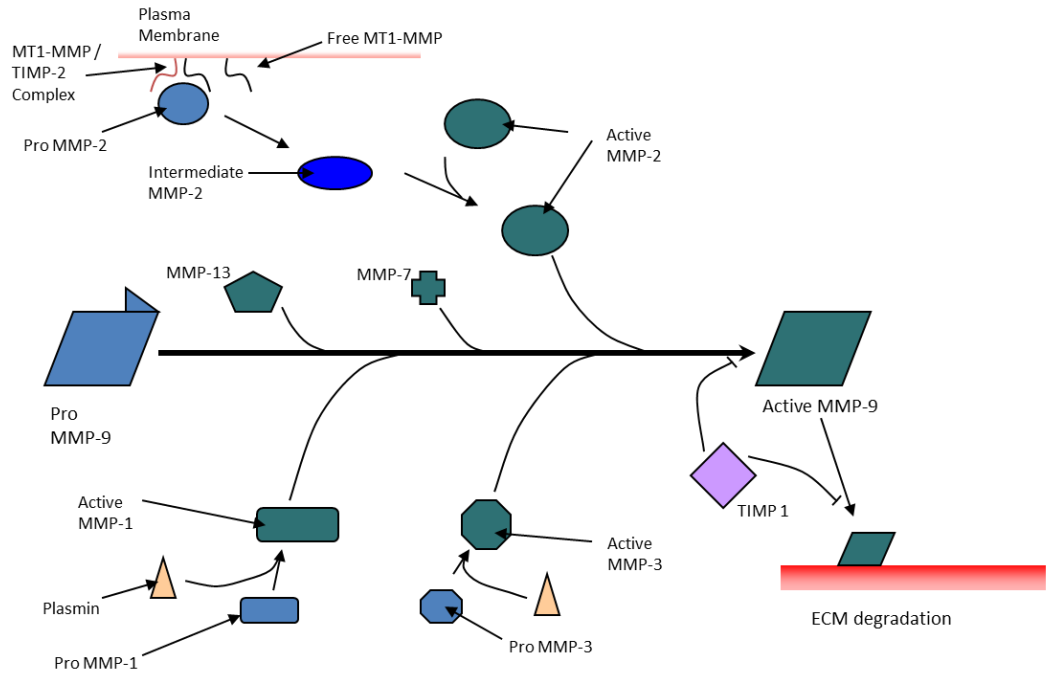

Figure 3.21. Schematic Representation of Osteoclast Pro MMP-9 Activation.

Activation of pro MMP-9 is accomplished via a cascade of MMP activation initiated by MT1-MMP and plasmin. Activation of pro MMP-1 and pro MMP-3 by plasmin and pro MMP-2 by MT1-MMP leads to the downstream cleavage of pro MMP-9 into the active form. MMP-7 and -13 have also been shown to be able to activate pro MMP-9. Additional control of MMP-9 activity is via the inhibitor TIMP1.

For the first time functional data has been shown highlighting how DR3/TL1A signalling affects OC formation and function; with DR3 involved in OC function and the addition of exogenous TL1A reducing OC formation. However, the overall results were in contrast to that published by Bull, Williams et al (242), who showed that the addition of TL1A to murine BMM directly promotes osteoclastogenesis. Comparison between the work performed in this study and the work by Bull, Williams et al highlighted the main difference in experimental procedure to be the strain of mouse used; DBA/1 versus C57BL/6. The exact difference between the DBA/1 and C57BL/6 mouse strains that would cause the observed differences are unknown. Work by Akhter et al (324) demonstrated breed related differences in bone histomorphometry between C57BL/6 and DBA/1 mice, with higher bone mineral content in the C57BL/6 mice, and a higher % osteoclast surface area at the distal femur in the DBA/1 mice. This data suggests that there is a difference between the strains in the bone cells and also the factors that control them. Variations in fracture healing (325), bone density (326), MSC growth kinetics, MSC differentiation potential and MSC surface epitope expression (134, 327) have also been reported between inbred strains. Studies into expression levels of the TNFSF between mouse strains have not been carried out. A study by Linkhart et al (328) however, comparing osteoclast formation between C57BL/6 and C3H/HeJ mice suggests that genes affecting the bone marrow osteoclast precursor population may contribute to the relative differences in bone density and OC formation. Whether there is a difference in baseline TL1A expression between the DBA/1 and C57BL/6 mice is also currently unknown, as reagents for the detection of the cytokine were unavailable at the time of the study. To determine whether the difference in the effect of TL1A was due to operator or mouse strain, osteoclast assays were performed using a C57BL/6 mouse under the same conditions as the DBA/1 work. As with the DBA/1 study DR3 was shown to have no effect on osteoclastogenesis. Addition of TL1A to the $DR3^{wt}$ cultures however, led to a trend towards an increase in osteoclast numbers/mm^2 confirming what was reported by Bull, Williams et al (242). Supernatant analysis highlighted that CCL3 levels were also 3-fold higher in $DR3^{wt}$ cultures following the addition of TL1A, demonstrating that CCL3 is still a target of TL1A signalling even though the effect on expression is different. These results confirm that the observed differences between the DBA/1 and C57BL/6 cultures are due to some intrinsic difference between the strains.

Further analysis into the mechanism of DR3 and TL1A signalling in murine osteoclasts, was terminated at this point. The differing results between the DBA/1 and C57BL/6 strains

highlighted that while murine studies provide a valuable system for the study of cellular activity and disease they may not reflect the human system. While some cell types and / or diseases can only be investigated in a murine model the isolation and culture of human osteoclasts is possible. In the human system OC precursors can be found circulating in the peripheral blood and are easily obtained, allowing the study of human OC directly. For these reasons the human model was used for further study into the mechanism of DR3/TL1A signalling on osteoclasts and their precursors.

3.4 **Conclusion**

At the conclusion of this chapter the following objectives have been met:

- The cellular phenotype of bone marrow isolated from DBA/1 $DR3^{wt}$ and $DR3^{ko}$ mice was charaterised.
- *In vitro* osteoclast cultures from BMCs isolated from DBA/1 $DR3^{wt}$ and $DR3^{ko}$ mice were developed on glass coverslips and ivory discs
- The impact of DR3 on OC formation and resorptive function, *in vitro,* was assessed.
- TL1A's effect on OC formation and resorptive function, *in vitro,* was determined.

The results have shown that while DR3 is not involved in the homeostasis of bone marrow, or osteoclast differentiation it plays a role in osteoclast resorptive function. $DR3^{ko}$ osteoclasts have been shown to have reduced resorptive activity in osteoclastogenesis assays and while the mechanism for this is not conclusive, the data suggests that DR3 has a role in the activation of the bone resorbing enzyme MMP-9. Further work is required however, to determine what effect DR3 may have on actin ring formation and Cathepsin K expression. DR3's only confirmed TNFSF ligand TL1A has been shown to play a key role in osteoclast differentiation; though its effects are dependent on the mouse strain used. In the DBA/1 model addition of TL1A significantly reduced osteoclast formation while in the C57BL/6 it had the opposite effect. The reasons for the difference in cellular response to TL1A are unknown but could be due to an intrinsic genetic variation between the two strains. TL1A has been shown to act mechanistically through either decreasing (DBA/1) or increasing (C57BL/6) levels of the chemokine CCL3. In the DBA/1 model TL1A has also been shown to exert an effect on CCL2, reducing the levels expressed in OC cultures, providing another possible mechanism of action. While the murine model of osteoclastogenesis has provided insight into the mechanism of DR3 and TL1A signalling the difference in DBA/1 and C57BL/6 response highlights the shortcomings. Whether either of these two responses to TL1A is comparable to the human system is unknown and will be investigated in chapter 4.

Chapter 4

Investigating the Regulation of Osteoclast Differentiation and Function by TL1A in Human Cells.

4.1 **Introduction**

The study into the effect of DR3 and TL1A on murine osteoclast differentiation and resorptive function in chapter 3 provided valuable insight into the mechanisms through which they act. The results demonstrated DR3 has an important role in osteoclast resorptive function; however the difference in response to TL1A between the two murine strains (DBA/1 and C57BL/6) highlighted the shortcomings in using mouse models. To gain a better understanding of the effects of TL1A on OC and their precursors, the system was transferred into a human model.

A number of studies have been carried out looking at the effect of TL1A on monocytes and macrophages, though the effect on OC is less understood. *In vitro,* TL1A has been shown to be involved in the activation and differentiation of monocytes / macrophages. Work by Kim et al (239) in 2001, using the human monocytic cell line THP-1, demonstrated that cross linking of DR3 resulted in the induction of MMP-9. This was further supported by Kang et al (278) who in 2005 showed that treatment of THP-1 cells with recombinant human TL1A dose-dependently induced MMP-9 expression. Co-stimulation of the THP-1 cells with IFN-γ was also observed to induce the expression of CXCL8 (Interleukin-8 (IL-8)), but failed to induce TNF or CCL2. In 2006 Su et al (240) investigated the effect of TL1A on CXCL8 expression from primary monocytes and macrophages. TL1A had no effect on CXCL8 secretion from monocytes though it was observed to stimulate CXCL8 expression by macrophages. A role for TL1A in macrophage differentiation was put forward by McLaren et al (270). In their study they demonstrated that TL1A signalling through DR3 promoted the differentiation of macrophages into foam cells through an increase in the uptake of acetylated low-density lipoprotein (LDL) and oxidized LDL. While the effect of TL1A on monocytes and macrophages has been investigated there are currently no papers that extensively look at the effect of TL1A on OC differentiation and function in a human system. In the Bull, Williams et al (242) study DR3-deficient mice were shown to be protected from bone erosions associated with AIA. *In vitro*, TL1A was shown to enhance osteoclastogenesis from bone marrow macrophages (BMM) in a DR3-dependent manner. When they looked in a human system TL1A significantly promoted osteoclastogenesis in PBMC cultures. However, the cell type that the TL1A was acting upon and the mechanism through which it was exerting its effect was not investigated. This raises the question as to whether TL1A is acting upon monocytes / macrophages (OC precursors) directly or indirectly via T-cells, which express DR3 (230,

248) and affect OC differentiation (58). To address this question the starting population of an OC assay would have to be comprised of just monocytes / macrophages, eliminating the effect of other cell types.

In vivo OC are derived from haematopoietic precursors; the most abundant source of these cells is the bone marrow. While it is acceptable to use BMM as a source of precursor cells in a murine model, ethical and practical difficulties mean that this is not a suitable method for an *in vitro* human system. Haematopoietic precursors are present in peripheral blood as mononuclear cells, which serve as a readily accessible alternative source of OC precursors (12, 35, 36). Until 15 years ago the subset of these cells that act as OC precursors was not entirely clear. Initial work on identifying the subset was performed by Quinn et al (37) who showed that adherent PBMCs that differentiated into OC expressed macrophage associated antigens CD68, CD11b and CD14. This suggested that osteoclasts can be derived from CD14-positive ($CD14^+$) monocytes. Further work by Massey and Flanagan (38) confirmed this by showing that selection of $CD14^+$ cells from PBMCs enhanced osteoclastic bone resorption, providing an easy source for the study of human OC. For this study, $CD14^+$ cells were isolated from female volunteers, as females are at an increased risk of OC related disease such as osteoporosis and rheumatoid arthritis (189-191, 329).

The aims of this chapter were to optimise culture of osteoclasts from human $CD14^+$ cells isolated from PBMCs and determine the effect of TL1A on osteoclast formation and function. Supernantants were collected across the culture period and analysed for specifc mediators that have a role in osteoclast differentiation and function. The data was used to determine the mechanism through which DR3/TL1A regulates osteoclastogenesis in humans. The specific objectives of this chapter are listed below:

- To define the purity of $CD14^+$ cells isolated from human PBMCs.
- To determine whether human osteoclast precursors cells express DR3.
- To develop a reproducible *in vitro* culture system for the generation of osteoclasts from human $CD14^+$ cells using ivory discs as the supporting matrix .
- To measure the effect and identify the mechanism through which TL1A modulates osteoclast differentiation and function.

4.2 **Results**

4.2.1 **Defining Base-line Purity and Expression of CD14 and DR3 on Freshly Isolated $CD14^+$ Cells**

Osteoclast precursors used in all osteoclastogenesis assays reported in this chapter were isolated from PBMCs using density gradient centrifugation and magnetic isolation (section 2.2.7). Blood was obtained from pre-menopausal females and precursor cells were identified on the basis of positive expression of CD14, as determined by flow cytometry (section 2.2.8). PBMC numbers obtained from 50ml of blood ranged from $1.74x10^7$ to $1.00x10^8$. Isolation, based on expression of CD14, resulted in the positive selection of approximately 10% of the starting cell number ($1.08x10^6$ to $8.25x10^6$). Initially using this method only 30% of the cells recovered were deemed to be $CD14^+$ by flow cytometry (Fig 4.1 (a, i)); this value was too low to perform the OC assays. Over subsequent assays the % $CD14^+$ cells isolated increased to $\geq$ 90% (Fig 4.1 (a, ii)). All assays in this chapter had a purity of $\geq$90% $CD14^+$ monocytes.

The morphology of the $CD14^+$ cells was studied by differential staining (section 2.2.5). Cells were identified by their size, granularity and nucleus size and shape. Cells in the $CD14^+$ isolate were found to be between 10 - 20µm in diameter and predominantly had a kidney-shaped nucleus, which occupied approximately half of the cell (Fig 4.1 (b)). The cytoplasm contained variable numbers of granules. The morphology of the $CD14^+$ cells, therefore, corresponded to that of monocytes (330).

DR3 expression on the $CD14^+$ cells was tested by flow cytometry and expression reported as a histogram for graphical presentation. No shift in signal was detected between the isotype control and the anti-DR3 antibody on the isolated $CD14^+$ cells (Fig 4.1 (c)) demonstrating that freshly isolated $CD14^+$ cells did not express DR3.

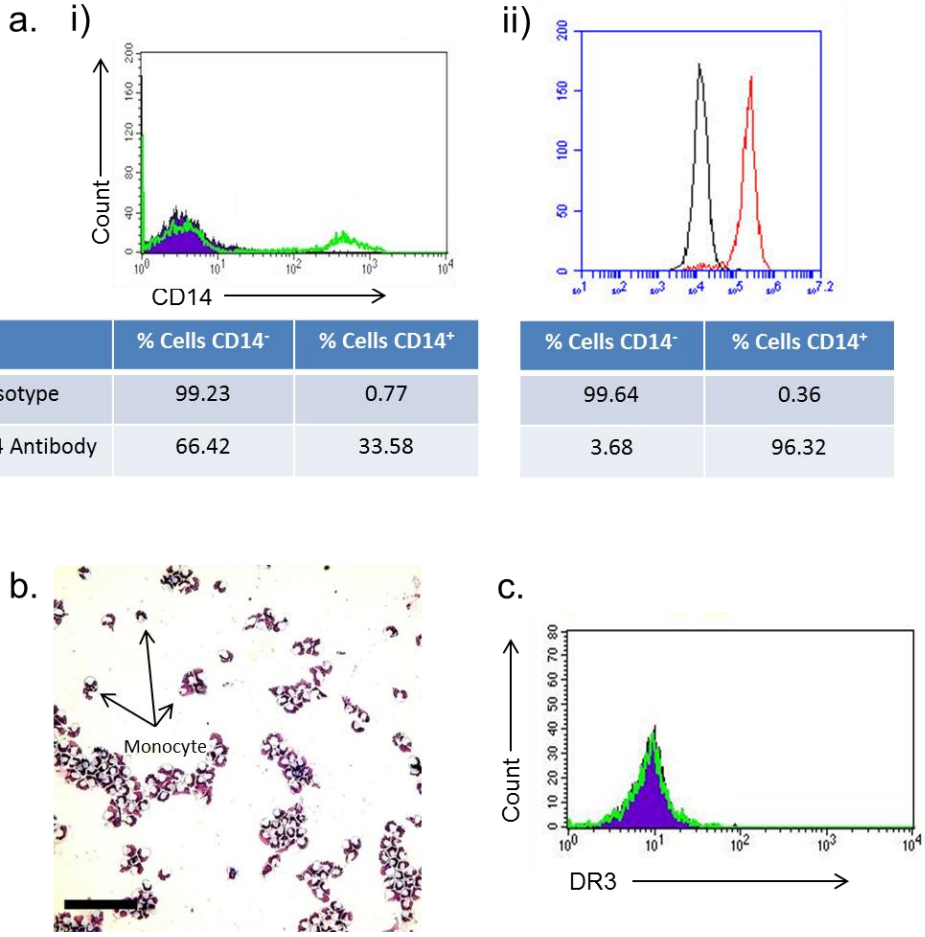

	% Cells CD14$^-$	% Cells CD14$^+$
Isotype	99.23	0.77
CD14 Antibody	66.42	33.58

% Cells CD14$^-$	% Cells CD14$^+$
99.64	0.36
3.68	96.32

Figure 4.1. CD14 Isolates are >90% CD14$^+$ and have a Monocyte Morphology, but do not Express DR3.

PBMCs were extracted from the peripheral blood of pre-menopausal females. CD14$^+$ cells were positively isolated by magnetic sorting. (a) Cells were stained for CD14 with an anti-human CD14 antibody (i – green, ii - red line) or isotype control (i – filled, ii - black line) and tested by flow cytometry. % CD14$^+$ cells was calculated. i) Initial attempts produced a population of only 30% CD14$^+$ monocytes. ii) Improvements to technique produced populations of >90% CD14$^+$ monocytes. (b) Cells were dried down onto glass coverslips and stained with May-Grünwald and Giemsa stain. CD14$^+$ cells predominantly expressed a monocyte morphology. (c) Cells were stained for DR3 with an anti-human DR3 antibody (green line) or isotype control (filled) and tested by flow cytometry. No DR3 expression was detected on the cells. Scale bar = 100µm.

4.2.2 **Assessing the Impact of Substrate on DR3 Expression**

The environment in which cells are grown can determine whether they express DR3. Su et al (240) and Kang et al (278) showed that $CD14^+$ cells expressed DR3; however, the expression was linked to activation of the cells by the pro-inflammatory cytokine TNF, bacterial LPS (278) or differentiation in RPMI medium for 6 – 7 days (240, 270, 278). OC can be grown on a variety of substratum; glass, plastic or bone (ivory). Initial experiments were performed to look at whether these substrates effect DR3 expression. $CD14^+$ cells were isolated (day -7) and grown for 7 days in culture medium supplemented with MCSF (section 2.2.9 and Fig 2.6). DR3 expression was gauged by flow cytometry and reported as fold-change in median fluorescent intensity (MFI) compared to the isotype control (day 0; section 2.2.10). No DR3 expression was detected on $CD14^+$ cells cultured on a glass substrate for 7 days (Fig 4.2 (a)), demonstrating that glass is not suitable for the induction of DR3. Culture of $CD14^+$ cells on plastic (Fig 4.2 (b)) and ivory (Fig 4.2 (c)) resulted in a marked up-regulation of DR3 expression (6.7-fold increase and 1.4-fold increase). The data shows that DR3 expression can be induced on $CD14^+$ cells when cultured in MCSF for 7 days on a plastic or ivory substrate.

4.2.3 **Maintenance of DR3 Expression over Time Course of Osteoclast Assay**

Osteoclast assays in this chapter were comprised of mixed cell populations; monocytes, macrophages, pre-OC and mature OC. It is currently unknown whether the addition of RANKL, to induce OC differentiation, affects DR3 expression on $CD14^+$ cells. $CD14^+$ cells were isolated (day -7) and cultured in MCSF for 7 days (n=1) on ivory discs. DR3 expression was confirmed (Fig 4.3 (a)) and RANKL added to cultures (day 0). DR3 expression was tested in the cultures on day 3, 7, 10 and 14 by flow cytometry (section 2.2.8) and MFI reported relative to the isotype control. DR3 was detected in cultures on day 3 with a 3.7-fold increase in fluorescence (Fig 4.3 (b)), day 7 (2.1-fold increase; Fig 4.3 (c)), day 10 (2.3-fold increase; Fig 4.3 (d)) and day 14 (2.8-fold increase; Fig 4.3 (e)). While levels of DR3 expression were variable due to only one rep being performed the data demonstrates that RANKL does not affect DR3 expression, and that TL1A can have a sustained effect on OC differentiation across the time course.

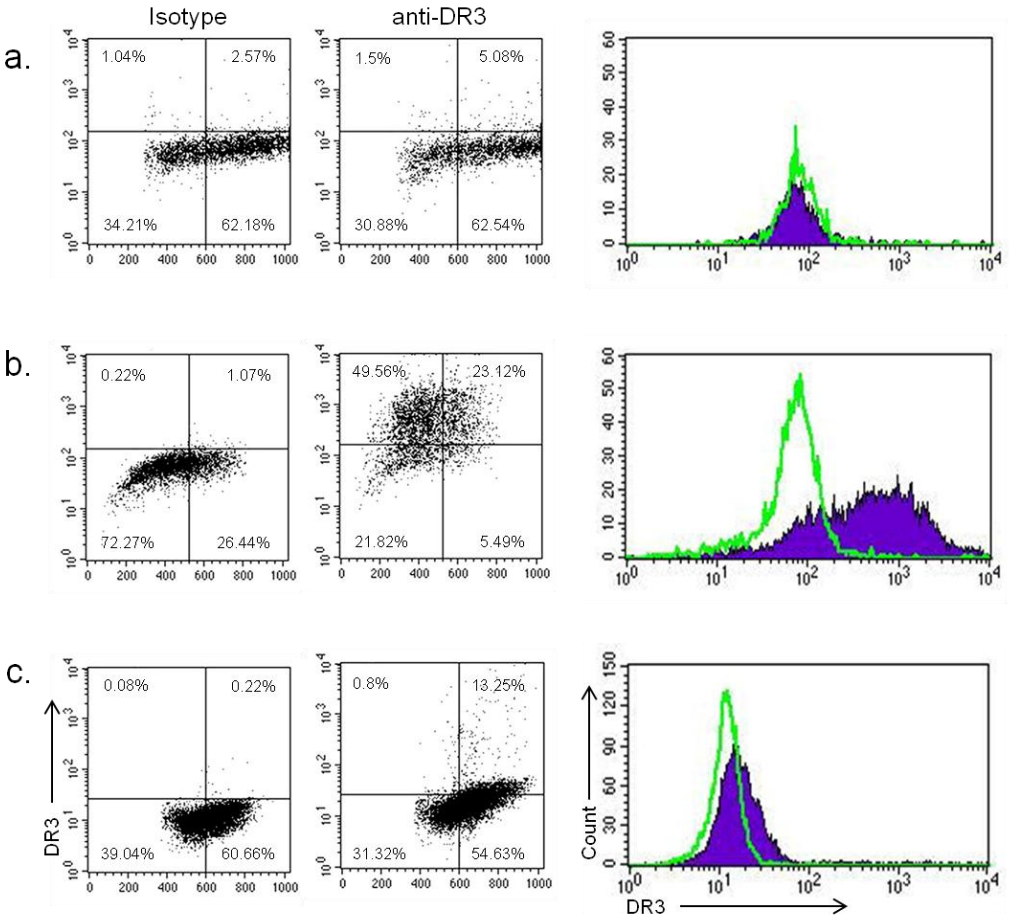

Figure 4.2. CD14⁺ Cells Express DR3 after 7 Days Culture in MCSF when Grown on a Plastic or Ivory Substrate.

PBMCs were extracted from the peripheral blood of a pre-menopausal female (n=1, 1 rep per condition). $CD14^+$ cells were positively isolated by magnetic sorting. Cells were plated onto either glass coverslips, plastic tissue culture flasks or ivory discs and cultured in MCSF for 7 days. Cells were stained with either an isotype control (green line) or with an anti-human DR3 antibody (filled) and tested by flow cytometry. (a) No DR3 expression was detected on cells cultured on glass coverslips. DR3 was detected on cells cultured on (b) plastic tissue culture flasks and (c) ivory discs.

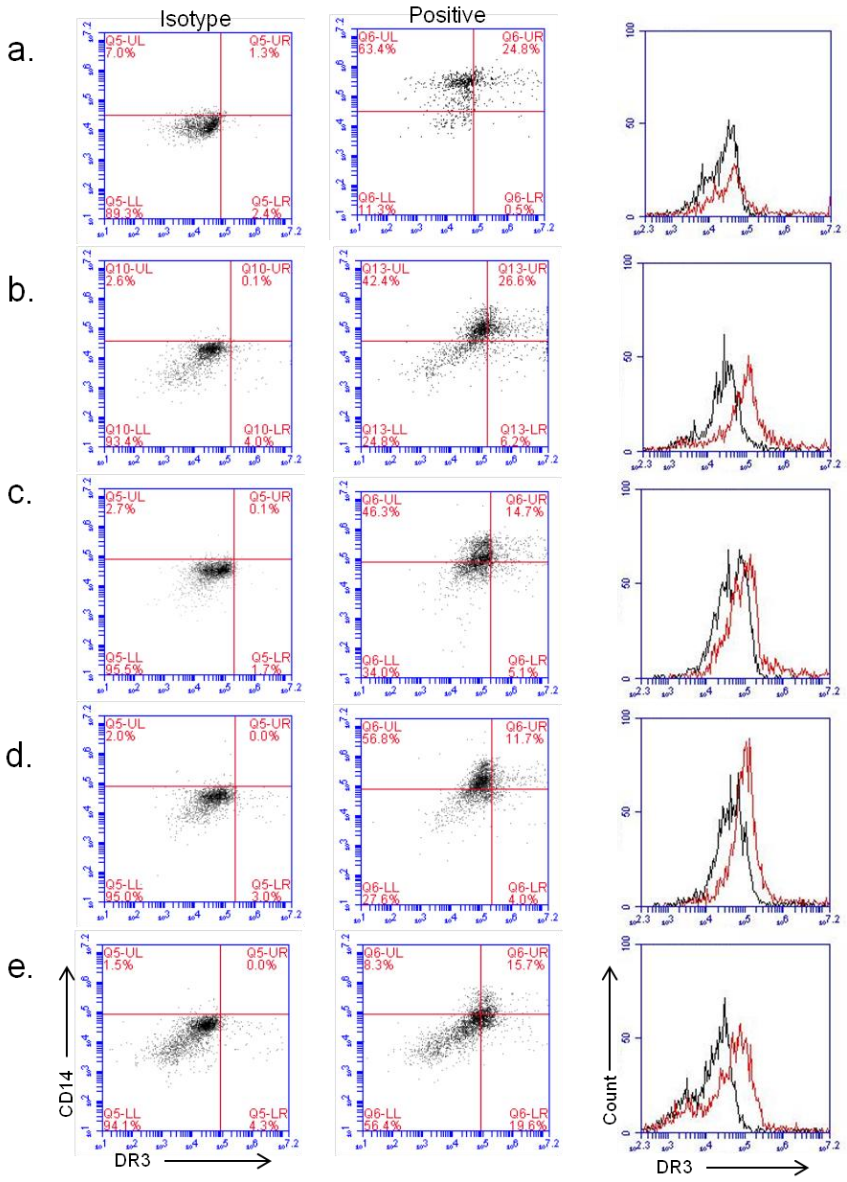

Figure 4.3. DR3 Expression is Maintained on Cells over the Time Course of Osteoclast Assay.

PBMCs were extracted from the peripheral blood of a pre-menopausal female (n=1, 1 rep per condition). $CD14^+$ cells were positively isolated by magnetic sorting. Cells were plated into a 48 well plate and cultured in MCSF for 7 days. Cells were stained with either an isotype control (black line) or with an anti-human DR3 antibody (red line) and tested by flow cytometry. (a) DR3 expression was detected after 7 days culture in MCSF. Cells were differentiated for a further 14 days in MCSF and RANKL and tested at (b) day 3, (c) day 7, (d) day 10 and (e) day 14. Expression of DR3 was confirmed across the time course of the experiment.

4.2.4 **Assessing the Impact of TL1A upon Osteoclast Differentiation in Plastic Tissue Culture Plates**

Flow cytometry of $CD14^+$ cells demonstrated induction of DR3 expression after culture in MCSF on a plastic substrate. To determine what effect this would have on OC formation TL1A was added to OC cultures, as described in section 2.2.10.1 (Fig 4.4). The total number of cells ($TRAP^+$ and $TRAP^-$) per well were counted and expressed as cells/mm^2 (mean±SEM) for graphical presentation (Fig 4.5 (a)). There was no significant difference in the total number of cells counted in the presence or absence of TL1A at day 1 (-TL1A = 498±54/mm^2 versus +TL1A 540±70/mm^2). Total cell number did not vary significantly across the time course. Differential cell counts were also performed on $TRAP^+$ cells. $TRAP^+$ cells were classified as mononuclear or multinucleated osteoclasts and were reported as $TRAP^+$/mm^2 (mean±SEM). The number of $TRAP^+$ cells increased from day 1 (-TL1A=1.9±0.3/mm^2 versus +TL1A=2.4±0.4/mm^2) to day 5 (-TL1A=13.9±1.8/mm^2 versus +TL1A=17.6±2.2/mm^2). TL1A significantly increased the number of $TRAP^+$ mononuclear cells (*P*=<0.01; Fig 4.5 (b)) present across the time course of the experiment though no significant differences were detected at individual time points. As with $TRAP^+$ cells the number of OC present in the cultures increased across the differentiation time course (day 1: -TL1A=0.07.5±0.03 versus +TL1A=0.05±0.03 and day 5: -TL1A=10.27.5±1.87 versus +TL1A=13.61±2.31). Addition of TL1A significantly increased osteoclast formation across the time course (*P*=≤0.05; Fig 4.5 (c)), though no significant differences were detected at individual time points. These results suggest that TL1A drives OC precursor differentiation and fusion into multinucleated OC.

4.2.5 **Assessing the Impact of TL1A upon Chemokine Release during Osteoclastogenesis in Plastic Tissue Culture Plates**

To determine the mechanism through which TL1A drives OC differentiation, supernatants were collected at every media change during the course of the experiments described in section 4.2.4. Soluble mediators known to be involved in OC fusion (CXCL8 and CCL2) were measured by ELISA. CXCL8 levels (mean±SEM) on day 0 were measured at 3.1±0.2ng/ml. Levels of CXCL8 were found to peak at day 1 following a significant increase (-TL1A = 11.9±2.2ng/ml; *P*<0.0001) before dropping significantly to background levels on day 2 (-TL1A = 1.8±0.1ng/ml; *P*<0.0001) and staying constant for the remainder of the time

course. CXCL8 levels were not altered by the addition of TL1A at any of the time points studied (Fig 4.6 (a)). Next CCL2 levels (mean±SEM) were measured. On day 0 CCL2 levels of 17.9±2.3ng/ml were detected. Levels were observed to drop to 11.5±2.4ng/ml on day 2. A moderate increase in CCL2 was observed on day 3 (17.1±3.7ng/ml) before dropping back down on day 4 (10.7±1.7ng/ml). CCL2 expression did not vary significantly between time points or following addition of TL1A (Fig 4.6 (b)). The results show that in this human system, TL1A does not affect osteoclastogenesis by targeting CXCL8 or CCL2.

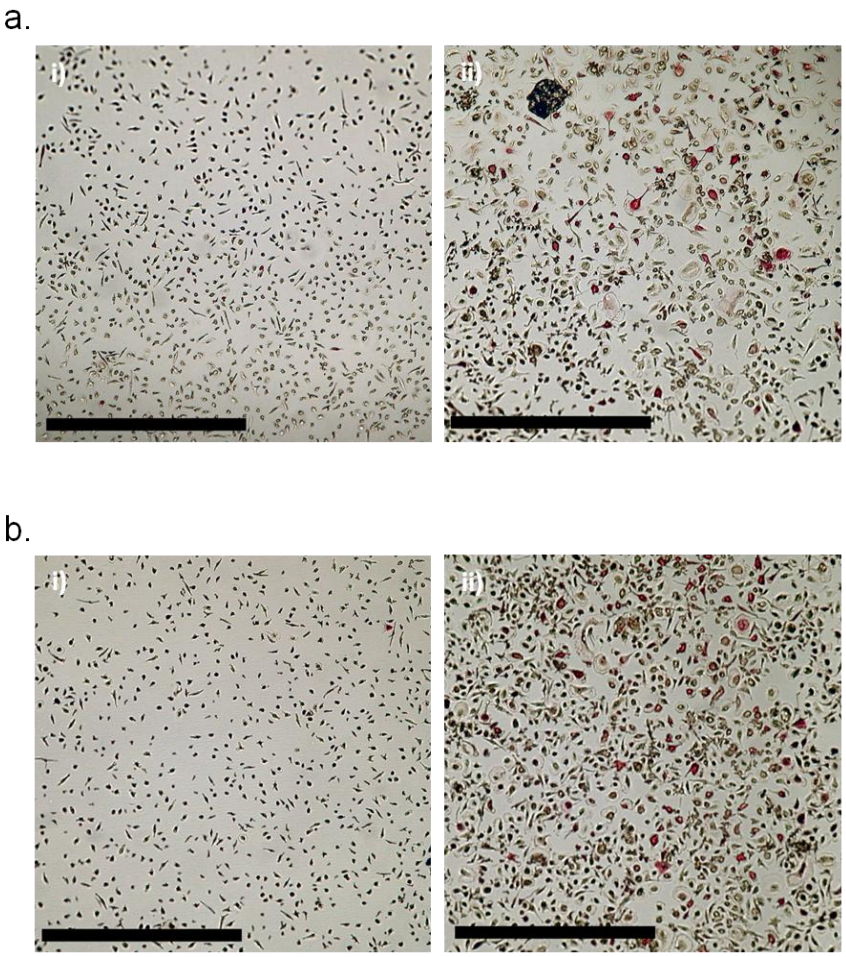

Figure 4.4. TRAP Stained Cells in Plastic Tissue Culture Plates.

PBMCs were extracted from the peripheral blood of pre-menopausal females (n=5). $CD14^+$ cells were positively isolated by magnetic sorting. Cells were plated into a 48 well plate and cultured in MCSF for 7 days and DR3 expression confirmed. Cells were differentiated for a further 5 days in MCSF and RANKL±TL1A 10ng/ml. At experiment end-points cells were stained for TRAP. Representative pictures of (a) MCSF+RANKL cultures at i) day 1 and ii) day 5 and (b) MCSF+RANKL+TL1A cultures at i) day 1 and ii) day 5. Scale bar = 1000µm.

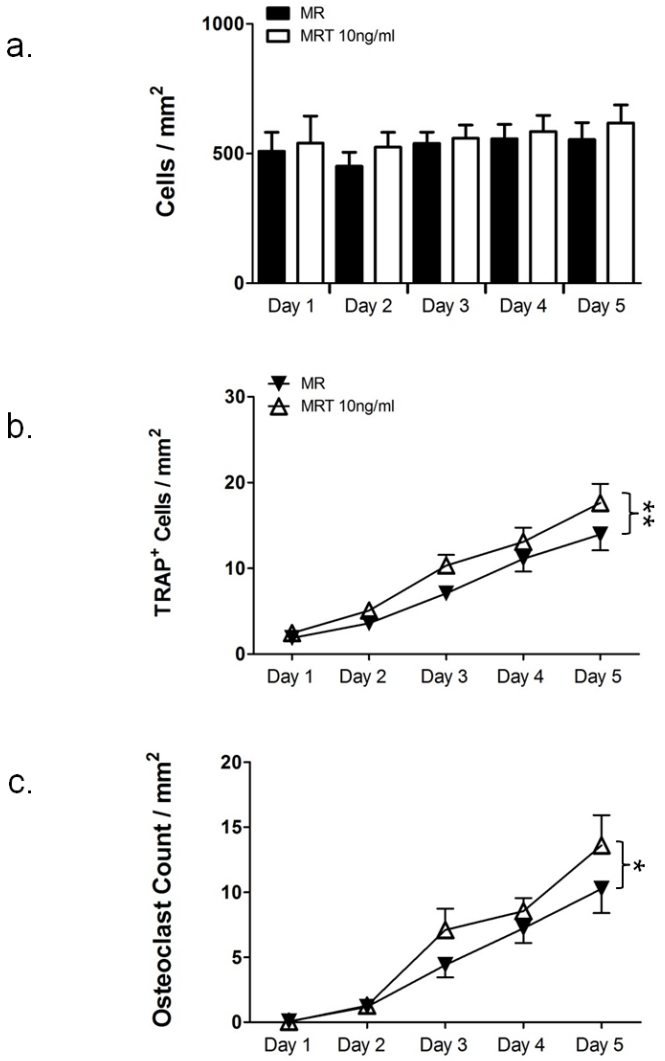

Figure 4.5. Addition of TL1A has No Effect on Total Cell Number but Significantly Increases TRAP$^+$ Cell and Osteoclast Number.

PBMCs were extracted from the peripheral blood of pre-menopausal females (n=5, 3 reps per condition). CD14$^+$ cells were positively isolated by magnetic sorting. Cells were plated into 48 well plates and cultured for 7 days in MCSF and DR3 expression confirmed (day 0). Cells were differentiated for a further 5 days in MCSF+RANKL (MR) or MCSF+RANKL+TL1A (MRT; 10ng/ml). At experiment end-points cells were stained for TRAP and (a) cell number, (b) TRAP$^+$ mononuclear cells and (c) OC counted. Addition of TL1A caused a significant increase in TRAP$^+$ cells (**P=<0.01) and OC (*P=<0.05) across the time course. No effect on cell number was observed. Statistical analysis was performed using a Kruskal-Wallis test.

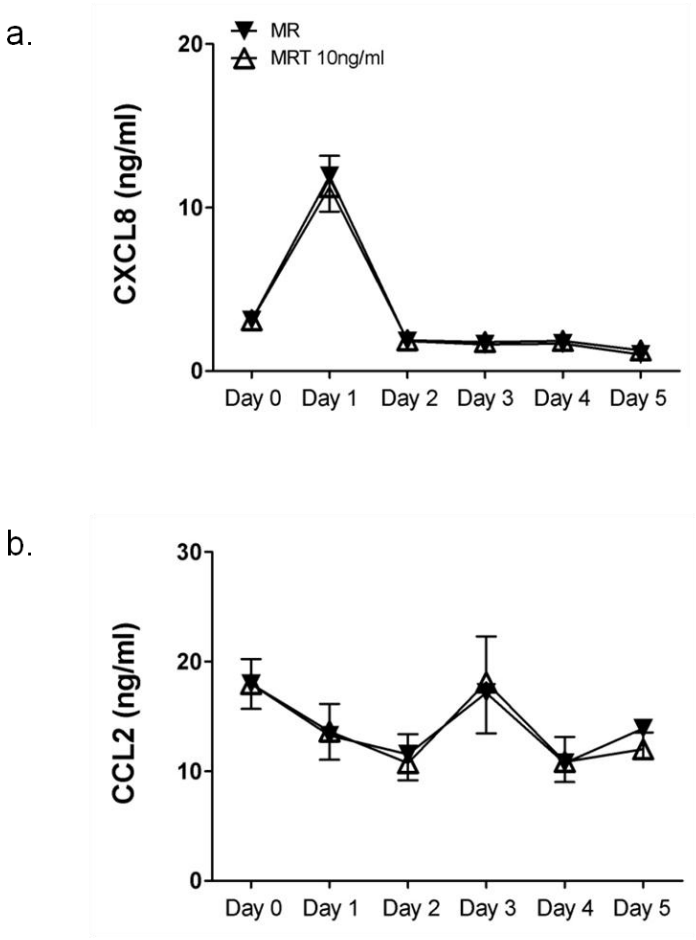

Figure 4.6. TL1A has No Effect on Levels of the Osteoclastic Chemokines CXCL8 and CCL2.

PBMCs were extracted from the peripheral blood of pre-menopausal females (n=5, 3 reps per condition). $CD14^+$ cells were positively isolated by magnetic sorting. Cells were plated into 48 well plates and cultured for 7 days in MCSF and DR3 expression confirmed (day 0). Cells were differentiated for a further 5 days in MCSF+RANKL (MR) or MCSF+RANKL+TL1A (MRT; 10ng/ml). Supernatants were collected at the indicated time points and tested for (a) CXCL8 and (b) CCL2 by ELISA. No significant differences were observed. Statistical analysis was performed using a Kruskal-Wallis test.

4.2.6 **Development of Osteoclast Cultures from CD14$^+$ Cells on Ivory Discs**

Before human OC assays on ivory discs could be performed, optimisation of the method was carried out to determine a time point that would provide the optimal balance between cells counted and area resorbed. OC were required to be established and functional, but numbers not to have reached a maximum level or plateaued. Ivory was selected as the bone-substrate of choice as it is composed of hydroxyapatite and was successfully utilised in the murine OC assays described in chapter 3. Osteoclasts (multinucleated TRAP$^+$ cells that contained $\geq$3 nuclei) were successfully cultured from the CD14$^+$ cells as described in section 2.2.10.2 and Fig 2.8. Cells were evenly distributed over the entire area of the 6mm diameter ivory disc used in these assays (Fig 4.7 (a i-vi)). The number of OC per mm^2 (mean±SEM) for each disc is presented graphically in Fig 4.7 (b). OC numbers were first analysed on day 7 of culture. A significant increase in OC numbers was detected between day 7 and 10 (0 versus 22±3; *P*=<0.01). OC numbers increased further between day 10 and 14 (22±3 versus 30±8), reaching a peak at day 18 (50±8) and plateauing at day 21 (48±6). Osteoclast function was measured by quantifying the area of disc resorbed (%, mean±SEM; Fig 4.8). At day 7 no resorption pits were identified on any of the discs evaluated. However, a significant increase in the area of the disc resorbed was detected by day 10 (7.5±1.3; *P*=<0.01). This increased further between day 14 and 18 (9.5±2.4 versus 40.4±4.9; *P*=<0.01) and between day 18 and 21 (40.4±4.9 versus 69.5±4.4; *P*=<0.01) when substantial surface erosion was detected. Day 14 was chosen as the time point for experiment termination for human OC assays based on the criteria for OC numbers.

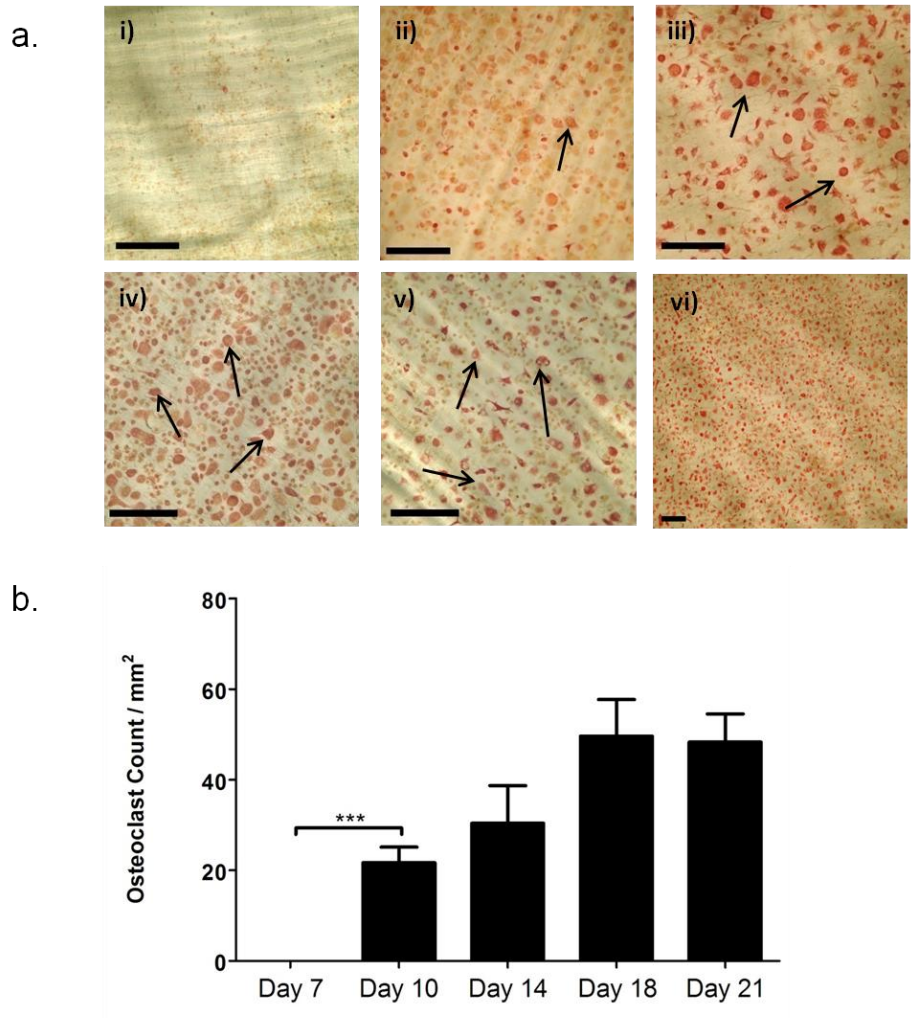

Figure 4.7. Osteoclast Numbers Increase from Day 7 to Day 18 when Cultured in MCSF and RANKL.

PBMCs were extracted from the peripheral blood of pre-menopausal female (n=1, 2 reps per time point). $CD14^+$ cells were positively isolated by magnetic sorting. Cells were plated onto ivory discs and cultured in MCSF and RANKL for 7 – 21 days. At experiment end-point cells were stained and $TRAP^+$ multinucleated OC counted. (a) Representative pictures (at x10 magnification) of i) day 7, ii) day 10, iii) day 14, iv) day 18 v) day 21 OC cultures and vi) day 21 at x4 magnification. Arrows indicate OC. A significant increase in (b) OC numbers was observed between days 7 and 10 (*** *P*=<0.01), with OC numbers increasing up to day 18. Scale bar = 250µm. Statistical analysis was performed using a Mann-Whitney test.

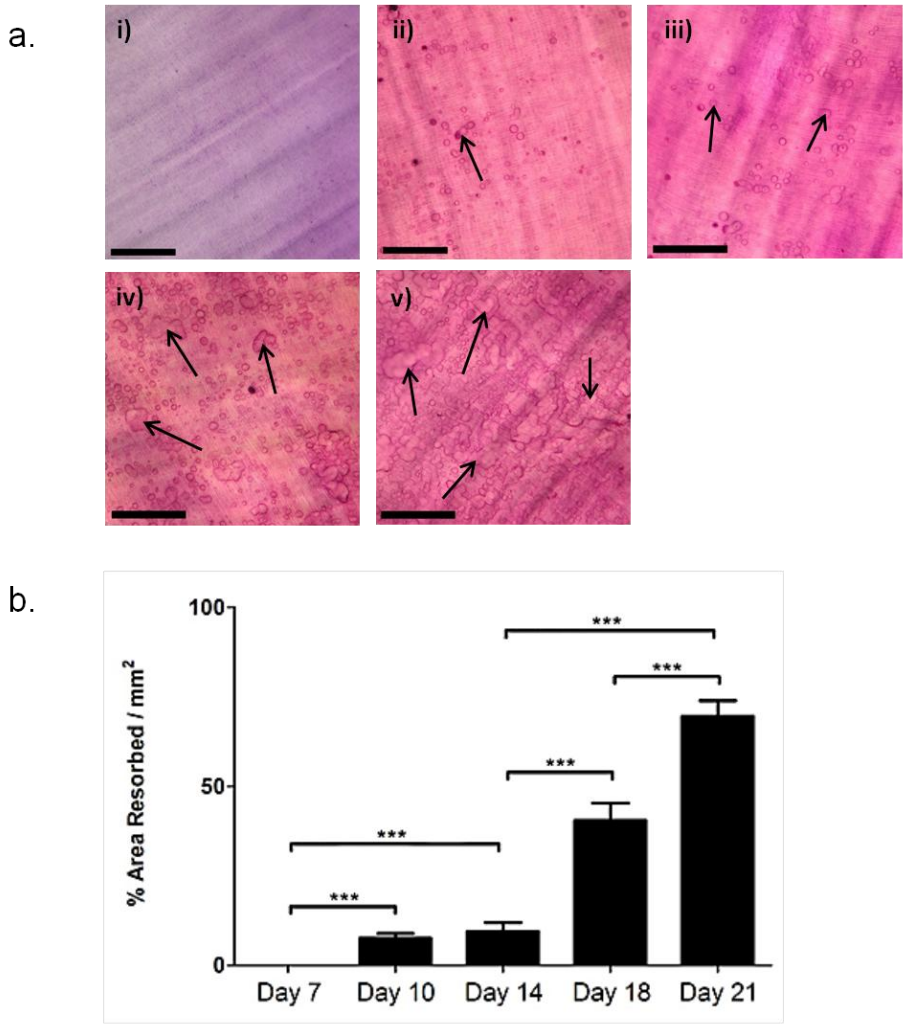

Figure 4.8. Osteoclast Resorption Increases from Day 7 to Day 21.

PBMCs were extracted from the peripheral blood of pre-menopausal female (n=1, 2 reps per time point). $CD14^+$ cells were positively isolated by magnetic sorting. Cells were plated onto ivory discs and cultured in MCSF and RANKL for 7 – 21 days. At experiment end-point cells were removed and discs stained with toluidine blue. (a) Representative pictures of i) day 7, ii) day 10, iii) day 14, iv) day 18 and v) day 21 resorption. Arrows indicate resorption pits. (b) % area resorbed was calculated. A significant increase in area resorbed was observed between days 7 and 10, 7 and 14, 14 and 18, 14 and 21 and 18 and 21 (***P=<0.01). Scale bar = 250µm. Statistical analysis was performed using a Mann-Whitney test.

4.2.7 **Assessing the Impact of TL1A Dose upon the Development of Osteoclasts on Ivory**

In order to assess the impact of TL1A on OC formation and resorptive function, subsequent assays were performed on ivory and terminated on day 14. As only modest effects of TL1A were observed at 10ng/ml an additional dose of 100ng/ml was investigated (methodology is described in section 2.2.10.2 and Fig 2.9). OC were detected in all cultures containing RANKL at days 7, 10 and 14. No OC were observed in control cultures (MCSF±TL1A; Fig 4.9). The total number of cells per mm^2 (mean±SEM) for each disc is presented graphically in Fig 4.10 (a) for control cultures and Fig 4.10 (b) for OC cultures. At day 7 in control cultures, cells expanded in MCSF in the presence or absence of TL1A; cell numbers were 0ng/ml TL1A=534±70 versus 10ng/ml TL1A=736±84 versus 100ng/ml TL1A=537±83. These did not change significantly over time. The total number of cells at day 7 in OC cultures was 518±33. This was comparable to the OC cultures with 10ng/ml TL1A (582±31) and 100ng/ml TL1A (569±26). Over the remaining time points assessed no significant difference within or between groups were detected. Differential counts were performed where $TRAP^+$ OC reported as OC per mm^2 (mean±SEM) showed TL1A to have a dose-dependent effect (Fig 4.10 (c)). At day 7 no significant difference was detected between the cultures (0ng/ml TL1A=5±1 versus 10ng/ml TL1A=6±1 versus 100ng/ml TL1A=7±1). OC numbers were observed to be increased in the 10ng/ml TL1A cultures and significantly in the 100ng/ml TL1A cultures at day 10 (0ng/ml TL1A=8±1 versus 10ng/ml TL1A=10±1 versus 100ng/ml TL1A=9±1, P=<0.05) and day 14 (0ng/ml TL1A=7±1 versus 10ng/ml TL1A=11±1 versus 100ng/ml TL1A=12±2, P=<0.05) when compared to cultures without TL1A. This translated into a significant increase in OC numbers across the time course in both the 10ng/ml TL1A cultures (P=<0.01) and the 100ng/ml TL1A cultures (P=<0.0001). No significant difference in OC number was detected between the 10ng/ml and 100ng/ml TL1A cultures.

4.2.8 **Assessing the Impact of TL1A Dose upon Osteoclast Resorptive Function**

TL1A has been demonstrated to increase OC formation. To assess whether TL1A affected OC resorptive function the area of the ivory disc resorbed was measured. Data was expressed as the % area resorbed (mean±SEM) for graphical presentation (Fig 4.11). Low levels of resorption were detected at day 7 in all cultures (0ng/ml TL1A=0.4±0.4%,

10ng/ml TL1A=0.6±0.2% and 100ng/ml TL1A=0.7±0.2%). At day 10 levels of resorption were observed to increase in the cultures containing TL1A (0ng/ml TL1A=0.9±0.3%, 10ng/ml TL1A=1.8±0.4% and 100ng/ml TL1A=1.6±0.4%). At day 14 a dose-dependent effect was observed with significantly increased resorption observed in cultures containing 10ng/ml and 100ng/ml TL1A, compared to those without (0ng/ml TL1A=1.3±0.3%, 10ng/ml TL1A=2.8±0.4% and 100ng/ml TL1A=5.2±1.6%, *P*=<0.001). This translated into a significant increase in % area resorbed across the time course in both the 10ng/ml TL1A cultures (*P*=<0.0001) and the 100ng/ml TL1A cultures (*P*=<0.01).

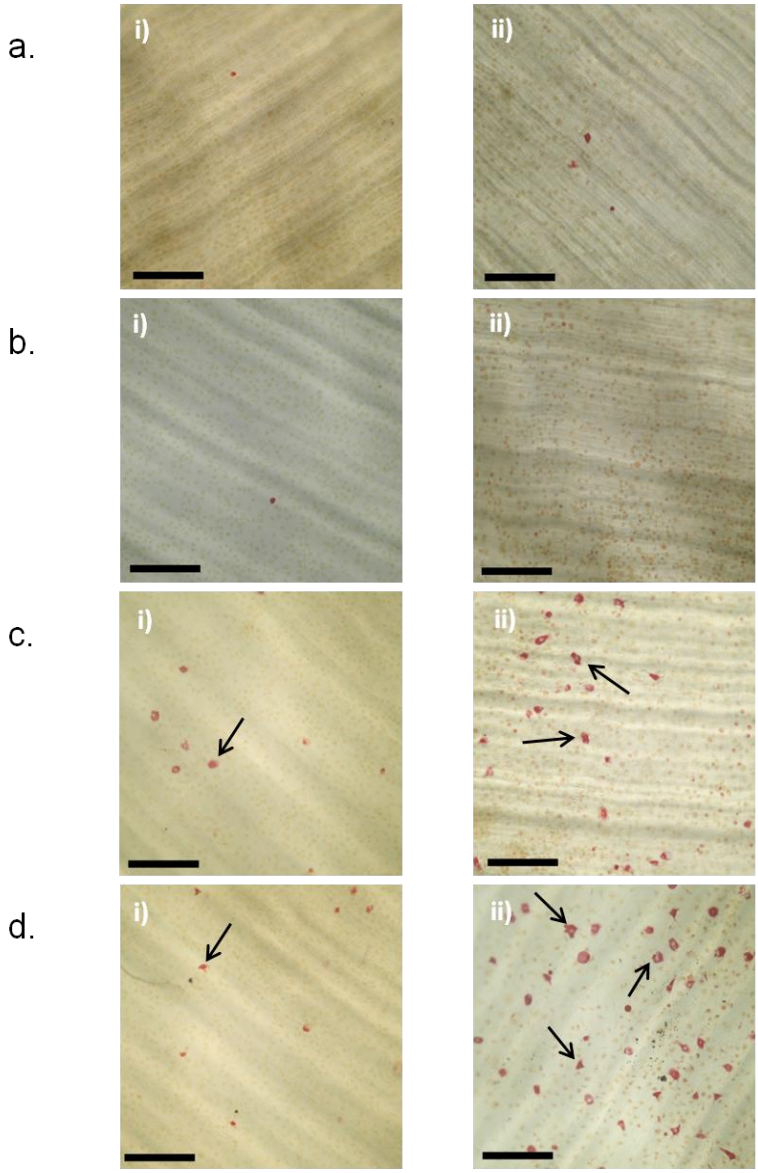

Figure 4.9. TRAP Stained Cells on Ivory Discs.

PBMCs were extracted from the peripheral blood of pre-menopausal females (n=6). $CD14^{+}$ cells were positively isolated by magnetic sorting. Cells were plated onto ivory discs (day -7) and cultured in MCSF for 7 days and DR3 expression confirmed (day 0). Cells were differentiated for a further 7, 10 or 14 days in MCSF±TL1A or MCSF and RANKL±TL1A at 10ng/ml or 100ng/ml. At experiment end-points cells were stained for TRAP. Representative pictures of (a) MCSF (b) MCSF+TL1A (100ng/ml) (c) MCSF+RANKL and (d) MCSF+RANKL+TL1A (100ng/ml) cultures at i) day 7 and ii) day 14. Arrows indicate OC. Scale bar = 250µm.

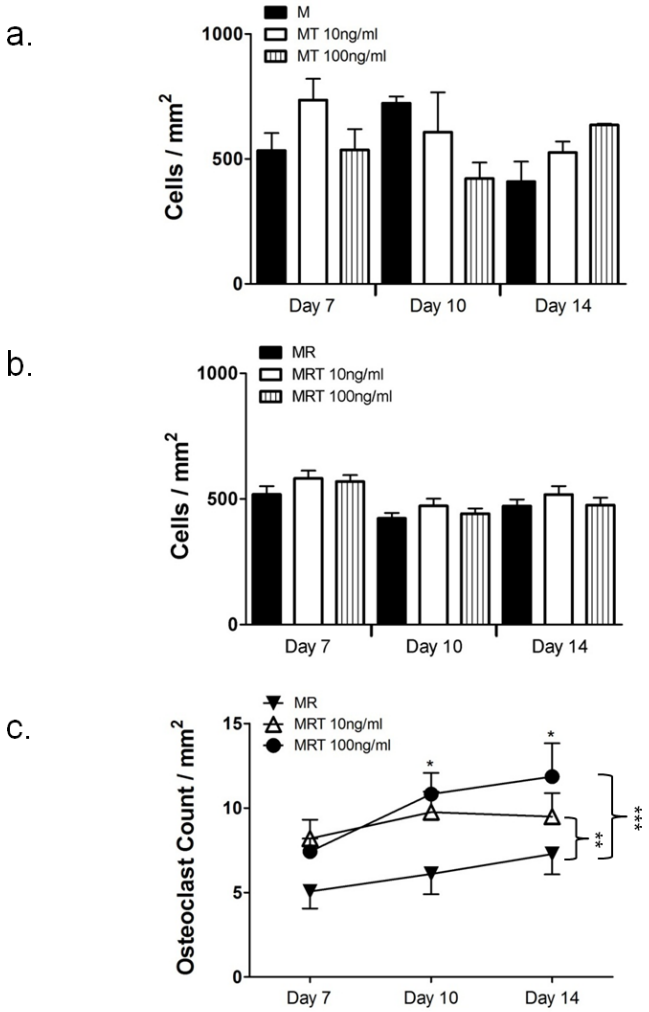

Figure 4.10. TL1A has No Effect on Total Cell Number in Control or Osteoclast Cultures. TL1A Significantly Increases Osteoclast Number in Osteoclast Cultures.

PBMCs were extracted from the peripheral blood of pre-menopausal females (n=6, 2 reps per condition). $CD14^+$ cells were positively isolated by magnetic sorting. Cells were plated onto ivory discs (day -7) and cultured for 7 days in MCSF and DR3 expression confirmed (day 0). Cells were differentiated for a further 7, 10 or 14 days in MCSF±TL1A (M/MT) or MCSF+RANKL±TL1A (MR/MRT) at 10ng/ml or 100ng/ml. At experiment end-points cells were stained for TRAP and total cell number in (a) control cultures and (b) OC cultures counted. Addition of TL1A had no effect on total cell number in control or OC cultures. (c) OC numbers in OC cultures were determined. A significant increase in OC numbers was observed in the 10ng/ml (**P=<0.01) and the 100ng/ml (***P=<0.0001) TL1A cultures across the time course. A significant increase in OC numbers was detected at day 10 (*P=<0.05) and day 14 (*P=<0.05) in the 100ng/ml TL1A cultures over cultures without TL1A. Statistical analysis was performed using a 2-way ANOVA and Bonferroni post test.

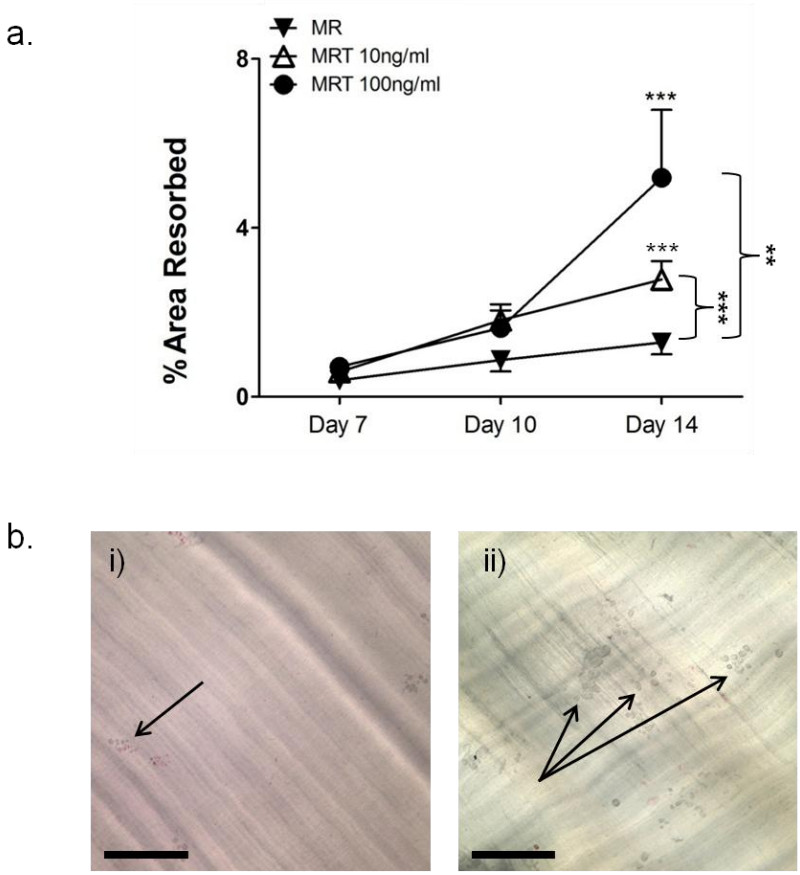

Figure 4.11. TL1A Significantly Increases Osteoclast Resorptive Function.

PBMCs were extracted from the peripheral blood of pre-menopausal females (n=6, 2 reps per condition). $CD14^+$ cells were positively isolated by magnetic sorting. Cells were plated onto ivory discs and cultured for 7 days in MCSF and DR3 expression confirmed (day 0). Cells were differentiated for a further 7, 10 or 14 days in MCSF+RANKL±TL1A (MR/MRT) at 10ng/ml or 100ng/ml. At experiment end-points discs were stained with toluidine blue, resorption pits analysed and (a) % area resorbed calculated. A significant increase in % area resorbed was observed in the 10ng/ml (***P=<0.0001) and 100ng/ml (**P=<0.01) TL1A cultures across the time course. A significant increase in resorption was detected at day 14 in cultures containing TL1A (***P=<0.0001) over cultures without TL1A. (b) Representative pictures of resorption at day 14 in i) MR and ii) MRT 100ng/ml cultures. Arrows indicate areas of resorption. Scale bar = 250µm. Statistical analysis was performed using a 2-way ANOVA and Bonferroni post test.

4.2.9 **Assessing the Impact of TL1A Dose upon Chemokine Production**

To explain the increase in OC formation observed in section 4.2.7, levels of the chemokines CXCL8, CCL2 and CCL3 were measured in control and OC culture supernatants (mean±SEM).

4.2.9.1 CXCL8

Stimulation of the macrophage cell line THP-1 with TL1A has been shown by Su et al (240) and Kang et al (278) to induce expression of CXCL8. To determine whether the same effect is observed in primary macrophages and OC cultures, levels of CXCL8 were measured. Levels of CXCL8 in control cultures (Fig 4.12 (a, i)) were found to be unaffected by the addition of TL1A. Levels were observed to be highest at day 0 (8.6±1.8ng/ml) dropping across the time course to their lowest point at day 10 (0ng/ml TL1A=2.3±0.5ng/ml versus 10ng/ml TL1A=1.8±0.3ng/ml versus 100ng/ml TL1A=3.0±1.5ng/ml). Levels of CXCL8 in OC cultures (Fig 4.12 (a, ii)) were highest at day 0 (9.0±0.8ng/ml) and fell across the time course to day 10 (0ng/ml TL1A=1.6±0.3ng/ml versus 10ng/ml TL1A=1.8±0.3ng/ml versus 100ng/ml TL1A=1.9±0.6ng/ml). No significant differences were detected in CXCL8 levels between the OC cultures.

4.2.9.2 CCL2

Analysis of murine OC culture supernatants in chapter 3 demonstrated that TL1A acts upon CCL2 expression, significantly reducing levels across the time course. In contrast to this result work by Su et al (240) and Kang et al (278) showed that stimulation of THP-1 cells with TL1A had no effect on CCL2 levels. TL1A was found to have no effect on CCL2 levels in control cultures (Fig 4.12 (b, i)) across the time course. Addition of TL1A had no effect on CCL2 expression in OC cultures (Fig 4.12 (b, ii)) with levels peaking at day 7 (0ng/ml TL1A=25.7±3.7ng/ml versus 10ng/ml TL1A=28.8±4.0ng/ml versus 100ng/ml TL1A=26.6±5.0ng/ml) before dropping at day 10 (0ng/ml TL1A=13.5±3.2ng/ml versus 10ng/ml TL1A=16.1±2.8ng/ml versus 100ng/ml TL1A=16.9±4.3ng/ml).

4.2.9.3 CCL3

Murine OC assay supernatant analysis in chapter 3 showed for the first time that CCL3 expression is affected by TL1A; inducing expression in the C57BL/6 model and reducing expression in the DBA/1 model. Levels of CCL3 in control cultures (Fig 4.12 (c, i)) showed no significant difference within or between groups across the time course. Levels of CCL3 in OC cultures (Fig 4.12 (c, ii)) were observed to increase across the time course, with TL1A

having a dose-dependent effect. Levels of CCL3 at day 0 were measured at 48.2±4.6pg/ml. Levels increased on day 7 (0ng/ml TL1A=70.9±20.1pg/ml versus 10ng/ml TL1A=73.2±16.2pg/ml versus 100ng/ml TL1A=147.6±37.0pg/ml) and day 10 (0ng/ml TL1A=78.0±21.7pg/ml versus 10ng/ml TL1A=101.1±28.8pg/ml versus 100ng/ml TL1A=156.0±56.0pg/ml). At day 14 levels of CCL3 in the 0ng/ml TL1A (79.5±22.4pg/ml) and 10ng/ml TL1A (118.0±35.9pg/ml) cultures continued to increase. A slight decrease was observed in the 100ng/ml TL1A cultures (137.4±20.6pg/ml). CCL3 levels in the 100ng/ml TL1A cultures were found to be significantly increased (*P*=<0.001) across the time course when compared to cultures without TL1A.

4.2.9.4 Correlation of Chemokines with OC Numbers and Resorptive Function

To determine whether OC numbers (Fig 4.13) or % area resorbed (Fig 4.14) are related to the chemokine levels found in the OC culture supernatants Spearman correlation analysis was performed. A significant and positive correlation between CCL3 and OC numbers on day 7 (r=0.53, *P*=<0.01), day 10 (r=0.51, *P*=<0.01) and day 14 (r=0.46, *P*=<0.05) was detected. No correlation was detected between CXCL8 or CCL2 and OC numbers at any of the time points tested. Analysis of % area resorbed and chemokine levels also demonstrated a significant and positive correlation with CCL3 on day 7 (r=0.42, *P*=<0.05), day 10 (r=0.52, *P*=<0.01) and day 14 (r=0.67, *P*=<0.001). No correlation was observed between % area resorbed and CXCL8 and CCL2. The results suggest that CCL3 is driving the increased OC formation and resorptive function observed in the OC cultures containing TL1A.

4.2.10 **Production of Pro-Inflammatory Cytokines TNF and TL1A by Osteoclast Cultures**

Upon activation, OC precursors (macrophages) can endogenously produce the pro-inflammatory cytokines TNF (173), a driver of OC formation and function, and TL1A (254). To ensure that the increase in OC formation and resorptive function observed in sections 4.2.7 and 4.2.8 could be attributed to the exogenous TL1A and not due to TL1A inducing TNF expression (278), levels of the cytokines were measured in supernatant by ELISA. Induction of TNF by TL1A was not demonstrated in any of the cultures tested. Endogenous TL1A was only tested in the MCSF+RANKL cultures. No endogenous TL1A was detected. This result confirms that the observed effects of TL1A are independent of TNF and endogenous TL1A.

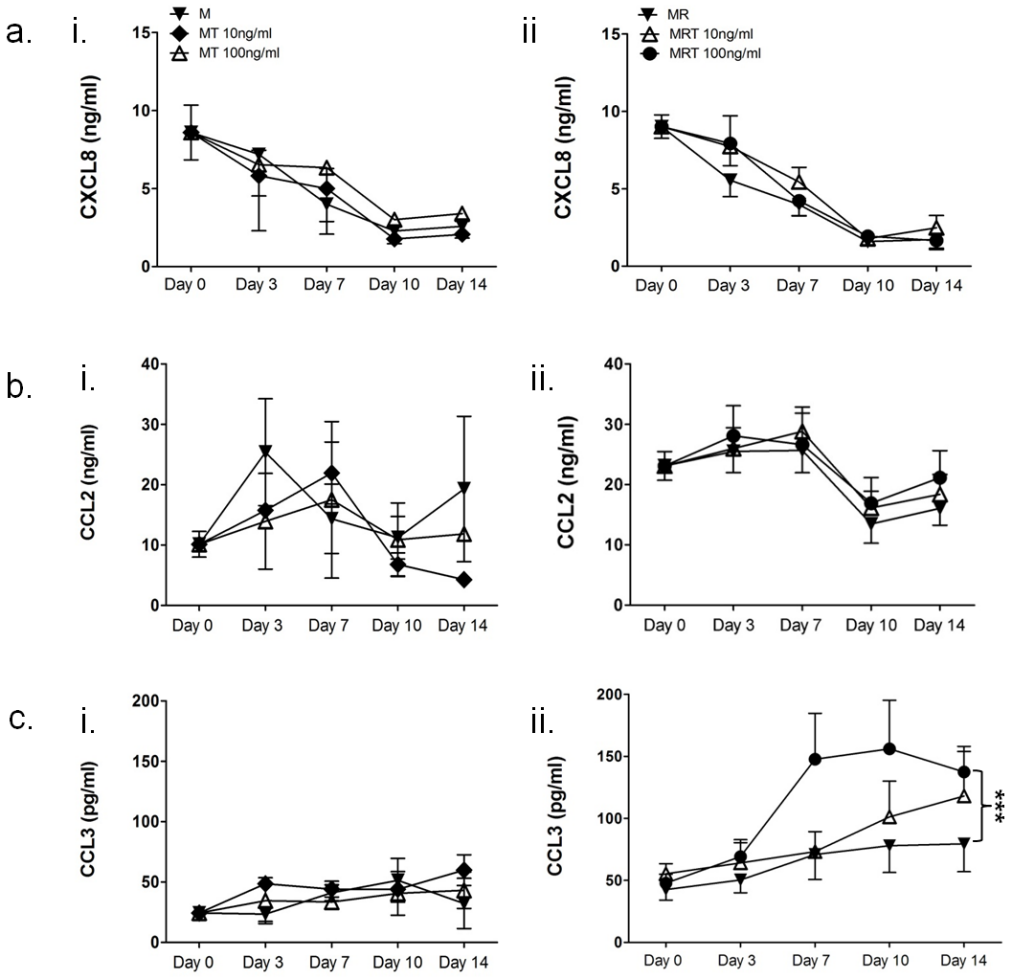

Figure 4.12. TL1A Significantly Increases Levels of the Chemokine CCL3 in Osteoclast Cultures.

PBMCs were extracted from the peripheral blood of pre-menopausal females (n=6, 2 reps per condition). CD14+ cells were positively isolated by magnetic sorting. Cells were plated onto ivory discs (day -7) and cultured for 7 days in MCSF and DR3 expression confirmed (day 0). Cells were differentiated for a further 7, 10 or 14 days in (i) MCSF±TL1A (M/MT) or (ii) MCSF+RANKL±TL1A (MR/MRT) at 10ng/ml or 100ng/ml. Supernatants were collected at the indicated time points and tested for (a) CXCL8, (b) CCL2 and (c) CCL3 by ELISA. A significant increase in CCL3 levels was detected across the time course (***P=<0.001) in 100ng/ml TL1A OC cultures. No significant differences were observed in chemokine expression in control and OC cultures for CXCL8 or CCL2. Statistical analysis was performed using a 2-way ANOVA and Bonferroni post test.

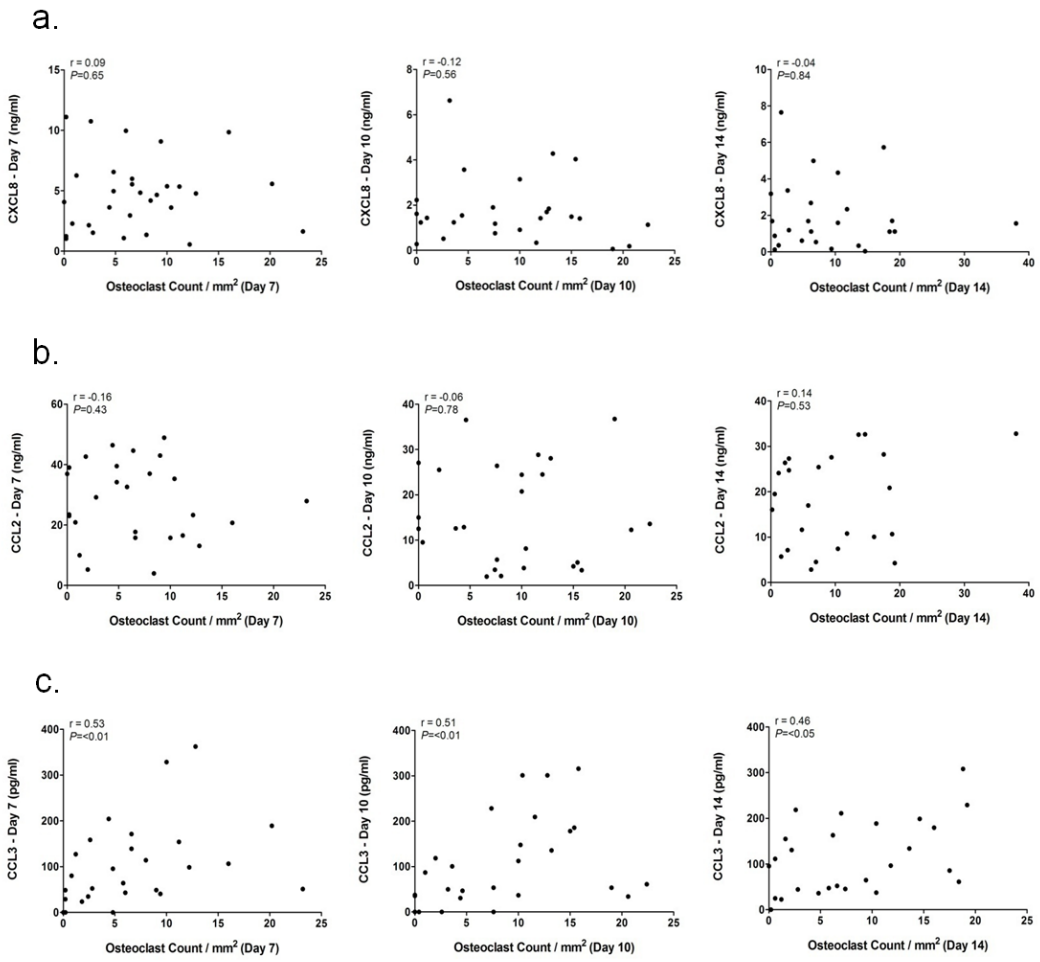

Figure 4.13. Levels of CCL3 in Osteoclast Cultures Significantly Correlates with OC Numbers.

PBMCs were extracted from the peripheral blood of pre-menopausal females (n=6, 2 reps per condition). $CD14^+$ cells were positively isolated by magnetic sorting. Cells were plated onto ivory discs (day -7) and cultured for 7 days in MCSF and DR3 expression confirmed (day 0). Cells were differentiated for a further 7, 10 or 14 days in MCSF and RANKL ± TL1A at 10ng/ml or 100ng/ml. Correlation between OC numbers and (a) CXCL8 levels, (b) CCL2 levels and (c) CCL3 levels were performed for day 7, 10 and 14. Levels of CCL3 were found to significantly correlate with OC numbers on day 7 (***P*=<0.01), day 10 (***P*=<0.01) and day 14 (**P*=<0.05). Statistical analysis was performed using Spearman Correlation.

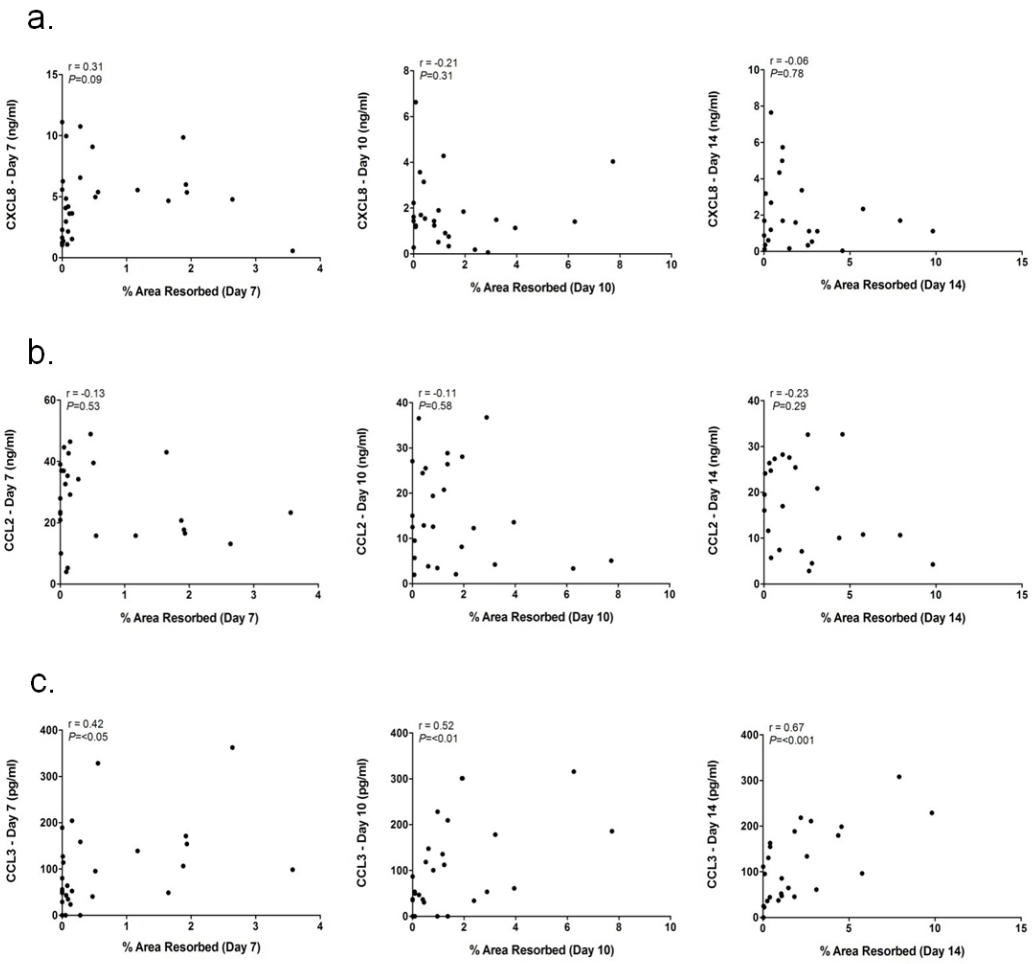

Figure 4.14. Levels of CCL3 in Osteoclast Cultures Significantly Correlates with % Area Resorbed.

PBMCs were extracted from the peripheral blood of pre-menopausal females (n=6, 2 reps per condition). $CD14^+$ cells were positively isolated by magnetic sorting. Cells were plated onto ivory discs (day -7) and cultured for 7 days in MCSF and DR3 expression confirmed (day 0). Cells were differentiated for a further 7, 10 or 14 days in MCSF and RANKL±TL1A at 10ng/ml or 100ng/ml. Correlation between % area resorbed and (a) CXCL8 levels, (b) CCL2 levels and (c) CCL3 levels were performed for day 7, 10 and 14. Levels of CCL3 were found to significantly correlate with % area resorbed on day 7 (*P=<0.05), day 10 (**P=<0.01) and day 14 (**P=<0.001). Statistical analysis was performed using Spearman Correlation.

4.2.11 **Assessing the Impact of TL1A Dose upon Total MMP-9 Expression**

To explain the increase in OC function levels of total MMP-9 were measured in OC culture supernatants by ELISA (mean±SEM, section 2.2.14.4.1). Levels of total MMP-9 (Fig 4.15 (a)) increased from day 0 (3.9±0.4µg/ml) to day 7 (0ng/ml TL1A=4.9±0.7µg/ml versus 10ng/ml TL1A=6.2±0.9µg/ml versus 100ng/ml TL1A=6.0±0.5µg/ml). A decrease was detected in all cultures at day 10 (0ng/ml TL1A=3.2±0.5µg/ml versus 10ng/ml TL1A=3.5±0.4µg/ml versus 100ng/ml TL1A=5.2±0.8µg/ml) followed by an increase in expression at day 14 (0ng/ml TL1A=4.8±1.1µg/ml versus 10ng/ml TL1A=5.2±0.5µg/ml versus 100ng/ml TL1A=7.5±1.0µg/ml). TL1A was observed to have a dose-dependent effect on total MMP-9 levels. A significant increase in total MMP-9 expression, across the time course, was detected in the 100ng/ml TL1A cultures compared to the 10ng/ml TL1A cultures (P=<0.05) and the cultures without TL1A (P=<0.001).

Comparison of total MMP-9 levels at day 14 with % area resorbed showed a significant correlation (Spearman r = 0.5, P=<0.01; Fig 4.15 (b)), inferring that TL1A is driving total MMP-9 expression and thus OC function.

4.2.12 **Levels of Pro and Active MMP-9 in OC Cultures**

While TL1A was shown to increase levels of total MMP-9, the ELISA used was unable to distinguish between the pro and active forms. To determine whether addition of TL1A increased levels of active MMP-9, a gelatine zymogram (section 2.2.14.4.1) was used to semi-quantitatively measure the levels of both pro and active MMP-9 in OC culture supernatants ±TL1A 100ng/ml (Fig 4.16). Levels of pro MMP-9 (Fig 4.17 (a)) detected at day 0 in cultures with and without TL1A were measured as 0.7±0.2ng/ml. These did not vary greatly over time with the exception of day 3; levels of pro MMP-9 in cultures without TL1A were observed to increase (1.2±0.4ng/ml) while levels of pro MMP-9 in the 100ng/ml TL1A cultures decreased (0.5±0.1ng/ml). A significant increase in active MMP-9 was detected across the time course in the cultures containing 100ng/ml TL1A (P=≤0.01; Fig 4.17 (b)). This significant increase in active MMP-9 across the time course was due to levels being detected in the 100ng/ml TL1A cultures from day 3 onwards (0ng/ml TL1A=0.0±0.0ng/ml versus 100ng/ml TL1A=0.07±0.06ng/ml), compared to day 7 in cultures without TL1A (0ng/ml TL1A=0.05±0.02ng/ml versus 100ng/ml TL1A=0.07±0.03ng/ml). From day 7 onwards levels of active MMP-9 did not differ significantly.

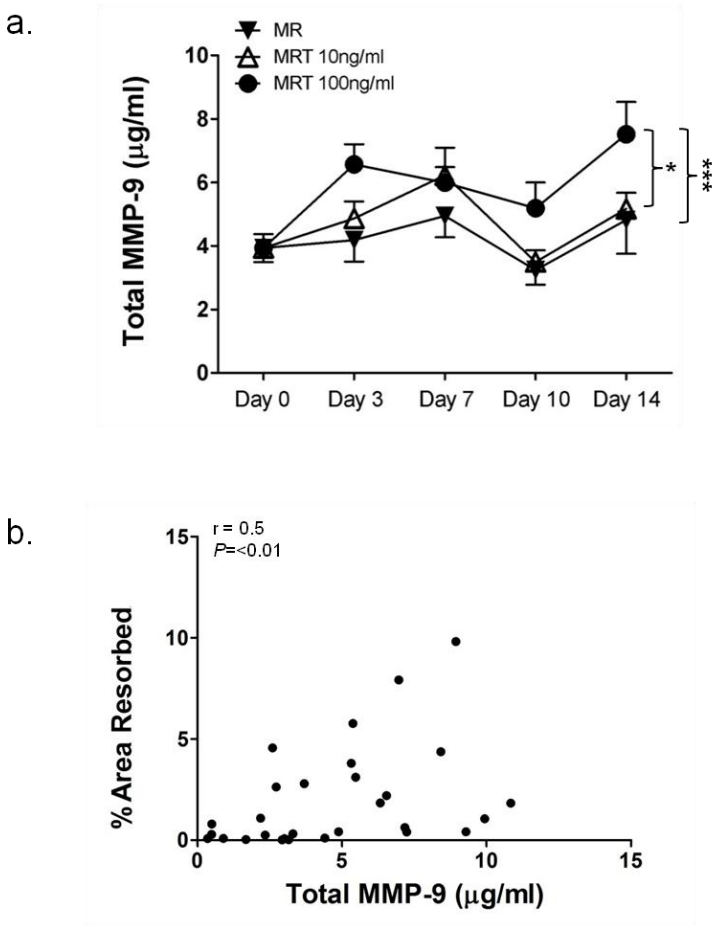

Figure 4.15. TL1A Significantly Increases Levels of Total MMP-9 in Osteoclast Cultures.

PBMCs were extracted from the peripheral blood of pre-menopausal females (n=6, 2 reps per condition). CD14+ cells were positively isolated by magnetic sorting. Cells were plated onto ivory discs and cultured for 7 days in MCSF and DR3 expression confirmed (day 0). Cells were differentiated for a further 7, 10 or 14 days in MCSF+RANKL±TL1A (MR/MRT) at 10ng/ml or 100ng/ml. Supernatants were collected at the indicated time points and tested for (a) total MMP-9 by ELISA. A significant increase in total MMP-9 was detected across the time course in the 100ng/ml TL1A cultures over the 10ng/ml TL1A cultures (*P=<0.05) and those without TL1A (***P=<0.001). (b) Levels of total MMP-9 were found to significantly correlate (r = 0.5, P=<0.01) with % area resorbed at day 14. Statistical analysis was performed using (a) 2-way ANOVA and Bonferroni post test and (b) Spearman Correlation. .

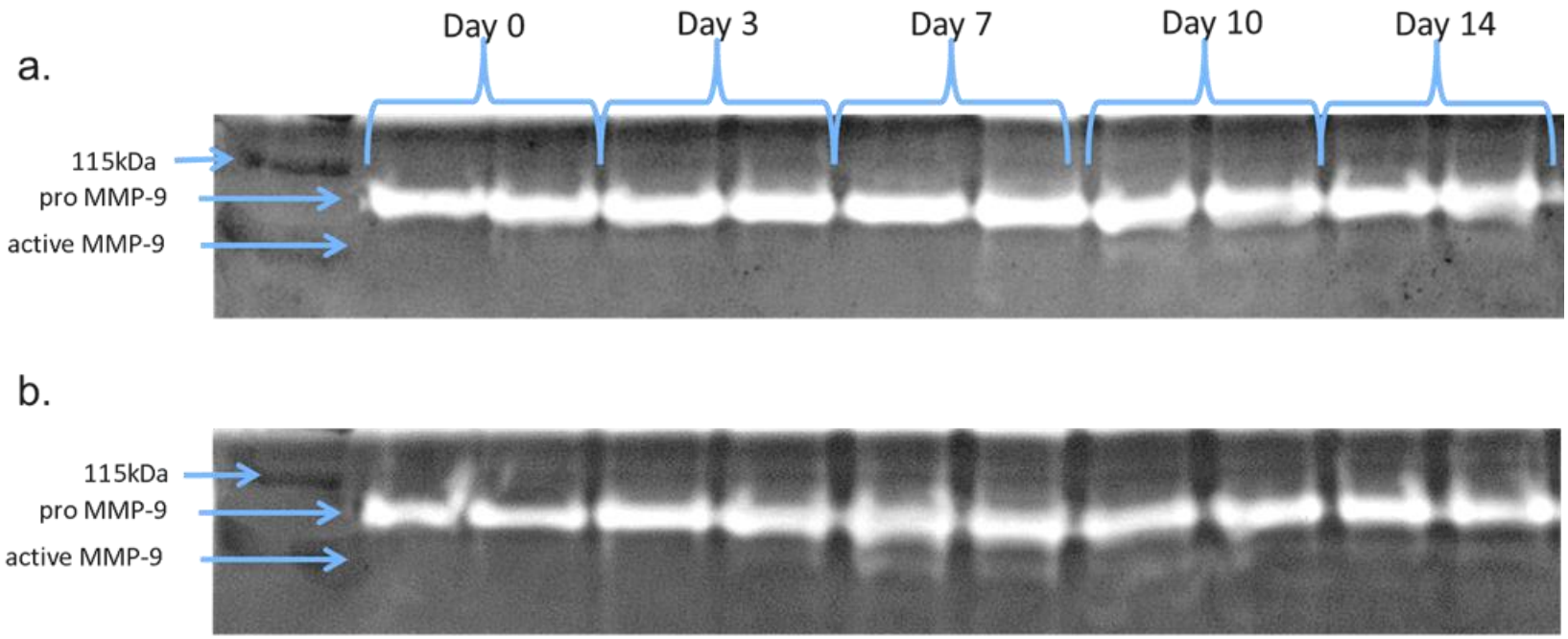

Figure 4.16. Levels of Pro and Active MMP-9 in Osteoclast Cultures.
Supernatants from osteoclast cultures were tested for levels of pro MMP-9 and active MMP-9 by gelatine zymography (n=4). Representative zymogram for (a) MR cultures. Pro MMP-9 (approx. 92kDa) was detected at all time points. Active MMP-9 (approx. 82kDa) was detected from day 7 onwards. Representative picture of (b) MR + TL1A 100ng/ml cultures. Pro MMP-9 was detected across the time course. Active MMP-9 was detected from day 3 onwards. A standard of MMP-9 at 10ng/ml was run on each gel.

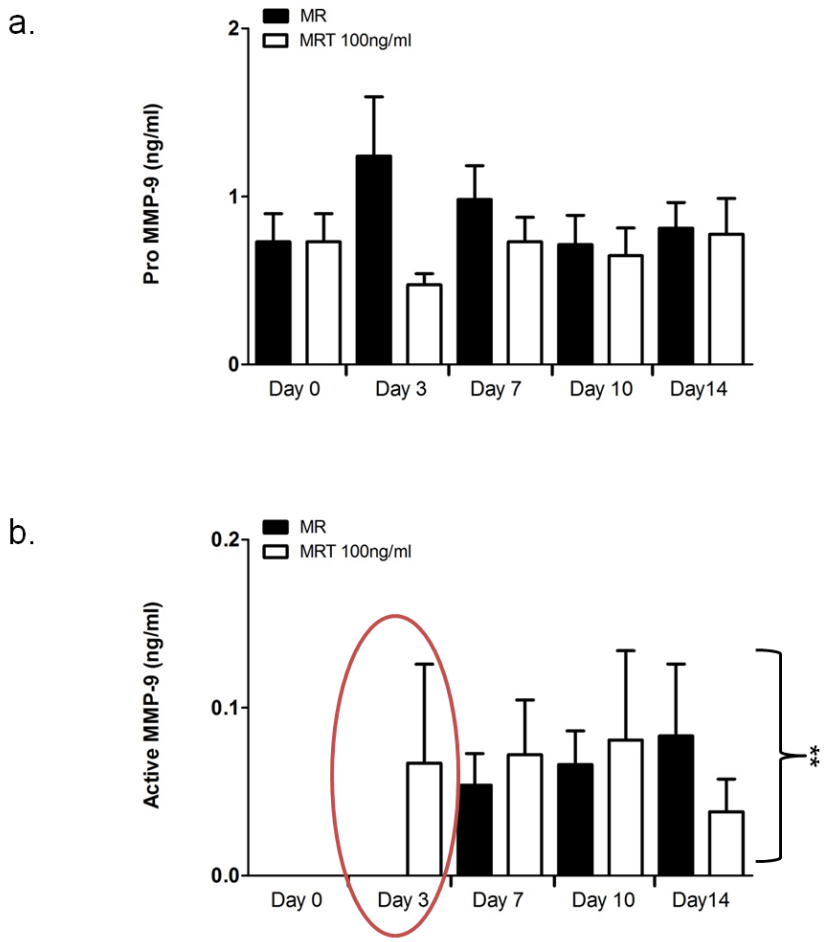

Figure 4.17. TL1A Increases Levels of Active MMP-9 in Osteoclast Cultures.

Supernatants were tested for levels of (a) pro MMP-9 and (b) active MMP-9 by gelatine zymogram. Levels were calculated semi-quantitatively using a standard at known concentration (10ng/ml). No significant difference was observed in pro MMP-9 levels. Active MMP-9 was detected earlier in cultures containing 100ng/ml TL1A. A significant increase (**$P \leq 0.01$) in active MMP-9 was observed in cultures supplemented with 100ng/ml TL1A across the time course. Statistical analysis was performed using a 1-way ANOVA.

4.3 **Discussion**

Comparison of $DR3^{wt}$ and $DR3^{ko}$ OC, and the effects of TL1A on OC differentiation and function in chapter 3 illustrated the possible roles that this receptor and ligand play in OC biology. Use of a murine model demonstrated that DR3 has an important role in OC resorptive function as very little resorption was observed in $DR3^{ko}$ cultures. Problems with the murine model however, were discovered when investigating the effect of TL1A. Using two different strains of mouse TL1A was found to produce opposing effects on OC differentiation; in a DBA/1 model TL1A reduced OC numbers while in a C57BL/6 model TL1A enhanced OC numbers. These differences led to the question: which, if either, was representative of what would happen in a human system. The study of TL1A and OC biology in a human system also provides a number of additional advantages over the murine model. A limiting factor in the murine system was the lack of specific reagents; e.g. antibodies for the detection of TL1A, specific monoclonal antibodies for the detection of DR3 and non-destructive methods for the detection of Cathepsin K, all of which are available for a human system. Current work into the effect of TL1A on human OC is very limited. Bull, Williams et al (242) are the only group who have investigated the effects of exogenous TL1A on OC differentiation *in vitro*. Their study showed that exogenous TL1A added to PBMC cultures significantly enhanced OC formation. Analysis of these results requires care, as there were limitations affecting the study. Firstly, only two repetitions of the experiment were carried out and so natural variation in response to TL1A between donors may have been missed. Secondly, osteoclastogenesis assays were carried out using PBMCs rather than isolated monocytes / macrophages. For this reason it is not clear whether the TL1A was acting upon the OC precursors directly or indirectly via T-cells. Thirdly, the mechanism through which DR3/TL1A signalling enhanced OC formation was not investigated. The aim of this chapter was to investigate whether, in a human system, TL1A could act directly upon OC precursors, what effect TL1A would have upon OC differentiation and function and the mechanisms involved.

The most abundant source of OC precursors can be found in the bone marrow however, ethical and practical difficulties mean that this is not a suitable source for a human system. Work by Fujikawa et al (331) demonstrated that *in vitro* $TRAP^+$ OC could be differentiated from circulating human monocytes ($CD14^+$, $CD11b^+$ and $HLA\text{-}DR^+$), though the exact subset was not clear. Human peripheral blood consists of two major subsets of monocyte, $CD16^+$ ($CX3CR1^{hi}CD14^{lo}CD16^{hi}CD11b^+CD11c^+CCR2^-CD62L^-$) and $CD16^-$

($CX3CR1^{lo}CD14^{hi}CD16^{-}CD11b^{hi}CCR2^{+}CD62L^{+}$), comprising 5-10% and 90-95% of the monocytes respectively (32, 332). Comparison of the $CD16^{-}$ and the $CD16^{+}$ monocyte subsets by Komano et al (39) found that only the $CD16^{-}$ subset differentiated into OC while the $CD16^{+}$ subset responded to RANKL by increasing expression of TNF and IL-6. The data shows that the $CD16^{-}$ subset of peripheral blood monocytes can be used as a source of OC precursors, though to be isolated from the $CD16^{+}$ monocytes a positive marker has to be chosen. Isolation of monocytes by the marker CD14, which has high expression on $CD16^{-}$ monocytes, has been shown to enhance osteoclastic bone resorption 2-4 fold compared to un-fractionated PBMCs (38). This demonstrates that CD14 can be used as a marker to isolate the subset of monocytes in the peripheral blood that are OC precursors.

An alternative to primary cells for the study of OC differentiation and function is the use of cell lines. Cell lines provide an almost unlimited supply of cells with similar genotypes and phenotypes. Their use avoids variation between individuals and bypasses ethical issues associated with human assays (333). A number of cell lines have been utilised for studying OC differentiation; these include the human pre-osteoclast cell line FLG 29.1 (334, 335), the monoblastic cell line UG3 (336, 337) and the monocyte cell line THP-1 (338, 339). Care must be taken when using cell lines however, as there are a number of limitations. As the cells have undergone a mutation to become immortal they may retain very little of the original *in vivo* characteristics of the cell that they are meant to represent, meaning that they have low biological relevance to the organism being studied. Low levels of variation between experiments, due to the homogeneity of the cells, also means that the data is not representative of the general population and could not be extrapolated out. For these reasons investigation into the effect of TL1A on human OC differentiation and function used primary cells ($CD14^{+}$ monocytes). This enabled levels of variation between individuals to be established and ensured that the results were as relevant to what occurs *in vivo* as possible

For the analysis of the effect of TL1A on human osteoclast differentiation and function a purified $CD14^{+}$ population was chosen over a PBMC population. Use of a purified $CD14^{+}$ population allowed for the specific analysis into the effects of TL1A on OC precursors and determination of the mechanisms involved; eliminating any possible indirect effects of TL1A on osteoclastogenesis through T cells (58, 230, 248) and other PBMCs. Flow cytometry, a powerful and accurate method for the analysis of cell types via the expression of cell surface markers, was used to determine the purity of the $CD14^{+}$ cells

isolated from the PBMCs. Initial attempts at isolation of $CD14^+$ cells from PBMCs generated a population that was only 30% pure, with the remaining 70% being composed of other PBMCs. Following improvement of the method the purity of the $CD14^+$ population was increased to $\geq$90%, consistent with the purity obtained by other groups using the same method (340, 341). Following culture in MCSF for 7 days the $CD14^+$ purity of the cell population was observed to slightly increase, though a small percentage of $CD14^-$ cells (less than 10%) were still present in the cultures. Histological analysis of the $CD14^+$ isolated cells showed that they had a monocytic morphology; 10 - 20µm in diameter with a kidney shaped nucleus (330). These results demonstrate that a highly pure mono-cellular population of monocytes can be obtained through positive selection of the marker CD14. The expression of DR3 on these cells was then investigated.

Expression of DR3 on primary human monocytes / macrophages and the macrophage cell line THP-1 has been shown by Su et al (240), Kang et al (278) and McLaren et al (270). However, the expression on primary human monocytes / macrophages was linked to activation of the cells by the pro-inflammatory cytokine TNF, bacterial LPS (278) or differentiation in RPMI medium for 6 – 7 days (240, 270, 278). To analyse the effect of TL1A on OC differentiation and function confirmation of DR3 expression on the $CD14^+$ cells isolated from the PBMCs was required. Flow cytometry upon $CD14^+$ cells obtained from the PBMC fraction revealed no DR3 expression. This data supports the observation made by Kang et al (278) that DR3 was not constitutively expressed on circulating monocytes. Whether expansion of monocytes in MCSF is sufficient to stimulate DR3 expression in $CD14^+$ cells has not been previously determined. $CD14^+$ cells were therefore cultured for a 7 day period in MCSF and 3 support matrices were tested (glass, plastic and ivory). Expression of membrane bound DR3 was detected (by flow cytometry) on day 7 on cells cultured on both plastic and ivory; though which splice variant of DR3 the JD3 antibody detects is unknown. DR3 was not detected on cells cultured on glass. Time points after day 7 were not investigated, so it cannot be ascertained as to whether there is a delay in DR3 expression on cells grown on glass or if they will never express DR3. The lack of DR3 expression on cells cultured on glass provides an explanation for the glass assay results in chapter 3, where no difference was observed between the $DR3^{wt}$ and $DR3^{ko}$ cultures following addition of TL1A. The failure of cells cultured on glass to induce DR3 expression meant that the $DR3^{wt}$ cells are effectively the same as the cells in the $DR3^{ko}$ cultures. TL1A is therefore unable to act upon the cells and have any effect on OC formation. The reasons for the differential substrate-dependent expression of DR3 are

not entirely clear. Saltel et al (309) demonstrated that osteoclasts grown on a glass substrate spread more than OC grown on an apatite substrate (mean surface area of approx. 14000μm^2 versus 3000μm^2). The podosome belt formed during the process of OC spreading enabled them to adhere to the glass surface however, the OC were unable to form a sealing zone. An explanation for the lack of sealing zone is provided by work by Nakamura et al (342) who suggests that actin ring formation is substrate-dependent. These data suggest that monocytes / macrophages will express DR3 when grown in MCSF and supported by an appropriate matrix. This may be particularly important when macrophages / monocytes are recruited to sites of bone resorption, informing them of their departure from the peripheral circulation and arrival at the bone surface. Having confirmed CD14$^+$ cells express membrane bound DR3 following culture in MCSF on a suitable substrate, the effect of TL1A on differentiation was investigated.

Initial work into the effect of TL1A on OC differentiation was performed using a plastic substrate. High levels of DR3 expression were observed on CD14$^+$ cells cultured on this substrate, so if TL1A was to have an effect then a difference should be observed between cultures. Studies generating OC from CD14$^+$ cells on plastic and ivory (or similar substrates such as dentine and bone) have used widely ranging levels of the recombinant cytokines MCSF and RANKL. Concentrations of RANKL used ranged from 3ng/ml to 100ng/ml (37, 343-348); as with the mouse recombinant cytokines this was dependent on the source of the cytokine and the levels required to induce OC differentiation. Levels of MCSF, required for cell proliferation and RANKL-induced osteoclastogenesis, ranged from 10ng/ml to 50ng/ml (37, 343-348). Again this was dependent on the supplier of the cytokine and ensuring that it was not a limiting factor in the experiment. In this study the concentrations of MCSF and RANKL used (5ng/ml and 5ng/ml) were taken from the supplier ED_{50} (effective dose at which the protein exhibits 50% of its maximum effect) and work previously carried out in the laboratory. No difference was observed in total cell number between cultures with and without TL1A across the time course. This would suggest that in this system, TL1A is not involved in the expansion of cells. However, as the experiment was only taken to 5 days, it cannot be ascertained whether this member of the TNFSF would increase the survival of the cells, as observed by Wen et al (246) in the TF-1 cell line. TL1A was found to significantly increase the number of TRAP$^+$ mononuclear cells and TRAP$^+$ multinucleated OC across the time course, demonstrating that TL1A can act directly on monocytes / macrophages in a manner similar to TNF, synergistically enhancing RANKL induced OC formation (282, 283). The results from this experiment

supported the work by Bull, Williams et al (242), that TL1A enhances OC formation, while showing for the first time that it does this via acting directly on the precursor cells. To determine the mechanism through which TL1A was enhancing the formation of OC, culture supernatants were analysed.

As discussed in section 1.3.5 chemokines are messengers that act upon OC precursors, inducing their migration from the blood stream to sites of bone resorption and subsequent formation of the multinucleated OC. To date there are no studies that examine the effect of TL1A on CCL2 and CXCL8 production by OC, though some work has been performed with monocytes and macrophages. Kang et al (278) and Su et al (240) demonstrated that TL1A induced CXCL8 expression in THP-1 cells and primary macrophages, though no effect was observed on CCL2 expression.

In the present study TL1A was found to have no effect CCL2 or CXCL8 expression in OC cultures grown on a plastic substrate. The lack of response observed in CCL2 levels is contrary to those observed in the murine cultures in chapter 3 where addition of TL1A significantly reduced CCL2 expression. This may be caused by the difference in substrate (plastic versus ivory) used to perform the assays, or due to a difference in the osteoclastogenic mechanism employed between the two species. However, the result does agree with the study by Su et al (240) who demonstrated that TL1A does not affect CCL2 expression in monocytes or macrophages. The reason for the difference in CXCL8 expression between this study and those by Kang et al (278) and Su et al (240) is unclear. Levels of TL1A used by Kang et al and Su et al (100 – 1μg/ml) were >10 times greater than those used in this study (10ng/ml), raising the possibility that the required signalling threshold to induce CXCL8 expression had not been reached. To address the questions raised in chemokine expression and to study the effect of TL1A on OC resorptive function, subsequent assays were performed on ivory discs; a substrate osteoclasts can recognise and resorb (41). Before any assays were carried out the method for the culture of human OC, on ivory discs, required optimisation.

To study the effect of TL1A on OC differentiation and resorptive function the assay was set-up to obtain a balance between OC numbers and resorptive activity. The time point selected for experiment termination required OC to have been established for at least one earlier time point and for numbers not to have peaked or plateaued. The OC were also required to demonstrate resorptive function on at least one earlier time point. A time point of day 14 was selected for experiment termination as all criteria were met. All

subsequent OC assays on ivory discs were terminated on day 14 of culture with RANKL. To address the contrasting effects of TL1A on CXCL8 expression between this study and those by Kang et al (278) and Su et al (240) a second concentration of 100ng/ml TL1A was also used.

Addition of TL1A to control cultures and OC cultures had no effect on total cell number across the time course. This supports the result observed in the plastic tissue culture plates that, in this system, TL1A is not involved in the proliferation and expansion of OC precursors. While TL1A did not affect total cell number it was observed to have a profound dose-dependent effect on OC number, in OC cultures. This supports the observation by Bull, Williams et al (242) that in PBMC cultures TL1A can enhance osteoclastogenesis, showing for the first time that it does this by acting directly on the $CD14^+$ OC precursors. The effect of TL1A on OC formation is in-line with other members of the TNFSF. Work by Lam et al (282) and Azuma et al (283) demonstrated that TNF (TNFSF2) can enhance OC formation in permissive levels of RANKL, acting directly on the precursor cells. Edwards et al (182) showed that LIGHT (TNFSF14) dose-dependently enhanced RANKL-induced osteoclastogenesis. A difference in the effect of TL1A compared to TNF and LIGHT in the above mentioned studies, however, is the effect on the control cultures. Azuma et al (283), Kobayashi et al (349) and Edwards et al (182) demonstrated that TNF and LIGHT induce OC in the absence of RANKL; while in this study TL1A was unable to induce osteoclastogenesis on its own. A possible explanation for this is that the other studies used PBMCs, so endogenous levels of RANKL would be present in the cultures. Having shown TL1A to have an effect on OC differentiation the effect on osteoclast resorptive function was investigated. TL1A had a dose-dependent effect on the % area resorbed, with a five-fold increase observed in the 100ng/ml cultures over those without. It is not clear from this study whether this increase in resorptive function is a result of the increase in OC numbers or as a result of an increase in the resorptive function of the OC.

To determine the mechanism through which TL1A was driving the increase in OC numbers and resorption, culture supernatants were analysed for soluble mediators. MMP-9 is a gelatinase involved in the degradation of bone by OC (106, 300, 301), whose increase in expression can potentially lead to an increase in area resorbed. This was shown by Grassi et al (350) who demonstrated when OC were grown in the presence of permanent CXCL12 they displayed a two-fold increase in the ability to resorb bone-like material and secreted

increased amounts of MMP-9. Studies by Kim et al (239) and Kang et al (278) have identified MMP-9 expression to be a target of TL1A signalling in the human macrophage THP-1 cell line, while results from chapter 3 demonstrated a role for DR3 in MMP-9 activation. Currently however, it is unknown what affect DR3/TL1A have on MMP-9 expression from human OC. To investigate the effect of TL1A on MMP-9 expression, supernatants were analysed from OC cultures for total MMP-9. TL1A was observed to have a dose-dependent effect on levels of total MMP-9. This result demonstrates for the first time that TL1A effects MMP-9 expression in OC cultures, adding support to the Kang et al (278) study, and providing an important mechanism to explain the increased resorption observed. Further support for the importance of the increase in total MMP-9 as a mechanism for the increase in resorption came from correlation of the two variables. Levels of total MMP-9 were found to significantly correlate with % area resorbed, demonstrating a positive relationship between the two. In chapter 3 DR3 was confirmed to have a role in the activation of murine MMP-9. To verify whether TL1A resulted in an increase in the active form of MMP-9 a gelatine zymogram was employed to measure inactive and active levels across the time course. Addition of TL1A (100ng/ml) to cultures was observed to activate MMP-9 at an earlier time point, leading to a significant increase in levels across the time course. The data shows a novel mechanism for DR3/TL1A signalling in human OC; increasing levels of total MMP-9 and inducing earlier activation of the enzyme.

While MMP-9 has a role in bone resorption, the key enzyme involved in the process is the proteinase Cathepsin K (104, 105). As with the murine assays in chapter 3, commercial methods for the quantitative measurement of CatK levels in culture require the total lysis of cells, releasing the CatK into the supernatant. Immunocytochemistry techniques were developed for staining the actin ring, nuclei and CatK *in situ* in OC cultures (Appendix II). An anti-CatK antibody was tested at a range of concentrations (1µg/ml - 4µg/ml) along with an equivalent isotype control, and binding visualised by counter staining with a FITC-conjugated secondary antibody. The anti-CatK antibody detected the presence of CatK at all concentrations; though levels of detection were observed to increase from 1µg/ml - 3µg/ml. Analysis of the isotype signal showed no non-specific binding at concentrations of 1µg/ml and 2µg/ml, with low levels being detected at 3µg/ml and 4µg/ml. Taken together the results suggested that the optimal concentration of antibody for the visualisation of CatK in OC, *in situ*, was 2µg/ml. The effect of TL1A on CatK expression is unknown and further experimentation would be required to potentially resolve this issue.

Having revealed a potential mechanism through which TL1A is driving the increase in OC resorptive function, the mechanism for the increase in OC formation was investigated.

Levels of endogenously expressed TNF and TL1A were measured in the cultures to ensure that the observed effects could be directly attributed to the exogenously added TL1A. In addition the chemokines CXCL8, CCL2 and CCL3 were measured to determine whether the change in substrate or TL1A concentration affected their expression. The observed effects of TL1A on OC formation in this study were proved to be independent of endogenous TNF and TL1A. Levels of CXCL8 were unaffected by the addition of TL1A in both control and OC cultures. This result supports the earlier observation in the plastic tissue culture plate assays, though again is contrary to that observed by Kang et al (278) and Su et al (240). The reason for the difference in CXCL8 expression between the studies is not clear; but may be down to the concentration of TL1A used or co-stimulation of the cells with IFNγ. Kang et al (278) only observed an increase in CXCL8 expression when a concentration of 250ng/ml TL1A was used in conjunction with IFNγ, while in the Su et al (240) study a level of 1μg/ml TL1A induced a change in CXCL8 expression. This level of TL1A is significantly higher compared to *in vivo* levels, even in a disease state; in RF^+ RA patients mean levels in serum were measured at 7.4±6.8ng/ml, over 100 times lower than that used in the Su et al study.

TL1A was demonstrated to have no effect on CCL2 levels in both control cultures and OC cultures. This result is different to that observed in the murine model in chapter 3, where TL1A led to a reduction in CCL2 levels, but is comparable to the Kang et al (278) and Su et al (240) studies. The difference in the human and murine model suggests a difference in the mechanisms through which TL1A effects osteoclastogenesis. This is not without precedent as there are a number of discrepancies between the immune system of mouse and man (351), highlighting again the caution that should be taken when extrapolating the data from one model to the other.

In contrast to CXCL8 and CCL2, TL1A was observed to have a dose-dependent effect on CCL3 expression in OC cultures with a significant increase observed in the 100ng/ml TL1A cultures across the time course. This supports the observation in chapter 3 that CCL3 expression is a target of TL1A signalling. This result, taken with the observations by Choi et al (87) and Han et al (88), suggests that the TL1A-induced increase in CCL3 is responsible for the increase in OC numbers observed. To prove this hypothesis however, an anti-CCL3 add back experiment would be required to determine whether OC numbers

could be returned to base-line in the 100ng/ml TL1A cultures, thus proving that the increase in CCL3 is the responsible factor. Levels of CCL3 in the control cultures were unaffected by TL1A, showing baseline expression. This shows that the increase in CCL3 expression by TL1A is a RANKL-mediated effect. Correlation of chemokine levels and OC numbers provides further evidence for the role of TL1A-induced CCL3 expression in enhancing osteoclastogenesis. Levels of CCL3 were found to significantly and positively correlate with OC numbers and % area resorbed on day 7, 10 and 14; no correlation was observed with levels of CXCL8 and CCL2. While correlation does not directly identify cause and effect it does demonstrate that the effects observed between TL1A-induced CCL3 expression, the increase in OC numbers and the % area resorbed are related.

4.4 **Conclusion**

At the conclusion of this chapter the following objectives were met:

- $CD14^+$ cells were isolated from human PBMCs and the purity defined.
- DR3 expression on OC pre-cursors was determined.
- An *in vitro* assay for the generation of OC from $CD14^+$ cells on plastic and ivory was developed.
- TL1A's effect on OC formation and resorptive activity was determined and the mechanism identified.

Results from the human osteoclast assays revealed a key role for TL1A in osteoclast biology. While its receptor DR3 was found not to be constitutively expressed on circulating $CD14^+$ monocytes / macrophages (OC pre-cursors), it could be induced *in vitro* by culture in the presence of MCSF on a plastic or ivory substrate. TL1A was proved to have a significant role in osteoclast differentiation and resorptive function, significantly increasing osteoclastogenesis and osteoclast resorptive function in a dose-dependent manner. For the first time in a human system TL1A was found to dose-dependently affect levels of the chemokine CCL3, total MMP-9 and active MMP-9 in OC cultures, providing a potential mechanism through which it drives increased OC formation and resorptive activity. The data has also shown that these effects on OC differentiation and resorptive function are independent of the cytokine TNF or endogenous TL1A. These results highlight the DR3/TL1A pathways as regulators of OC differentiation and activity. However, whether DR3/TL1A have a role in the pathogenesis of diseases characterised by hyper OC activity is currently unknown and will be investigated in chapter 5.

Chapter 5

Investigating the Role of DR3/TL1A in Human Bone-Related Disease

5.1 **Introduction**

In Chapter 4 the effect of TL1A upon OC differentiation from human precursor cells was analysed and its impact upon *in vitro* OC function quantified. TL1A increased OC numbers and promoted resorptive function in a DR3- and dose- dependent manner. Biological responses attributed to DR3 and TL1A were discovered through *in vivo* studies into the pathogenesis of a number of inflammatory conditions for instance: inflammatory bowel disease (254, 263) and psoriasis (269). Whether DR3 and TL1A are implicated in the pathology of diseases associated with OC hyper-activity, such as the inflammatory arthritides and post-menopausal osteoporosis (OP), has not been established. In this chapter the potential impact of DR3 and TL1A upon the adverse bone pathology associated with human diseases such as rheumatoid arthritis (RA) and osteoporosis are explored.

A number of diseases are characterised by phenotypic OC hyper-activity that leads to focal bone erosions, generalised reduction in bone mineral density and systemic osteoporosis. These diseases included both inflammatory arthritides such as RA (352, 353), the spondyloartritides (ankylosing spondylitis (AS) (354) and psoriatic arthritis (PsA) (355)), as well as non-inflammatory conditions such as OP (52, 197) and Paget's disease of bone (356). The exact aetiology of these diseases are unknown and very likely different. However, evidence from recent studies implies that the DR3/TL1A pathway is implicated in disease pathogenesis. In the last year Konsta et al (267) demonstrated that TL1A levels in ankylosing spondylitis were 2.6-fold higher in anti-TNF treatment-naïve patients (581±175.5pg/ml) compared to healthy controls (226.7±48.24pg/ml). The association between DR3/TL1A and RA is stronger and has been reported several times in the literature (264-266). Finally, work by Bamias et al (3) demonstrated an increase in DR3 levels in psoriatic skin lesions compared with healthy controls; and that TL1A expression was primarily localised to keratinocytes and macrophages. Whilst these studies were not linked to the pathology of psoriatic arthritis, TL1A could well contribute to the development of skin lesions and/or joint pathology associated with PsA. Well designed, clinical studies are required to prove this conclusively. In this proof-of-concept study, archived serum samples were used to identify inflammatory arthritides potentially modulated by TL1A.

The greatest number of samples available had been collected from cohorts of RA patients. RA is a disease characterised by persistent inflammation of multiple joints and infiltration by immune cells (171). The uncontrolled inflammatory response leads to structural changes within the joint: hyperplasia of the synovial lining and damage to cartilage and bone. While the factors that trigger the onset of RA are unknown, members of the TNFSF certainly play critical roles in its pathogenesis (180-182, 357, 358). Levels of RANKL (TNFSF11) (180), TNF (TNFSF2) (181) and LIGHT (TNFSF14) (182, 183) have all been shown to be up-regulated in the serum and synovial tissue of RA patients, compared to healthy controls. The importance of RANKL in osteoclast formation and resorptive activity is well established (15, 16, 60). Studies by Thomson et al (184), Kudo et al (185) and Edwards et al (182) demonstrated that TNF and LIGHT were also able to act either independently or synergistically with RANKL to increase OC formation and function. This data highlights the importance of the TNFSF in RA pathogenesis. The association between DR3/TL1A and RA was first established in 2004 by Osawa et al (265). He revealed that duplication of the DR3 gene was more prevalent in RA patients than healthy individuals. Bamias et al (264) and Zhang et al (266) subsequently showed that TL1A levels were elevated five-fold (4.55±5.96ng/ml versus 0.89+0.86ng/ml) in RA patient serum (264) and increased (up to 600pg/ml versus 0pg/ml) in RA synovial fluid (266). The functional significance of raised TL1A levels in RA was not studied, although Bamias et al (264) suggested that TL1A could constitute a measure of disease activity. Currently there is a body of published data that supports a pathogenic role for TL1A in RA (264-267, 269), however there is no such foundation for OP. For this reason, in the second part this chapter, osteoclastogenesis by the TL1A pathway was evaluated in precursor cells isolated from OP patient blood samples. TL1A expression was also quantified in serum specimens.

OP is a disease defined by a generalised low bone mineral density (BMD), which leads to an increased risk of fracture (187). The decrease in BMD can be unproblematic. However, osteoporotic fracture can lead to a loss of mobility, increased morbidity and eventual mortality (192). The aetiology and pathogenesis of osteoporotic fractures are not fully defined. A major contributing factor is an imbalance in the bone remodelling process, where bone resorption exceeds bone formation. How this relates to the *in vivo* pathogenesis of the disease, the mechanisms which drive it and the potential implications for fracture formation and repair have barely been considered. However, given the post-menopausal status of the majority of OP patients with fractures; oestrogen deficiency is considered a primary cause (359, 360). Studies by D'Amelio et al (200, 201) also

demonstrated an up-regulation of the TNFSF members RANKL (0.32 – 2.0pg/ml versus 0.036 – 0.14pg/ml) and TNF (53 - 178.25pg/ml versus 32.9 - 53.7pg/ml) in osteoporotic PBMC cultures compared to post-menopausal controls. This suggests that changes in expression of the TNFSF may contribute to the imbalance in bone remodelling and increased risk of fracture associated with OP. The role of DR3/TL1A in fracture and OP has not been previously studied. The proof-of-concept study in this chapter will provide the first evidence assessing whether changes in expression of DR3 and / or TL1A are associated with fracture and / or OP. Evidence will be provided via recruitment and comparison of three post-menopausal patient cohorts: non-osteoporotic with / without fracture and osteoporotic with fracture.

The aims of this chapter were two-fold. Firstly, to analyse levels of TL1A in serum of patients with different forms of arthritis. Secondly, to determine whether expression of DR3 and / or TL1A are altered in the pathogenesis of fracture and / or OP. The specific objectives are listed below:

- To measure TL1A levels in serum from patients with rheumatoid arthritis, psoriatic arthritis, osteoarthritis (OA) and healthy controls.
- To analyse TL1A levels in seropositive and seronegative RA patient serum.
- To determine the effect of anti-TNF treatment on serum TL1A levels in RA patients.
- To investigate whether serum TL1A levels are linked to erosive RA.
- To obtain ethical approval for the collection and analysis of blood samples from 3 cohorts of treatment-naïve, post-menopausal patients
- To recruit sufficient patients from 3 defined cohorts (up to a maximum of 15 patients per group) for this proof-of-concept study. These were defined as:-:
    1. Patients without osteoporosis or fracture (OP^-Frac^-)
    2. Patients without osteoporosis but with fracture (OP^-Frac^+)
    3. Patients with osteoporosis and fracture (OP^+Frac^+)

- To measure TL1A and TNF levels in serum samples collected from the three patient groups.
- To isolate and culture sufficient $CD14^+$cells (osteoclast precursor cells) from 45 ml of patient blood samples and define DR3 expression.
- To design and conduct osteoclast differentiation assays with adequate replicates and controls for statistical evaluation to fulfil the aim of the chapter.
- To measure the effect of TL1A upon $CD14^+$ precursor cells isolated from the three groups of post-menopausal patient (above) in osteoclast differentiation assays.

5.2 Results

5.2.1 Assessing Serum TL1A Levels in Patients with Arthritis

Levels of TL1A were measured in the serum of patients with the following arthritides: RA (n=75), PsA (n=11) and OA (n=5). Serum obtained from healthy volunteers was used as normal controls (n=12). Results (reported as mean±SEM) are presented graphically in Fig 5.1 (a)). TL1A was detected in serum from all four patient cohorts, though levels were observed to vary within and between groups. Levels were significantly elevated in the RA cohort (1.99±0.3ng/ml, min=0ng/ml and max=14.2ng/ml; *P*=<0.05). A small, but non-significant, increase was observed in the PsA cohort (0.43±0.2ng/ml, min=0ng/ml and max=1.67ng/ml). TL1A levels in normal controls was consistently low (0.23±0.02ng/ml, min=0.16ng/ml and max=0.34ng/ml). Serum concentration of TL1A in the OA cohort (0.23±0.2ng/ml. min=0ng/ml and max=0.85ng/ml) was not significantly different from controls.

5.2.2 Analysing Levels of TL1A in Rheumatoid Arthritis Rheumatoid Factor Subgroups

Rheumatoid factor (RF) was measured in RA patient serum by ELISA (section 2.2.15.2). RA patient samples were sub-divided into two groups according to their rheumatoid factor status (i.e. positive (RF^+; $\geq$ 20units/ml) or negative (RF^-; < 20units/ml)). TL1A levels measured in section 5.2.1 were analysed to determine whether the presence of RF affected serum concentration. Results are reported as mean±SEM in Figure 5.1 (b). Levels of TL1A were significantly elevated in the RF^+ group (2.83±0.5ng/ml) compared to the RF^- group (0.42±0.1ng/ml; *P*=<0.01) and normal controls (0.23±0.02ng/ml; *P*=<0.01). There was no difference between the RF^- subgroup and normal controls. A significant correlation between TL1A and RF was detected (r =0.70, *P*=<0.0001).

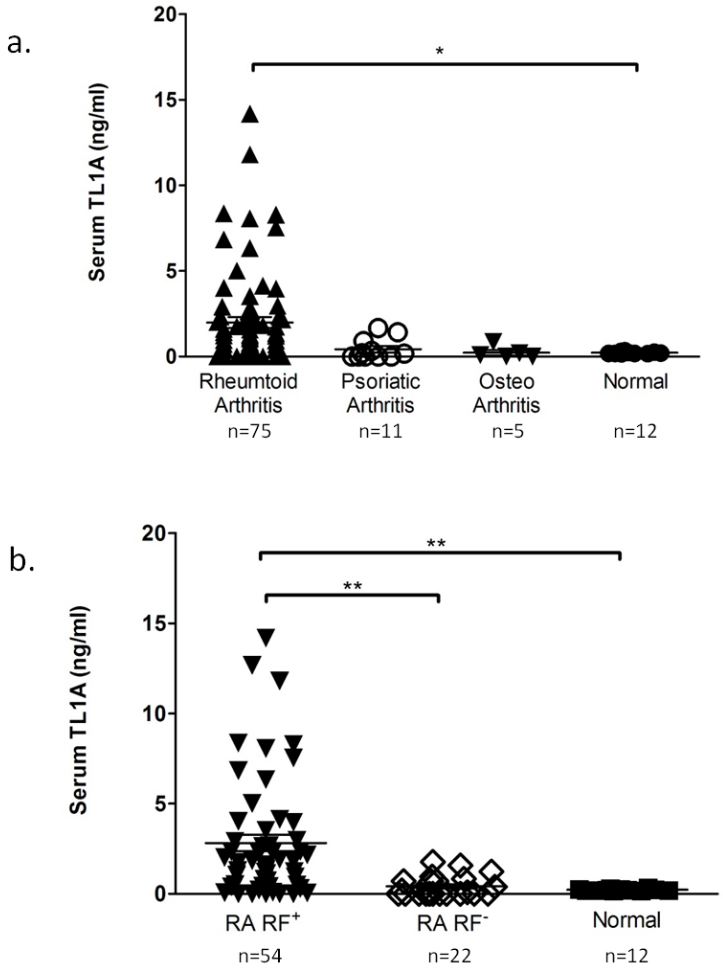

Figure 5.1. Serum TL1A is Significantly Elevated in Rheumatoid Factor$^+$ Rheumatoid Arthritis Patients

Serum was obtained from arthritis patients and healthy controls. Levels of TL1A was measured in the serum by ELISA. (a) TL1A was significantly elevated in RA serum over healthy controls. (*P=<0.05). (b) Grouping of RA patients into rheumatoid factor positive (RF^+) or rheumatoid factor negative (RF^-) demonstrated significantly elevated levels of TL1A in the RF^+ cohort, compared to the RF^- cohort (**P=<0.01) and healthy controls (**P=<0.01). Statistical analysis was performed with a One-way ANOVA with Bonferroni post test.

5.2.3 **Determining the Effect of Anti-TNF Treatment on Serum TL1A Levels in Rheumatoid Arthritis**

To determine whether anti-TNF treatment affects serum TL1A levels, RA patient samples from section 5.2.2 (RF^+ and RF^-) were divided into two groups: patients treated with TNF antagonists versus standard disease-modifying anti-rheumatic drugs (DMARDs). A small, but non-significant reduction in TL1A was observed in the RF^+ anti-TNF patient cohort (anti-TNF=2.33±0.6 versus DMARDs=3.40±0.7ng/ml). TL1A levels in the RF^- patients treated with TNF antagonists also demonstrated a slight, non-significant, reduction compared to those treated with DMARDs (anti-TNF=0.36±0.1 versus DMARDs=0.49±0.2ng/ml; Fig 5.2 (a)). Serum TL1A levels were significantly lower in the RF^- anti-TNF cohort compared to the RF^+ anti-TNF cohort (*P*=<0.05).

5.2.4 **Assessing TL1A Levels in Erosive and Non-Erosive Rheumatoid Arthritis**

To determine whether TL1A levels were linked to erosive status, RA samples from section 5.2.2 were grouped depending on the radiological presence of erosive disease at the time of sampling. TL1A levels were significantly elevated in RF^+ samples displaying erosive disease (4.34±1.0ng/ml; *P*=<0.01) compared to non-erosive disease (2.00±0.6ng/ml). No significant difference was observed in the RF^- subgroup (erosive=0.39±0.1ng/ml versus non-erosive=0.1±0.1ng/ml; Fig 5.2 (b)).

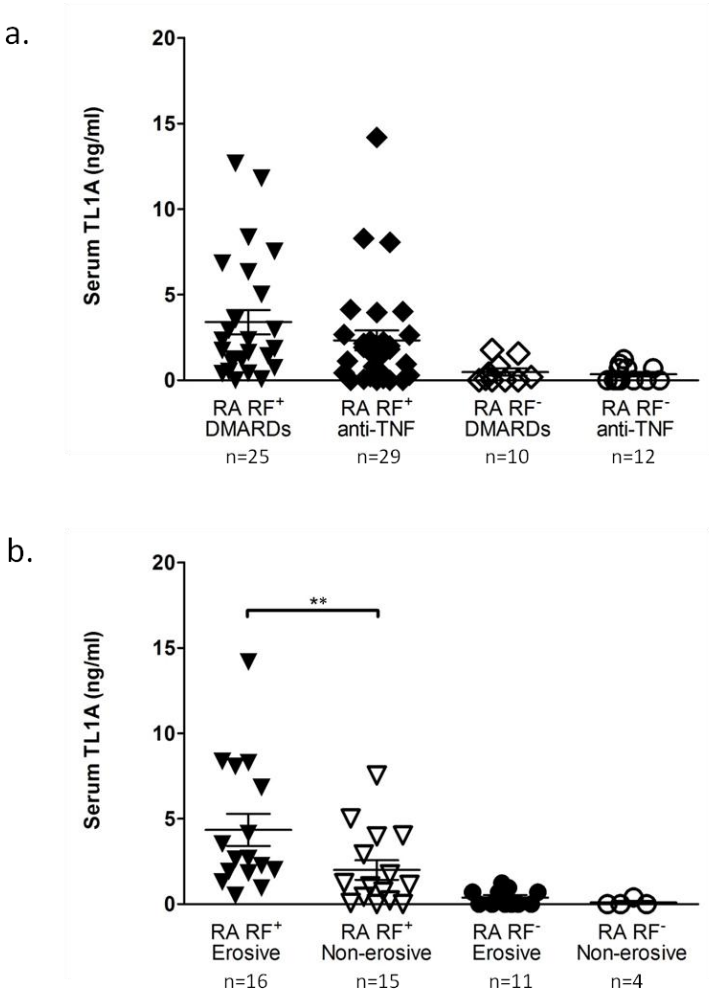

Figure 5.2. Anti-TNF Treatment has no Effect on Serum TL1A Concentrations. Serum TL1A is Significantly Elevated in RF+ Patients with Erosive Disease

Serum was obtained from RA patients. Patients were grouped according to (a) treatment and (b) erosive status at time of sampling. No difference in serum TL1A was detected between patients receiving anti-TNF treatment and DMARDs. Levels of TL1A were found to be significantly elevated in RF+ patients displaying erosive disease (**P=<0.01). Statistical analysis was performed with a One-way ANOVA with Bonferroni post test.

5.2.5 **Assessing TL1A and TNF Levels in Serum from Three Cohorts of Post-Menopausal Patients**

TL1A and TNF concentration were measured by ELISA in serum harvested from blood samples obtained in clinic. Three groups of post-menopausal women who presented in fracture clinic were studied; those with osteoporosis and recent fracture (OP^+Frac^+, n=3), those without osteoporosis but with recent fracture (OP^-Frac^+, n=6) and those without osteoporosis and fracture (OP^-Frac^-, n=6). Patients were recruited to the study based on the following inclusion / exclusion criteria:

Inclusion criteria

- Attending for first bone density scan; Adult; Female; Post-Menopausal

Exclusion criteria

- Recent fracture (in the past 3 months); History of corticosteroid use (except inhaled or topical) or anti-TNF therapy; Patients with known seropositive rheumatoid arthritis, inflammatory bowel disease; Recent history of continuous treatment with bisphosphonate, calcitonin, Strontium ranelate or parathyroid hormone (i.e. for more than 3 months); Patients with known primary hyperparathyroidism; Currently taking part in another study.

Levels of TL1A (mean±SEM; Fig 5.3) were elevated in patients with fracture (OP^-Frac^- =47.2±29.0pg/ml versus OP^-Frac^+=90.8±4.5pg/ml and OP^+Frac^+=103.1±2.3pg/ml), though this difference was not significant. The presence of OP had no significant effect on serum TL1A levels. TNF was not detected in the OP^-Frac^-, OP^-Frac^+ and OP^+Frac^+ serum samples as levels were below the limit of detection for the ELISA (8pg/ml).

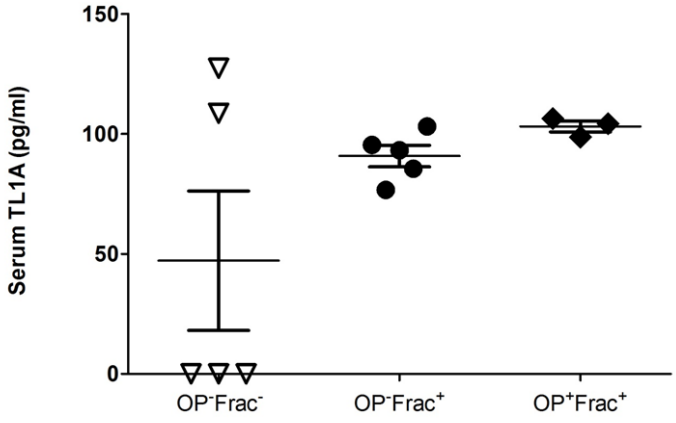

Figure 5.3. Serum TL1A is Elevated in the +Fracture Patient Cohorts.

Serum was obtained from the peripheral blood of the patient cohorts. Levels of TL1A were measured by ELISA. Levels of serum TL1A were observed to be elevated in the +fracture patient cohort samples, though this difference was not significant. Statistical analysis was performed using a 1-way ANOVA and Bonferroni post test.

5.2.6 **Defining Baseline Expression of CD14 and DR3 on Freshly Isolated Patient-Derived $CD14^+$ Cells**

Expression of CD14 and DR3 on freshly isolated $CD14^+$ cells from three cohorts of post-menopausal patients was assessed by flow cytometry (section 2.2.8); OP^-Frac^-, OP^-Frac^+ and OP^+Frac^+. Expression is represented graphically as fold increase in MFI relative to the isotype control (mean±SEM; Fig 5.4). High levels of variation in CD14 expression was detected within the OP^+Frac^+ cohort. The presence of fracture had no significant effect on CD14 expression: OP^-Frac^-=7.7±1.9 versus OP^-Frac^+=4.1±1.0. Comparison between the fracture cohorts demonstrated no significant effect of osteoporosis on CD14 expression: OP^-Frac^+=4.1±1.0 versus OP^+Frac^+=16.4±8.1. DR3 was not expressed on freshly isolated $CD14^+$ cells from the post-menopausal patient cohorts (Fig 5.4 (b)).

5.2.7 **Assessing Expression of CD14 and DR3 on Patient-Derived $CD14^+$ Cells after 7 Days Culture in MCSF**

Patient-derived $CD14^+$ cells were isolated (day -7) and cultured on ivory for 7 days in medium supplemented with MCSF. Expression of CD14 (Fig 5.5 (a)) varied greatly within each group. Comparison of CD14 expression (fold increase relative to isotype; mean±SEM) between the cohorts without osteoporosis demonstrated no significant effect of fracture (OP^-Frac^-=11.1±4.2, OP^-Frac^+=11.3±3.1). Osteoporosis also had no significant effect on CD14 expression (OP^-Frac^+=11.3±3.1 and OP^+Frac^+=11.8±8.2). Expression of DR3 (Fig 5.5 (b)) was only detected on one patient sample (OP^-Frac^+, 1.8-fold increase). No significant difference in DR3 expression was detected between the patient cohorts.

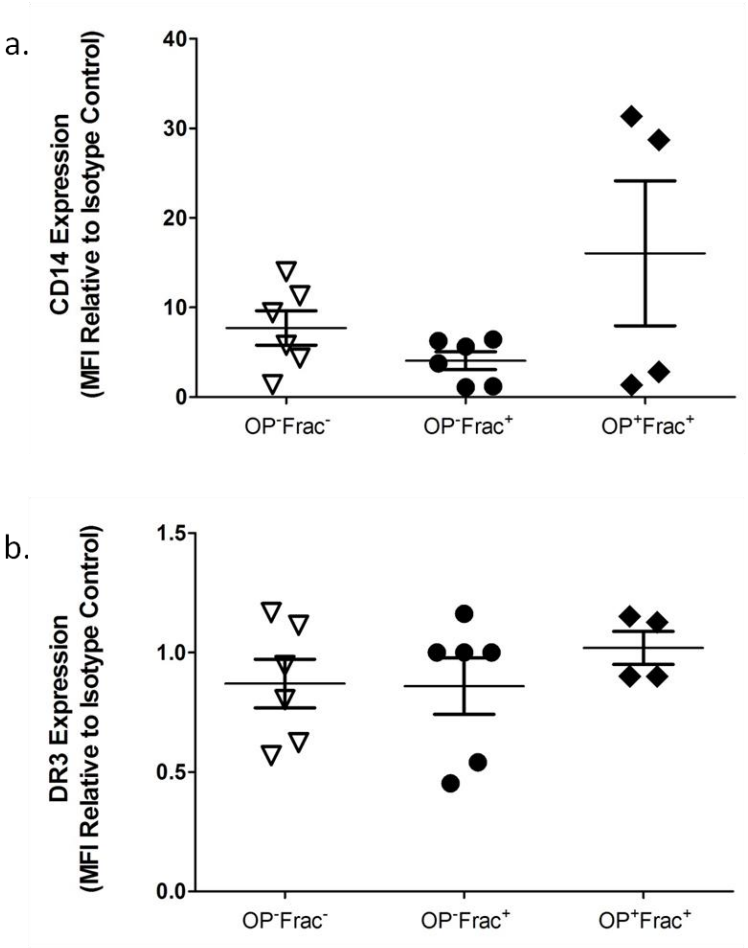

Figure 5.4. Expression of CD14 and DR3 on Patient-derived CD14⁺ Cells.

PBMCs were extracted from the peripheral blood of the patient cohorts and CD14⁺ cells isolated by magnetic sorting. Cells were stained with either an isotype control or with an anti-human CD14 / DR3 antibody and analysed by flow cytometry. MFI was calculated relative to the isotype control for (a) CD14 and (b) DR3. No significance in CD14 expression was detected between the groups. No DR3 expression was detected. Statistical analysis was performed with a One-way ANOVA with Bonferroni post test.

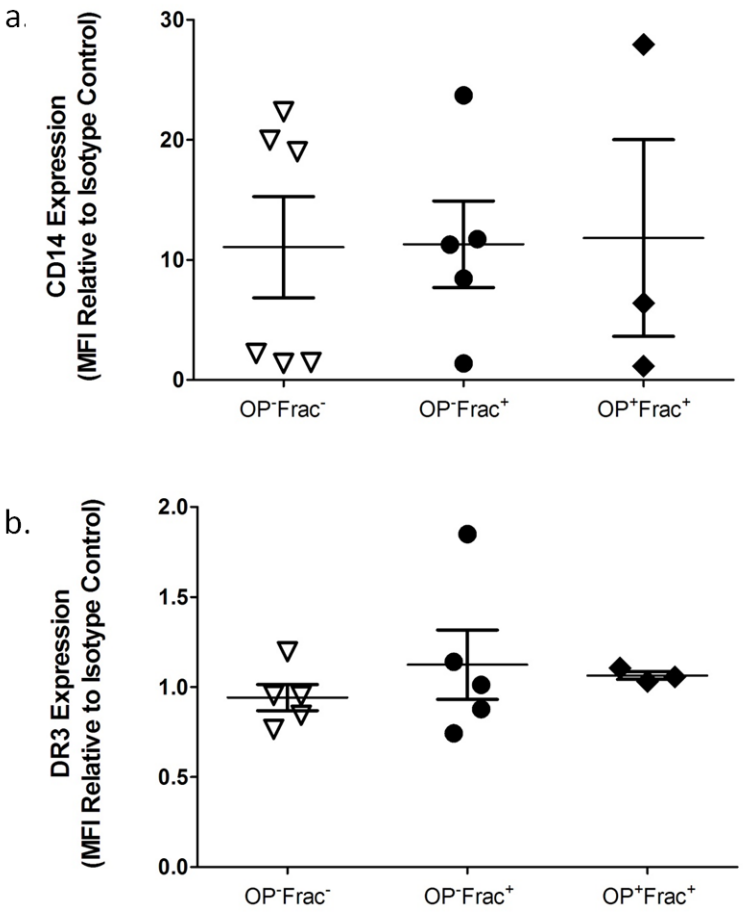

Figure 5.5. Expression of CD14 and DR3 on Patient-derived CD14$^+$ Cells after 7 Days Culture in MCSF .

PBMCs were extracted from the peripheral blood of the patient cohorts and CD14$^+$ cells isolated by magnetic sorting . CD14$^+$ cells were plated onto ivory discs and cultured for 7 days in MCSF. Cells were removed and stained with either an isotype control or with a anti-human CD14 / DR3 antibody and analysed by flow cytometry. MFI was calculated relative to the isotype control for (a) CD14 and (b) DR3. No significant difference in CD14 expression or DR3 expression was detected between the groups. Statistical analysis was performed with a One-way ANOVA with Bonferroni post test.

5.2.8 **Assessing the Ability of Patient-Derived CD14$^+$ Cells to Differentiate into Osteoclasts**

Osteoporosis is a disease characterised by increased osteoclast activity leading to a reduction in bone mineral density (200). For this reason, the ability of the patient-derived CD14$^+$ cells to differentiate into osteoclasts (Fig 5.6) was investigated under our pre-defined culture conditions (section 2.2.12). Total cell and specific osteoclast counts were determined for each experimental disc at each time point investigated.

The total number of cells per mm^2 (mean±SEM) for each disc is presented graphically in Fig 5.7 (a, i) for control cultures (MCSF) and Fig 5.7 (a, ii) for OC cultures (MCSF+RANKL). In the control cultures fracture had no significant effect on total cell number. OP however, was demonstrated to have a significant effect on total cell number across the time course (*P*=<0.0001). Comparison of total cell number in the fracture cohorts showed elevated cell numbers at day 3 in OP cultures (OP$^-$Frac$^+$=174±39/mm^2 versus OP$^+$Frac$^+$=399±75/mm^2); these did not change significantly over time. In the OC cultures fracture was demonstrated to have no significant effect on total cell number. OP resulted in significantly increased cell numbers across the time course (*P*=<0.0001). Total cell number at day 3 was measured as OP$^-$Frac$^+$=244±46/mm^2 versus OP$^+$Frac$^+$=446±68/mm^2 and did not vary significantly over time.

Differential counts were performed and TRAP$^+$ OC, reported as OC / mm^2 (Fig 5.7 (b)) and % OC (Fig 5.7 (c)). Very low levels of spontaneous OC formation were detected in control (MCSF) cultures across the time course. The presence of fracture or osteoporosis did not affect spontaneous OC formation. In OC cultures (MCSF+RANKL), OC were first detected 3 days after addition of RANKL. Numbers increased between day 3 and day 7 and remained constant at day 14. Fracture had no significant effect on OC number or % OCs. Comparison between fracture cohorts showed no significant effect of OP on OC number and % OCs across the time course.

5.2.9 **Assessing the Resorptive Function of the Patient-Derived Osteoclasts**

To determine whether fracture or osteoporosis is associated with an increase in OC resorptive activity the area resorbed by patient-derived OC was measured. OC resorptive activity was expressed as % area resorbed (mean±SEM) for graphical presentation (Fig 5.7 (d)). Osteoclastogenic resorptive function was observed in cultures from the three patient cohorts. Levels of resorption in cultures derived from patients without OP at day 10 and

day 14 were: $OP^{-}Frac^{-}$=0.13±0.06% and 0.66±0.52% versus $OP^{-}Frac^{+}$=0.33±0.22% and 0.39±0.30%. No significant difference was detected demonstrating that OC resorptive activity is not affected by fracture. The presence of OP was determined not to affect OC activity, with no significant difference in resorption at day 10 and day 14 between the fracture cohorts: $OP^{-}Frac^{+}$=0.33±0.22% and 0.39±0.30% versus $OP^{+}Frac^{+}$=0.09±0.06% and 0.18±0.09%.

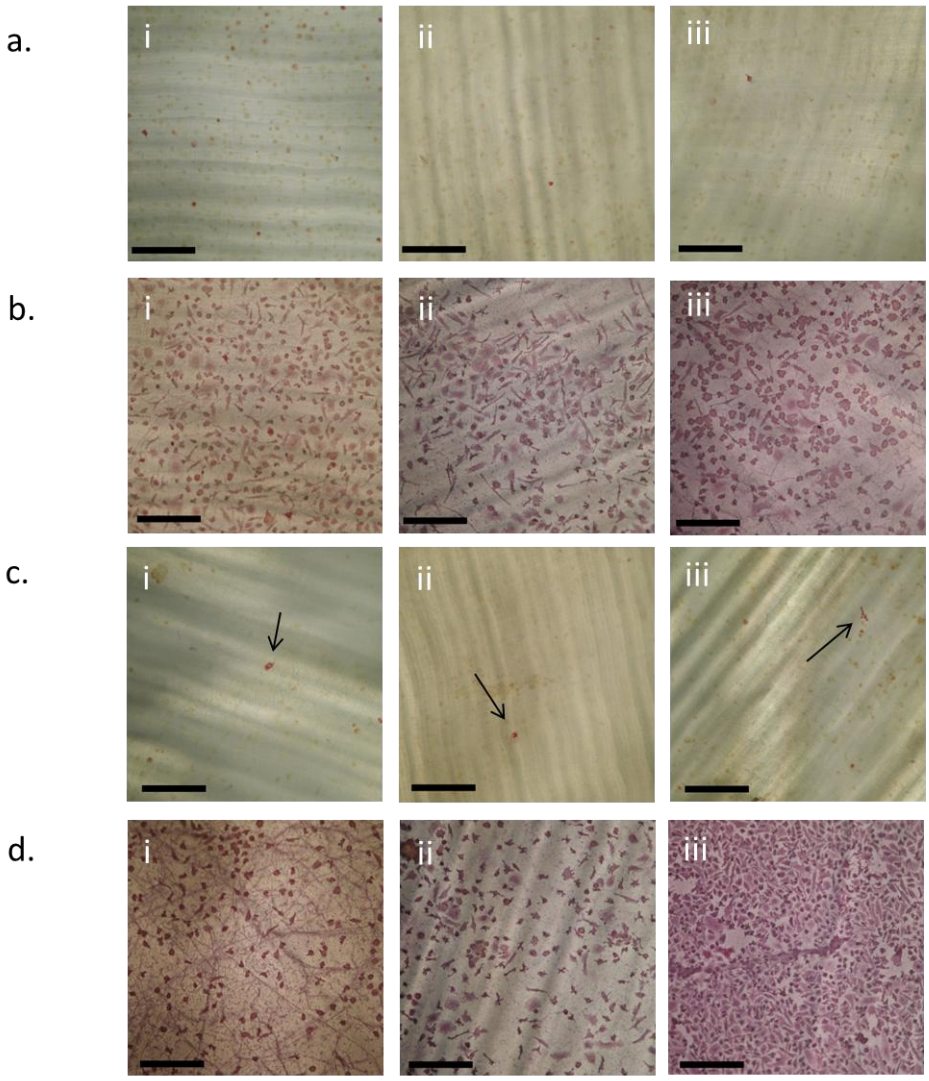

Figure 5.6. Representative Pictures of TRAP and Haematoxylin Stained Control and Osteoclast Cultures from Patient-Derived CD14$^+$ Cells.

PBMCs were extracted from the peripheral blood of the three post-menopausal patient cohorts. CD14$^+$ cells were positively isolated by magnetic sorting (day -7). Cells were plated onto ivory discs and cultured in MCSF for 7 days (day 0) before differentiation in MCSF±TL1A or MCSF+RANKL±TL1A (100ng/ml) for 14 days. At experiment end points cells were stained for TRAP and with haematoxylin. Representative pictures of (i) OP$^-$Frac$^-$, (ii) OP$^-$Frac$^+$ and (iii) OP$^+$Frac$^+$ (a and b) control and (c and d) OC cultures. Arrows indicate osteoclasts. Scale bar = 250µm.

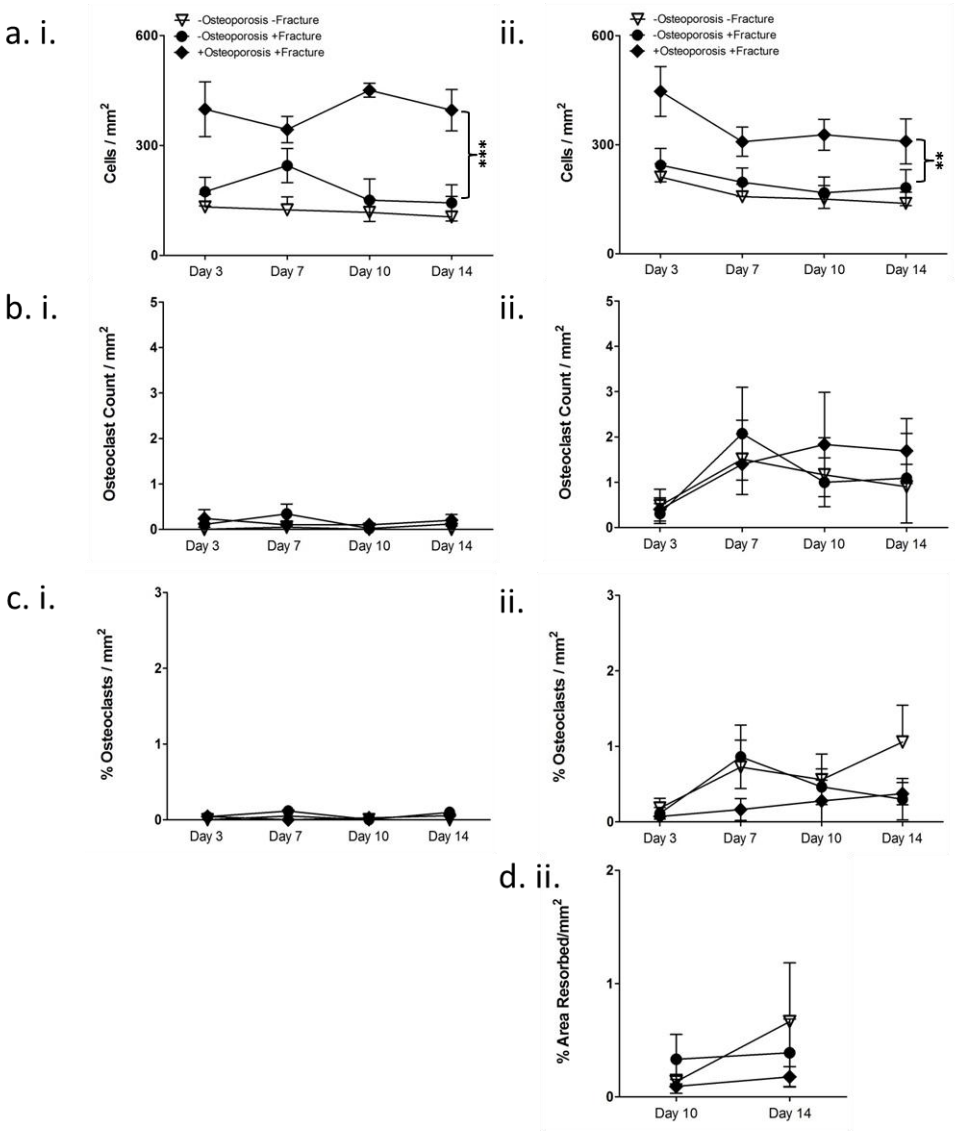

Figure 5.7. Cultures Derived from Osteoporotic Patients have Significantly Higher Total Cell Numbers.

PBMCs were extracted from the peripheral blood. $CD14^+$ cells were positively isolated by magnetic sorting. Cells were plated onto ivory discs and cultured in MCSF for 7 days before differentiation in MCSF or MCSF+RANKL. At experiment end-point cells were stained for TRAP and with Haematoxylin and discs with toluidine blue. (a) Total cell number, (b) OC number, (c) % OC and (d) % area resorbed were calculated in (i) control and (ii) OC cultures. Total cell numbers were significantly elevated across the time course in osteoporotic patient-derived control (*** P=<0.0001) and OC cultures (** P=<0.01). Fracture and OP had no significant effect on OC numbers or OC resorptive activity. Statistical analysis was performed with a Two-way ANOVA.

5.2.10 **Assessing CCL3 Expression in Patient-Derived Osteoclast Cultures**

As an assessment of osteoclast formation the chemokine CCL3 (361) was measured in the supernatants of the patient-derived OC cultures (Fig 5.8 (a)). The presence of fracture had no significant effect on CCL3 expression across the time course. At day 0 levels of CCL3, in the non-OP cohorts, were measured at $OP^{-}Frac^{-}$=89.8±23.7pg/ml versus $OP^{-}Frac^{+}$=76.0±18.0pg/ml. These remained constant at day 7. At day 10 levels in the $OP^{-}Frac^{-}$ cultures dropped significantly compared to the $OP^{-}Frac^{+}$ cultures (23.1±9.9pg/ml versus 98.5±24.6, *P*=<0.05). At day 14, levels of CCL3 were observed to increase in the $OP^{-}Frac^{-}$ cultures (36.7±10.0pg/ml) and decrease in the $OP^{-}Frac^{+}$ cultures (86.9±6.5pg/ml). Analysis of CCL3 levels in the fracture cohorts demonstrated no effect of OP on CCL3 levels. CCL3 expression in the $OP^{+}Frac^{+}$ at day 0 were measured as 78.4±21.6pg/ml and remained relatively constant across the time course.

5.2.11 **Assessing Total MMP-9 Expression in Patient-Derived Osteoclast Cultures**

As an assessment of OC resorptive function expression of total MMP-9 was measured in supernatants from patient-derived OC cultures by ELISA (Fig 5.8 (b)). Levels of total MMP-9 (mean±SEM) were significantly elevated (*P*=<0.0001) in the fracture cohort cultures ($OP^{-}Frac^{+}$) across the time course, compared to the non-fracture cohort cultures ($OP^{-}Frac^{-}$). At day 0 levels of total MMP-9 were measured at; $OP^{-}Frac^{-}$=0.89±0.2µg/ml versus $OP^{-}Frac^{+}$=1.66±0.6µg/ml. Levels were observed to increase at day 7, with significantly elevated total MMP-9 detected in the fracture cohort ($OP^{-}Frac^{-}$=1.58±0.4µg/ml versus $OP^{-}Frac^{+}$ 3.23±0.7µg/ml; *P*=<0.05). Total MMP-9 levels in the $OP^{-}Frac^{-}$ dropped at day 10 (1.15±0.4µg/ml) and remained low at day 14 (0.53±0.2µg/ml). In the fracture cohort, $OP^{-}Frac^{+}$, levels at day 10 were observed to decrease (1.89±0.4µg/ml) but were significantly higher at day 14 (2.68±0.6µg/ml; *P*=<0.01).

Comparison of the fracture cohorts demonstrated no effect of OP on total MMP-9 expression. Levels of total MMP-9 were comparable between the fracture cohorts at each time point tested.

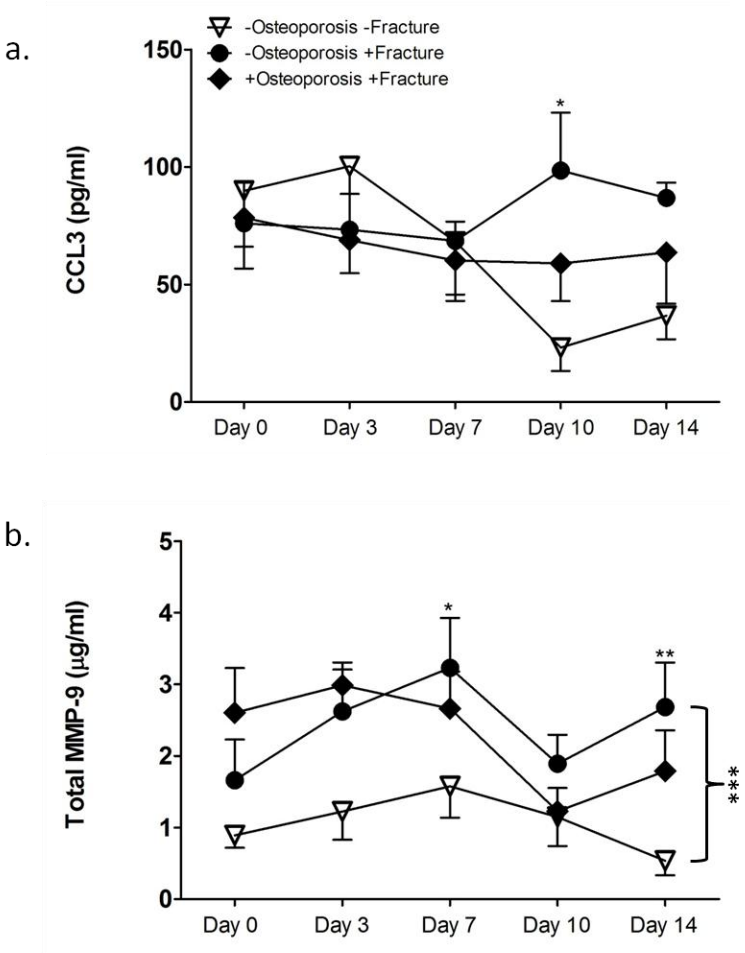

Figure 5.8. Total MMP-9 is Significantly Elevated in Fracture Patient-Derived Cultures.

PBMCs were extracted from the peripheral blood of the patient cohorts and $CD14^+$ cells isolated by magnetic sorting. $CD14^+$ cells were plated onto ivory discs (day -7) and cultured in MCSF for 7 days before differentiation in MCSF+RANKL. Supernatants were collected at the indicated time points and tested for (a) CCL3 and (b) Total MMP-9 by ELISA. (a) Fracture and OP had no significant effect on CCL3 expression across the time course. A significant increase in CCL3 expression was detected at day 10 in the OP^-Frac^+ cultures compared to the OP^-Frac^- cultures (*P=<0.05). (b) Fracture patient-derived cultures exhibited significantly increased total MMP-9 expression across the time course (***P=<0.0001). Significant increases were observed at day 7 (*P=<0.05) and day 14 (**P=<0.01). A change in total MMP-9 expression caused by osteoporosis was not detected. Statistical analysis was performed using a Two-way ANOVA and Bonferroni post test.

5.2.12 **Assessing the Impact of TL1A on the Ability of Patient-Derived CD14$^+$ Cells to Differentiate into Osteoclasts**

In Chapter 4, TL1A (100ng/ml) enhanced OC formation (over control levels) when added to precursor cells isolated from the blood of normal (pre-menopausal) human volunteers. In this chapter, precursor cells were harvested from post-menopausal patients with / without fracture and osteoporosis. The effect of fracture and OP on OC formation and resorptive function in response to TL1A (100ng/ml) was measured. Serious unidentified microbial infection was noted in 48% of cultures 3 – 5 days after the addition of TL1A. All reagents used in the assay were tested (MCSF, RANKL, TL1A, polyHistidine and human OC medium) separately in human OC medium (no cells) to determine the source of the infection. After 1 week in culture (37°C, 5% CO_2), no infection was detected in any of the samples tested. This confirmed that the reagents were not the source of the infection. The likely source of the infection was the patient cells; although this was not tested.

In the remaining (52%) of viable cell cultures containing TL1A, there was no effect on cell expansion or survival. Total cell number (mean±SEM) in control and OC cultures (±TL1A) were comparable (Fig 5.9). In control cultures (MCSF±TL1A) fracture had no effect on OC precursor response to TL1A. Total cell numbers at day 3 in the non-OP cultures (OP^-Frac^-: -TL1A=132.4±34 versus +TL1A=131.1±38 and OP^-Frac^+: -TL1A=174.0±39 versus +TL1A=235.5±42) were not significantly different following the addition of TL1A, and showed minimal variation across the time course. Total cell numbers in the fracture cohort cultures were also unaffected by the addition of TL1A. Numbers at day 3 (OP^-Frac^+: -TL1A=174.0±39 versus +TL1A=235.5±42 and OP^+Frac^+: -TL1A=398.7±75 versus +TL1A=412.8±66) were consistent across the time course. The data demonstrated that OP does not change precursor proliferation or survival in response to TL1A. In OC cultures (MCSF+RANKL±TL1A) fracture and OP were again shown to have no significant effect on cell survival and proliferation in response to TL1A. Total cell numbers in the non-OP cultures were constant from day 3 onwards (OP^-Frac^-: -TL1A=211.2±36 versus +TL1A=159.6±35 and OP^-Frac^+: -TL1A=243.7±46 versus +TL1A=241.6±39). This trend was also observed when comparing the fracture cohorts: total cell numbers at day 3 were OP^-Frac^+: -TL1A=243.7±46 versus +TL1A=241.6±39 and OP^+Frac^+: -TL1A=446.4±68 versus +TL1A=482.6±103.

Differential counts of $TRAP^+$ OC (OC / mm^2 and % OC; mean±SEM) demonstrated that TL1A does not affect spontaneous or RANKL-induced OC formation in fracture or OP patient-derived cultures (Fig 5.10 and Fig 5.11).

Across the time course low levels of spontaneous OC formation were detected in the control cultures (MCSF±TL1A). The presence of fracture or OP had no significant effect on spontaneous OC precursor differentiation in response to TL1A. The presence of fracture had no significant effect on RANKL-induced osteoclastogenesis following addition of TL1A. OP was also demonstrated to have no significant effect on RANKL-induced OC differentiation in response to TL1A. OC were detected in the fracture cohort cultures from day 3 onwards however, no significant difference was detected between the cohorts at any of the time points tested or across the time course.

5.2.13 **Assessing the Impact of TL1A on Patient-Derived Osteoclast Resorptive Function**

To determine whether fracture or osteoporosis affects OC resorptive function in response to TL1A, the area resorbed by patient-derived OC was analysed. OC resorptive activity is presented graphically as % area resorbed (mean±SEM; Fig 5.12). Addition of TL1A had no effect on OC resorptive function in fracture and OP patient-derived cultures.

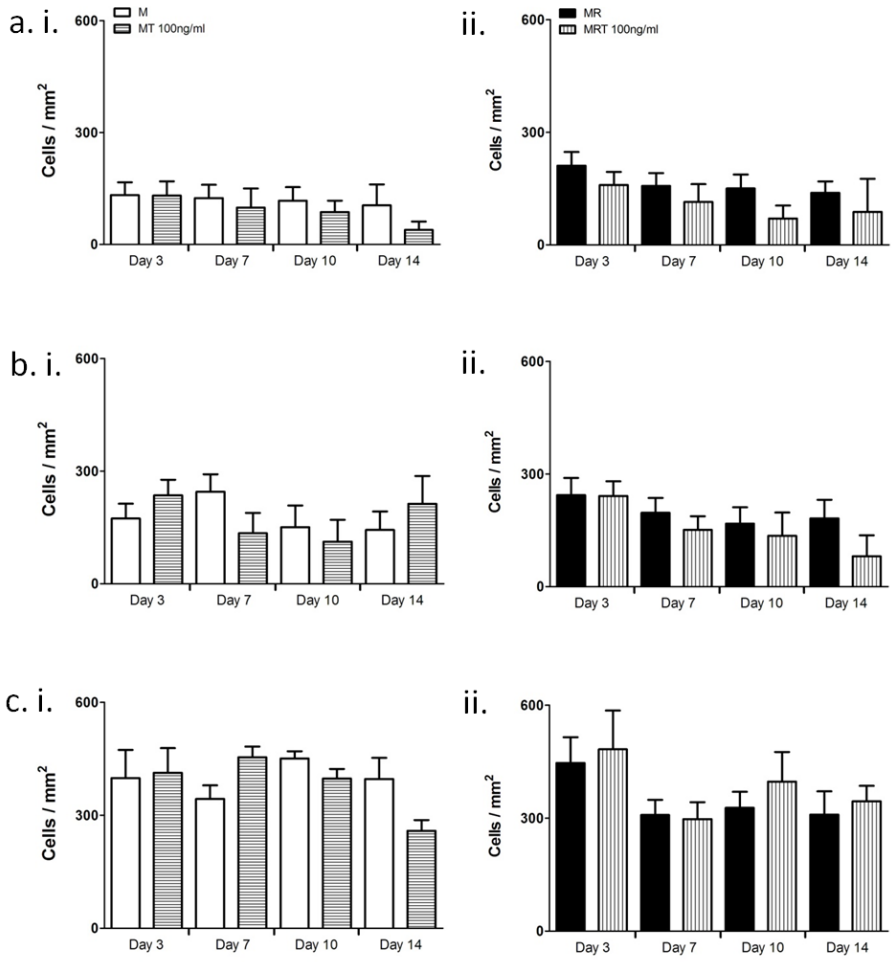

Figure 5.9. TL1A has No Effect on Total Cell Number in Patient-Derived Control and OC Cultures.

PBMCs were extracted from the peripheral blood of the $OP^{-}Frac^{-}$ (n=6), $OP^{-}Frac^{+}$ (n=6) and $OP^{+}Frac^{+}$ (n=4) patient cohorts and $CD14^{+}$ cells isolated by magnetic sorting. $CD14^{+}$ cells were plated onto ivory discs (day -7) and cultured in MCSF for 7 days before differentiation in MCSF±TL1A or MCSF+RANKL±TL1A @ 100ng/ml (2 reps per condition). At experiment end-point cells were stained for TRAP and with Haematoxylin. Total cell number was counted in (i) control and (ii) OC cultures from (a) $OP^{-}Frac^{-}$, (b) $OP^{-}Frac^{+}$ and (c) $OP^{+}Frac^{+}$ cohorts. Addition of TL1A had no effect on total cell number. Statistical analysis was performed with a Two-way ANOVA.

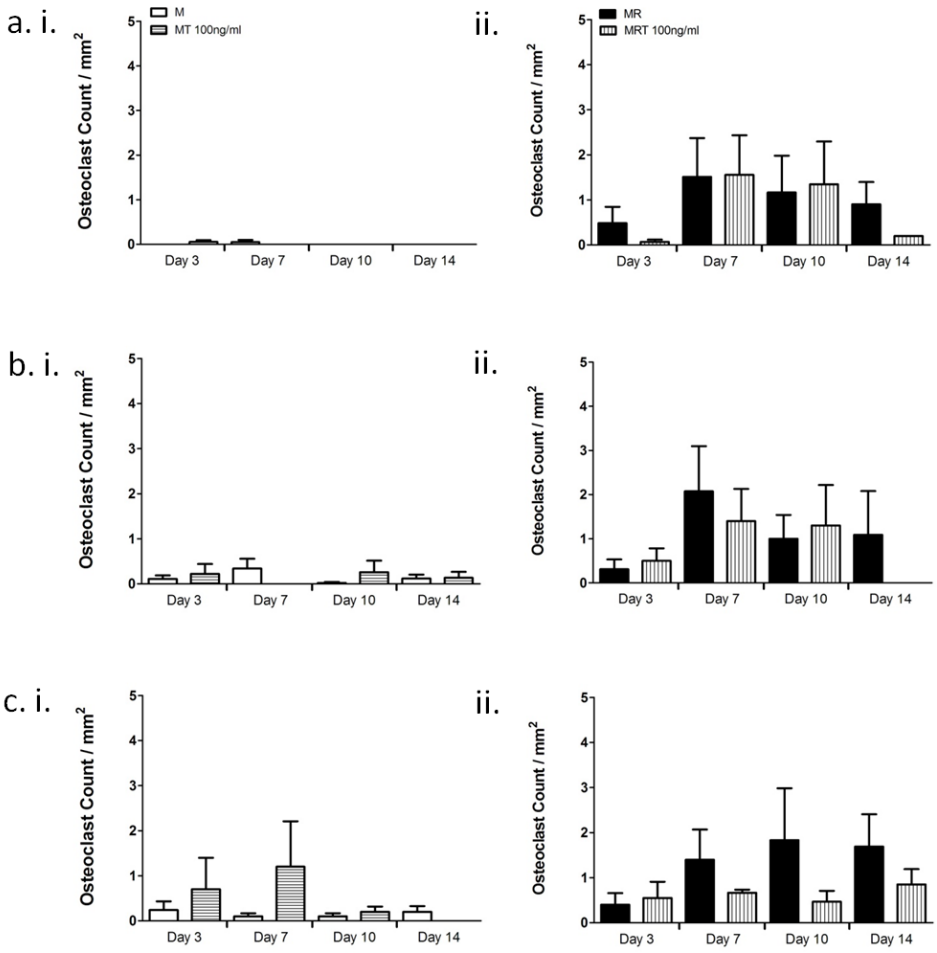

Figure 5.10. TL1A has No Effect on Osteoclast Numbers in Patient-Derived Control and OC Cultures.

PBMCs were extracted from the peripheral blood of the $OP^{-}Frac^{-}$ (n=6), $OP^{-}Frac^{+}$ (n=6) and $OP^{+}Frac^{+}$ (n=4) patient cohorts and $CD14^{+}$ cells isolated by magnetic sorting. $CD14^{+}$ cells were plated onto ivory discs (day -7) and cultured in MCSF for 7 days before differentiation in MCSF±TL1A or MCSF+RANKL±TL1A @ 100ng/ml (2 reps per condition). At experiment end-point cells were stained for TRAP and osteoclasts counted in (i) control and (ii) OC cultures from (a) $OP^{-}Frac^{-}$, (b) $OP^{-}Frac^{+}$ and (c) $OP^{+}Frac^{+}$ cohorts. TL1A had no effect on osteoclast numbers. Statistical analysis was performed with a Two-way ANOVA.

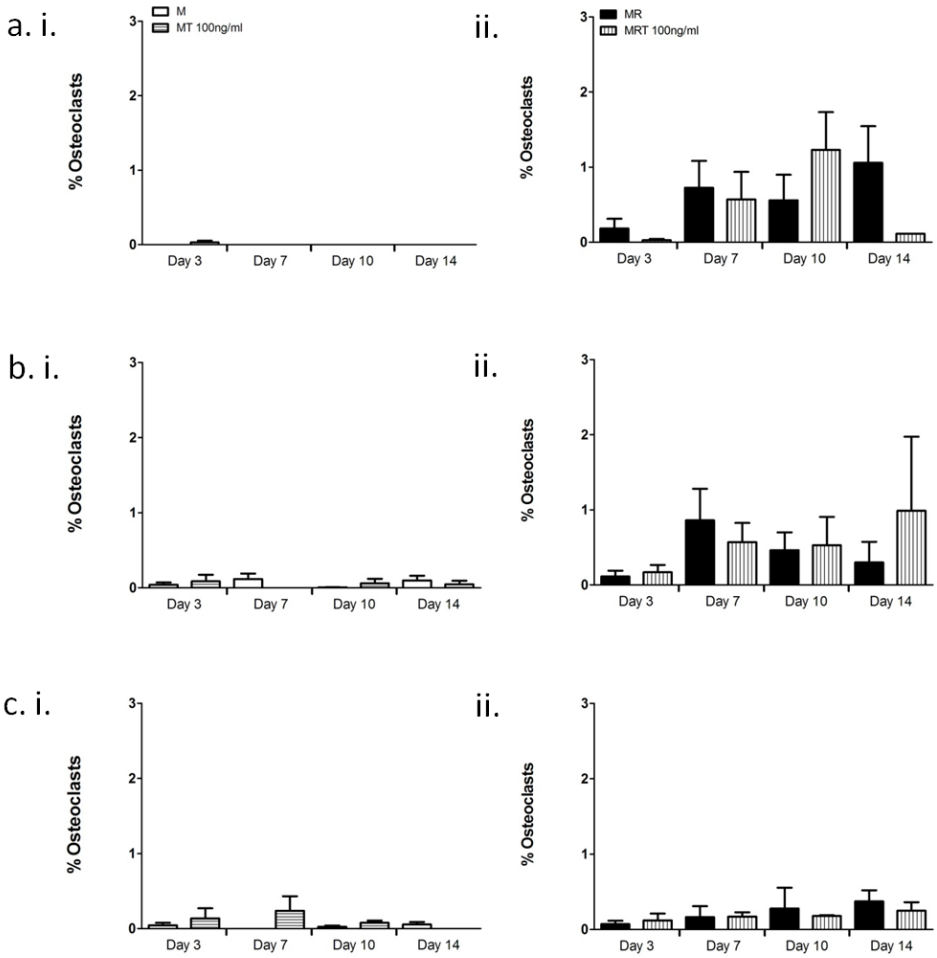

Figure 5.11. TL1A has No Effect on % Osteoclasts in Patient-Derived Cultures

PBMCs were extracted from the peripheral blood of the $OP^{-}Frac^{-}$ (n=6), $OP^{-}Frac^{+}$ (n=6) and $OP^{+}Frac^{+}$ (n=4) patient cohorts and $CD14^{+}$ cells isolated by magnetic sorting. $CD14^{+}$ cells were plated onto ivory discs (day -7) and cultured in MCSF for 7 days before differentiation in MCSF±TL1A or MCSF+RANKL±TL1A @ 100ng/ml (2 reps per condition). At experiment end-point cells were stained for TRAP and % OCs calculated in (i) control and (ii) OC cultures from (a) $OP^{-}Frac^{-}$, (b) $OP^{-}Frac^{+}$ and (c) $OP^{+}Frac^{+}$ cohorts. TL1A had no effect on % osteoclasts. Statistical analysis was performed with a Two-way ANOVA.

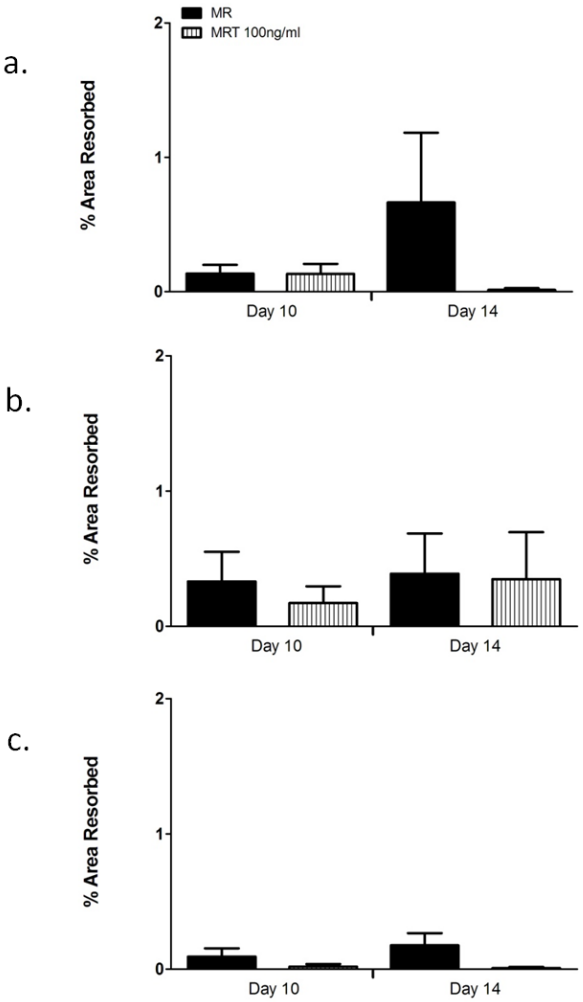

Figure 5.12. TL1A has No Effect on Osteoclast Resorptive Function in Patient-Derived Cultures

PBMCs were extracted from the peripheral blood of the $OP^{-}Frac^{-}$ (n=6), $OP^{-}Frac^{+}$ (n=6) and $OP^{+}Frac^{+}$ (n=4) patient cohorts and $CD14^{+}$ cells isolated by magnetic sorting. $CD14^{+}$ cells were plated onto ivory discs (day -7) and cultured in MCSF for 7 days before differentiation in MCSF±TL1A or MCSF+RANKL±TL1A @ 100ng/ml (2 reps per condition). At experiment end-points discs were stained with toluidine blue, resorption pits analysed and % area resorbed calculated in (a) $OP^{-}Frac^{-}$, (b) $OP^{-}Frac^{+}$ and (c) $OP^{+}Frac^{+}$ cultures. TL1A had no effect on osteoclast resorptive function. Statistical analysis was performed with a Two-way ANOVA

5.3 **Discussion**

OC over-activity is associated with focal bone erosions and the generalised bone loss that is observed in a number of diseases including RA (352, 353), AS (354) , PsA (355) and post-menopausal OP (52, 197). While the exact aetiology of these diseases remains unknown, cytokines belonging to the TNFSF such as RANKL (TNFSF11), TNF (TNFSF2) and LIGHT (TNFSF14) are up-regulated. Furthermore, published literature has identified key roles for the TNFSF cytokines in promoting OC activity (180-183, 200, 201). It is therefore entirely feasible that excess production of TNFSF cytokines drive osteoclast-dependent pathology in diseases like RA and OP. In the last 10 years a role for the TNFRSF / TNFSF members DR3 (TNFRSF25) and TL1A (TNFSF15) was proposed. Elevated levels of TL1A were detected in serum samples obtained from AS (267) and RA (264) patients. TL1A was not linked with bone pathology in these papers; furthermore TL1A has not been previously studied in the context of OP. The aim of this chapter was two-fold:

1. To analyseTL1A levels in the serum of patients with different forms of arthritis.
2. To determine whether DR3 and TL1A were implicated in the pathogenesis of osteoporosis and/or fractures in patients without osteoporosis.

Serum TL1A levels were increased 8.7-fold in RA patients (1.99±0.3ng/ml) compared to healthy controls (0.23±0.02ng/ml). This result adds support to the work published by Bamias et al (264). His study demonstrated that TL1A levels in serum were increased 5-fold in RA patients (4.55±5.96ng/ml) over age- and sex-matched controls (0.89±0.86ng/ml). In the present study, TL1A was also increased 1.9-fold in PsA patient serum (0.43±0.2ng/ml). Although TL1A was raised in the serum from PsA patients the level was not significantly different to the controls. In a study by Bamias et al (269) DR3 and TL1A expression were shown to be significantly induced in psoriatic skin lesions. TL1A expression was demonstrated to primarily localise to keratinocytes and macrophages within the psoriatic lesions. Bamias also identified in several cases of psoriasis nuclear localisation of TL1A in inflammatory and fibroblast-like cells, which did not occur under steady state conditions. Nuclearisation of TL1A was also detected in the synovial membrane of RA patients suggesting a potential common pathway between skin and synovial inflammation (269). Taken with the results from this current study the increase in serum TL1A and subsequent nuclear localisation may provide a possible explanation why a subgroup of patients with psoriasis develop arthritis. Additional studies are required to determine whether the up-regulation of DR3/TL1A is linked to the

development and bone pathology associated with psoriatic arthritis: osteolysis, ankylosing, formation of spurs, paramarginal erosions and calcification within the area of enthesitis (362). A detailed study examining serum TL1A in psoriasis patients and following disease progression would provide a number of important observations. Cell studies looking at OC and OB response to any increase in TL1A would also provide a mechanism through which the bone pathology associated with PsA progresses. RA and PsA are inflammatory arthritides characterised by bone pathology. To determine whether serum TL1A levels were also elevated in an arthritides not primarily associated with bone pathology, samples obtained from OA patients were studied.

OA is a chronic joint disease characterised by focal and progressive hyaline articular cartilage loss. Concomitant changes in the bone underneath the cartilage also occur including marginal outgrowths and osteophytes. Modest inflammation may also be present in and around the soft tissue of the joint (363, 364). In this study levels of serum TL1A measured in OA patients (0.23±0.2ng/ml) were not significantly different to that of the controls (0.23±0.02ng/ml). This suggests that persistent inflammation, as observed in RA and PsA, is a driving factor in the elevation of serum TL1A expression. This elevation in serum TL1A is subsequently linked to the bone pathology associated with the inflammatory arthritides. If persistent inflammation were the only contributing factor to the increased TL1A expression then levels between the RA and PsA cohorts should be consistent. However, TL1A levels in the RA cohort (1.99±0.3ng/ml) were 4.7-fold higher than their PsA counterparts (0.43±0.2ng/ml). This suggests that additional factors in RA, such as the presence of rheumatoid factor (RF), may be driving the increase in TL1A expression.

An explanation for the difference in TL1A levels between the RA and PsA samples was gained from work by Moll, Wright (365), Cassatella et al (366) and Prehn et al (253). In 1973 Moll, Wright (365) recognised that PsA patients were seronegative for rheumatoid factor (RF), whereas patients with RA were typically seropositive. The importance of this in relation to TL1A expression was demonstrated by Cassatella et al (366) and Prehn et al (253). In their studies, stimulation of monocytes with immunocomplexes such as RF, significantly induced the expression of TL1A by the cells. The data suggests that RF present in RA patients stimulates expression of TL1A by monocytes, increasing serum levels over that of PsA patients. To determine whether the presence of RF is a significant factor in serum TL1A levels, the RA patient cohort was split into seropositive and

seronegative sub-groups. Patients were deemed to be seropositve if RF was $\geq$ 20units/ml. Levels of TL1A were found to be significantly increased in the RF^+ sub-group over the RF^- sub-group (6.7-fold) and the normal controls (12.3-fold). The study by Bamias et al (264) also demonstrated an increase in TL1A levels in the RF^+ sub-group, when compared to the controls (6.9-fold), adding support to the results in this study. In this study and the Bamias et al study (264) a strong significant correlation between TL1A and RF was discovered, demonstrating an important link between RF and TL1A *in vivo*. Treatment of RA is routinely through DMARDS though those with severe arthritis can be treated with an anti-TNF biological. Whether anti-TNF treatment affects serum TL1A levels is currently unknown.

RA patients (RF^+ and RF^-) were grouped depending on their treatment; DMARDs versus anti-TNF treatment. Anti-TNF treatment led to a slight reduction in serum TL1A levels compared to the DMARDs in both the RF^+ and RF^- cohorts. However, these reductions were not significant, demonstrating that anti-TNF treatment does not affect serum TL1A. This result is in contrast to that observed in the Bamias et al (264) study. In the Bamias et al study TL1A levels were measured in patients before treatment with a TNF inhibitor, adalimumab, (6.77ng/ml) and 3 months post-treatment (2.8ng/ml). A significant reduction in serum TL1A was observed suggesting that anti-TNF treatment did have an effect on TL1A expression. There were a number of differences between the Bamias et al study and the study performed in this thesis however. The Bamias et al study measured TL1A in a group of patients both pre- and post- treatment while in this study levels in the patients pre-treatment were unknown; meaning that the Bamias et al study has greater statistical power. The duration that the patients were on anti-TNF treatment in this study before being sampled were also unknown; meaning that some if not all of the patients in the anti-TNF treatment group could have started treatment well over three months before being tested. This does raise an interesting possibility however, that following anti-TNF treatment serum TL1A levels could initially drop but rise again over time. It should be noted that in the Bamias et al study levels of TL1A in the anti-TNF treated group were still 3.1-fold higher than those observed in the normal controls, suggesting that TL1A could still exert a significant effect on the pathogenesis of the disease. While TL1A levels have been shown to be affected by the presence of RF and the effect of anti-TNF treatment debatable its link to erosive disease remains unknown.

To determine whether serum TL1A levels were linked to erosive disease the RA patient samples (RF^+ and RF^-) were grouped depending on whether they displayed erosions at the time of sampling. TL1A levels were significantly elevated (2.2-fold) in the RF^+ group displaying erosive disease over the non-erosive RF^+ group. Levels of TL1A were also 3.9-fold higher in RF^- patients with erosive disease over non-erosive disease, though this was not significant. This data adds support to the work by Bamias et al (264) which revealed that TL1A was significantly elevated in the RF^+ patients with active disease over those in remission (8.2±8.7ng/ml versus 4.1±4.1ng/ml). In the Bamias et al study however, no difference was observed in the RF^- patients (active=1.93±1.08ng/ml versus remission=1.96±1.58ng/ml). The data from this study and the Bamias et al (264) study provides evidence for a role of TL1A in the pathogenesis of erosive disease. This is further supported with the results from chapter 4, where addition of TL1A to *in vitro* OC cultures significantly enhanced OC formation and resorptive activity. Additional support for the role of TL1A in erosive pathology came from studies by Zhang et al (266) and Bull, Williams et al (242) in murine models of CIA and AIA. Administration of TL1A to a CIA model significantly aggravated CIA induction (266). Clinical score in CIA-TL1A treated mice were significantly elevated compared to the CIA-PBS control group. Histopathologically CIA-TL1A treated mice displayed increased cartilage loss, severe pannus formation and bone destruction and deformation (266). In the AIA model co-administration of TL1A resulted in significant dose-dependent exacerbation of disease (242), increasing the size of bone erosions and severity of bone destruction. The data, taken as a whole, suggests a significant role for TL1A in the pathogenesis of RA, with increased levels responsible for increased bone destruction. The link between TL1A and RA raises a number of interesting possibilities: could TL1A levels be used as a prognostic marker for erosive disease and is increased TL1A responsible for the non-responders to anti-TNF treatment?

Currently there are no reliable prognostic markers for RA at disease onset. RF and anti – CCP have been shown to be associated with more severe joint damage. However, an increase in RF and anti-CCP is typical of a relatively advanced stage of disease; therefore they are of limited use in the very early stages (367, 368). Whether TL1A serum levels could be used as a prognostic marker for erosive RA remains to be tested. The RA patients used in this study all had established disease, so it is not known whether TL1A levels are up-regulated before the onset of RA or after disease progression has started. To answer this question a long term study would be required with patients who display at clinic with signs of early arthritis. Serum TL1A levels would then have to be measured and

monitored over time to determine whether there is any direct link between TL1A, pathogenesis of RA and erosive disease. Possibly of even more importance is the effect of anti-TNF treatment on TL1A. While anti-TNF treatment has made it possible for many RA patients to have a better quality of life, there are those who do not respond to the treatment. The reasons behind the lack of response to treatment are unknown; however it is plausible that in these individuals the erosive damage is being driven by increased TL1A and not TNF. Through studying the cells of these patients and measuring their TL1A and DR3 expression it should be possible to obtain a better understanding of the complexities of RA and, in the long term, develop better treatments for the management of the disease. While this study and those by Osawa et al (265), Bamias et al (264) and Zhang et al (266), have revealed a role for DR3 and TL1A in the pathogenesis of RA nothing is currently known about their involvement in fracture or post-menopausal OP. This was investigated in the second half of this chapter.

To determine whether DR3/TL1A have a role in the development of post-menopausal osteoporosis and / or fracture, patients were recruited to one of three cohorts, depending if they met the criteria set out in section 2.2.15. The three patient cohorts were defined as:

- Patients without osteoporosis or fracture (OP^-Frac^-)
- Patients without osteoporosis but with fracture (OP^-Frac^+)
- Patients with osteoporosis and fracture (OP^+Frac^+)

The role of DR3/TL1A in the pathogenesis of fracture could be identified through comparison of the non-OP cohorts (OP^-Frac^- and OP^-Frac^+). The role of DR3/TL1A in the pathogenesis of OP could then be determined through comparison of the fracture cohorts (OP^-Frac^+ and OP^+Frac^+). The number of patients recruited to each group for this proof-of-concept study was lower than hoped, with 6 recruited to both the OP^-Frac^- and OP^-Frac^+ cohorts and only 4 recruited to the OP^+Frac^+ cohort. The reason for the lower than expected recruitment can be attributed to a low number of patients presenting at clinic in the time frame of the study, who conformed to the inclusion and exclusion criteria. The study also presented a number of limitations, meaning a certain degree of care must be taken with interpretation of the results. The low patient numbers in each group mean that any differences may be masked by the inherent variation between individuals. The lack of a with osteoporosis without fracture cohort also means that it is difficult to fully

identify the effect of fracture and the effect of OP in the $OP^{+}Frac^{+}$ cohort results. While all post-menopausal, the exact age of the patients recruited to the study are unknown; due to causes outside of the operators control resulting in the patient data being lost. This raises the possibility that the mean age in the cohorts could be significantly different and any observed effects could be due to this rather than fracture or OP. Having recruited patients to the study, levels of TL1A and TNF, a member of the TNFSF associated with increased OC activity (184), were measured in the serum.

The role of the TNFSF following the menopause in fracture and post-menopausal osteoporotic fracture has not been fully elucidated. Oestrogen deficiency associated with the menopause has been linked to a subtle increase in expression of the TNFSF members RANKL and TNF in *ex vivo* cultures of PBMCs (200, 201), circulating monocytes (202) and bone marrow macrophages (203, 204). Whether expression of TL1A and TNF is altered *in vivo* in post-menopausal women following fracture or OP is unknown and was investigated. TL1A was detected in serum from 10 out of 13 patients. Comparison of the non-OP cohorts demonstrated an up-regulation of TL1A following recent fracture (1.9-fold); while no difference was observed between the fracture cohorts. This result suggests that TL1A is up-regulated following fracture but not as a consequence of OP. Support for fracture leading to an increase in TNFSF members is provided by a study by Kon et al (369). They showed that TNFSF members RANKL, OPG and TNF are temporally up-regulated during fracture healing, with levels related to the stage of repair. While still unknown, up-regulation of TL1A expression in response to fracture could be part of the complex array of signalling molecules and pro-inflammatory cytokines involved in skeletal repair. In contrast serum TNF was not detected in any of the patient samples. This suggests three possibilities: i) the up-regulation of TNF is localised to the site of skeletal repair and is not systemic, ii) TNF was not required at the stage of skeletal repair when the samples were obtained and iii) elevated serum TNF is not a contributing factor in the pathogenesis of fracture and / or OP. Further studies with increased numbers are required to conclusively say either way. Characterisation of CD14 and DR3 expression on cells from the post-menopausal cohorts was then carried out to determine whether fracture or OP change the cellular phenotype of the OC precursor.

Analysis of the freshly isolated patient-derived cells demonstrated a high level of variation in CD14 expression in the $OP^{+}Frac^{+}$ cohort. Comparison of the non-OP cohorts and the fracture cohorts demonstrated fracture and OP had no significant effect on CD14

expression, with approx. 60% of the isolated cells showing moderate to high expression. After 7 days culture in MCSF the variation in CD14 expression on the cells increased greatly, though no significant difference between the cohorts was observed. The reason behind the high variation in CD14 expression between and within the patient cohorts is not clear but may be due to age. Work by Sadeghi et al (370) demonstrated that monocytic CD14 expression alters during aging, with cells changing from a $CD14^{bright}/CD16^{dim}$ phenotype to a $CD14^{dim}/CD16^{bright}$ phenotype. This change in CD14 expression during aging is further supported by work from Kósa et al (371). In their study they showed that there is a significant down-regulation in transcriptional activity of the CD14 gene in post-menopausal bone when compared to pre-menopausal bone. DR3 expression was found to be non-existent on the freshly isolated cells. This supports the observation by Kang et al (278) and the work in chapter 4: that DR3 is not constitutively expressed on circulating monocytes. In contrast to the results in chapter 4, DR3 expression was not detected on the cells after 7 days culture in MCSF on ivory; with the exception of one patient in the $OP^{-}Frac^{+}$ cohort. As with CD14 expression the absence of DR3 may also be due to changes in the immune system as a person ages. While currently there are no papers looking at the effects of aging on monocyte / macrophage DR3 expression, it has been documented that some functions of these cells are impaired in aged animal models (372) and elderly individuals (373). However, the menopause has been linked to an increase in the expression of some receptors, such as soluble IL-6 receptor (374). Further work is required to determine the effects of aging and the menopause on DR3 expression. Though the patient-derived cells exhibited no DR3 expression and variable CD14 expression osteoclastogenesis assays were continued, to determine what effect this may have on the ability of the cells to undergo OC differentiation.

Comparison of the total cell number in both the control (MCSF) and OC cultures (MCSF+RANKL) demonstrated a significant effect of OP. Total cell numbers were significantly increased in the $OP^{+}Frac^{+}$ cohort compared to the non-OP cohorts, suggesting a change in cell viability. Studies into cell viability in patients with osteoporosis are limited. In a study by D'Amelio et al (200) PBMC viability between post-menopausal controls and osteoporotic patients were analysed by the 3-(4,5-dimethylthiazol-2-yl)-2,5,diphenyltetrazolium bromide (MTT) assay. Viability of PBMC's obtained from osteoporotic patients were found to be slightly increased over the post-menopausal controls, when cultured in MCSF and MCSF+RANKL; however, this increase in viability was

not significant. This data, taken in conjunction with the results from this study, suggest that a fundamental change in cell viability is part of the pathogenesis of osteoporosis. The mechanism behind this change in cell viability is currently is unknown. Survival of monocytes / macrophages is dependent on signalling from the cytokine MCSF through its receptor c-FMS (375, 376). Levels of MCSF added to the cultures of the patient-derived cells were constant. This means that the ability of the cells to survive and proliferate in culture should be equal. The differences in total cell number observed suggested that the non-osteoporotic monocytes / macrophages received reduced survival signals compared to their osteoporotic counterparts. This could be due to altered levels of c-FMS expression on the cohort cells, though further work would be required to confirm this. Differential cell counts were then performed on the cultures to determine if there was a difference in the ability of the cells to undergo spontaneous OC formation or RANKL-induced OC formation.

Fracture and OP had no effect on spontaneous OC formation. This result is in contrast to work published by D'Amelio et al (200). In their study they demonstrated significantly higher levels of 'spontaneous' osteoclast formation from osteoporotic patient PBMC cultures (45.5±13.4 OC/10^5 cells) compared to pre-menopausal controls (15.1±10.5 OC/10^5 cells). Differences in experimental procedure between this study and that by D'Amelio et al (200) could explain the observed differences in osteoporotic spontaneous OC formation. In the D'Amelio et al study PBMC cultures were used, compared to CD14 cultures used in this study. The set of experiments in the D'Amelio study were also performed without the addition of MCSF and RANKL to the cultures. However, the presence of other PBMCs in the cultures would produce the cytokines required for cell survival and OC differentiation (377-379). Increases in RANKL and MCSF production by PBMCs post-menopause has also been demonstrated by a number of groups (380-382), providing an explanation for the high levels of spontaneous OC formation observed in the D'Amelio et al study. Comparison of the OC cultures from non-OP and fracture cohorts also demonstrated no effect of the two conditions on RANKL-induced osteoclastogenesis. This suggested that a fundamental change in the ability of $CD14^+$ cells to undergo osteoclast formation is not responsible for the increased OC activity associated with OP. This is supported by an additional set of experiments in the D'Amelio et al (200) study and a study by Jevon et al (383). In these studies PBMCs cultured from osteoporotic patients demonstrated no increase in osteoclastogenic potential, compared to post-menopausal controls, when cultured in the presence of exogenous MCSF and RANKL. The results

demonstrated that a change in the ability of $CD14^+$ cells to undergo spontaneous or RANKL-induced OC formation is not related to fracture or the pathogenesis of OP. The resorptive activity of the OC was then investigated to determine whether fracture or OP increased the ability of the OC to resorb bone.

In the 2003 study by Jevon et al (383) OC derived from PBMCs from osteoporotic patients demonstrated increased OC resorptive activity, with respect to pre-menopausal controls. Interestingly this was not due to an increase in OC numbers, suggesting a fundamental change in OC resorptive activity. In this present study a low level of resorption was detected in the patient OC cultures. However, fracture and OP had no effect on OC resorptive function. As with OC formation in the D'Amelio et al (200) study, the key factor in the increased resorption observed in the Jevon et al (383) study seems to be the presence of PBMCs in the cultures. Factors released by the PBMCs can exert a direct effect on the formation and function of the OC. This would lead to the difference in results observed between the present study and those by D'Amelio et al (200) and Jevon et al (383). Fracture and OP have been demonstrated to have no effect on the ability of post-menopausal-derived $CD14^+$ OC precursors to undergo osteoclastogenesis. To determine whether they have any effect on mediators of OC formation and function, levels of CCL3 and total MMP-9 were evaluated in the culture supernatants.

Published studies have demonstrated CCL3 (87, 88) and total MMP-9 (350) to be mediators of OC formation and resorptive activity; with CCL3 expression involved in OC formation (87, 88) and MMP-9 involved in OC resorption (350). Levels of CCL3 were comparable between the three cohorts across the time course: consistent with the comparable levels of OC formation observed between the cultures. In contrast to CCL3, fracture was found to have a significant effect on expression of total MMP-9. The increase in total MMP-9 observed in the fracture cultures is supported by studies from Colnot et al (384) and Uusitalo et al (385). In the study by Colnot et al (384) MMP-9 was demonstrated to regulate crucial events in fracture repair. MMP-9-deficient mice were found to have non-union and delayed union of fractures due to dysregulation of cartliage remodelling and impaired ossification. In the work published by Uusitalo et al (385) MMP-9 production was demonstrated to be significantly up-regulated following fracture. Immunohistochemistry identified MMP-9 to be predominantly localised in osteoclasts and chondroclasts at the osteochondral junction. Taken with the data from the current study the results demonstrate that the presence of fracture has a significant effect on total

MMP-9 release from OC and their precursors. The results reported in this chapter have demonstrated that fracture and OP have no direct effect on osteoclast formation or OC resorptive activity. While DR3 expression was not identified on the $CD14^+$ cells, the effect of fracture and OP on cellular response to TL1A was investigated.

When TL1A was added to the cultures expression of DR3 was not detected on the surface of the cells. It cannot be conclusively ascertained however, whether induction of DR3 expression was delayed, appearing on the surface of the cells after the TL1A had been added to the cultures. Addition of TL1A to the non-OP and fracture cultures had no effect on total cell number, osteoclast number, % osteoclasts or resorptive function. This suggested that DR3 expression on the $CD14^+$ cells was not delayed and induced at a later time point

The investigation into the role of DR3/TL1A into the pathogenesis of fracture and OP has revealed some surprising results. However, care must be taken with their interpretation as the study was limited in both patient numbers and cohorts recruited. TL1A was elevated in the fracture cohorts; however, increased sample numbers are required to conclusively prove whether this difference is significant. A post-study power calculation indicated that a sample size of 18 patients per cohort is required to obtain a conclusive result. Comparison between the fracture cohorts also demonstrated no difference in serum TL1A, suggesting that OP has no effect on TL1A expression. Without a 'with osteoporosis without fracture' cohort however, this conclusion cannot be confidently made. Cellular studies also revealed that DR3 is not expressed on OC precursors isolated from post-menopausal women. While OP led to an increase in OC precursor cell viability there was no difference in their ability to undergo osteoclastogenesis or increased resorptive function. This data was in contrast to that by D'Amelio et al (200) and Jevon et al (383); highlighting the importance of all cell types in the pathogenesis of osteoporosis. While an increase in OC activity has been highlighted as a key factor in the progression of OP, decreased bone formation by the OB also plays a significant role (198, 199). The presence of DR3 on osteoblasts has been shown by Borysenko et al (241) and Bu et al (261). The role that DR3 plays in OB differentiation and activation has not been fully investigated, though it was shown by Borysenko et al (241) to have a potential role in normal OB function. The effect of DR3 on OB differentiation and function will be investigated in chapter 6.

5.4 **Conclusion**

At the conclusion of this chapter the following objectives were met:

- Serum TL1A was identified as being significantly elevated in RF^+ RA patients.
- Anti-TNF treatment was determined to have no significant effect on RA patient serum TL1A levels.
- Serum TL1A levels were demonstrated to be linked to erosive pathology in RA.
- Ethical approval for the collection and analysis of blood samples, from 3 cohorts of post-menopausal treatment-naïve patients was acquired and patients were recruited to the cohorts.
- Serum TL1A was identified as being raised in post-menopausal fracture patients.
- DR3 expression was revealed to be absent from post-menopausal OC precursors.
- Fracture and OP were identified as not having a direct effect on OC formation and resorptive activity, or altering cellular response to TL1A.

The aim of this chapter was to examine the role of DR3/TL1A in the pathogenesis of diseases characterised by OC hyper-activity. The results have demonstrated that TL1A is elevated in arthritides associated with persistent inflammation; significantly so in patients with RA over healthy controls. Further breakdown of the RA patients into sub-groups according to their RF status (RF^+ and RF^-) revealed that the presence of RF had a significant effect on TL1A levels, causing increased expression of the cytokine by stimulated macrophages (253, 366). The effect of anti-TNF treatment on serum TL1A is debatable and requires further work. Results from this study fail to demonstrate anti-TNF treatment having a significant effect on TL1A levels. A study by Bamias et al (264), however, showed a significant reduction in TL1A following anti-TNF treatment. It is interesting to note that TL1A levels in the anti-TNF treatment patients in the Bamias et al (264) study were still considerably higher than healthy controls; suggesting that TL1A still exerts a significant effect on the pathogenesis of the disease. This would provide a possible explanation for why some people do not respond to anti-TNF treatment. Comparison of TL1A levels in RA patients with non-erosive and erosive disease also pointed to a role of the cytokine in driving erosive pathology. Further work into whether serum TL1A could be used as an early prognostic marker for RA disease severity, however, remains to be seen. For the first time this study has also examined the role of DR3 and TL1A in the pathogenesis of

fracture and OP through a proof-of-concept analysis of three post-menopausal patient cohorts:

- -osteoporosis –fracture
- -osteoporosis +fracture
- +osteoporosis +fracture

Fracture patients were demonstrated to have increased levels of serum TL1A; however, this increase was not statistically significant. Whether serum TL1A is therefore up-regulated following fracture and the significance of this requires further testing with much larger patient numbers. Culture of the patient-derived $CD14^+$ cells demonstrated OP to have a significant effect on cell viability. Interestingly, however, this increase in cell viability did not translate into increased OC formation or resorptive activity. These results were in contrast to work published by D'Amelio et al (200) and Jevon et al (383) who showed an increase in osteoclast differentiation and activity, respectively, in cultures from osteoporotic patients. These studies however, used PBMCs as a source of cells and highlight the important role of other cell types in the pathogenesis of osteoporosis. Fracture and OP were also deemed to have no effect on OC precursor response to TL1A. TL1A had no effect on cell survival, OC formation or resorptive activity in any of the cultures tested. The most intriguing aspect of this study was the demonstration that patient-derived $CD14^+$ cells, cultured for 7 days in MCSF, showed no expression of DR3. The reasons for the lack of expression, when compared to the results from chapter 4, suggests a fundamental change in the cells with aging. However, there are currently no studies looking at the expression of death receptors on the surface of immune cells and how these change with age. This finding could have important implications not only in the pathogenesis of adverse bone pathology but also with the impaired immune response associated with aging. Further research is required to elucidate the importance of DR3 expression on normal monocyte / macrophage / T cell immune function. In addition to OC precursor's expression of DR3 has also been demonstrated on the surface of OB. However, whether it has a role in OB differentiation and bone formation is unknown and will be investigated in the next chapter.

Chapter 6

The Role of Death Receptor 3 in Murine Osteoblast Function

6.1 **Introduction**

Investigations in chapter 5, which studied the potential role of the DR3/TL1A pathway in the pathogenesis of RA and OP, produced a number of intriguing findings. Serum TL1A levels were frequently higher in seropositive RA patients with erosive bone disease than in RA patients without bone changes detectable by X-ray. However, there was no link between DR3/TL1A and increased fracture risk or OP. This was a surprising finding as each condition is characterised by OC-over activity, and both TL1A and DR3 were found to promote OC differentiation and increase bone-matrix resorption (Chapter 4). Increased OC activity is a causal factor in reducing BMD and bone quality associated with OP. However, reduced OB activity and increased differentiation of mesenchymal stem cells into adipocytes rather than OB also plays a significant role (198, 199, 386). As discussed in the introduction OB activity is regulated by a number of factors within its microenvironment, including members of the TNFSF and their receptors. Recent studies by Bu et al (261) and Borysenko et al (241) identified expression of DR3 on the surface of human OB and the MG63 OB cell line, revealing it as a potential regulator of bone formation. This chapter will therefore investigate whether DR3 and TL1A are expressed by murine OB, and assess the functional role they play in OB differentiation and bone formation *in vitro*.

The function of the death receptor group of the TNFRSF in OB differentiation, function and survival has not been fully defined, with studies demonstrating opposing effects of signalling on OB differentiation and survival. Osteoblasts express the death receptors Fas (CD95, TNFRSF6) (261, 387), DR4 (TNFRSF10A), DR5 (TNFRSF10B) (261, 388), TNFR1 (TNFRSF1A) (261) and DR3 (TNFRSF25) (241, 261) at varying levels throughout their differentiation. Studies into the effects of these receptors and their ligands on OB biology have demonstrated roles in inhibition of OB differentiation (261, 387, 389-392), induction of apoptosis (261, 388, 393, 394) and stimulation of early OB proliferation (389, 395). These data highlight the complex role that death receptors play in OB homeostasis, simultaneously affecting survival and differentiation. Expression of full-length DR3 on primary human OB and the MG63 cell line was initially shown by Bu et al (261). This finding was supported by Borysenko et al (241), who additionally investigated the role of DR3 and TL1A in OB survival.

In the Borysenko et al (241) study cross-linking of DR3 with an anti-DR3 monoclonal antibody (mAb) on the osteoblastic MG63 cell line was demonstrated to result in the

apoptosis of a large proportion of cells. This effect however, was only observed at low cell densities ($1x10^3$ cells/cm^2). At higher cell densities ($3x10^3$ cells/cm^2 and $9x10^3$ cells/cm^2) the effects of DR3 cross-linking on survival were lost in a graded manner; with % viable cells comparable between the naïve and anti-DR3 treated cultures. Intriguingly, addition of TL1A to primary OB cultures had no effect on apoptosis, suggesting that the primary role of DR3/TL1A in OB biology is not cell survival. This is supported by the results from long-term antibody cross-linking of DR3 on MG63 cells. These experiments showed that antibody cross-linking resulted in altered growth pattern of the cells to a monotonous monolayer and reduced matrix synthesis, suggesting that activation of DR3 inhibits OB differentiation. This role of DR3 in inhibition of OB differentiation was not conclusive, the effects were not reproducible with TL1A or in primary human OB (241). Therefore, activation of DR3 expressed on OB can result in a number of effects: inducing apoptosis, or inhibiting differentiation of MG63 cells. The study by Borysenko et al only investigated activation of DR3 by cross-linking or with non-physiological levels of TL1A (0.1µg/ml) on an OB cell line. The potential role of DR3 in the regulation of normal primary OB differentiation and function was not investigated. To address this question the role of DR3 in OB differentiation and function was analysed in this chapter using primary OB isolated from male $DR3^{wt}$ and $DR3^{ko}$ mice.

Analysis of OB alkaline phosphatase (ALP) activity and mineral deposition can provide valuable insight into their differentiation and function (396-402). ALP is an early marker of OB differentiation and is highly synthesised by the cells. It is initially expressed in the cytoplasm of the OB, though it is soon observed on the cell surface and in matrix vesicles that interact with the mineralised matrix (403, 404). Deletion of the tissue non-specific form of ALP in mice results in abnormal calcification, indicating the importance of the enzyme in the formation of the osteoid and in mineral deposition (405). As part of the mineralisation process the OB is required to break down organic components of the bone matrix; either removing old collagen fragments from the surface of the resorption pit or as part of matrix maturation (18-20, 166). This process has been demonstrated to be mediated by members of the MMP family (19). Work by Parikka et al (19) demonstrated that the osteoprogenitor population express MMP-2, -8, -13 and -14. Further work by Ben David et al (402) revealed the presence of the gelatinase MMP-9 in mesenchymal stem cell-derived cultures. Investigations in chapter 3 and chapter 4, which studied the effect of DR3 in OC differentiation and function, demonstrated that DR3/TL1A affects MMP-9 activation. The effect of DR3 on OB-derived MMP activation has never been investigated.

The aim of this chapter was to explore the role of DR3 in regulating OB differentiation and mineral deposition using precursor cells derived from the bone marrow of $DR3^{wt}$ and $DR3^{ko}$ mice. The effect of DR3 on OB differentiation was investigated by monitoring ALP levels over the time course of the experiments. Supernatants were collected across the culture period. MMP-2 and -9 were measured to determine DR3's effect on OB MMP expression. DR3's role in regulating the function of mature OB was examined by quantifying levels of mineral deposition. The specific objectives of this chapter are:

- To isolate and culture osteoprogenitor cells from DBA/1 mice.
- To characterise DR3 and TL1A expression by osteoprogenitors and mineralising osteoblasts.
- To assess the impact of DR3 on alkaline phosphatase, mineralisation and pro MMP-9 expression by osteoblasts grown from two mouse strains (DBA/1 and C57BL/6).
- To determine the effect of DR3 on osteoblast-derived MMP-2 and MMP-9 levels.
- To characterise the *in vivo* bone phenotype of $DR3^{wt}$ and $DR3^{ko}$ mice, bred on a DBA/1 background. Male and female mice were evaluated aged 8 weeks and 20 weeks.

6.2 **Results**

6.2.1 **Isolation and Culture of Osteoprogenitors from DBA/1 Mice**

For *in vitro* functional analyses, OB are frequently derived from mesenchymal stem cells that are isolated from BM and bone explants (398, 406, 407). OB assays from DBA/1 mice had not been established previously in the laboratory. In the first instance the best source of progenitor cells was identified, BM cells (from femora) and homogenised epiphysis/metaphysis explants from one mouse were tested (section 2.2.16). Bone marrow cultures produced significantly increased numbers of OPCs compared to the explant cultures across the time course (P=<0.0001; Fig 6.1 (a)). Significant differences were noted in confluence at every time point from day 26 to day 36 (58±3% versus 43±3%, P=<0.01). Cells isolated from the BM and explant cultures never reached 100% confluence.

Since BM cells produced the more efficient culture system, they were adopted as the cell source of choice for all subsequent assays. Next BM were isolated from the femora of 3 animals ($DR3^{wt}$ and $DR3^{ko}$; Fig 6.1 (b)) to determine whether increased numbers of starting mesenchymal stem cells would give rise to sufficient healthy OPCs for functional assessments. After only 3 days in culture, OPC confluence was calculated as 63±3% in $DR3^{wt}$ and 58±3% in $DR3^{ko}$ cultures, and reached near 100% confluence at day 10 ($DR3^{wt}$=95±5% versus $DR3^{ko}$=98±3%).

All subsequent OB assays using DBA/1 mouse cells used BM isolated from the femora of three 3 animals as the initial source of MSCs.

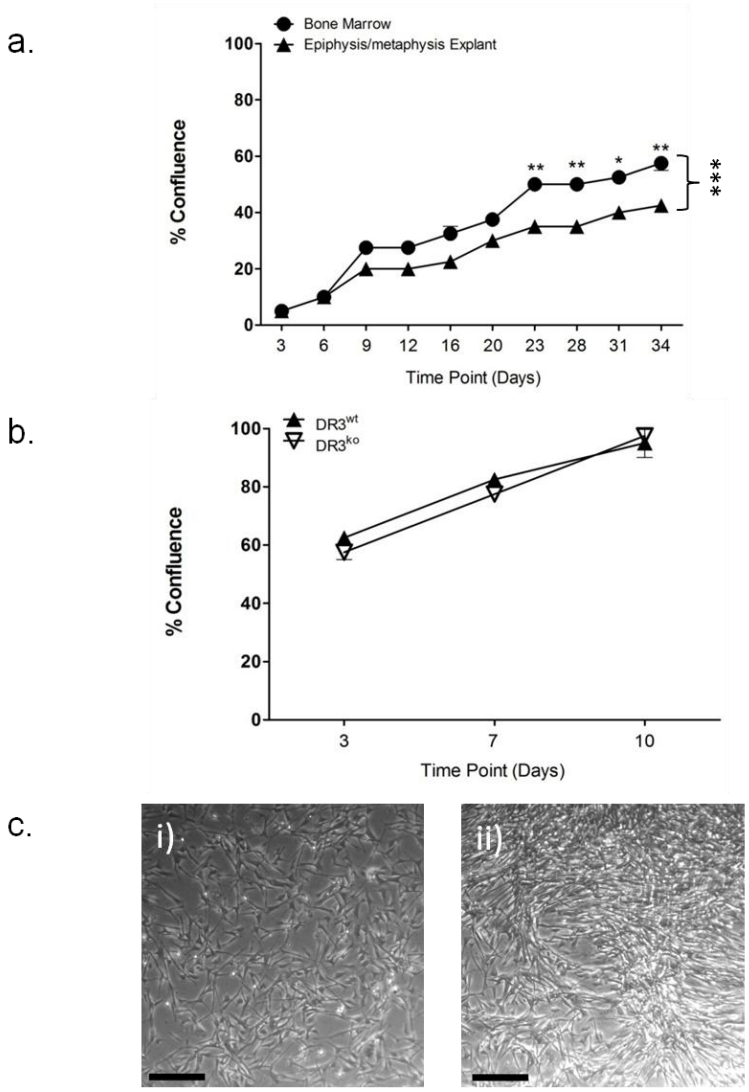

Figure 6.1. Identification and Development of DBA/1 Osteoprogenitor Source and Culture

Osteoprogenitor cells were used as the starting cell population for all OB mineralisation assays. Initial work focused on obtaining a suitable source and culture methodology. (a) Comparison of BM and epiphysis / metaphysis explants as a source of OPCs (n=1, 1 rep). Increased numbers of OPCs were observed in the bone marrow cultures (****P*=<0.0001) across the time course; significant increases were observed at time points day 23 (***P*=<0.01), day 28 (***P*=<0.01), day 31 (**P*=<0.05) and day 34 (***P*=<0.01). (b) Isolated BM from 3 DR3^{wt} and 3 DR3^{ko} DBA mice was added to a T75 tissue culture flask. OPCs reached confluence after 10 days culture. (c) Representative pictures of DR3^{wt} cultures at i) 60% and ii) 100% confluence. Scale bar = 250µm. Statistical analysis was performed using a one-way ANOVA and Bonferroni post test.

6.2.2 **Expression of DR3 on Osteoprogenitors and Mineralising Osteoblasts**

Borysenko et al (241) demonstrated expression of DR3 on the MG63 osteoblast cell line and human osteoblasts cultured from mesenchymal stem cells by flow cytometry and western analysis. However, expression of DR3 on murine OPCs and mature mineralising OB has not been demonstrated previously. CD44 and RANKL are expressed at all stages of OB differentiation (408-413); they were tested alongside DR3 as surrogate markers of OB differentiation. Expression levels of DR3, CD44 and RANKL were measured by flow cytometry (section 2.2.17) and reported as fold increase in median fluorescent intensity (MFI) of the isotype control (mean±SEM).

DR3 expression was detected on the surface of $DR3^{wt}$ OPCs (1.8±0.2). A small sub-population of $DR3^{wt}$ cells demonstrated increased levels of DR3 expression, visualised by the shoulder present on the flow cytometry histogram. Levels of DR3 expression were reduced on $DR3^{wt}$ mineralising OB (1.4±0.8; Fig 6.2 (a)) compared to the OPCs. Negligible levels of DR3 were detected on the surface of $DR3^{ko}$ OPCs and mineralising OB. The diminutive expression detected was attributed to non-specific binding of the polyclonal antibody used for analysis.

Comparable levels of CD44 ($DR3^{wt}$=14.7±1.6, $DR3^{ko}$=13.3±2.4) and RANKL ($DR3^{wt}$=3.0±0.8, $DR3^{ko}$=2.6±0.8) expression were detected on the surface of OPCs from $DR3^{wt}$ and $DR3^{ko}$ mice. Analysis of the $DR3^{wt}$ and $DR3^{ko}$ mineralising OB demonstrated no significant difference in CD44 ($DR3^{wt}$=12.4±3.8, $DR3^{ko}$=13.0±5.3) or RANKL ($DR3^{wt}$=5.6±2.3%, $DR3^{ko}$=5.5±2.4) expression between the genotypes (Fig 6.2 (b) and Fig 6.2 (c))

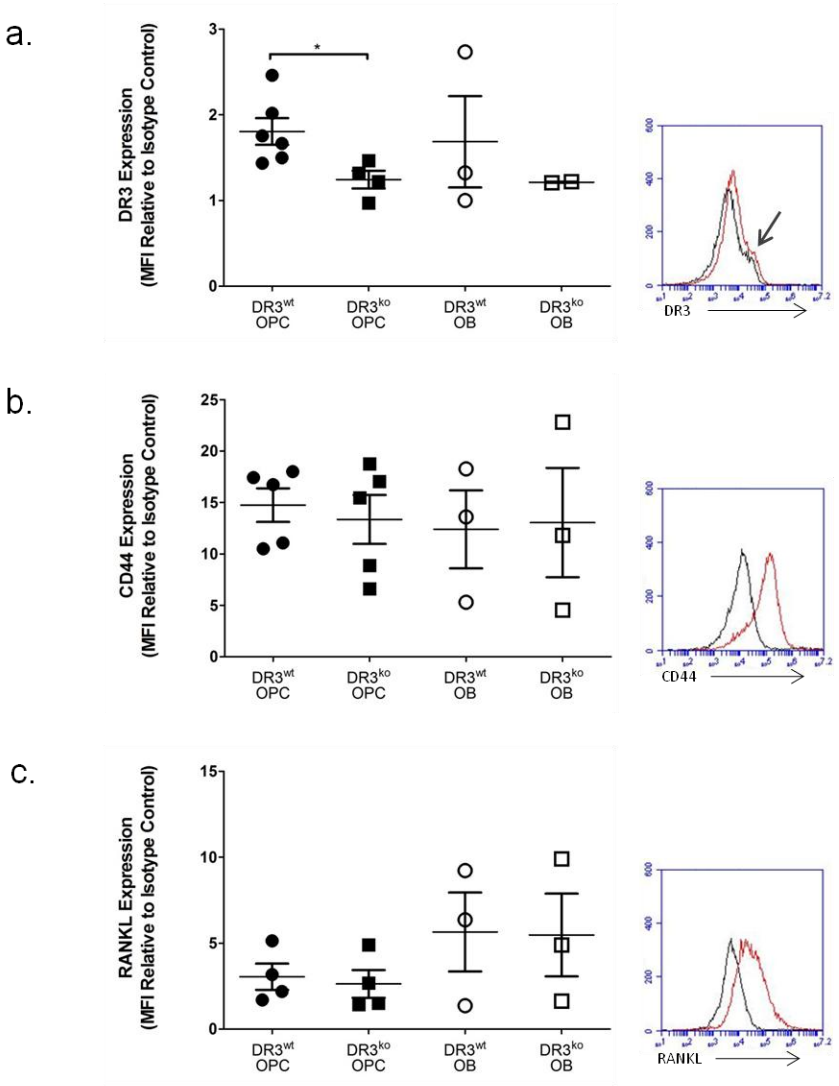

Figure 6.2. DR3 is Expressed on DR3^{wt} Osteoprogenitors and Mineralising Osteoblasts

Bone marrow was isolated from the femora of DR3^{wt} and DR3^{ko} DBA mice and re-suspended in T25 tissue culture flasks. Osteoprogenitors were cultured to 80% confluence and mineralisation medium added to half the flasks. Cells were stained with either an isotype control (black line) or with an anti-mouse DR3 antibody, anti-mouse CD44 antibody or anti-mouse RANKL antibody (red line) and tested by flow cytometry (a) Specific DR3 expression was detected on DR3^{wt} osteoprogenitors (*P=<0.01), arrow represents sub-population of cells displaying increased DR3 expression. On DR3^{wt} mineralising OB and DR3^{ko} cells no specific DR3 expression was detected. No difference in (b) CD44 and (c) RANKL expression was detected between DR3^{wt} and DR3^{ko} cells. Statistical analysis was performed with a two tail unpaired t-test.

6.2.3 **Development of Primers for the Detection of TL1A**

TL1A expression by OPCs and mineralising OB has not been determined previously. At the time this study was conducted, commercial antibodies for the detection of murine TL1A were unavailable. For this reason, four primers for the detection of murine TL1A mRNA (by PCR) were designed and tested *in-house*. As a positive control TL1A expression was induced by stimulation with immune complexes (IC) in RAW cells. mRNA was isolated and converted to cDNA (section 2.2.18.1). TL1A gradient PCR was performed according to section 2.2.18.2. Estimated TL1A product sizes for each of the four primers were calculated as follows: primer 1 – 75bp**,** primer 2 – 149bp**,** primer 3 – 166bp**,** and primer 4 – 91bp. No bands were detected at any temperatures for primer 1. At 53°C and 60°C no product was detected for primer 2 and 3, while multiple bands were detected at 55.6°C (primer 2 = 200bp, 250bp and ~300bp; primer 3 = 150bp and 300bp), 58°C (primer 2 = 200bp, 250bp and ~300bp; primer 3 = 150bp and 100bp) and 59°C (primer 2 = 100bp, 200bp and 300bp; primer 3 = 150bp and 100bp)**,** suggesting a level of non-specific amplification (Fig 6.3 (a)). A band at ~96bp was detected at all temperatures for primer 4, corresponding to the estimated TL1A product size (Fig 6.3 (b)). All subsequent murine TL1A PCR reactions were performed with primer 4 and an annealing temperature of 59°C.

6.2.4 **Assessing the Specificity of Primer 4 for the Amplification of TL1A mRNA**

To assess the specificity of primer 4 for TL1A, amplified product from section 6.2.3 was excised from the electrophoresis gel (Fig 6.4 (a)) and sent to Eurofins MWG Operon (Ebersberg, Germany) for sequencing. Results from the sequencing and subsequent BLAST analysis revealed the product to be a 94% match to murine TL1A (Fig 6.4 (b)), with the remaining 6% error possibly due to mis-reading by the sequencer. The results confirm the specificity of primer 4 for TL1A.

6.2.5 **Determining Expression of TL1A by Osteoprogenitors and Differentiating Osteoblasts**

Investigation into the effect of DR3/TL1A in OC formation and resorptive function in chapter 3 revealed contrasting effects of TL1A in the DBA/1 and C57BL/6 strains. Subsequent assays in this chapter were performed using cells derived from DBA/1 and C57BL/6 mice, to determine whether there were strain-specific differences in OB biology.

DBA/1 OPCs were isolated and cultured according to section 6.2.1. C57BL/6 OPCs were isolated and cultured according to work previously carried out in the laboratory by Anja Bloom (308). To assess whether OPC or differentiating OB express TL1A, mRNA was isolated from C57BL/6 and DBA/1 $DR3^{wt}$ and $DR3^{ko}$ cells. mRNA was tested by RT-PCR using primer 4 (section 2.2.24.3). A band at ~96bp was detected for OPCs (day 0) and differentiating OB (days 5, 10 and 15) corresponding to the size of TL1A (Fig 6.5). The result demonstrates that OPCs and differentiating osteoblasts produce TL1A mRNA.

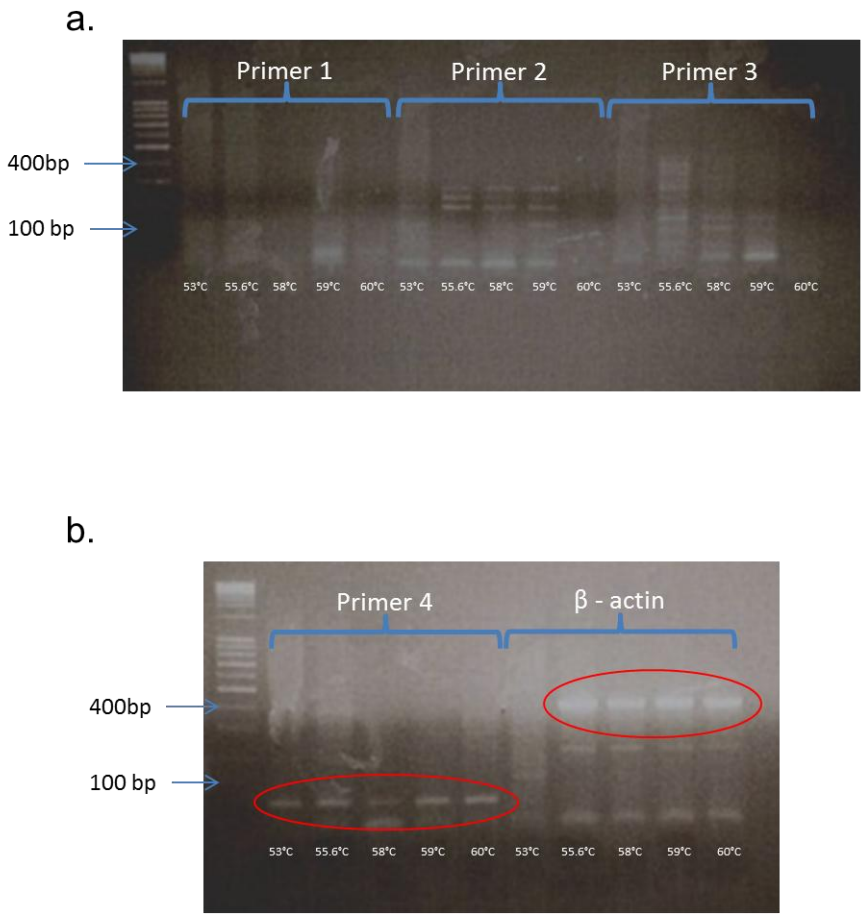

Figure 6.3. TL1A Primer 4 Produces a Product Equivalent to Calculated TL1A Product Size

RAW cells were stimulated with immune complexes and mRNA extracted and converted to cDNA by RT-PCR. Gradient PCR was performed on the cDNA using primers designed for the amplification of TL1A. A β-actin primer was used as a positive control. (a) Primers 1, 2 and 3 failed to produce bands that corresponded to the calculated size of the TL1A product, for the respective primer, at any of the temperatures tested. (b) Bands were observed, at all temperatures, for primer 4 at a molecular weight of approx. 90bp corresponding to the calculated size of the TL1A product – 91bp. The β – actin primer produced a band at a molecular weight of 450bp corresponding to the calculated product size.

a.

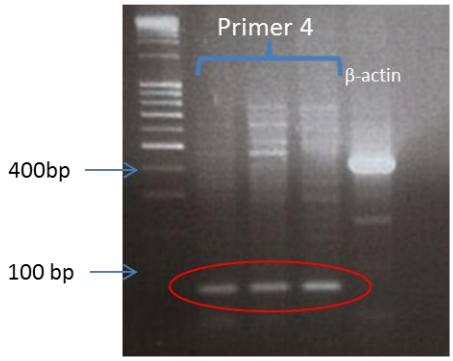

b.

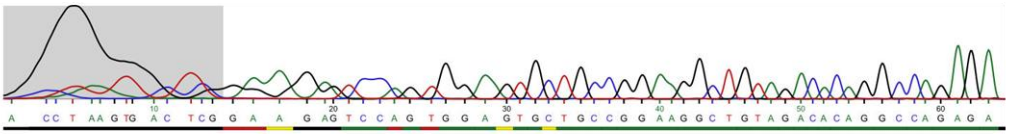

Features in this part of subject sequence:
tumor necrosis factor ligand superfamily member 15

Score = 75.0 bits (40), Expect = 6e-12
Identities = 48/51 (94%), Gaps = 3/51 (6%)
Strand=Plus/Minus

```
Query  1         GAA-GAGT-CCAGTGG-AGTGCTGCCGGAAGGCTGTAGACACAGGCCAGAG  48
                 ||| |||| ||||||| ||||||||||||||||||||||||||||||||||
Sbjct  60695000  GAAGGAGTCCCAGTGGAAGTGCTGCCGGAAGGCTGTAGACACAGGCCAGAG  60694950
```

Figure 6.4. TL1A Primer 4 is Specific to and Amplifies TL1A cDNA

RAW cells were stimulated with immune complexes and mRNA extracted and converted to cDNA by RT-PCR. PCR was performed on the cDNA using primer 4 for the amplification of TL1A. A β-actin primer was used as a positive control. (a) PCR of the cDNA produced a band size corresponding to the calculated size of the TL1A product . Bands were excised from the gel and sent for DNA sequencing. (b) BLAST analysis of the sequence confirmed that primer 4 is specific to and amplifies TL1A cDNA.

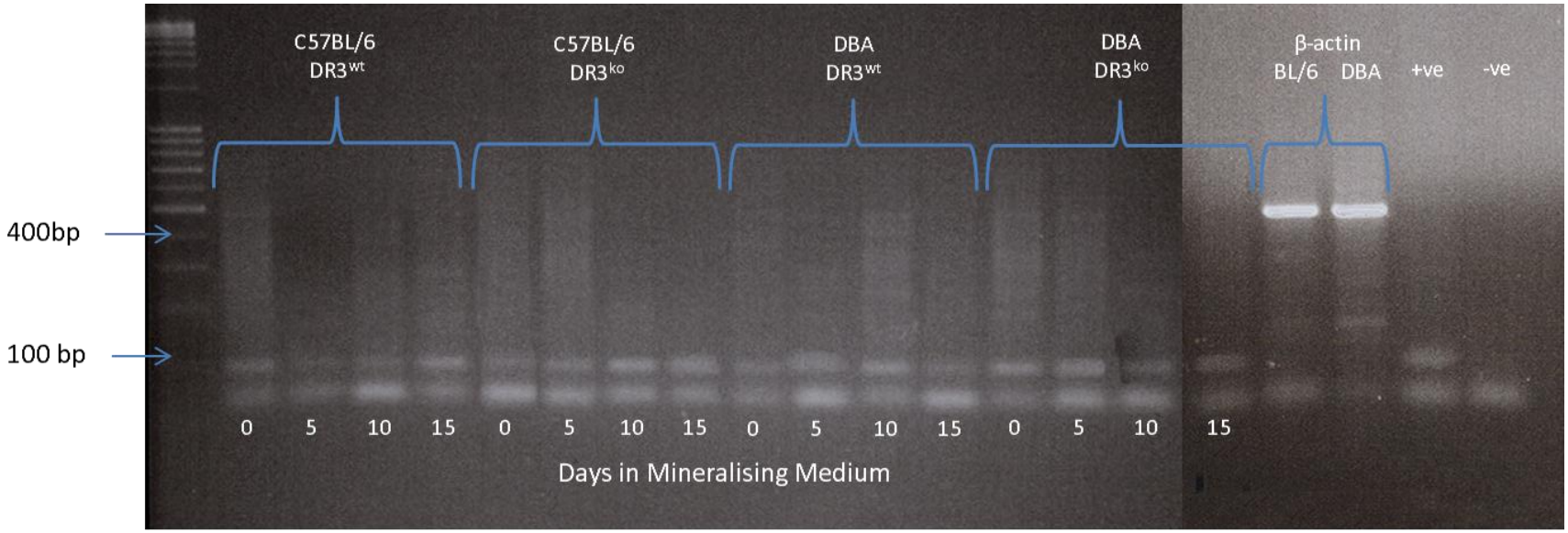

Figure 6.5. TL1A mRNA is Constitutively Expressed by Pre-osteoblasts and Mineralising Osteoblasts

Bone marrow was isolated from the femora of DR3^{wt} and DR3^{ko} DBA and C57BL/6 mice and osteoprogenitors grown to confluence. Cells were split and mineralisation medium added. At designated time points mRNA was extracted and converted to cDNA by RT-PCR. TL1A PCR, using primer 4, was performed on cDNA from all samples. A band corresponding to 90bp was detected for all samples, demonstrating constitutive expression of TL1A by osteoblasts during differentiation.

6.2.6 **Assessing the Impact of DR3 on Osteoblast Alkaline Phosphatase Activity**

To assess the effect of DR3 on OB differentiation, mineralisation assays were performed using DBA/1 and C57BL/6-derived cells and levels of the early OB differentiation marker ALP were analysed (section 2.2.16.1). ALP activity was expressed as % staining (mean±SEM) for graphical presentation (Fig 6.6).

Levels of ALP staining were significantly elevated in DBA/1 $DR3^{wt}$ cultures across the time course compared to the $DR3^{ko}$ cultures (*P*=<0.05; Fig 6.7 (a)). At the earliest time point assessed (day 17) levels were raised in the $DR3^{wt}$ cultures (43±8%) over the $DR3^{ko}$ cultures (32±7%), however this difference was not significant. These levels did not vary significantly over the remaining time points assessed: day 20, day 23 and day 26.

In C57BL/6 cultures (Fig 6.7 (b)) levels of ALP staining at day 17 were significantly elevated in the $DR3^{wt}$ (66±2%) versus $DR3^{ko}$ (34±3%; *P*=<0.0001) cultures. These levels remained relatively constant to day 23. At day 26 a significant increase in ALP staining was observed in the $DR3^{wt}$ (76±3%; *P*=<0.001) compared to $DR3^{ko}$ (44±4%; *P*= <0.01) cultures. Significantly elevated ALP staining was detected in the in $DR3^{wt}$ cultures (*P*=<0.0001) across the time course.

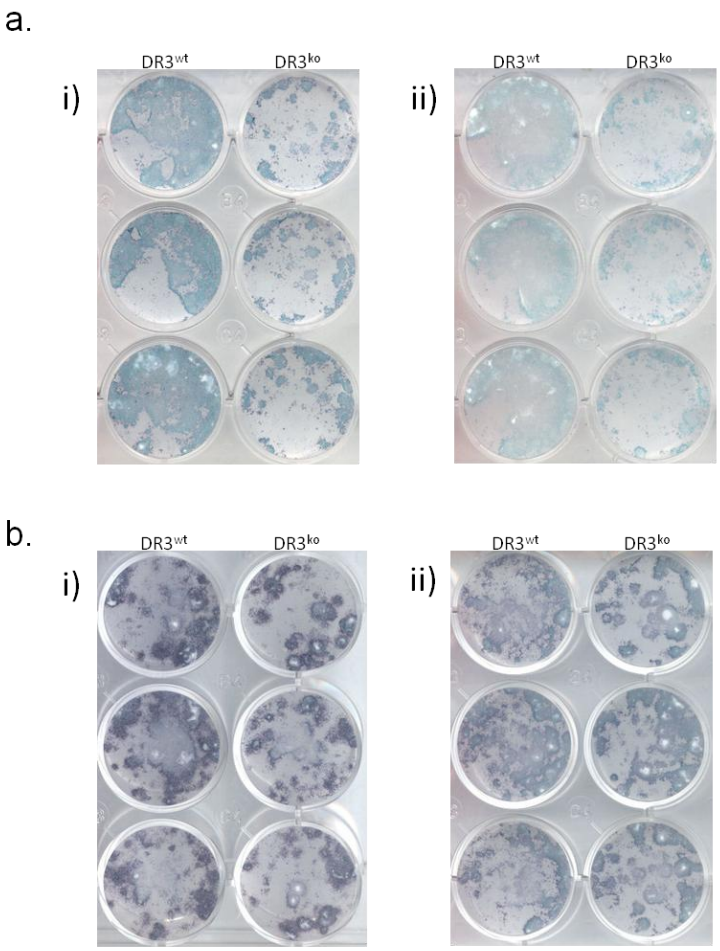

Fig 6.6. Representative Pictures of DBA/1 and C57BL/6 Alkaline Phosphatase Staining

Bone marrow was isolated from the femora of $DR3^{wt}$ and $DR3^{ko}$ DBA/1 and C57BL/6 mice and osteoprogenitors grown to confluence. Cells were split and plated at $4x10^4$ cells / well. Mineralisation medium was added and cells cultured for up to 26 days before being stained with ALP stain, for detection of alkaline phosphatase. Representative pictures of (a) DBA/1 and (b) C57BL/6 cultures at (i) day 17 and (ii) day 26.

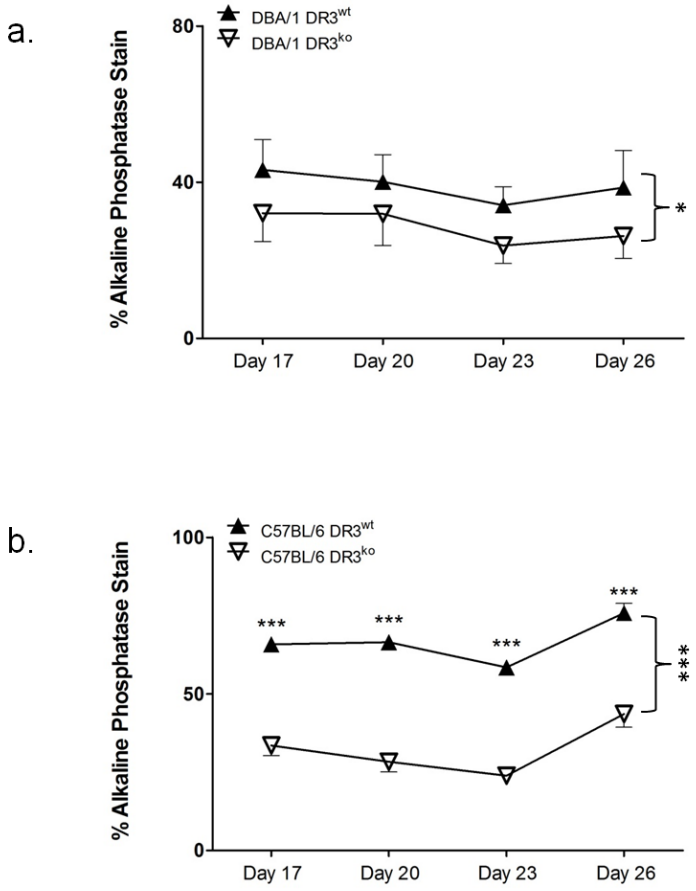

Figure 6.7. DBA/1 and C57BL/6 DR3^{wt} Osteoblasts Exhibit Significantly Increased Alkaline Phosphatase Staining

Bone marrow was isolated from the femora of DR3^{wt} and DR3^{ko} DBA/1 (n=3) and C57BL/6 (n=4) mice and osteoprogenitors grown to confluence (3 reps per condition). Cells were split and plated at 4x10^4 cells / well. Mineralisation medium was added and cells cultured for up to 26 days before being stained with ALP stain, for detection of alkaline phosphatase activity. % area exhibiting ALP activity was calculated. ALP activity was significantly elevated across the time course in (a) DBA/1 DR3^{wt} cultures (*P=<0.05) and (b) C57BL/6 DR3^{wt} cultures (***P=<0.0001); with significant differences observed at all time points (***P=<0.0001). Statistical analysis was performed with a two-way ANOVA and Bonferroni post test.

6.2.7 **Determining the Effect of DR3 on Osteoblast Cell Number**

The increase in ALP staining observed in section 6.2.6 could be due to increased cell number in the $DR3^{wt}$ cultures. To identify whether DR3 affected cell proliferation, cells were stained with DAPI and cell number calculated (section 2.2.14.5; Fig 6.8(a)). Comparison of cell number (cell / mm^2, mean±SEM) demonstrated no significant difference between $DR3^{wt}$ (34.5±3.2) and $DR3^{ko}$ (35.8±3.6) cultures (Fig 6.8 (b)). The data indicates that DR3 does not affect OPC / OB proliferation or cell survival.

6.2.8 **Determining the Effect of DR3 on the Expression of Pro MMP-9**

Degradation of the ECM and matrix maturation by OB-lineage cells during bone remodelling is regulated by members of the matrix metalloproteinase family, which include MMP-9 (121, 414). As a primary functional measure, the effect of DR3 upon pro MMP-9 expression by OB was determined. Levels were measured (by ELISA) across the differentiation time course in supernatants harvested from both DBA/1 and C57BL/6 cultures (section 2.2.14.4.1).

In DBA/1 cultures, levels of pro MMP-9 (Fig 6.9 (a)); mean±SEM) were significantly elevated at day 3 when $DR3^{wt}$ and $DR3^{ko}$ were compared (3.45±0.67ng/ml versus 1.47±0.19ng/ml; *P*=<0.0001). At day 7 pro MMP-9 levels in both $DR3^{wt}$ and $DR3^{ko}$ cultures dropped (0.80±0.16ng/ml versus 0.68±0.23ng/ml) and continued to decline to day 26 (0.21±0.18ng/ml versus 0.16±0.16ng/ml), when levels were comparable. Nevertheless, levels of pro MMP-9 were significantly elevated in the $DR3^{wt}$ versus $DR3^{ko}$ cultures across the time course (*P*=<0.05).

In C57BL/6 cultures (Fig 6.9 (b)) levels of pro MMP-9 at day 3 were 0.31±0.10ng/ml and 0.03±0.02ng/ml for $DR3^{wt}$ and $DR3^{ko}$ respectively. These levels were lower than those observed in the DBA/1 cultures. Pro MMP-9 levels remained low and relatively consistent until day 14**,** when they increased significantly to 0.51±0.17ng/ml for $DR3^{wt}$ and 4.09±1.00ng/ml for $DR3^{ko}$ (*P*=<0.05). Maximum pro MMP-9 levels were observed in $DR3^{wt}$ on day 23 (2.49±0.72ng/ml) and $DR3^{ko}$ on day 20 (7.44±1.24ng/ml). This translated into significantly elevated pro MMP-9 in $DR3^{ko}$ over $DR3^{wt}$ cultures across the time course (*P*=<0.0001).

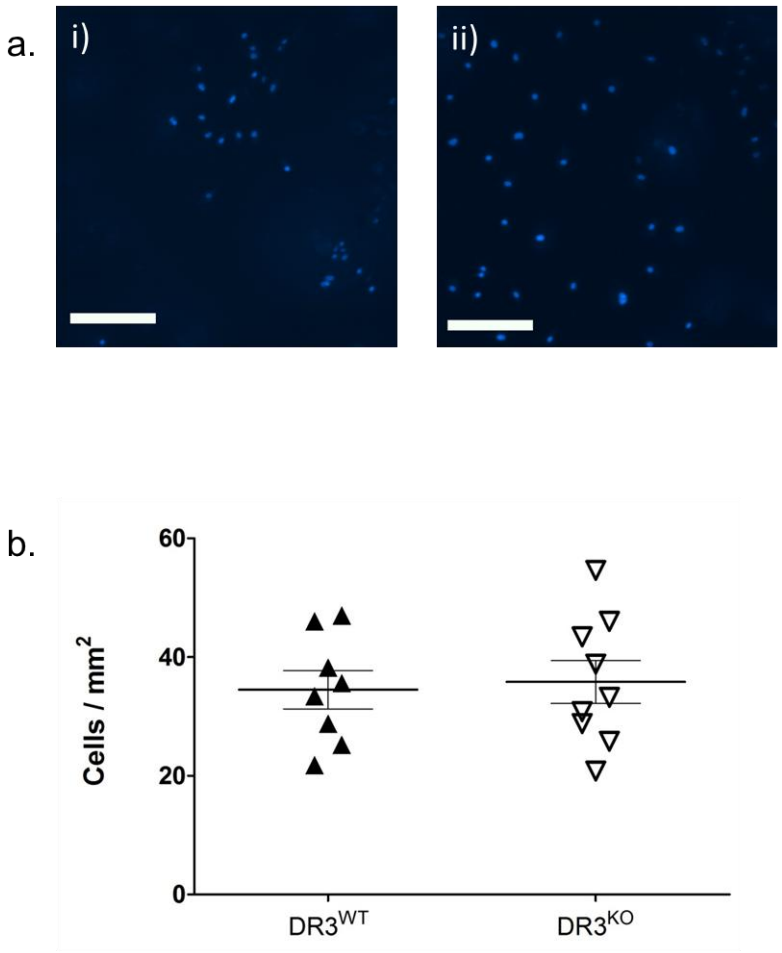

Figure 6.8. Cell Number is Comparable between DR3^{WT} and DR3^{KO} Osteoblast Cultures at Day 26

Bone marrow was isolated from the femora of DR3^{wt} and DR3^{ko} DBA/1 mice and osteoprogenitors grown to confluence. Cells were split and plated at 4x10^4 cells / well. Mineralisation medium was added and cells cultured for 26 days. Cells were stained with DAPI and the number of cells / mm^2 calculated. (a) Representative pictures of DAPI stained (i) DR3^{wt} and (ii) DR3^{ko} cultures. (b) No difference in cell number was detected between DR3^{wt} and DR3^{ko} cultures. Scale bar = 250µm. Statistical analysis was performed with a two tail unpaired t-test.

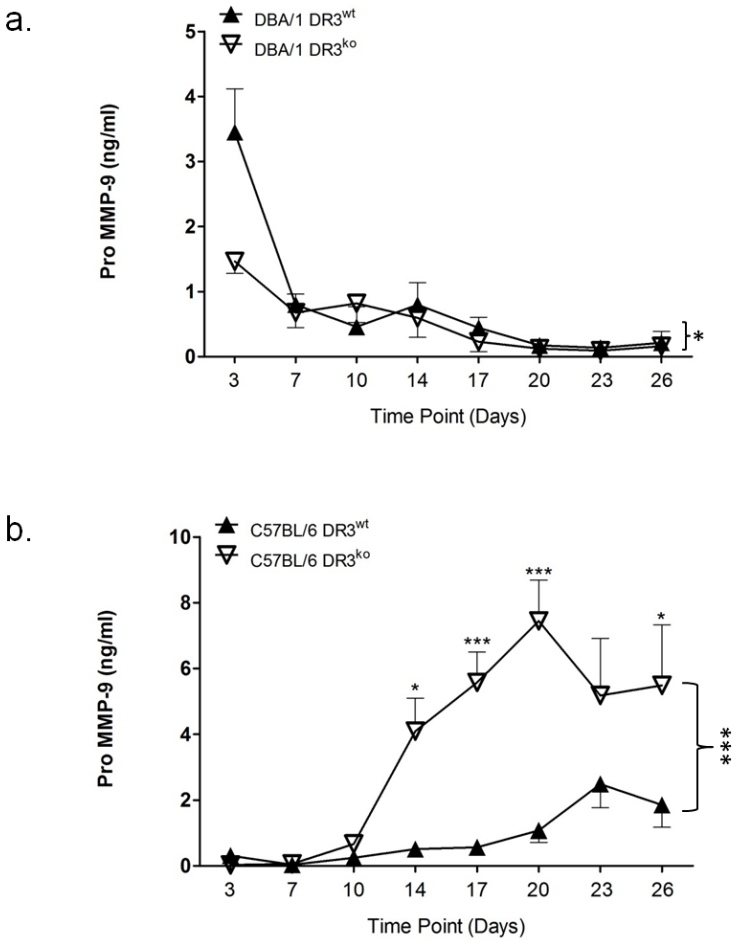

Figure 6.9. DBA/1 and C57BL/6 Osteoblasts Exhibit Different pro MMP-9 Expression Profiles

Bone marrow was isolated from the femora of DR3^{wt} and DR3^{ko} DBA/1 (n=3) and C57BL/6 (n=4) mice and osteoprogenitors grown to confluence (3 reps per condition). Cells were split and plated at 4x10^4 cells / well. Mineralisation medium was added and cells cultured for 26 days. Supernatants were collected across the time course and tested for levels of pro MMP-9. Levels of pro MMP-9 were significantly elevated across the time course in (a) DBA/1 DR3^{wt} cultures (*P=<0.05); with a significant difference observed at day 3 (***P=<0.0001). In (b) C57BL/6 cultures levels of pro MMP-9 were significantly elevated in DR3^{ko} cultures (***P=<0.0001) across the time course; with significant differences observed at day 14 (*P=<0.05), day 17 and day 20 (***P=<0.0001) and day 26 (**P=<0.01). Statistical analysis was performed with a two-way ANOVA and Bonferroni post test.

6.2.9 **Identifying the Effect of DR3 on Activation of Osteoblast-Derived MMPs in C57BL/6 Cultures**

Analysis of $DR3^{wt}$ and $DR3^{ko}$ cultures in section 6.2.8 showed a significant increase in pro MMP-9 in the $DR3^{ko}$ cultures. To ascertain whether DR3 was involved in the activation of OB-derived MMPs, a gelatine zymogram (section 2.2.14.4.1) was used to semi-quantitatively measure levels of pro and active MMP-2 and MMP-9 in C57BL/6 $DR3^{wt}$ and $DR3^{ko}$ OB cultures (n=1; Fig 6.10). Results are reported graphically as band intensity relative to a pro MMP-9 standard at a known concentration (10ng/ml). Further testing of C57BL/6 assays and DBA/1 assays was not performed due to time constraints of the project and ending of the AR UK studentship that funded this study.

Levels of pro MMP-2 detected at day 3 were low in both $DR3^{wt}$ (0.002) and $DR3^{ko}$ (0.002) cultures (Fig 6.11 (a, i)). At day 7 the relative levels of pro MMP-2 in both $DR3^{wt}$ and $DR3^{ko}$ cultures increased (0.10 versus 0.08) and showed minor variation across the differentiation time course. In contrast to pro MMP-2, at day 3 levels of active MMP-2 (Fig 6.11 (a, ii)) were 5.8-fold higher in the $DR3^{wt}$ (0.64) cultures compared to the $DR3^{ko}$ (0.11) cultures. Levels of active MMP-2 increased in the $DR3^{ko}$ cultures up to day 14 (0.53), where they were comparable to the $DR3^{wt}$ (0.56). Expression of active MMP-2 followed a similar pattern in $DR3^{wt}$ and $DR3^{ko}$ cultures for the remainder of the time course.

Relative band intensity of pro MMP-9 at day 3 was calculated at 0.06 and 0.05 in $DR3^{wt}$ and $DR3^{ko}$ cultures respectively (Fig 6.11 (b, i)). Levels of pro MMP-9 remained comparable and relatively low across the time course, peaking at day 23 in the $DR3^{wt}$ (0.10) and day 17 in the $DR3^{ko}$ (0.09) cultures. This result differs to the result in section 6.2.8 as DR3 had no effect on pro MMP-9 expression. DR3 was demonstrated to have an important role in the activation of OB-derived MMP-9. Stark differences in levels of active MMP-9 were observed between the $DR3^{wt}$ and $DR3^{ko}$ cultures across the time course (Fig 6.11 (b, ii)). Levels of active MMP-9 were highest at day 3 in the $DR3^{wt}$ cultures (0.19) and declined to day 20 (0.03). In contrast, active MMP-9 was not detected in the $DR3^{ko}$ cultures until day 20 (0.05), where levels were similar to the $DR3^{wt}$.

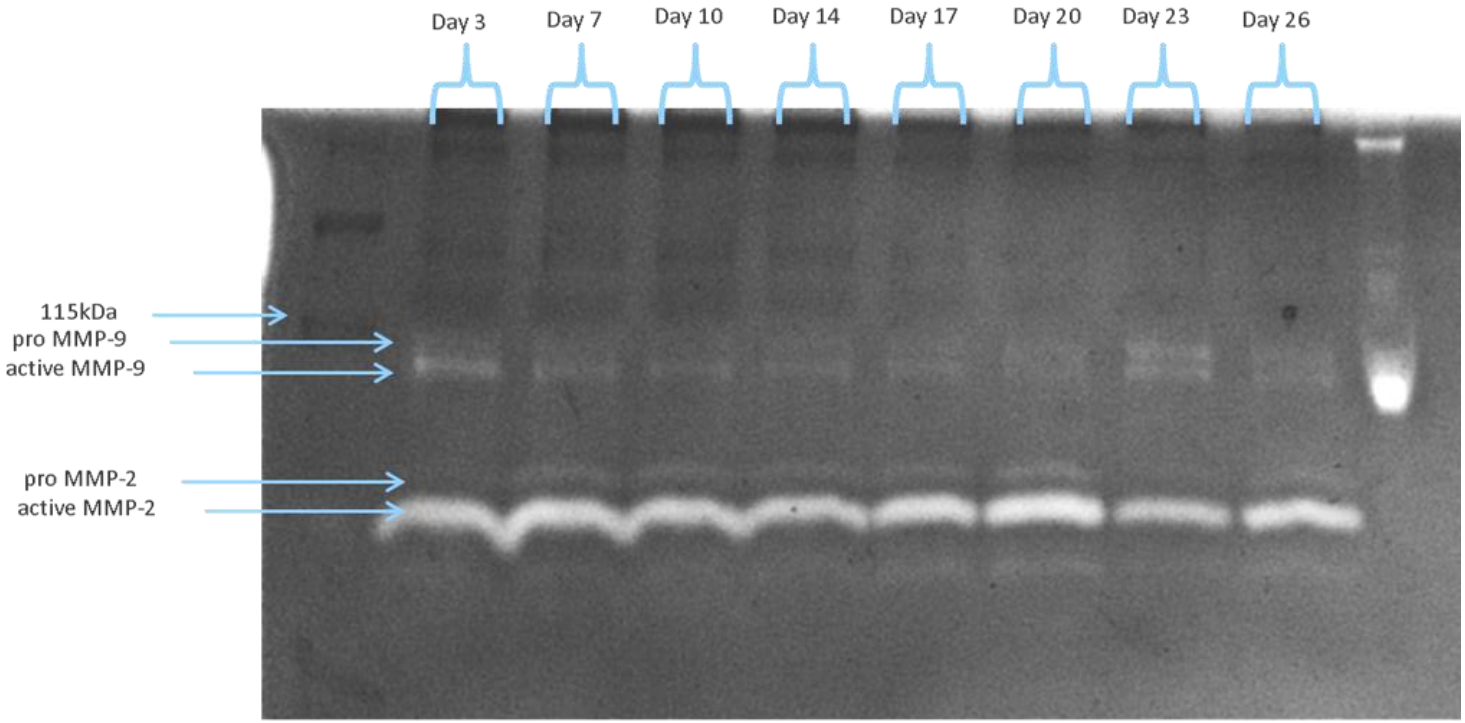

Figure 6.10. Levels of Pro and Active MMP-2 and -9 in C57BL/6 Osteoblasts Cultures

Supernatants from C57BL/6 DR3^{wt} and DR3^{ko} OB cultures were tested for levels of pro and active MMP-2 and MMP-9 by gelatine zymogram (n=1). Representative DR3^{wt} zymogram. Bands were detected at MW of approx. 92KDa (pro MMP-9), 82kDa (active MMP-9), 72kDa (pro MMP-2) and 68kDa (active MMP-2). A standard of 10ng/ml MMP-9 was run on each gel.

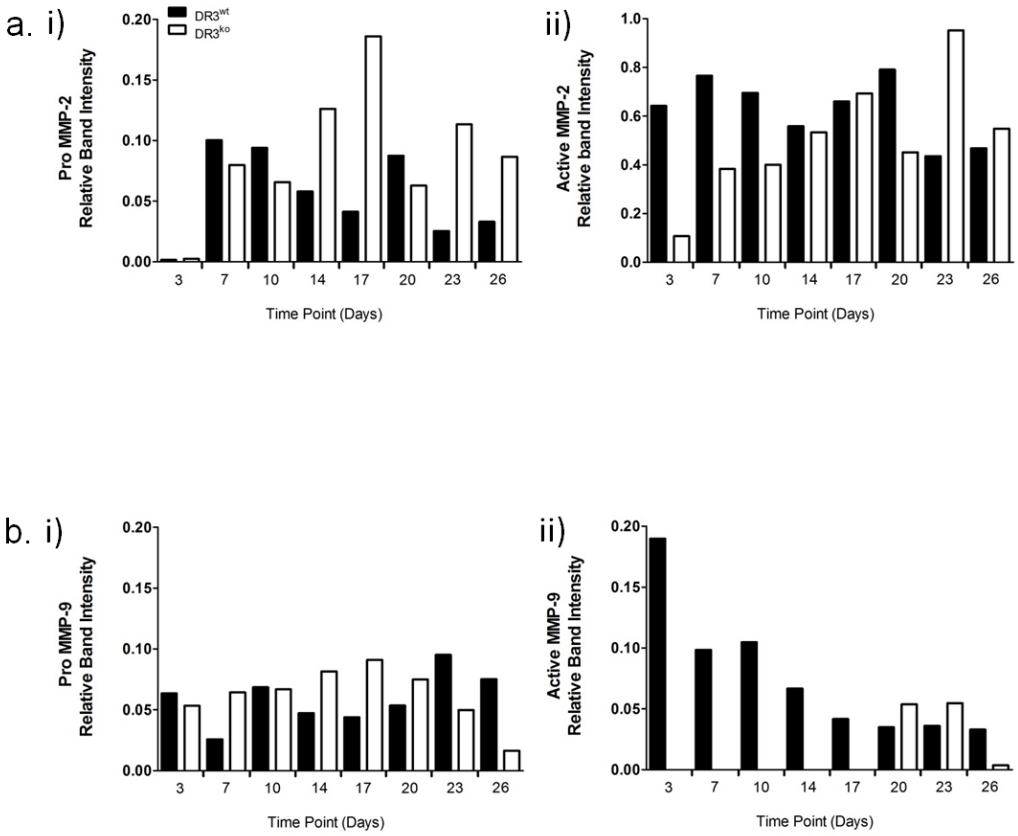

Figure 6.11. Levels of Active MMP-2 and MMP-9 are Elevated Early in C57BL/6 DR3^{wt} Osteoblast Cultures

Supernatants from C57BL/6 DR3^{wt} and DR3^{ko} OB cultures were tested for levels of i) pro and ii) active (a) MMP-2 and (b) MMP-9 by gelatine zymogram (n=1). Band intensities were compared to a pro MMP-9 standard at known concentration (10ng/ml). Levels of active MMP-2 and active MMP-9 in DR3^{wt} cultures were elevated early in the time course compared to DR3^{ko} cultures. No trend was observed in pro MMP-2 - 9 expression.

6.2.10 **Assessing the Effect of DR3 on Osteoblast Mineralisation**

The results from sections 6.2.6 and 6.2.9 showed that the presence of DR3 was linked to increased levels of OB differentiation and MMP activation. To determine what affect this had on OB mineral deposition, levels of mineralisation in DBA/1 and C57BL/6 cultures were analysed (Fig 6.12).

Levels of mineralisation (%; mean±SEM) in DBA/1 cultures (Fig 6.13 (a)) at day 17 were calculated at 2.6±0.4% ($DR3^{wt}$) and 1.8±0.3% ($DR3^{ko}$). Mineralisation increased at day 20 in the $DR3^{wt}$ cultures (4.5±0.7%), while levels remained constant in the $DR3^{ko}$ (1.8±0.3%). Significantly elevated levels of mineralisation were detected in $DR3^{wt}$ cultures at day 23 ($DR3^{wt}$=8.8±2.3% versus $DR3^{ko}$=3.0±0.6%; P=<0.0001). This resulted in significantly increased levels of mineralisation across the time course in the $DR3^{wt}$ cultures (P=<0.0001).

In C57BL/6 cultures levels of mineralisation were observed to be elevated compared to the DBA/1 cultures (Fig 6.13 (b)). At day 17 mineralisation in the $DR3^{wt}$ and $DR3^{ko}$ cultures were 19.1±4.0% and 2.5±0.9% respectively. Levels of mineralisation significantly increased in $DR3^{wt}$ (29.1±6.5%) cultures at day 20 compared to the $DR3^{ko}$ (3.5±1.1%; P=<0.01). Both $DR3^{wt}$ and $DR3^{ko}$ cultures displayed increased mineralisation over the remaining time points tested, resulting in significantly elevated mineralisation in the $DR3^{wt}$ over the $DR3^{ko}$ cultures (P=<0.0001).

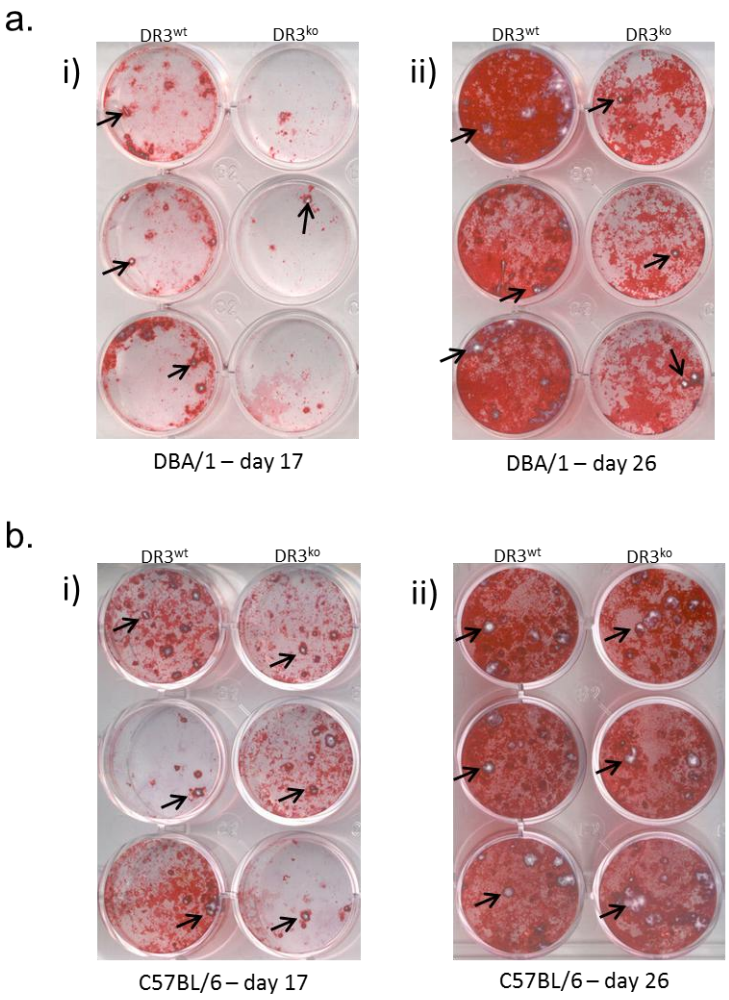

Fig 6.12. Representative Pictures of DBA/1 and C57BL/6 Mineralisation Staining

Bone marrow was isolated from the femora of $DR3^{wt}$ and $DR3^{ko}$ DBA/1 and C57BL/6 mice and osteoprogenitors grown to confluence. Cells were split and plated at $4x10^4$ cells / well. Mineralisation medium was added and cells cultured for up to 26 days before being stained with alizarin red, for detection of mineralisation. Representative pictures of (a) DBA/1 and (b) C57BL/6 cultures at (i) day 17 and (ii) day 26. Arrows indicate areas of high mineralisation

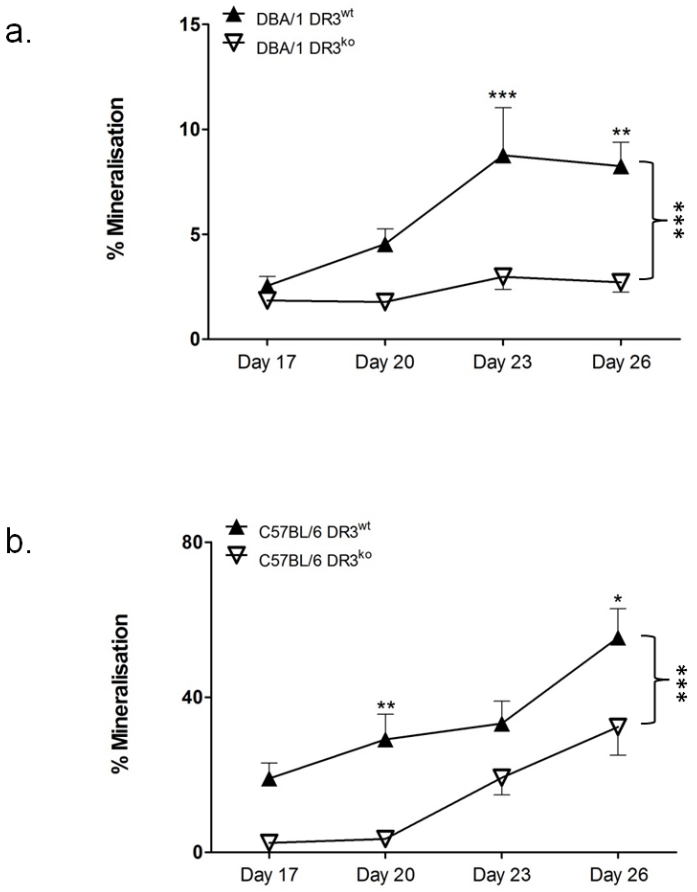

Figure 6.13. DBA/1 and C57BL/6 DR3^{wt} Osteoblasts Exhibit Significantly Increased Mineralisation

Bone marrow was isolated from the femora of DR3^{wt} and DR3^{ko} DBA/1 (n=3) and C57BL/6 (n=4) mice and osteoprogenitors grown to confluence. Cells were split and plated at 4x10^4 cells / well. Mineralisation medium was added and cells cultured for up to 26 days before being stained with alizarin red, for detection of mineralisation (3 reps per condition). % area mineralised was significantly elevated across the time course in (a) DBA/1 DR3^{wt} cultures (***P=<0.0001); with significant differences observed at day 23 (***P=<0.0001) and day 26 (**P=<0.01), and (b) C57BL/6 DR3^{wt} cultures (***P=<0.0001); with significant differences observed at day 20 (**P=<0.01) and day 26 (*P=<0.05). Statistical analysis was performed with a two-way ANOVA and Bonferroni post test.

6.2.11 **Comparison of DBA/1 and C57BL/6 Osteoblast Phenotype**

Differences in *in vivo* fracture healing and adult bone density have been demonstrated between inbred stains of mice (325, 326). The causes of these differences are unknown but variations *in vitro* MSC growth kinetics have been reported, suggesting dissimilarities in OB behaviour between strains (134, 327). To assess whether there was any fundamental variation in differentiation and function between DBA/1 and C57BL/6-derived OB, ALP staining (section 6.2.6), pro MMP-9 expression (section 6.2.8) and mineralisation (section 6.2.10) were compared in $DR3^{wt}$ cultures.

ALP activity was presented graphically as % of well displaying positive staining (mean±SEM). At day 17 levels of ALP staining (section 6.2.6) were significantly elevated in the C57BL/6 $DR3^{wt}$ cultures compared to the DBA/1 $DR3^{wt}$ cultures (66±2% versus 43±8%; *P*=<0.01). Levels of ALP staining remained relatively constant in the DBA/1 $DR3^{wt}$ cultures across the time course. In the C57BL/6 cultures ALP staining remained constant up to day 23, a significant increase in staining was observed at day 26 (76±3%; *P*=<0.001). Significantly elevated levels of ALP were detected across the time course in the C57BL/6 $DR3^{wt}$ compared to the DBA/1 $DR3^{wt}$ cultures (P=<0.0001; Fig 6.14 (a)).

The expression profile of pro MMP-9 (section 6.2.8) was observed to differ between the DBA/1 and C57BL/6 $DR3^{wt}$ cultures across the time course (Fig 6.14 (b)), with levels peaking early in the DBA/1 (day 3) and late in the C57BL/6 (day 23) cultures. At day 3 levels of pro MMP-9 were 10 times higher in the DBA/1 cultures over the C57BL/6 (3.45±0.67ng/ml versus 0.31±0.10ng/ml; *P*=<0.0001). Levels were comparable between the two strains from day 10 to day 17. At day 20 the expression of pro MMP-9 reversed with increased levels detected in the C57BL/6 cultures compared to the DBA/1 (1.08±0.36ng/ml versus 0.17±0.12ng/ml). Expression of pro MMP-9 peaked in the C57BL/6 cultures at day 23 with levels displaying a significant 17-fold increase compared to the DBA/1 cultures (2.49±0.72ng/ml versus 0.14±0.09ng/ml; *P*=<0.0001). Across the time course no significant difference in pro MMP-9 expression was detected between the DBA/1 and C57BL/6 cultures.

Mineral deposition was expressed as a % of the well surface with positive staining for alizarin red (mean±SEM). Levels of mineralisation (section 6.2.10) in the C57BL/6 $DR3^{wt}$ cultures were significantly elevated across the time course compared to the DBA/1 $DR3^{wt}$ (*P*=<0.0001; Fig 6.14 (c)). Mineralisation at day 17 was calculated at 19±4% (C57BL/6) and

3±0.4% (DBA/1). Levels of mineralisation increased in both the C57BL/6 and DBA/1 cultures across the differentiation time course. Mineralisation peaked at day 26, where significantly elevated levels were detected in the C57BL/6 compared to the DBA/1 cultures (55±8% versus 8±1%; *P*=<0.0001).

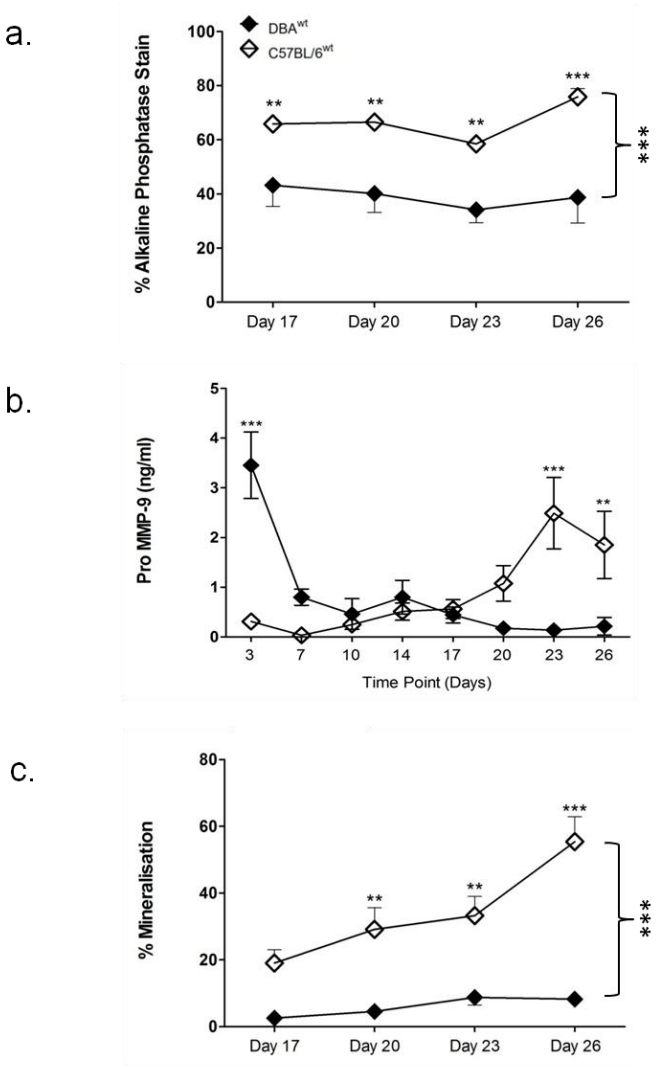

Figure 6.14. C57BL/6 DR3^{wt} Osteoblast Exhibit Significantly Increased Alkaline Phosphatase Activity and Mineralisation Compared to DBA/1 DR3^{wt} Osteoblasts

Bone marrow was isolated from the femora of DR3^{wt} DBA/1 (n=3) and C57BL/6 (n=4) mice and osteoprogenitors grown to confluence. Cells were split and plated at 4x10^4 cells / well. Mineralisation medium was added and cells cultured for up to 26 days (3 reps per condition). Across the time course C57BL/6 OB demonstrated significantly elevated (a) ALP activity (***P=<0.0001); with significant increases on day 17, 20, 23 (**P=<0.01) and day 26 (***P=<0.0001). Levels of pro MMP-9 (b) were elevated at day 3 in DBA/1 cultures (***P=<0.0001) and in C57BL/6 cultures at day 23 (***P<0.0001) and day 26 (**P=<0.01). No significant difference was detected across the time course. Mineralisation (c) was significantly increased in the C57BL/6 cultures across the time course (***P=<0.0001); with significant increases on day 20, 23 (**P=<0.01) and day 26 (***P=<0.0001). Statistical analysis was performed with a two-way ANOVA and Bonferroni post test.

6.2.12 **Phenotypic Analysis of Weight, Femur Length and Bone Density in DBA/1 DR3^{wt} and DR3^{ko} Mice**

The results from the *in vitro* OB mineralisation assays demonstrated differences in differentiation (section 6.2.6) and mineral deposition (section 6.2.10) between DBA/1 and C57BL/6 DR3^{wt}- and DR3^{ko}-derived OB. To determine whether these differences had an effect on the *in vivo* bone phenotype, mouse weight, femur length, femur bone density and vertebra bone density were measured. Male and female DBA/1 mice were used for the study to correspond with the OC assays (chapter 3) and OB assays (section 2.2.20; Fig 6.15). Measurements were taken in mice aged 8 and 20 weeks to identify any changes that occur during aging.

6.2.12.1 Mouse Weight

Mouse weights are reported as grams (mean±SEM) for graphical presentation. At 8 weeks (Fig 6.16 (a)) DR3^{wt} male mice were significantly heavier than their DR3^{ko} counterparts (21.3±0.6g versus 18.5±0.6g; *P*=<0.01). In the female cohort no difference was detected between the DR3^{wt} and DR3^{ko} mice (15.3±0.3g versus 16.5±0.2g). Male DR3^{wt} (*P*=<0.0001) and DR3^{ko} (*P*=<0.05) mice were significantly heavier than their female counterparts. At 20 weeks of age (Fig 6.17 (a)) no significant difference in weight was detected between male DR3^{wt} and DR3^{ko} mice (30.7±1.6g versus 29.3±0.7g). In the female cohort DR3^{wt} mice weighed significantly more than the DR3^{ko} mice (25.5±0.8g versus 20.3±1.1g; *P*=<0.05). Male DR3^{wt} (*P*=<0.05) and DR3^{ko} (*P*=<0.0001) mice were significantly heavier than their female counterparts at 20 weeks.

6.2.12.2 Femur Length

X-rays of disassociated murine femora were taken using the Carestream In Vivo FX Pro (section 2.2.20). Femur lengths were calculated using Carestream Molecular Imaging Software and presented graphically in mm (mean±SEM). At 8 weeks of age (Fig 6.16 (b)) no significant differences were observed in femora length between the DR3^{wt} and the DR3^{ko} male (12.4±0.2mm versus 11.8±0.4mm) and female (11.7±0.3mm versus 11.8±0.2mm) cohorts. At 20 weeks (Fig 6.17 (b)) no significant difference in femur length was detected in the male cohort (11.4±0.3mm versus 10.7±0.2mm) or the female cohort (9.5±0.4mm versus 10.5±0.1mm; *P*=<0.05). Male DR3^{wt} femora were significantly longer than the female DR3^{wt} femora (*P*=<0.0001) at 20 weeks.

6.2.12.3 Femur and Vertebra Bone Density

Femur and spine bone density (g/cm^3, mean±SEM) were calculated from X-rays according to section 2.2.26. At 8 weeks of age male femur bone densities were 1.63±0.15 (DR3^{wt}) and 1.50±0.09 (DR3^{ko}). Female femora bone densities were calculated as 1.52±0.09 and 1.61±0.03 in DR3^{wt} and DR3^{ko} mice respectively. Comparison of the data revealed no significant difference in femora bone density between the DR3^{wt} and DR3^{ko} mice. As with the femora, no significant difference was detected in vertebra bone density at 8 weeks in male and female mice. Vertebra bone densities in male mice were 2.56±0.39 (DR3^{wt}) and 2.83±0.30 (DR3^{ko}). Female vertebra bone density at 8 weeks was 2.57±0.11 in the DR3^{wt} and 2.77±0.16 in the DR3^{ko} (Fig 6.16 (c, ii)).

Femora bone density at 20 weeks (Fig 6.17 (c, i)) in male DBA/1 mice were 1.71±0.06 and 1.73±0.04 (DR3^{wt} and DR3^{ko}). In females, femora bone density in the DR3^{wt} was 1.70±0.02 and 1.72±0.03 in the DR3^{ko}. Differences in femora bone density in the males and females at 20 weeks were not significant. Comparison of vertebra bone density at 20 weeks (Fig 6.17 (c, ii)) revealed no significant difference between the DR3^{wt} and DR3^{ko} in both male (2.72±0.27 versus 3.39±0.32) and female (3.29±0.15 versus 3.05±0.49) DBA/1 mice.

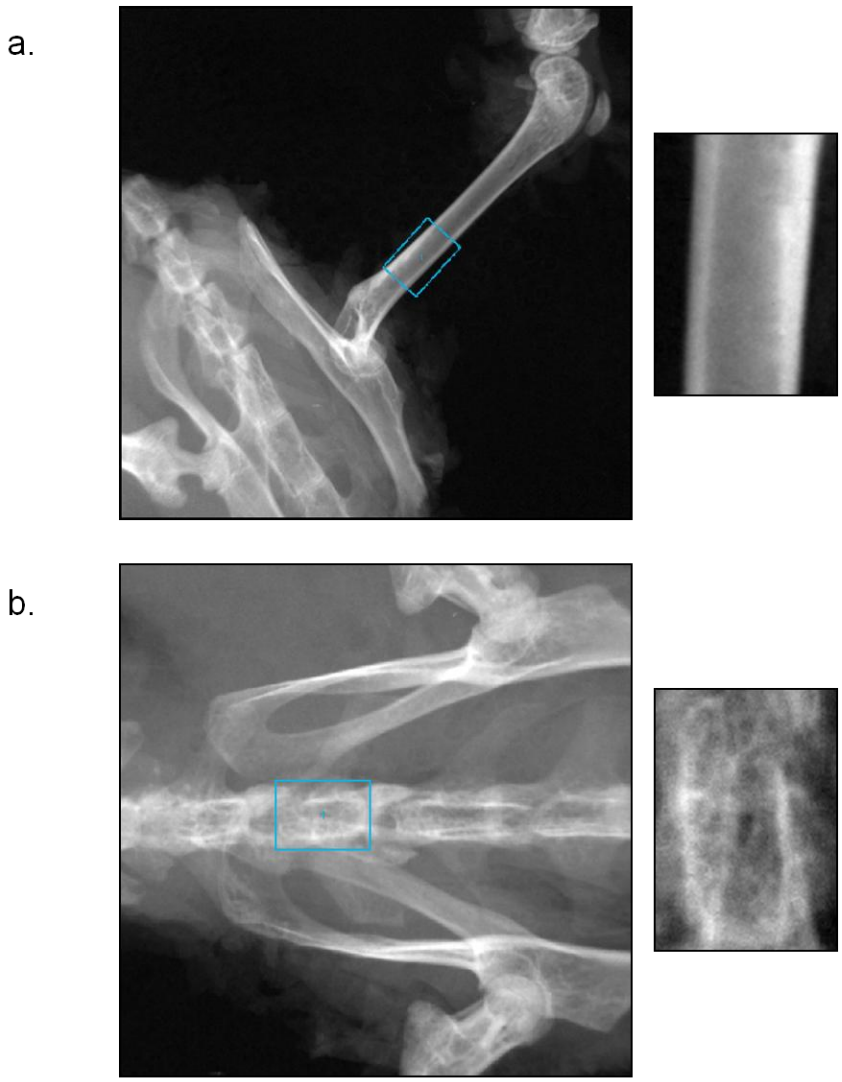

Figure 6.15. Representative X-rays of DBA/1 Mice used for Calculation of Femur Length and Bone Density

DBA/1 DR3^{wt} and DR3^{ko} mice (male and female) were aged for 8 and 20 weeks. Following sacrifice X-rays of the femur and spine were taken and used for calculation of femur length, and femur and spine bone density. Representative images of (a) femur bone density region of interest (ROI) and (b) spine bone density ROI.

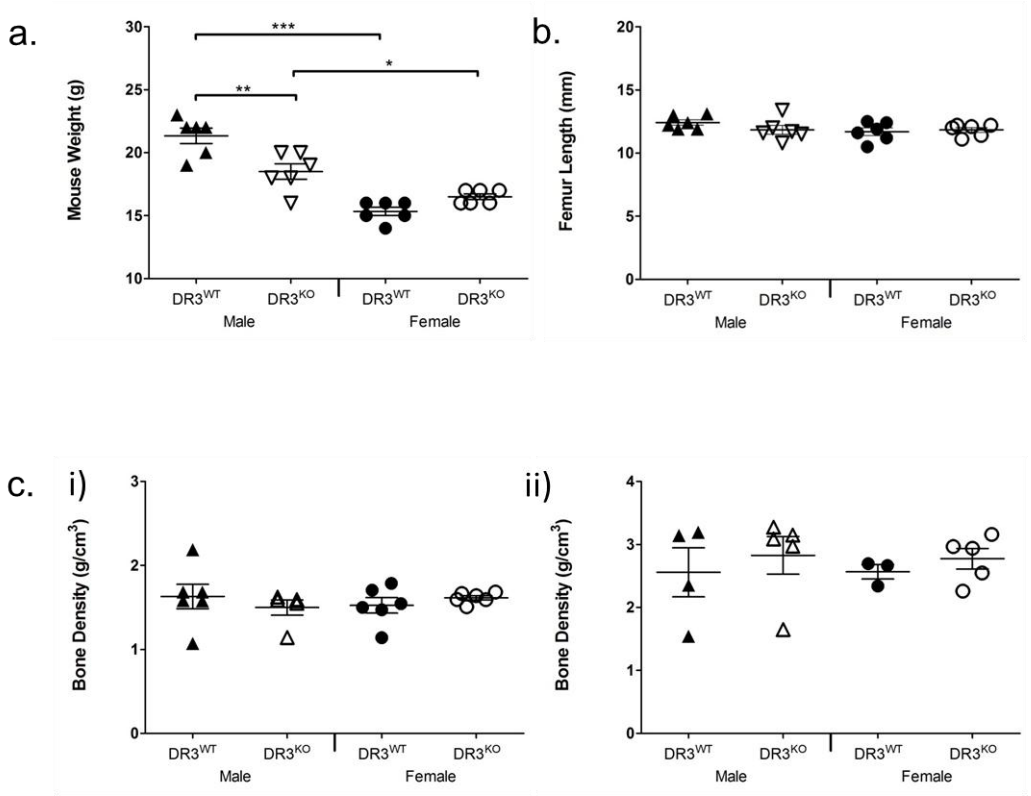

Figure 6.16. DBA/1 Weight and Bone Phenotype at 8 Weeks

DBA/1 DR3^{wt} and DR3^{ko} mice (male and female) were aged for 8 weeks. Following sacrifice (a) mouse weight, (b) femur length and (c) (i) femur (ii) and vertebra bone density were calculated. A significant difference in weight was observed between male DR3^{wt} and DR3^{ko} mice (**P=<0.01), male and female DR3^{wt} mice (***P=<0.0001) and male and female DR3^{ko} mice (*P=<0.05). No difference in femur length or femur and spine bone density was observed. Statistical analysis was performed with a two-way ANOVA and Bonferroni post test.

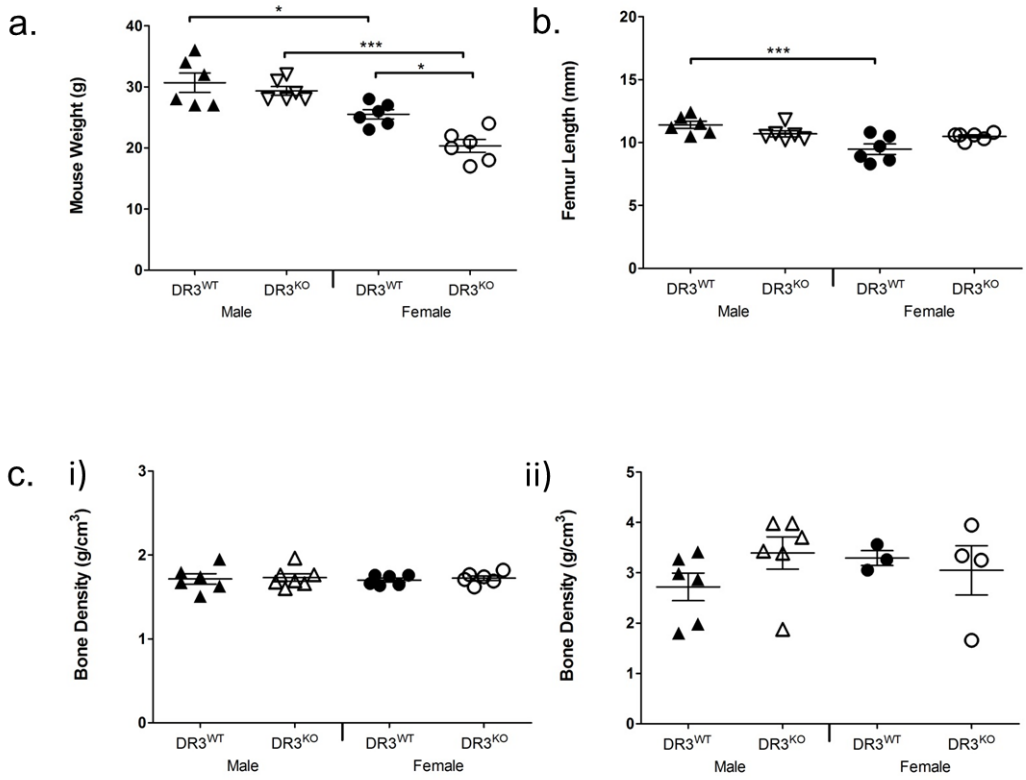

Figure 6.17. DBA/1 Weight and Bone Phenotype at 20 Weeks

DBA/1 DR3^{wt} and DR3^{ko} mice (male and female) were aged for 20 weeks. Following sacrifice (a) mouse weight, (b) femur length and (c) (i) femur (ii) and vertebra bone density were calculated. A significant difference in weight was observed between male and female DR3^{wt} mice (*P=<0.05), male and female DR3^{ko} mice (***P=<0.0001) and female DR3^{wt} and DR3^{ko} mice (*P=<0.05) . A significant difference in femur length was detected between male and female DR3^{wt} mice (***P=<0.0001). No difference in femur and spine bone density was observed. Statistical analysis was performed with a two-way ANOVA and Bonferroni post test.

6.3 **Discussion**

Formation of new bone is the principal function of the OB (130). OB bone formation is coupled to OC resorptive activity, resulting in a balanced cycle of bone remodelling. Aberrant OB activity has been linked to the pathogenesis of a number of diseases: decreased bone formation in OP (198, 199); and increased bone formation in the spondyloartritides, such as ankylosing spondylitis (AS) (288, 354, 415, 416). The effects of the TNFRSF death receptors on OB activity are poorly understood, with much debate on their exact role. Members have been demonstrated to induce apoptosis, inhibit differentiation or have no effect at all (261, 387-390, 417, 418). Work published by Bu et al (261) and Borysenko et al (241) showed positive expression of DR3 on the surface of the human OB MG63 cell line and primary human OB. Whether DR3 is expressed by murine primary OB and the role that it plays in normal OB function has never been investigated. TL1A, the TNFSF ligand for DR3, is known to be expressed by endothelial cells as well as activated monocytes, dendritic cells and T cells (237, 252, 253). No studies have been performed however, investigating whether TL1A is produced by OPCs or mineralising OB. The aims of this chapter were to firstly assess whether murine OPCs and OB express DR3 and TL1A. Secondly, to investigate the role of DR3 in OB differentiation, matrix maturation and mineral deposition.

Osteoblasts originate from mesenchymal stem cells (MSCs). The MSC differentiates into the mature mineralising OB through a number of intermediary stages; the progenitor cell, the osteoprogenitor, the immature OB and finally the mature OB. In studies where murine OBs are required BM is commonly used as the source of MSCs (398, 399, 401, 419, 420). However, other MSC sources have been employed, including epiphysis explants (421), compact bone and adipose tissue (422). In the present study DBA/1 BM and epiphysis / metaphysis explants were investigated to determine which MSC source produced the higher number of OPCs for use in subsequent mineralisation assays. Increased numbers of OPCs were observed in the BM cultures. This result was in contrast to that by Cheng et al (421) who revealed epiphysis-derived MSCs had increased cell proliferation and differentiation potential over BM-derived MSCs. The difference in results between the two studies can be explained by the method in which the BM was isolated. In the Cheng et al (421) study BM was isolated exclusively from the diaphysis, as the epiphyses were completely removed. In the present study the epiphyses were still present when the BM was isolated from the femora, meaning that MSCs present in the

epiphysis, as well as the BM, were obtained. This 'dual' source of MSCs in the BM cultures also provides an explanation for the difference in OPC numbers generated in the BM and epiphysis cultures in the current study; with a higher starting MSC number in the BM cultures compared to the epiphysis cultures. BM was chosen as the MSC source for all subsequent experiments. BM isolated from the femora of one mouse, however, produced inadequate numbers of OPCs for the mineralisation assays (between $4x10^5$ and $7x10^5$ cells required; confluent T75 tissue culture flask). The effect of increasing the starting MSC population on OPC generation was investigated by increasing the number of mice and femora from which BM was isolated.

In the BM versus epiphysis explant experiment OPCs reached ~60% confluence after 34 days culture. This suggested that the starting population of MSC was too low to sufficiently proliferate to the required number of cells. In a study by DiGirolamo et al (423) human MSCs were demonstrated to lose some of their proliferative capacity and differentiation potential over time. This raised the possibility that this may also occur in the murine system. The effect of increasing the MSC starting concentration on OPC confluence was investigated. Increasing the starting population of MSCs, using BM isolated from the femora of 3 DBA/1 mice, resulted in the generation of OPC confluence after 10 days culture. The number of mice used for the isolation of BM and time taken for the generation of confluent OPCs is not generally reported. The time taken for the OPCs to reach confluence in the present study was comparable to that reported by Baddoo et al (5-7 days; (398)). However, in the Baddoo et al (398) study the number of mice used to generate the OPCs was not stated. In previous work from our laboratory the femora from one C57BL/6 mouse had been shown to produce comparable numbers of OPCs in the same timeframe (308) as the current study. A number of possible reasons exist for the difference between the inbred strains of mice. C57BL/6 mice are generally larger than DBA/1 mice and as such have more BM: this equates to increased MSC numbers obtained per femur. Work published by Phinney et al (327) and Peister et al (134) has also described differences in MSC growth kinetics between C57BL/6 and DBA/1 mice. There is still some debate regarding whether MSC proliferation potential is greater in the DBA/1 or C57BL/6 strains: with Phinney et al (327) showing DBA/1-derived MSCs, and Peister et al (134) showing C57BL/6-derived MSCs to expand more rapidly. Having determined the conditions required for MSC culture, DR3 expression on OPCs and mineralising OB was explored.

Expression of DR3 on MG63 cells and primary human OB has been demonstrated by Bu et al (261) and Borysenko et al (241). However, there are currently no papers examining DR3 expression on murine OPCs or OB. This gap in knowledge of murine DR3 expression is most likely due to the limited availability of quality reagents for its detection. In the present study DR3 expression was demonstrated for the first time on the surface of murine OPCs. The majority of cells exhibited a 2-fold MFI signal over the isotype; however, a small sub-population of OPCs exhibited an increased level of DR3 expression. This supports the observation by Borysenko et al (241) who showed that while the majority of MG63 cells displayed a two-fold increase in signal compared to the isotype control, there was a small population that expressed DR3 eight times above the isotype. Why DR3 expression is increased in a small subpopulation of OPCs is not clear. The differing levels of expression may be due to the cells being at different stages of differentiation. Studies by Colter et al (424) and Sekiya et al (425) identified a subpopulation of cells in MSC cultures that were smaller, displayed increased proliferation and were precursors for the more mature larger cells, demonstrating the heterogeneity of the cultures. Additional, more detailed flow cytometric analyses of the murine OPC cultures are required to identify the population of stem cells that express DR3. DR3 expression in mineralising OB was observed to be reduced when compared to the OPCs; mineralising OB only exhibited a 1.4-fold increase in expression over the isotype. Changes in DR3 expression may be due to the temporal regulation of receptor expression during OB differentiation. This is supported by work by Bonnelye et al (426) and Deckers et al (427). In their respective studies differential expression of the oestrogen receptors α and β (426) and the VEGF receptors (427) were revealed during OB differentiation with levels changing depending on the maturation stage of the OB.

In addition to DR3, expression of CD44 and RANKL on the surface of the OB was investigated. CD44, a receptor for hyaluronan involved in cell-cell and cell-matrix adhesion, and RANKL, are expressed by OB at all stages of differentiation: MSC, OPC and mature OBs (408-413, 428, 429). Levels of osteoblast RANKL expression are variable and dependent upon which receptors on the cell surface are activated. For example, OBs derived from mice lacking CD44 and the PGE_2 receptors, EP_2 and EP_4, have been shown to have reduced expression of RANKL (430, 431). The effect on OB differentiation and function was not investigated in these studies, though *in vivo* fewer OB and subtle increases in cortical thickness were observed in $CD44^{-/-}$ mice compared to wild-type (431). In contrast, signalling through TNFR1 by TNF up-regulated RANKL expression on the OB

(432). To examine whether ablation of DR3 affected levels of CD44 and RANKL, cell-surface expression was analysed on OPCs and mineralising OB. Comparable expression of CD44 and RANKL were detected on the surface of $DR3^{wt}$ and $DR3^{ko}$ OPCs and mineralising OB. This result demonstrated that absence of DR3 does not affect homeostatic expression of RANKL and CD44. After demonstrating the expression of CD44, RANKL and DR3, the expression of TL1A by OB was investigated.

TL1A mRNA has been detected in murine total tissue RNA extracts (255), mouse joints (266) and murine myeloid and T cells (433). Detection of TL1A mRNA in the OB however, has never been previously demonstrated in human or murine OB. The result from this study revealed for the first time the production of TL1A mRNA by OB. Some caution must be taken with the data, however, as many regulatory mechanisms occur after the manufacture of mRNA affecting the translation of the message into protein (434). Addition of a poly(A) tail to mRNA extends its half-life by protecting it from degradation. In contrast, transcriptional regulation of mRNA can lead to the termination of protein synthesis. Examples of these can be seen in the control of OB pro-collagen mRNA by cortisol. In the study by Delany et al (435) cortisol was shown to decrease the stability of alpha 1 (I) pro-collagen mRNA, resulting in decreased production of type I collagen. Additional investigation by qPCR is required to determine whether TL1A mRNA is temporally regulated providing insight into the stage of OB differentiation in which TL1A acts. The results thus far in this chapter have established constitutive expression of TL1A and expression of DR3 on OPCs, and to a lesser extent, mineralising OB. What effect, if any, this exerted on OB differentiation and function was then explored in OB mineralisation assays using MSCs derived from both DBA/1 and C57BL/6 mice.

ALP is highly expressed by OB and is an early marker of OB differentiation. In both DBA/1 and C57BL/6 mineralisation assays DR3 significantly increased levels of ALP staining. This result showed similar parallels to those reported by Frost et al (389) with TNF. In the Frost et al study addition of low doses of TNF (<10pmol) to OB cultures increased ALP activity by stimulating early OB proliferation (389) and implied that the increased ALP expression in the $DR3^{wt}$ over the $DR3^{ko}$ cultures could be explained by more efficient cell expansion in $DR3^{wt}$ assays. Comparison of cell number between the $DR3^{wt}$ and $DR3^{ko}$ cultures however, did not reveal any significant difference. Thus the data suggests that DR3 has an autocrine role in regulating early OB differentiation, which is being driven by the constitutive expression of TL1A. To prove that DR3/TL1A are driving this autocrine

effect add back experiments, using either anti-TL1A or soluble DR3 (sDR3), are required to neutralise this outcome. If DR3/TL1A are responsible, then following addition of anti-TL1A or sDR3 to $DR3^{wt}$ and $DR3^{ko}$ cultures, levels of ALP staining in the $DR3^{wt}$ cultures should be comparable to the $DR3^{ko}$ cultures. The differences observed in the rate of differentiation between the $DR3^{wt}$ and $DR3^{ko}$ cultures had the potential to affect levels of mineral apposition in the cultures. For mineralisation to occur maturation of the matrix is required; this process is performed in part by OB-derived MMPs.

While the OB is the cell responsible for the formation of new bone it does display some collagen degradation characteristics. In 1986 Takahashi et al (20) described osteoblastic phagocytosis of collagen fibrils and mineralised bone matrix *in vitro*. The mechanism of how the OB degraded these components was not investigated in this study. Further support for the bone degradation ability of OB was provided by Everts et al (18) and Mulari et al (436). In these studies OC-independent organic bone degradation and cleaning of resorption pits was observed by ALP-, osteopontin-, and osteocalcin-positive cells of mesenchymal origin. These observations were further built upon by Parikka et al (19), who confirmed that human MSC-derived OB thoroughly removed exposed collagen fibres from the bottom of resorption lacunae. This was shown to be by MMPs rather than cysteine proteases; use of an MMP inhibitor inhibited degradation of the organic bone matrix while a cysteine protease inhibitor had no effect. Which MMPs are the most crucial in OB bone degradation, however, remains unknown. Parikka et al (19) demonstrated by western blot and gelatine zymography the presence of MMP-2, -8, -13 and -14 in OB cultures. MMP-9 has also been shown by zymogram and PCR to be produced by OB (402), though the functional significance of this in OB bone degradation has not been investigated. A suggested role for OB-derived MMPs in matrix maturation was put forward by Filanti et al (166). In their study levels of MMP-2, -9 and -14 were revealed to increase in cultures up to the time of nodule formation. These observations lead to the proposal that the MMPs are involved in the process of maturing the matrix ready for mineral deposition. The results from chapter 3 and chapter 4 have identified osteoclastic MMP-9 expression and activation to be a target of DR3 signalling. The effect of DR3 on OB-derived MMP-2 and MMP-9 was therefore assessed.

Analysis of DBA/1 and C57BL/6 OB culture supernatants produced contrasting results in pro MMP-9 expression. Pro MMP-9 was significantly elevated in DBA/1 $DR3^{wt}$ cultures, while levels were highest in the C57BL/6 $DR3^{ko}$ cultures. The data suggested an intrinsic

difference between the inbred strains in their mechanistic approach to bone formation. While the ELISA provided detail on the levels of the inactive form of MMP-9 it had a number of limitations. The ELISA was not able to distinguish whether the DBA/1 $DR3^{wt}$ and C57BL/6 $DR3^{ko}$ cultures produced more pro MMP-9, or if activation of MMP-9 was increased in the DBA/1 $DR3^{ko}$ and C57BL/6 $DR3^{wt}$ cultures; active MMP-9 being responsible for the cleavage of collagen. To determine whether DR3 affected the activation of OB-derived MMP-9, a gelatine zymogram was used to discern levels of the inactive and active forms. Levels of pro and active MMP-2 were also analysed in the zymogram to determine whether DR3 affected the activation of additional MMPs. Limitations on time, due to the end of the AR UK studentship that funded this project, meant that culture supernatants from only one C57BL/6 assay were analysed.

Levels of pro MMP-2 were found to be comparable between $DR3^{wt}$ and $DR3^{ko}$ cultures and showed minimal variation across the time course of the experiment when measured by zymography. This was also true for pro MMP-9. Comparison of pro MMP-9 expression by ELISA and zymogram revealed a discrepancy in results; with the ELISA revealing a significant difference in $DR3^{wt}$ and $DR3^{ko}$ pro MMP-9 expression, while only a slight difference was observed in the zymogram. The discrepancy in pro MMP-9 expression is potentially due to the semi-quantitative nature of zymogram analysis. For accurate quantification of enzyme levels enzyme titrations and standard curves are required (437). The analysis performed in this study compared the samples to just one pro MMP-9 control, and so only an approximation of enzyme levels could be calculated.

Analysis of active MMP-2 and MMP-9 showed elevated levels in the $DR3^{wt}$ cultures compared to the $DR3^{ko}$ cultures. The active forms of MMP-2 and MMP-9 were detected across the full duration of the time course. In the current study supernatant from only one C57BL/6 experiment was tested by zymography, meaning that it was insufficiently powered to draw firm conclusions on the effect of DR3 on MMP activation. Comparison of active MMP-2 and MMP-9 in the DBA/1 and C57BL/6 cultures would provide important information as to whether the expression profiles differ between the strains, as with pro MMP-9. The increased levels of active MMP-2 and MMP-9 detected in the C57BL/6 cultures led to the hypothesis that DR3 has an important, novel role in activation of OPC and OB-derived MMP-2 and MMP-9. The mechanism through which DR3 signalling results in the activation of MMP2 and MMP-9 is unknown. A possible mechanism for how DR3 leads to the activation of MMP-2 and MMP-9 can be gained from looking at the molecules

known to be involved in this process. Activation of MMP-2 is a two-step process resulting in an intermediate 64kDa form generated by MMP-14 (MT1-MMP) / TIMP-2 activity, and a mature form generated by the action of the plasmin system (438). Activation of MMP-9 is performed by a number of factors including: MMP-2, -3, -14 and plasmin (316-320). This raises the possibility that DR3 acts upon either MMP-14 or plasmin expression controlling the activation of MMP-2 and subsequently MMP-9. Addition to OB cultures of a plasmin inhibitor or selective inhibition of MMP-14 and MMP-2 with specific inhibitory antibodies would demonstrate which of the molecules DR3 signalling targets. A review of the current literature does not yield any examples of a homeostatic role of death receptors in MMP activation. However, in the study by Ben David et al (402), addition of TNF to OB cultures resulted in increased release of active MMP-9 and -2 into the supernatants, as determined by gelatine zymography. This study demonstrated that signalling through death receptors by their ligands induced the expression and activation of MMPs. To conclusively prove the significant role of DR3 in MMP activation add-back experiments using sDR3 or anti-TL1A to neutralise DR3 signalling are required. If DR3 signalling is critical for MMP activation then following addition of sDR3 or anti-TL1A, levels of active MMP-2 and MMP-9 in $DR3^{wt}$ cultures should be comparable to that of the $DR3^{ko}$ cultures. Measurement of the degradation products (c-telopeptide fragments) of type I, type II and type V collagen in the $DR3^{wt}$ and $DR3^{ko}$ cultures with / without sDR3 or anti-TL1A would also provide evidence of DR3's role in MMP-2 and MMP-9 activity (19). The relationship between MMPs and mineralisation could also be deduced by the use of MMP inhibitors in $DR3^{wt}$ OB assays. If MMP-2 and MMP-9 are crucial for mineralisation then inhibition of these MMPs should result in a reduction in levels of mineral deposition. Through comparison of the effects of the MMP inhibitors on mineralisation it may be possible to deduce which MMP has the more significant role in matrix maturation and mineral deposition. Having shown that DR3 enhanced OB differentiation and MMP activation, DR3's effect on mineral deposition was examined.

Levels of mineralisation were significantly decreased in both DBA/1 and C57BL/6-derived $DR3^{ko}$ cultures compared to the respective $DR3^{wt}$ cultures. This difference between the $DR3^{wt}$ and $DR3^{ko}$ cultures in mineralisation highlights an important role of DR3 in the process of normal OB mineralisation. There are currently no reported studies that examine the effects of death receptor ablation on osteoblast mineral apposition. A number of studies however, have demonstrated similar effects on *in vitro* mineral apposition in extracellular Ca^{2+}-sensing receptor knockout mice ($CaR^{-/-}$) (439) and type 2

cannabinoid receptor-deficient mice ($CB2^{-/-}$) (440). In these studies reduced nodule formation and mineral deposition were shown in the respective knockouts compared to their wild-type counterparts. The levels of mineralisation reported were also comparable to the $DR3^{ko}$ cultures in this study. The mechanism through which CaR and CB2 receptors regulated mineralisation was not fully defined, though Sophocleous et al (440) demonstrated CB2 signalling controlled OB function through activation of the MAPK-ERK signalling pathway. DR3 has also been identified to be able to activate the MAPK signalling pathway in TF-1 cells (246), whether DR3 signalling regulates OB function in the same manner remains to be explored.

In the only other study exploring the effect of DR3 signalling on OB function, Borysenko et al (241) demonstrated that cross-linking of DR3 with an anti-DR3 mAb inhibited differentiation and function of the MG63 OB cell line. Cross-linking of receptors, however, may cause activation that is significantly different to that of the natural ligand. This was highlighted in the Borysenko et al study as they were not able to reproduce the result with TL1A or in primary human OB. Signalling through DR3 by TL1A was also demonstrated to induce apoptosis. This was only observed in the MG63 cell line using high levels of TL1A (0.1µg/ml) and was not reproducible with primary human OB. Taken together the data from the current study and that by Borysenko et al (241) suggests a possible dual function of DR3/TL1A in OB biology, similar to that of TNFR1 and TNF (389-392), where low levels of stimulation drive OB differentiation but higher levels inhibit differentiation or induce apoptosis. Comparison of OB derived from TL1A-deficient mice and wild-types would produce valuable evidence for the role of TL1A signalling in OB differentiation. Addition of anti-TL1A to $DR3^{wt}$ cultures would also demonstrate the specific activation effect of TL1A in OB differentiation, if OB differentiation and mineralisation levels are reduced to that of the $DR3^{ko}$. This finding could have important implications in the bone pathology of a number of diseases, such as AS and RA, where changes in DR3/TL1A expression potentially lead to aberrant OB function; this is discussed in more detail in chapter 7.

Comparison between the DBA/1 and C57BL/6 cultures demonstrated a comparable role of DR3 in OB differentiation, matrix maturation and mineralisation. Levels of ALP staining and mineral deposition, however, were significantly elevated in the C57BL/6 cultures. The potential reasons for the differences between the two inbred strains are discussed in chapter 7. Having demonstrated a difference in OB differentiation and function between

DR3^{wt} and DR3^{ko} mice *in vitro,* the *in vivo* consequences on weight, size and bone density were investigated.

In vitro DR3 was demonstrated to play an important role in normal OB differentiation and mineral deposition. Whether this had any effect on the *in vivo* bone phenotype was unknown and was investigated in male and female DBA/1 mice. At 8 and 20 weeks male mice were observed to be significantly heavier than their female counterparts. This was consistent with weight-sex characteristics observed by a number of groups (441, 442). Differences in weight between the DR3^{wt} and DR3^{ko} mice were observed in males at 8 weeks and females at 20 weeks. Whether these differences in weight were caused by reduced bone formation, however, was not certain as no difference in femur or vertebra bone density were detected at any of the time points tested. While bone density between the DR3^{wt} and DR3^{ko} mice were comparable, differences in other factors such as fat or muscle could produce the observed disparity in weight. OB, adipocytes (fat cells) and myocytes (muscle cells) are all derived from mesenchymal stem cells. While DR3 has been demonstrated to affect OB differentiation nothing is currently known about its role in adipocyte and myocyte proliferation, differentiation and function. To address this gap in the literature, culture of DR3^{wt} and DR3^{ko} MSCs in medium specific for adipocyte differentiation (serum free, insulin, high density lipoprotein and Dex; (443)) or myocyte differentiation (5% FCS, VEGF, bFGF, and IGF-1; (444)) is required. By comparing the ability of the DR3^{wt} and DR3^{ko} cells to differentiate into these cells and analysing the activation of the adipocyte specific transcription factor, peroxisome proliferator-activated receptor-γ (PPAR-γ) and myocyte specific transcription factor, MyoD the role of DR3 can be deduced.

The *in vitro* studies performed in this chapter demonstrated increased bone mineralisation by male DR3^{wt}-derived OB. However, this did not translate into an increase in *in vivo* bone density in the DR3^{wt} mice compared to the DR3^{ko} mice. A possible explanation for this discrepancy is that while OB activity is reduced in the DR3^{ko} animals a balance in bone remodelling is still retained due to reduced OC activity. Analysis of OB-derived soluble RANKL and OPG, in DR3^{wt} and DR3^{ko} OB assay supernatants, would provide evidence as to whether the absence of DR3 alters levels of mediators involved in OC differentiation. Co-culture assays would also demonstrate whether OB induced OC differentiation is reduced in the DR3^{ko} mice compared to the DR3^{wt}. Comparison of relative levels of *in vivo* bone formation using fluorescent calcium-chelating compounds

and *in vivo* bone resorption using urinary excretion of [^{3}H]tetracycline (445) would also highlight whether there are any significant differences in the balance of bone remodelling between the DR3^{wt} and DR3^{ko} mice. A second possible explanation for the observed discrepancy is that while the amount of mineral between the DR3^{wt} and DR3^{ko} mice is the same, other related factors such as bone quality (BQ), bone volume to total volume (BV/TV), trabecular thickness (Tb Th) and bone surface density (BS/TV) may be different. Additional work is required before it can be confidently said that there are no differences in bone phenotype between the DR3^{wt} and DR3^{ko} mice. Analysis of the bones with micro CT would allow very accurate 3D recreation and calculation of BV/TV, TB Th, BS/TV and BQ (446). Analysis of the bones by histomorphometry would also reveal what cells are present at sites of bone remodelling, what stage of differentiation they are at**,** and where they are in conjunction to one another. Bone histomorphometry has the additional advantage of providing detailed information about bone turnover (measured by tetracycline labelling) and mineralisation (measured by osteoid seam width and mineralisation lag time) (447).

6.4 **Conclusion**

At the conclusion of this chapter the following objectives were met:

- Expression of DR3 was demonstrated on the surface of primary murine osteoprogenitors and mineralising osteoblasts.
- TL1A mRNA was constitutively expressed by DBA/1 and C57BL/6 osteoprogenitors and differentiating osteoblasts.
- DR3 was revealed to be involved in homeostatic osteoblast differentiation and mineral deposition.
- DR3 was confirmed to be involved in the activation of osteoblast-derived MMP-2 and MMP-9.
- Initial analysis on the *in vivo* bone phenotype of male and female DBA/1 $DR3^{wt}$ and $DR3^{ko}$ mice was performed.

The results from this study have revealed a novel homeostatic role for DR3 in OB function. Expression of DR3 by murine OPC and mineralising OB was demonstrated, with higher levels detected in OPCs compared to mineralising OB. For the first time this study has also shown constitutive expression of TL1A by OPCs and differentiating OB. Levels of ALP were significantly elevated in $DR3^{wt}$ cultures compared to $DR3^{ko}$ cultures, identifying a role of DR3 in OB differentiation. The lower levels of OB differentiation observed in the $DR3^{ko}$ cultures had the knock-on effect of reducing matrix maturation and mineral deposition. Expression of pro MMP-9 was affected by DR3, though intrinsic differences were observed between the two mouse strains: levels of pro MMP-9 were higher in DBA/1 $DR3^{wt}$ cultures and C57BL/6 $DR3^{ko}$ cultures. Analysis of inactive and active MMP-2 and -9 in C57BL/6 cultures showed a potential novel role for DR3 in the activation of osteoblast-derived MMPs; providing a possible mechanism for the increased mineralisation observed in the $DR3^{wt}$ cultures. These results highlight, for the first time, DR3 as an important autocrine regulator of OB differentiation and function. These findings could have important implications in the elucidation of the mechanisms involved in diseases characterised by aberrant OB activity, such as osteoporosis and ankylosing spondylitis.

Chapter 7

General Discussion

7 General Discussion

Bone remodelling is a balanced process that is carried out by the OC and the OB. An imbalance in the activity of either of these two cells can result in a number of bone pathologies that are detrimental to a person's quality of life. Increased OC activity leads to excessive bone resorption giving rise to diseases that are characterised by generalised bone loss and focal erosions, such as osteoporosis and RA. Increased bone formation by the OB can have equally devastating effects, as seen in ankylosing spondylitis, where the spinal vertebra can become fused. The aetiology of these diseases and what causes the change in OC, OB behaviour is complex and multifactorial. Members of the TNFSF and their receptors have been shown to have a pivotal role in control of bone remodelling. The TNFSF member RANKL (TNFSF11), its receptor RANK (TNFRSF11A) and soluble decoy receptor OPG (TNFRSF11B) are critical for regulating OC differentiation (54). TNF (TNFSF2) and LIGHT (TNFSF14) have also been demonstrated to act synergistically with RANKL *in vitro*, enhancing OC formation (182, 282, 283). *In vivo* changes in expression of the TNFSF and TNFRSF members have been linked to the pathogenesis of a number of diseases characterised by adverse bone pathology. An up-regulation of RANKL, TNF and LIGHT have been identified in the serum and synovial fluid of RA patients (180-183), while in post-menopausal OP increases in TNF expression have been identified (448). The exact function of all TNFSF and TNFRSF members in bone however, is unknown. Recent *in vitro* studies have demonstrated that signalling through DR3 (TNFRSF25) by its ligand TL1A (TNFSF15) can increase OC formation (242) and induce OB apoptosis (241). Changes in DR3/TL1A expression have also been linked to diseases characterised by adverse bone pathology such as RA (264, 265) and AS (267). The mechanisms through which DR3/TL1A affected OC, OB biology and contributed to the pathology of adverse bone disease, however, remained undetermined. This thesis set out to explore three main aims:

1. To determine the effect of DR3/TL1A on OC formation and resorptive function and identify the mechanisms involved.
2. To assess the role of DR3/TL1A in RA and OP; diseases characterised by increased OC activity.
3. To identify the role of DR3 in OB differentiation and function.

7.1 **Effect of DR3/TL1A on Murine and Human Osteoclast Differentiation and Resorptive Function**

The study by Bull, Williams et al (242) in 2008 was the first to demonstrate an effect of DR3/TL1A on OC formation and function. In their study murine BM and human PBMC cultures were used as the primary cell sources for OC assays. This meant that it could not be determined whether DR3/TL1A were enhancing OC formation directly via the OC precursor or indirectly by altering the production of RANKL and TNF by T cells, which also express DR3 (236, 237). This study set out to determine whether DR3/TL1A affected OC differentiation directly and to identify the mechanisms involved, in both murine and human models.

Isolation of OC precursors from the BM of $DR3^{wt}$ and $DR3^{ko}$ mice demonstrated DR3 to have an important role in OC resorptive function; with very low levels of resorption detected in the $DR3^{ko}$ cultures. This difference in resorption suggested a number of possibilities including; delayed maturation of the OC resulting in a delay in resorptive activity or a fundamental difference in OC attachment, cytoskeleton rearrangement or bone degrading enzyme release. Analysis into the mechanism through which DR3 regulated bone resorption demonstrated an increase in levels of active MMP-9 in $DR3^{wt}$ compared to $DR3^{ko}$ culture supernatants. This increase corresponded with the increase in bone resorption and revealed for the first time a role of DR3 in MMP-9 activation. Whether the link between active MMP-9 and resorption observed in the murine assays was due to a causal relationship was not clear from this study. Determining the answer to this question may not be straight forward, as specific MMP-9 inhibitors are not readily available. The thiirane MMP inhibitor SB-3CT has been demonstrated by Gu et al (449) to be a selective inhibitor of MMP-2 and MMP-9. In their studies SB-3CT was found to reduce MMP-9 degradation of the ECM protein laminin, providing significant protection against brain damage in an experimental model of focal cerebral ischaemia. Addition of SB-3CT to $DR3^{wt}$ OC cultures and analysis of resorptive function by quantification of the area of the ivory disc resorbed and measurement of collagen degradation products (c-telopeptide fragments) in the supernatants would provide important information on the role of MMP-9 in OC resorption. In addition to regulation of MMP-9 activation DR3 may also regulate additional aspects of OC resorptive function, such as cytoskeleton rearrangement, CatK expression or c-Src kinase activity.

Initiation of OC resorption requires the OC to rearrange its cytoskeleton, forming an actin ring (101). Disruption to the formation of the actin ring results in the inhibition of bone resorption, as a sealed zone around the ruffled membrane is unable to form (450). In the current study an immunocytochemical method for the visualisation of actin ring formation was developed in $DR3^{wt}$ cells (appendix I), though the study into actin ring formation in $DR3^{ko}$ OC was not performed. Comparison of actin ring formation in $DR3^{wt}$ and $DR3^{ko}$-derived OC would identify whether this process is regulated by DR3. If differences are observed then the mechanism for how DR3 regulates actin ring formation would require elucidation.

The investigation in this thesis into the effect of DR3 on murine CatK production by an *in-house* developed bioassay and zymography were inconclusive. Using the developed methods the protease was not detected in the culture supernatants due to cross-reactivity with FCS. Additional follow up experimentation analysing CatK mRNA levels in $DR3^{wt}$ and $DR3^{ko}$ OC by qPCR and protein levels by SDS-PAGE and Western blot (451) should be performed to demonstrate involvement of DR3 in CatK regulation. C-Src is the dominant src family kinase expressed in OC and acts as an adaptor protein through its enzymatic activity (452, 453). In a study by Miyazaki et al (99) c-Src activity was identified as being essential for OC function, with disruption of c-Src by adenovirus induced Src mutants resulting in significantly decreased OC resorption. Targeted disruption of the c-Src proto-oncogene in mice was also demonstrated to lead to the development of an osteopetrotic phenotype due to defects in OC resorptive function (100). These data present variations in c-Src activity as a potential cause for the stark difference in OC resorptive function observed between the $DR3^{wt}$ and $DR3^{ko}$ OC. Immunoprecipitation of c-Src from $DR3^{wt}$ and $DR3^{ko}$ cultures and visualisation by SDS-PAGE and Western blot would identify whether levels are comparable between the two genotypes. Analysis of the immunoprecipitated c-Src activity (454) *in vitro* would also reveal if c-Src activity is potentially regulated by DR3.

In the course of this study TL1A was demonstrated to have opposing effects on OC formation in DBA/1 and C57BL/6 OC cultures. Addition of TL1A to DBA/1 cultures significantly inhibited OC formation in a DR3-dependent manner, while addition of TL1A to the C57BL/6 cultures enhanced OC formation. The result from the C57BL/6 OC assay supported the published results by Bull, Williams et al (242); who demonstrated addition of TL1A significantly enhanced C57BL/6 OC development from $DR3^{wt}$ but not $DR3^{ko}$ BMC.

To explain the mechanism through which TL1A was regulating OC formation, culture supernatants were analysed for soluble mediators known to be involved in OC migration.

Formation of the multinucleated OC is dependent on the action of chemokines inducing the migration of OC precursors. The investigation into the mechanism through which DR3/TL1A affected OC formation revealed a contemporary role for murine TL1A in regulating the expression of the chemokines CCL2 and CCL3. In the DBA/1 model TL1A significantly reduced expression of CCL2 and lowered expression of CCL3 in a DR3-dependent manner. In contrast, CCL3 expression in the C57BL/6 cultures was elevated. Whether CCL2 and CCL3 were the only two factors regulated by TL1A and were fully responsible for the changes in osteoclastogenesis observed remains to be tested. Work by Lean et al (361) and Okamatsu et al (455) identified CCL9 as the main chemokine expressed by murine OC and that it promoted RANKL induced OC formation. Regulation of CCL9 expression by TL1A could therefore have a significant effect on osteoclastogenesis. Likewise changes in the expression of CCL5, also known to stimulate the migration of OC precursors (85), would affect OC formation. Analysis of chemokine receptor expression (CCR1, CCR2, CCR4 and CCR5) by flow cytometry would provide evidence of an additional possible mechanism by which TL1A could regulate OC formation. While chemokines are essential for OC precursor migration, to form the multinucleated OC the mononuclear cells must undergo a process of fusion. The process of OC fusion is not fully understood, though a number of molecules have been identified to mediate this process. E-cadherin (456) and macrophage fusion receptor (MFR; (457) have been shown through the use of neutralising antibodies to be involved in monocyte / macrophage fusion. In a study by Yagi et al (458) ablation of dendritic cell-specific transmembrane protein (DC-STAMP) resulted in the complete abrogation of OC cell fusion. Overexpression of DC-STAMP in RAW-D cells however, significantly enhanced RANKL-induced OC formation (459). Analysis of the expression of these fusion proteins by immunological staining and qPCR (459) could reveal additional targets of DR3/TL1A regulation of OC formation.

The investigation into the effect of TL1A on OC formation and the mechanism of action revealed contrasting results between the DBA/1 and C57BL/6 strains (table 7.1). The cause of this inherent difference in cellular response to TL1A is unknown. Intrinsic differences between inbred strains of mice have been shown by a number of groups and are discussed in chapter 3. Variations in DR3 and TL1A expression between DBA/1 and C57BL/6 OC precursors could also provide a possible explanation for the opposing effect

of TL1A on OC differentiation. Flow cytometric analysis of DR3 expression on the surface of the OC precursors and analysis of TL1A levels in OC culture supernatants would determine whether there is a difference in DR3/TL1A expression between the strains. Currently however, specific monoclonal antibodies for the detection of murine DR3 on monocytes / macrophages and soluble TL1A are not commercially available

The murine models of osteoclastogenesis used in this thesis provided important insights into the role of DR3/TL1A in OC formation and function. The opposing effects of TL1A in the DBA/1 and C57BL/6 strains however raised a problem; which, if either, of the two mouse models was representative of the human system. Additionally, the lack of specific murine reagents meant that levels of DR3 and TL1A expressed by OC and their precursors could not be measured. To address these limitations in the murine assays the study was transferred into a human model; as the direct effect of TL1A on OC precursors ($CD14^+$ monocytes) could be examined and reagents for the detection of DR3 by flow cytometry and TL1A by ELISA were readily available.

In the current study expression of DR3 was demonstrated to be induced on $CD14^+$ monocytes following culture in MCSF for 7 days (chapter 4). Addition of TL1A to the $DR3^+$ $CD14^+$ cultures identified for the first time a direct and dose-dependent effect on human OC formation and resorptive function. The increase in OC formation correlated with a significant increase in levels of the chemokine CCL3 and suggested that this was the main target of DR3/TL1A signalling in the human system. Further experimentation is required as outlined above for the murine system to determine whether TL1A signalling also regulates expression of chemokine receptors, RANK or the fusion proteins involved in OC formation. The increase in OC resorptive function observed in the human assays correlated with an increase in total MMP-9 release. This supported the results published by Kim et al (239) and Kang et al (278) who identified MMP-9 expression to be a target of TL1A signalling in the human macrophage THP-1 cell line. TL1A was further identified to have a role in the activation of human osteoclastic MMP-9. How DR3/TL1A signalling regulated MMP-9 activation was not investigated in this study and should be investigated as previously discussed for the murine assays. While MMP-9 is known to have a role in bone resorption the principal enzyme involved is CatK (104, 127). An *in situ* immunocytochemistry method was developed for the detection of CatK in OC cultures, however due to time constraints brought about by the end of the AR UK funding the effect of TL1A on CatK expression was not fully investigated (Appendix II). To fully explore whether DR3/TL1A signalling regulates CatK expression analysis of CatK mRNA levels by

qPCR and detection of protein levels by Western blot and immunocytochemistry should be performed.

In the human (chapter 4) and murine (chapter 3) *in vitro* assays performed in this thesis DR3/TL1A were shown to have an effect on OC resorptive function, by increasing the area of the ivory disc resorbed. The analysis of resorption pits throughout the course of this thesis (chapters 3, 4 and 5) employed a standard method; discs were stained with toluidine blue and the area resorbed analysed by light microscopy (460). A limitation of this method was that it did not provide any detail on pit depth or pit volume. Alternative methods for the analysis of resorption pits have been described in the literature including confocal microscopy (129) and scanning electron microscopy (461). At the end of this study a portion of time was spent on the development of a method for the analysis of resorption pits by confocal microscopy (Appendix V).

Comparison of the human and murine studies, used to determine the mechanism of DR3/TL1A in regulating OC differentiation and function, demonstrated a number of similarities and differences between the two systems (table 7.1). In both the murine and human models DR3 was identified as having a significant role in OC resorptive function and MMP-9 activation. The effect of TL1A on chemokine expression however, varied between species. In the human system CCL3 was identified as being a key target of TL1A signalling with expression of CCL2 unaffected. This was in contrast to the murine system where CCL2 was identified as a key target of TL1A. Differences in chemokine and chemokine receptor expression between mouse and human systems are not uncommon; e.g. CXCR1, CXCL8, CXCL7 and CCL13 are expressed in humans but not mice, while CCL9 and CCL12 have been identified in mice but not humans (351). The significance of these differences cannot be conclusively determined as there is considerable redundancy built into the system. This result further highlighted the care that must be taken when extrapolating results from a murine system into a human system, as subtle differences in mechanisms may be present.

Outcome	DBA/1 (DR3^{wt})	C57BL/6 (DR3^{wt})	Human
Total Cell Number	↓	↔	↔
OC Formation	↓	↑	↑
OC Resorption	↓	Not tested	↑
CCL2	↓	Not tested	↔
CCL3	↓	↑	↑
CXCL8	-	Not tested	↔
CXCL1	↔	Not tested	-
Active MMP-9	↑ (DR3 only)	Not tested	↑

Table 7.1. The Effect of TL1A on OC Function in murine and human *in vitro* OC Assays

7.2 Role of DR3/TL1A in Inflammatory Arthritis

As discussed in the introduction aberrant expression of DR3 and TL1A have been linked to the pathogenesis of a number of inflammatory conditions including inflammatory arthritides such as RA (264-266) and AS (267, 268). The consequence of the aberrant expression of TL1A in the pathogenesis of these diseases was not investigated in any of the above mentioned studies. The present study set out to clarify the significance of increased TL1A expression in RA and to determine whether TL1A levels were also elevated in patients with psoriatic arthritis.

In the current study TL1A levels in RA patients were elevated 8.6-fold over normal controls, significantly correlated to levels of RF, and revealed for the first time to be linked to the presence of erosive disease (chapter 5). Taken in conjunction with the results reported by Bamias et al (264), Zhang et al (266) and the *in vitro* data from chapter 4 the result suggested that TL1A is a significant driving factor in the increased bone resorption associated with RA. Further support for this theory is provided by work performed in murine models of AIA (242) and CIA (266). In these experiments administration of TL1A significantly exacerbated disease, increasing the size of bone erosions and the severity of bone destruction. The RA patients used in this study all had established disease, so it was unknown whether TL1A levels were elevated before the onset of RA or after the disease

was established. A long-term study measuring serum TL1A in patients who present at clinic with signs of early arthritis would determine whether there is a direct link between TL1A levels and the pathogenesis of erosive disease. The outcome of this study would thus predict whether TL1A could be used as a prognostic marker of disease severity.

Treatment of RA is routinely through the prescription of DMARDs, though patients with severe arthritis can be treated with anti-TNF biological such as adalimumab, etanercept and infliximab. Clinical investigations into anti-TNF therapy in RA have provided evidence that TNF regulates the expression of other pro-inflammatory cytokines such as IL-6 and IL-8 (462). Migone et al (248) reported that TL1A mRNA was up-regulated in HUVEC cells following TNF stimulation suggesting that TL1A is also under TNF regulation. However, there is still some debate over this as Cassatella et al (366) revealed that production of TL1A by immune complex stimulate monocytes was unaffected following treatment with TNF neutralising antibodies. In the present study RA patients on anti-TNF therapy were shown to have comparable levels of serum TL1A when compared to patients on DMARDs, suggesting that control of TL1A expression is independent of TNF. This result was in contrast to that reported by Bamias et al (264), who demonstrated that anti-TNF treatment significantly reduced serum TL1A levels. However, in the Bamias et al (264) study TL1A levels in the anti-TNF treatment cohort were still significantly higher than the normal controls. These data provide a possible explanation why some RA patients do not respond to anti-TNF therapy. Studies examining expression of TL1A levels in anti-TNF responders and non-responders would help determine whether TL1A levels could predict the likelihood of successful treatment. If TL1A levels are significantly elevated in the non-responder cohort over the responder cohort then it could be reasonably assumed that the erosive pathology in the non-responder patients is primarily being driven by TL1A.

The relationship between TL1A and bone degradation reported in this thesis and in the studies mentioned above (242, 264, 266) present TL1A as an attractive target for therapy. In the Bull, Williams et al (242) study administration of TL1A neutralising antibodies to the CIA model of RA, the industry standard for assessing potential therapies, resulted in reduced disease activity. While this result was very promising further testing is required to characterise the efficacy and safety of anti-TL1A treatment. The current biological treatment of RA, anti-TNF, is associated with a significant 80% increase in the risk of serious infection in the first 6 months which reduces to a significant 20% increase over subsequent years (463). The numbers of studies looking at the role of DR3/TL1A in

infections however are limited. In a 2008 study, Meylan et al (256) showed that control of *Toxoplasma gondii* parasitic infection was not dependent on DR3, as DR3-deficient mice displayed an immune response comparable to the wild-type. However, in recent studies by Buchan et al (464) and Twohig et al (243) DR3/TL1A were shown to have important roles in the development of optimal T cell immunity against *Salmonella* (464) and efficient development of antiviral T cell immunity (243). In the Buchan et al (464) study, infected DR3-deficient mice had reduced numbers of antigen-experienced and proliferating $CD4^+$ T cells compared to wild-type littermates, resulting in impaired bacterial clearance. The impaired immunity to viral infection reported by Twohig et al (243) in the DR3-deficient mice, was associated with a reduction of up to 90% in T cell response and impaired anti-MCMV NK response during acute infection, which became lethal. Further investigation is required into the role of DR3/TL1A in infection and the effects of DR3/TL1A blockade on infection occurrence before anti-TL1A can be considered as a therapeutic treatment for RA and moved into clinical trials.

While there is a growing body of evidence linking DR3/TL1A to RA a number of studies have suggested that TL1A may also be linked to the pathogenesis of the SpAs. In the current study the potential role of TL1A in PsA was investigated. Analysis of PsA patient serum in the current study revealed for the first time an increase in levels of TL1A. This increase was of a much smaller magnitude than observed in the RA patients (1.9-fold versus 8.6-fold). The data in conjunction with the study by Konsta et al (267), who showed increased levels of serum TL1A in AS patients, points to a potentially important role of DR3/TL1A in the pathogenesis of the SpAs. These studies are limited in that they do not look at the consequences of the increased TL1A expression on the bone pathology. A number of animal models of spondylitis exist and should be utilised to further understand the role of DR3/TL1A in the progression of the disease. Spontaneous ankylosing enthesopathy has been described in DBA/1 group-housed male mice, with onset occurring as early as 2-3 months of age and prevalence ranging from 50% to 100% (465). Histological analysis of grouped male DBA/1 $DR3^{wt}$ and $DR3^{ko}$ mice would provide information on incidence and severity of the disease and show whether $DR3^{ko}$ mice are protected against spontaneous SpA. Visualisation of DR3 and TL1A in the joints by immunohistochemistry would identify the cells through which DR3/TL1A exert an effect. In addition to the experimental mouse models of disease more detailed clinical studies are required to elucidate the role of TL1A in the SpAs. The current study into TL1A levels in PsA patients was inadequately powered due to the low number of patients recruited. To

conclusively demonstrate that TL1A levels are elevated in PsA a larger cohort of patients are required. PsA is also related to the skin condition psoriasis, with studies reporting that between 5% and 42% of psoriasis sufferers develop PsA (362). Elevated expression of DR3 and TL1A have been reported by Bamias et al (269) in skin lesions of patients with psoriasis, raising the possibility that DR3/TL1A may have a role in the development of PsA from psoriasis. Studies into serum TL1A and DR3 expression in psoriasis patients and follow up to see whether they develop PsA would provide proof-of-concept of DR3/TL1A's involvement in the onset of PsA.

The data presented in this thesis adds to a growing body of evidence (264-267) identifying a role for DR3/TL1A in the pathogenesis of the inflammatory arthritides (table 7.2) however, no such groundwork has been established for OP. OP is a disease characterised by a generalised bone loss due to OC over activity. This thesis provided the first proof-of-concept study investigating the role of DR3/TL1A in the pathogenesis of OP.

Arthritis	**Serum TL1A**
Ankylosing Spondylitis	↑
Psoriatic Arthritis	↑
Osteoarthritis (control)	↔
Rheumatoid Arthritis (Seropositive - erosive)	↑↑↑
Rheumatoid Arthritis (Seropositive – non-erosive)	↑↑
Rheumatoid Arthritis (Seronegative - erosive)	↑
Rheumatoid Arthritis (Seronegative – non-erosive)	↔

Table 7.2. Relative Changes in Serum TL1A Levels in Inflammatory Arthritides Compared to Normal Controls

7.3 **Role of DR3/TL1A in Post-Menopausal Osteoporosis and Fracture**

As discussed in the introduction OP is characterised by low BMD and an increased risk of fracture. This thesis provided the first proof-of-concept study investigating the role of DR3/TL1A in fracture and / or post-menopausal OP; by comparing serum TL1A levels, DR3 expression on OC precursors and osteoclastogenesis in pre-menopausal controls and three post-menopausal patient cohorts: non-osteoporotic with / without fracture and osteoporotic with fracture.

TL1A levels were reduced in the post-menopausal $OP^{-}Frac^{-}$ cohort compared to the pre-menopausal controls. However, levels of TL1A in the post-menopausal fracture cohorts (with/without OP) were comparable to the pre-menopausal controls (Appendix III). This suggested that like the TNFSF members RANKL, OPG and TNF (369), TL1A is temporally up-regulated during fracture healing. This is the first time that changes in TL1A expression have been linked to fracture repair. Further testing is required to demonstrate this link conclusively. Recruitment of additional patients to each cohort and the recruitment of a pre-menopausal fracture cohort would add power to the current study and also reveal whether changes in TL1A expression following fracture are observed across all ages. To demonstrate the importance of TL1A in *in vivo* fracture healing murine fracture models can be utilised. Induction of fracture in wild-type and TL1A-deficient mice and analysis of healing by dorsal-ventral radiographs and histological analysis of total fracture area, cartilage area and mineralised tissue area (325) would demonstrate if TL1A is an integral part of fracture repair.

Probably the most intriguing aspect of this study was the discovery that OC precursors derived from post-menopausal patients expressed negligible levels of DR3 compared to pre-menopausal–derived OC precursors (Appendix III). The reasons for the difference in DR3 expression between the pre- and post-menopausal cohorts were not clear from this study. The effect of aging, fracture and OP on OC precursor expression of death receptors is unknown, as no studies have been performed looking at this specific aspect. A detailed flow cytometric study looking at the expression of the death receptors on OC precursors isolated from pre- and post- menopausal patients with / without fracture and OP patient cohorts would identify changes in the expression profiles associated with age, fracture and disease. Another possibility for the variation in DR3 expression between the pre-and post-menopausal cohorts is that the expressed isoform of DR3 changes following the menopause. In humans there are at least 13 DR3 splice variants (230, 244), while in mice there are 3 (280). Studies by Twohig et al (466) and Bamias et al (467) have demonstrated differential expression of the murine DR3 splice variants between naïve and activated T cells. This raises the possibility that the post-menopausal-derived cells may be expressing an alternative isoform of DR3 that is not detected by the JD3 monoclonal antibody used for flow cytometry in this study. Analysis of the DR3 transcripts by RT-PCR cloning and sequencing would provide additional evidence on the effects of the menopause on DR3 expression. What effect the absence of DR3 on post-menopausal human OC precursors

had on osteoclastogenesis has never been previously investigated and was subsequently explored.

Analysis of the pre- and post-menopausal OC cultures revealed significantly reduced cell viability and OC formation in the post-menopausal cultures compared to the pre-menopausal cultures (appendix IV). This suggested that DR3 may have a role in the regulation of OC precursor cell viability and optimal OC differentiation. To explore the role of DR3 in maintaining OC precursor cell viability and differentiation further investigation is required. The reduced cell number observed in the post-menopausal cultures suggests that DR3 is required to either sustain proliferative potential or inhibit apoptosis in the OC precursors. Measurement of cell proliferation through the incorporation of 5-bromo-2'-deoxyuridine (Brdu) or ^{3}H-Thymidine; flow cytometric analysis of early and late apoptosis using Annexin V and propidium iodide (468); and measurement of caspase-3 activity in cell culture lysates would determine whether the difference in cell viability is due to changes in proliferative potential or apoptosis. The mechanism of how DR3 regulates OC precursor cell viability also remains to be explored. Levels of MCSF used in the human assays in this study were identical. This raises the possibility that DR3 may indirectly regulate c-FMS expression or c-FMS affinity for MCSF. Comparison of c-FMS expression in pre- and post-menopausal OC precursors by flow cytometry would reveal whether expression is indirectly regulated by DR3. To determine how the absence of DR3 on post-menopausal OC precursors may affect OC formation a number of studies should be performed; testing of RANK and chemokine receptor expression by flow cytometry; testing of fusion protein expression by qPCR and immunostaining; and testing for expression of the master transcription regulator of osteoclasts, NFATc1 (64), by qPCR and immunofluorescence. A reduction in expression of any of the aforementioned would result in the decreased OC formation observed in the post-menopausal cultures.

Comparison of the pre- and post-menopausal OC cultures performed in this thesis presented some intriguing findings and indicated that DR3/TL1A are not directly responsible for the increased OC activity associated with post-menopausal OP (table 7.3). Increased OC activity however, is just one key factor in the pathogenesis of OP. Histomorphometric analysis of iliac and cancellous bone from osteoporotic patients demonstrated decreased OB activity and bone formation (198, 199, 469). The presence of DR3 on the surface of human OB has been shown by Bu et al (261) and Borysenko et al

(241) though the role of DR3 in OB biology is uncertain. Whether DR3 was also expressed on the surface of murine OB and its homeostatic function were unknown and therefore investigated.

Outcome	OP^-Frac^-	OP^-Frac^+	OP^+Frac^+
Serum TL1A	↓*	↔	↔
$CD14^+$ DR3 Expression	↓↓	↓↓	↓↓
Total Cell Number	↓↓	↓↓	↓
OC Number	↓↓	↓↓	↓
% OC	↓*	↓	↓
% Resorption	↓*	↓*	↓*

Table 7.3. Comparison of the Post-Menopausal OC Assay Outcomes to Pre-Menopausal Assays (*=Change not significant)

7.4 Role of DR3 in Osteoblast Differentiation and Function

In the only previous study into the effect of DR3 on OB biology Borysenko et al (241) demonstrated that activation of DR3 on the MG63 cell line by cross-linking could induce apoptosis or inhibit MG63 OB differentiation. In their study however, the effect of DR3 on normal OB differentiation and mineral deposition was not investigated. This was addressed in the current study through analysis of primary OB cultured from the BM of $DR3^{wt}$ and $DR3^{ko}$ mice.

Cell surface expression of DR3 on primary murine OPCs and mineralising OB was demonstrated for the first time (chapter 6). DR3 expression on murine OPCs was demonstrated to be equivalent to that shown by Borysenko et al (241) on human OB, with an approximately 2-fold increase of signal over the isotype control. DR3 expression on mineralising OB was reduced compared to the OPCs. This raised the question as to whether the reduction in DR3 expression was due to a loss of receptor or whether the DR3 isoform expressed had changed as discussed in section 7.3.

This study was the first to identify production of TL1A mRNA by OPCs and differentiating OB. While constitutive expression of TL1A mRNA was detected in OPCs and mineralising OB it is not known whether levels were temporally regulated during differentiation.

Analysis of OPC and OB TL1A mRNA levels by qPCR at varying stages of differentiation would identify if transcriptional activity of TL1A increases or decreases depending on the stage of OB maturity. A limitation of the study into OB TL1A expression however, was that actual protein levels could not be measured as specific commercial antibodies for the detection of soluble TL1A or membrane-bound TL1A were not available at the time of study. Generation of these reagents would allow the measurement of TL1A in the culture supernatants by ELISA or membrane-bound TL1A by flow cytometry. The expression profile of TL1A and DR3 on OPCs and OB also suggested a potential autocrine role for DR3 in OB differentiation; this was supported by the results obtained from the mineralisation assays.

Analysis of the mineralisation assays performed in this study demonstrated DR3 to have a significant role in DBA/1 and C57BL/6 OB differentiation, MMP-2 and -9 activation and mineral deposition. Levels of ALP, an early marker of OB differentiation, were significantly elevated in the $DR3^{wt}$ cultures over the $DR3^{ko}$ cultures. A number of possibilities exist by which DR3 may regulate OB differentiation. Early stages of OB differentiation are driven by the autocrine action of Wnt proteins signalling through LRP5 and the serpentine frizzled receptors. In a study by Rawadi et al (396) signalling through the Wnt autocrine loop was demonstrated to mediate the induction of ALP. Blockade of Wnt signalling by overexpression of DKK1 or LRP5ΔC inhibited induction of ALP, demonstrating the importance of this signalling pathway in OB differentiation. Loss of function of LRP5 was also found to lead to the development of OP due to decreased bone formation (147). Analysis of Wnt and LRP5 expression by qPCR would demonstrate any changes induced by the ablation of DR3, identifying a possible mechanism through which the receptor may regulate OB differentiation. Differentiation of the MSC into the early immature OB is also dependent on the induction of the transcription factors Runx2 (137) and Osx (138). Variations in expression of these transcription factors caused by the ablation of DR3 would result in the differences in ALP activity observed.

In addition to enhancing ALP levels, DR3 was shown to have a role in the regulation of OB-derived MMP activation; with levels of active MMP-2 and MMP-9 elevated in the $DR3^{wt}$ C57BL/6 cultures compared to the $DR3^{ko}$. Taken together with the results from the OC assays this identified MMP activation as a key target of DR3 signalling. The processes of MMP-2 and MMP-9 activation are discussed in chapters 6 and 3 respectively. Selective inhibition of the molecules involved in MMP activation with specific inhibitory antibodies

or shRNA and measurement of MMP-2 and MMP-9 activation by quantitative zymography would reveal important insights into the regulatory mechanisms of osteoblastic MMP-2 and MMP-9 activation by DR3.

Analysis of mineral deposition in the DBA/1 and C57BL/6 $DR3^{wt}$ and $DR3^{ko}$ cultures demonstrated DR3 to have an important role in the regulation of OB mineralisation; with levels in the $DR3^{ko}$ cultures significantly reduced compared to the $DR3^{wt}$. Whether the variation in mineralisation was due to the difference in OB differentiation and matrix maturation or due to a specific effect of DR3 on mineral deposition is still unclear. In a study by Sophocleous et al (440) activation of the MAPK-ERK signalling pathway by the type 2 cannabinoid receptor was demonstrated to control OB function. DR3 has also been shown to activate MAPK in TF-1 cells (246) suggesting a possible mechanism through which DR3 regulates bone formation. In a study by Albers et al (399) the frizzled receptor FZD9 was also revealed to have an important role in bone formation, as FZD9-deficient mice displayed a low bone mass caused by impaired bone formation. Analysis of FZD9 transcription in $DR3^{wt}$ and $DR3^{ko}$ OB would identify whether DR3 indirectly regulates OB mineralisation through FZD9 expression. The final stages of OB differentiation and mineralisation are dependent on the induction of the transcription factors Osx and *ATF4* (139), leading to the generation of the mature bone forming OB. Analysis of these transcription factors by qPCR in $DR3^{wt}$ and $DR3^{ko}$ OB would identify whether they are under the influence of DR3 regulation and provide important mechanistic insights into OB differentiation and function.

In the current study DR3 has been demonstrated to regulate OB differentiation and function in both the DBA/1 and C57BL/6 cultures; however levels of ALP and mineral deposition were significantly elevated in the C57BL/6 cultures compared to the DBA/1 cultures (table 7.4). As discussed in chapter 3 fundamental differences in bone biology between inbred strains of mice have been reported (134, 325-327), though the exact reasons for these differences are unknown. In the last 10 years 5-HT (serotonin) has been reported as being a key regulator of bone homeostasis (470, 471). Expression of the 5-HT receptors and transporters (5-HTT) has been demonstrated on the surface of OPCs and mineralising OB (471, 472). In $5\text{-}HT_{2B}$ receptor knockout mice Collet et al (471) demonstrated reduced OB differentiation as measured by ALP activity. This subsequently resulted in fewer mineralisation nodules. This was built upon by Baudry et al (470) who demonstrated that tissue nonspecific alkaline phosphatase is a target of $5\text{-}HT_{2B}$ signalling.

Differences in 5-HT receptor expression have been demonstrated in the brains of inbred mice (473). It is currently not known whether OB 5-HT_{2B} expression also differs between strains but this does present a possible explanation for the differences observed between the DBA/1 and C57BL/6 mice in normal OB function. The data presented in this thesis and published studies (264, 266, 267) demonstrates a complex role of DR3/TL1A in OC and OB biology and in the pathogenesis of various adverse bone pathologies; these are discussed below in section 7.5.

Outcome	**DBA/1**	**C57BL/6**
ALP Activity	↑	↑↑
Mineral Deposition	↑	↑↑
Cell Proliferation	↔	-
Pro MMP-9	↑	↓
Active MMP-9	-	↑↑
Active MMP-2	-	↑↑
RANKL	↔	↔
CD44	↔	↔

Table 7.4. Effect of Autocrine DR3/TL1A Signalling on DBA/1 and C57BL/6 $DR3^{wt}$ OB Differentiation and Function

7.5 **DR3/TL1A in Adverse Bone Pathology**

The *in vitro* and *ex vivo* studies performed in this thesis suggest three models of how changes to DR3/TL1A expression can lead to an imbalance in the bone remodelling cycle, resulting in diseases characterised by adverse bone pathology.

1. Rheumatoid Arthritis

In vitro assays have shown that high levels of TL1A significantly enhance OC formation and resorptive function (chapter 4). This is supported by the work in chapter 5, and the study by Bamias et al (264), that demonstrated high levels of serum TL1A was linked to the presence of erosive disease in RA. In the Borysenko et al (241) study long–term stimulation of DR3 on MG63 cells inhibited OB differentiation or induced OB apoptosis, suggesting that high levels of TL1A may also produce the same effect *in vivo*. *In vivo* this

dual action of DR3/TL1A would shift the bone remodelling balance towards excessive bone erosion, resulting in the joint destruction and generalised osteopenia observed in diseases such as RA (Fig 7.1).

2. Spondyloarthritis

AS and PsA are diseases characterised by increased bone formation. TL1A levels were revealed to be elevated in both PsA patient (chapter 5) and AS patient serum (267). In chapter 6, DR3 was demonstrated to have a role in the regulation of OB differentiation and mineral deposition. The data raises the possibility that small increases in TL1A, as observed in AS and PsA, could stimulate bone formation leading to the formation of syndesmophytes and fusion of spinal vertebra (Fig 7.1). TL1A titration studies are required however, to conclusively determine what effect increasing levels of TL1A have on OB differentiation and mineral deposition.

3. Osteoporosis

DR3 expression has been shown to be lost on the surface of post-menopausal-derived OC precursors, suggesting that expression of the receptor disappears with aging (chapter 5). In the investigation into the role of DR3 in OB function (chapter 6) decreased OB differentiation and mineral deposition were observed in $DR3^{ko}$ mice. This raises the possibility that loss of DR3 on the OB post-menopause may be responsible for the reduced bone formation seen in OP. This would shift the balance of bone remodelling away from bone formation towards increased resorption (Fig 7.2). To prove this hypothesis further human work and animal models should be utilised. Characterisation of DR3 on pre- and post-menopausal OPCs and mineralising OB would determine whether DR3 expression is lost post-menopause. Generation of an inducible OPC / OB DR3 conditional knockout rodent (474) would also allow for the *in vivo* effects of OB DR3 ablation on the pathogenesis of OP to be studied.

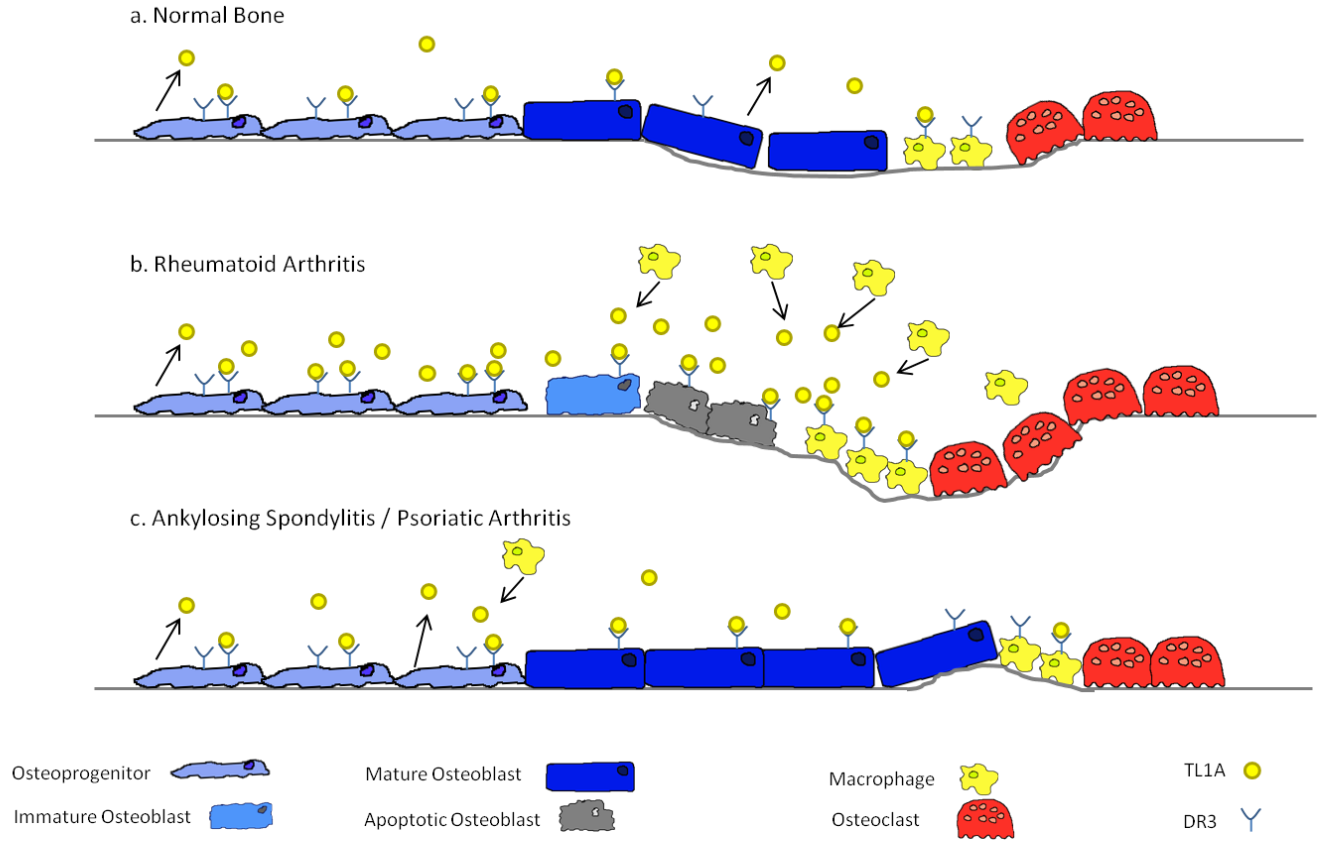

Figure 7.1. **Schematic Representation of the Possible Role of DR3, TL1A in the Pathogenesis of Bone Pathology in Inflammatory Arthritides**

Under a) normal conditions signalling through DR3 by TL1A on osteoprogenitors and macrophages results in the balanced turnover of bone. (b) In rheumatoid arthritis TL1A levels are significantly elevated due to infiltrating macrophages and T cells. Increased TL1A inhibits the differentiation of osteoprogenitors and leads to the apoptosis of mature OB. Signalling by TL1A on OC precursors results in an up-regulation of OC differentiation and resorptive activity leading to increased bone resorption. (c) Subtle increases in TL1A levels in ankylosing spondylitis and psoriatic arthritis increase OB differentiation resulting in increased bone formation and the generation of syndesmophytes.

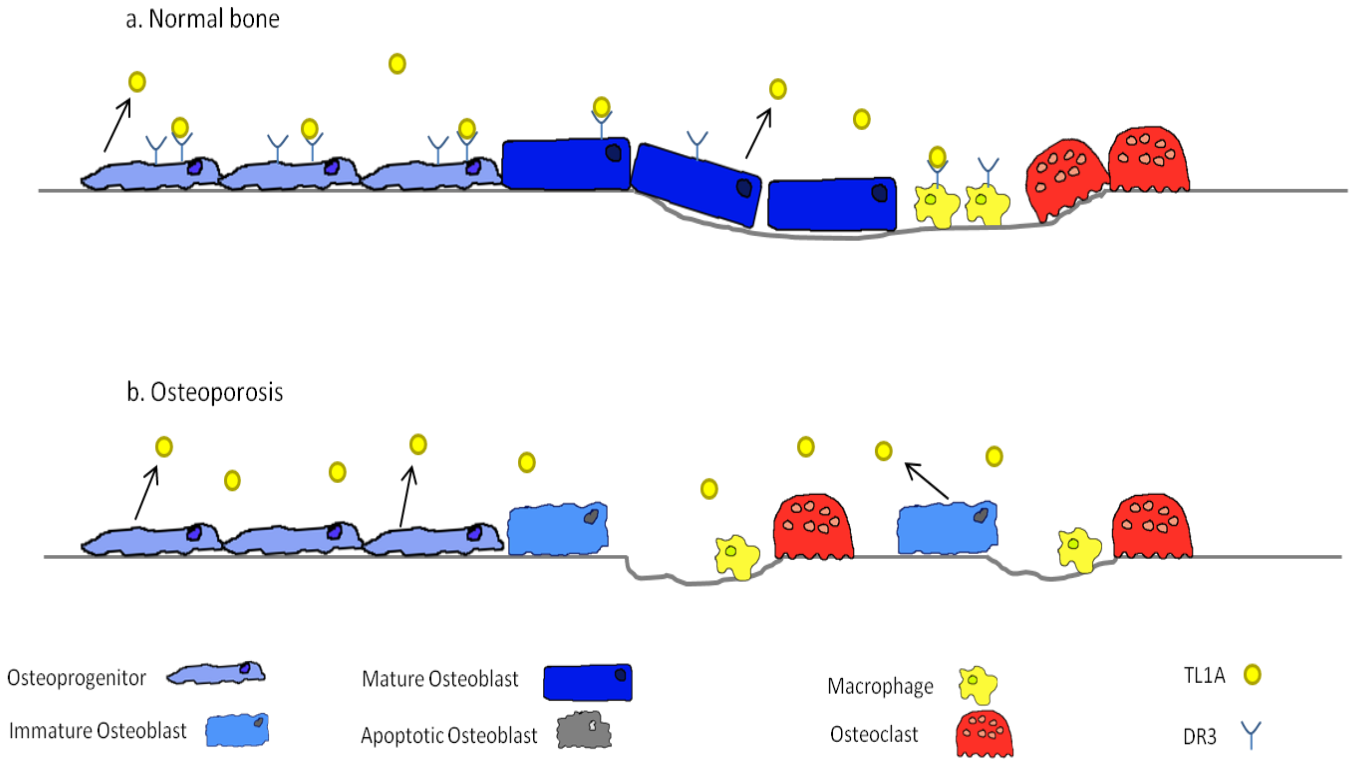

Figure 7.2. **Schematic Representation of the Possible Role of DR3, TL1A in the Pathogenesis of Bone Pathology in Post-Menopausal Osteoporosis**

Under a) normal conditions signalling through DR3 by TL1A on osteoprogenitors and macrophages results in the balanced turnover of bone. (b) In post-menopausal osteoporosis DR3 expression is absent from the OB and OC. Absence of DR3, TL1A signalling on OB results in inhibited OB differentiation and bone formation. Absence of DR3, TL1A signalling on the OC does not effect OC formation or function resulting in an imbalance in the bone remodelling cycle.

7.6 **Future Work**

The work performed in this thesis has revealed many novel aspects of the role of DR3/TL1A in the regulation of bone biology. A number of important questions still remain to be answered and require further investigation.

- The exact mechanism through which DR3/TL1A regulates OC resorption still remains unknown. The effect of DR3/TL1A on actin ring formation, CatK expression and c-Src activity requires elucidating to identify what aspects of OC resorptive function DR3/TL1A may regulate.
- DR3 has been demonstrated to increase activation of OC and OB MMPs. The mechanism how DR3 regulates the activation of these MMPs remains elusive and requires investigation.
- Serum TL1A is increased in RA patients with erosive disease, whether TL1A can be used as a prognostic marker for disease severity however is unknown. Assessment of serum TL1A levels in patients who display at clinic with early signs of arthritis and follow up throughout the course of the disease would provide valuable information. An in-depth study into the effects of anti-TNF treatment on serum TL1A levels could also provide answers as to why some patients do not respond to treatment.
- DR3/TL1A were revealed to have no direct effect on the increased OC activity associated with OP. Analysis of post-menopausal OC assays using PBMCs as a starting population would determine whether DR3/TL1A have an indirect effect on increased OC activity in post-menopausal OP.
- DR3 has been shown to potentially regulate OB differentiation and function in an autocrine manner. Investigation into its effect on the OB specific transcription factors Runx2, OSX and ATF4, would provide valuable insight into the mechanism and time frame of its action. Titration of TL1A into OB cultures would also reveal the effect of raised cytokine levels on OB function, producing a possible mechanism for the adverse bone pathology observed in AS and PsA.
- *In vivo* OC differentiation is controlled by OB expression of RANKL and OPG. To determine whether DR3/TL1A signalling on the OB can indirectly regulate OC formation expression of soluble RANKL and OPG should be analysed in $DR3^{wt}$ and $DR3^{ko}$ OB cultures. Co-culture assays using OC and OB derived from $DR3^{wt}$ and $DR3^{ko}$ mice would further reveal whether DR3/TL1A signalling on the OB is required for optimal OC differentiation and function.

7.7 **Concluding Remarks**

At the outset of this thesis the role of DR3/TL1A in OC and OB biology and disease characterised by adverse bone pathology were unknown. This study has identified a potentially important role of DR3/TL1A in OC and OB differentiation and function. DR3 has been shown to be involved in OC resorptive function through the activation of MMP-9, while TL1A has been demonstrated to effect OC formation through regulation of osteoclastogenic chemokine expression. *In vitro* DR3 has been revealed to have a role in normal OB differentiation and bone formation affecting levels of ALP expression, activation of MMP-2, -9 and mineral deposition. *In vivo* TL1A has been linked to the pathogenesis of erosive RA, with levels unaffected by anti-TNF treatment. Intriguingly DR3/TL1A were shown to have no direct effect on the increased OC activity associated with OP, with DR3 expression not induced on $CD14^+$ cells isolated from post-menopausal females. Further research is required to fully elucidate the mechanisms through which DR3/TL1A act however, the data presented in thesis demonstrates for the first time DR3/TL1A to be potentially important regulators of bone remodelling.

Chapter 8

Appendix

Appendix I **Visualisation of Actin Ring Formation by Immunocytochemistry**

When resorbing bone, OC undergo rearrangement of their actin. This forms a ring, which surrounds the ruffled border and is involved in the creation of the sealed zone (17, 475). A possible mechanism for the observed difference in $DR3^{wt}$ and $DR3^{ko}$ resorptive function (section 3.2.8) could be an inability of the $DR3^{ko}$ mice to rearrange their actin. Optimisation of actin ring and nucleus immunocytochemistry (ICC) was performed to enable the visualisation of the actin and nucleus in OC cultures (section 2.2.6). Analysis of stained osteoclasts under the fluorescent microscope showed that a 1:100 dilution (0.5units/ml) of the Alexa Fluor® 594 phalloidin stain was sufficient to visualise the cellular actin. Actin (red) was observed as diffuse staining in mononuclear precursors cells and non-bound multinucleated osteoclasts. In fully differentiated OC the actin was visualised as a highly organised ring around the outer edge of the cell. Staining with DAPI (blue) at 300nM was found to be suitable for the visualisation of the nuclei in both precursor cells and multinucleated osteoclasts.

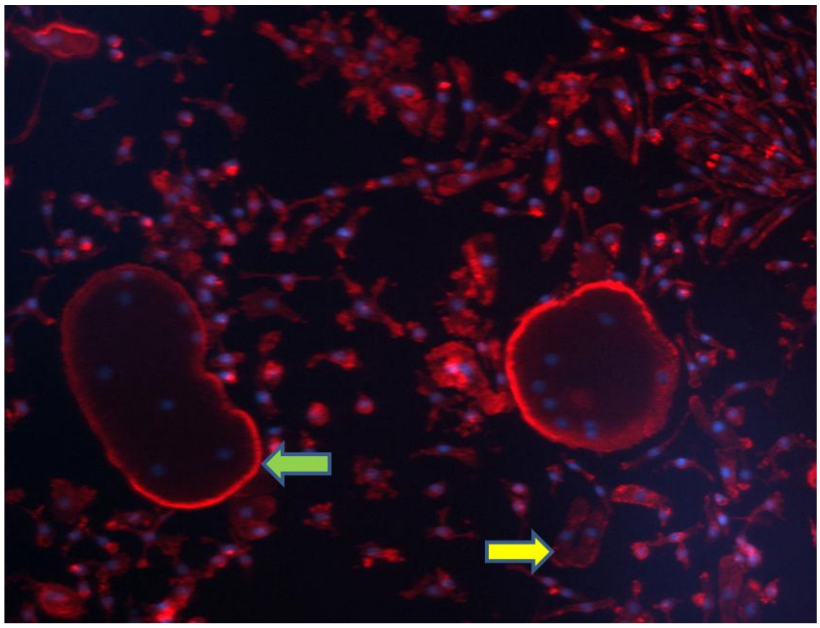

Appendix I. Alexa Fluor® 594 Phallodin and DAPI Staining of Actin and Nuclei in an Osteoclast Culture.

BMCs were extracted from the femora of DR3^{wt} DBA/1 mice and cultured for 10 days, in a 48 well tissue culture plate, in the presence of MCSF and RANKL. Cells were stained with Alexa Fluor 594 phalloidin and DAPI for the visualisation of actin and nuclei. Actin was visualised as red in both osteoclasts and their precursors. In precursor cells actin was diffuse throughout the cell (yellow arrow), in differentiated osteoclasts actin was highly organised into a ring structure (green arrow). Nuclei, stained with DAPI, were visualised as blue.

Appendix II **Visualisation of Cathepsin K by Immunocytochemistry**

While the gelatinase MMP-9 has been shown to be involved in osteoclastic bone resorption (300, 301) it is not the main factor; the proteinase Cathepsin K has been shown to be the key enzyme involved in this process (104, 105). Detection of Cathepsin K by ELISA was not possible without lysis of the cells, as Cathepsin K release is restricted to the sealed zone under the OC. To enable detection of Cathepsin K, within the OC and the sealed zone, a method was established for the immunocytochemical staining of the enzyme. The immunocytochemistry methodology is outlined in section 2.2.19. An anti-Cathepsin K antibody was tested at concentrations of 1µg/ml, 2µg/ml, 3µg/ml and 4µg/ml, along with an isotype control at equivalent concentrations. For visualisation an anti-rabbit FITC conjugated antibody was employed. A signal, representing the presence of Cathepsin K, was visible at all concentrations. The % of luminosity of the green signal image was calculated per image. The luminosity of the Cathepsin K signal was observed to increase from 1µg/ml to 3µg/ml (9.8% versus 12.5% versus 15.1%). At 4µg/ml the level of luminosity decreased to 7.8%. No non-specific signal from the isotype control was detected at concentrations of 1µg/ml and 2µg/ml. A non-specific signal was detected when the isotype control was used at 3µg/ml (2.7%), increasing slightly when used at 4µg/ml (3.1%). The results suggest that the optimum concentration for the visualisation of Cathepsin K is 2µg/ml.

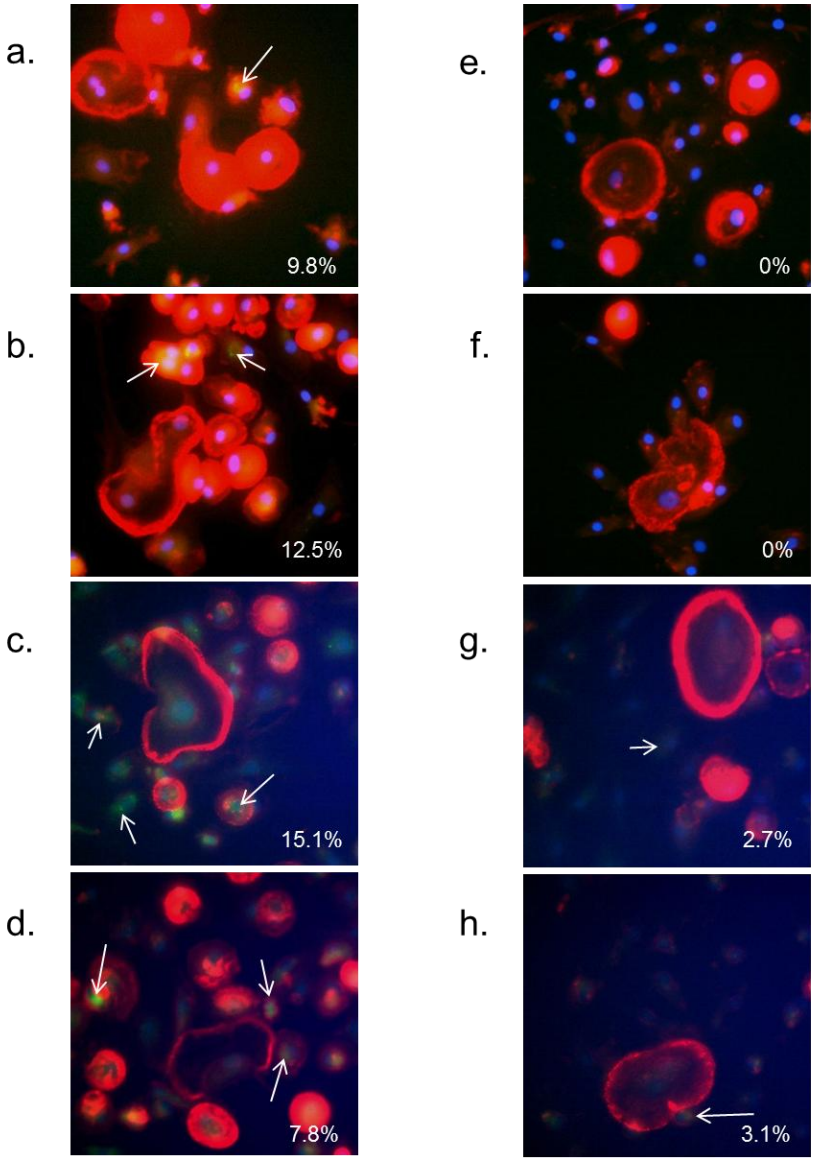

Appendix II. Visualisation of Cathepsin K with anti-Cathepsin K / anti-Rabbit FITC in a Human Osteoclast Culture.

$CD14^+$ cells were differentiated for 14 days in MCSF and RANKL. Cells were stained with Alexa Fluor 594 phalloidin, DAPI and anti-cathepsin K or isotype control with anti-rabbit-FITC for visualisation. Representative pictures of cathepsin K staining at (a) 1µg/ml (b) 2µg/ml (c) 3µg/ml (d) 4µg/ml and isotype at (e) 1µg/ml (f) 2µg/ml (g) 3µg/ml (h) 4µg/ml. Actin was visualised as red. Nuclei were visualised as blue. Cathepsin K / non-specific binding was visualised as green or yellow (white arrow). Percentages indicate luminosity of cathepsin K staining.

Appendix III **Comparison of Serum TL1A and DR3 and CD14 Expression on $CD14^+$ Cells Isolated from Pre-Menopausal Controls and Post-Menopausal Patients**

Serum and $CD14^+$ cells were isolated from the peripheral blood of pre-menopausal controls (chapter 4) and post-menopausal patient cohorts (chapter 5). Serum TL1A levels were measured by ELISA and reported graphically as pg/ml (mean±SEM). Isolated $CD14^+$ cells (day -7) were cultured on ivory for 7 days in medium supplemented with MCSF to determine whether there is a fundamental difference in expression following the menopause. Expression is presented as fold increase in MFI relative to the isotype control (mean±SEM). Levels of serum TL1A in the pre-menopausal controls were measured at (117.3±29.3pg/ml). These were comparable to the post-menopausal fracture cohorts (OP^-Frac^+=90.8±4.5pg/ml and OP^+Frac^+=103.1±2.3pg/ml). Serum TL1A levels in the non-OP non-fracture cohort were reduced (OP^-Frac^-=47.2±29.0pg/ml), however, this difference was not significant (Fig Appendix III (a)).

Pre-menopausal $CD14^+$ cells demonstrated a 10.0±2.3-fold increase in CD14 expression over the isotype (Fig Appendix III (b)). No significant difference in CD14 expression was observed compared to the post-menopausal OP^-Frac^- (11.1±4.2), OP^-Frac^+ (11.3±3.1) and OP^+Frac^+ (11.8±8.2) patient cohorts. DR3 expression increased 5.1±1.6-fold on the pre-menopausal control-derived cells. This was significantly elevated compared to the OP^-Frac^- (0.9±0.1; P<0.01), OP^-Frac^+ (1.1±0.2; P=<0.01) and OP^+Frac^+ (1.1±0.0; P=<0.05) patient-derived cells (Fig Appendix III (c)).

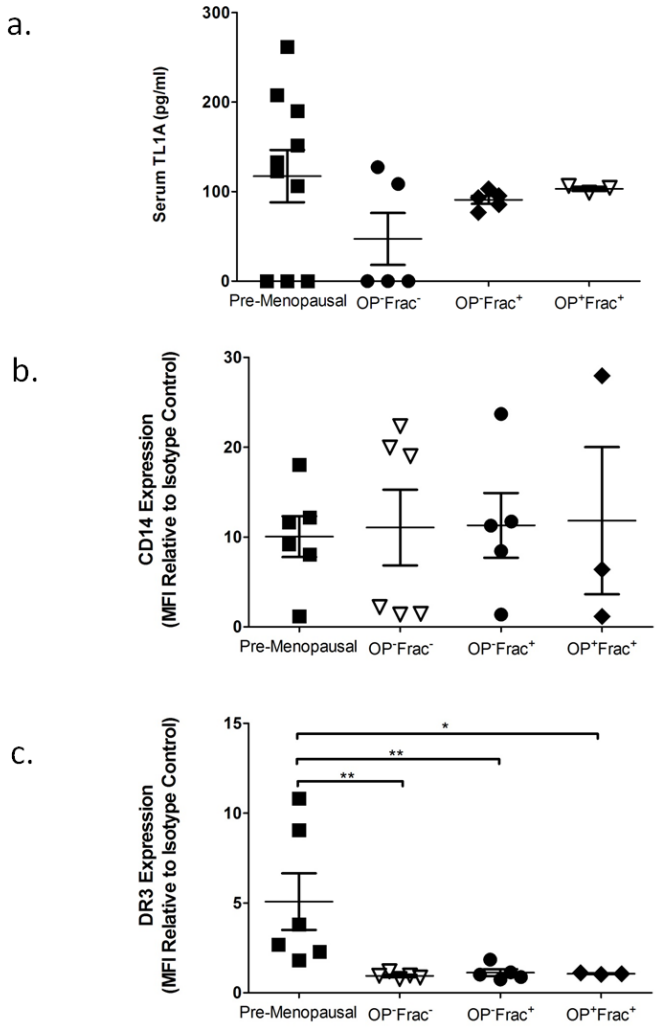

Appendix III. Comparison of Serum TL1A and DR3 / CD14 Expression on CD14⁺ Cells Isolated from Pre-Menopausal Controls and Post-Menopausal Patients after 7 Days Culture.

Serum and $CD14^+$ cells were isolated from the peripheral blood of pre-menopausal controls and post-menopausal patients. Levels of serum TL1A were observed to be comparable between the pre-menopausal controls and post-menopausal cohorts. $CD14^+$ cells were plated onto ivory discs and cultured for 7 days in MCSF. Cells were removed and stained with either an isotype control or with an anti-human CD14 / DR3 antibody and tested by flow cytometry . Fold increase in MFI relative to the isotype control was calculated for (a) CD14 and (b) DR3 expression. No significant difference in CD14 expression was detected. DR3 expression was significantly elevated in the pre-menopausal controls compared to the OP^-Frac^- (**P=<0.01), OP^-Frac^+ (**P=<0.01) and OP^+Frac^+ (*P=<0.05) cohorts. Statistical analysis was performed with a 2-way ANOVA and Bonferroni post test and Mann Whitney test.

Appendix IV **Comparing the Differentiation and Resorptive Function of Pre-Menopausal and Post-Menopausal Patient–Derived Osteoclasts**

Following culture in MCSF for 7 days DR3 expression was not induced on the surface of post-menopausal patient-derived $CD14^+$ cells, this was in stark contrast to the pre-menopausal control cells (Appendix III). To determine whether there was a fundamental difference in the ability of patient-derived $CD14^+$ cells and pre-menopausal-derived $CD14^+$ cells to differentiate into osteoclasts, results from chapter 4 (pre-menopausal) and chapter 5 (post-menopausal) were compared.

The total number of cells per mm^2 (mean±SEM) for each disc is presented graphically in Fig Appendix IV (a). Total cell number in the pre-menopausal cultures were observed to be significantly increased across the time course compared to the post-menopausal OP^-Frac^-, OP^-Frac^+ (P=<0.0001) and OP^+Frac+ (P=<0.01) cultures. At day 7 total cell numbers in the cultures were calculated as; pre-menopausal=534±70, OP^-Frac^-=211±36, OP^-Frac^+=244±46 and OP^+Frac^+=446±68. These did not change significantly over time.

Differential counts were performed and $TRAP^+$ OC reported as OC / mm^2 (Fig Appendix IV (b)). OC numbers in the pre-menopausal cultures increased across the time course from 5±1 at day 7 to 7±1 at day 14. OC numbers in the post-menopausal cultures at day 7 were; OP^-Frac^-=2±1, OP^-Frac^+=2±1 and OP^+Frac^+=1±1, these did not vary significantly across the time course. A significant increase in OC numbers was detected in the pre-menopausal cultures across the time course compared to the OP^-Frac^-, OP^-Frac^+ (P=<0.01) and OP^+Frac^+ (P=<0.05) cultures.

OC resorptive activity was expressed as % area resorbed (mean±SEM) for graphical presentation (Fig Appendix IV (c)). Levels of resorption in cultures at day 10 were; pre-menopausal=0.9±0.3%, OP^-Frac^-=0.1±0.1%, OP^-Frac^+=0.3±0.2% and OP^+Frac^+=0.1±0.1%. Levels in the pre-menopausal cultures increased at day 14 (1.3±0.3%) while remaining relatively constant in the post-menopausal cultures (OP^-Frac^-=0.7±0.5%, OP^-Frac^+=0.4±0.3% and OP^+Frac^+=0.2±0.1%). Across the time course no significant difference was detected in OC resorptive function.

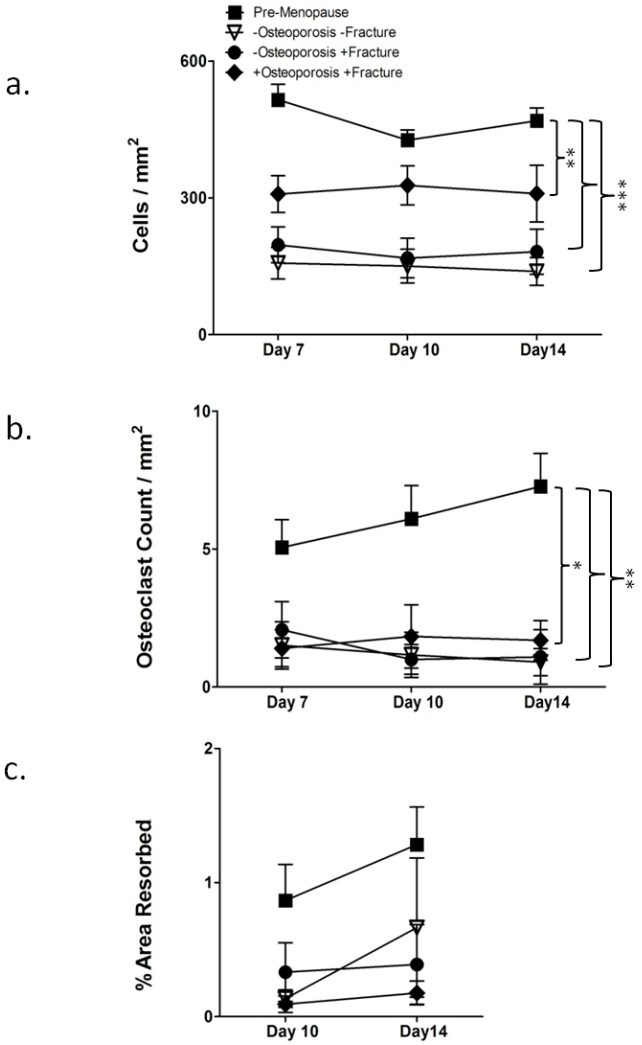

Appendix IV. Comparison of Pre-Menopausal OC cultures (Chapter 4) to Post-Menopausal Patient-Derived OC Cultures (chapter 5)

PBMCs were extracted from the peripheral blood and $CD14^+$ cells isolated by magnetic sorting. Pre-menopausal (chapter 4) and patient-derived $CD14^+$ cells were plated onto ivory discs and cultured in MCSF for 7 days before differentiation in MCSF+RANKL. (a) Total cell number was significantly increased across the time course in the pre-menopausal cultures over the non-OP (***P=<0.0001) and OP cohorts (**P=<0.01). (b) Across the time course OC numbers were significantly elevated in the pre-menopausal cultures compared to the non-OP (**P=<0.01) and OP (*P=<0.05) cultures. (c) No significant difference was found in % area resorbed. Statistical analysis was performed with a two-way ANOVA and Bonferroni post test.

Appendix V **Improving the Methodology of Analysing Resorption Pits on Ivory Discs - Results**

The current method employed for the functional assessment of counting resorption pits (toluidine blue staining, photographing, highlighting resorption pits and calculation of the % area resorbed) is time consuming, taking 6 hours to fully analyse an experiment (12 discs). While this method provides the surface area of the disc that is resorbed it does not provide any indication of the depth of the resorption pit. At the end of this project a portion of time was spent on developing a more sensitive method for the analysis of pit area and depth in 3D. Use of confocal microscopy was optimised for the accurate analysis of resorption pit depth; the methodology is described in section 2.2.18.

Discs were initially placed onto a glass slide and scanned using reflective light (Appendix V a (a)). Images produced were of a higher quality and resolution than those produced using a standard light microscope. However, the reflectance of the discs was relatively low, so resolution of the pits was not at the highest level that can be produced with the equipment. Discs were also prone to distortion under the lens of the microscope due to drying out. This had the knock-on effect of changing the focus, meaning that the accuracy of pit depth measurement could not be relied upon. To address the reflectance and distortion problems, discs were stained with the fluorescent dye calcein and mounted onto glass slides using DPX. Discs were scanned using a laser of wavelength 495nm. Images produced had a higher resolution than those scanned with reflective light (Appendix V a (b)). The high resolution of the scan allowed for accurate 3D reconstruction of the pits (Appendix V b (a)) as well as analysis of pit area and depth (Appendix V B (b)). In the samples tested resorption pits were found to have a depth ranging from 3µm to 20µm. These results are within the range observed by other groups using laser scanning confocal microscopy and scanning surface profiling (476-478) for pit measurement. Optimisation of the confocal microscope for the analysis of resorption pits showed that accurate high resolution pictures, in 2D and 3D, could be obtained, allowing the accurate calculation of pit area and pit volume.

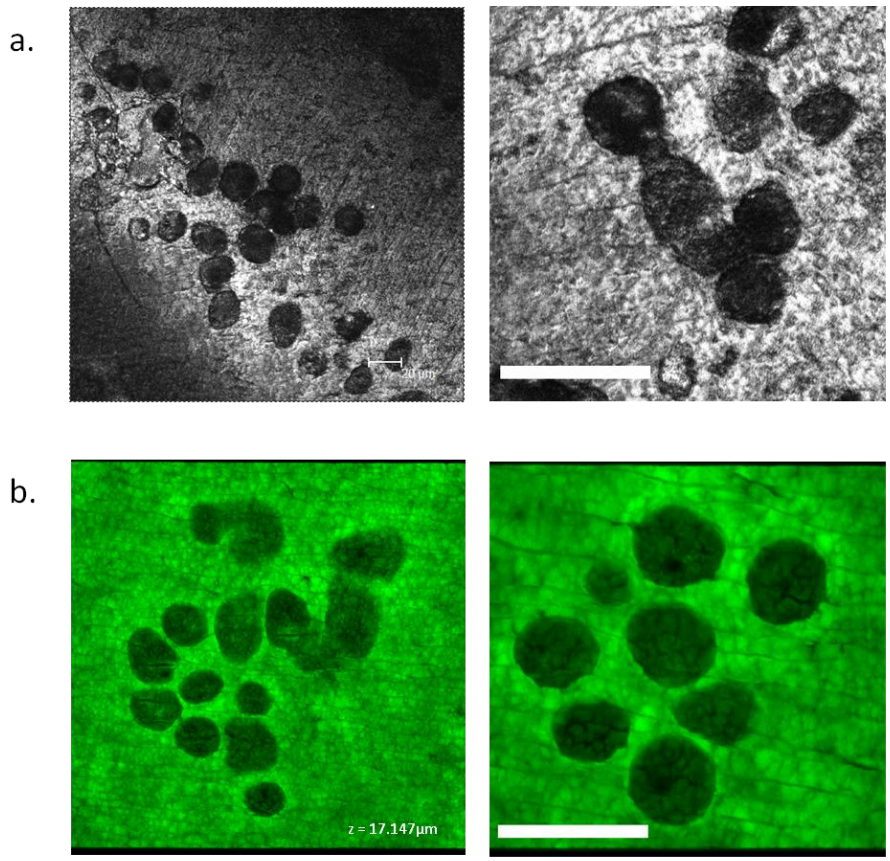

Appendix V (a). Optimisation of Confocal Microscope for Ivory Disc Resorption Analysis.

Ivory discs were scanned using a confocal microscope for the analysis of osteoclast resorption pits. Representative pictures of discs scanned and analysed with (a) refelctive light and (b) discs stained with calcein and scanned using a 495 nm wavelength laser. Scale bar = 10µm.

a.

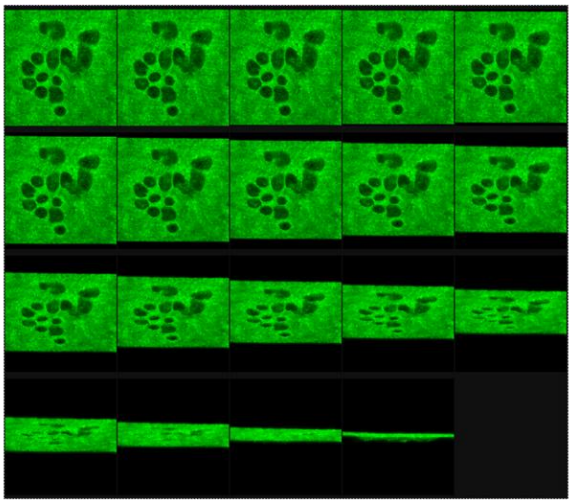

b.

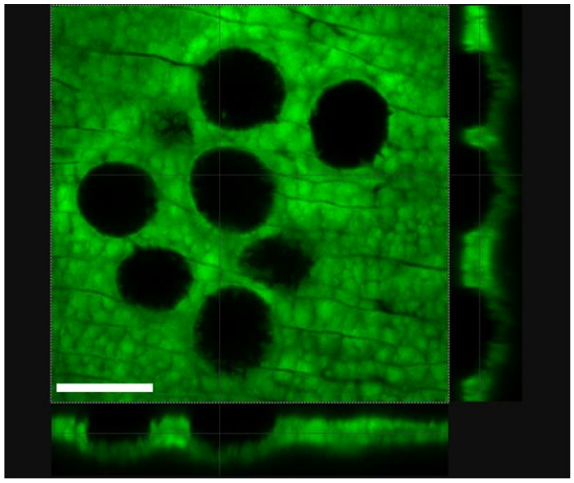

Appendix V (b). Optimisation of Confocal Microscope for Ivory Disc Resorption Analysis.

Ivory discs were scanned using a confocal microscope for the analysis of resorption pits. Representative snapshot of (a) images used to create 3D video of resorption pits. Representative (b) cross sectional analysis of resorption pits showing pits in profile and face on for the analysis of area and depth. Scale bar = 10µm.

Appendix V **Improving the Methodology of Analysing Resorption Pits on Ivory Discs - Discussion**

A standard method for the analysis of resorption pits was employed throughout this thesis; sonication of discs, staining with toluidine blue and analysis of resorption pit area by light microscopy (460). However, a number of alternative methods have been used by other groups including confocal microscopy (129) and scanning electron microscopy (461). Use of a confocal microscope for the analysis of resorption pits was selected and a method developed (comparison between the standard method and confocal is found in Table 8.1). Initial work on the confocal microscope using reflective light produced higher resolution images than those seen with just a light microscope. However, the images were not as 'sharp' or detailed as is possible to obtain with a confocal microscope, due to the low reflectance of ivory (Appendix V). To overcome this, discs were stained with the fluorescent dye calcein, which binds to calcium. To visualise the discs a laser of wavelength of 495nm was required to excite the calcein. When excited calcein emitted light at a wavelength of 515nm (green), this was then used to visualise the disc surface. The images produced via this method were of a higher resolution and more detailed than those generated using reflective light and light microscopy. Pits were clearly visible on the surface of the discs with the edges clearly defined. Creating a 'z-series' stack (multiple images through a section) allowed for the 3D recreation of the resorption pit. Further analysis could then be performed using the images, such as depth measurements and cross-sectional analysis. Using this method of 3D recreation, pit depth was found to range between 3µm and 20µm (Appendix V). These pit depths were found to be within the range observed by other groups, validating the method; Inui et al (477) (approx. 6µm using a scanning surface profiler), and Parikka et al (476) and Jeon et al (478) (approx. 10µm and 5µm - 25µm respectively, using scanning confocal microscopy). However, a number of issues were identified that required further development before the method could be used for high throughput analysis of resorption pits.

Ivory discs were found to dry out under the confocal; this created distortion in the disc and had the knock-on effect of altering the focus. Occurrence of this during the generation of a 'z-series' would lead to inaccurate measurements. Some work was done on mounting the ivory discs onto glass slides using DPX and covering with a coverslip. While this did help with the drying out and distortion it was not without its own problems. The thickness (0.3-0.7mm) and inherent roughness of the ivory discs meant that mounting

was not straight forward, as a large percentage of the glass coverslip was not supported and could crack if put under too much pressure. While this wouldn't affect the disc, the cracked glass was a risk to the lens of the confocal microscope so broken slides could not be analysed. Development of a method to mount the ivory discs safely would allow the use of the confocal microscope for analysis.

	Standard Method	**Confocal Microscopy Reflective Light**	**Confocal Microscopy 495nm Laser**
Time Taken to Analyse 1 Experiment (12 Discs)	Approx. 6 hours	Approx. 4 hours	Approx. 4 hours
Relative Picture Resolution	Low	Medium	High
Calculation of Pit Area	Yes	Yes	Yes
Calculation of Pit Depth	No	Yes – Low Accuracy	Yes – High Accuracy

Table 8.1. Comparison of methods for the analysis of osteoclast resorption pits on ivory discs.

Appendix VI **Presentations**

F. Collins, A. Bloom, M. Stone, E. Wang, A. Williams (2012). *Death Receptor 3 and TNF-like Ligand 1A – A Driving Force in Osteoclast Differentiation and Potential Target for Rheumatoid Arthritis Therapy*. Bone Research Society Conference 2012. Oral presentation.

F. Collins, E. Wang, A. Williams (2012). *Death Receptor 3 and TL1A: A Regulatory Pathway Of Bone Turnover*. MITReG Postgraduate Day. Oral presentation.

A. S. Williams, **F. Collins**, Z. Newton , R. M. Goodfellow , R. Rajak , C. Calder , E. C. Y. Wang (2012). *TNF-Like Protein 1A/Death Receptor 3 Pathway Regulates Osteoclastogenesis and Is Associated with Erosive Disease in Rheumatoid Arthritis*. ACR annual meeting 2012. Poster presentation.

F. Collins, A. Bloom, E.Wang, A.S.Williams (2011). *DR3 - TL1A Pathway – Effect on Osteoclast Differentiation and Function*. ASBMR Conference 2011. Poster presentation.

F. Collins, A. Bloom, E.Wang, A.S.Williams (2011). *Death Receptor 3 – Effect on Osteoclast Differentiation and Function*. BSI Summer School 2011. Poster presentation.

A. C. Bloom, **F. L. Collins**, B. A. J. Evans, D. P. Aeschlimann, B. P. Morgan, A. S. Williams (2011). *CD59 An Unexpected Protective Role In Bone*. ECTS 2011. Poster presentation.

A. S. Williams, **F. Collins**, Z. Newton, R. Goodfellow, C. Calder, E. Wang. *Targeting TL1A To Prevent Bone Damage In Rheumatoid Arthritis*. British Society for Rheumatology (BSR) Conference 2011. Poster presentation.

E. Wang, Z. Newton, **F. Collins**, O. Hayward, R. Singh, W. Perks, J. Twohig and A. S. Williams (2011). *Control Of Early Cartilage Destruction In Inflammatory Arthritis By Death Receptor 3*. BSI Congress 2011. Poster presentation.

A. S. Williams, **F. Collins**, Z. Newton , R. M. Goodfellow , R. Rajak , C. Calder , E. C. Y. Wang (2010). *Death Receptor 3 Orchestrates Erosive Pathology In Rheumatoid Arthritis*. BSI Congress 2010. Poster presentation.

Chapter 9

References

1. Steele DG, Bramblett CA. *The anatomy and biology of the human skeleton*: TAMU Press.; 1988.
2. Takayanagi H. Osteoimmunology: shared mechanisms and crosstalk between the immune and bone systems. Nat Rev Immunol. [Review]. 2007 Apr;7(4):292-304.
3. Karsenty G, Kronenberg HM, Settembre C. Genetic control of bone formation. Annual Review of Cell and Developmental. 2009;25:629-48.
4. Teitelbaum SL. Osteoclasts: What do they do and how do they do it? Am J Pathol. [Proceedings Paper]. 2007 Feb;170(2):427-35.
5. Bonewald LF, Johnson ML. Osteocytes, mechanosensing and Wnt signaling. Bone. 2008;42(4):606-15.
6. Andersen TL, Sondergaard TE, Skorzynska KE, Dagnaes-Hansen F, Plesner TL, Hauge EM, et al. A physical mechanism for coupling bone resorption and formation in adult human bone. The American journal of pathology. 2009;174(1):239-47.
7. Dempster DW. Anatomy and Functions of the Adult Skeleton. Primer on the Metabolic Bone Diseases and Disorders of Mineral Metabolism. 2006:7–11.
8. Chambers TJ, Darby JA, Fuller K. Mammalian collagenase predisposes bone surfaces to osteoclastic resorption. Cell Tissue Res. 1985;241(3):671-5.
9. Henriksen K, Sørensen MG, Nielsen RH, Gram J, Schaller S, Dziegiel MH, et al. Degradation of the organic phase of bone by osteoclasts: a secondary role for lysosomal acidification. Journal of Bone and Mineral Research. 2005;21(1):58-66.
10. Delaisse J-M, Eeckhout Y, Vaes G. Bone-resorbing agents affect the production and distribution of procollagenase as well as the activity of collagenase in bone tissue. Endocrinology. 1988;123(1):264-76.
11. Mizoguchi T, Muto A, Udagawa N, Arai A, Yamashita T, Hosoya A, et al. Identification of cell cycle–arrested quiescent osteoclast precursors in vivo. The Journal of cell biology. 2009;184(4):541-54.
12. Chambers TJ. Regulation of the differentiation and function of osteoclasts. Journal of Pathology. 2000 Sep;192(1):4-13.
13. Yoshida H, Hayashi SI, Kunisada T, Ogawa M, Nishikawa S, Okamura H, et al. THE MURINE MUTATION OSTEOPETROSIS IS IN THE CODING REGION OF THE MACROPHAGE COLONY STIMULATING FACTOR GENE. Nature. [Article]. 1990 May;345(6274):442-4.
14. Lagasse E, Weissman IL. Enforced expression of Bcl-2 in monocytes rescues macrophages and partially reverses osteopetrosis in op/op mice. Cell. [Article]. 1997 Jun;89(7):1021-31.
15. Yasuda H, Shima N, Nakagawa N, Yamaguchi K, Kinosaki M, Mochizuki S, et al. Osteoclast differentiation factor is a ligand for osteoprotegerin osteoclastogenesis-inhibitory factor and is identical to TRANCE/RANKL. Proc Natl Acad Sci U S A. [Article]. 1998 Mar;95(7):3597-602.
16. Fuller K, Wong B, Fox S, Choi YW, Chambers TJ. TRANCE is necessary and sufficient for osteoblast-mediated activation of bone resorption in osteoclasts. J Exp Med. [Article]. 1998 Sep;188(5):997-1001.
17. Teitelbaum SL. Bone resorption by osteoclasts. Science. 2000 Sep;289(5484):1504-8.
18. Everts V, Delaisse JM, Korper W, Jansen DC, Tigchelaar-Gutter W, Saftig P, et al. The bone lining cell: Its role in cleaning Howship's lacunae and initiating bone formation. Journal of Bone and Mineral Research. 2002 Jan;17(1):77-90.
19. Parikka V, Väänänen A, Risteli J, Salo T, Sorsa T, Väänänen HK, et al. Human mesenchymal stem cell derived osteoblasts degrade organic bone matrix in vitro by matrix metalloproteinases. Matrix biology. 2005;24(6):438-47.

20. Takahashi T, Kurihara N, Takahashi K, Kumegawa M. AN ULTRASTRUCTURAL-STUDY OF PHAGOCYTOSIS IN BONE BY OSTEOBLASTIC CELLS FROM FETAL MOUSE CALVARIA INVITRO. Arch Oral Biol. 1986;31(10):703-6.
21. Pierce AM, Lindskog S, Hammarstrom L. OSTEOCLASTS - STRUCTURE AND FUNCTION. Electron Microscopy Reviews. 1991;4(1):1-45.
22. Walker DG. OSTEOPETROSIS CURED BY TEMPORARY PARABIOSIS. Science. 1973;180(4088):875-.
23. Walker DG. BONE-RESORPTION RESTORED IN OSTEOPETROTIC MICE BY TRANSPLANTS OF NORMAL BONE-MARROW AND SPLEEN-CELLS. Science. [Article]. 1975;190(4216):784-5.
24. Maggiani F, Forsyth R, Hogendoorn PCW, Krenacs T, Athanasou NA. The immunophenotype of osteoclasts and macrophage polykaryons. Journal of Clinical Pathology. 2011;64(8):701-5.
25. Katagiri T, Takahashi N. Regulatory mechanisms of osteoblast and osteoclast differentiation. Oral Dis. [Review]. 2002 May;8(3):147-59.
26. Fujikawa Y, Quinn JMW, Sabokbar A, McGee JO, Athanasou NA. The human osteoclast precursor circulates in the monocyte fraction. Endocrinology. 1996 Sep;137(9):4058-60.
27. Lorenzo J, Choi Y, Horowitz M, Takayanagi H. *Osteoimmunology: interactions of the immune and skeletal systems*: Academic Press.; 2010.
28. Kurihara N, Suda T, Miura Y, Nakauchi H, Kodama H, Hiura K, et al. GENERATION OF OSTEOCLASTS FROM ISOLATED HEMATOPOIETIC PROGENITOR CELLS. Blood. 1989 Sep;74(4):1295-302.
29. Arai F, Miyamoto T, Ohneda O, Inada T, Sudo T, Brasel K, et al. Commitment and differentiation of osteoclast precursor cells by the sequential expression of c-Fms and receptor activator of nuclear factor kappa B (RANK) receptors. J Exp Med. 1999 Dec;190(12):1741-54.
30. Jacquin C, Gran DE, Lee SK, Lorenzo JA, Aguila HL. Identification of multiple osteoclast precursor populations in murine bone marrow. Journal of Bone and Mineral Research. 2006 Jan;21(1):67-77.
31. de Vries TJ, Schoenmaker T, Hooibrink B, Leenen PJM, Everts V. Myeloid blasts are the mouse bone marrow cells prone to differentiate into osteoclasts. J Leukoc Biol. 2009 Jun;85(6):919-27.
32. Geissmann F, Jung S, Littman DR. Blood monocytes consist of two principal subsets with distinct migratory properties. Immunity. 2003;19(1):71-82.
33. Mbalaviele G, Jaiswal N, Meng A, Cheng LZ, Van den Bos C, Thiede M. Human mesenchymal stem cells promote human osteoclast differentiation from CD34(+) bone marrow hematopoietic progenitors. Endocrinology. 1999 Aug;140(8):3736-43.
34. Koizumi K, Saitoh Y, Minami T, Takeno N, Tsuneyama K, Miyahara T, et al. Role of CX3CL1/Fractalkine in Osteoclast Differentiation and Bone Resorption. J Immunol. 2009 Dec;183(12):7825-31.
35. Suda T, Takahashi N, Martin TJ. MODULATION OF OSTEOCLAST DIFFERENTIATION. Endocr Rev. [Review]. 1992 Feb;13(1):66-80.
36. Roodman GD. Cell biology of the osteoclast. Experimental Hematology. 1999 Aug;27(8):1229-41.
37. Quinn JMW, Elliott J, Gillespie MT, Martin TJ. A combination of osteoclast differentiation factor and macrophage-colony stimulating factor is sufficient for both human and mouse osteoclast formation in vitro. Endocrinology. 1998 Oct;139(10):4424-7.
38. Massey HM, Flanagan AM. Human osteoclasts derive from CD14-positive monocytes. British Journal of Haematology. 1999 Jul;106(1):167-70.

39. Komano Y, Nanki T, Hayashida K, Taniguchi K, Miyasaka N. Identification of a human peripheral blood monocyte subset that differentiates into osteoclasts. Arthritis Research and Therapy. 2006;8(5):152.
40. Boyle WJ, Simonet WS, Lacey DL. Osteoclast differentiation and activation. Nature. [Review]. 2003 May;423(6937):337-42.
41. Vaananen HK, Zhao H, Mulari M, Halleen JM. The cell biology of osteoclast function. J Cell Sci. [Article]. 2000 Feb;113(3):377-81.
42. Bar-Shavit Z. The osteoclast: A multinucleated, hematopoietic-origin, bone-resorbing osteoimmune cell (vol 102, pg 1130, 2007). J Cell Biochem. [Correction]. 2008 Aug;104(5):1946-7.
43. Udagawa N, Takahashi N, Yasuda H, Mizuno A, Itoh K, Ueno Y, et al. Osteoprotegerin produced by osteoblasts is an important regulator in osteoclast development and function. Endocrinology. 2000;141(9):3478-84.
44. Suda T, Takahashi N, Udagawa N, Jimi E, Gillespie MT, Martin TJ. Modulation of osteoclast differentiation and function by the new members of the tumor necrosis factor receptor and ligand families. Endocr Rev. [Article]. 1999 Jun;20(3):345-57.
45. Manolagas SC. Birth and death of bone cells: basic regulatory mechanisms and implications for the pathogenesis and treatment of osteoporosis. Endocr Rev. 2000;21(2):115-37.
46. Jimi E, Nakamura I, Amano H, Taguchi Y, Tsurukai T, Tamura M, et al. Osteoclast function is activated by osteoblastic cells through a mechanism involving cell-to-cell contact. Endocrinology. 1996 May;137(5):2187-90.
47. Takahashi N, Akatsu T, Udagawa N, Sasaki T, Yamaguchi A, Moseley JM, et al. OSTEOBLASTIC CELLS ARE INVOLVED IN OSTEOCLAST FORMATION. Endocrinology. [Note]. 1988 Nov;123(5):2600-2.
48. Tanaka S, Takahashi N, Udagawa N, Tamura T, Akatsu T, Stanley ER, et al. MACROPHAGE COLONY-STIMULATING FACTOR IS INDISPENSABLE FOR BOTH PROLIFERATION AND DIFFERENTIATION OF OSTEOCLAST PROGENITORS. J Clin Invest. 1993 Jan;91(1):257-63.
49. Dai XM, Ryan GR, Hapel AJ, Dominguez MG, Russell RG, Kapp S, et al. Targeted disruption of the mouse colony-stimulating factor 1 receptor gene results in osteopetrosis, mononuclear phagocyte deficiency, increased primitive progenitor cell frequencies, and reproductive defects. Blood. 2002 Jan;99(1):111-20.
50. Simonet WS, Lacey DL, Dunstan CR, Kelley M, Chang MS, Luthy R, et al. Osteoprotegerin: A novel secreted protein involved in the regulation of bone density. Cell. [Article]. 1997 Apr;89(2):309-19.
51. Tsuda E, Goto M, Mochizuki S, Yano K, Kobayashi F, Morinaga T, et al. Isolation of a novel cytokine from human fibroblasts that specifically inhibits osteoclastogenesis. Biochemical and Biophysical Research Communications. 1997 May;234(1):137-42.
52. Bucay N, Sarosi I, Dunstan CR, Morony S, Tarpley J, Capparelli C, et al. osteoprotegerin-deficient mice develop early onset osteoporosis and arterial calcification. Genes Dev. [Article]. 1998 May;12(9):1260-8.
53. Mizuno A, Amizuka N, Irie K, Murakami A, Fujise N, Kanno T, et al. Severe osteoporosis in mice lacking osteoclastogenesis inhibitory factor osteoprotegerin. Biochemical and Biophysical Research Communications. [Article]. 1998 Jun;247(3):610-5.
54. Lacey DL, Timms E, Tan HL, Kelley MJ, Dunstan CR, Burgess T, et al. Osteoprotegerin ligand is a cytokine that regulates osteoclast differentiation and activation. Cell. [Article]. 1998 Apr;93(2):165-76.
55. Wong BR, Rho JR, Arron J, Robinson E, Orlinick J, Chao M, et al. TRANCE is a novel ligand of the tumor necrosis factor receptor family that activates c-Jun N-terminal kinase in T cells. Journal of Biological Chemistry. [Article]. 1997 Oct;272(40):25190-4.

56. Anderson DM, Maraskovsky E, Billingsley WL, Dougall WC, Tometsko ME, Roux ER, et al. A homologue of the TNF receptor and its ligand enhance T-cell growth and dendritic-cell function. Nature. [Article]. 1997 Nov;390(6656):175-9.
57. Blair HC, Athanasou NA. Recent advances in osteoclast biology and pathological bone resorption. Histology and Histopathology. 2004 Jan;19(1):189-99.
58. Kong YY, Yoshida H, Sarosi I, Tan HL, Timms E, Capparelli C, et al. OPGL is a key regulator of osteoclastogenesis, lymphocyte development and lymph-node organogenesis. Nature. 1999;397(6717):315-23.
59. Hsu HL, Lacey DL, Dunstan CR, Solovyev I, Colombero A, Timms E, et al. Tumor necrosis factor receptor family member RANK mediates osteoclast differentiation and activation induced by osteoprotegerin ligand. Proc Natl Acad Sci U S A. [Proceedings Paper]. 1999 Mar;96(7):3540-5.
60. Dougall WC, Glaccum M, Charrier K, Rohrbach K, Brasel K, De Smedt T, et al. RANK is essential for osteoclast and lymph node development. Genes Dev. [Article]. 1999 Sep;13(18):2412-24.
61. Ross FP, Teitelbaum SL. alpha(v)beta(3) and macrophage colony-stimulating factor: partners in osteoclast biology. Immunol Rev. [Review]. 2005 Dec;208:88-105.
62. Faccio R, Takeshita S, Zallone A, Ross FP, Teitelbaum SL. c-Fms and the alpha(v)beta(3) integrin collaborate during osteoclast differentiation. J Clin Invest. [Article]. 2003 Mar;111(5):749-58.
63. Kobayashi N, Kadono Y, Naito A, Matsumoto K, Yamamoto T, Tanaka S, et al. Segregation of TRAF6-mediated signaling pathways clarifies its role in osteoclastogenesis. Embo J. [Article]. 2001 Mar;20(6):1271-80.
64. Takayanagi H, Kim S, Koga T, Nishina H, Isshiki M, Yoshida H, et al. Induction and activation of the transcription factor NFATc1 (NFAT2) integrate RANKL signaling in terminal differentiation of osteoclasts. Dev Cell. [Article]. 2002 Dec;3(6):889-901.
65. Wagner EF, Eferl R. Fos/AP-1 proteins in bone and the immune system. Immunol Rev. [Review]. 2005 Dec;208:126-40.
66. Asagiri M, Sato K, Usami T, Ochi S, Nishina H, Yoshida H, et al. Autoamplification of NFATc1 expression determines its essential role in bone homeostasis. J Exp Med. [Article]. 2005 Nov;202(9):1261-9.
67. Crotti TN, Flannery M, Walsh NC, Fleming JD, Goldring SR, McHugh KP. NFATc1 regulation of the human beta(3) integrin promoter in osteoclast differentiation. Gene. [Article]. 2006 May;372:92-102.
68. Matsumoto M, Kogawa M, Wada S, Takayanagi H, Tsujimoto M, Katayama S, et al. Essential role of p38 mitogen-activated protein kinase in cathepsin K gene expression during osteoclastogenesis through association of NFATc1 and PU.1. Journal of Biological Chemistry. [Article]. 2004 Oct;279(44):45969-79.
69. Xing LP, Schwarz EM, Boyce BF. Osteoclast precursors, RANKL/RANK, and immunology. Immunol Rev. 2005 Dec;208:19-29.
70. Lapidot T, Kollet O. The essential roles of the chemokine SDF-1 and its receptor CXCR4 in human stem cell homing and repopulation of transplanted immune-deficient NOD/SCID and NOD/SCID/B2m(null) mice. Leukemia. 2002 Oct;16(10):1992-2003.
71. Hattori K, Heissig B, Tashiro K, Honjo T, Tateno M, Shieh JH, et al. Plasma elevation of stromal cell-derived factor-1 induces mobilization of mature and immature hematopoietic progenitor and stem cells. Blood. 2001 Jun;97(11):3354-60.
72. Rothe L, Collin-Osdoby P, Chen Y, Sunyer T, Chaudhary L, Tsay A, et al. Human osteoclasts and osteoclast-like cells synthesize and release high basal and inflammatory stimulated levels of the potent chemokine interleukin-8. Endocrinology. 1998 Oct;139(10):4353-63.

73. Fuller K, Owens JM, Chambers TJ. MACROPHAGE INFLAMMATORY PROTEIN-1-ALPHA AND IL-8 STIMULATE THE MOTILITY BUT SUPPRESS THE RESORPTION OF ISOLATED RAT OSTEOCLASTS. J Immunol. 1995 Jun;154(11):6065-72.
74. Bendre MS, Montague DC, Peery T, Akel NS, Gaddy D, Suva LJ. Interleukin-8 stimulation of osteoclastogenesis and bone resorption is a mechanism for the increased osteolysis of metastatic bone disease. Bone. 2003 Jul;33(1):28-37.
75. Bendre MS, Margulies AG, Walser B, Akel NS, Bhattacharrya S, Skinner RA, et al. Tumor-derived interleukin-8 stimulates osteolysis independent of the receptor activator of nuclear factor-kappa B ligand pathway. Cancer Research. 2005 Dec;65(23):11001-9.
76. Onan D, Allan EH, Quinn JMW, Gooi JH, Pompolo S, Sims NA, et al. The Chemokine Cxcl1 Is a Novel Target Gene of Parathyroid Hormone (PTH)/PTH-Related Protein in Committed Osteoblasts. Endocrinology. 2009 May;150(5):2244-53.
77. Boisvert WA, Rose DM, Johnson KA, Fuentes ME, Lira SA, Curtiss LK, et al. Up-regulated expression of the CXCR2 ligand KC/GRO-α in atherosclerotic lesions plays a central role in macrophage accumulation and lesion progression. The American journal of pathology. 2006;168(4):1385-95.
78. Rollins BJ. Chemokines. Blood. 1997 Aug;90(3):909-28.
79. Kim MS, Magno CL, Day CJ, Morrison NA. Induction of chemokines and chemokine receptors CCR2b and CCR4 in authentic human osteoclasts differentiated with RANKL and osteoclast like cells differentiated by MCP-1 and RANTES. J Cell Biochem. [Article]. 2006 Feb;97(3):512-8.
80. Wise GE, Frazier-Bowers S, D'Souza RN. Cellular, molecular, and genetic determinants of tooth eruption. Crit Rev Oral Biol Med. [Review]. 2002;13(4):323-34.
81. Que BG, Wise GE. Colony-stimulating factor-1 and monocyte chemotactic protein-1 chemotaxis for monocytes in the rat dental follicle. Arch Oral Biol. [Article]. 1997 Dec;42(12):855-60.
82. Kim MS, Day CJ, Morrison NA. MCP-1 is induced by receptor activator of nuclear factor-kappa B ligand, promotes human osteoclast fusion, and rescues granulocyte macrophage colony-stimulating factor suppression of osteoclast formation. Journal of Biological Chemistry. [Article]. 2005 Apr;280(16):16163-9.
83. Kim MS, Day CJ, Selinger CI, Magno CL, Stephens SRJ, Morrison NA. MCP-1-induced human osteoclast-like cells are tartrate-resistant acid phosphatase, NFATc1, and calcitonin receptor-positive but require receptor activator of NF B ligand for bone resorption. Journal of Biological Chemistry. 2006;281(2):1274.
84. Miyamoto K, Ninomiya K, Sonoda KH, Miyauchi Y, Hoshi H, Iwasaki R, et al. MCP-1 expressed by osteoclasts stimulates osteoclastogenesis in an autocrine/paracrine manner. Biochemical and Biophysical Research Communications. [Article]. 2009 Jun;383(3):373-7.
85. Yu XF, Huang YF, Collin-Osdoby P, Osdoby P. CCR1 chemokines promote the chemotactic recruitment, RANKL development, and motility of osteoclasts and are induced by inflammatory cytokines in osteoblasts. Journal of Bone and Mineral Research. [Article]. 2004 Dec;19(12):2065-77.
86. Oba Y, Lee JW, Ehrlich LA, Chung HY, Jelinek DF, Callander NS, et al. MIP-1 alpha utilizes both CCR1 and CCR5 to induce osteoclast formation and increase adhesion of myeloma cells to marrow stromal cells. Experimental Hematology. 2005 Mar;33(3):272-8.
87. Choi SJ, Cruz JC, Craig F, Chung H, Devlin RD, Roodman GD, et al. Macrophage inflammatory protein 1-alpha is a potential osteoclast stimulatory factor in multiple myeloma. Blood. [Article]. 2000 Jul;96(2):671-5.
88. Han JH, Choi SJ, Kurihara N, Koide M, Oba Y, Roodman GD. Macrophage inflammatory protein-1 alpha is an osteoclastogenic factor in myeloma that is independent of receptor activator of nuclear factor kappa B ligand. Blood. 2001 Jun;97(11):3349-53.

89. Watanabe T, Kukita T, Kukita A, Wada N, Toh K, Nagata K, et al. Direct stimulation of osteoclastogenesis by MIP-1 alpha: evidence obtained from studies using RAW264 cell clone highly responsive to RANKL. Journal of Endocrinology. 2004 Jan;180(1):193-201.
90. Lee JE, Shin HH, Lee EA, Van Phan T, Choi HS. Stimulation of osteoclastogenesis by enhanced levels of MIP-1 alpha in BALB/c mice in vitro. Experimental Hematology. 2007 Jul;35(7):1100-8.
91. Scheven BAA, Milne JS, Hunter I, Robins SP. Macrophage-inflammatory protein-1 alpha regulates preosteoclast differentiation in vitro. Biochemical and Biophysical Research Communications. [Article]. 1999 Jan;254(3):773-8.
92. Terpos E, Politou M, Szydlo R, Goldman JM, Apperley JF, Rahemtulla A. Serum levels of macrophage inflammatory protein-1 alpha (MIP-1 alpha) correlate with the extent of bone disease and survival in patients with multiple myeloma. British Journal of Haematology. 2003 Oct;123(1):106-9.
93. Koch AE, Kunkel SL, Harlow LA, Mazarakis DD, Haines GK, Burdick MD, et al. MACROPHAGE INFLAMMATORY PROTEIN-1-ALPHA - A NOVEL CHEMOTACTIC CYTOKINE FOR MACROPHAGES IN RHEUMATOID-ARTHRITIS. J Clin Invest. 1994 Mar;93(3):921-8.
94. Ishii T, Kikuta J, Kubo A, Ishii M. Control of osteoclast precursor migration: A novel point of control for osteoclastogenesis and bone homeostasis. IBMS BoneKEy. 2010;7(8):279-86.
95. McHugh KP, Hodivala-Dilke K, Zheng MH, Namba N, Lam J, Novack D, et al. Mice lacking beta 3 integrins are osteosclerotic because of dysfunctional osteoclasts. J Clin Invest. [Article]. 2000 Feb;105(4):433-40.
96. Stenbeck G. Formation and function of the ruffled border in osteoclasts. Seminars in Cell & Developmental Biology. 2002 Aug;13(4):285-92.
97. AbuAmer Y, Ross FP, Schlesinger P, Tondravi MM, Teitelbaum SL. Substrate recognition by osteoclast precursors induces c-src/microtubule association. J Cell Biol. [Article]. 1997 Apr;137(1):247-58.
98. Pavlos NJ, Xu J, Riedel D, Yeoh JS, Teitelbaum SL, Papadimitriou JM, et al. Rab3D regulates a novel vesicular trafficking pathway that is required for osteoclastic bone resorption. Journal of Bone and Mineral Research. [Meeting Abstract]. 2005 Sep;20(9):S375-S.
99. Miyazaki T, Sanjay A, Neff L, Tanaka S, Horne WC, Baron R. Src kinase activity is essential for osteoclast function. Journal of Biological Chemistry. [Article]. 2004 Apr;279(17):17660-6.
100. Soriano P, Montgomery C, Geske R, Bradley A. TARGETED DISRUPTION OF THE C-SRC PROTOONCOGENE LEADS TO OSTEOPETROSIS IN MICE. Cell. [Article]. 1991 Feb;64(4):693-702.
101. Vaananen K. Mechanism of osteoclast mediated bone resorption - rationale for the design of new therapeutics. Adv Drug Deliv Rev. [Review]. 2005 May;57(7):959-71.
102. Vaananen HK, Horton M. THE OSTEOCLAST CLEAR ZONE IS A SPECIALIZED CELL-EXTRACELLULAR MATRIX ADHESION STRUCTURE. J Cell Sci. 1995 Aug;108:2729-32.
103. Li YP, Chen W, Liang YQ, Li E, Stashenko P. Atp6i-deficient mice exhibit severe osteopetrosis due to loss of osteoclast-mediated extracellular acidification. Nature Genet. [Article]. 1999 Dec;23(4):447-51.
104. Gowen M, Lazner F, Dodds R, Kapadia R, Feild J, Tavaria M, et al. Cathepsin K knockout mice develop osteopetrosis due to a deficit in matrix degradation but not demineralization. Journal of Bone and Mineral Research. [Article]. 1999 Oct;14(10):1654-63.
105. Drake FH, Dodds RA, James IE, Connor JR, Debouck C, Richardson S, et al. Cathepsin K, but not cathepsins B, L, or S, is abundantly expressed in human osteoclasts. Journal of Biological Chemistry. [Article]. 1996 May;271(21):12511-6.

106. Tezuka K, Nemoto K, Tezuka Y, Sato T, Ikeda Y, Kobori M, et al. IDENTIFICATION OF MATRIX METALLOPROTEINASE-9 IN RABBIT OSTEOCLASTS. Journal of Biological Chemistry. [Article]. 1994 May;269(21):15006-9.
107. Mulari MTK, Zhao H, Lakkakorpi PT, Vaananen HK. Osteoclast ruffled border has distinct subdomains for secretion and degraded matrix uptake. Traffic. [Article]. 2003 Feb;4(2):113-25.
108. Salo J, Lehenkari P, Mulari M, Metsikko K, Vaananen HK. Removal of osteoclast bone resorption products by transcytosis. Science. [Article]. 1997 Apr;276(5310):270-3.
109. Halleen JM, Raisanen S, Salo JJ, Reddy SV, Roodman GD, Hentunen TA, et al. Intracellular fragmentation of bone resorption products by reactive oxygen species generated by osteoclastic tartrate-resistant acid phosphatase. Journal of Biological Chemistry. [Article]. 1999 Aug;274(33):22907-10.
110. Hayman AR, Jones SJ, Boyde A, Foster D, Colledge WH, Carlton MB, et al. Mice lacking tartrate-resistant acid phosphatase (Acp 5) have disrupted endochondral ossification and mild osteopetrosis. Development. [Article]. 1996 Oct;122(10):3151-62.
111. Zhao C, Irie N, Takada Y, Shimoda K, Miyamoto T, Nishiwaki T, et al. Bidirectional ephrinB2-EphB4 signaling controls bone homeostasis. Cell Metabolism. 2006 Aug;4(2):111-21.
112. Mundy GR, Elefteriou F. Boning up on ephrin signaling. Cell. 2006 Aug;126(3):441-3.
113. Nagase H, Woessner JF. Matrix metalloproteinases. Journal of Biological Chemistry. [Review]. 1999 Jul;274(31):21491-4.
114. Krane SM, Inada M. Matrix metalloproteinases and bone. Bone. [Review]. 2008 Jul;43(1):7-18.
115. Andersen TL, Ovejero MD, Kirkegaard T, Lenhard T, Foged NT, Delaisse JM. A scrutiny of matrix metalloproteinases in osteoclasts: evidence for heterogeneity and for the presence of MMPs synthesized by other cells. Bone. 2004 Nov;35(5):1107-19.
116. Blavier L, Delaisse JM. MATRIX METALLOPROTEINASES ARE OBLIGATORY FOR THE MIGRATION OF PREOSTEOCLASTS TO THE DEVELOPING MARROW CAVITY OF PRIMITIVE LONG BONES. J Cell Sci. [Article]. 1995 Dec;108:3649-59.
117. Reponen P, Sahlberg C, Munaut C, Thesleff I, Tryggvason K. HIGH EXPRESSION OF 92-KDA TYPE-IV COLLAGENASE (GELATINASE) IN THE OSTEOCLAST LINEAGE DURING MOUSE DEVELOPMENT. In: Greenwald RA, Golub LM, editors. Inhibition of Matrix Metalloproteinases: Therapeutic Potential. New York: New York Acad Sciences; 1994. p. 472-5.
118. Everts V, Delaisse JM, Korper W, Beertsen W. Cysteine proteinases and matrix metalloproteinases play distinct roles in the subosteoclastic resorption zone. Journal of Bone and Mineral Research. [Proceedings Paper]. 1998 Sep;13(9):1420-30.
119. Everts V, Beertsen W, Schroder R. EFFECTS OF THE PROTEINASE-INHIBITORS LEUPEPTIN AND E-64 ON OSTEOCLASTIC BONE-RESORPTION. Calcif Tissue Int. [Article]. 1988 Sep;43(3):172-8.
120. Chen QJ LL, Lenhard T, Engsig M, Winding B, Therkildsen B, Pedersen AC, Larsen D, Werb Z, Foged NT, Delaisse JM. MMP-9 is a regulator of osteoclast recruitment as demonstrated by targeted mutagenesis. Bone. 1998;23:S548.
121. Vu TH, Shipley JM, Bergers G, Berger JE, Helms JA, Hanahan D, et al. MMP-9/gelatinase B is a key regulator of growth plate angiogenesis and apoptosis of hypertrophic chondrocytes. Cell. [Article]. 1998 May;93(3):411-22.
122. Cackowski FC, Anderson JL, Patrene KD, Choksi RJ, Shapiro SD, Windle JJ, et al. Osteoclasts are important for bone angiogenesis. Blood. 2010 Jan;115(1):140-9.

123. Sato T, Foged NT, Delaisse JM. The migration of purified osteoclasts through collagen is inhibited by matrix metalloproteinase inhibitors. Journal of Bone and Mineral Research. [Article]. 1998 Jan;13(1):59-66.
124. Delaisse JM, Engsig MT, Everts V, Ovejero MD, Ferreras M, Lund L, et al. Proteinases in bone resorption: obvious and less obvious roles. Clin Chim Acta. [Article]. 2000 Feb;291(2):223-34.
125. Rice DPC, Kim HJ, Thesleff I. Detection of gelatinase B expression reveals osteoclastic bone resorption as a feature of early calvarial bone development. Bone. [Article]. 1997 Dec;21(6):479-86.
126. Kamiya T, Kobayashi Y, Kanaoka K, Nakashima T, Kato Y, Mizuno A, et al. Fluorescence microscopic demonstration of cathepsin K activity as the major lysosomal cysteine proteinase in osteoclasts. Journal of Biochemistry. 1998 Apr;123(4):752-9.
127. Delaisse JM, Andersen TL, Engsig MT, Henriksen K, Troen T, Blavier L. Matrix metalloproteinases (MMP) and cathepsin K contribute differently to osteoclastic activities. Microscopy Research and Technique. 2003 Aug;61(6):504-13.
128. Gelb BD, Shi GP, Chapman HA, Desnick RJ. Pycnodysostosis, a lysosomal disease caused by cathepsin K deficiency. Science. [Article]. 1996 Aug;273(5279):1236-8.
129. Saftig P, Hunziker E, Wehmeyer O, Jones S, Boyde A, Rommerskirch W, et al. Impaired osteoclastic bone resorption leads to osteopetrosis in cathepsin-K-deficient mice. Proc Natl Acad Sci U S A. 1998 Nov;95(23):13453-8.
130. Aubin JE. Advances in the osteoblast lineage. Biochemistry and Cell Biology-Biochimie Et Biologie Cellulaire. 1998;76(6):899-910.
131. Pittenger MF, Mackay AM, Beck SC, Jaiswal RK, Douglas R, Mosca JD, et al. Multilineage potential of adult human mesenchymal stem cells. Science. 1999 Apr;284(5411):143-7.
132. Jiang YH, Jahagirdar BN, Reinhardt RL, Schwartz RE, Keene CD, Ortiz-Gonzalez XR, et al. Pluripotency of mesenchymal stem cells derived from adult marrow. Nature. 2002 Jul;418(6893):41-9.
133. Gronthos S, Graves SE, Ohta S, Simmons PJ. THE STRO-1(+) FRACTION OF ADULT HUMAN BONE-MARROW CONTAINS THE OSTEOGENIC PRECURSORS. Blood. 1994 Dec;84(12):4164-73.
134. Peister A, Mellad JA, Larson BL, Hall BM, Gibson LF, Prockop DJ. Adult stem cells from bone marrow (MSCs) isolated from different strains of inbred mice vary in surface epitopes, rates of proliferation, and differentiation potential. Blood. [Article]. 2004 Mar;103(5):1662-8.
135. Harada S-i, Rodan GA. Control of osteoblast function and regulation of bone mass. Nature. 2003;423(6937):349-55.
136. Aubin JE, Lian JB, Stein GS. Bone Formation: Maturation and Functional Activities of Osteoblast Lineage Cells. 6th ed. Washington D.C: American Society for Bone and Mineral Research; 2006.
137. Ducy P, Zhang R, Geoffroy V, Ridall AL, Karsenty G. Osf2/Cbfa1: A transcriptional activator of osteoblast differentiation. Cell. 1997 May;89(5):747-54.
138. Nakashima K, Zhou X, Kunkel G, Zhang ZP, Deng JM, Behringer RR, et al. The novel zinc finger-containing transcription factor Osterix is required for osteoblast differentiation and bone formation. Cell. 2002 Jan;108(1):17-29.
139. Yang XG, Matsuda K, Bialek P, Jacquot S, Masuoka HC, Schinke T, et al. ATF4 is a substrate of RSK2 and an essential regulator of osteoblast biology: Implication for Coffin-Lowry syndrome. Cell. 2004 Apr;117(3):387-98.
140. Schoeters GER, Saint-Georges L, Heuvel R, Vanderborght O. Mineralization of adult mouse bone marrow in vitro. Cell Proliferation. 1988;21(5):363-74.

141. Franceschi RT, Iyer BS, Cui Y. Effects of ascorbic acid on collagen matrix formation and osteoblast differentiation in murine MC3T3-E1 cells. Journal of Bone and Mineral Research. 2009;9(6):843-54.
142. Buttery LDK, Bourne S, Xynos JD, Wood H, Hughes FJ, Hughes SPF, et al. Differentiation of osteoblasts and in vitro bone formation from murine embryonic stem cells. Tissue engineering. 2001;7(1):89-99.
143. Igarashi M, Kamiya N, Hasegawa M, Kasuya T, Takahashi T, Takagi M. Inductive effects of dexamethasone on the gene expression of Cbfa1, Osterix and bone matrix proteins during differentiation of cultured primary rat osteoblasts. Journal of molecular histology. 2004;35(1):3-10.
144. Beresford JN, Joyner CJ, Devlin C, Triffitt JT. The effects of dexamethasone and 1, 25-dihydroxyvitamin D< sub> 3</sub> on osteogenic differentiation of human marrow stromal cells< i> in vitro</i>. Arch Oral Biol. 1994;39(11):941-7.
145. Boyden LM, Mao JH, Belsky J, Mitzner L, Farhi A, Mitnick MA, et al. High bone density due to a mutation in LDL-receptor-related protein 5. N Engl J Med. 2002 May;346(20):1513-21.
146. Little RD, Carulli JP, Del Mastro RG, Dupuis J, Osborne M, Folz C, et al. A mutation in the LDL receptor-related protein 5 gene results in the autosomal dominant high-bone-mass trait. American Journal of Human Genetics. 2002 Jan;70(1):11-9.
147. Gong YQ, Slee RB, Fukai N, Rawadi G, Roman-Roman S, Reginato AM, et al. LDL receptor-related protein 5 (LRP5) affects bone accrual and eye development. Cell. 2001 Nov;107(4):513-23.
148. Hill TP, Spater D, Taketo MM, Birchmeier W, Hartmann C. Canonical Wnt/beta-catenin signaling prevents osteoblasts from differentiating into chondrocytes. Dev Cell. 2005 May;8(5):727-38.
149. Day TF, Guo XZ, Garrett-Beal L, Yang YZ. Wnt/beta-catenin signaling in mesenchymal progenitors controls osteoblast and chondrocyte differentiation during vertebrate skeletogenesis. Dev Cell. 2005 May;8(5):739-50.
150. Logan CY, Nusse R. The Wnt signaling pathway in development and disease. Annual Review of Cell and Developmental Biology. 2004;20:781-810.
151. ten Dijke P, Fu JY, Schaap P, Roelen BAJ. Signal transduction of bone morphogenetic proteins in osteoblast differentiation. J Bone Joint Surg-Am Vol. [Article; Proceedings Paper]. 2003;85A:34-8.
152. Canalis E, Economides AN, Gazzerro E. Bone morphogenetic proteins, their antagonists, and the skeleton. Endocr Rev. 2003 Apr;24(2):218-35.
153. Winnier G, Blessing M, Labosky PA, Hogan BLM. BONE MORPHOGENETIC PROTEIN-4 IS REQUIRED FOR MESODERM FORMATION AND PATTERNING IN THE MOUSE. Genes & Development. 1995 Sep;9(17):2105-16.
154. Zhang HB, Bradley A. Mice deficient for BMP2 are nonviable and have defects in amnion chorion and cardiac development. Development. 1996 Oct;122(10):2977-86.
155. Akiyama H, Kim J-E, Nakashima K, Balmes G, Iwai N, Deng JM, et al. Osteo-chondroprogenitor cells are derived from Sox9 expressing precursors. Proc Natl Acad Sci U S A. 2005;102(41):14665-70.
156. Komori T, Yagi H, Nomura S, Yamaguchi A, Sasaki K, Deguchi K, et al. Targeted disruption of Cbfa1 results in a complete lack of bone formation owing to maturational arrest of osteoblasts. Cell. 1997 May;89(5):755-64.
157. Otto F, Thornell AP, Crompton T, Denzel A, Gilmour KC, Rosewell IR, et al. < i> Cbfa1</i>, a Candidate Gene for Cleidocranial Dysplasia Syndrome, Is Essential for Osteoblast Differentiation and Bone Development. Cell. 1997;89(5):765-71.

158. Mundlos S, Otto F, Mundlos C, Mulliken JB, Aylsworth AS, Albright S, et al. Mutations involving the transcription factor CBFA1 cause cleidocranial dysplasia. Cell. 1997;89(5):773-9.
159. Ducy P, Starbuck M, Priemel M, Shen J, Pinero G, Geoffroy V, et al. A Cbfa1-dependent genetic pathway controls bone formation beyond embryonic development. Genes & development. 1999;13(8):1025-36.
160. Zhou X, Zhang Z, Feng JQ, Dusevich VM, Sinha K, Zhang H, et al. Multiple functions of Osterix are required for bone growth and homeostasis in postnatal mice. Proceedings of the National Academy of Sciences. 2010;107(29):12919-24.
161. Robey PG, Boskey AL. The Composition of Bone. 7th ed. Rosen CJ, editor. Washington D.C: American Society for Bone and Mineral Research; 2008.
162. Robey PG, Boskey AL. Extracellular Matrix and Biomineralization of Bone. 6th ed. Washington D.C: American Society of Bone and Mineral Research; 2006.
163. Termine JD, Kleinman HK, Whitson SW, Conn KM, McGarvey ML, Martin GR. Osteonectin, a bone-specific protein linking mineral to collagen. Cell. 1981;26(1):99-105.
164. Anderson HC, Sipe JB, Hessle L, Dhamyamraju R, Atti E, Camacho NP, et al. Impaired calcification around matrix vesicles of growth plate and bone in alkaline phosphatase-deficient mice. The American journal of pathology. 2004;164(3):841-7.
165. Onodera S, Nishihira J, Iwabuchi K, Koyama Y, Yoshida K, Tanaka S, et al. Macrophage migration inhibitory factor up-regulates matrix metalloproteinase-9 and-13 in rat osteoblasts - Relevance to intracellular signaling pathways. Journal of Biological Chemistry. 2002 Mar;277(10):7865-74.
166. Filanti C, Dickson GR, Di Martino D, Ulivi V, Sanguineti C, Romano P, et al. The expression of metalloproteinase-2,-9, and-14 and of tissue inhibitors-1 and-2 is developmentally modulated during osteogenesis in vitro, the mature osteoblastic phenotype expressing metalloproteinase-14. Journal of Bone and Mineral Research. 2000 Nov;15(11):2154-68.
167. (US). OotSG. Diseases of the Bone. In: General OotS, editor. Bone Health and Osteoporosis: A Report of the Surgeon General. Rockville: Office of the Surgeon General (US); 2004.
168. Moll JMH, Wright V. Psoriatic arthritis. *Seminars in arthritis and rheumatism*,. 1973;vol. 3,(no. 1,):pp. 55-78.
169. Khan MA. Update on spondyloarthropathies. Annals of Internal Medicine. 2002 Jun;136(12):896-907.
170. Feldmann M, Brennan FM, Maini RN. Rheumatoid arthritis. Cell. 1996 May;85(3):307-10.
171. Scrivo R, Di Franco M, Spadaro A, Valesini G. The immunology of rheumatoid arthritis. In: Shoenfeld Y, Gershwin ME, editors. Autoimmunity, Pt D: Autoimmune Disease, Annus Mirabilis2007. p. 312-22.
172. Aletaha D, Neogi T, Silman AJ, Funovits J, Felson DT, Bingham CO, et al. 2010 Rheumatoid Arthritis Classification Criteria An American College of Rheumatology/European League Against Rheumatism Collaborative Initiative. Arthritis Rheum. 2010 Sep;62(9):2569-81.
173. Feldmann M, Brennan FM, Maini RN. Role of cytokines in rheumatoid arthritis. Annual Review of Immunology. 1996;14:397-440.
174. McInnes IB, Schett G. Cytokines in the pathogenesis of rheumatoid arthritis. Nat Rev Immunol. 2007 Jun;7(6):429-42.
175. Buchan G, Barrett K, Turner M, Chantry D, Maini RN, Feldmann M. INTERLEUKIN-1 AND TUMOR NECROSIS FACTOR MESSENGER-RNA EXPRESSION IN RHEUMATOID-ARTHRITIS - PROLONGED PRODUCTION OF IL-1-ALPHA. Clinical and Experimental Immunology. 1988 Sep;73(3):449-55.

176. Brennan FM, Chantry D, Jackson AM, Maini RN, Feldmann M. CYTOKINE PRODUCTION IN CULTURE BY CELLS ISOLATED FROM THE SYNOVIAL-MEMBRANE. Journal of Autoimmunity. 1989 Jun;2:177-86.
177. Brennan FM, Jackson A, Chantry D, Maini R, Feldmann M. INHIBITORY EFFECT OF TNF-ALPHA ANTIBODIES ON SYNOVIAL CELL INTERLEUKIN-1 PRODUCTION IN RHEUMATOID-ARTHRITIS. Lancet. 1989 Jul;2(8657):244-7.
178. Butler DM, Maini RN, Feldmann M, Brennan FM. Modulation of proinflammatory cytokine release in rheumatoid synovial membrane cell cultures. Comparison of monoclonal anti TNF-alpha antibody with the interleukin-1 receptor antagonist. European Cytokine Network. 1995 Jul-Dec;6(4):225-30.
179. Alvarogracia JM, Zvaifler NJ, Brown CB, Kaushansky K, Firestein GS. CYTOKINES IN CHRONIC INFLAMMATORY ARTHRITIS .6. ANALYSIS OF THE SYNOVIAL-CELLS INVOLVED IN GRANULOCYTE-MACROPHAGE COLONY-STIMULATING FACTOR PRODUCTION AND GENE-EXPRESSION IN RHEUMATOID-ARTHRITIS AND ITS REGULATION BY IL-1 AND TUMOR-NECROSIS-FACTOR-ALPHA. J Immunol. 1991 May;146(10):3365-71.
180. Crotti TN, Smith MD, Weedon H, Ahern MJ, Findlay DM, Kraan M, et al. Receptor activator NF-kappa B ligand (RANKL) expression in synovial tissue from patients with rheumatoid arthritis, spondyloarthropathy, osteoarthritis, and from normal patients: semiquantitative and quantitative analysis. Ann Rheum Dis. [Article]. 2002 Dec;61(12):1047-54.
181. Saxne T, Palladino MA, Heinegard D, Talal N, Wollheim FA. DETECTION OF TUMOR NECROSIS FACTOR-ALPHA BUT NOT TUMOR NECROSIS FACTOR-BETA IN RHEUMATOID-ARTHRITIS SYNOVIAL-FLUID AND SERUM. Arthritis Rheum. 1988 Aug;31(8):1041-5.
182. Edwards JR, Sun SG, Locklin R, Shipman CM, Adamopoulos IE, Athanasou NA, et al. LIGHT (TNFSF14), a novel mediator of bone resorption, is elevated in rheumatoid arthritis. Arthritis Rheum. [Article]. 2006 May;54(5):1451-62.
183. Kang YM, Kim SY, Kang JH, Han SW, Nam EJ, Kyung HS, et al. LIGHT up-regulated on B lymphocytes and monocytes in rheumatoid arthritis mediates cellular adhesion and metalloproteinase production by synoviocytes. Arthritis Rheum. [Article]. 2007 Apr;56(4):1106-17.
184. Thomson BM, Mundy GR, Chambers TJ. TUMOR NECROSIS FACTORS-ALPHA AND FACTORS-BETA INDUCE OSTEOBLASTIC CELLS TO STIMULATE OSTEOCLASTIC BONE-RESORPTION. J Immunol. 1987 Feb;138(3):775-9.
185. Kudo O, Fujikawa Y, Itonaga I, Sabokbar A, Torisu T, Athanasou NA. Proinflammatory cytokine (TNF alpha/IL-1 alpha) induction of human osteoclast formation. Journal of Pathology. 2002 Oct;198(2):220-7.
186. Smolen JS, Aletaha D, Koeller M, Weisman MH, Emery P. New therapies for treatment of rheumatoid arthritis. Lancet. 2007 Dec;370(9602):1861-74.
187. Consensus conference: Osteoporosis. JAMA : the journal of the American Medical Association. 1984 1984 Aug;252(6):799-802.
188. Cooper C, Atkinson EJ, Ofallon WM, Melton LJ. INCIDENCE OF CLINICALLY DIAGNOSED VERTEBRAL FRACTURES - A POPULATION-BASED STUDY IN ROCHESTER, MINNESOTA, 1985-1989. Journal of Bone and Mineral Research. [Article]. 1992 Feb;7(2):221-7.
189. Melton LJ, Chrischilles EA, Cooper C, Lane AW, Riggs BL. HOW MANY WOMEN HAVE OSTEOPOROSIS. Journal of Bone and Mineral Research. [Article]. 1992 Sep;7(9):1005-10.
190. Burge R, Dawson-Hughes B, Solomon DH, Wong JB, King A, Tosteson A. Incidence and economic burden of osteoporosis-related fractures in the United States, 2005-2025. Journal of Bone and Mineral Research. [Article]. 2007 Mar;22(3):465-75.

191. Khosla S, Amin S, Orwoll E. Osteoporosis in men. Endocr Rev. [Review]. 2008 Jun;29(4):441-64.
192. Center JR, Nguyen TV, Schneider D, Sambrook PN, Eisman JA. Mortality after all major types of osteoporotic fracture in men and women: an observational study. Lancet. [Article]. 1999 Mar;353(9156):878-82.
193. Riggs BL, Melton LJ. THE WORLDWIDE PROBLEM OF OSTEOPOROSIS - INSIGHTS AFFORDED BY EPIDEMIOLOGY. Bone. 1995 Nov;17(5):S505-S11.
194. Cohen B, Rushton N. ACCURACY OF DEXA MEASUREMENT OF BONE-MINERAL DENSITY AFTER TOTAL HIP-ARTHROPLASTY. J Bone Joint Surg-Br Vol. [Article]. 1995 May;77B(3):479-83.
195. Unnanuntana A, Gladnick BP, Donnelly E, Lane JM. The Assessment of Fracture Risk. J Bone Joint Surg-Am Vol. [Review]. 2010 Mar;92A(3):743-53.
196. Vestergaard P, Rejnmark L, Mosekilde L. Osteoporosis is markedly underdiagnosed: a nationwide study from Denmark. Osteoporosis Int. [Article]. 2005 Feb;16(2):134-41.
197. Jilka RL, Hangoc G, Girasole G, Passeri G, Williams DC, Abrams JS, et al. INCREASED OSTEOCLAST DEVELOPMENT AFTER ESTROGEN LOSS - MEDIATION BY INTERLEUKIN-6. Science. [Article]. 1992 Jul;257(5066):88-91.
198. Eriksen EF, Hodgson SF, Eastell R, Cedel SL, Ofallon WM, Riggs BL. CANCELLOUS BONE REMODELING IN TYPE-I (POSTMENOPAUSAL) OSTEOPOROSIS - QUANTITATIVE ASSESSMENT OF RATES OF FORMATION, RESORPTION, AND BONE LOSS AT TISSUE AND CELLULAR-LEVELS. Journal of Bone and Mineral Research. 1990 Apr;5(4):311-9.
199. Kragstrup J, Melsen F, Mosekilde L. THICKNESS OF BONE FORMED AT REMODELING SITES IN NORMAL HUMAN ILIAC TRABECULAR BONE - VARIATIONS WITH AGE AND SEX. Metabolic Bone Disease & Related Research. 1984;5(1):17-21.
200. D'Amelio P, Grimaldi A, Pescarmona GP, Tamone C, Roato I, Isaia G. Spontaneous osteoclast formation from peripheral blood mononuclear cells in postmenopausal osteoporosis. Faseb Journal. 2004 Dec;18(15):410-+.
201. D'Amelio P, Grimaldi A, Di Bella S, Brianza SZM, Cristofaro MA, Tamone C, et al. Estrogen deficiency increases osteoclastogenesis up-regulating T cells activity: A key mechanism in osteoporosis. Bone. 2008 Jul;43(1):92-100.
202. Pacifici R, Brown C, Puscheck E, Friedrich E, Slatopolsky E, Maggio D, et al. EFFECT OF SURGICAL MENOPAUSE AND ESTROGEN REPLACEMENT ON CYTOKINE RELEASE FROM HUMAN BLOOD MONONUCLEAR-CELLS. Proc Natl Acad Sci U S A. [Article]. 1991 Jun;88(12):5134-8.
203. Bismar H, Diel I, Ziegler R, Pfeilschifter J. INCREASED CYTOKINE SECRETION BY HUMAN BONE-MARROW CELLS AFTER MENOPAUSE OR DISCONTINUATION OF ESTROGEN REPLACEMENT. J Clin Endocrinol Metab. [Article]. 1995 Nov;80(11):3351-5.
204. Passeri G, Girasole G, Jilka RL, Manolagas SC. INCREASED INTERLEUKIN-6 PRODUCTION BY MURINE BONE-MARROW AND BONE-CELLS AFTER ESTROGEN WITHDRAWAL. Endocrinology. [Article]. 1993 Aug;133(2):822-8.
205. Kanis JA. Diagnosis of osteoporosis and assessment of fracture risk. Lancet. 2002 Jun 1;359(9321):1929-36.
206. Compston J, Cooper A, Cooper C, Francis R, Kanis JA, Marsh D, et al. Guidelines for the diagnosis and management of osteoporosis in postmenopausal women and men from the age of 50 years in the UK. Maturitas. [Article]. 2009 Feb;62(2):105-8.
207. Royal College of Physicians NOGobotBRS, British Geriatrics Society, British Orthopaedic Association, British Society of Rheumatology, National Osteoporosis Society, Osteoporosis 2000, Osteoporosis Dorset, Primary Care Rheumatology Society, Society for Endocrinology. Osteoporosis. Clinical guideline for prevention and treatment, Executive Summary.2008.

208. Papapoulos SE. Bisphosphonates: how do they work? Best Practice & Research Clinical Endocrinology & Metabolism. 2008 Oct;22(5):831-47.
209. Rosen CJ, Rackoff PJ. Emerging anabolic treatments for osteoporosis. Rheum Dis Clin North Am. 2001 Feb;27(1):215-+.
210. Marie PJ. Strontium ranelate: New insights into its dual mode of action. Bone. 2007 May;40(5):S5-S8.
211. Schwarz EM, Ritchlin CT. Clinical development of anti-RANKL therapy. Arthritis Research & Therapy. 2007;9.
212. McClung MR, Lewiecki EM, Cohen SB, Bolognese MA, Woodson GC, Moffett AH, et al. Denosumab in postmenopausal women with low bone mineral density. N Engl J Med. 2006 Feb;354(8):821-31.
213. O'Malley WE, Achinstein B, Shear MJ. Action of bacterial polysaccharide on tumors. II. Damage of sarcoma 37 by serum of mice treated with Serratia marcescens polysaccharide, and induced tolerance. Journal of the National Cancer Institute. 1962;29(6):1169-75.
214. Carswell EA, Old LJ, Kassel R, Green S, Fiore N, Williamson B. An endotoxin-induced serum factor that causes necrosis of tumors. Proceedings of the National Academy of Sciences. 1975;72(9):3666-70.
215. Williams TW, Granger GA. Lymphocyte in vitro cytotoxicity: lymphotoxins of several mammalian species. 1968.
216. Aggarwal BB, Moffat B, Harkins RN. Human lymphotoxin. Production by a lymphoblastoid cell line, purification, and initial characterization. Journal of Biological Chemistry. 1984;259(1):686-91.
217. Aggarwal BB, Kohr WJ, Hass PE, Moffat B, Spencer SA, Henzel WJ, et al. Human tumor necrosis factor. Production, purification, and characterization. Journal of Biological Chemistry. 1985;260(4):2345-54.
218. Bodmer JL, Schneider P, Tschopp J. The molecular architecture of the TNF superfamily. Trends in Biochemical Sciences. 2002 Jan;27(1):19-26.
219. Aggarwal BB. Signalling pathways of the TNF superfamily: A double-edged sword. Nat Rev Immunol. 2003 Sep;3(9):745-56.
220. MacEwan DJ. TNF ligands and receptors–a matter of life and death. British journal of pharmacology. 2009;135(4):855-75.
221. Bossen C, Ingold K, Tardivel A, Bodmer JL, Gaide O, Hertig S, et al. Interactions of tumor necrosis factor (TNF) and TNF receptor family members in the mouse and human. Journal of Biological Chemistry. 2006 May;281(20):13964-71.
222. Dempsey PW, Doyle SE, He JQ, Cheng G. The signaling adaptors and pathways activated by TNF superfamily. Cytokine Growth Factor Rev. 2003;14(3):193-209.
223. Lavrik I, Golks A, Krammer PH. Death receptor signaling. J Cell Sci. 2005;118(2):265-7.
224. Mackay F, Kalled SL. TNF ligands and receptors in autoimmunity: an update. Curr Opin Immunol. 2002;14(6):783.
225. Hsu HL, Huang JN, Shu HB, Baichwal V, Goeddel DV. TNF-Dependent recruitment of the protein kinase RIP to the TNF receptor-1 signaling complex. Immunity. 1996 Apr;4(4):387-96.
226. Chinnaiyan AM, Orourke K, Tewari M, Dixit VM. FADD, A NOVEL DEATH DOMAIN-CONTAINING PROTEIN, INTERACTS WITH THE DEATH DOMAIN OF FAS AND INITIATES APOPTOSIS. Cell. 1995 May;81(4):505-12.
227. Hsu HL, Xiong J, Goeddel DV. THE TNF RECEPTOR 1-ASSOCIATED PROTEIN TRADD SIGNALS CELL-DEATH AND NF-KAPPA-B ACTIVATION. Cell. 1995 May;81(4):495-504.

228. Stanger BZ, Leder P, Lee TH, Kim E, Seed B. RIP - A NOVEL PROTEIN CONTAINING A DEATH DOMAIN THAT INTERACTS WITH FAS/APO-1 (CD95) IN YEAST AND CAUSES CELL-DEATH. Cell. 1995 May;81(4):513-23.
229. Kitson J, Raven T, Jiang YP, Goeddel DV, Giles KM, Pun KT, et al. A death-domain-containing receptor that mediates apoptosis. Nature. [Article]. 1996 Nov;384(6607):372-5.
230. Screaton GR, Xu XN, Olsen AL, Cowper AE, Tan RS, McMichael AJ, et al. LARD: A new lymphoid-specific death domain containing receptor regulated by alternative pre-mRNA splicing. Proc Natl Acad Sci U S A. [Article]. 1997 Apr;94(9):4615-9.
231. Marsters SA, Sheridan JP, Donahue CJ, Pitti RM, Gray CL, Goddard AD, et al. Apo-3, a new member of the tumor necrosis factor receptor family, contains a death domain and activates apoptosis and NF-kappa B. Curr Biol. [Article]. 1996 Dec;6(12):1669-76.
232. Chinnaiyan AM, Orourke K, Yu GL, Lyons RH, Garg M, Duan DR, et al. Signal transduction by DR3, a death domain-containing receptor related to TNFR-1 and CD95. Science. [Article]. 1996 Nov;274(5289):990-2.
233. Bodmer JL, Burns K, Schneider P, Hofmann K, Steiner V, Thome M, et al. TRAMP, a novel apoptosis-mediating receptor with sequence homology to tumor necrosis factor receptor 1 and Fas(Apo-1/CD95). Immunity. [Article]. 1997 Jan;6(1):79-88.
234. Wang ECY, Kitson J, Thern A, Williamson J, Farrow SN, Owen MJ. Genomic structure, expression, and chromosome mapping of the mouse homologue for the WSL-1 (DR3, Apo3, TRAMP, LARD, TR3, TNFRSF12) gene. Immunogenetics. [Article]. 2001 Feb;53(1):59-63.
235. Tan KB, Harrop J, Reddy M, Young P, Terrett J, Emery J, et al. Characterization of a novel TNF-like ligand and recently described TNF ligand and TNF receptor superfamily genes and their constitutive and inducible expression in hematopoietic and non-hematopoietic cells. Gene. [Article]. 1997 Dec;204(1-2):35-46.
236. Jones GW, Stumhofer JS, Foster T, Twohig JP, Hertzog P, Topley N, et al. Naive and activated T cells display differential responsiveness to TL1A that affects Th17 generation, maintenance, and proliferation. Faseb Journal. 2011 Jan;25(1):409-19.
237. Fang L, Adkins B, Deyev V, Podack ER. Essential role of TNF receptor superfamily 25 (TNFRSF25) in the development of allergic lung inflammation. J Exp Med. [Article]. 2008 May;205(5):1037-48.
238. Park MH, Song MJ, Cho MC, Moon DC, Yoon DY, Han SB, et al. Interleukin-32 enhances cytotoxic effect of natural killer cells to cancer cells via activation of death receptor 3. Immunology. 2012 Jan;135(1):63-72.
239. Kim SH, Lee WH, Kwon BS, Oh GT, Choi YH, Park JE. Tumor necrosis factor receptor superfamily 12 may destabilize atherosclerotic plaques by inducing matrix metalloproteinases. Jpn Circ J-Engl Ed. [Article]. 2001 Feb;65(2):136-8.
240. Su WB, Chang YH, Lin WW, Hsieh SL. Differential regulation of interleukin-8 gene transcription by death receptor 3 (DR3) and type I TNF receptor (TNFRI). Exp Cell Res. [Article]. 2006 Feb;312(3):266-77.
241. Borysenko CW, Garcia-Palacios V, Griswold RD, Li YN, Iyer AKV, Yaroslavskiy BB, et al. Death receptor-3 mediates apoptosis in human osteoblasts under narrowly regulated conditions. J Cell Physiol. [Article]. 2006 Dec;209(3):1021-8.
242. Bull MJ, Williams AS, Mecklenburgh Z, Calder CJ, Twohig JP, Elford C, et al. The Death Receptor 3-TNF-like protein 1A pathway drives adverse bone pathology in inflammatory arthritis. J Exp Med. [Article]. 2008 Oct;205(11):2457-64.
243. Twohig JP, Marsden M, Cuff SM, Ferdinand JR, Gallimore AM, Perks WV, et al. The death receptor 3/TL1A pathway is essential for efficient development of antiviral CD4(+) and CD8(+) T-cell immunity. Faseb Journal. 2012 Aug;26(8):3575-86.
244. Warzocha K, Ribeiro P, Charlot C, Renard N, Coiffier B, Salles G. A new death receptor 3 isoform: Expression in human lymphoid cell lines and non-Hodgkin's

lymphomas. Biochemical and Biophysical Research Communications. 1998 Jan;242(2):376-9.
245. Pobezinskaya YL, Choksi S, Morgan MJ, Cao XM, Liu ZG. The Adaptor Protein TRADD Is Essential for TNF-Like Ligand 1A/Death Receptor 3 Signaling. J Immunol. 2011 May;186(9):5212-6.
246. Wen L, Zhuang L, Luo X, Wei P. TL1A-induced NF-kappa B activation and c-IAP2 production prevent DR3-mediated apoptosis in TF-1 cells. Journal of Biological Chemistry. [Article]. 2003 Oct;278(40):39251-8.
247. Marsters SA, Sheridan JP, Pitti RM, Brush J, Goddard A, Ashkenazi A. Identification of a ligand for the death-domain-containing receptor Apo3. Curr Biol. [Article]. 1998 Apr;8(9):525-8.
248. Migone TS, Zhang J, Luo X, Zhuang L, Chen C, Hu BG, et al. TL1A is a TNF-like ligand for DR3 and TR6/DcR3 and functions as a T cell costimulator. Immunity. [Article]. 2002 Mar;16(3):479-92.
249. Gout S, Morin C, Houle F, Huot J. Death receptor-3, a new E-selectin counter-receptor that confers migration and survival advantages to colon carcinoma cells by triggering p38 and ERK MAPK activation. Cancer Research. 2006 Sep;66(18):9117-24.
250. Chicheportiche Y, Bourdon PR, Xu HD, Hsu YM, Scott H, Hession C, et al. TWEAK, a new secreted ligand in the tumor necrosis factor family that weakly induces apoptosis. Journal of Biological Chemistry. 1997 Dec;272(51):32401-10.
251. Kaptein A, Jansen M, Dilaver G, Kitson J, Dash L, Wang E, et al. Studies on the interaction between TWEAK and the death receptor WSL-1/TRAMP (DR3). FEBS Lett. [Article]. 2000 Nov;485(2-3):135-41.
252. Kim S, Zhang LR. Identification of naturally secreted soluble form of TL1A, a TNF-like cytokine. Journal of Immunological Methods. 2005 Mar;298(1-2):1-8.
253. Prehn JL, Thomas LS, Landers CJ, Yu QT, Michelsen KS, Targan SR. The T cell costimulator TL1A is induced by Fc gamma R signaling in human monocytes and dendritic cells. J Immunol. [Article]. 2007 Apr;178(7):4033-8.
254. Bamias G, Martin C, Marini M, Hoang S, Mishina M, Ross WG, et al. Expression, localization, and functional activity of TL1A, a novel Th1-polarizing cytokine in inflammatory bowel disease. J Immunol. 2003 Nov;171(9):4868-74.
255. Bamias G, Mishina M, Nyce M, Ross WG, Kollias G, Rivera-Nieves J, et al. Role of TL1A and its receptor DR3 in two models of chronic murine ileitis. Proceedings of the National Academy of Sciences of the United States of America. 2006 May;103(22):8441-6.
256. Meylan F, Davidson TS, Kahle E, Kinder M, Acharya K, Jankovic D, et al. The TNF-family receptor DR3 is essential for diverse T cell-mediated inflammatory diseases. Immunity. [Article]. 2008 Jul;29(1):79-89.
257. Papadakis KA, Zhu DC, Prehn JL, Landers C, Avanesyan A, Lafkas G, et al. Dominant role for TL1A/DR3 pathway in IL-12 plus IL-18-induced IFN-gamma production by peripheral blood and mucosal CCR9(+) T lymphocytes'. J Immunol. 2005 Apr;174(8):4985-90.
258. Papadakis KA, Prehn JL, Landers C, Han QW, Luo X, Cha SC, et al. TL1A synergizes with IL-12 and IL-18 to enhance IFN-gamma production in human T cells and NK cells. J Immunol. 2004 Jun;172(11):7002-7.
259. Slebioda TJ, Rowley TF, Ferdinand JR, Willoughby JE, Buchan SL, Taraban VY, et al. Triggering of TNFRSF25 promotes CD8(+) T-cell responses and anti-tumor immunity. European Journal of Immunology. 2011 Sep;41(9):2606-11.
260. Heidemann SC, Chavez V, Landers CJ, Kucharzik T, Prehn JL, Targan SR. TL1A Selectively Enhances IL-12/IL-18-Induced NK Cell Cytotoxicity against NK-Resistant Tumor Targets. J Clin Immunol. 2010 Jul;30(4):531-8.

261. Bu RF, Borysenko CW, Li YN, Cao LH, Sabokbar A, Blair HC. Expression and function of TNF-family proteins and receptors in human osteoblasts. Bone. [Article]. 2003 Nov;33(5):760-70.
262. Barrett R, Zhang XL, Koon HW, Vu M, Chang JY, Yeager N, et al. Constitutive TL1A Expression under Colitogenic Conditions Modulates the Severity and Location of Gut Mucosal Inflammation and Induces Fibrostenosis. Am J Pathol. 2012 Feb;180(2):636-49.
263. Bamias G, Kaltsa G, Siakavellas SI, Papaxoinis K, Zampeli E, Michopoulos S, et al. High intestinal and systemic levels of decoy receptor 3 (DcR3) and its ligand TL1A in active ulcerative colitis. Clinical Immunology. 2010 Nov;137(2):242-9.
264. Bamias G, Siakavellas SI, Stamatelopoulos KS, Chryssochoou E, Papamichalel C, Sfikakis PP. Circulating levels of TNF-like cytokine 1A (TL1A) and its decoy receptor 3 (DcR3) in rheumatoid arthritis. Clinical Immunology. [Article]. 2008 Nov;129(2):249-55.
265. Osawa K, Takami N, Shiozawa K, Hashiramoto A, Shiozawa S. Death receptor 3 (DR3) gene duplication in a chromosome region 1p36.3: gene duplication is more prevalent in rheumatoid arthritis. Genes and Immunity. 2004 Sep;5(6):439-43.
266. Zhang J, Wang XH, Fahmi H, Wojcik S, Fikes J, Yu YH, et al. Role of TL1A in the Pathogenesis of Rheumatoid Arthritis. J Immunol. [Article]. 2009 Oct;183(8):5350-7.
267. Konsta M, Bamias G, Tektonidou MG, Christopoulos P, Iliopoulos A, Sfikakis PP. Increased levels of soluble TNF-like cytokine 1A in ankylosing spondylitis. Rheumatology - Advance Access. 2012.
268. Zinovieva E, Bourgain C, Kadi A, Letourneur F, Izac B, Said-Nahal R, et al. Comprehensive Linkage and Association Analyses Identify Haplotype, Near to the TNFSF15 Gene, Significantly Associated with Spondyloarthritis. Plos Genetics. 2009 Jun;5(6).
269. Bamias G, Evangelou K, Vergou T, Tsimaratou K, Kaltsa G, Antoniou C, et al. Upregulation and nuclear localization of TNF-like Cytokine 1A (TL1A) and its receptors DR3 and DcR3 in psoriatic skin lesions. Experimental Dermatology. 2011 Sep;20(9):725-31.
270. McLaren JE, Calder CJ, McSharry BP, Sexton K, Salter RC, Singh NN, et al. In vitro promotion of macrophage foam cell formation by Death Receptor 3 and its ligand TL1A. Immunology. 2010 Dec;131:103-.
271. Kim WJ, Kang YJ, Suk K, Park JE, Kwon BS, Lee WH. Comparative analysis of the expression patterns of various TNFSF/TNFRSF in atherosclerotic plaques. Immunol Invest. [Article]. 2008;37(4):359-73.
272. Al-Lamki RS, Wang J, Tolkovsky AM, Bradley JA, Griffin JL, Thiru S, et al. TL1A both promotes and protects from renal inflammation and injury. J Am Soc Nephrol. [Article]. 2008 May;19(5):953-60.
273. Prehn JL, Mehdizadeh S, Landers CJ, Luo X, Cha SC, Wei P, et al. Potential role for TLlX the new TNF-family member and potent costimulator of IFN-gamma, in mucosal inflammation. Clinical Immunology. 2004 Jul;112(1):66-77.
274. Yamazaki K, McGovern D, Ragoussis J, Paolucci M, Butler H, Jewell D, et al. Single nucleotide polymorphisms in TNFSF15 confer susceptibility to Crohn's disease. Human Molecular Genetics. 2005 Nov;14(22):3499-506.
275. Michelsen KS, Thomas LS, Taylor KD, Yu QT, Mei L, Landers CJ, et al. IBD-Associated TL1A Gene (TNFSF15) Haplotypes Determine Increased Expression of TL1A Protein. Plos One. 2009 Mar;4(3).
276. Picornell Y, Mei L, Taylor K, Yang HY, Torgan SR, Rotter JI. TNFSF15 is an ethnic-specific IBD gene. Inflammatory Bowel Diseases. 2007 Nov;13(11):1333-8.
277. Takedatsu H, Michelsen KS, Wei B, Landers CJ, Thomas LS, Dhall D, et al. TL1A (TNFSF15) regulates the development of chronic colitis by modulating both T-helper 1 and T-helper 17 activation. Gastroenterology. 2008 Aug;135(2):552-67.

278. Kang YJ, Kim WJ, Bae HU, Kim DI, Park YB, Park JE, et al. Involvement of TL1A and DR3 in induction of pro-inflammatory cytokines and matrix metalloproteinase-9 in atherogenesis. Cytokine. 2005 Mar;29(5):229-35.
279. Bamias G, Stamatelopoulos K, Sigala F, Zampeli E, Protogerou A, Papamichael C, et al. Circulating levels of TNF-like Cytokine 1A correlate with the progression of atheromatous lesions in patients with Rheumatoid Arthritis. Clinical Immunology. 2013.
280. Wang ECY, Thern A, Denzel A, Kitson J, Farrow SN, Owen MJ. DR3 regulates negative selection during thymocyte development. Molecular and Cellular Biology. 2001 May;21(10):3451-61.
281. Li WA, Barry ZT, Cohen JD, Wilder CL, Deeds RJ, Keegan PM, et al. Detection of femtomole quantities of mature cathepsin K with zymography. Anal Biochem. [Article]. 2010 Jun;401(1):91-8.
282. Lam J, Takeshita S, Barker JE, Kanagawa O, Ross FP, Teitelbaum SL. TNF-alpha induces osteoclastogenesis by direct stimulation of macrophages exposed to permissive levels of RANK ligand. J Clin Invest. 2000 Dec;106(12):1481-8.
283. Azuma Y, Kaji K, Katogi R, Takeshita S, Kudo A. Tumor necrosis factor-alpha induces differentiation of and bone resorption by osteoclasts. Journal of Biological Chemistry. 2000 Feb;275(7):4858-64.
284. Brand DD, Latham KA, Rosloniec EF. Collagen-induced arthritis. Nat Protoc. [Article]. 2007;2(5):1269-75.
285. Lories RJU, Matthys P, De Vlam K, Derese I, Luyten FP. Ankylosing enthesitis, dactylitis, and onychoperiostitis in male DBA/1 mice: a model of psoriatic arthritis. Ann Rheum Dis. 2004;63(5):595-8.
286. Braem K, Deroose CM, Luyten FP, Lories RJ. Inhibition of inflammation but not ankylosis by glucocorticoids in mice: further evidence for the entheseal stress hypothesis. Arthritis Research & Therapy. 2012;14(2):R59.
287. Lories RJ, Derese I, Luyten FP. Modulation of bone morphogenetic protein signaling inhibits the onset and progression of ankylosing enthesitis. J Clin Invest. 2005;115(6):1571-9.
288. Grisar J, Bernecker PM, Aringer M, Redlich K, Sedlak M, Wolozcszuk W, et al. Ankylosing spondylitis, psoriatic arthritis, and reactive arthritis show increased bone resorption, but differ with regard to bone formation. The Journal of rheumatology. 2002;29(7):1430-6.
289. El Maghraoui A, Borderie D, Cherruau B, Edouard R, Dougados M, Roux C. Osteoporosis, body composition, and bone turnover in ankylosing spondylitis. The Journal of rheumatology. 1999;26(10):2205.
290. Joffe I, Epstein S, editors. Osteoporosis associated with rheumatoid arthritis: pathogenesis and management. Seminars in arthritis and rheumatism; 1991: Elsevier.
291. Woolf AD. Osteoporosis in rheumatoid arthritis—the clinical viewpoint. Rheumatology. 1991;30(2):82-4.
292. Walsh NC, Crotti TN, Goldring SR, Gravallese EM. Rheumatic diseases: the effects of inflammation on bone. Immunol Rev. 2005;208(1):228-51.
293. Li X, Qin L, Bergenstock M, Bevelock LM, Novack DV, Partridge NC. Parathyroid hormone stimulates osteoblastic expression of MCP-1 to recruit and increase the fusion of pre/osteoclasts. Journal of Biological Chemistry. 2007;282(45):33098.
294. Hounoki H, Sugiyama E, Mohamed SGK, Shinoda K, Taki H, Abdel-Aziz HO, et al. Activation of peroxisome proliferator-activated receptor [gamma] inhibits TNF-[alpha]-mediated osteoclast differentiation in human peripheral monocytes in part via suppression of monocyte chemoattractant protein-1 expression. Bone. 2008;42(4):765-74.

295. Burgess TL, Qian Y, Kaufman S, Ring BD, Van G, Capparelli C, et al. The ligand for osteoprotegerin (OPGL) directly activates mature osteoclasts. The Journal of cell biology. 1999;145(3):527-38.
296. Kaye M, Zucker SW, Leclerc YG, Prichard S, Hodsman AB, Barre PE. OSTEOCLAST ENLARGEMENT IN ENDSTAGE RENAL-DISEASE. Kidney Int. [Article]. 1985;27(3):574-81.
297. Makris GP, Saffar JL. QUANTITATIVE RELATIONSHIP BETWEEN OSTEOCLASTS, OSTEOCLAST NUCLEI AND THE EXTENT OF THE RESORBING SURFACE IN HAMSTER PERIODONTAL-DISEASE. Arch Oral Biol. [Article]. 1982;27(11):965-9.
298. Piper K, Boyde A, Jones SJ. THE RELATIONSHIP BETWEEN THE NUMBER OF NUCLEI OF AN OSTEOCLAST AND ITS RESORPTIVE CAPABILITY INVITRO. Anat Embryol. [Article]. 1992 Sep;186(4):291-9.
299. Lees RL, Heersche JNM. Macrophage colony stimulating factor increases bone resorption in dispersed osteoclast cultures by increasing osteoclast size. Journal of Bone and Mineral Research. [Proceedings Paper]. 1999 Jun;14(6):937-45.
300. Hill PA, Murphy G, Docherty AJP, Hembry RM, Millican TA, Reynolds JJ, et al. THE EFFECTS OF SELECTIVE INHIBITORS OF MATRIX METALLOPROTEINASES (MMPS) ON BONE-RESORPTION AND THE IDENTIFICATION OF MMPS AND TIMP-1 IN ISOLATED OSTEOCLASTS. J Cell Sci. [Article]. 1994 Nov;107:3055-64.
301. Hill PA, Reynolds JJ, Meikle MC. INHIBITION OF STIMULATED BONE-RESORPTION INVITRO BY TIMP-1 AND TIMP-2. Biochimica Et Biophysica Acta. [Article]. 1993 May;1177(1):71-4.
302. Walker DG. CONTROL OF BONE-RESORPTION BY HEMATOPOIETIC TISSUE - INDUCTION AND REVERSAL OF CONGENITAL OSTEOPETROSIS IN MICE THROUGH USE OF BONE-MARROW AND SPLENIC TRANSPLANTS. J Exp Med. 1975;142(3):651-63.
303. Itonaga I, Fujikawa Y, Sabokbar A, Murray DW, Athanasou NA. Rheumatoid arthritis synovial macrophage-osteoclast differentiation is osteoprotegerin ligand-dependent. Journal of Pathology. 2000 Sep;192(1):97-104.
304. Crotti TN, O'Sullivan RP, Shen ZX, Flannery MR, Fajardo RJ, Ross FP, et al. Bone Matrix Regulates Osteoclast Differentiation and Annexin A8 Gene Expression. J Cell Physiol. 2011 Dec;226(12):3413-21.
305. Destaing O, Saltel F, Geminard JC, Jurdic P, Bard F. Podosomes display actin turnover and dynamic self-organization in osteoclasts expressing actin-green fluorescent protein. Molecular Biology of the Cell. 2003 Feb;14(2):407-16.
306. Ikeda F, Nishimura R, Matsubara T, Tanaka S, Inoue J, Reddy SV, et al. Critical roles of c-Jun signaling in regulation of NFAT family and RANKL-regulated osteoclast differentiation. J Clin Invest. [Article]. 2004 Aug;114(4):475-84.
307. de Vries TJ, Schoenmaker T, Beertsen W, van der Neut R, Everts V. Effect of CD44 deficiency on in vitro and in vivo osteoclast formation. J Cell Biochem. 2005 Apr;94(5):954-66.
308. Bloom AC. The Role of CD59a in Bone: Cardiff University; 2012.
309. Saltel F, Destaing O, Bard F, Eichert D, Jurdic P. Apatite-mediated actin dynamics in resorbing osteoclasts. Molecular Biology of the Cell. 2004 Dec;15(12):5231-41.
310. Redey SA, Razzouk S, Rey C, Bernache-Assollant D, Leroy G, Nardin M, et al. Osteoclast adhesion and activity on synthetic hydroxyapatite, carbonated hydroxyapatite, and natural calcium carbonate: relationship to surface energies. Journal of biomedical materials research. 1999;45(2):140-7.
311. Zhang D, Udagawa N, Nakamura I, Murakami H, Saito S, Yamasaki K, et al. The small GTP-binding protein, rho p21, is involved in bone resorption by regulating cytoskeletal organization in osteoclasts. J Cell Sci. 1995;108(6):2285-92.

312. Lakkakorpi PT, Väänänen HK. Calcitonin, prostaglandin E2, and dibutyryl cyclic adenosine 3', 5'-monophosphate disperse the specific microfilament structure in resorbing osteoclasts. Journal of Histochemistry & Cytochemistry. 1990;38(10):1487-93.
313. Nakamura I, Takahashi N, Sasaki T, Tanaka S, Udagawa N, Murakami H, et al. Wortmannin, a specific inhibitor of phosphatidylinositol-3 kinase, blocks osteoclastic bone resorption. FEBS Lett. 1995;361(1):79-84.
314. Zhao H, Laitala-Leinonen T, Parikka V, Väänänen HK. Downregulation of small GTPase Rab7 impairs osteoclast polarization and bone resorption. Journal of Biological Chemistry. 2001;276(42):39295-302.
315. Repeke CE, Ferreira SB, Claudino M, Silveira EM, de Assis GF, Avila-Campos MJ, et al. Evidences of the cooperative role of the chemokines CCL3, CCL4 and CCL5 and its receptors CCR1+ and CCR5+ in RANKL+ cell migration throughout experimental periodontitis in mice. Bone. 2010;46(4):1122-30.
316. Toth M, Chvyrkova I, Bernardo MM, Hernandez-Barrantes S, Fridman R. Pro-MMP-9 activation by the MT1-MMP/MMP-2 axis and MMP-3: role of TIMP-2 and plasma membranes. Biochemical and Biophysical Research Communications. 2003;308(2):386-95.
317. Ramos-DeSimone N, Hahn-Dantona E, Sipley J, Nagase H, French DL, Quigley JP. Activation of matrix metalloproteinase-9 (MMP-9) via a converging plasmin/stromelysin-1 cascade enhances tumor cell invasion. Journal of Biological Chemistry. 1999;274(19):13066-76.
318. Dreier R, Grässel S, Fuchs S, Schaumburger J, Bruckner P. Pro-MMP-9 is a specific macrophage product and is activated by osteoarthritic chondrocytes via MMP-3 or a MT1-MMP/MMP-13 cascade. Exp Cell Res. 2004;297(2):303-12.
319. Sang Q-X, Birkedal-Hansen H, Van Wart HE. Proteolytic and non-proteolytic activation of human neutrophil progelatinase B. Biochimica et Biophysica Acta (BBA)-Protein Structure and Molecular Enzymology. 1995;1251(2):99-108.
320. Knäuper V, Smith B, López-Otin C, Murphy G. Activation of progelatinase B (proMMP-9) by active collagenase-3 (MMP-13). Eur J Biochem. 2004;248(2):369-73.
321. Uría JA, López-Otín C. Matrilysin-2, a new matrix metalloproteinase expressed in human tumors and showing the minimal domain organization required for secretion, latency, and activity. Cancer Research. 2000;60(17):4745-51.
322. Dodds RA, James IE, Rieman D, Ahern R, Hwang SM, Connor JR, et al. Human osteoclast cathepsin K is processed intracellularly prior to attachment and bone resorption. Journal of Bone and Mineral Research. [Article]. 2001 Mar;16(3):478-86.
323. Yamaza T, Goto T, Kamiya T, Kobayashi Y, Sakai H, Tanaka T. Study of immunoelectron microscopic localization of cathepsin K in osteoclasts and other bone cells in the mouse femur. Bone. 1998 Dec;23(6):499-509.
324. Akhter MP, Iwaniec UT, Covey MA, Cullen DM, Kimmel DB, Recker RR. Genetic variations in bone density, histomorphometry, and strength in mice. Calcif Tissue Int. 2000;67(4):337-44.
325. Manigrasso MB, O'Connor JP. Comparison of fracture healing among different inbred mouse strains. Calcif Tissue Int. 2008;82(6):465-74.
326. Beamer WG, Donahue LR, Rosen CJ, Baylink DJ. Genetic variability in adult bone density among inbred strains of mice. Bone. 1996;18(5):397-403.
327. Phinney DG, Kopen G, Isaacson RL, Prockop DJ. Plastic adherent stromal cells from the bone marrow of commonly used strains of inbred mice: variations in yield, growth, and differentiation. J Cell Biochem. 1999;72(4):570-85.
328. Linkhart TA, Linkhart SG, Kodama Y, Farley JR, Dimai HP, Wright KR, et al. Osteoclast formation in bone marrow cultures from two inbred strains of mice with different bone densities. Journal of Bone and Mineral Research. 1999;14(1):39-46.

329. Lawrence RC, Helmick CG, Arnett FC, Deyo RA, Felson DT, Giannini EH, et al. Estimates of the prevalence of arthritis and selected musculoskeletal disorders in the United States. Arthritis & Rheumatism. 1998;41(5):778-99.
330. Bain BJ, MBBSFRACPMRC aP. *Blood cells: a practical guide*: Blackwell; 2006.
331. Fujikawa Y, Quinn JM, Sabokbar A, McGee JO, Athanasou NA. The human osteoclast precursor circulates in the monocyte fraction. Endocrinology. 1996;137(9):4058-60.
332. Hornung V, Rothenfusser S, Britsch S, Krug A, Jahrsdörfer B, Giese T, et al. Quantitative expression of Toll-like receptor 1–10 mRNA in cellular subsets of human peripheral blood mononuclear cells and sensitivity to CpG oligodeoxynucleotides. The Journal of Immunology. 2002;168(9):4531-7.
333. Masters JRW. Human cancer cell lines: fact and fantasy. Nature Reviews Molecular Cell Biology. 2000;1(3):233-6.
334. Gattei V, Bernabei PA, Pinto A, Bezzini R, Ringressi A, Formigli L, et al. Phorbol ester induced osteoclast-like differentiation of a novel human leukemic cell line (FLG 29.1). The Journal of cell biology. 1992;116(2):437-47.
335. Aldinucci D, Quinn JMW, Degan M, Juzbasic S, De Luliis A, Importa S, et al. In vitro cellular systems for studying OC function and differentiation. Methods in molecular medicine: human cell culture protocols Totowa: Human Press Inc. 1996.
336. Ikeda T, Sasaki K, Ikeda K, Yamaoka G, Kawanishi K, Kawachi Y, et al. A new cytokine-dependent monoblastic cell line with t (9; 11)(p22; q23) differentiates to macrophages with macrophage colony-stimulating factor (M-CSF) and to osteoclast-like cells with M-CSF and interleukin-4. Blood. 1998;91(12):4543-53.
337. Ikeda T, Ikeda K, Sasaki K, Kawakami K, Hatake K, Kaji Y, et al. IL-13 as well as IL-4 induces monocytes/macrophages and a monoblastic cell line (UG3) to differentiate into multinucleated giant cells in the presence of M-CSF. Biochemical and Biophysical Research Communications. 1998;253(2):265-72.
338. Soares-Schanoski A, Gómez-Piña V, del Fresno C, Rodríguez-Rojas A, García F, Glaría A, et al. 6-Methylprednisolone down-regulates IRAK-M in human and murine osteoclasts and boosts bone-resorbing activity: a putative mechanism for corticoid-induced osteoporosis. J Leukoc Biol. 2007;82(3):700-9.
339. Jakob F, Siggelkow H, Homann D, Köhrle J, Adamski J, Schütze N. Local estradiol metabolism in osteoblast-and osteoclast-like cells. The Journal of steroid biochemistry and molecular biology. 1997;61(3):167-74.
340. Kzhyshkowska J, Mamidi S, Gratchev A, Kremmer E, Schmuttermaier C, Krusell L, et al. Novel stabilin-1 interacting chitinase-like protein (SI-CLP) is up-regulated in alternatively activated macrophages and secreted via lysosomal pathway. Blood. 2006;107(8):3221-8.
341. Gratchev A, Kzhyshkowska J, Utikal J, Goerdt S. Interleukin-4 and Dexamethasone Counterregulate Extracellular Matrix Remodelling and Phagocytosis in Type-2 Macrophages. Scandinavian journal of immunology. 2005;61(1):10-7.
342. Nakamura I, Takahashi N, Sasaki T, Jimi E, Kurokawa T, Suda T. Chemical and physical properties of the extracellular matrix are required for the actin ring formation in osteoclasts. Journal of Bone and Mineral Research. 1996 Dec;11(12):1873-9.
343. Nose M, Yamazaki H, Hagino H, Morio Y, Hayashi SI, Teshima R. Comparison of osteoclast precursors in peripheral blood mononuclear cells from rheumatoid arthritis and osteoporosis patients. Journal of Bone and Mineral Metabolism. 2009 Jan;27(1):57-65.
344. Kudo O, Sabokbar A, Pocock A, Itonaga I, Athanasou NA. Isolation of human osteoclasts formed in vitro: Hormonal effects on the bone-resorbing activity of human osteoclasts. Calcif Tissue Int. 2002 Dec;71(6):539-46.

345. Grassi F, Piacentini A, Cristino S, Toneguzzi S, Cavallo C, Facchini A, et al. Human osteoclasts express different CXC chemokines depending on cell culture substrate: molecular and immunocytochemical evidence of high levels of CXCL10 and CXCL12. Histochem Cell Biol. [Article]. 2003 Nov;120(5):391-400.
346. Nicholson GC, Malakellis M, Collier FM, Cameron PU, Holloway WR, Gough TJ, et al. Induction of osteoclasts from CD14-positive human peripheral blood mononuclear cells by receptor activator of nuclear factor kappa B ligand (RANKL). Clinical Science. 2000 Aug;99(2):133-40.
347. Holloway WR, Collier FML, Aitken CJ, Myers DE, Hodge JM, Malakellis M, et al. Leptin inhibits osteoclast generation. Journal of Bone and Mineral Research. 2002;17(2):200-9.
348. Michael H, Härkönen PL, Väänänen HK, Hentunen TA. Estrogen and testosterone use different cellular pathways to inhibit osteoclastogenesis and bone resorption. Journal of Bone and Mineral Research. 2005;20(12):2224-32.
349. Kobayashi K, Takahashi N, Jimi E, Udagawa N, Takami M, Kotake S, et al. Tumor necrosis factor alpha stimulates osteoclast differentiation by a mechanism independent of the ODF/RANKL-RANK interaction. J Exp Med. 2000 Jan;191(2):275-85.
350. Grassi F, Cristino S, Toneguzzi S, Piacentini A, Facchini A, Lisignoli G. CXCL12 chemokine up-regulates bone resorption and MMP-9 release by human osteoclasts: CXCL12 levels are increased in synovial and bone tissue of rheumatoid arthritis patients. J Cell Physiol. [Article]. 2004 May;199(2):244-51.
351. Mestas J, Hughes CCW. Of mice and not men: Differences between mouse and human immunology. J Immunol. 2004 Mar;172(5):2731-8.
352. Gravallese EM, Harada Y, Wang JT, Gorn AH, Thornhill TS, Goldring SR. Identification of cell types responsible for bone resorption in rheumatoid arthritis and juvenile rheumatoid arthritis. Am J Pathol. 1998 Apr;152(4):943-51.
353. Stewart A, Mackenzie LM, Black AJ, Reid DM. Predicting erosive disease in rheumatoid arthritis. A longitudinal study of changes in bone density using digital X-ray radiogrammetry: a pilot study. Rheumatology. 2004 Dec;43(12):1561-4.
354. Braun J, Sieper J. Ankylosing spondylitis. Lancet. 2007 Apr;369(9570):1379-90.
355. Ritchlin CT, Haas-Smith SA, Li P, Hicks DG, Schwarz EM. Mechanisms of TNF-alpha- and RANKL-mediated osteoclastogenesis and bone resorption in psoriatic arthritis. J Clin Invest. 2003 Mar;111(6):821-31.
356. Siris ES. Paget's disease of bone. Journal of Bone and Mineral Research. 1998;13(7):1061-5.
357. Choy EHS, Panayi GS. Mechanisms of disease: Cytokine pathways and joint inflammation in rheumatoid arthritis. N Engl J Med. 2001 Mar;344(12):907-16.
358. Smith JB, Haynes MK. Rheumatoid arthritis - A molecular understanding. Annals of Internal Medicine. 2002 Jun;136(12):908-22.
359. Burger HG, Dudley EC, Hopper JL, Groome N, Guthrie JR, Green A, et al. Prospectively measured levels of serum follicle-stimulating hormone, estradiol, and the dimeric inhibins during the menopausal transition in a population-based cohort of women. J Clin Endocrinol Metab. [Article]. 1999 Nov;84(11):4025-30.
360. Riggs BL, Khosla S, Melton LJ. A unitary model for involutional osteoporosis: Estrogen deficiency causes both type I and type II osteoporosis in postmenopausal women and contributes to bone loss in aging men. Journal of Bone and Mineral Research. [Article]. 1998 May;13(5):763-73.
361. Lean JM, Murphy C, Fuller K, Chambers TJ. CCL9/MIP-1 gamma and its receptor CCR1 are the major chemokine ligand/receptor species expressed by osteoclasts. J Cell Biochem. 2002;87(4):386-93.

362. Mease P, Goffe BS. Diagnosis and treatment of psoriatic arthritis. Journal of the American Academy of Dermatology. 2005;52(1):1-19.
363. Hirsch R, Helmick CG, Jordan JM, Kington RS, Lane NE, Nevitt MC, et al. Osteoarthritis: new insights. *Annuals Internal Medicine*,. 2000;*133*,:635-46.
364. Sarzi-Puttini P, Cimmino MA, Scarpa R, Caporali R, Parazzini F, Zaninelli A, et al. Osteoarthritis: An overview of the disease and its treatment strategies. Seminars in Arthritis and Rheumatism. 2005 Aug;35(1):1-10.
365. Moll JMH, Wright V. Psoriatic arthritis *Seminars in arthritis and rheumatism*, . 1973;vol. 3,(no. 1,): pp. 55-78.
366. Cassatella MA, da Silva GP, Tinazzi I, Facchetti F, Scapini P, Calzetti F, et al. Soluble TNF-like cytokine (TL1A) production by immune complexes stimulated monocytes in rheumatoid arthritis. J Immunol. [Article]. 2007 Jun;178(11):7325-33.
367. Vencovský J, Macháček S, Šedová L, Kafkova J, Gatterova J, Pešáková V, et al. Autoantibodies can be prognostic markers of an erosive disease in early rheumatoid arthritis. Ann Rheum Dis. 2003;62(5):427-30.
368. Lindqvist E, Eberhardt K, Bendtzen K, Heinegård D, Saxne T. Prognostic laboratory markers of joint damage in rheumatoid arthritis. Ann Rheum Dis. 2005;64(2):196-201.
369. Kon T, Cho TJ, Aizawa T, Yamazaki M, Nooh N, Graves D, et al. Expression of Osteoprotegerin, Receptor Activator of NF-κB Ligand (Osteoprotegerin Ligand) and Related Proinflammatory Cytokines During Fracture Healing. Journal of Bone and Mineral Research. 2001;16(6):1004-14.
370. Sadeghi HM, Schnelle JF, Thomas JK, Nishanian P, Fahey JL. Phenotypic and functional characteristics of circulating monocytes of elderly persons. Experimental Gerontology. 1999 Dec;34(8):959-70.
371. Kosa JP, Balla B, Kiss J, Podani J, Takacs I, Lazary A, et al. Postmenopausal Expression Changes of Immune System-Related Genes in Human Bone Tissue. J Clin Immunol. [Article]. 2009 Nov;29(6):761-8.
372. De la Fuente M, Medina S, Del Rio M, Ferrandez MD, Hernanz A. Effect of aging on the modulation of macrophage functions by neuropeptides. Life Sciences. 2000 Sep;67(17):2125-35.
373. Fietta A, Merlini C, Debernardi PM, Gandola L, Piccioni PD, Grassi C. NONSPECIFIC IMMUNITY IN AGED HEALTHY-SUBJECTS AND IN PATIENTS WITH CHRONIC-BRONCHITIS. Aging-Clinical and Experimental Research. 1993 Oct;5(5):357-61.
374. Girasole G, Giuliani N, Modena AB, Passeri G, Pedrazzoni M. Oestrogens prevent the increase of human serum soluble interleukin-6 receptor induced by ovariectomy in vivo and decrease its release in human osteoblastic cells in vitro. Clin Endocrinol. [Article]. 1999 Dec;51(6):801-7.
375. Metcalf D. THE GRANULOCYTE MACROPHAGE COLONY STIMULATING FACTORS. Cell. [Article]. 1985;43(1):5-6.
376. Sieff CA. HEMATOPOIETIC GROWTH-FACTORS. J Clin Invest. [Editorial Material]. 1987 Jun;79(6):1549-57.
377. Horwood NJ, Kartsogiannis V, Quinn JMW, Romas E, Martin TJ, Gillespie MT. Activated T lymphocytes support osteoclast formation in vitro. Biochemical and Biophysical Research Communications. 1999 Nov;265(1):144-50.
378. Praloran V, Gascan H, Papin S, Chevalier S, Trossaert M, Boursier MC. INDUCIBLE PRODUCTION OF MACROPHAGE COLONY-STIMULATING FACTOR (CSF-1) BY MALIGNANT AND NORMAL HUMAN T-CELLS. Leukemia. 1990 Jun;4(6):411-4.
379. Praloran V. STRUCTURE, BIOSYNTHESIS AND BIOLOGICAL ROLES OF MONOCYTE-MACROPHAGE COLONY STIMULATING FACTOR (CSF-1 OR M-CSF). Nouvelle Revue Francaise D Hematologie. 1991;33(4):323-33.

380. Shanker G, Sorcithomas M, Adams MR. ESTROGEN MODULATES THE EXPRESSION OF TUMOR-NECROSIS-FACTOR-ALPHA MESSENGER-RNA IN PHORBOL ESTER-STIMULATED HUMAN MONOCYTIC THP-1 CELLS. Lymphokine and Cytokine Research. 1994 Dec;13(6):377-82.
381. Srivastava S, Weitzmann MN, Kimble RB, Rizzo M, Zahner M, Milbrandt J, et al. Estrogen blocks M-CSF gene expression and osteoclast formation by regulating phosphorylation of Egr-1 and its interaction with Sp-1. J Clin Invest. 1998 Nov;102(10):1850-9.
382. Eghbali-Fatourechi G, Khosla S, Sanyal A, Boyle WJ, Lacey DL, Riggs BL. Role of RANK ligand in mediating increased bone resorption in early postmenopausal women. J Clin Invest. [Article]. 2003 Apr;111(8):1221-30.
383. Jevon M, Hirayama T, Brown MA, Wass JAH, Sabokbar A, Ostelere S, et al. Osteoclast formation from circulating precursors in osteoporosis. Scandinavian Journal of Rheumatology. 2003;32(2):95-100.
384. Colnot C, Thompson Z, Miclau T, Werb Z, Helms JA. Altered fracture repair in the absence of MMP9. Development. 2003 Sep;130(17):4123-33.
385. Uusitalo H, Hiltunen A, Soderstrom M, Aro HT, Vuorio E. Expression of cathepsins B, H, K, L, and S and matrix metalloproteinases 9 and 13 during chondrocyte hypertrophy and endochondral ossification in mouse fracture callus. Calcif Tissue Int. 2000 Nov;67(5):382-90.
386. Rosen CJ, Bouxsein ML. Mechanisms of disease: is osteoporosis the obesity of bone? Nature Clinical Practice Rheumatology. 2006 Jan;2(1):35-43.
387. Kovacic N, Lukic IK, Grcevic D, Katavic V, Croucher P, Marusic A. The Fas/Fas ligand system inhibits differentiation of murine osteoblasts but has a limited role in osteoblast and osteoclast apoptosis. The Journal of Immunology. 2007;178(6):3379-89.
388. Young AB, Cooley ID, Chauhan VS, Marriott I. Causative agents of osteomyelitis induce death domain-containing TNF-related apoptosis-inducing ligand receptor expression on osteoblasts. Bone. 2011;48(4):857-63.
389. Frost A, Jonsson KB, Nilsson O, Ljunggren Ö. Inflammatory cytokines regulate proliferation of cultured human osteoblasts. Acta Orthopaedica. 1997;68(2):91-6.
390. Abbas S, Zhang Y-H, Clohisy JC, Abu-Amer Y. Tumor necrosis factor-α inhibits pre-osteoblast differentiation through its type-1 receptor. Cytokine. 2003;22(1):33-41.
391. Gilbert L, He X, Farmer P, Boden S, Kozlowski M, Rubin J, et al. Inhibition of osteoblast differentiation by tumor necrosis factor-α. Endocrinology. 2000;141(11):3956-64.
392. Mukai T, Otsuka F, Otani H, Yamashita M, Takasugi K, Inagaki K, et al. TNF-α inhibits BMP-induced osteoblast differentiation through activating SAPK/JNK signaling. Biochemical and Biophysical Research Communications. 2007;356(4):1004-10.
393. Hill PA, Tumber A, Meikle MC. Multiple extracellular signals promote osteoblast survival and apoptosis. Endocrinology. 1997;138(9):3849-58.
394. Kitajima I, Soejima Y, Takasaki I, Beppu H, Tokioka T, Maruyama I. Ceramide-induced nuclear translocation of NF-κB is a potential mediator of the apoptotic response to TNF-α in murine clonal osteoblasts. Bone. 1996;19(3):263-70.
395. Gerstenfeld LC, Cho TJ, Kon T, Aizawa T, Cruceta J, Graves BD, et al. Impaired intramembranous bone formation during bone repair in the absence of tumor necrosis factor-alpha signaling. Cells Tissues Organs. 2001;169(3):285-94.
396. Rawadi G, Vayssière B, Dunn F, Baron R, Roman-Roman S. BMP-2 controls alkaline phosphatase expression and osteoblast mineralization by a Wnt autocrine loop. Journal of Bone and Mineral Research. 2003;18(10):1842-53.

397. Beck GR, Sullivan EC, Moran E, Zerler B. Relationship between alkaline phosphatase levels, osteopontin expression, and mineralization in differentiating MC3T3-E1 osteoblasts. J Cell Biochem. 1998;68(2):269-80.
398. Baddoo M, Hill K, Wilkinson R, Gaupp D, Hughes C, Kopen GC, et al. Characterization of mesenchymal stem cells isolated from murine bone marrow by negative selection. J Cell Biochem. [Article]. 2003 Aug;89(6):1235-49.
399. Albers J, Schulze J, Beil FT, Gebauer M, Baranowsky A, Keller J, et al. Control of bone formation by the serpentine receptor Frizzled-9. The Journal of cell biology. 2011;192(6):1057-72.
400. Van Der Horst G, Van Bezooijen RL, Deckers MML, Hoogendam J, Visser A, Lwik C, et al. Differentiation of murine preosteoblastic KS483 cells depends on autocrine bone morphogenetic protein signaling during all phases of osteoblast formation. Bone. 2002;31(6):661-9.
401. Rauch A, Seitz S, Baschant U, Schilling AF, Illing A, Stride B, et al. Glucocorticoids suppress bone formation by attenuating osteoblast differentiation via the monomeric glucocorticoid receptor. Cell Metabolism. 2010;11(6):517-31.
402. Ben David D, Reznick AZ, Srouji S, Livne E. Exposure to pro-inflammatory cytokines upregulates MMP-9 synthesis by mesenchymal stem cells-derived osteoprogenitors. Histochem Cell Biol. 2008;129(5):589-97.
403. Golub EE, Boesze-Battaglia K. The role of alkaline phosphatase in mineralization. Current Opinion in Orthopaedics. 2007;18(5):444-8.
404. Bilezikian JP, Raisz LG, Rodan GA. Principles of Bone Biology: Academic Press; 2002.
405. Anderson HC, Sipe JB, Hessle L, Dhamyamraju R, Atti E, Camacho NP, et al. Impaired calcification around matrix vesicles of growth plate and bone in alkaline phosphatase-deficient mice. Am J Pathol. 2004 Mar;164(3):841-7.
406. Nöth U, Osyczka AM, Tuli R, Hickok NJ, Danielson KG, Tuan RS. Multilineage mesenchymal differentiation potential of human trabecular bone-derived cells. J Orthop Res. 2002;20(5):1060-9.
407. Yameen Z, Leavesley D, Upton Z, Xiao Y. Multilineage differentiation potential of bone and cartilage cells derived from explant culture. The Open Stem Cell Journal. 2009;1:10-9.
408. Fujii Y, Fujii K, Nakano K, Tanaka Y. Crosslinking of CD44 on human osteoblastic cells upregulates ICAM-1 and VCAM-1. FEBS Lett. 2003;539(1):45-50.
409. Huang JC, Sakata T, Pfleger LL, Bencsik M, Halloran BP, Bikle DD, et al. PTH differentially regulates expression of RANKL and OPG. Journal of Bone and Mineral Research. 2003;19(2):235-44.
410. Thomas GP, Baker SU, Eisman JA, Gardiner EM. Changing RANKL/OPG mRNA expression in differentiating murine primary osteoblasts. Journal of Endocrinology. 2001;170(2):451-60.
411. Atkins GJ, Kostakis P, Pan B, Farrugia A, Gronthos S, Evdokiou A, et al. RANKL expression is related to the differentiation state of human osteoblasts. Journal of Bone and Mineral Research. 2003;18(6):1088-98.
412. Jamal HH, Aubin JE. CD44 Expression in Fetal Rat Bone:< i> In Vivo</i> and< i> in Vitro</i> Analysis. Exp Cell Res. 1996;223(2):467-77.
413. Nakamura H, Kenmotsu S-i, Sakai H, Ozawa H. Localization of CD44, the hyaluronate receptor; on the plasma membrane of osteocytes and osteoclasts in rat tibiae. Cell Tissue Res. 1995;280(2):225-33.
414. Lorenzo JA, Pilbeam CC, Kalinowski JF, Hibbs MS. PRODUCTION OF BOTH 92-KDA AND 72-KDA GELATINASES BY BONE-CELLS. Matrix. 1992 Aug;12(4):282-90.

415. Dakwar E, Reddy J, Vale FL, Uribe JS. A review of the pathogenesis of ankylosing spondylitis. Neurosurgical Focus. 2008 Jan;24(1).
416. Sieper J, Appel H, Braun J, Rudwaleit M. Critical appraisal of assessment of structural damage in ankylosing spondylitis. Arthritis Rheum. 2008 Mar;58(3):649-56.
417. Katavić V, Lukić IK, Kovačić N, Grčević D, Lorenzo JA, Marušić A. Increased bone mass is a part of the generalized lymphoproliferative disorder phenotype in the mouse. The Journal of Immunology. 2003;170(3):1540-7.
418. Atkins GJ, Bouralexis S, Evdokiou A, Hay S, Labrinidis A, Zannettino ACW, et al. Human osteoblasts are resistant to Apo2L/TRAIL-mediated apoptosis. Bone. 2002;31(4):448-56.
419. Sreejit P, Dilip KB, Verma RS. Generation of mesenchymal stem cell lines from murine bone marrow. Cell and Tissue Research. 2012 Oct;350(1):55-68.
420. Anjos-Afonso F, Siapati EK, Bonnet D. In vivo contribution of murine mesenchymal stem cells into multiple cell-types under minimal damage conditions. Journal of Cell Science. 2004 Nov;117(23):5655-64.
421. Cheng CC, Lian WS, Hsiao FSH, Liu IH, Lin SP, Lee YH, et al. Isolation and Characterization of Novel Murine Epiphysis Derived Mesenchymal Stem Cells. Plos One. 2012 Apr;7(4).
422. Sung JH, Yang HM, Park JB, Choi GS, Joh JW, Kwon CH, et al. Isolation and Characterization of Mouse Mesenchymal Stem Cells. Transplantation Proceedings. 2008 Oct;40(8):2649-54.
423. DiGirolamo CM, Stokes D, Colter D, Phinney DG, Class R, Prockop DJ. Propagation and senescence of human marrow stromal cells in culture: a simple colony-forming assay identifies samples with the greatest potential to propagate and differentiate. British Journal of Haematology. 2001;107(2):275-81.
424. Colter DC, Class R, DiGirolamo CM, Prockop DJ. Rapid expansion of recycling stem cells in cultures of plastic-adherent cells from human bone marrow. Proceedings of the National Academy of Sciences. 2000;97(7):3213-8.
425. Sekiya I, Larson BL, Smith JR, Pochampally R, Cui JG, Prockop DJ. Expansion of human adult stem cells from bone marrow stroma: conditions that maximize the yields of early progenitors and evaluate their quality. Stem cells. 2002;20(6):530-41.
426. Bonnelye E, Aubin JE. Differential expression of estrogen receptor-related receptor alpha and estrogen receptors alpha and beta in osteoblasts in vivo and in vitro. Journal of Bone and Mineral Research. 2002 Aug;17(8):1392-400.
427. Deckers MML, Karperien M, van der Bent C, Yamashita T, Papapoulos SE, Lowik C. Expression of vascular endothelial growth factors and their receptors during osteoblast differentiation. Endocrinology. 2000 May;141(5):1667-74.
428. Zhu H, Mitsuhashi N, Klein A, Barsky LW, Weinberg K, Barr ML, et al. The role of the hyaluronan receptor CD44 in mesenchymal stem cell migration in the extracellular matrix. Stem Cells. 2006 Apr;24(4):928-35.
429. Nakamura H, Ozawa H. Immunolocalization of CD44 and the ERM family in bone cells of mouse tibiae. Journal of Bone and Mineral Research. 1996 Nov;11(11):1715-22.
430. Li X, Pilbeam CC, Pan L, Breyer RM, Raisz LG. Effects of prostaglandin E< sub> 2</sub> on gene expression in primary osteoblastic cells from prostaglandin receptor knockout mice. Bone. 2002;30(4):567-73.
431. Cao JJ, Singleton PA, Majumdar S, Boudignon B, Burghardt A, Kurimoto P, et al. Hyaluronan increases RANKL expression in bone marrow stromal cells through CD44. Journal of Bone and Mineral Research. 2005;20(1):30-40.
432. Steeve KT, Marc P, Sandrine T, Dominique H, Yannick F. IL-6, RANKL, TNF-alpha/IL-1: interrelations in bone resorption pathophysiology. Cytokine Growth Factor Rev. 2004;15(1):49-60.

433. Shih DQ, Barrett R, Zhang XL, Yeager N, Koon HW, Phaosawasdi P, et al. Constitutive TL1A (TNFSF15) Expression on Lymphoid or Myeloid Cells Leads to Mild Intestinal Inflammation and Fibrosis. Plos One. 2011 Jan;6(1).
434. Vogel C, Marcotte EM. Insights into the regulation of protein abundance from proteomic and transcriptomic analyses. Nature Reviews Genetics. 2012;13(4):227-32.
435. Delany AM, Gabbitas BY, Canalis E. CORTISOL DOWN-REGULATES OSTEOBLAST ALPHA-1(I) PROCOLLAGEN MESSENGER-RNA BY TRANSCRIPTIONAL AND POSTTRANSCRIPTIONAL MECHANISMS. Journal of Cellular Biochemistry. 1995 Mar;57(3):488-94.
436. Mulari MTK, Qu Q, Harkonen PL, Vaananen HK. Osteoblast-like cells complete osteoclastic bone resorption and form new mineralized bone matrix in vitro. Calcif Tissue Int. 2004 Sep;75(3):253-61.
437. Vandooren J, Geurts N, Martens E, Van den Steen PE, Opdenakker G. Zymography methods for visualizing hydrolytic enzymes. Nature methods. 2013;10(3):211-20.
438. Baramova EN, Bajou K, Remacle A, L'Hoir C, Krell HW, Weidle UH, et al. Involvement of PA/plasmin system in the processing of pro-MMP-9 and in the second step of pro-MMP-2 activation. FEBS Lett. 1997;405(2):157-62.
439. Dvorak-Ewell MM, Chen TH, Liang N, Garvey C, Liu B, Tu CL, et al. Osteoblast Extracellular Ca2+-Sensing Receptor Regulates Bone Development, Mineralization, and Turnover. Journal of Bone and Mineral Research. 2011 Dec;26(12):2935-47.
440. Sophocleous A, Landao-Bassonga E, van't Hof RJ, Idris AI, Ralston SH. The type 2 cannabinoid receptor regulates bone mass and ovariectomy-induced bone loss by affecting osteoblast differentiation and bone formation. Endocrinology. 2011;152(6):2141-9.
441. Porter G, Festing M. EFFECTS OF DAILY HANDLING AND OTHER FACTORS ON WEIGHT GAIN OF MICE FROM BIRTH TO SIX WEEKS OF AGE. Laboratory Animals. 1969;3:7 - 16.
442. Gall GAE, Kyle WH. Growth of the Laboratory Mouse. Theoretical and Applied Genetics. 1968;38(7):304-8.
443. Gregoire FM, Smas CM, Sul HS. Understanding adipocyte differentiation. Physiological Reviews. 1998 Jul;78(3):783-809.
444. Muguruma Y, Reyes M, Nakamura Y, Sato T, Matsuzawa H, Miyatake H, et al. IN vivo and in vitro differentiation of myocytes from human bone marrow-derived multipotent progenitor cell. Experimental Hematology. 2003 Dec;31(12):1323-30.
445. König A, Mühlbauer RC, Fleisch H. Tumor necrosis factor α and interleukin-1 stimulate bone resorption in vivo as measured by urinary [3H] tetracycline excretion from prelabeled mice. Journal of Bone and Mineral Research. 1988;3(6):621-7.
446. van't Hof RJ. Analysis of Bone Architecture in Rodents Using Microcomputed Tomography. Bone Research Protocols: Springer; 2012. p. 461-76.
447. Compston J. Bone histomorphometry [mdash] the renaissance? BoneKey-Osteovision. 2004;1(5):9-12.
448. Deswal A, Petersen NJ, Feldman AM, Young JB, White BG, Mann DL. Cytokines and cytokine receptors in advanced heart failure - An analysis of the cytokine database from the vesnarinone trial (VEST). Circulation. [Article]. 2001 Apr;103(16):2055-9.
449. Gu Z, Cui J, Brown S, Fridman R, Mobashery S, Strongin AY, et al. A highly specific inhibitor of matrix metalloproteinase-9 rescues laminin from proteolysis and neurons from apoptosis in transient focal cerebral ischemia. The Journal of neuroscience. 2005;25(27):6401-8.
450. Nakamura I, Pilkington MF, Lakkakorpi PT, Lipfert L, Sims SM, Dixon SJ, et al. Role of alpha(v)beta(3) integrin in osteoclast migration and formation of the sealing zone. J Cell Sci. 1999 Nov;112(22):3985-93.

451. Zhang F, Tanaka H, Kawato T, Kitami S, Nakai K, Motohashi M, et al. Interleukin-17A induces cathepsin K and MMP-9 expression in osteoclasts via celecoxib-blocked prostaglandin E-2 in osteoblasts. Biochimie. 2011 Feb;93(2):296-305.
452. Destaing O, Sanjay A, Itzstein C, Horne WC, Toomre D, De Camilli P, et al. The tyrosine kinase activity of c-Src regulates actin dynamics and organization of podosomes in osteoclasts. Molecular Biology of the Cell. 2008;19(1):394-404.
453. Schwartzberg PL, Xing L, Hoffmann O, Lowell CA, Garrett L, Boyce BF, et al. Rescue of osteoclast function by transgenic expression of kinase-deficient Src insrc-/- mutant mice. Genes & development. 1997;11(21):2835.
454. Miyazaki T, Takayanagi H, Isshiki M, Takahashi T, Okada M, Fukui Y, et al. In Vitro and In Vivo Suppression of Osteoclast Function by Adenovirus Vector–Induced csk Gene. Journal of Bone and Mineral Research. 2000;15(1):41-51.
455. Okamatsu Y, Kim D, Battaglino R, Sasaki H, Spate U, Stashenko P. MIP-1 gamma promotes receptor activator of NF-kappa B ligand-induced osteoclast formation and survival. J Immunol. 2004 Aug;173(3):2084-90.
456. Mbalaviele G, Chen H, Boyce BF, Mundy GR, Yoneda T. THE ROLE OF CADHERIN IN THE GENERATION OF MULTINUCLEATED OSTEOCLASTS FROM MONONUCLEAR PRECURSORS IN MURINE MARROW. Journal of Clinical Investigation. 1995 Jun;95(6):2757-65.
457. Saginario C, Sterling H, Beckers C, Kobayashi R, Solimena M, Ullu E, et al. MFR, a putative receptor mediating the fusion of macrophages. Molecular and Cellular Biology. 1998 Nov;18(11):6213-23.
458. Yagi M, Miyamoto T, Sawatani Y, Iwamoto K, Hosogane N, Fujita N, et al. DC-STAMP is essential for cell-cell fusion in osteoclasts and foreign body giant cells. J Exp Med. [Article]. 2005 Aug;202(3):345-51.
459. Kukita T, Wada N, Kukita A, Kakimoto T, Sandra F, Toh K, et al. RANKL-induced DC-STAMP is essential for osteoclastogenesis. Journal of Experimental Medicine. 2004 Oct;200(7):941-6.
460. Boyce BF, Yoneda T, Lowe C, Soriano P, Mundy G. Requirement of pp60c-src expression for osteoclasts to form ruffled borders and resorb bone in mice. J Clin Invest. 1992;90(4):1622.
461. Arnett TR, Dempster DW. EFFECT OF PH ON BONE-RESORPTION BY RAT OSTEOCLASTS INVITRO. Endocrinology. 1986 Jul;119(1):119-24.
462. Feldmann M, Maini RN. Anti-TNF alpha therapy of rheumatoid arthritis: what have we learned? Annual Review of Immunology. 2001;19:163-96.
463. Galloway JB, Hyrich KL, Mercer LK, Dixon WG, Fu B, Ustianowski AP, et al. Anti-TNF therapy is associated with an increased risk of serious infections in patients with rheumatoid arthritis especially in the first 6 months of treatment: updated results from the British Society for Rheumatology Biologics Register with special emphasis on risks in the elderly. Rheumatology. 2011 Jan;50(1):124-31.
464. Buchan SL, Taraban VY, Slebioda TJ, James S, Cunningham AF, Al-Shamkhani A. Death receptor 3 is essential for generating optimal protective CD41 T-cell immunity against Salmonella. European Journal of Immunology. 2012 Mar;42(3):580-8.
465. Taurog JD. Animal Models of Spondyloarthritis. Molecular Mechanisms of Spondyloarthropathies. 2009;649:245-54.
466. Twohig JP, Marsden M, Cuff SM, Ferdinand JR, Gallimore AM, Perks WV, et al. The death receptor 3/TL1A pathway is essential for efficient development of antiviral CD4+ and CD8+ T-cell immunity. The FASEB journal. 2012;26(8):3575-86.
467. Bamias G, Mishina M, Nyce M, Ross WG, Kollias G, Rivera-Nieves J, et al. Role of TL1A and its receptor DR3 in two models of chronic murine ileitis. Proceedings of the National Academy of Sciences. 2006;103(22):8441-6.

468. Vermes I, Haanen C, Steffens-Nakken H, Reutellingsperger C. A novel assay for apoptosis flow cytometric detection of phosphatidylserine expression on early apoptotic cells using fluorescein labelled annexin V. Journal of Immunological Methods. 1995;184(1):39-51.
469. Rehman MTA, Hoyland JA, Denton J, Freemont AJ. HISTOMORPHOMETRIC CLASSIFICATION OF POSTMENOPAUSAL OSTEOPOROSIS - IMPLICATIONS FOR THE MANAGEMENT OF OSTEOPOROSIS. Journal of Clinical Pathology. 1995 Mar;48(3):229-35.
470. Baudry A, Bitard J, Mouillet-Richard S, Locker M, Poliard A, Launay JM, et al. Serotonergic 5-HT2B Receptor Controls Tissue-nonspecific Alkaline Phosphatase Activity in Osteoblasts via Eicosanoids and Phosphatidylinositol-specific Phospholipase C. Journal of Biological Chemistry. 2010 Aug;285(34):26066-73.
471. Collet C, Schiltz C, Geoffroy V, Maroteaux L, Launay JM, de Vernejoul MC. The serotonin 5-HT2B receptor controls bone mass via osteoblast recruitment and proliferation. Faseb Journal. 2008 Feb;22(2):418-27.
472. Bliziotes MM, Eshleman AJ, Zhang XW, Wiren KM. Neurotransmitter action in osteoblasts: Expression of a functional system for serotonin receptor activation and reuptake. Bone. 2001 Nov;29(5):477-86.
473. Yilmazer-Hanke DM, Roskoden T, Zilles K, Schwegler H. Anxiety-related behavior and densities of glutamate, GABA(A), acetylcholine and serotonin receptors in the amygdala of seven inbred mouse strains. Behavioural Brain Research. 2003 Oct;145(1-2):145-59.
474. Friedel RH, Wurst W, Wefers B, Kühn R. Generating conditional knockout mice. Transgenic Mouse Methods and Protocols: Springer; 2011. p. 205-31.
475. Teitelbaum SL, Tondravi MM, Ross FP. Osteoclasts, macrophages, and the molecular mechanisms of bone resorption. J Leukoc Biol. [Review]. 1997 Apr;61(4):381-8.
476. Parikka V, Lehenkari P, Sassi ML, Halleen J, Risteli J, Harkonen P, et al. Estrogen reduces the depth of resorption pits by disturbing the organic bone matrix degradation activity of mature osteoclasts. Endocrinology. 2001 Dec;142(12):5371-8.
477. Inui T, Ishibashi O, Inaoka T, Origane Y, Kumegawa M, Kokubo T, et al. Cathepsin K antisense oligodeoxynucleotide inhibits osteoclastic bone resorption. Journal of Biological Chemistry. 1997 Mar;272(13):8109-12.
478. Jeon OH, Jeong SH, Yoo YM, Kim KH, Yoon DS, Kim CH. Quantification of Temporal Changes in 3D Osteoclastic Resorption Pit using Confocal Laser Scanning Microscopy. Tissue Eng Regen Med. [Article]. 2012 Feb;9(1):29-35.